

**Solid-State NMR Spectroscopy Studies of Human N-
Ras Protein
and
Synthesis and Biochemical Studies of Rab GGTase
Inhibitors**

**Zur Erlangung des akademischen Grades eines
Doktors der Naturwissenschaften
vom Fachbereich Chemie der
Universität Dortmund
angenommene**

Dissertation

von B. Sc. (Honours)-Chemiker

Kui Thong Tan

aus

Perak (Malaysia)

- 1. Gutachter: Prof. Dr. Herbert Waldmann**
- 2. Gutachter: Prof. Dr. Roger S. Goody**

Tag der mündlichen Prüfung: 17.09.2007

Die vorliegende Arbeit wurde unter Anleitung von Prof. Dr. Herbert Waldmann am Fachbereich Chemie der Universität Dortmund und am Max-Planck-Institut für molekulare Physiologie in der Zeit von August 2003 bis Mai 2007 angefertigt.

For My Family and Xiaoai

Table of Contents

Chapter A

1	Introduction	2
2	Background	3
2.1.1	Cancer and oncogenes	3
2.1.2	Ras proteins and cancers	4
2.1.3	Upstream ligands and downstream effectors of Ras proteins	5
2.1.4	CAAX modification and membrane targeting of Ras proteins	7
2.1.5	Microlocalization of Ras proteins at the plasma membrane	10
2.1.6	Dynamic regulation of Ras microlocalization and activity	11
2.2.1	Solid-state nuclear magnetic resonance (NMR) spectroscopy	13
2.2.2	Solid-state magic-angle spinning	14
2.2.3	^2H quadrupole coupling	16
2.2.4	Relaxation measurement	17
3	Aim of the Dissertation	19
4	Results and Discussion	22
4.1	Synthesis of Isotope Labeled N-Ras Proteins	22
4.1.1	Synthetic plan	22
4.1.2	Selection of linker for the preparation of peptides	25
4.1.3	Preparation of building blocks	26
4.1.4	Synthesis of isotopically labeled lipidated peptides	30
4.1.5	Coupling of MIC-incorporated isotope labeled lipidated peptides on truncated N-Ras protein	32
4.2	Structural Studies of Membrane-Associated C-Terminus of Lipid-Modified Human N-Ras Protein by Solid-State NMR Spectroscopy	36
4.2.1	Solid-state NMR spectroscopy study of phospholipids phases	36
4.2.2	Measurement of proton and carbon NMR for N-Ras proteins 1 and 2	38
4.2.3	Two dimensional (2D) NMR	42
4.2.4	Torsion angle prediction by TALOS	46
4.2.5	Structural model of membrane-associated C-terminus of N-Ras	

protein	49
4.3 Dynamical Studies of Membrane-Associated C-Terminus of Lipid-Modified Human N-Ras Protein by Solid-State NMR Spectroscopy	52
4.3.1 Lipid chain dynamics of membrane bound Ras protein	52
4.3.2 Molecular dynamics of the C-terminus of membrane-associated Ras protein.	62
4.3.3 Summary of the dynamic study for the membrane-associated N-Ras protein C-terminus	66
5 Experimental Part	70
6 References	83

Chapter B

1 Introduction	89
2 Background	90
2.1 Vesicular Transport in Eukaryotic Cell	90
2.2 The Roles of Rab Proteins in Protein Trafficking	92
2.2.1 Rab proteins assisted vesicle formation	93
2.2.2 Rab proteins mediated vesicle motility	94
2.2.3 Rab proteins regulate vesicle docking	94
2.2.4 Rab proteins regulate vesicle fusion	95
2.3.1 Upstream regulation of Rab proteins	96
2.4.1 Post-translational modification of Rab proteins	98
2.5.1 Rab pathway as a target for disease therapy	98
2.6.1 Rab GGTase as an apoptotic target	100
2.7.1 Regulation of Rab GGTase activity to study endosomal vesicular trafficking and cancer	101
3 Aim of the Dissertation	103
4 Results and Discussion	105
4.1.1 Fluorescence assay of Rab GGTase	105
4.1.2 Synthesis of fluorescence substrate NBD-FPP 1	107

4.2	Synthesis of Rab GGTase Inhibitors	112
4.2.1	Synthetic plan	112
4.2.2	Choice of linkers	113
4.2.3	Synthesis of hydrazine linker 21 and loading to resin	115
4.2.4	Incorporation of amino acids and the N-terminus substrates	117
4.2.5	Oxidative cleavage by NBS	119
4.2.6	Oxidative cleavage by Cu(OAc) ₂	124
4.2.7	Comparison of the NBS and the Cu(OAc) ₂ oxidative cleavage condition	127
4.2.8	Summary and discussion of the peptide library synthesis	128
4.3	Biochemical Investigation of Rab GGTase Inhibitors	130
4.3.1	<i>In vitro</i> screening of peptide library	130
4.3.2	Structure activity relationships (SAR) of inhibitors	133
4.3.3	<i>In vivo</i> study of peptide inhibitors	139
4.3.4	Selectivity studies of inhibitors towards Rab GGTase, FTase and GGTase I	140
4.3.5	Kinetic analysis of compound 81 towards Rab GGTase inhibition	143
4.3.6	Summary and discussion of biochemical investigation of Rab GGTase inhibitors	148
5	Conclusions and Outlook	149
6	Appendix	150
7	Experimental Part	187
8	References	336

Abbreviation

Summary of the Dissertation

Zusammenfassung der Dissertation

Acknowledgement

Curriculum Vitae

Chapter A

Solid-State NMR Spectroscopy Studies of Human N-Ras Protein

1 Introduction

A lot of publicity has been rightly accorded to the Human Genome Project, which has now been completed.¹ The success of this work has been hailed as a breakthrough that will lead to a new era in medicinal research. However, it is important to appreciate that this knowledge forms only the tip of the iceberg. As proteins ‘speak’ for DNA and phenotypes of all living organism on earth, the study of the proteins has become the more significant task in this post genomic era. This is far more challenging than understanding the genome, because of the complexity of interactions that can take place between proteins. Moreover, the structure and function of proteins present in a cell depend on the type of cell. In the diseased state, the structure and hence the function of the proteins can be altered. Currently and even in the future, drugs that interact with proteins will remain the most important target in medicine and provide treatment for ailments such as cancer, pain, depression, asthma and many other problems.

The race is now on to analyze the structure and function of proteins, many of which are completely new to science, and to see whether they can act as novel drug targets for the future. This is not an easy task, and it is made all the more difficult by the fact that it is simply not possible to derive the structure of proteins based on the known gene sequences alone. This is because different proteins can be derived from a single gene, and proteins are often modified following their synthesis (post-translational modification).

The analysis of secondary and tertiary structure of proteins is painstaking work. If the protein can be crystallized, it is then possible to determine its structure by X-ray crystallography. However, not all proteins can be crystallized, and even if they are, it is possible that the conformation in the crystal form is different from that in solution. In this aspect, NMR spectroscopy has become an important complementary tool to X-ray crystallography in identifying the structure of proteins, especially in the study of membrane proteins that cannot be crystallized easily.²

2 Background

2.1.1 Cancer and oncogenes

Cancer is a class of diseases or disorders characterized by uncontrolled division of cells and the ability of these cells to spread, either by direct growth into adjacent tissue through invasion, or by implantation into distant sites by metastasis (where cancer cells are transported through the bloodstream or lymphatic system). Cancer may affect people of all ages, but risk tends to increase with age. It is one of the principal causes of death in developed countries. In the USA and other developed countries, cancer is presently responsible for about 25% of all deaths. On a yearly basis, 0.5% of the population is diagnosed with cancer.³

Cell division or cell proliferation is a physiological process that occurs in almost all tissues. Normally the balance between proliferation and apoptosis (programmed cell death) is tightly regulated to ensure the integrity of organs and tissues (Figure 1A). Cancer cells avoid apoptosis and continue to multiply in an unregulated manner. One of the most profound features of cancer cell is the growth properties in laboratory culture dish. Tumor cells grow in multilayers, with higher cell densities, and they continue to grow even when the surface of the culture dish is completely covered (Figure 1B). The reason of this uncontrolled cell growth is normally attributed to the mutation or damage of genes. Cancer is, ultimately, a disease of genes.

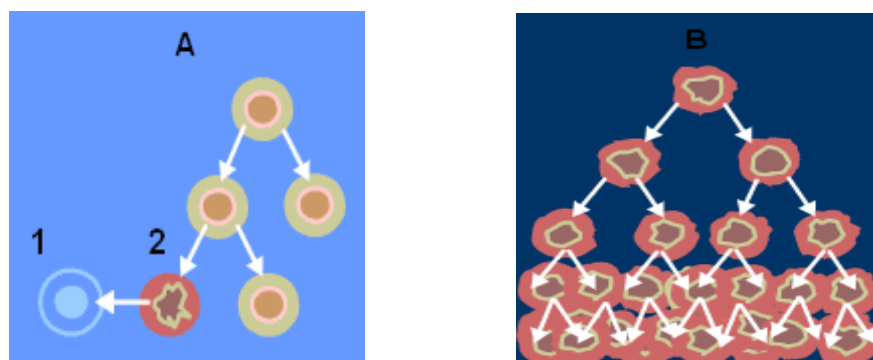


Figure 1. A) Normal cell division and apoptosis of damage cells **2** leading to cell death **1**; **B)** Non-stop division of cancer cells⁴

Cancer formation is initiated *via* the conversion of normal cellular genes, called proto-oncogenes, into oncogenes. This results in the alteration of growth properties that is characterized as oncogenic transformation. The biological function of proto-oncogenes is not to cause cancer. Rather these genes encode proteins that are part of the regular process of signal transduction pathways, which control normal cellular growth and differentiation.⁵

Cellular growth, division and differentiation are all controlled by signal transduction pathways triggered mainly by proteins called growth factors. Many growth factor receptors are membrane spanning proteins with protein tyrosine kinase activity. Binding of the ligand (growth factor) to its receptor leads to activation of the tyrosine kinase activity and the subsequent activation of a number of cytoplasmic proteins. These proteins form a cascade in which the activation of one molecule causes activation of its downstream effector until the final target is reached.

Oncogenic transformation of cells can be caused by constitutive activation of these pathways in a number of ways. For example, over- or inappropriate expression of a growth factor can result in inappropriate activation of a signal transduction pathway causing cells to grow and divide under conditions where they would not otherwise divide. Mutation of an intermediate component in the cascade, which results in the protein getting accumulated in its activated form results in a pathway whose output is always "on" and is independent of the original extracellular signal. This also leads to uncontrolled growth of cells.

One component of the signal transduction cascade involved in growth regulation is the protein encoded for by the ***Ras*** (rat sarcoma) gene.⁶

2.1.2 Ras proteins and cancers

Ras proteins are the prototype members of a large family of ~ 21 kDa GTP-regulated molecular switches for signaling pathways that modulate many aspects of cell behavior,

including proliferation,⁷ differentiation,⁸ motility⁹ and death.¹⁰ The Ras superfamily of GTPases can be subdivided into the Ras, Rho, Rab, ARF, and Ran subfamilies. The tumor oncoproteins H-Ras, K-Ras, and N-Ras are the founding members of a larger family of at least 35 related human proteins.¹¹

Ras genes were first identified and characterized as transduced oncogenes in the Harvey and Kirsten strains of acutely transforming retroviruses.¹² Mutationally activated forms of H-Ras, K-Ras, and N-Ras were subsequently isolated from human tumor cells using transfection-based assays.

The H-, N-, and K-Ras proteins are ubiquitously expressed in mammalian cells. About 30% of human tumors exhibit activating mutations in one or more of the Ras genes, and of these, K-Ras is most frequently found to be mutated (about 85% of the total), followed by N-Ras (15%) and H-Ras (less than 1%).¹³ High rates of K-Ras-activating mutations have been detected in non-small cell lung cancer (15 to 20% of tumors)¹⁴, colon adenomas (40%)¹⁵, and pancreatic adenocarcinomas (95%)¹⁶. More than half of the most malignant thyroid tumors, characterized as poorly differentiated or undifferentiated, harbor a mutation in K-Ras, H-Ras, or N-Ras. In addition to mutational activation, Ras genes are amplified or over-expressed in some tumors. In contrast, Ras mutations are rarely seen in some neoplasms, such as breast cancer (< 5%). Despite this low frequency, there is considerable experimental evidence that aberrant Ras activation and signaling may promote breast cancer formation.¹⁷

2.1.3 Upstream ligands and downstream effectors of Ras proteins

Ras proteins require binding of GTP to develop functional activity. Switching between the active GTP-bound and the inactive GDP-bound state is regulated by binding to the guanine nucleotide.¹⁸ Although Ras proteins possess intrinsic GTPase and GDP/GTP exchange activities, they are too low to account for the rapid and transient GDP/GTP cycling that occurs during mitogenic stimulation. Instead, a complete model for Ras function includes regulatory proteins that control the GTP/GDP cycling rate. These

regulatory proteins include GTPase activating proteins (GAPs), which stimulate hydrolysis of bound GTP to GDP, and guanine nucleotide exchange factor proteins (GEFs), which promote the replacement of bound GDP with GTP (Figure 2).

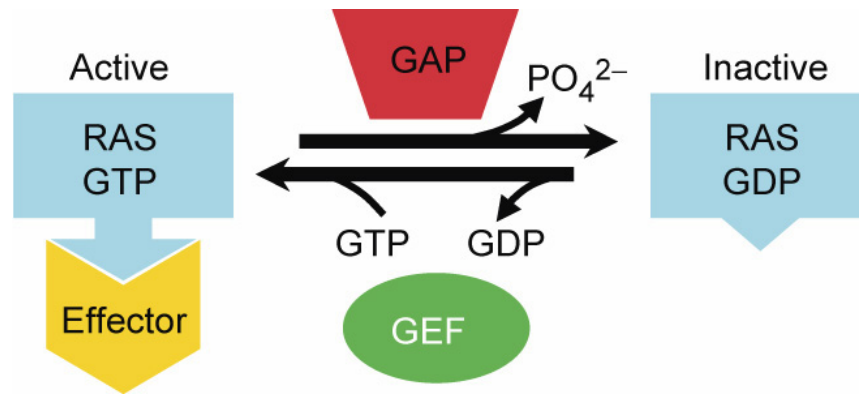


Figure 2. Activation and deactivation of Ras by GAP and GEF¹⁹. Ras GTP is deactivated by GAP and Ras GDP is activated by GEF.

Active Ras-GTP induces a wide variety of cellular processes, such as transcription, translation, cell-cycle progression, apoptosis or cell survival, through direct interaction with various effectors (Figure 3). One of the best characterized Ras signaling pathways is the Raf/MEK/ERK pathway.²⁰ The outcome of this signaling pathway can be either anti- or proapoptotic depending on the circumstances, thus determine the life or death of the cell. As shown in Figure 3, through interaction with Raf, Ras activates the MEK kinases and, in turn, the ERK kinases. ERKs phosphorylate cytoplasmic targets such as Rsk, Mnk, and phospholipase A2 which are then translocated to the nucleus, where they stimulate the activity of various transcription factors and cell-cycle progression.

It has recently been found that Ras homologues vary in their ability to activate the key effectors Raf and PI3K, with K-Ras being more effective as a recruiter and activator of Raf to the plasma membrane than does H-Ras, and H-Ras being more effective as an activator of PI3K.²¹ This indicates that activation of different Ras isoforms can have distinct biochemical consequences for the cell. Furthermore, it has been suggested that

the subcellular distribution of Ras proteins could be related to differential participation of various Ras homologues in signaling process.²²

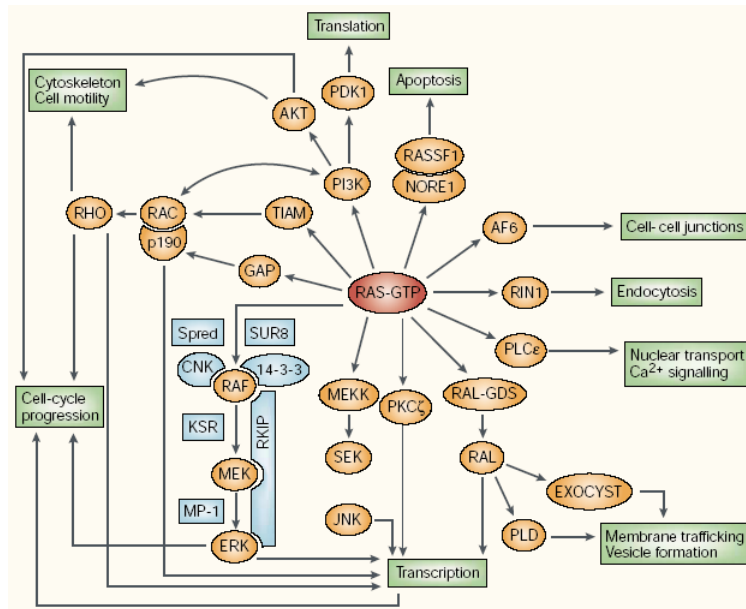


Figure 3. Ras signal transduction cascade of different downstream effectors²³. Ras proteins regulate many biological processes such as transcription, cell-cycle progression and etc.

2.1.4 CAAX modification and membrane targeting of Ras proteins

An important question for the studies of Ras is whether the ubiquitously expressed, almost identical Ras homologues have distinct functions. It has long been assumed that due to the high degree of sequence homology (>90%) shared by the three main expressed isoforms H-Ras, N-Ras and K-Ras, the identical sequences are functionally redundant. This view is reinforced by observations that all Ras homologues share common sets of downstream effectors, upstream GEFs and GAPs.

It was until recently that the biological differences in the cellular requirements of these Ras homologues which have identical sequences covering the effectors, exchange factors and guanine-nucleotide-binding domains were detected, where signaling through each Ras homologue can result in distinct biochemical outcomes.²⁴

The only region of the Ras homologues that exhibits significant sequence divergence is the final 24 residues of the protein, known as the hypervariable region (HVR), which exhibits approximately 10-15% conservation as compared with > 90% similarity over the N-terminal of 165 residues. HVR can be divided into two domains: the membrane-targeting domain and the linker domain. The membrane-targeting domain comprises the C-terminal CAAX motif, common to all Ras proteins plus a second signal sequence. The CAAX box (C = cysteine, A = aliphatic amino acids, X = serine or methionine) is sequentially modified after translation to render it more hydrophobic. The second signal sequence consists of a polybasic stretch of six lysine residues (175-180) in K-Ras, or palmitoylation of cysteine 181 and farnesylation of cysteine 186 in N-Ras, palmitoylation of cysteine 181 and 184, and farnesylation of cysteine 186 in H-Ras (Figure 4).²⁵

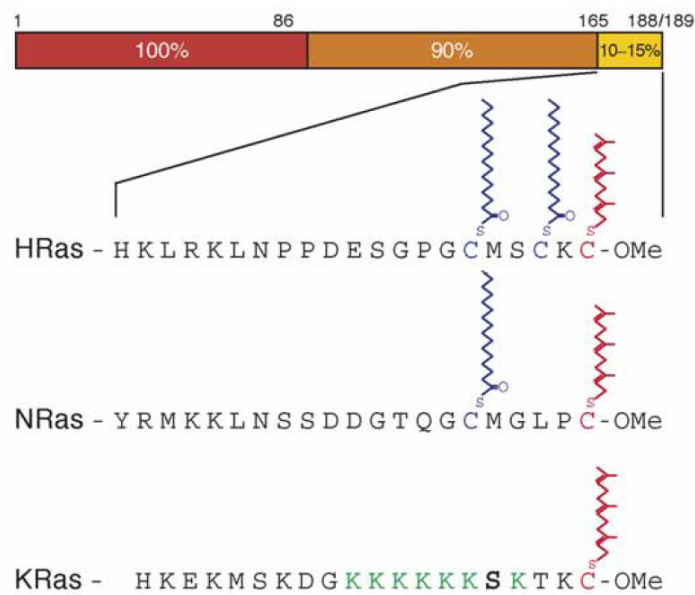


Figure 4. Amino acid sequences and lipid modification of the C-termini of different Ras homologues.²⁶

The post-translational modification of the CAAX motif is common to all Ras proteins. Figure 5 shows the schematic processing of post-translational modification of the CAAX motif after the biosynthesis of Ras proteins. First, protein farnesyltransferase (FTase), a cytosolic enzyme, attaches a farnesyl group to the cysteine residue of the CAAX motif.

Following that, an endopeptidase, Rce1 (Ras and a-factor converting enzyme) located on the cytosolic surface of the ER, removes the AAX tripeptide.²⁷ The α -carboxyl group on the carboxy-terminus of the farnesyl cysteine is then methylated by isoprenylcysteine carboxyl methyltransferase (Icmt).²⁸ K-Ras is more efficiently methylated than H-Ras or N-Ras.²⁹ Finally, after methylation, Ras proteins take one of two routes to the cell surface, which is dictated by a second targeting signal that is located immediately after the amino-terminal of the farnesylated cysteine.³⁰ H-Ras and N-Ras undergo palmitoylation on cysteine residues in their HVRs and enter the exocytic pathway, trafficking through the Golgi to the plasma membrane. In contrast, K-Ras, which has a polylysine sequence instead of cysteine residues, bypasses the Golgi and reaches the plasma membrane by an as-yet-unknown mechanism.³¹ The correct processing of the CAAX motif is essential for the efficient forward transport of Ras, because deletion of Rce1 or Icmt impairs the ability of Ras to engage both trafficking pathways, which results in mislocalization to the cytosol.^{32, 33}

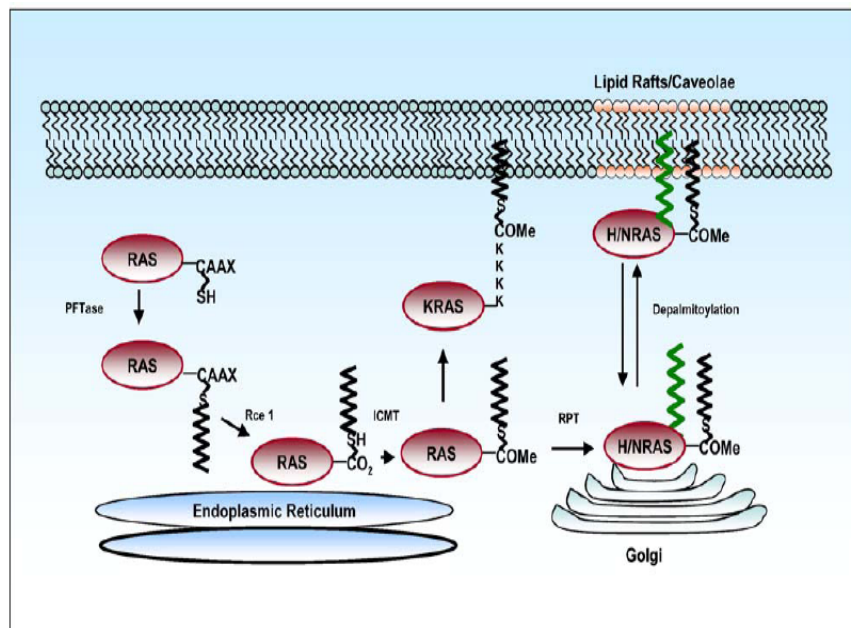


Figure 5. Schematic processing of post-translational modification of the CAAX motif after the biosynthesis of Ras proteins.^{6b}

Farnesylation is an irreversible process and stable modification of Ras. However palmitoylation, which results in the formation of a labile thioester bond is reversible in cells. At present, three palmitoyltransferase Akr1, Erf2 and Ykt6 have been identified to palmitoylate Ras proteins in yeast *Saccharomyces cerevisiae*.³⁴

2.1.5 Microlocalization of Ras proteins at the plasma membrane

Once Ras proteins have been delivered to the plasma membrane, their spatial microlocalization is dictated by a complex interplay between the Ras protein and the plasma membrane. Critical determinants of Ras microlocalization include the lipid anchor, the adjacent hypervariable region, and properties of the plasma membrane such as phospholipids/cholesterol composition of the membrane.

The plasma membrane comprises a complex mosaic of microdomains.³⁵ The best characterized of these are lipid rafts and caveolae, although it has been proposed that there are other lipid-based microdomains. For the lipid anchor, palmitoylated peripheral membrane proteins can associate with lipid rafts because the saturated palmitoyl chain packs well into the liquid order raft structure, whereas unsaturated, branched chain prenyl groups stays mostly in non-raft domains. This division of the plasma membrane into raft and non-raft compartments clearly presents a framework for differential lateral segregation of the Ras isoforms. As shown in Figure 6, K-Ras is associated predominantly with non-raft plasma membrane, irrespective of its activation state. H-Ras is distributed approximately equally between raft and non-raft plasma membrane, but GTP loading increases the fraction of H-Ras in non-raft membrane. It is important to stress that H-Ras and K-Ras are highly mobile in the plasma membrane, so the localizations shown need to be thought of more in terms of residence time.

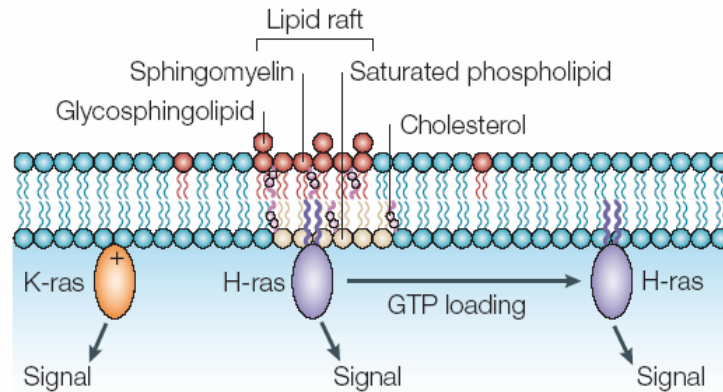


Figure 6. Microlocalization of Ras proteins in different phospholipids domains.³³

2.1.6 Dynamic regulation of Ras microlocalization and activity

Mature, fully processed Ras proteins that reached the plasma membrane were believed to remain on this compartment until degraded. However, two recent studies have uncovered a dynamic palmitoylation pathway that regulates H- and N-Ras trafficking. This pathway operates constitutively and is essential for maintaining the correct Ras localization.³⁶

This dynamic palmitoylation of Ras proteins results in a constant flux of the proteins between endomembranes and the plasma membrane. Palmitoylation at Golgi membranes directs Ras to the plasma membrane, whereas depalmitoylation at the plasma membrane releases the protein into the cytosol, allowing it to rebind to Golgi membranes, where it is once again palmitoylated and traffics to the plasma membrane (Figure 7).

This mechanism confers high accuracy in protein localization, because any mislocalization into other membrane compartments is prevented by the de-/re-palmitoylation cycle that continuously resets the systems. The precise localization is lost when the palmitate thioester is replaced by a thioether bond which cannot undergo dynamic palmitoylation. This finding suggests that the reversible cycle of de-/re-palmitoylation is crucial for allowing Ras proteins (H-Ras and N-Ras) to be properly localized in the cell.

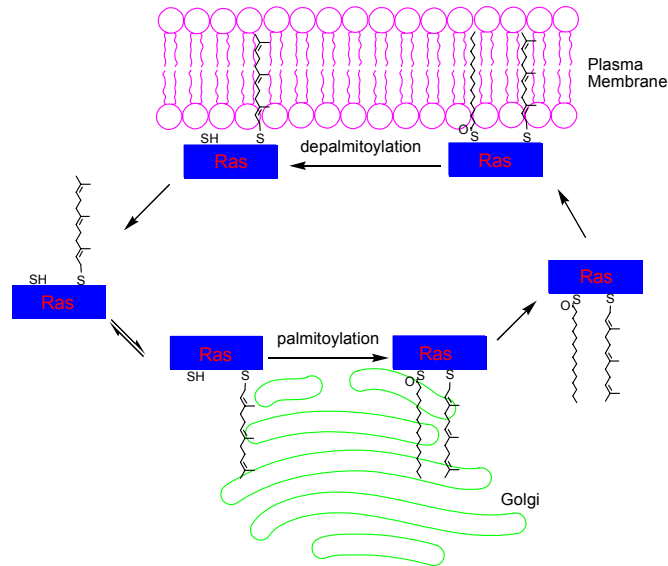


Figure 7. Dynamic palmitoylation of Ras proteins. Ras proteins are depalmitoylated at plasma membrane and palmitoylated at Golgi.

The discovery of the highly dynamic nature of Ras membrane interaction has changed the perception of compartmentalized Ras signaling. In addition to the existence of different signaling and regulatory environments in a cell, continuous shuttling of Ras between plasma membrane and Golgi has provided yet another additional regulatory mechanism. Its signaling activity from a particular membrane system is therefore not simply regulated by the timing of local GAP/GEF recruitment but also by the dynamics of its inter-membrane trafficking.

Different membrane compartments, such as the plasma membrane and Golgi, supply unique sets of GAPs and GEFs and downstream effector pathways. The three Ras homologues have similar preferences for effector proteins or regulators. In a given compartment, all Ras homologues are thus subject to the same regulation and encounter the same effectors. What makes Ras signaling distinct between various homologues is the differential access to and residence time in a particular membrane compartments. The stability of palmitoylation (H-Ras and N-Ras) or controlled membrane desorption (K-Ras) allows fine-tuning of the onset, duration and amplitude of signaling from specific compartments.

2.2.1 Solid-state nuclear magnetic resonance (NMR) spectroscopy

Determining three-dimensional structures and gaining information on the dynamics of membrane-associated proteins are fundamental to the understanding of many biological functions. Approximately 30% of all genes in a genome code for integral membrane-associated proteins, such as ion channel and receptor proteins, which are involved in a wide range of functional activities essential for the cell. Hence, knowledge of their structural and dynamical information is therefore an essential in deciphering the information from the various genome projects.

The two principal experimental methods, X-ray crystallography and solution NMR spectroscopy, are complementary to each other for the study of proteins structure and dynamics, and have contributed more than 98% of protein structures to the Protein Data Bank (85% and 13% of structures are determined by X-ray and NMR spectroscopy, mostly solution NMR spectroscopy, respectively). However, the fact that only around 1% of the protein structures in the Protein Data Bank correspond to membrane-associated proteins reflects the significant challenge posed by this class of proteins.

The structure determination of membrane-bound proteins remains difficult even with advanced methodologies. X-ray crystallography analysis is hampered by the difficulty in preparing high-quality crystals. Solution NMR analysis of membrane-associated proteins is very difficult due to the slow tumbling motion of the large membrane complexes causing the severe resonance line broadening effect. Thus solution NMR analyses of membrane proteins have been largely conducted under membrane-mimicking environments of micelles, and less in water condition. The information obtained under these conditions, however, may not reflect the real structures in the membrane-bound states.

In contrast to the solution NMR, solid-state NMR has several advantages in determining the structures and dynamics of membrane-bound proteins. Application of solid-state NMR is not limited by slow molecular motions of these large protein complexes.

Structures of numerous membrane-associated proteins have been determined by magic-angle spinning (MAS) method. Solid-state MAS NMR has been used for structural analysis of a small uniformly isotope-labeled membrane protein and for signal assignments of semi-selectively labeled membrane proteins. Further, solid-state NMR techniques provide the unique possibility to study molecular dynamics in a broad window of correlation times.

2.2.2 Solid state magic-angle spinning

Magic-angle spinning is used routinely in the vast majority of solid-state NMR experiments, where its primary task is to remove the effects of chemical shift anisotropy (chemical shifts due to different orientations of a nucleus and its electron cloud with respect to the external magnetic field B_0) and to assist in the removal of heteronuclear dipolar coupling effects. It is also used to narrow lines from quadrupolar nuclei (nuclei with spin quantum number ≥ 1 , such as deuterium), and is increasingly the method of choice for removing the effects of homonuclear dipolar coupling from NMR spectra.

In solution NMR spectra, effects of chemical shift anisotropy, dipolar coupling, and etc., are rarely observed. This is because the rapid isotropic tumbling of the molecules in a solution averages the molecular orientation dependence of the transition frequencies to zero on the NMR timescale, i.e. the rate of change of molecular orientation is fast relative to the magnitude of the chemical shift anisotropy, dipole-dipole coupling, and etc., in frequency units.

Spinning of a sample in the magnetic field during an NMR experiment leads to a reduction (scaling) of the anisotropic interaction tensor. The interaction is scaled by the second Legendré polynomial $\frac{1}{2}(3\cos^2\theta-1)$, where θ is the angle between the spinning axis and the external magnetic field. If this angle is 54.7° , the second Legendré polynomial equals zero and the anisotropic interaction vanishes, the result is a narrow NMR line and a set of spinning sidebands occurring at integer multiples of the spinning frequency. Magic-angle spinning removes the effects of chemical shielding anisotropy. In

combination with high power decoupling heteronuclear, dipolar couplings are averaged out, which provides spectra with better resolution. In addition to the magic-angle, another factor which determines the resolution of spectra is the spinning speed. In order for magic-angle spinning to reduce a powder pattern to a single line at the isotropic chemical shift, the rate of the sample spinning must be around a factor of 3 or 4 greater in comparison to the anisotropy. Figure 8a shows the broad NMR resonance of ^{13}C at a static sample. Figure 8b and 8c illustrate the effect of magic-angle spinning at 5 kHz and 10 kHz respectively. At higher spinning rate, the spectrum consist of fewer spinning sidebands, which further increases the resolution of the spectrum and provides a better resolution-to-noise ratio. At present, spinning rates of up to 50 kHz are achievable, with 30 kHz being routine on a modern spectrometer.³⁷

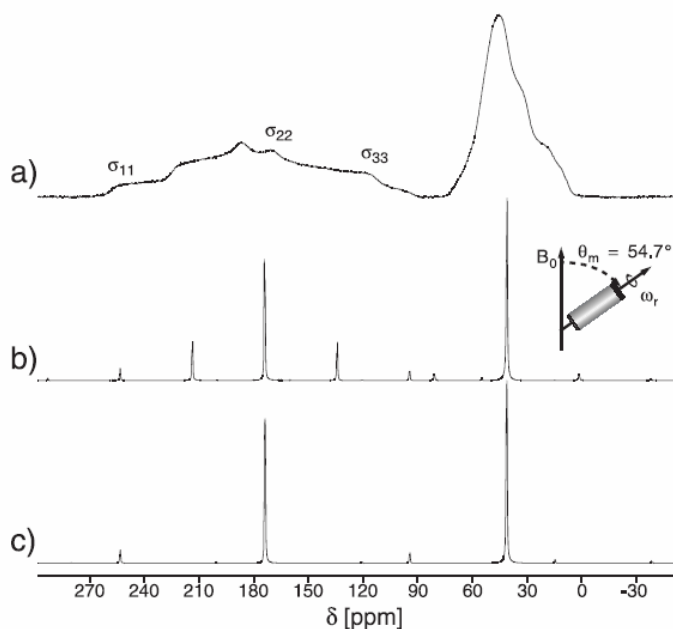


Figure 8. Effect of magic-angle spinning on the ^{13}C NMR spectrum of powdered Gly; a) The static NMR spectrum of Gly is characterized by two broad anisotropic line shapes, Magic angle spinning at b) 5 kHz and; c) 10 kHz removes the anisotropic line shapes and yields narrow lines plus a set of spinning side bands.³⁸

2.2.3 ^2H quadrupole coupling

An interaction that is never directly seen in liquid spectra but can dominate solid-state spectra is the quadrupole interaction. Figure 9A shows the energy level scheme for a spin quantum number $I = 1$ nuclei, such as deuterium, ^2H . Nuclei with $I > \frac{1}{2}$ behave as if their electric charge distribution is nonspherical. This uneven distribution of electric charge produces two different energy states under magnetic field B_0 . In ^2H powder NMR spectra of static samples, the doublet arising from the two possible transitions: $+1 \leftrightarrow 0$ and $0 \leftrightarrow -1$ (Figure 9B). Because in a powdered sample, a spherical distribution of the spins with respect to the laboratory frame occurs, so called *Pake patterns* are observed, because the position of an NMR line in the spectrum depends on the orientation of the respective crystallite. Magic-angle spinning can also be used to narrow the line broadening effect arising from quadrupolar coupling.

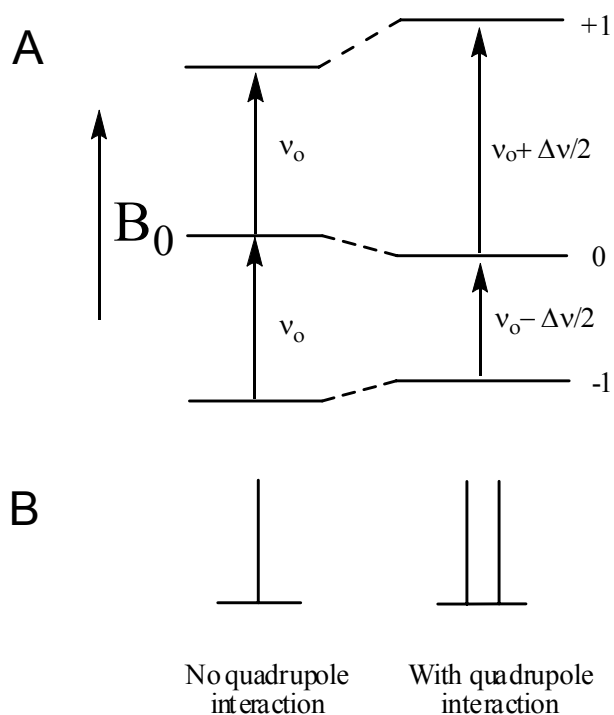


Figure 9. Nuclear spin/electric quadrupolar coupling. A) Energy levels of nuclei with spin quantum number $I = 1$; B) Splitting pattern in the absence and in the presence of the quadrupolar interaction.

It has been realized that quadrupolar splitting features arising from nuclei with spin quantum number $I > \frac{1}{2}$, especially deuterium, is a powerful nucleus for studies of molecular dynamics in solids, polymers, lipids and liquid crystals. The moderate quadrupole-coupling constant, in the range 140-220 kHz in organic compounds, and moderate width of *Pake patterns*, in the range 105-165 kHz make this nucleus relatively easy to deal with experimentally. Moreover, the lineshapes are sensitive to molecular motions with correlation times of the order of ~ 100 ps to ~ 100 μ s. Furthermore, ^2H exchange experiments can also provide information about millisecond correlation time motions. Because of this, ^2H has been extensively used in motional studies, primarily *via* lineshape analyses, but also through relaxation time measurement. Normally in ^2H quadrupolar measurement, the larger coupling constant always indicates the presence of atoms in more rigid condition and *vice versa*.

2.2.4 Relaxation measurement

NMR possesses another facet, the nuclear relaxation times (T_1 , spin lattice relaxation and spin-spin relaxation T_2 , respectively), which allow measurement of dynamic parameters such as correlation times, activation energies, and etc. All nuclear relaxation processes are induced by fluctuating nuclear spin interactions, with the fluctuations arising from molecular motion. Relaxation describes the return of the magnetization vector into equilibrium from some non-equilibrium state imposed, for instance prepared by a sequence of radiofrequency (rf) pulses.³⁹

At equilibrium, the net magnetization vector lies along the direction of the applied magnetic field B_0 and is called the equilibrium magnetization M_0 (Figure 10). In this configuration, the Z component of magnetization M_z equals M_0 . The time constant which describes how M_z returns to its equilibrium value M_0 is called the spin lattice relaxation time (T_1). In general, T_1 is inversely proportional to the spectral density of molecular motions at the Larmor frequency. The rotation frequency distribution depends on the temperature and viscosity of the surrounding environment. Therefore T_1 will vary as a function of temperature.

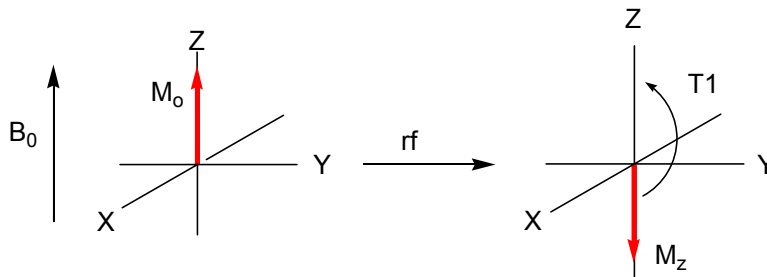


Figure 10. The cartoon describes T_1 relaxation. A 180° pulse inverts the magnetization vector along the $-z$ direction. T_1 relaxation describes the flipping back of the magnetization vector into the equilibrium state.

Another parameter which can be used to measure dynamic properties of corresponding molecules is spin-spin relaxation T_2 . T_2 is the time constant that describes the dephasing of the magnetization in the XY plane completely before growing back up to Z axis (Figure 11). Actually, both processes T_1 and T_2 occur simultaneously with the only restriction being that T_2 is smaller than or equal to T_1 . Two factors contribute to the decay of spin-spin magnetization: 1) molecular interactions (due to a pure T_2 molecular effect) and 2) variations in B_0 (due to an inhomogeneous T_2 effect). The combination of these two factors is what actually results in the decay of spin-spin magnetization.

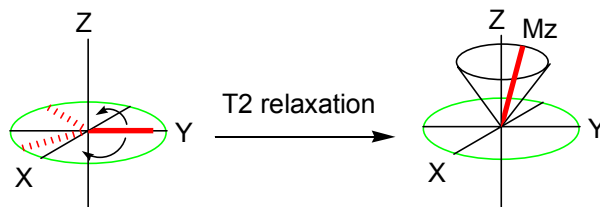


Figure 11. T_2 relaxation describes the dephasing of the magnetization vector in the xy-plane.

By measuring the relaxation times of T_1 and T_2 , a detailed analysis of intramolecular, molecular and collective motions that occur in a membrane with temperature change may be observed. Normally, correlation times are plotted in a log scale as a function of the reciprocal of temperature in order to have a direct reading of activation energies from the slopes of the lines; the steeper the slope, the higher the activation energy.

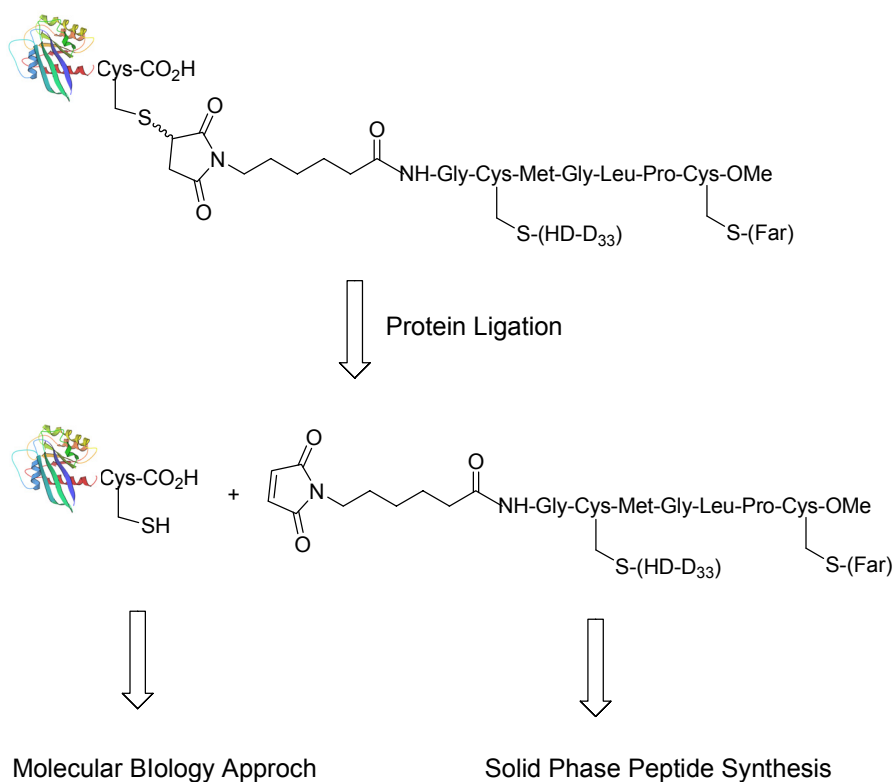
3 Aim of the Dissertation

It is worth noting that while the structure of the soluble part of N-Ras proteins (residues 1-166) has been solved by both X-ray diffraction and solution NMR spectroscopy in the absence of a membrane,⁴⁰ there are no structural data for the C-terminal membrane binding region (residues 180-186). The difficulties of crystallizing membrane attached Ras protein and the line broadening effect in solution NMR due to slow molecular motion of protein while associated with lipid bilayer have resulted in the lack of full structural data of this protein. It is therefore of general significance that the structural information of residues 180-186 can be obtained in the membrane-associated form, in order not only to understand the biological important domain (membrane-associated region) but also to establish the full N-Ras protein structure.

While structure data on N-Ras protein is scarce, the information about their mobility is even more limited. Though several studies have addressed the dynamics of the soluble N-terminus of Ras protein,⁴¹ little is known about the dynamic aspects of the membrane anchor of membrane-associated Ras protein. This part of the molecule not only attaches to the membrane bilayer but also determines the sorting of Ras into rafts or liquid crystalline domains. Recent work unveiled a dynamic pathway that is based on dynamic de-/re-palmitoylation of H-Ras protein to regulate Ras trafficking and has significantly raised the level of understanding of the dynamic information for the membrane anchor domain to another important level.³⁶

Recent advancement in solid-state NMR has prompted us to consider using this technique to investigate the structural and dynamic information for the C-terminal membrane binding region of the N-Ras protein. In addition to providing the sophisticated methodology required for measuring structural parameters, solid-state NMR spectroscopy has unique capabilities for studying the molecular dynamics of membrane proteins in their natural environment in a broad time window.

The aim of this dissertation is to study the dynamic and structural information of the membrane-bound domain (residues 180-186) of the N-Ras protein in a lipid bilayer.⁴² Lipidated N-Ras proteins can be produced by ligating the expressed water-soluble N-terminal Ras protein with lipophilic chemically synthesized C-terminal peptides (residues 180-186) to obtain a fully functional hybrid protein. In this way, isotopically labeled amino acids (¹³C, ¹⁵N) should be introduced into specific positions of the lipidated C-terminus. The N-terminus of chemically synthesized lipopeptides should be incorporated with a thiol accepting group such as maleimidocaproyl (MIC) to facilitate protein ligation. In order to maintain the stability of the protein, the labile thioester palmitoyl lipid chain at cysteine should be displaced by more stable thioether hexadecyl chain which should be labeled by deuterium ²H to study the dynamic information of lipid chain in lipid bilayer (Scheme 1).



Scheme 1. General synthetic scheme to yield the ²H, ¹³C and ¹⁵N labeled lipidated N-Ras protein.

For the solid-state NMR study, three chemically modified N-Ras proteins **1**, **2** and **3** with different ^{13}C - and ^{15}N - labeling patterns containing one S-hexadecylated (HD) and one S-farnesylated (Far) cysteine should be synthesized (Figure 12). The hexadecyl lipid chain of Cys 181 should be fully labeled with deuterium. The alternating labeling pattern should preclude most of the signal superposition and enabled well-resolved peaks to be observed. The chemically modified N-Ras proteins should be subjected to different solid-state NMR measurements all conducted under magic angle spinning (for instance ^{13}C - ^{13}C and ^{13}C - ^1H correlation experiments) and static ^2H measurements to probe the structural and dynamic information of the N-Ras C-terminus.

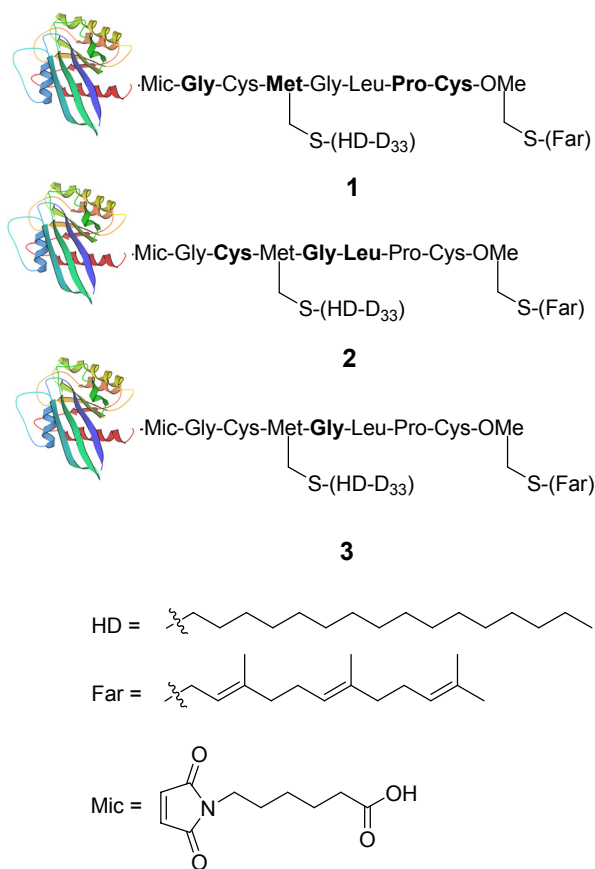


Figure 12. Three chemically modified N-Ras proteins. **Bold:** fully ^{13}C , ^{15}N labeled amino acids; HD: hexadecyl.

4 Results and Discussion

4.1 Synthesis of Isotope Labeled N-Ras Proteins

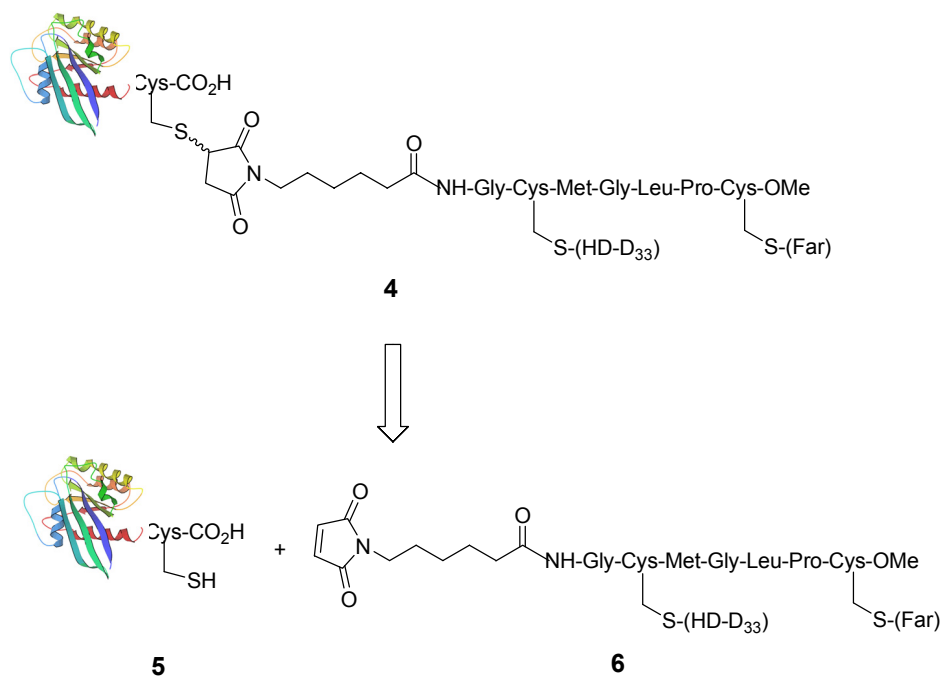
4.1.1 Synthetic plan

The biochemical generation of fully functionalized and modified lipidated protein conjugates is difficult, time consuming, and limited to only certain protein conjugates. Enzymatic lipidation of entire Ras proteins can be achieved by means of farnesyltransferase (FTase) together with the corresponding farnesyl pyrophosphate. FTase was successfully used to synthesize a Ras protein and peptides carrying analogues of the farnesyl group.⁴³ Although these methods can be used to generate Ras proteins embodying farnesyl groups and analogues, they do not allow for the synthesis of fully processed and correctly lipidated Ras proteins.

The biosynthesis of Ras proteins proceeds through farnesylation of a precursor protein carrying the C-terminal CAAX sequence, followed by proteolytic removal of the AAX tripeptide and methyl esterification of the resulting C-terminal cysteine residue. Only then is the palmitic acid thioesters introduced. Despite numerous and intense attempts, the mammalian Ras palmitoyltransferase has not yet been identified. Thus the enzymatic synthesis of fully processed and correctly lipidated Ras protein is currently not feasible. The attachment of hexadecyl lipid to form the thioether to afford a more stable adduct instead of chemically unstable palmitoyl lipid chain has rendered the use of an enzymatic approach not possible. Furthermore, in our case, ¹³C and ¹⁵N could not be incorporated specifically into the residues 180-186 at the C-terminus of N-Ras protein by using the molecular biology approach alone.

The synthesis of fully chemically decorated N-Ras proteins therefore has to be achieved by combining the techniques of organic synthesis and methods of molecular biology.⁴⁴ Normally, this approach involves the expression of suitable Ras mutants lacking the lipidatable C-terminus and their subsequent coupling with different corresponding lipidated peptides to the C-terminus of Ras by means of a protein ligation strategy.

C-terminally truncated N-Ras proteins **5** were generated by introducing stop codons at position 182 of wild-type human N-Ras. These mutants carried a cysteine at the C-terminal position 181, which lies on the surface of the protein and is therefore accessible to external reagents and peptides. The N-Ras mutant protein **5** was then allowed to react with the maleimido modified peptides **6** in stoichiometric amounts. The maleimidocaproyl (MIC) group is a well-established functionality for the covalent modification of proteins. It is known to react specifically with mercapto groups of proteins by conjugate addition of the thiol to the α , β -unsaturated carbonyl compound to form the desired protein conjugate **4** (Scheme 2).⁴⁵



Scheme 2. Ligation of truncated N-Ras protein **5** and Mic-containing lipidated peptide **6** via Michael reaction.

As compared to wild type N-Ras protein, the synthesized protein conjugate **4** consists of an extra glycine residue, maleimidocaproyl and hexadecyl chain instead of palmitoyl group. The analogues of this semi-synthetic Ras protein **4** have been verified to be biologically active in PC12 cells.⁴⁴ Although the thioether hexadecyl lipid chain behaves differently from the thioester palmitoyl chain *in vivo*, the structural and dynamic

information should be similar to each other in NMR studies with the thioether hexadecyl chain conferring higher stability. The chemical stability of these three protein conjugates is critical to the structural and dynamical studies by NMR spectroscopy, as in general, NMR measurement requires very long measuring time (one day to a week). The easily hydrolyzed thioester makes the palmitoyl lipid unsuitable for NMR experiment.

Three lipidated peptides **7**, **8** and **9** with different sites of isotope incorporated amino acids were prepared for the coupling to the truncated N-Ras protein **5** (Figure 13). Lipidated ^{13}C , ^{15}N and ^2H labeled peptides carrying a MIC group at the N-terminus were synthesized by means of Solid Phase Peptide Synthesis (SPPS) employing Fmoc-protection strategy. In this synthesis, a building block strategy will be conducted to obtain the three desired products. The lipidated chains, farnesyl and deuterium-labeled hexadecyl, will be attached to the cysteine side chain before the beginning of solid-phase synthesis.

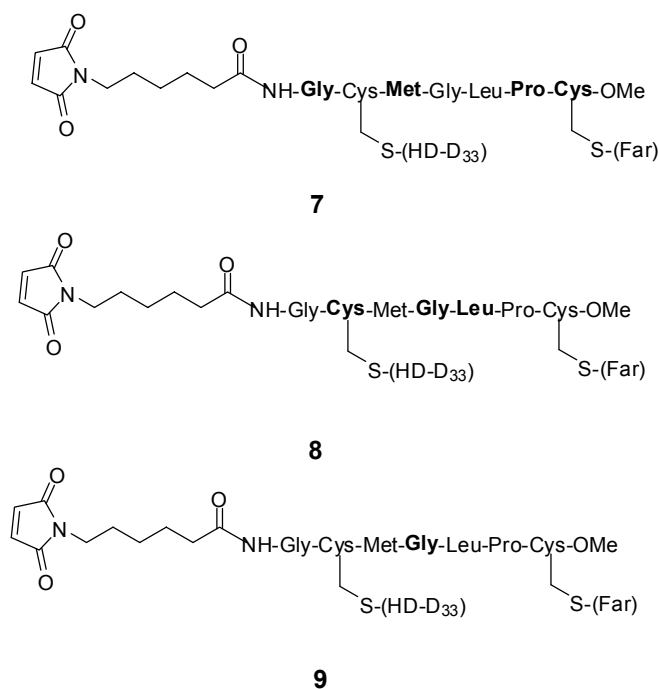
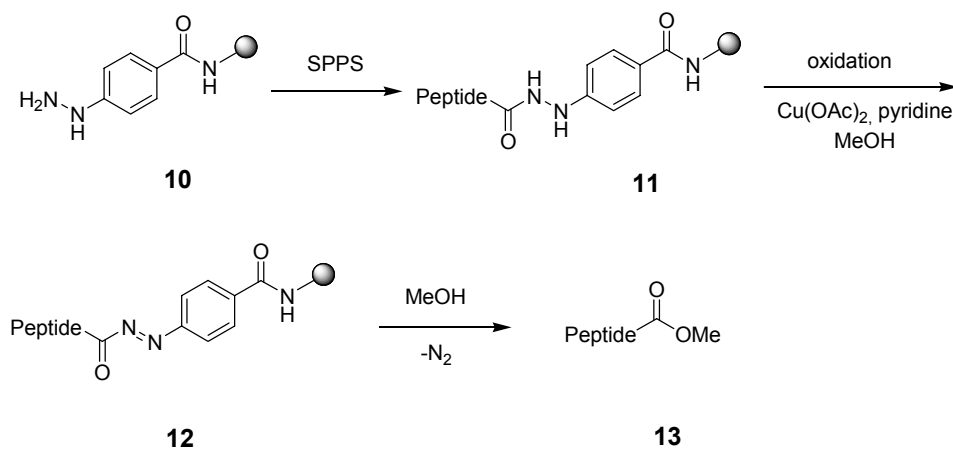


Figure 13. Three chemically synthesized isotopically labeled lipidated peptides. Fully ^{13}C and ^{15}N labeled amino acids are highlighted in bold.

4.1.2 Selection of linker for the preparation of peptides

The major challenge to be met in the synthesis of lipidated peptides is the selection of a set of suitable orthogonally stable protecting groups and a linker, which allows for the selective introduction of different lipids and other functional groups. Typical solid-phase linkers such as the Wang linker and Rink amide linker are not compatible with these requirements, as the strong acid required for release of peptide from the solid support will destroy the acid sensitive farnesyl group. Other linkers such as those based on the trityl group or the Sasrin resin that allow release of product under very mild acid conditions are compatible with the farnesyl group, but do not meet the requirements for introduction of methyl ester at the C-terminus. In addition, the nucleophilic release of peptide from resin under strong basic conditions such as sodium methoxide to form methyl ester at the C-terminus will cause the hydrolysis of maleimidocaproyl group.

The oxidation sensitive aryl hydrazine group **10** has been known for more than 30 years. Although used previously for peptide synthesis, the special utility of the hydrazine linker really came to light when applied to the synthesis of lipidated peptides.⁴⁶ The linker is cleaved by oxidation to an acyldiazene, which is then displaced by a suitable nucleophile (Scheme 3). The oxidation method which is suitable for the preparation of lipidated peptide is carried out *in situ*, employing catalytic Cu(OAc)₂, pyridine and methanol in CH₂Cl₂. Methanol serves as a nucleophile to give the desired lipidated peptide with methyl ester at the C-terminus **13**.

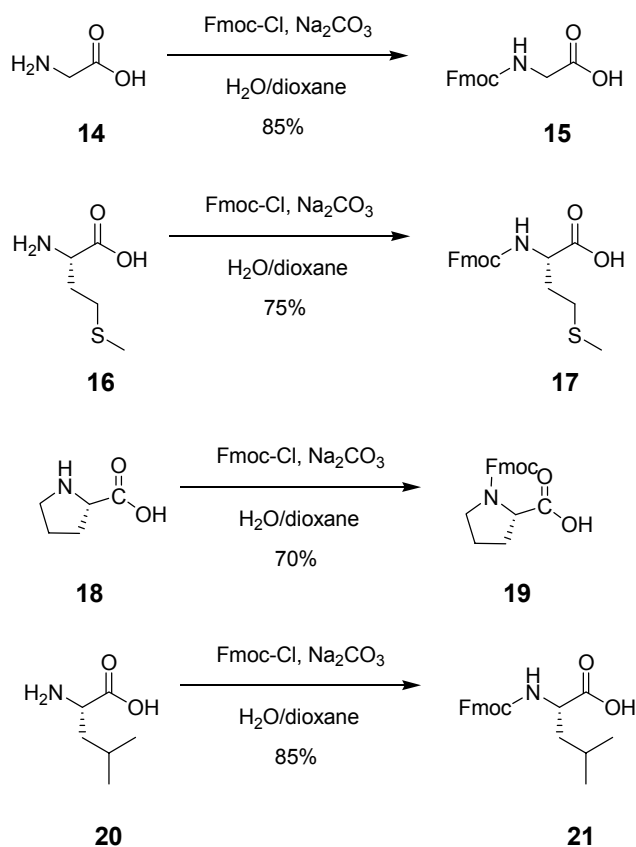


Scheme 3. General scheme for the synthesis of peptide methyl ester using the hydrazine linker.

The linker is orthogonal to classical urethane protecting groups such as Boc, Fmoc and Alloc. Moreover, racemization does not occur upon release of peptides from the resin. In this work, the aryl hydrazine linker will be used for the construction of three isotope labeled lipidated peptides **7**, **8** and **9**. The Fmoc protecting group was chosen as a standard protecting group strategy in the preparation of lipidated peptides.

4.1.3 Preparation of building blocks

To prepare labeled lipidated peptides **7**, **8** and **9**, different building blocks containing the Fmoc protecting group must be first synthesized. Commercially available and fully ^{13}C and ^{15}N decorated amino acids, leucine, proline, glycine, methionine, were protected with the Fmoc group using Fmoc-Cl and Na_2CO_3 in H_2O /dioxane as a solvent at room temperature overnight (Scheme 4). In general, the yields of the Fmoc protection on the four above mentioned amino acids ranged from 70% to 85% after purification. The unlabeled Fmoc protected amino acids were obtained from commercial sources and used without further purification.

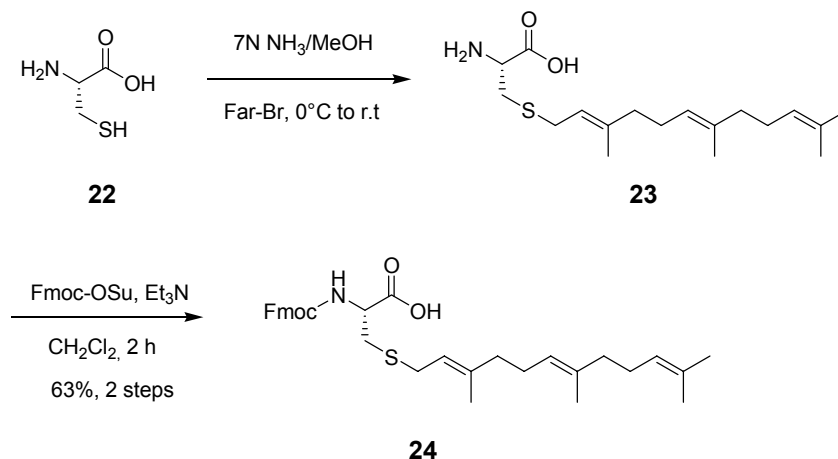


Scheme 4. Synthesis of Fmoc-protected fully ^{13}C and ^{15}N labeled building blocks.

Though the introduction of the Fmoc group on glycine, methionine, proline and leucine is straight forward, the synthesis of Fmoc protected lipidated cysteine is relatively challenging. The thiol group presents on the cysteine side chain made the Fmoc protection of the amine group followed by alkylation impossible. The better nucleophilicity of sulfur compared to oxygen and nitrogen means that the Fmoc group will be loaded on cysteine side chain instead of amine group. The synthesis of Fmoc protected lipidated cysteine therefore must start prior to the introduction of lipid group to the cysteine side chain followed by Fmoc protection.

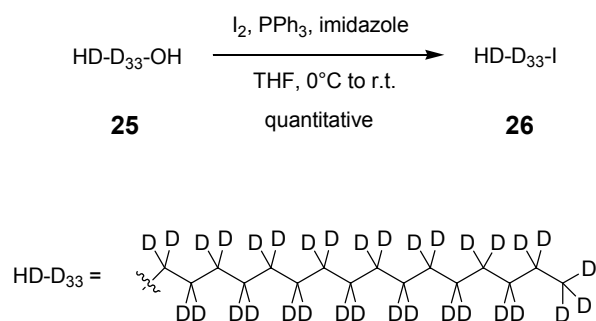
For the synthesis of ^{13}C and ^{15}N labeled Fmoc-Cys(Far)-OH **24**, the isotope decorated cysteine **22** was reacted with farnesyl bromide in 7N NH_3 in methanol from 0°C to room temperature overnight. The resulting NH_2 -Cys(Far)-OH **23** was proceeded to next step without purification and subjected to Fmoc protection using Fmoc-OSu and Et_3N in

CH₂Cl₂ for 2 hours to afford the desired product **24** in 63% yield as a colorless liquid after purification (Scheme 5). The synthesis of unlabeled Fmoc-Cys(Far)-OH **35** followed the same protocol.



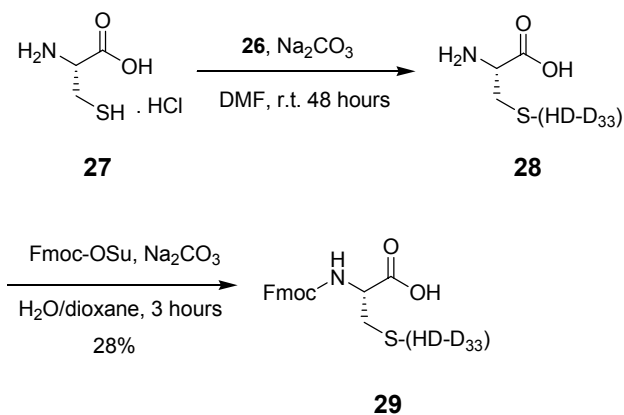
Scheme 5. Synthesis of ¹³C and ¹⁵N labeled lipidated Fmoc-Cys(Far)-OH **24** building block.

The synthesis of ¹³C, ¹⁵N and ²H labeled Fmoc-Cys(HD-D₃₃)-OH **29** can not be performed using the same protocol as for the preparation of compound **24**. The unreactive hexadecyl halide can not be linked to the sulfur atom of cysteine in 7N NH₃ in methanol. Therefore an alternative method was developed to obtain the desired product Fmoc-Cys(HD-D₃₃)-OH **29**. The synthesis of underlying compound **29** started from commercially available labeled cysteine hydrochloride and D₃₃-hexadecyl alcohol **25**. Starting material **25** was transformed to D₃₃-hexadecyl iodide **26** employing I₂, PPh₃ and imidazole in CH₂Cl₂ at 0°C to room temperature overnight to afford the desired product **26** in quantitative yield (Scheme 6).



Scheme 6. Synthesis of deuterium labeled hexadecyl iodide **26**.

Initial attempts to introduce compound **26** to labeled cysteine followed by Fmoc protection failed to yield any product **29**, although a trial reaction using unlabeled cysteine hydrochloride gave the desired product in 30% yield. This was quite surprising as the conditions and reagents used for the synthesis of Fmoc protected hexadecylated cysteine were the same, with the only exception being that the isotope decorated cysteine was not used as a hydrochloride salt. In order to perform the reaction under identical conditions, the labeled cysteine was pretreated with 1M HCl in water and ether respectively, before alkylation and protection. The alkylation of compound **26** to isotope labeled cysteine hydrochloride **27** was achieved by using Na₂CO₃ in DMF at room temperature for 48 hours to yield **28**. Protection of resulted unpurified hexadecylated cysteine **28** was performed by using Fmoc-OSu and Na₂CO₃ in H₂O/dioxane overnight to afford the desired product **29** in 28% yield (Scheme 7). The synthesis of unlabeled Fmoc-Cys(HD-D₃₃)-OH **36** followed the same protocol.



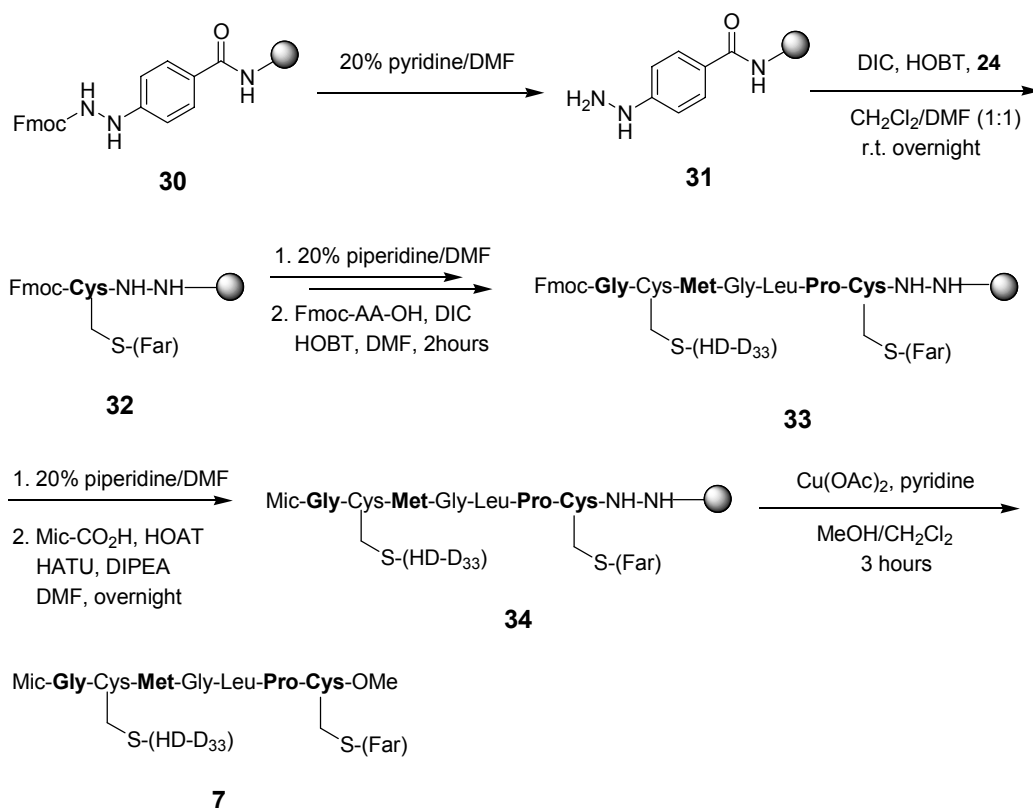
Scheme 7. Synthesis of ^{13}C , ^{15}N and ^2H labeled lipidated Fmoc-Cys(HD-D₃₃) **29** building block.

4.1.4 Synthesis of isotopically labeled lipidated peptides

The synthesis of isotope labeled lipidated peptide **7** was carried out on hydrazine resin using commercially available Fmoc hydrazine linker **30**. Fmoc group of resin **30** was deprotected using 20% piperidine in DMF to give free amino group **31** which can be used later for the coupling of the first amino acid. The loading of the first building block, ^{13}C and ^{15}N decorated Fmoc-Cys(Far)-OH **24**, was achieved using the coupling reagent DIC and HOBT in $\text{CH}_2\text{Cl}_2/\text{DMF}$ at room temperature overnight to afford **32**. The addition of CH_2Cl_2 as a co-solvent was necessary as compound **24** exhibits poor solubility in DMF. A longer coupling time was required for the coupling of the first amino acid **24** to the resin due to the bulky farnesyl side chain.

The subsequent elongation of the peptide chain and deprotection of the Fmoc group were achieved by employing standard coupling reagents DIC and HOBT in DMF for two hours and 20% piperidine in DMF respectively to give **33**. Compound **33** was deprotected and coupled to MIC carboxylic acid using the coupling reagent HOAT, HBTU and DIPEA in DMF overnight to obtain **34**. Peptide **34** on resin was released from the solid support by oxidation using $\text{Cu}(\text{OAc})_2$, pyridine and excess methanol in CH_2Cl_2 for 3 hours to afford the desired isotope incorporated lipidated peptide **7** in 23% yield after purification (Scheme 8).

In general, the synthesis of MIC-modified isotope labeled lipidated peptides **7** on hydrazine resin gave reasonable amounts of products (11 mg) for the subsequent coupling to truncated N-Ras protein. The generally low yield (23% in this case) of employing hydrazine linker was not attributed to the inefficient coupling of amino acid building blocks to the resin or formation of side products. Instead, it was believed that during the oxidative release of peptide from the solid support, the formation of radical species *in situ* by $\text{Cu}(\text{OAc})_2$ caused a radical derived from the hydrazide to be trapped by the polystyrene polymer. Upon formation of hydrazine and polystyrene bond, the peptides therefore would not be released from the solid support.



Scheme 8. Synthesis of MIC-incorporated isotope labeled lipidated peptide **7**. **Bold** = fully ¹³C and ¹⁵N labeled amino acids.

Figure 14 shows the LC-MS trace for peptide 7. The HPLC peak at 10.69 minute corresponds to the correct peptide 1 mass peak of 1367 $[M+H]^+$.

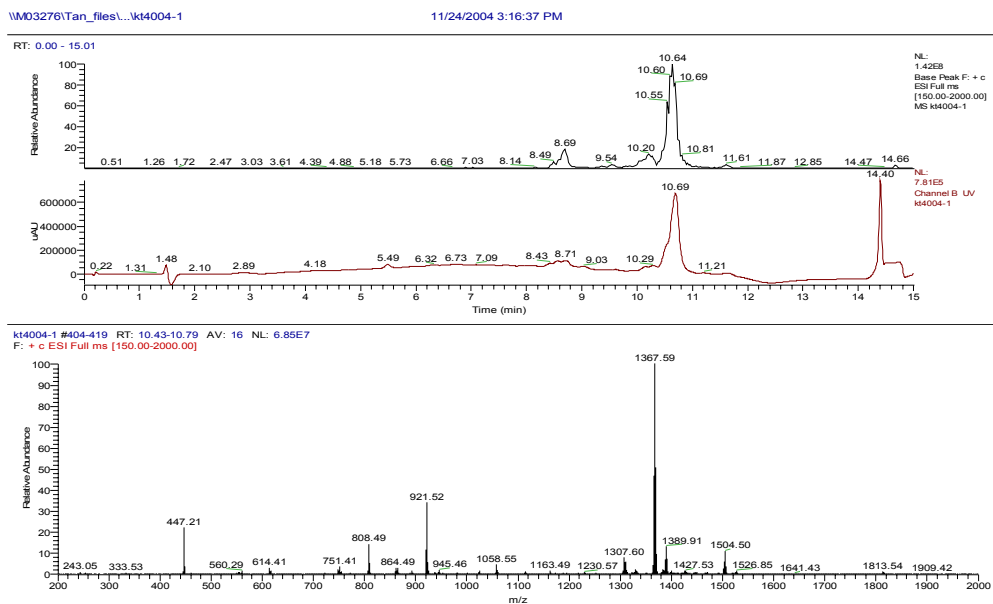


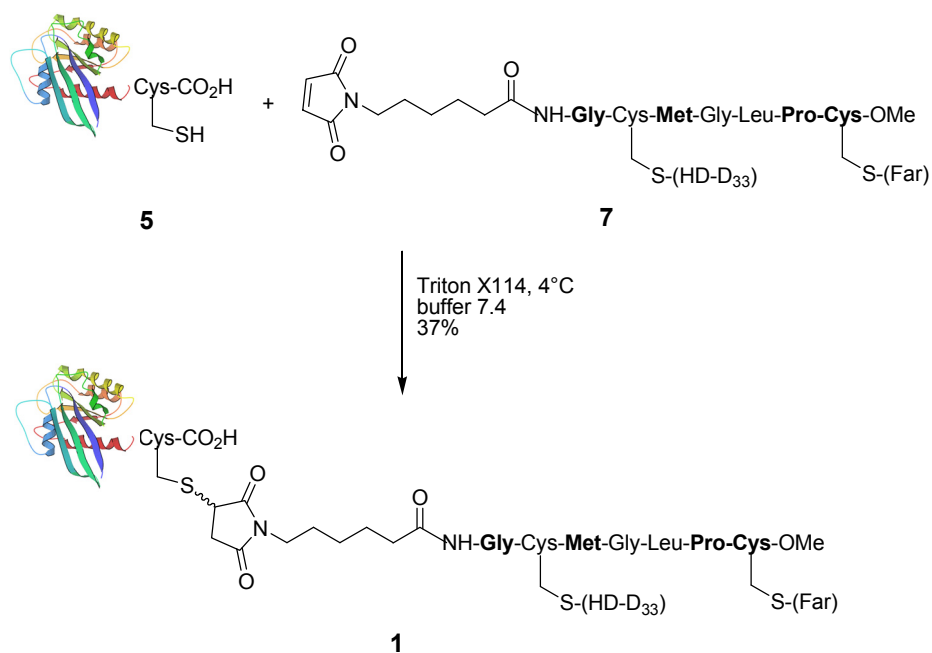
Figure 14. HPLC_MS trace of isotope decorated lipidated peptide 7 after purification.

MIC-incorporated peptide 8 and 9 were prepared by means of the same procedure as peptide 7 in 10% and 17% yield respectively.

4.1.5 Coupling of MIC-incorporated isotope labeled lipidated peptides to truncated N-Ras protein

The protein ligation between cysteine side chain of the truncated Ras mutant and the maleimidocaproyl (MIC) group at the N-terminus of lipopeptide was developed in 2002.⁴⁴ This ligation technique allows the presence of base and acid sensitive lipid groups in peptide. Under suitable reaction conditions, the thiol group of cysteine side chain reacts specifically with the maleimido group to form a thioether bond.

The ligation reaction was conducted by Christine Nowak in the group of Jürgen Kuhlmann, Max-Plank Institute of Molecular Physiology. The coupling was performed with stoichiometric amounts of isotope labeled lipidated peptide **7** and truncated N-Ras protein **5**. The coupling mixture was incubated in Triton X114 containing Tris buffer at 4°C overnight under argon to give product **1** (Scheme 9). The addition of nonionic detergent enables to dissolve the lipophilic peptide **7** and hydrophilic truncated N-Ras mutant **5**. The purification of the reaction mixture can be assisted by this detergent. The hydrophobic coupling product and lipidated peptide **7** was extracted to Triton X114 phase, and unreacted protein **5** remained in the water phase.



Scheme 9. Synthesis of chemical modified N-Ras protein **1** by protein ligation of truncated N-Ras protein **5** and isotope labeled lipidated peptide **7**. **Bold** : fully ¹³C and ¹⁵N labeled amino acids.

The protein extract was diluted to 2% Triton and applied on a DEAE-sepharose column to give semi-synthetic protein **1** in 37% yield. Figure 15 shows the SDS-page characterization of protein **1**.

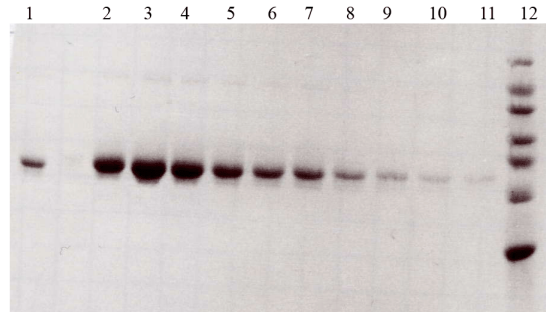


Figure 15. SDS-PAGE gel of semi-synthetic N-Ras protein **1**. The bands represented as the following, **1**: truncated N-Ras protein **5**, **12**: Marker, **2-11**: Product fraction after purification.

The resulting semi-synthetic lipidated protein **1** was further characterized by MALDI-TOF measurement. Figure 16 shows the MALDI-TOF spectrum of semi-synthetic protein **1**.

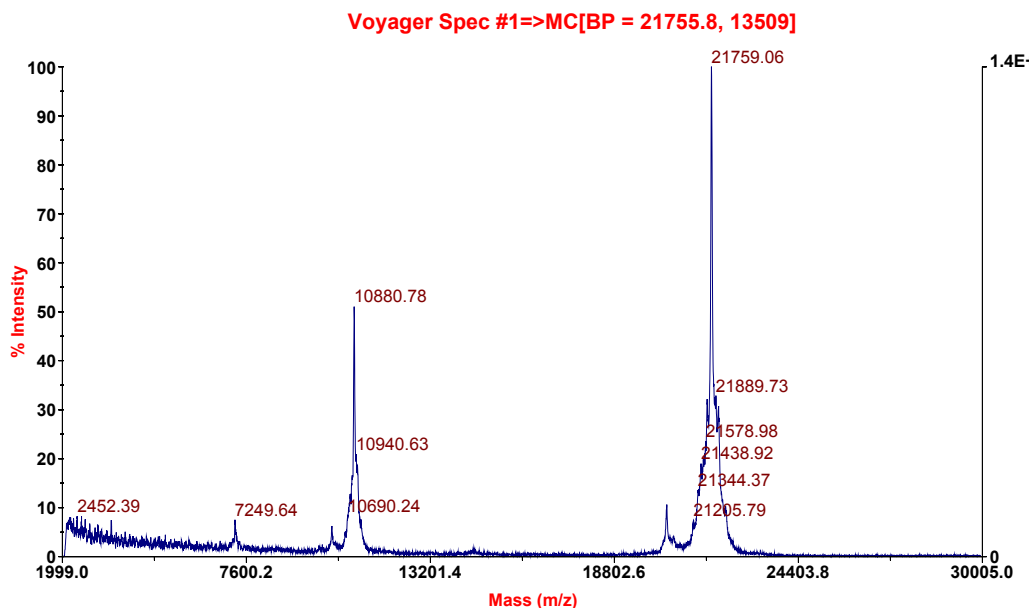


Figure 16. MALDI-TOF spectrum of semi-synthetic protein **1**. The mass peak at 10880 and 21759 corresponds to the mass of coupling protein **1**.

Isotope labeled lipidated proteins **2** and **3** were prepared under the same ligation condition as protein **1** to give 15% and 30% yield respectively (Scheme 9). The isotope labeled pattern of protein **2** is complementary to protein **1**.

In summary, three ^{13}C , ^{15}N and ^2H labeled lipidated semi-synthetic proteins **1**, **2**, and **3** have been synthesized by combining techniques of organic synthesis and molecular biology. In general, the amount of the proteins obtained from the ligation reaction (5 to 10 mg) was sufficient to carry out the NMR measurement. The NMR experiments of the three semi-synthetic proteins were performed in collaboration with the group of PD Dr. Daniel Huster at the University of Leipzig to study the structural and dynamical information of the membrane associated C-terminus of the underlying N-Ras proteins **1**, **2** and **3**.

4.2 Structural Studies of Membrane-Associated C-terminus of Lipid-Modified Human N-Ras Protein by Solid-State NMR Spectroscopy

4.2.1 Solid-state NMR spectroscopy study of phospholipid phases

The key to NMR studies of membrane proteins is the preparation of the phospholipid membrane. Phospholipids can form numerous self-assembled superstructures,⁴⁷ like micellar, bilayer, hexagonal, and other phases. Figure (17a, b) displays the molecular arrangements of phospholipids in micelle and bilayer structure. Each micelle typically formed from lysolipids, contains approximately 50-60 single chain lipid molecules and a single polypeptide. In contrast, lipid bilayers are very large supramolecular structures with many phospholipids and polypeptide molecules in extended two-dimensional arrays.

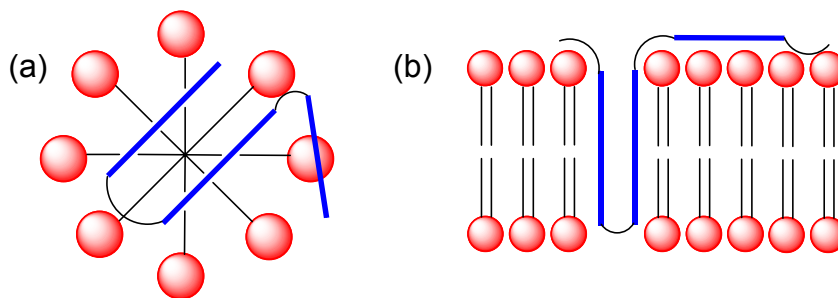


Figure 17. Typical self-assembled phospholipids structures with incorporated membrane protein. a) micelle, b) bilayer.

Proteins in micelles re-orientate relatively slowly, while those in bilayers are immobile on the relevant NMR timescales, enabling them to be treated spectroscopically as solids. The association of membrane proteins with these two phospholipids configuration gives rise to different results and conclusions. The existence of different phospholipid phases can be identified by phosphorous ^{31}P NMR. Depending on the phase state of the phospholipids, ^{31}P NMR spectra display different peak patterns, as shown in Figure 18. In bilayers, rapid axial diffusion leads to a partial motional averaging of the ^{31}P chemical shift tensor. Hence, an axially symmetric powder pattern is observed, characteristic of phospholipids bilayers.

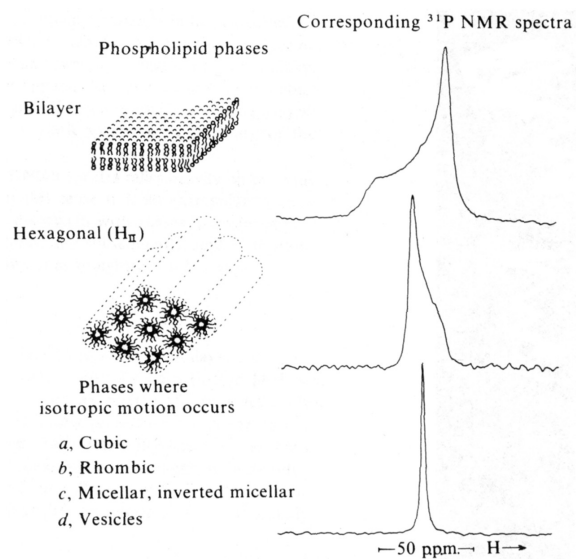


Figure 18. ^{31}P NMR spectra of different phospholipids phases.⁴⁸

In this dissertation, the dynamical and structural information of membrane-bound N-Ras proteins were studied in phospholipids bilayers, which reflect the basic structural motive of a cellular membrane. Figure 19 shows the ^{31}P NMR spectra of phospholipid bilayers of DMPC- D_{54} and DMPC- D_{54} with N-Ras protein prepared using the described protocol.⁶² The ^{31}P NMR spectrum of DMPC- d_{54} with or without N-Ras proteins corresponds well with the ^{31}P NMR peak pattern of lipid bilayer shown in Figure 18. Protein binding does not interfere with the bilayer structure of DMPC.

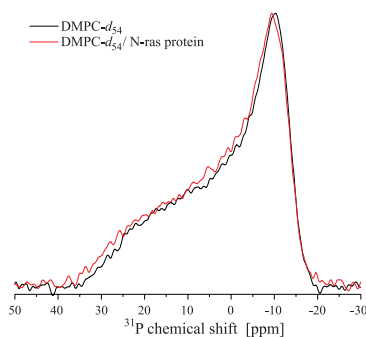


Figure 19. ^{31}P NMR spectra of DMPC- D_{54} and DMPC- D_{54} in the presence of N-Ras protein at a molar ratio of 1:150.

4.2.2 Measurement of proton and carbon NMR for N-Ras proteins 1 and 2

The structural analysis of the membrane-bound N-Ras protein was conducted together with Dr. Daniel Huster and Guido Reuther at the University of Leipzig. From empirical analysis it is known that the secondary chemical shift, in other words, the difference between the measured isotropic chemical shift and the corresponding value in the random coil, strongly correlate with protein secondary structure.⁴⁹ Thus the secondary structure of a protein can be deduced by determination of ^{13}C and ^1H chemical shift of the given protein. For example, the chemical shifts of valine show distinctive chemical shifts changes in different secondary structures (Figure 20). The chemical shift of valine $\text{C}\alpha$ in a β -sheet shifts downfield, while chemical shift of α -helix moves upfield when compared with the value of the random coil.

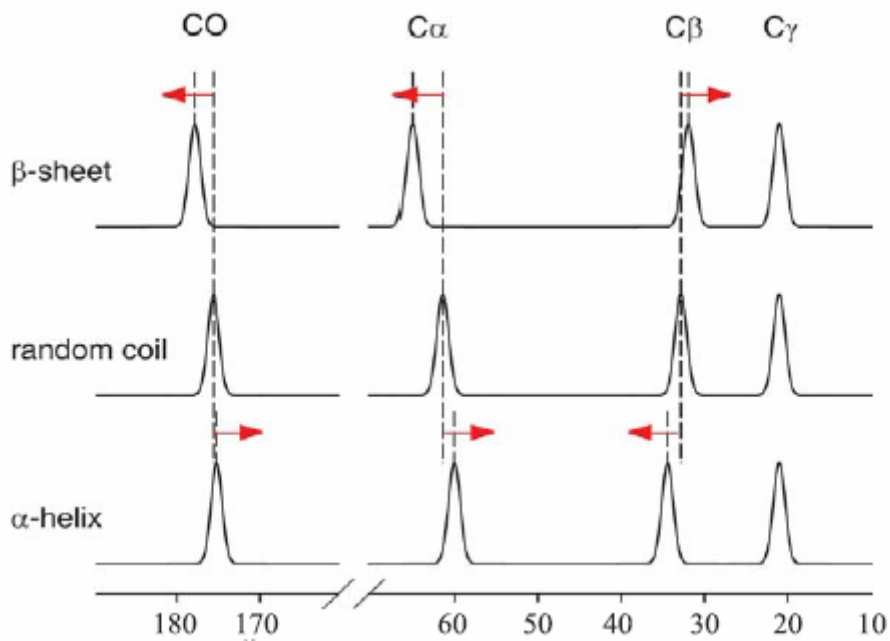


Figure 20. Simulated ^{13}C NMR spectra of valine in different secondary structures.⁵⁰ Noticeable shifts in the isotropic peak positions depending on secondary structures are observed.

By using this characteristic feature of chemical shifts for different protein secondary structures, two isotopically labeled lipid-modified N-Ras proteins **1** and **2** were subjected

to NMR spectroscopy measurement to determine their chemical shifts. Different MAS NMR experiments such as ^{13}C experiment, ^{13}C - ^{13}C and ^{13}C - ^1H correlation experiments were performed to establish the $^{13}\text{C}\alpha$, $^{13}\text{C}\beta$, ^{13}CO and $^1\text{H}\alpha$ chemical shifts for the C-terminus of the membrane-bound N-Ras protein. There are two possible approaches to obtain the ^{13}C NMR of the underlying lipidated N-Ras proteins **1** and **2**.

The first of the two approaches involves the investigation of ^{13}C chemical shifts of N-Ras proteins using a Bloch-decay experiment. In this NMR experiment, the ^{13}C nucleus is directly irradiated. Since isotopic enrichment in the C-terminus of the Ras protein was prepared, the delivery of well-resolved spectra and identification of chemical shifts of each carbon from the lipidated N-Ras C-terminus are possible. The mixing ratio of 150 equivalents of phospholipids DMPC to the protein would affect the NMR spectra of the N-Ras C-terminal region due to the relatively high intensity of DMPC peaks at natural abundance in ^{13}C (1.1%). Furthermore the chemical shifts of DMPC might lie in the same region as the N-Ras C-terminus, which would pose a serious problem in the identification of N-Ras C-terminus ^{13}C peaks. Another obvious disadvantage of using the Bloch-decay measurement will be the low sensitivity of ^{13}C due to the small gyromagnetic ratio of ^{13}C compared to ^1H . This shortcoming may reduce the intensity of ^{13}C signal of the N-Ras proteins.

Figure 21 shows the ^{13}C NMR spectrum of semi-synthetic N-Ras protein **1** determined by the Bloch-decay method. From the ^{13}C spectra, each chemical shift of the N-Ras C-terminus can be identified and characterized easily by comparing with the literature values. Fortunately, the ^{13}C chemical shifts of DMPC do not overlap with the N-Ras protein **1** as shown by the spectra and the intensity of Ras **1** peaks are at an acceptable range. However, the line widths of each ^{13}C peak are quite broad showing that the ^{13}C chemical shifts obtained from this method might not be very accurate. In addition, the methionine β and γ ^{13}C chemical shifts overlap with a prominent lipid natural abundance peak, which makes this method alone not very accurate for getting the ^{13}C chemical shifts of both N-Ras proteins **1** and **2**. A complementary method called cross-polarization was therefore applied to compare the ^{13}C chemical shift with Bloch-decay measurement.

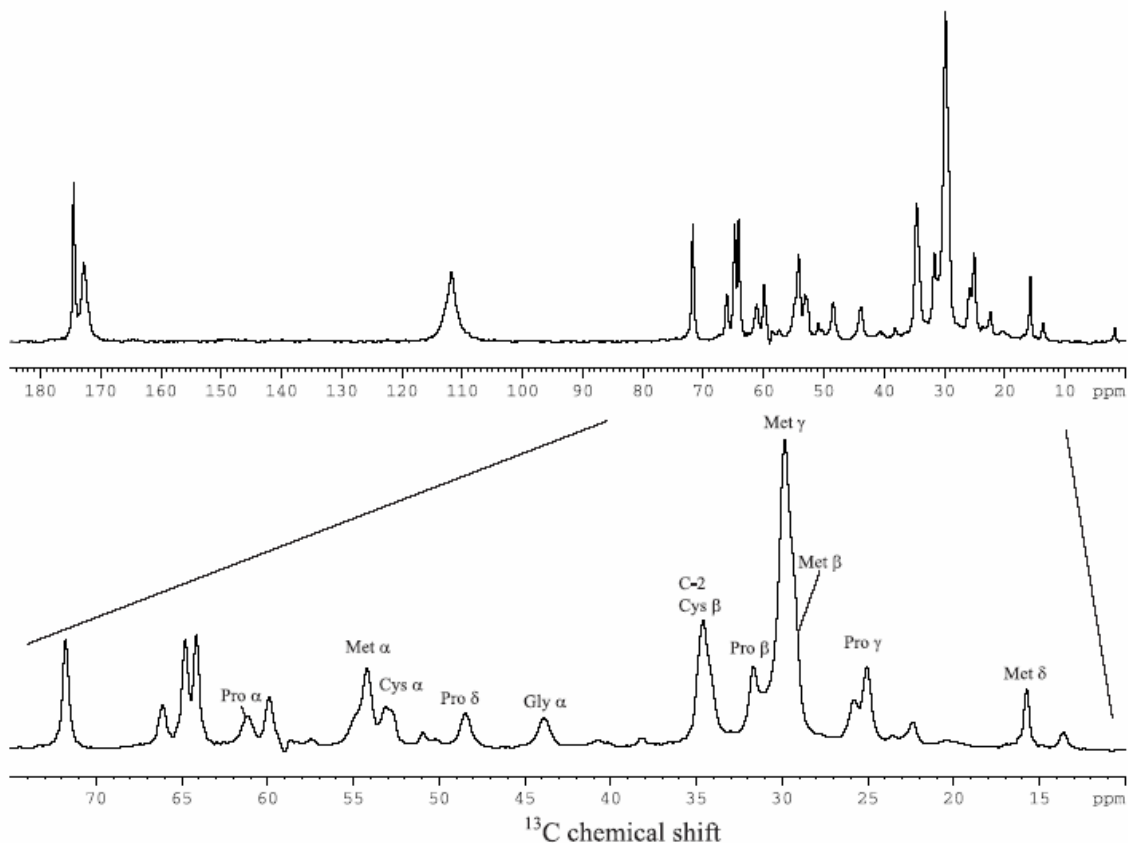


Figure 21. ^{13}C NMR spectrum of semi-synthetic N-Ras protein **1** in a DMPC matrix (1:150, mol/mol) at 30°C using direct polarization (Bloch-decay method).

Cross polarization (CP) measurement makes use of the high gyromagnetic ratio of ^1H . In the ^{13}C CP experiments, ^1H was irradiated instead of ^{13}C . Through a special pulse sequence, the magnetizations are transferred to its adjacent carbon atoms using dipolar couplings thus obtaining the ^{13}C NMR spectrum. By using this method, the intensity of a ^{13}C signal can be enhanced up to 4 times as compared to the Bloch-decay experiment. CP is one of the most widely used techniques in solid-state NMR. Figure 22 shows the spectrum of a ^{13}C CP experiment⁵¹ of the semi-synthetic N-Ras protein **1**.

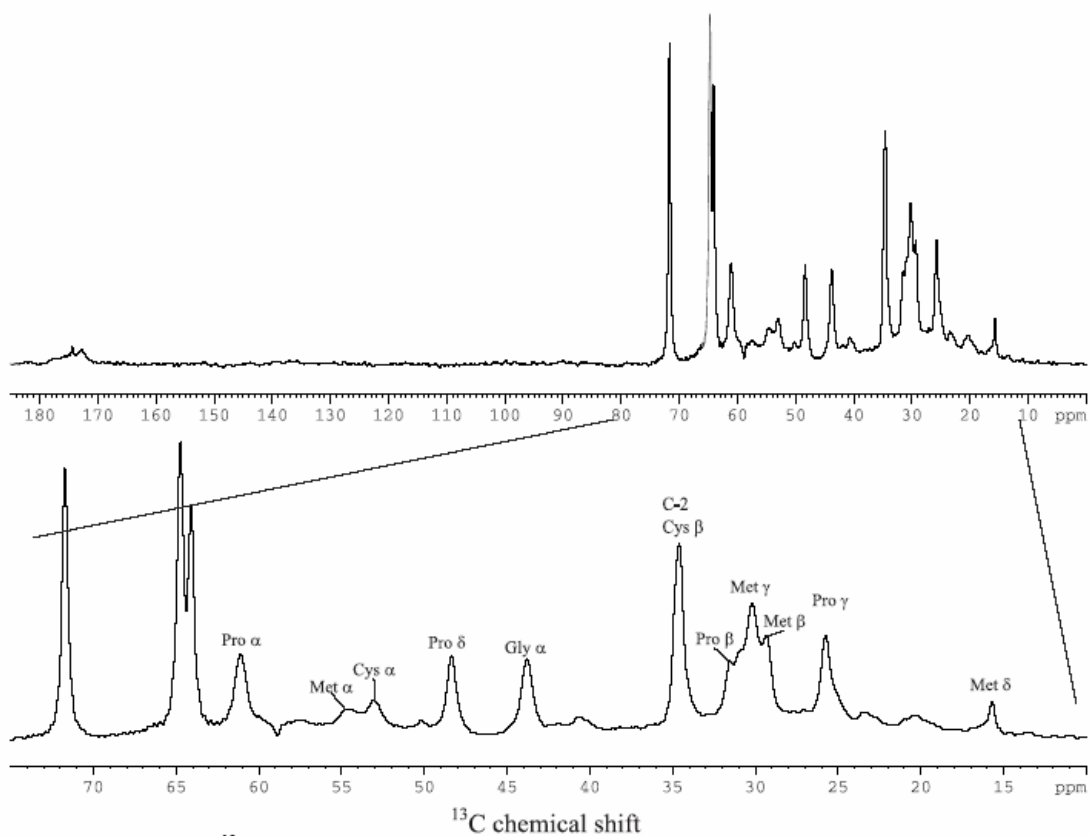


Figure 22 ^{13}C NMR spectrum of semi-synthetic N-Ras protein **1** in a DMPC lipid matrix using cross polarization.

The intensity and resolution of the peaks have increased significantly as compared to the Bloch-decay measurement. Due to the small dipolar couplings in the highly mobile lipid matrix, the methionine peaks can be identified in the spectra. The disadvantage of this measurement is that the chemical shifts of ^{13}CO can not be detected due to the absence of adjacent ^1H . Bloch-decay and cross polarization measurement of ^{13}C chemical shifts of membrane-bound lipid modified N-Ras C-terminus were therefore used complementary to each other.

The peaks in the Bloch-decay and cross polarization experiment were assigned with reference to literature values.⁵² However, the assignment can be ambiguous due to the overlay of several signals from different ^{13}CO and ^{13}C α of protein. Therefore,

measurement of 2D NMR spectroscopy is essential to establish the correct assignment of each peak. This is very important for the subsequent determination of torsion angles.

4.2.3 Two dimensional (2D) NMR

The 2D NMR technique is a very powerful method to identify signals and characterize the relationship between two atoms. Signals arise in the 2D NMR spectrum only if a coupling between two atoms exists. In solid-state NMR spectroscopy, the correlation between atoms is produced by dipolar couplings instead of, J coupling as in solution NMR spectroscopy. In 2D NMR, the x and y axis correspond to the frequency of two investigated nuclei. A cross peak will be observed only if the dipole couplings between two nuclei occur. Towards the analysis of membrane-bound N-Ras proteins, several 2D NMR experiments have been carried out such as ^{13}C - ^{13}C proton-driven spin diffusion and ^1H - ^{13}C HetCor measurements.⁵³

In Figure 23 relevant regions of the ^1H - ^{13}C of two isotopic labeled N-Ras proteins **1**, **2** correlation spectra are shown. The alternating labeling pattern precludes most of the signal superposition, and well-resolved peaks are observed. In the spectra all correlation peaks for directly bonded ^1H - ^{13}C pairs are present. Typical line widths for the $\text{C}\alpha$ and $\text{H}\alpha$ signals are ≈ 1 ppm and ≈ 0.15 - 0.25 ppm, respectively. This suggests that dipolar couplings are reduced by molecular motion but still sufficiently large to allow for polarization transfer by cross-polarization and proton-driven spin diffusion.⁵⁴

The ^1H - ^{13}C correlation spectra also provide different crosspeak patterns depending on the labeling scheme of the protein investigated. ^{13}C and ^{15}N labeled amino acids are shown in bold italics. In addition to the protein signals, crosspeaks of the non-deuterated glycerol (G) and lipid chain signals (C-2, CH_2) from the membrane are detected.

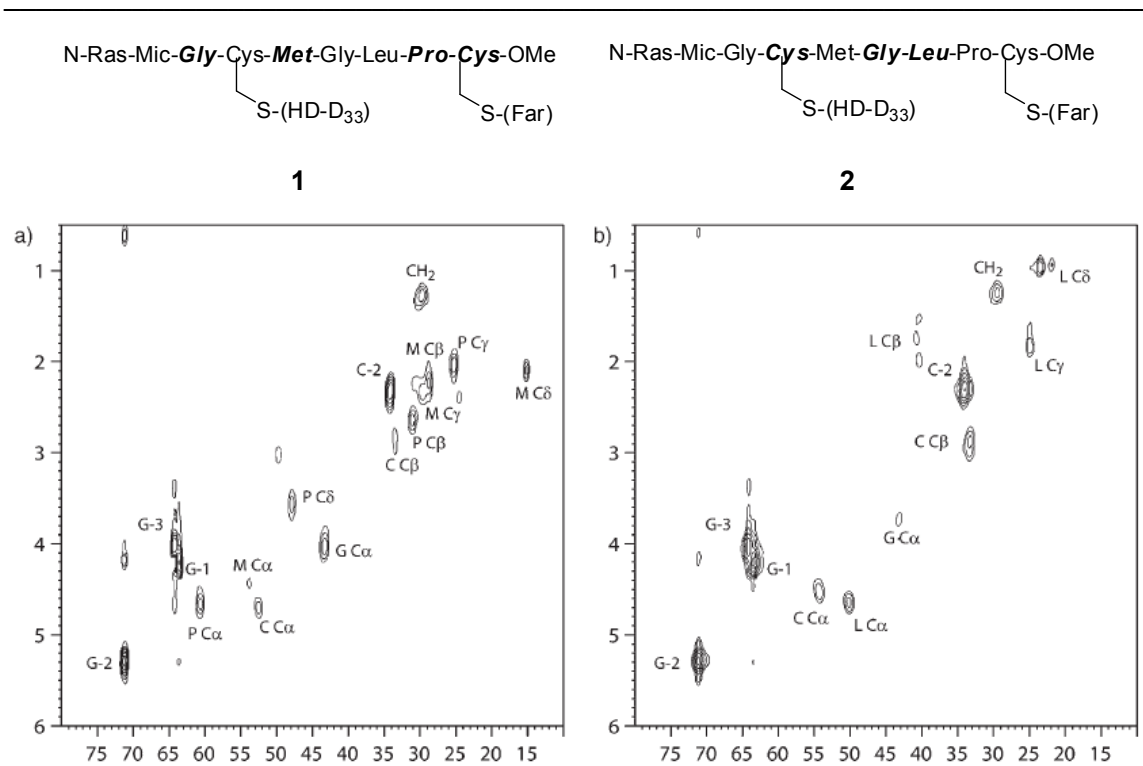


Figure 23. Contour plots of ^{13}C - ^1H MAS NMR spectra of the lipitated membrane-bound Ras proteins. a) N-Ras **1**, b) N-Ras **2**, **Bold** and *italic*: ^{13}C and ^{15}N labeled amino acids.

The ^{13}C - ^{13}C correlation spectra show all correlations within the labeled amino acid between $\text{C}\alpha$ and CO (Figure 24). In the carbonyl region of the ^{13}C - ^{13}C correlation spectra six out of seven $\text{C}\alpha$ - CO crosspeaks are resolved. Thus, the complete assignment was possible from this set of MAS NMR experiments. A table containing the assignments and chemical-shift values is given in Table 1.

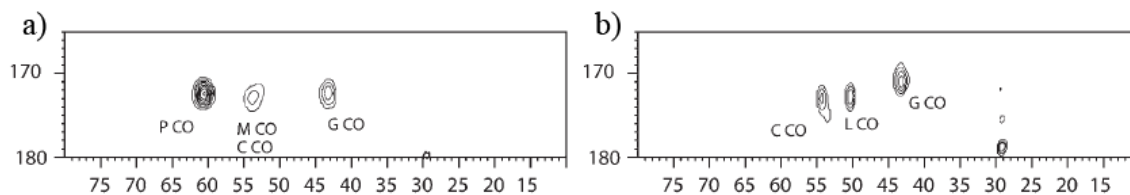


Figure 24. Contour plots of ^{13}C - ^{13}C MAS NMR spectra of the lipitated membrane-bound Ras proteins. a) N-Ras **1**, b) N-Ras **2**.

Table 1. ^1H and ^{13}C chemical shifts, signal assignment, and deviation from random coil values for the C-terminus of membrane-associated N-Ras.

Residue	Signal	δ [ppm]	$\delta_{\text{random coil}} - \delta_{\text{experiment}}$ [ppm]
Gly 180	C α	45.4	-0.3
	CO	173.8	1.1
	H α	4.02	-0.06
Cys 181	C α	56.5	1.9
	CO	174.6	0.1
	C β	35.5	-7.1
	H α	4.53	0.03
	H β	2.87	n.r.
Met 182	C α	56.0	-0.7
	CO	174.4	1.9
	C β	30.9	1.7
	C γ	31.4	n.r.
	C δ	17.3	n.r.
	H α	4.42	0.06
	H β	2.20	n.r.
	H γ	2.32	n.r.
	H δ	2.10	n.r.
Gly 183	C α	45.4	-0.3
	CO	173.6	1.3
	H α	3.73	0.23
Leu 184	C α	52.3	2.6
	CO	174.7	2.4
	C β	42.6	-0.3
	C γ	27.1	n.r.
	C δ	25.6	n.r.
	H α	4.65	-0.31
	H β	1.99	n.r.
	H γ	1.84	n.r.
H δ	0.96	n.r.	
Pro 185	C α	62.7	0.5
	CO	174.4	2.9
	C β	33.1	-1.4
	C γ	27.3	n.r.
	C δ	49.9	n.r.
	H α	4.65	-0.23
	H β	2.65	n.r.
	H γ	2.07	n.r.
	H δ	3.57	n.r.

Residue	Signal	δ [ppm]	$\delta_{\text{random coil}} - \delta_{\text{experiment}}$ [ppm]
Cys 186	C α	54.6	3.8
	C β	35.6	-7.2
	H α	4.68	-0.13
	H β	2.82	n.r.

n.r. : not relevant for structural analysis.

4.2.4 Torsion angle prediction by TALOS

The $^{13}\text{C}\alpha$, $^{13}\text{C}\beta$, ^{13}CO , and $^1\text{H}\alpha$ chemical shifts for the C-terminus of the membrane-bound N-Ras proteins **1** and **2** determined in the MAS NMR experiments provided the input parameters for the structural calculations. The program package TALOS was used to determine a model for the backbone structure of the membrane-binding domain of Ras from the isotopic chemical shifts. The deviations of the observed chemical shifts from those of the random coil increase towards the C-terminus of Ras, indicating that the TALOS prediction is also better for the C-terminal amino acids.

TALOS⁵⁵ is a database system used for the empirical prediction of Φ and Ψ backbone torsion angles by using the input of five isotropic chemical shifts ($\text{H}\alpha$, $\text{C}\alpha$, $\text{C}\beta$, CO , N). The goal of TALOS is to use secondary chemical shift and sequence information in order to make quantitative predictions for the protein backbone angles Φ and Ψ , and to provide a measure of the uncertainties in these predictions.

This program searches a database containing 78 proteins of known X-ray structure for chemical-shift and sequence homology. The TALOS database, while small, was constructed using the most well-defined parts of high resolution (2.2 Å or better) X-ray crystal structures to define the Φ and Ψ angles. TALOS finds chemical-shift identities for triplets of amino acids and yields the backbone torsion angles as output. The idea behind TALOS is that if one can find some triplet of residues in a protein of known structure with similar secondary shifts and sequence to a triplet in a target protein, then the Φ and Ψ angles in the known structure will be useful predictors for the angles in the target. The information obtained from TALOS calculation will provide a basis for calculating a structural model of the molecule in question.⁵⁶

In practice, TALOS searches a database for the 10 best matches to a given triplet in the target protein. If these 10 matches indicate consistent values for Φ and Ψ angles, then their average and standard deviations are used as a prediction. However, if the 10 best

matches have mutually inconsistent value of Φ and Ψ angles, the matches are declared ambiguous and not prediction is made for the central residue.

The output of TALOS database is given in a Ramachandran plot. The Ramachandran plot shows the Φ/Ψ distributions of the 10 best database matches for the selected residue. The graph is shaded to show the most populated regions of the TALOS database. In the graph, each match from the database is drawn as a small square at a particular Φ/Ψ coordinate. The squares are colored according to this scheme: Green ■, this match is good and included in the prediction. Red ■, outlier; not included in the prediction. Blue ■, reference (Φ/Ψ taken from “-ref” structure). The Ramachandran plot of TALOS calculation was given in Figure 25.

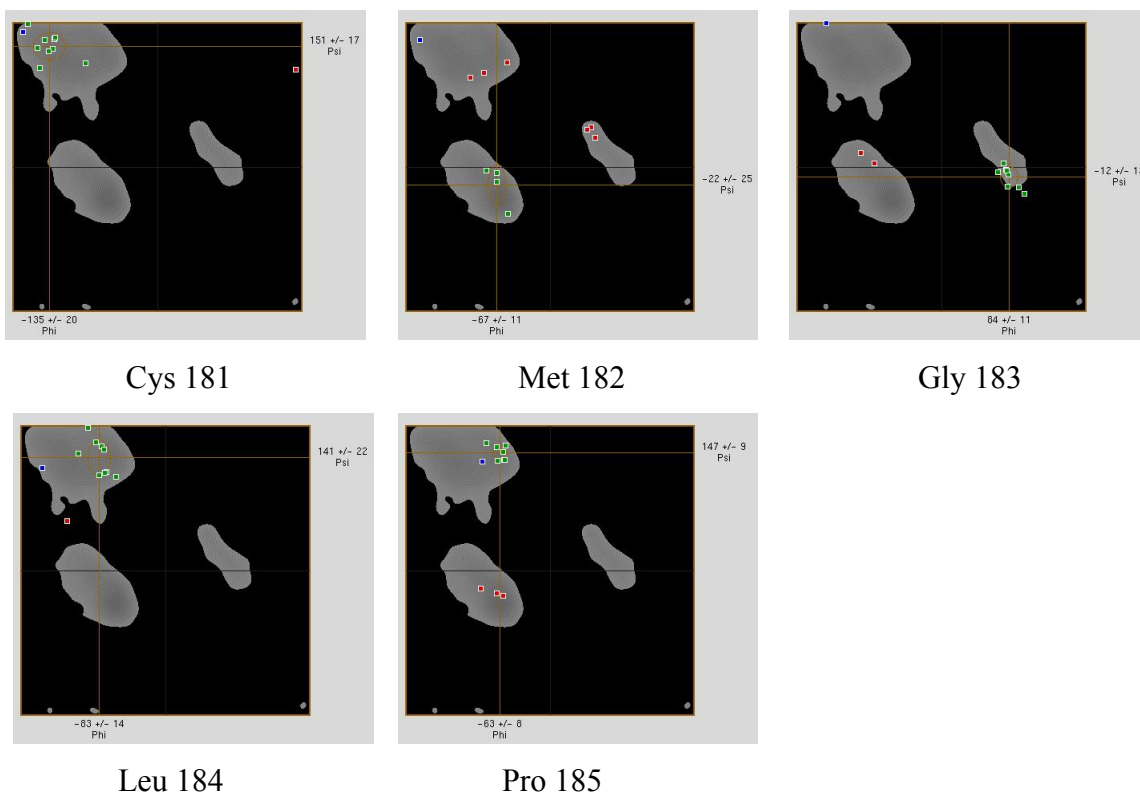


Figure 25. TALOS results for membrane bound Ras-protein as a Ramachandran plot of the 5 amino acids in the C-terminus of the molecule.

No torsion angles for glycine 180 and cysteine 186 could be predicted by TALOS because glycine 180 and cysteine 186 are, respectively, the first and the terminal labeled amino acids in the sequence of interest. TALOS requires the input of chemical-shift data for three consecutive residues. With the exception of methionine 182, the torsion angles for the backbone geometry determined were conclusive. For this residue, three equally populated subsets of backbone torsion angles were found. From the Ramachandran plot, one can immediately conclude that cysteine 181, leucine 184 and proline 185 lies in the β -sheet region, while glycine 183 stays in a left handed helix.

The TALOS program also gave the average and standard deviation of Φ and Ψ angles for the selected residue matched. The average backbone torsion angles and standard deviation for the amino acids 181-185 of the C terminus of N-Ras are given in Table 2. The standard deviation for the predicted torsion angles is approximately 15%. This is reasonable given that TALOS is just a small database containing NMR chemical shifts correlation of only 78 proteins structures.

Table 2. Backbone torsions angles of the membrane-binding domain of the lipidated human N-Ras protein.

Residue	Φ	Ψ
Cys 181	$-135^\circ \pm 20^\circ$	$151^\circ \pm 17^\circ$
Met 182	$-67^\circ \pm 11^\circ$	$-22^\circ \pm 25^\circ$
	$-79^\circ \pm 23^\circ$	$121^\circ \pm 10^\circ$
	$51^\circ \pm 5^\circ$	$45^\circ \pm 7^\circ$
Gly 183	$84^\circ \pm 11^\circ$	$-12^\circ \pm 13^\circ$
Leu 184	$-83^\circ \pm 14^\circ$	$141^\circ \pm 22^\circ$
Pro 185	$-63^\circ \pm 8$	$147^\circ \pm 9^\circ$

4.2.5 Structural model of membrane-associated C-terminus of N-Ras protein

A simulated annealing protocol was used for structural calculations of the C-terminus of the membrane-bound lipidated Ras protein. Because of the ambiguity in the TALOS result for methionine 182, three families of structural models were calculated. Figure 26 shows the structural model for the lipidated C-terminus of the membrane-bound N-Ras protein derived from solid-state NMR data.

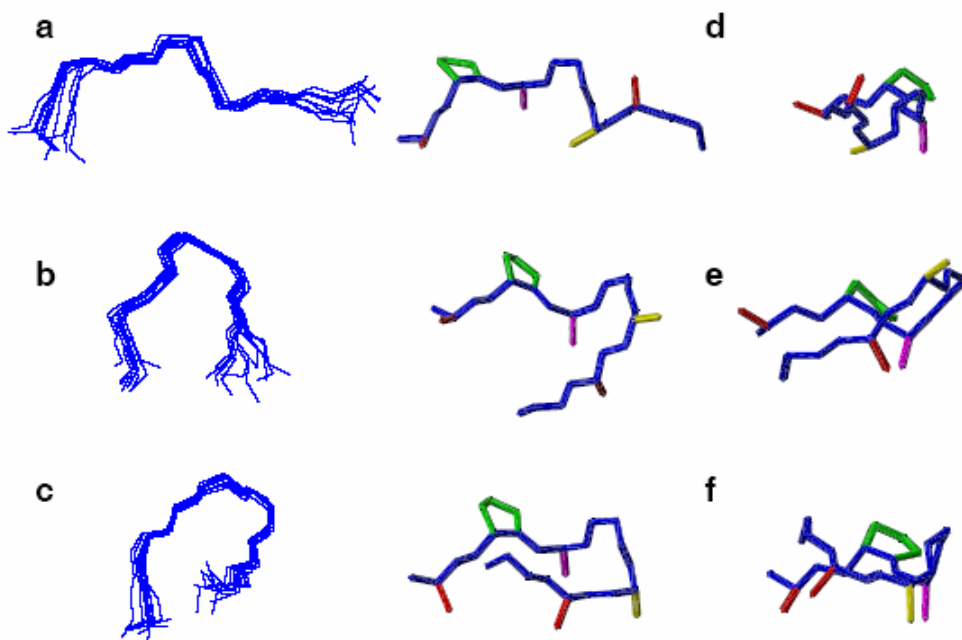


Figure 26. Possible structural model for the lipidated C-terminus of the membrane-bound N-Ras protein.

The superposition of the 10 lowest energy backbone models are displayed for the three sets of methionine 182 torsion angles in the left column shown in Figure 26 **a-c**. The $C\alpha$ coordinates of the five amino acid stretch, for which the torsion angles have been predicted, show a root mean square deviation (rmsd) of a) 0.56, b) 0.51 and c) 0.63 Å (calculated from 200 structural models). Figure 26 **d-f** show different views of the averaged structural model with the backbone in blue and proline in green. The $C\beta$ atoms

for the cysteine, leucine and methionine are shown in red, yellow, and magenta, respectively.

The global fold of the C-terminus of the N-Ras protein in the membrane resembles a horseshoe. The membrane anchor of Ras protein has no regular α -helical or β -sheet motifs. This is not surprising because the sequence investigated here contains two glycine residues and one proline residue, which are well-known turn promoters and helix breakers.⁵⁷ As a result of the lack of structural information for glycine 180 and cysteine 186, the ends of the sequence appear disordered in the images.

The TALOS results for methionine 182 show that the relationship between torsion angles and chemical shift is not unique. Therefore, additional spectroscopic information is required to determine the most likely structural model of membrane-bound Ras protein, perhaps through torsion angle measurement.⁵⁸ Studies of membrane binding of the lipidated Ras heptapeptide (residues 180-186) by ¹H MAS NOESY and neutron diffraction spectroscopy have been reported.⁵⁹ Strong intermolecular crosspeaks indicated that the hydrophobic side chains (cysteine, leucine, and methionine) insert into the membrane interior. The polar five-membered ring of proline points towards the aqueous phase. These results provide additional information for the selection of the most likely structural models of the three possible for the membrane-binding domain of N-Ras.

It should be noted that the torsion angle predictions by TALOS do not provide information about the side chains of the protein. However, the tetrahedral geometry of the C α atom in the backbone determines the direction of the side chain with respect to the protein backbone. In the middle and right columns of Figure 26, two views of the average backbone conformational model of the Ras membrane-binding domain are shown for each set of methionine torsion angles. These structural models also include the C β sites. For two of the three models, the hydrophobic side chains point in different directions, which appears to be a rather unlikely conformation based on thermodynamic considerations and is not in line with the NOEs between Ras peptide side chains and the membrane. Thus one structural model remains, in which the lipidated and hydrophobic

side chains point in the same direction, suggesting the orientation of the membrane-binding domain of the protein (Figure 26 c and f). In agreement with the hydrophobicity scale⁶⁰ in this model, proline would point away from the membrane into the aqueous phase. Therefore, the interaction of the protein with the membrane stabilizes its conformation.

From these results, a model of the structure of the membrane-bound lipidated N-Ras protein was constructed (Figure 27). The membrane topology of the protein is determined by hydrophobic interactions between the lipidated cysteine and hydrophobic side chains. Further, hydrogen bonds between the peptide backbone and the phospholipids in the interface region of the membrane are likely to occur. The lipid-binding domain is linked to the GTP-binding N-terminal region of the protein by a linker domain, which is putatively flexible.⁶¹ In contrast to H-Ras, there is currently no structure available for the N-terminus of N-Ras. However, considering that there is 92 % sequence homology between H-Ras and N-Ras it can be assumed that these structures are very similar.

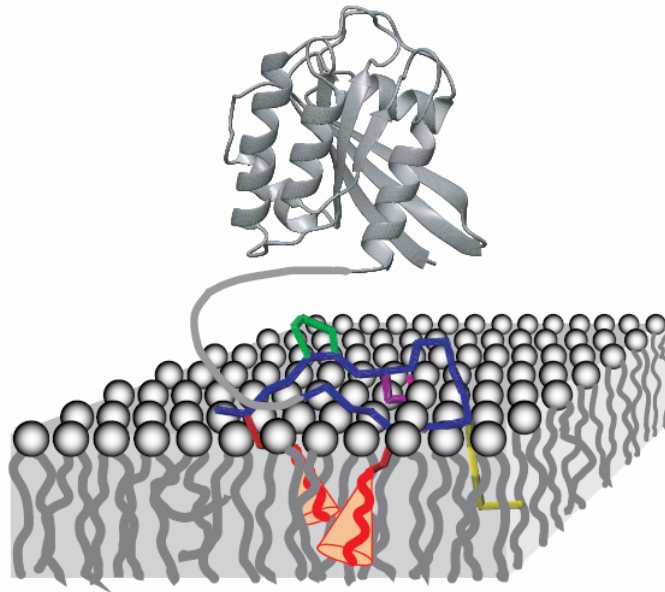


Figure 27. Structural model for membrane-associated C-terminus of N-Ras protein.

4.3 Dynamical Studies of Membrane-Associated C-Terminus of Lipid-Modified Human N-Ras Protein by Solid-State NMR Spectroscopy

4.3.1 Lipid chain dynamics of membrane bound Ras protein

Deuterium labeled hexadecyl lipid chain at cysteine 181 of N-Ras protein **3**, was used to obtain the dynamical information of the N-Ras lipid chain's interaction with phospholipid membranes. This provides the essential key to study the dynamical information of lipid chain, where deuterium in a C-²H bond has quadrupolar coupling constant of 167 kHz. This moderate interaction strength makes this nucleus very valuable for dynamical studies of lipid chains in the membrane. Moreover, the lineshapes are sensitive to molecular motions with correlation times between approximately 100 ps and 100 μs, which coincidentally corresponds well with the motion of membrane-bound proteins.

The dynamical data of the membrane-bound N-Ras proteins was analyzed together with Dr. Daniel Huster and Guido Reuther at Leipzig University. The Ras proteins **3** were reconstituted into DMPC or chain perdeuterated DMPC-D₅₄ membranes and investigated by static ²H NMR methods.⁶² To gain insights into the molecular dynamics of the lipid modifications of membrane-associated N-Ras, the properties of the lipid chains were compared in three different samples: (i) pure DMPC-D₅₄, (ii) DMPC-D₅₄/N-Ras (non-deuterium labeled) at a 150:1 molar ratio, and (iii) DMPC/N-Ras **3** at a 150:1 molar ratio. Thus, structural and dynamical information about the Ras hexadecyl chain attached to cysteine 181 in comparison to the phospholipid chains can be extracted. Furthermore, the effect of the Ras protein on the bilayer properties of the host DMPC matrix was determined using the same combination of samples.

Figure 28 shows the ²H NMR powder spectrum of the three samples. The blue DMPC/N-Ras **3** spectrum shows the quadrupole splitting of N-Ras lipid chain, which provides dynamical information of the protein lipid chain in lipid bilayer. Further dynamic information of the lipid bilayer under the influence of Ras proteins can be obtained from the measurement of DMPC-D₅₄/N-Ras (Red line). The final black line DMPC-D₅₄ spectrum was measured without N-Ras.

From the raw ^2H NMR powder spectra, it is very difficult to obtain any useful information due to the poorly resolved deuterium peaks. A mathematical algorithm called de-Paking⁶³ was employed to convert the ^2H raw spectra to the spectra which can be read and calculated.

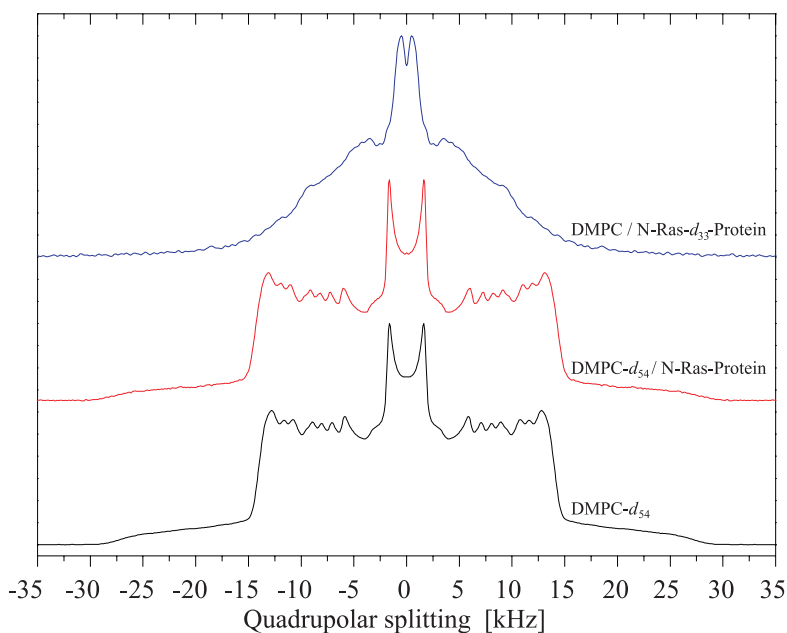


Figure 28. ^2H NMR powder spectra of Ras/membrane preparations. **Blue:** N-Ras protein **3** in DMPC, **Red:** N-Ras protein in DMPC- D_{54} , **Black:** DMPC- D_{54} .

The spectra shown in Figure 29 are symmetric and well resolved after de-Paking procedure was conducted. The quadrupole splitting of each deuterium atom is assigned such that the smallest splitting belongs to the deuterium attached at C_{16} , and the next splitting is the deuterium at C_{15} . The following splitting corresponds to C_{14} , C_{13} and so on.

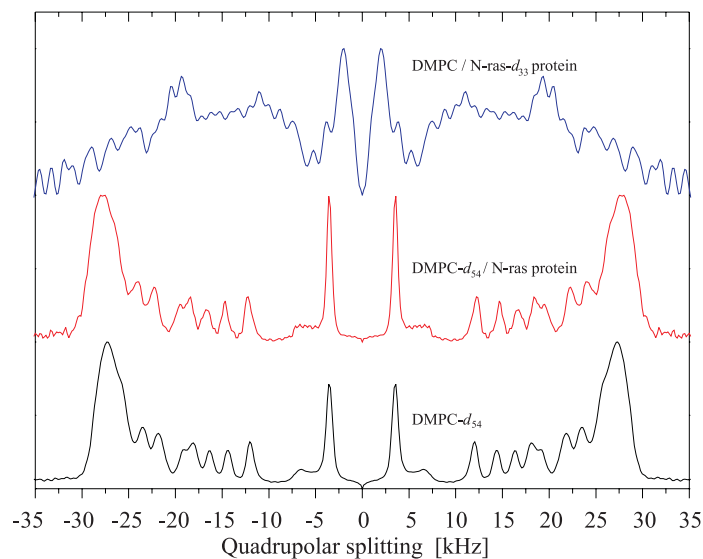


Figure 29. Depacked spectra from Figure 29. **Blue:** N-Ras protein **3** in DMPC, **Red:** N-Ras protein in DMPC-D₅₄, **Black:** DMPC-D₅₄.

Dynamical information of the lipid chain can be extracted from the value of ²H quadrupolar splitting. A smaller quadrupolar splitting represents a more flexible carbon in a CH₂ bond while a bigger quadrupolar splitting means a more rigid bond. In order to compare the flexibility of each carbon chain easily, the quadrupolar splitting of each Pake doublet was converted into an order parameter according to Eq. (1).⁶⁴

The order parameter, S, provides information about the amplitude of motion of the corresponding C-²H bond and varies between 1 to 0. When S is 1, it means that the respective C-H bond is completely rigid. If S is 0, it means that the bond is isotropically mobile. The value of the order parameter can be calculated from the experimental quadrupolar splitting based on the equation (1).

$$\Delta\nu_Q = \frac{3}{4} \frac{e^2 q Q}{h} S(n) \quad (1)$$

Where, $S(n)$ is order parameter of the corresponding atom, and $\Delta\nu_Q$ is the quadrupolar splitting of that particular deuterium and e^2qQ/h is the quadrupolar coupling constant (167 kHz in a C-²H bond).

Smoothed order parameter profiles showing the dependence of the order parameter on the position of the carbon segment in the acyl chain are presented in Figure 30. The segments are numbered consecutively starting from the carbonyl group of the lipid or the carbon directly connected to the sulfur atom of cysteine 181 of N-Ras, respectively. The red and black lines in the graph correspond to DMPC-D₅₄ in the presence and in the absence of N-Ras protein, respectively. The blue line corresponds to N-Ras **3** in DMPC.

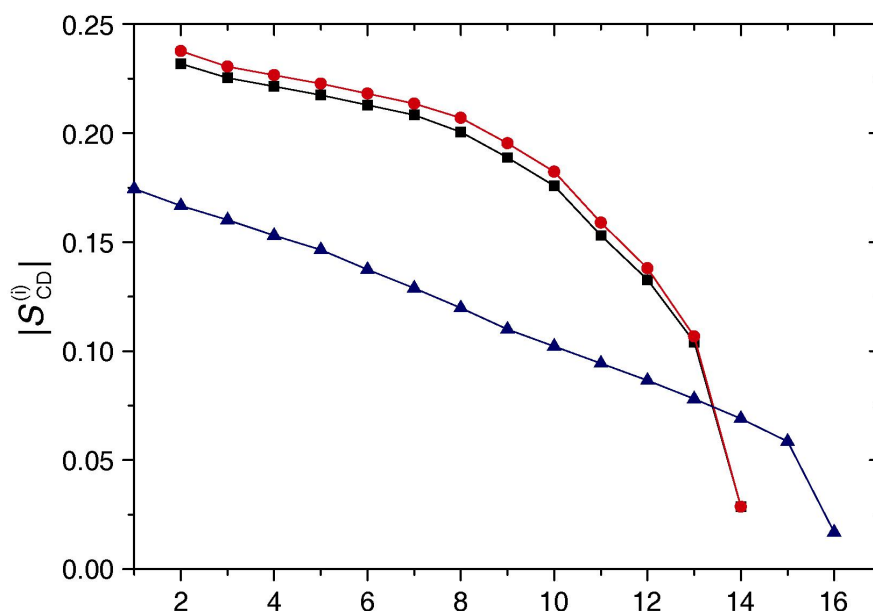


Figure 30. Comparison of order parameter of N-Ras hexadecyl lipid chain **Blue**: N-Ras protein **3** in DMPC, **Red**: non isotope labeled N-Ras protein in DMPC-D₅₄, **Black**: DMPC-D₅₄.

Striking differences between the chain order parameters of DMPC-D₅₄ and N-Ras are observed. The dramatically narrower ²H NMR spectrum of the N-Ras **3** chains illustrates that the order parameter of N-Ras **3** is significantly lower than DMPC. This indicates that the hydrocarbon chains of the Ras protein occupy a substantially greater conformational space than the DMPC hydrocarbon chains and the lipid chain of the protein is less orderly packed in the DMPC lipid bilayer. It can therefore be deduced that the Ras protein lipid

chain is very mobile inside the DMPC phospholipid membrane. In contrast, the order parameter profiles for DMPC- D_{54} in the presence and in the absence of Ras are very similar. This shows clearly that the addition of N-Ras protein **3** does not affect the mobility and structure of DMPC lipid bilayer.

The order parameter of N-Ras protein **3** lipid chain was compared with the previously studied C-terminal N-Ras heptapeptide (residues 180-186)^{59, 65} to understand the influence of the globular part of N-Ras protein on the dynamics of the lipid chain. The results of the comparison are summarized and shown in Figure 31.

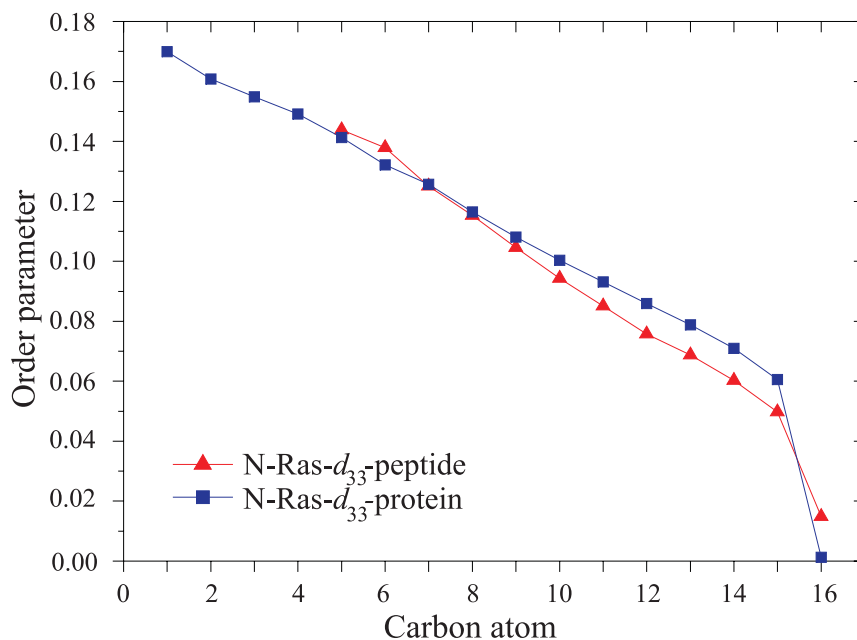


Figure 31. Comparison of N-Ras protein **3** lipid chain and N-Ras C-terminal heptapeptide lipid chain.

Interestingly, the order parameters for C-terminal N-Ras heptapeptide and N-Ras protein **3** were found to be highly similar. These similar dynamical features of the lipid chain of the peptide and protein indicate that the lipid chain modifications of Ras protein may move relatively independent to the rest of the protein.

From the ^2H NMR data, the average area per hydrocarbon chain $\langle A \rangle$ and the chain length of the hydrocarbon region D_C can be calculated.⁶⁵ Figure 32 shows the length of each lipid chain (for the phospholipids as well as for the Ras lipid chain modifications). Table 3 reports the values of the average area per hydrocarbon chain $\langle A \rangle$ and the summary of the length of lipid chain.

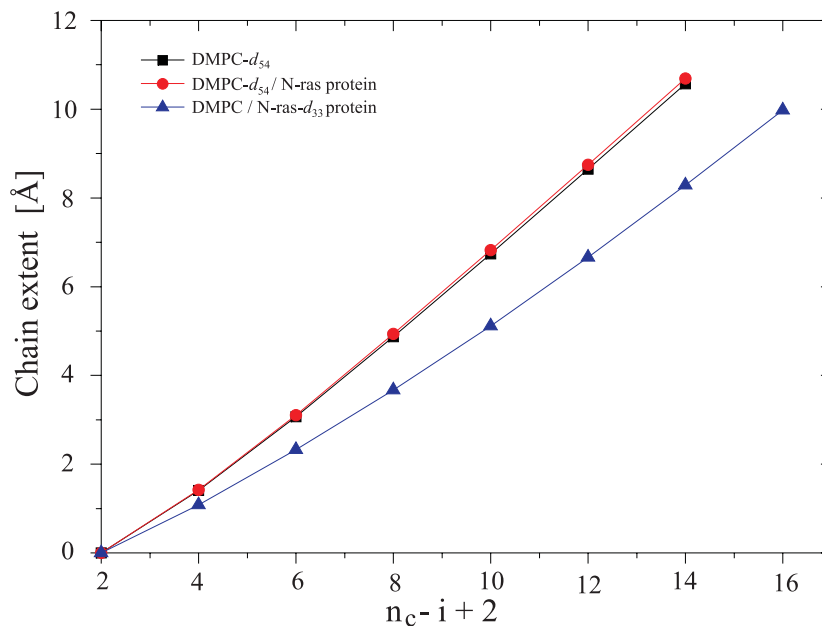


Figure 32. Comparison of chain extension of N-Ras protein **3**. **Blue**: N-Ras protein **3** in DMPC, **Red**: N-Ras protein in DMPC- D_{54} , **Black**: DMPC- D_{54} .

Table 3. Summary of the chain length and average area results for DMPC- D_{54} , DMPC- D_{54} /Ras, and DMPC/N-Ras **3** at 30°C.

	$\langle A \rangle / \text{Å}^2$	$D_C / \text{Å}$
DMPC- D_{54}	29.7 ± 0.4	12.9 ± 0.2
DMPC- D_{54} /Ras	29.5 ± 0.4	13.0 ± 0.2
DMPC/N-Ras 3	33.8 ± 0.8	13.0 ± 0.4

The hydrocarbon thickness for DMPC-D₅₄ is in good agreement with X-ray results.⁶⁶ The slightly higher absolute magnitudes of the order parameters for DMPC-D₅₄ in the presence of N-Ras protein indicate a slightly thicker hydrocarbon core, so that the interfacial area per chain is somewhat smaller compared to pure DMPC-D₅₄. It is very interesting to note that N-Ras protein lipid chain has 16 carbon atoms and DMPC-D₅₄ has only 14 carbon atoms but they share similar chain extension value, which are 13.0 Å and 12.9 Å long respectively. This is in good agreement with previously reported studies on a lipidated Ras heptapeptide (residues 180-186), which also showed the C-terminal Ras peptide and DMPC lipid chains to match in their lengths.^{59,65} In contrast, the average area per hydrocarbon chain for N-Ras **3** is more than 4 Å² larger. The large cross-sectional area of the Ras chain provides space for the peptide backbone, which takes up a substantial area in the lipid-water interface of the membrane. In the space beneath the peptide backbone in the membrane core, lies the hydrophobic peptide side chains (leucine and methionine) and the Ras lipid chains, which undergo large amplitude motion. Thus, the polar protein backbone forms an "umbrella" shielding the hydrophobic side chains and lipid modifications of Ras from the water medium.⁶⁷

To provide dynamics information of the lipid at chemically modified N-Ras protein in DMPC constructed lipid bilayer, ²H NMR spin-lattice relaxation time (T_{1Z}) or longitudinal relaxation time measurements were performed for the various samples studied. The inverse of T_{1Z} defines the spin-lattice relaxation rate R_{1Z} . While order parameters provide information about the motional amplitude of a C-H bond vector, the correlation time of motion can be deduced from relaxation times.

Figure 33 shows the inversion recovery of the magnetization vector that is used to measure the spin-lattice relaxation time T_{1Z} . At equilibrium state, most of the nuclei spin point towards the direction of Z axis, which is parallel to the direction of magnetic field B_0 . When a 180° pulse is applied to the magnetization vector, it is inverted to the $-Z$ axis. The loss of energy to the surrounding environment renders the nuclear spins to return to their equilibrium state where the direction of the magnetization is parallel to magnetic

field B_0 . By simple definition, the relaxation time T_{1z} of nuclei is the time by which nuclei spin requires to return to its equilibrium state from excited state.

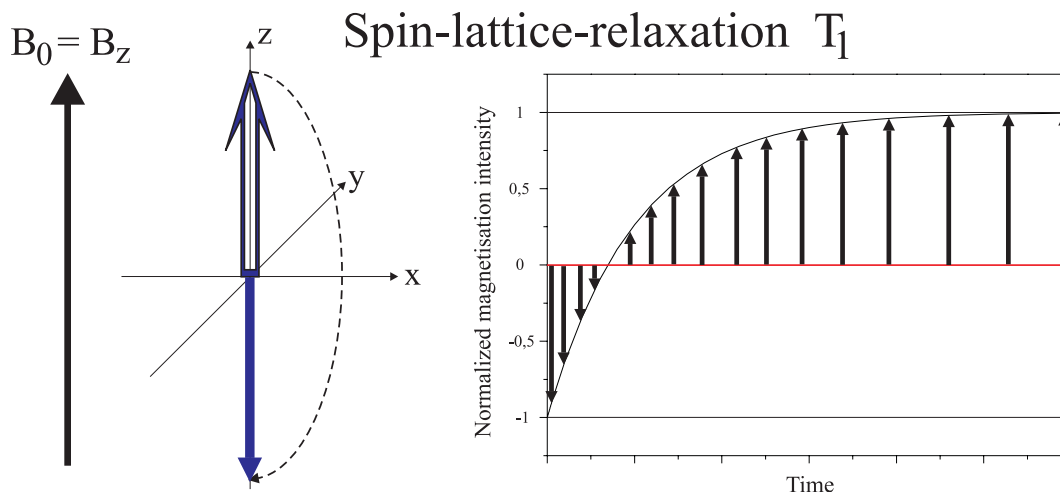


Figure 33. The principle of inversion recovery to measure the spin-lattice relaxation time T_1 .

The relaxation Time T_{1z} is dependant on the mobility of the nucleus in the sample. As mobility increases, the vibrational and rotational frequencies increase, making it more likely for a component of the sample to be able to interact with excited nuclei. However, at extremely high mobility, the probability of a component of the surrounding environment being able to interact with excited nuclei decreases, therefore lengthening the relaxation time. From the study of the relaxation time for N-Ras **3**, the dynamical information about the amplitude motion of lipid chain can be understood.

The relaxation study for DMPC-D₅₄ in the presence and in the absence of the Ras as well as for N-Ras **3** in a DMPC matrix is shown in Figure 34. For DMPC-D₅₄ in the presence as well as in the absence of Ras protein, the dependence is linear. However, the relaxation rate $R_{1z}^{(i)}$ versus order parameter $|S_{CD}^{(i)}|^2$ plot for the N-Ras **3** hexadecyl chain departs from the linear dependence and shows a bent shape with a steeper slope. The relaxation rates for the N-Ras **3** hexadecyl chain are generally higher than for DMPC-D₅₄. The steeper slope of N-Ras **3** implies that the Ras lipid chain is much more flexible and

mobile than that of DMPC-D₅₄. In previous analyses of pure phospholipid membranes, it has been found that the relaxation rate often exhibits a linear dependence on the square of the order parameter.⁶⁸ While the physical reason for this interesting behavior is still under discussion, it has been shown to be a common feature for non-saturated phospholipids.

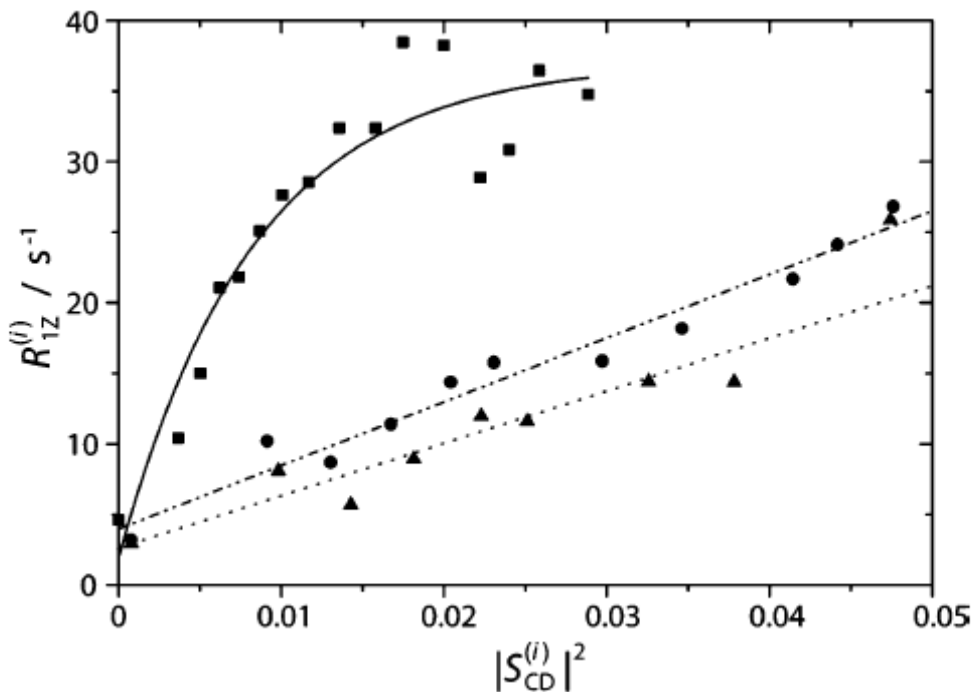


Figure 34. Dependence of the $R_{1Z}^{(i)}$ relaxation rates on the corresponding order parameter squared for DMPC-D₅₄ (◆), DMPC-D₅₄/N-Ras (150:1 mol/mol) (▲), and DMPC/N-Ras **3** (150:1 mol/mol) (■) at 115.1 MHz (17.6 T).

These R_{1Z} versus S_{CD}^2 plots report the elastic properties of the lipid chains in a membrane.⁶⁹ In softer materials, the lipid chains are undergoing large amplitude motions, which are expressed in a steeper slope in the square-law plots with a nonlinear dependence. This is exactly the behavior observed for the Ras hexadecyl chain modification at cysteine 181. This Ras lipid modification is not only more loosely packed as expressed by low order parameters, it also appears to be highly flexible and dynamic, undergoing motions with large angular amplitudes. A material made of such highly mobile chains would be soft and very elastic. Interestingly, the lipid chains of the host

matrix show a somewhat shallower slope in the square-law plots, which means, that the elasticity of the host membrane is actually slightly reduced. This again underlines that the changes in the membrane caused by the insertion of the Ras protein are mostly compensated for by the mobility of the Ras chains rather than by the host matrix.

The relaxation time T_{1z} of N-Ras protein **3** was also compared with the C-terminal N-Ras heptapeptide. A plot of quadrupolar relaxation time T_1 of each carbon atom was shown in Figure 35.

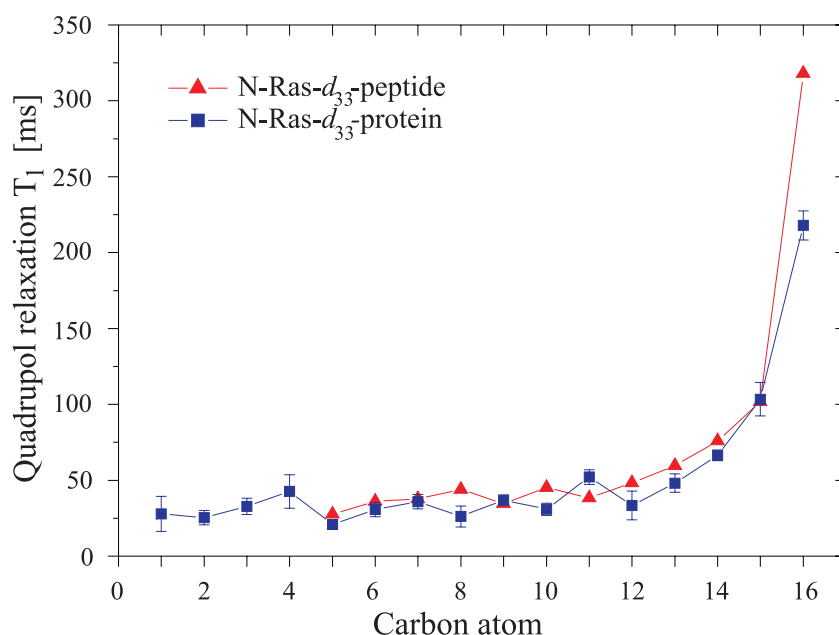


Figure 35. Comparison of the relaxation time for N-Ras protein **3** and C-terminal N-Ras- D_{33} heptapeptide.

The relaxation time of N-Ras protein **3** and C-terminal N-Ras- D_{33} heptapeptide shows similar trend with increasing relaxation time from carbon close to protein/peptide back to carbon far away from the backbone. The absolute value of relaxation time ranges from around 25 ms to 300 ms for N-Ras- D_{33} heptapeptide and 200 ms for N-Ras-protein **3**. The relaxation time determined for the hexadecyl chain of the Ras protein are about 100ms longer, which can be understood by considering the molecular mass difference between peptide and protein, which results in somewhat slower motions of the later.

4.3.2 Molecular dynamics of the C-terminus of membrane-associated Ras protein.

In addition to the dynamics information for the Ras protein lipid modification at cysteine 181, the backbone and side chain molecular mobility of the seven isotopic labeled C-terminal amino acids of Ras were studied by ^{13}C MAS NMR spectroscopy. The order parameter of backbone and side chain can be determined by 2D *dipolar coupling chemical-shift correlation experiment* (DIPSHIFT).⁷⁰

In DIPSHIFT measurement, the motional averaged dipolar coupling strength between ^1H and its directly bonded ^{13}C is measured. Similar to the motional averaged quadrupolar interaction, the actually measured dipolar coupling can be used to determine the molecular order parameter of the ^{13}C - ^1H bond vector. The order parameter of the backbone can thus be calculated from the motionally averaged dipolar coupling. Large dipolar coupling of ^1H and its neighboring ^{13}C implies that the ^{13}C and ^1H bond has a small motional amplitude angle θ and large order parameter and vice versa. Figure 36 shows the ^{13}C - ^1H bond motional amplitude angle.

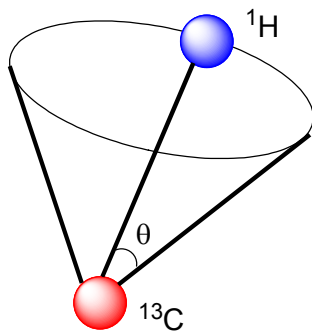


Figure 36. ^{13}C - ^1H bond motional amplitude angle.

To avoid overlapping of the NMR signals, two complementary ^{13}C labeled Ras proteins, N-Ras proteins **1** and **2**, were subjected to DIPSHIFT measurements. The good resolution of the 1D ^{13}C NMR spectra performed in the structure investigation of C-terminal N-Ras protein allows determining the strength of the ^1H - ^{13}C dipolar couplings in a DIPSHIFT experiment. Fast anisotropic molecular motions partially average these couplings.

Therefore, the amplitude of the motion of the bond vectors can be assessed from the order parameter defined by the ratio of the motionally averaged and full dipolar coupling. Figure 37A shows order parameters for the protein backbone and side chains of the seven isotopic labeled terminal amino acids residues. Filled bars correspond to the order parameters of $C\alpha$ sites, open bars to the $C\beta$, hatched bars to the $C\gamma$, and crossed bars to the $C\delta$ sites. Figure 37B shows the combined plot of the order parameters of cysteine 181 starting at the $C\alpha$ site and continuing into the lipid chain of the membrane anchor.

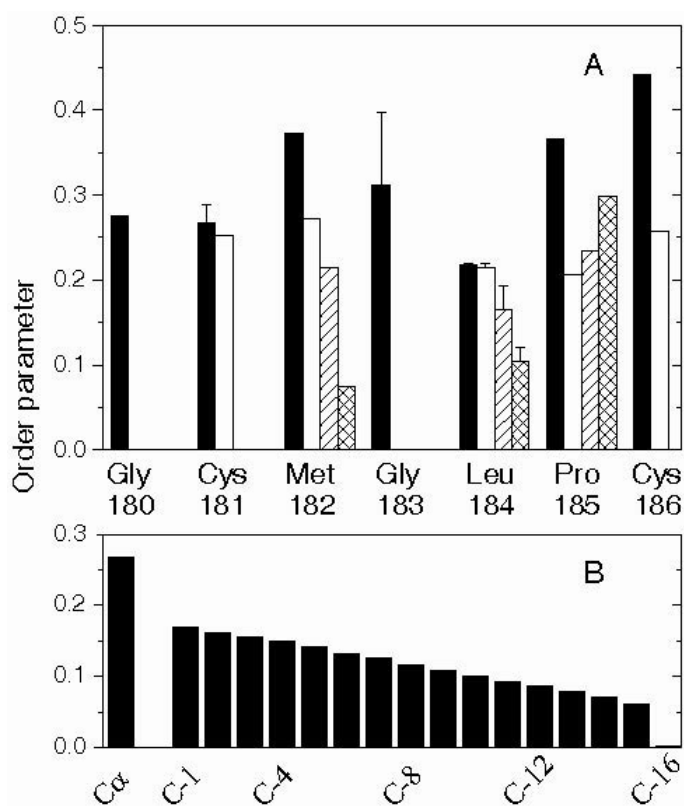


Figure 37. ^1H - ^{13}C order parameters of the membrane bound C-terminus of Ras. (A) Order parameters for the protein backbone and side chains are given for the seven terminal residues. (B) Combined plot of the order parameters of cysteine 181 starting at the $C\alpha$ site and continuing into the lipid chain membrane anchor. The hexadecyl chain order parameters were taken from Figure 30

The absolute values for these order parameters are relatively low indicating large amplitude motions in the C-terminus of membrane bound Ras. A monotonic decrease of

the order parameters along the side and lipid chains is observed indicating that the amplitude of motions increases along the chain. Only for Pro 185, order parameters decrease for $C\beta$ and increase again for $C\gamma$ and $C\delta$ as expected for the five-membered ring that folds back to the main chain. In general, lipid chain attached cysteine 181 and cysteine 186 show higher order parameter. This can be recognized by the anchor of lipid chain to the phospholipids in which render higher rigidity of these two amino acids residues in the study. There is no conclusive trend in the amplitude of the backbone motions of the membrane bound Ras protein. It is interesting that the two lipid modified cysteine residues exhibit very different order parameters suggesting that the farnesylated Cys 186 is more rigid than the hexadecylated Cys 181.

Finally, it is important to know the correlation times of the molecular motions studied. To this end, ^{13}C MAS NMR T_1 and T_2 relaxation times as a function of temperature was measured for membrane-bound N-Ras protein **3**, shown in Figure 38.

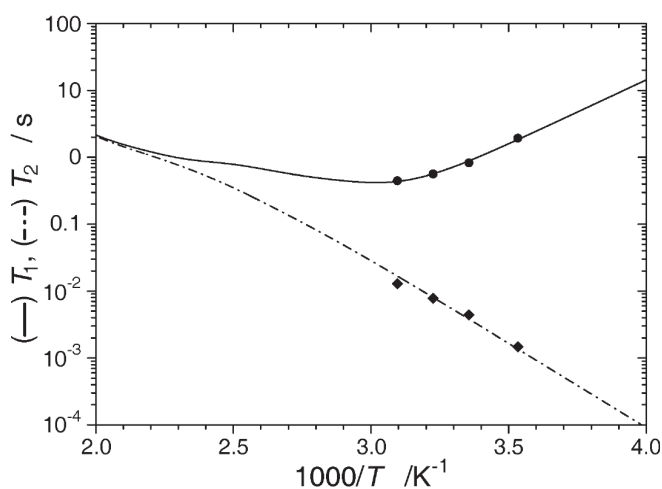


Figure 38. Experimental and simulated relaxation times vs inverse temperature data for the $^{13}\text{C}\alpha$ signal of Gly 183 of membrane-bound Ras protein. The symbols refer to the experimental T_1 (■) and T_2 (◆) relaxation times, and the lines are the best fit simulation using a modified Lipari-Szabo approach.

With increasing temperature, T_1 relaxation times decrease while T_2 relaxation times increase as typical for samples exhibiting molecular motions that are not in the extreme narrowing limit. To calculate correlation times for the backbone motions of membrane bound Ras, a modified Lipari-Szabo formalism⁷¹ was used with an Arrhenius temperature dependence of the correlation time with $\tau_0 = 10^{-15}$ s.⁷² It was further considered that two directly bonded hydrogens relax the $^{13}\text{C}\alpha$ spin of glycine 183. Since membrane binding restricts the mobility of the Ras protein, the spectral density functions contained one anisotropic term for the overall and one for the internal protein motions. The anisotropy is represented in an order parameter for the fast internal (S_f) and slower (S_s) overall motions of membrane-associated Ras. The spectral density functions of the modified Lipari-Szabo equation are given in equation (2).

$$J(\omega) = \frac{2}{5} \left[\frac{(1 - S_f^2)}{1 + (\omega\tau_f)^2} + \frac{(S_f^2 - S_s^2)\tau_s}{1 + (\omega\tau_s)^2} \right] \quad (2)$$

The product S of S_f and S_s represents the order parameter measured in the DIPSHIFT experiments. For the temperature dependence of the correlation times, an Arrhenius behavior was assumed. These parameters could be determined from the experimentally measured temperature dependence of the relaxation times. The results of the analysis are shown in Table 4.

Table 4. Correlation times for the slow and fast motions of glycine 183 in membrane-associated lipidated Ras protein

Temperature/K	τ_s/ns	τ_f/ns
283	864.0 ± 22.2	7.4 ± 0.3
298	306.7 ± 7.9	3.3 ± 0.1
310	143.9 ± 3.7	1.9 ± 0.1
323	67.6 ± 1.6	1.0 ± 0.05

Depending on temperature, the correlation times are between ~ 70 and 900 ns for the overall and between ~ 1 and 7 ns for the internal motions. The order parameters for these dynamic processes are 0.445 and 0.70 , respectively, and $S_{\text{DIPSHIFT}} = S_s \times S_f = 0.312$.

4.3.3 Summary of the dynamic study for the membrane-associated N-Ras protein C-Terminus

The dynamical results calculated from the ^2H NMR indicates that the lipid modification at cysteine 181 adjusts its length to that of the host membrane. Instead of the membrane adjusting to the longer protein chain by local curvature, which costs free energy, the chain inserts into the hydrophobic membrane interior with almost no energy cost, thereby largely retaining its configurational entropy and leaving the host matrix relatively unchanged. This requires the protein chain to be flexible in order to insert into a fluid membrane that is characterized by a large amount of molecular disorder.

This may indicate that the matching between the Ras and the DMPC chain lengths happened by chance and the low order parameter of the Ras lipid modifications result from the insertion of the protein backbone and side chains into the lipid water interface of the membrane. Thereby, the phospholipids molecules are spaced apart, which decreases the lateral pressure in the membrane underneath.

The lipid chain modifications of Ras can fill the volume below the protein backbone by assuming very low order parameters, which means high amplitude motions for these chains. Therefore, the matching of the length of the Ras hydrocarbon chains with those of the phospholipid matrix is a result of energetically favorable hydrophobic contacts between the Ras and the DMPC chains as well as the accommodation of the interfacial area of the Ras chains to the area that the peptide backbone occupies in the membrane interface.

The dynamic properties of this lipid chain completely differ from that of the phospholipid membrane. Interestingly, the dynamic properties of the Ras lipid chain at cysteine 181 resemble those of phospholipid chains in very soft membranes. Such bilayers are

characterized by very flexible and mobile hexadecyl chains described by low order parameters and large amplitude motions. In other words, the lipid chain of cysteine 181 is characterized by a high amount of flexibility.

Although an immobile lipid chain would provide maximal hydrophobic interactions with the membrane, the entropic contribution to the free energy of protein binding would be unfavorable. For stable membrane insertion, two lipid modifications are necessary.⁷³ While the farnesyl moiety appears to be more rigid as inferred from the higher order parameter of cysteine 186, the highly flexible and mobile Ras hexadecyl chain modification contributes sufficient hydrophobic binding energy but also configurational entropy, which both reduces the free energy of the membrane bound Ras protein and contributes to stable membrane insertion. According to this model, the branched farnesyl chain provides the more rigid membrane anchor while the second flexible chain modification can contribute both hydrophobic energy but also favorable configurational entropy and therefore reduce the free energy of the membrane ensemble.

The motional amplitudes of the seven terminal amino acids of the membrane-associated Ras protein were determined using ¹³C CP MAS NMR experiments. It is particularly noteworthy that the order parameter of farnesylated cysteine 186 is about 60% higher than that of hexadecylated cysteine 181. Considering the high degree of flexibility of the chain of cysteine 181, this would suggest that the farnesyl modification of cysteine 186 is relatively rigid. Currently, very little is known about the mobility of farnesyl moieties in membranes; however, molecular dynamics and NMR results suggest that they exist primarily in an extended conformation⁷⁴ and have no effect on the lipid chain order in phospholipids membranes.⁷⁵ The higher order of cysteine 186 compared to cysteine 181 suggests that the farnesyl chain may not show the high degree of flexibility that was observed for the hexadecyl chain. From its branched structure, the farnesyl chain represents a barbed hook that may more stably insert into the membrane than the very flexible hexadecyl chain.

The protein order parameters are relatively low compared to other membrane proteins.⁷⁶ However, it should be recalled that the membrane anchor of Ras is not folded into a

regular secondary structure. Further, the order parameters need to be related to the time scale on which they are measured. Correlation times from the analysis of ^{13}C relaxation rates of glycine 183 in membrane-associated Ras **3** were studied by relaxation measurement. According to the modified Liparid-Szabo model, the molecular mobility of the membrane-associated Ras protein **3** can be separated into a fast segmental and a slower overall process. The order parameter for the fast motion of the glycine 183 $\text{C}\alpha\text{-H}\alpha$ bond vector is 0.70 and for the slow motions of the membrane anchor it is 0.445.

At 37 °C the fast bond vector fluctuations of glycine 183 occur with a correlation time of 1.9 ns and a motional amplitude angle of $\sim 40^\circ$. Such segmental fluctuations are quite common for amino acids in somewhat flexible loop structures of soluble proteins. This agrees with the structural model of membrane-associated Ras protein that showed no regular secondary structure.⁷⁷ On the other hand, the membrane anchor of Ras inserts into the lipid water interface of the membrane where it experiences a highly dynamic structural assembly of lipids and water molecules.⁷⁸ This suggests that membrane binding of Ras stabilizes the structure of its membrane anchor presumably by hydrogen bonds between the protein backbone and phospholipids segments in the membrane interface. In addition to the segmental mobility, the membrane anchor of Ras undergoes slower motions with large amplitudes (order parameter of 0.445). The correlation time for this motion is ~ 140 ns at 37 °C.

In summary, the C-terminus of membrane-associated full length Ras protein shows a versatile dynamics (Figure 39).

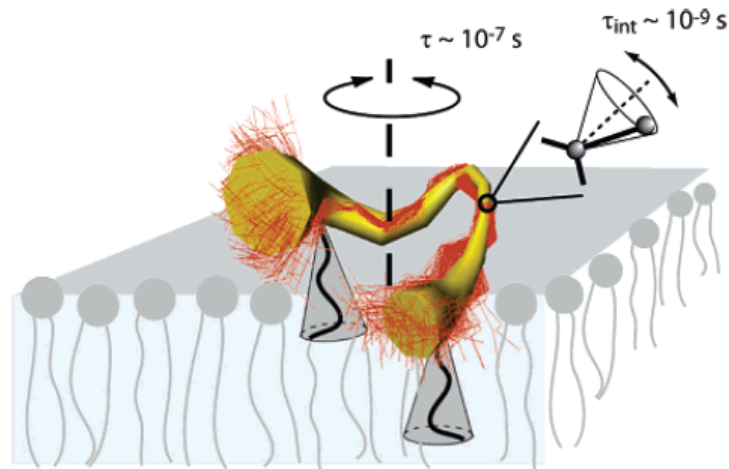


Figure 39. Cartoon illustrates the results of dynamical studies of N-Ras proteins.⁴²

The protein backbone is shown as the 200 lowest energy structures (orange). The flexibility of the structure is represented by the yellow tube. Fast segmental motions of the protein backbone and side chains occur with correlation times in the nanosecond range. The entire C-terminus of Ras undergoes axially symmetric motions on the membrane surface with correlation times of several 100 ns. The lipid modifications are also highly mobile and flexible in the membrane.

The segmental motions of the protein backbone are similar to those of loop structures of soluble proteins. It is suggested that binding to the lipid membrane stabilizes the structure of the C-terminus of Ras. Further, the membrane anchor of Ras undergoes slower motions with axial symmetry, which may apply to the entire protein. In fact, NMR study of full-length farnesylated Ras also indicated that the motions of the N-terminal domain are influenced by the lipidated C-terminus in solution.⁷⁹ The lipid chain modification at cysteine 181 is highly mobile in the liquid-crystalline membrane.

5 Experimental Part

5.1.1 Materials and Methods

Nuclear Magnetic Resonance Spectroscopy

^1H and ^{13}C NMR spectra were recorded on one of the following instruments: Varian Mercury 400, Bruker DRX 400 and Bruker DRX 500 with tetramethylsilane as the internal reference. The chemical shifts are provided in ppm and the coupling constants in Hz. The following abbreviations for multiplicities are used: *s*, singlet; *d*, doublet; *dd*, double doublet; *dt*, doublet triplet; *t*, triplet; *q*, quadruplet; *m*, multiplet; *br*, broad. The ^1H and ^{13}C spectra are calibrated to the solvent signals of CDCl_3 (7.26 ppm and 77.00 ppm) and MeOH (3.31 ppm, 49.05 ppm).

Solid State NMR Spectroscopy

^1H , ^2H and ^{13}C NMR spectra were acquired with a Bruker Avance 750 widebore NMR spectrometer (Bruker BioSpin GmbH, Rheinstetten, Germany) at a resonance frequency of 749.8 for ^1H , 188.5 MHz for ^{13}C and 115.1 MHz for ^2H .

Sample Preparation

Large unilamellar vesicles were prepared by extrusion in buffer (10mM, HEPES, 10mM NaCl, 1mM MgCl_2 , pH 7.4). Aliquots of soluble Ras molecules were added to the liposome solution at a 1:150 protein to lipid molar ratio. After incubation at 37°C for 4 hours, the sample was ultracentrifuged at $\sim 90,000$ for 10 hours. Subsequently, the pellet was lyophilized and then hydrated to 35 wt% water content. After equilibration by several freeze-thaw cycles and gentle centrifugation the sample was transferred into 4 mm MAS rotors with Teflon insert.

Mass Spectrometry

Gas chromatography-mass spectrometry (GC-MS) were measured from a Hewlett Packard 6890 GC system coupled to a Hewlett Packard 5973 Mass Selective Detector. A HP 5TA capillary column (0.33 μm x 25 m x 0.2 mm) and helium flow rate of 2 mL/ min were used. High resolution mass spectra (HR-MS, 70 eV) were measured on a Jeol SX 102A spectrometer by using fast atom bombardment (FAB) techniques. The matrix used for FAB was 3-nitrobenzylalcohol (3-NBA). The MALDI-TOF spectra were recorded on a Voyager-DE Pro

MALDI-TOF and with 2,5-dihydroxybenzoic acid (DHB) as the matrix (20 mg DHB, 900 μ l H₂O, 90 μ l ethanol, 10 μ l TFA).

Reversed-Phase High-Pressure Liquid Chromatography

Analytical HPLC was recorded on an Agilent HPLC (1100 series machine). The standard gradient began at 10% acetonitrile and was raised to 90% over 15 min. After 3 min at 90% acetonitrile, the column was washed for 5 min with 100% acetonitrile. The column was then equilibrated for 3 min with 10% acetonitrile. TFA (0.1% v/v) was added to the HPLC solvents. Analytical HPLC-MS measurements were recorded on an Agilent HPLC (1100 series) coupled to a Finnigan LCQ ESI spectrometer. The column used is indicated in parenthesis.

Thin-Layer Chromatography (TLC)

Thin-layer chromatography (TLC) plates were obtained from Merck (Silica gel 60, F254). The TLCs were visualized by UV light ($\lambda = 254$ nm, 366 nm) or by staining with KMnO₄ solution. The solvent system and R_f values are noted for the synthesized compounds.

Flash Chromatography

Flash column chromatography was performed using flash silica gel (Merck, Darmstadt, 40-64 μ M) with pressure ranging from 0.5 - 1.0 bar.

Chemicals

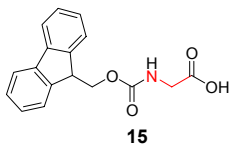
Chemicals were obtained from the following suppliers and used without further purification: Acros, Aldrich, Fluka, Novabiochem, Senn Chemicals. The solid support was purchased from Novabiochem. Uniformly ¹³C and ¹⁵N labeled amino acids were purchased from Euriso-Top GmbH (Saarbrücken, Germany).

5.2.1 Experimental procedures and analytical data

General procedure (GP 1) for the synthesis of building blocks 15, 17, 19 and 21

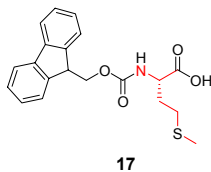
To isotope labeled amino acid (0.64 mmol, 1.0 equivalent) in Na₂CO₃ solution (1.6 mmol, 2.5 equivalents, 2 mL) and dioxane (4 mL) mixture was added Fmoc-Cl (0.64 mmol, 1.0 equivalent) at 0°C. The reaction mixture was stirred at room temperature overnight. The reaction mixture was extracted with diethyl ether (10 mL x 2), and the organic layer was discarded. The pH of the aqueous layer was adjusted to pH 1 with 1 M HCl. The aqueous solution was extracted with ethyl acetate (10 mL x 2). The combined organic layers were washed with brine, dried over MgSO₄, filtered and concentrated under reduced pressure. The crude product was purified by flash chromatography.

Analytical data of N-(9-Fluorenylmethoxycarbonyl) glycine-¹³C₂, ¹⁵N 15



Yield = 85 %; **R_f** = 0.1 (CH₂Cl₂ / MeOH : 9/1); **LRMS** (FAB, *m*-NBA) *m/z* calc. for C₁₅¹³C₂H₁₅¹⁵N¹⁵O₄ 300.1, found 300.0 [M+H]⁺; **¹H NMR** (400 MHz, CDCl₃): δ = 7.77 (d, *J* = 7.5 Hz, 2H), 7.60 (d, *J* = 7.0 Hz, 2H), 7.41 (t, *J* = 7.5, 7.5 Hz, 1H), 7.32 (dt, *J* = 7.5, 1.2 Hz, 2H), 4.44 (dd, *J* = 7.0, 0.6 Hz, 2H), 4.24 (t, *J* = 7.0 Hz, 1H), 3.90-3.86 (m, 1H) ppm; **¹³C NMR** (100 MHz, CDCl₃): δ = 171.9 (d, *J* = 59.2 Hz, 1C), 156.5, 143.7, 140.6, 127.5, 127.0, 125.0, 120.0, 65.6, 46.5, 42.5 (dd, *J* = 59.6, 14.3 Hz, 1C) ppm.

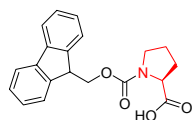
Analytical data of N-(9-Fluorenylmethoxycarbonyl) L-Methionine-¹³C₅, ¹⁵N 17



Yield = 75 %; **R_f** = 0.32 (CH₂Cl₂ / MeOH : 9/1); **LC-MS** (C18, ESI_MS) 378.1 [M+H]⁺; **R_t** = 8.82 min; **¹H NMR** (400 MHz, CDCl₃): δ = 7.76 (d, *J* = 7.5 Hz, 2H), 7.6 (d, *J* = 7.6 Hz, 2H), 7.40 (t, *J* = 7.4 Hz, 2H), 7.31 (t, *J* = 7.44 Hz, 2H), 4.72 (br, 1H), 4.44 (d, *J* = 6.8 Hz, 1H), 4.23 (t,

$J = 6.8$ Hz, 2H), 2.39 (br, 1H), 2.27 (br, 1H), 2.10 (s, 3H), 1.93 (br, 2H) ppm; ^{13}C NMR (100 MHz, CDCl_3): $\delta = 176.87$ (d, $J = 58.8$ Hz, 1C), 155.9, 143.6, 141.3, 127.7, 127.0, 125.0, 120.0, 67.1, 52.9 (ddd, $J = 58.7, 34.3, 12.9$ Hz, 1C), 47.1, 31.5 (t, $J = 35.0$ Hz, 1C), 29.9 (d, $J = 35.7$ Hz, 1C), 15.4 (s, 1C) ppm.

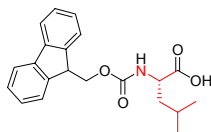
Analytical data of N-(9-Fluorenylmethoxycarbonyl) L-Proline- $^{13}\text{C}_5$, ^{15}N 19



19

Yield = 70 %; **R_f** = 0.38 (CH_2Cl_2 / MeOH : 9/1); **LC-MS** (C18, ESI_MS) 343.9 $[\text{M}+\text{H}]^+$; **R_t** = 8.51 min; ^1H NMR (400 MHz, CDCl_3): $\delta = 7.77$ (d, $J = 7.4$ Hz, 2H, trans), 7.72 (d, $J = 7.4$ Hz, 2H, cis), 7.60 (d, $J = 7.4$ Hz, 2H, trans), 7.56 (d, $J = 8.2$ Hz, 2H, cis), 7.45-7.35 (m, 2H), 7.35-7.27 (m, 2H), 4.60 (br, 1H), 4.54-4.45 (m, 1H), 4.44-4.34 (m, 1H), 4.30-4.20 (m, 2H), 3.75 (br, 1H), 3.65 (br, 1H), 3.39 (br, 1H), 3.29 (br, 1H), 2.45 (br, 1H), 2.29 (br, 1H), 2.13 (br, 2H), 1.94-1.63 (m, 2H) ppm (cis-trans isomers); ^{13}C NMR (101 MHz, CDCl_3): $\delta = 176.8$ (d, $J = 60.4$ Hz, 1C), 174.46 (d, $J = 58.7$ Hz, 1C), 156.5, 154.1, 143.760, 143.6, 141.3, 127.7, 127.6, 127.0, 125.0, 124.9, 120.0, 119.9, 60.27-57.55 (m, 1C), 68.0, 67.3, 47.85-45.91 (m, 1C), 30.9 (t, $J = 30.6, 30.6$ Hz, 1C), 28.7 (t, $J = 31.9, 31.9$ Hz, 1C), 24.3 (t, $J = 32.0, 32.0$ Hz, 1C), 23.3 (t, $J = 32.0, 32.0$ Hz, 1C) ppm (cis-trans isomers).

Analytical data of N-(9-Fluorenylmethoxycarbonyl) L-Leucine- $^{13}\text{C}_6$, ^{15}N 21



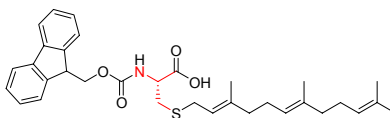
21

Yield = 85 %; **R_f** = 0.45 (CH_2Cl_2 / MeOH : 9/1); ^1H NMR (400 MHz, CDCl_3): $\delta = 7.76$ (d, $J = 7.59$ Hz, 2H), 7.64-7.54 (m, 2H), 7.40 (t, $J = 7.36$ Hz, 2H), 7.31 (t, $J = 7.33$ Hz, 2H), 4.60 (br, 1H), 4.51-4.35 (m, 2H), 4.23 (t, $J = 7.02$ Hz, 1H), 2.03-1.64 (m, 2H), 1.63-1.34 (m, 2H), 1.12 (d, $J = 5.5$ Hz, 3H), 0.81 (d, $J = 3.6$ Hz, 3H) ppm; ^{13}C NMR (101 MHz, CDCl_3): $\delta = 177.48$ (d, $J = 58.8$ Hz, 1C), 143.6, 141.3, 127.7, 127.0, 125.0, 119.9, 67.0, 52.29 (ddd, $J = 58.7, 34.2, 12.2$ Hz, 1C), 47.1, 41.3 (t, $J = 34.4, 34.4$ Hz, 1C), 24.76 (q, $J = 34.6, 34.6, 34.4$ Hz, 1C), 22.81 (d, $J = 34.8$ Hz, 1C), 21.67 (d, $J = 34.5$ Hz, 1C) ppm.

General procedure (GP 2) for the synthesis of compound 24, 35

To isotope labeled cysteine **22** (71 mg, 0.57 mmol) in methanol (5 mL) was added 7N NH₃ in methanol (2 mL) and farnesyl bromide (340 mg, 0.60 mmol) respectively at 0°C. The reaction mixture was slowly warmed to room temperature and stirred overnight. The reaction mixture was evaporated to dryness under reduced pressure. CH₂Cl₂ (10 mL) and Et₃N (115 mg, 1.14 mmol) were added to the remained white solid flask followed by Fmoc-OSu (230 mg, 0.68 mmol) at 0°C. The reaction mixture was slowly warmed to room temperature and stirred for 3 hours. 1M HCl (5 mL) was added to the reaction mixture, and extracted twice with CH₂Cl₂. The combined organic phase was washed with brine, dried over MgSO₄, filtered and concentrated *in vacuo*. The crude was purified by flash chromatography.

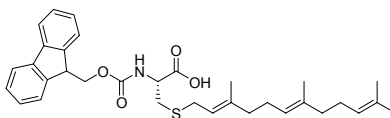
Analytical data of N-(9-Fluorenylmethoxycarbonyl) S-Hexadecyl L-Cysteine-¹³C₃, ¹⁵N **24**



24

Yield = 63 %; **R_f** = 0.7 (CH₂Cl₂ / MeOH : 9/1); **LC-MS** (C4, ESI_MS) 552.2 [M+H]⁺; **R_t** = 9.15 min; **¹H NMR** (400 MHz, CDCl₃): δ = 7.76 (d, *J* = 7.4 Hz, 2H), 7.60 (d, *J* = 6.8 Hz, 2H), 7.40 (t, *J* = 7.66 Hz, 2H), 7.31 (t, *J* = 7.45 Hz, 2H), 5.22 (t, *J* = 7.34 Hz, 1H), 5.13-5.01 (m, 2H), 4.63 (m, 1H), 4.55-4.32 (m, 2H), 4.24 (t, *J* = 7.00 Hz, 1H), 3.46-2.98 (m, 2H), 2.92-2.66 (m, 2H), 2.18-2.00 (m, 6H), 2.00-1.91 (m, 2H), 1.67 (s, 3H), 1.65 (s, 3H), 1.59 (s, 6H) ppm; **¹³C NMR** (100 MHz, CDCl₃): δ = 173.0 (d, *J* = 57.7 Hz, 1C), 156.5, 144.0, 141.5, 140.2, 135.5, 131.4, 127.9, 127.4, 125.4, 124.7, 124.1, 120.2, 11.9, 67.7, 54.30-52.43 (m, 1C), 47.3, 40.0, 39.9, 33.7, 33.1 (d, *J* = 35.6 Hz, 1C), 30.4, 27.2, 26.7, 26.0, 18.0, 16.4, 16.3 ppm.

Analytical data of N-(9-Fluorenylmethoxycarbonyl) S-Farnesyl L-Cysteine **35**



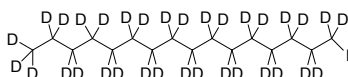
35

Yield = 60 %; **R_f** = 0.7 (CH₂Cl₂ / MeOH : 9/1); **LC-MS** (C4, ESI_MS) 548.4 [M+H]⁺; R_t = 9.69 min; **¹H NMR** (400 MHz, CDCl₃): δ = 7.76 (d, *J* = 7.4 Hz, 2H), 7.60 (t, *J* = 6.47 Hz, 2H), 7.40 (t, *J* = 7.42 Hz, 2H), 7.31 (t, *J* = 7.38 Hz, 2H), 5.61 (d, *J* = 7.86 Hz, 1H), 5.22 (t, *J* = 7.46 Hz, 1H), 5.08 (t, *J* = 6.80 Hz, 2H), 4.62 (dd, *J* = 12.50, 5.55 Hz, 1H), 4.41 (t, *J* = 7.03 Hz, 2H), 4.24 (t, *J* = 7.07 Hz, 1H), 3.45-3.07 (m, 2H), 3.06-2.87 (m, 2H), 2.08-2.00 (m, 6H), 2.00-1.92 (m, 2H), 1.67 (s, 3H), 1.65 (s, 3H), 1.59 (6, 3H) ppm; **¹³C NMR** (100 MHz, CDCl₃): δ = 173.0, 156.5, 144.0, 141.5, 140.2, 135.5, 131.4, 127.9, 127.4, 125.4, 124.7, 124.1, 120.2, 11.9, 67.7, 53.0, 47.3, 40.0, 39.9, 33.7, 33.1, 30.4, 27.2, 26.7, 26.0, 18.0, 16.4, 16.3 ppm.

General procedure (GP 3) for the synthesis of compound 26

To a solution of imidazole (99 mg, 1.45 mmol) and PPh₃ (285 mg, 1.09 mmol) in CH₂Cl₂ (2 mL) at 0°C was added I₂ (276 mg, 1.09 mmol). Cetyl alcohol **25** (200 mg, 0.72 mmol) in CH₂Cl₂ (1 mL) was then added and the reaction mixture was warmed to room temperature after 0.5 hour stirring. The reaction flask was covered with aluminum foil and stirred overnight. The reaction mixture was quenched with 5 % Na₂S₂O₃ (20 mL). The organic layer was separated and the aqueous layer was washed with CH₂Cl₂. The combined organic phase was washed with brine, dried over MgSO₄, filtered and concentrated *in vacuo*. The crude product was purified by column chromatography.

Analytical data of Hexadecyl-D₃₃ iodide 26



26

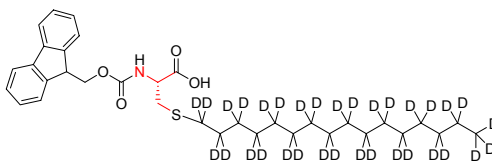
Yield = Quantitative; **R_f** = 0.9 (cyclohexane / ethyl acetate : 4/1); **GC-MS**: 6.66 min, 385 [M]⁺, 258 [M-I]⁺; **¹³C NMR** (100 MHz, CDCl₃): δ = 32.1, 29.8, 29.5, 22.9, 14.3, 8.2 ppm.

General procedure (GP 4) for the synthesis of compound 29

¹³C and ¹⁵N labeled cysteine (42 mg, 0.34 mmol) was treated with 1M HCl (3 mL) for 1 hour and dried under reduced pressure, the procedure was repeated once to afford **27**. Deuterated hexadecyl iodide **26** (132 mg, 0.34) in ether was added to **27** and the ether was evaporated under

reduced pressure. DMF (1 mL) and Na₂CO₃ (76 mg, 0.72 mmol) were added to the reaction flask and the reaction mixture was stirred at room temperature for 60 hours. The reaction mixture was evaporated to dryness under reduce pressure. H₂O (1 mL) and dioxane (2 mL) were added to the reaction mixture, followed by Na₂CO₃ (36 mg, 0.34 mmol) and Fmoc-OSu (114 mg, 0.34 mmol) at 0°C. The reaction mixture was stirred for 3 hours at room temperature. 1M HCl (5 mL) was added to the reaction mixture, and extracted twice with CH₂Cl₂. The combined organic phase was washed with brine, dried over MgSO₄, filtered and concentrated *in vacuo*. The crude was purified by flash chromatography.

Analytical data of N-(9-Fluorenylmethoxycarbonyl) S-Hexadecyl-D₃₃ L-Cysteine-¹³C₃, ¹⁵N 29



29

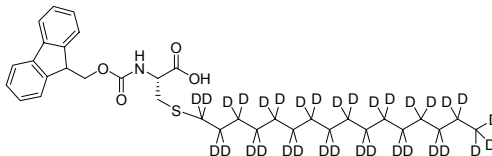
Yield = 35 %; **R_f** = 0.5 (CH₂Cl₂ / MeOH : 9/1); **¹H NMR** (400 MHz, CDCl₃): δ = 7.69 (d, *J* = 7.6 Hz, 2H), 7.53 (d, *J* = 7.2 Hz, 2H), 7.33 (t, *J* = 7.4 Hz, 2H), 7.24 (t, *J* = 7.3 Hz, 2H), 5.68 (d, *J* = 7.9 Hz, 1H), 5.45 (d, *J* = 7.5 Hz, 1H), 4.73 (br, 1H), 4.34 (d, *J* = 6.5 Hz, 2H), 4.17 (t, *J* = 7.00 Hz, 1H), 3.14 (br, 1H), 2.78 (br, 1H) ppm; **¹³C NMR** (100 MHz, CDCl₃): δ = 174.57 (d, *J* = 59.5 Hz, 1C), 155.92 (dd, *J* = 26.7, 1.9 Hz, 1C), 143.65, 141.31, 127.75, 127.09, 125.08, 120.00, 67.40, 53.41 (ddd, *J* = 50.0, 35.0, 12.8 Hz, 1C), 47.11, 33.99 (d, *J* = 35.8 Hz, 1C) ppm.

General procedure (GP 5) for the synthesis of compound 36

To Fmoc-Cys(Trt)-OH (200 mg, 0.35 mmol) in CH₂Cl₂ (15 mL) was added 3% TES (0.45 mL) and 5% TFA (0.75 mL). The reaction mixture was stirred for 2 hours at room temperature. The solvent was co-evaporated with toluene two times under reduced pressure. To the resulted white solid in DMF (5 mL) was added K₂CO₃ (145 mg, 1.05 mmol) and deuterated hexadecyl iodide **26** (135 mg, 0.35 mmol) respectively. The reaction mixture was stirred at room temperature for 4 hours. The solvent was poured into diethyl ether (20 mL) and extracted with 1M HCl (5 mL) twice. The collected organic layer was washed with brine, dried over MgSO₄, filtered and

concentrated in vacuo. The crude product was purified by silica gel chromatography to obtain 50 mg **36** as white solid (23% yield).

Analytical data of N-(9-Fluorenylmethoxycarbonyl) S-Hexadecyl-D₃₃ L-Cysteine **36**



36

Yield = 23 %; R_f = 0.5 (CH₂Cl₂ / MeOH : 9/1); LC-MS (C4, ESI_MS) 601.4 [M+H]⁺; R_t = 10.53 min; ¹H NMR (400 MHz, CDCl₃): δ = 7.70 (d, J = 7.3 Hz, 2H), 7.53 (d, J = 7.1 Hz, 2H), 7.34 (t, J = 7.4 Hz, 2H), 7.24 (t, J = 7.3 Hz, 2H), 5.56 (d, J = 7.5 Hz, 1H), 4.64 (br, 1H), 4.37 (d, J = 7.8 Hz, 2H), 4.17 (t, J = 7.04 Hz, 1H), 3.15-2.91 (m, 2H) ppm; ¹³C NMR (101 MHz, CDCl₃): δ = 174.5, 155.9, 143.6, 141.2, 127.6, 127.0, 125.1, 119.9, 67.4, 47.0 ppm.

General procedure (GP 5) for the synthesis of isotope labeled lipidated peptides **7**, **8** and **9**

Coupling using DIC/HOBT activation. The Fmoc-amino acid to be coupled (3 equivalents relative to resin loading) was dissolved in dry DMF (For lipidated amino acids, same volume of CH₂Cl₂ was added), followed by addition of HOBT (3 equivalents) and DIC (3 equivalents). The mixture was stirred for 1 minute and added to the hydrazine resin **31** at room temperature. The mixture was shaken at room temperature for 2 hours (For lipidated amino acids, the mixture was shaken overnight). The solvent was filtered off and the resin was washed three times with DMF, three times with CH₂Cl₂, and three times with DMF.

Determination of Fmoc-loading. Resin (1-2 mg) was weighed into a volumetric flask and filled with 3 mL 20% piperidine in DMF. After 20 minutes of gentle agitation, 1 mL was transferred to a quartz UV cuvette and diluted to 3 mL with DMF. The absorbance was measured against reference at λ = 301 nm. The loading C_L is determined according to Beer's Law, $A = \epsilon cd$, where ϵ = 7800 at 301 nm.

$$C_L = \frac{Cv \times V}{M} = \frac{A \times 9 \times 1000}{7800 \times M}$$

where C_V is the volume concentration, A is the absorbance, d is the path length of the UV cuvette, V is the total volume, M is the mass of the resin.

Determination of Theoretical Loading. The theoretical loading of the resin was determined according to the following formula:

$$\text{Loading}_{\text{new}} (\text{mol/g}) = \frac{\text{loading}_{\text{old}} (\text{mol/g})}{1 + \Delta \times \text{loading}_{\text{old}} (\text{mol/g})}$$

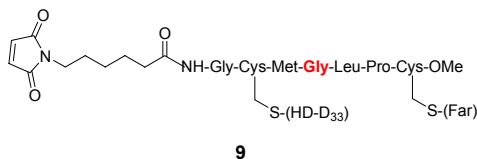
Where $\text{loading}_{\text{old}}$ is the previous loading and Δ is the mass difference of the added compound to the resin.

Removal of Fmoc protecting group. The resin was washed 3 times with 3 mL 20% piperidine/DMF (5 minutes each time) to remove the Fmoc group from the amino acid. Subsequently, the resin was washed again three times with DMF, three times with CH_2Cl_2 , three times with DMF (each time 2 to 5 mL).

Coupling of MIC group using HATU/HOAT. The Fmoc-amino acid to be coupled (3 equivalents relative to resin loading) was dissolved in dry DMF followed by addition of HOAT (3 equivalents) and HATU (3 equivalents). DIPEA (6 equivalents) was lastly added and the resulting solution was stirred for 1 minute and added to the peptidyl hydrazine resin at room temperature. The mixture was shaken at room temperature for 2 hours. The solvent was filtered off and the resin was washed three times with DMF, three times with CH_2Cl_2 , and three times with DMF. Finally, the resin was dried *in vacuo*.

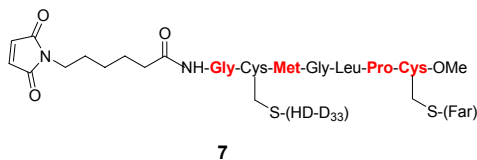
Release of Peptides using $\text{Cu}(\text{OAc})_2$ /pyridine/Methanol. To MIC-containing peptidyl hydrazine resin (initial loading 3.4 mmol) in CH_2Cl_2 (2 mL) was added $\text{Cu}(\text{OAc})_2$ (3mg, 1.7 mmol), pyridine (26 mg, 0.34 mmol) and methanol (0.1mL, 2.4 mmol) mixture in CH_2Cl_2 (2 mL). The reaction mixture was shaken for 3 hours at room temperature under oxygen. The reaction solvent was collected and washed with CH_2Cl_2 . The collected solvent was extracted twice with 1M HCl (5 mL each), washed with brine, dried with MgSO_4 , filtered and concentrated *in vacuo*. The crude product was purified by silica gel chromatography.

Analytical data of MIC-Gly-Cys(HD-D₃₃)-Met-Gly(¹³C₂, ¹⁵N)-Leu-Pro-Cys(Far)-OMe 9



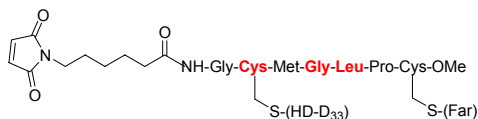
Yield = 17 %; **R_f** = 0.4 (CH₂Cl₂ / MeOH : 9/1); **LC-MS** (C4, ESI_MS) 1351.8 [M+H]⁺, 1374.0 [M+Na]⁺; **R_t** = 11.13 min; **¹H NMR** (400 MHz, CDCl₃): δ = 6.68 (s, 2H), 5.15 (t, *J* = 7.6 Hz, 1H), 5.11-5.04 (m, 2H), 4.75 (t, *J* = 9.5 Hz, 1H), 4.72-4.61 (m, 2H), 4.62-4.52 (m, 2H), 4.30-4.23 (m, 1H), 3.95 (t, *J* = 5.0 Hz, 1H), 3.74 (s, 3H), 3.54-3.45 (m, 4H), 3.16 (dd, *J* = 13.3, 8.2 Hz, 1H), 3.05 (dd, *J* = 13.3, 7.1 Hz, 1H), 2.94 (dd, *J* = 13.8, 4.8 Hz, 1H), 2.84 (dd, *J* = 11.5, 6.7 Hz, 1H), 2.71 (dd, *J* = 13.6, 6.6 Hz, 1H), 2.64-2.52 (m, 3H), 2.29 (t, *J* = 7.4 Hz, 1H), 2.25-2.17 (m, 4H), 2.13-1.92 (m, 12H), 1.66 (s, 3H), 1.65 (s, 3H), 1.59 (s, 6H), 0.93 (d, *J* = 4.7 Hz, 3H), 0.92 (d, *J* = 4.4 Hz, 3H) ppm; **¹³C NMR** (100 MHz, CDCl₃): δ = 170.8, 170.5, 170.0, 169.59 (d, *J* = 53.0 Hz, 1C), 169.5, 169.4, 169.3, 169.0, 168.9, 140.0, 135.3, 134.0, 131.2, 124.2, 123.6, 119.4, 60.0, 53.3, 52.5, 51.9, 49.0, 47.3, 42.98 (dd, *J* = 53.0, 10.8 Hz, 1C), 39.6, 37.5, 35.8, 30.5, 30.5, 29.6, 28.1, 26.7, 26.5, 26.2, 25.6, 24.9, 24.8, 24.8, 24.5, 23.2, 21.6, 17.6, 16.1, 15.9, 15.0 ppm.

Analytical data of MIC-Gly(¹³C₂, ¹⁵N)-Cys(HD-D₃₃)-Met(¹³C₅, ¹⁵N)-Gly-Leu-Pro(¹³C₅, ¹⁵N)-Cys(Far, ¹³C₃, ¹⁵N)-OMe 7



Yield = 23 %; **R_f** = 0.4 (CH₂Cl₂ / MeOH : 9/1); **LC-MS** (C4, ESI_MS) 1367.6 [M+H]⁺, 1389.7 [M+Na]⁺; **R_t** = 10.69 min; **¹³C NMR** (100 MHz, CDCl₃): δ = 171.83-170.33 (m, 4C), 60.03 (dd, *J* = 54.9, 32.2 Hz, 1C), 53.69-51.29 (m, 2C), 43.99 (dd, *J* = 52.6, 11.8 Hz, 1C), 47.41 (dd, *J* = 31.2, 9.4 Hz, 1C), 33.18 (d, *J* = 35.8 Hz, 1C), 30.60 (d, *J* = 35.2 Hz, 2C), 28.05 (td, *J* = 65.0, 35.2, Hz, 1C), 24.90 (t, *J* = 31.7 Hz, 1C), 15.03 (s, 1C) ppm.

Analytical data of MIC-Gly-Cys(HD-D₃₃, ¹³C₃, ¹⁵N)-Met-Gly(¹³C₂, ¹⁵N)-Leu(¹³C₆, ¹⁵N)-Pro-Cys(Far)-OMe 8



8

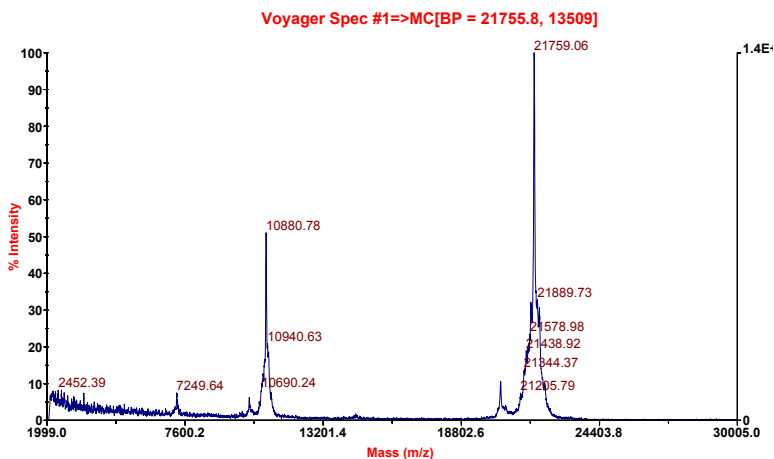
Yield = 5.4 mg (10%); **R_f** = 0.4 (CH₂Cl₂ / MeOH : 9/1); **LC-MS** (C4, ESI_MS) 1362.9 [M+H]⁺, 1384.8 [M+Na]⁺; **R_t** = 10.53 min.

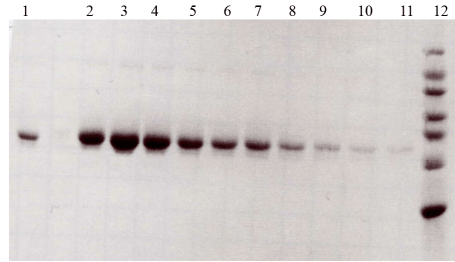
General procedure (GP 6) for the ligation of isotope labeled lipidated peptides with truncated N-Ras protein 1, 2 and 3

The coupling of labeled lipidated peptide and truncated N-Ras protein (¹⁻¹⁸²N-RasG12V) was performed by Christine Nowak following the previously reported protocol.⁴⁴ The product of the ligation was analyzed by MALDI-TOF MS and SDS-PAGE.

Analytical Data of N-Ras Δ 181MIC-Gly-Cys(HD-D₃₃)-Met-Gly-Leu-Pro-Cys(Far)-OMe 1

Yield = 37%; The mass peak at 21759 corresponds to the ligation product 1

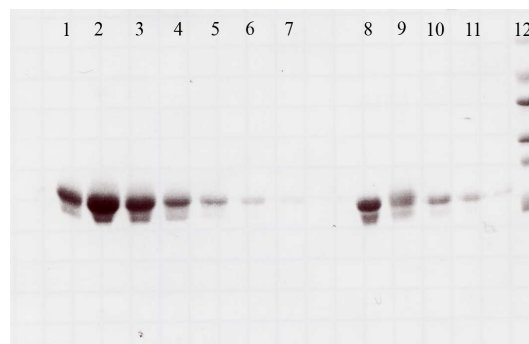
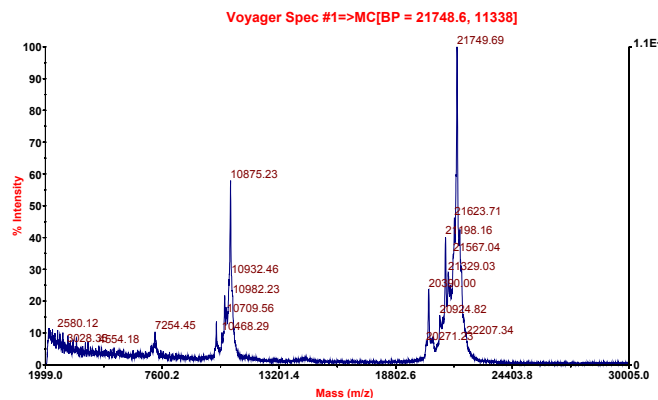




1: truncated N-Ras protein $^{1-182}$ N-RasG12V, 12: marker, 2-11: product fraction after purification

Analytical Data of N-Ras Δ 181MIC-Gly-Cys(HD-D₃₃)-Met-Gly-Leu-Pro-Cys(Far)-OMe 2

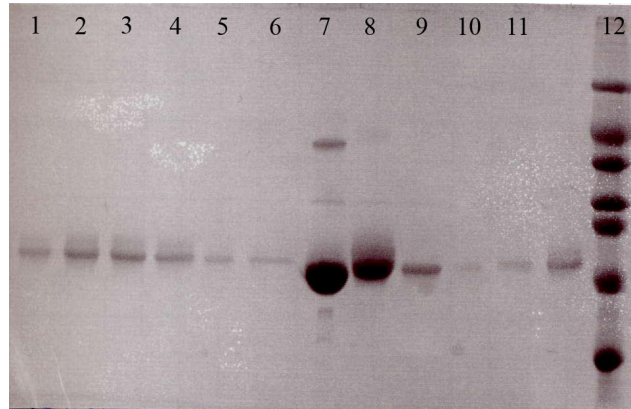
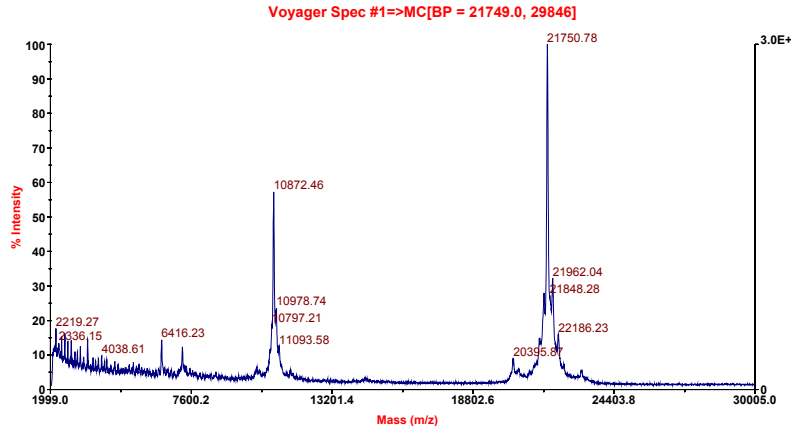
Yield = 15%; The mass peak at 21749 corresponds to the ligation product 2.



8: truncated N-Ras protein $^{1-182}$ N-RasG12V, 12: marker, 1-7: product fraction after purification, 9: crude mixture.

Analytical Data of N-Ras Δ 181MIC-Gly-Cys(HD-D₃₃)-Met-Gly-Leu-Pro-Cys(Far)-OMe 3

Yield = 30 %; The mass peak at 21750 corresponds to the ligation product 3.



7: truncated N-Ras protein ¹⁻¹⁸²N-RasG12V, 12: marker, 1-6: product fraction after purification, 8: crude mixture.

6 References

- [1] (a) E. S. Lander, et. al. *Nature*, **2001**, *409*, 860-921; (b) J. C. Venter, et. al. *Science*, **2001**, *291*, 1304-1351.
- [2] Some reviews about membrane protein structures solved by NMR. (a) F. M. Marassi, S. J. Opella, *Curr. Opin. Struct. Biol.*, **1998**, *8*, 640-648; (b) S. J. Opella, F. M. Marassi, *Chem. Rev.*, **2004**, *104*, 3587-3606; (c) R. Fu, T. A. Cross, *Annu. Rev. Biophys. Biomol. Struct.*, **1999**, *28*, 235-268.
- [3] (a) A. Jemal, T. Murray, E. Ward, A. Samuels, R. C. Tiwari, A. Ghafoor, E. J. Feuer, M. J. Thun, *CA Cancer J. Clin.*, **2005**, *55*, 10-30.
- [4] <http://en.wikipedia.org/wiki/Cancer>.
- [5] (a) E. R. Fearon, *Tumor suppressor genes*. In: B. Vogelstein, K. W. Kinzler, editors. *The genetic basis of human cancer*. McGraw-Hill Companies; **1998**. p. 229-236; (b) J. Yokota, *Carcinogenesis*, **2000**, *21*, 497-503; (c) R. Bernards, R. A. Weinberg, *Nature*, **2002**, *418*, 823.
- [6] (a) J. L. Bos, *Cancer Res.*, **1989**, *49*, 4682-4689; (b) K. Rajalingam, R. Schreck, U. R. Rapp, S. Albert, *Biochim. Biophys. Acta.*, 2007, *in press*.
- [7] A. Bounacer, A. McGregor, J. Skinner, J. Bond, Z. Poghosyan, D. W. Thomas, *Oncogene*, **2004**, *23*, 7839 -7845.
- [8] (a) P. Crespo, J. Leon, *Cell Mol. Life Sci.*, **2000**, *57*, 1613-1636; (b) D. Bar-Sagi, J. R. Feramisco, *Cell*, **1985**, *42*, 841-848.
- [9] G. Oxford, D. Theodorescu, *Cancer Lett.*, **2003**, *189*, 117-128.
- [10] (a) A. D. Cox, C. J. Der, *Oncogene*, **2003**, *22*, 8999-9006; (b) G. H. Fisherm, S. L. Wellen, D. Klimstra, J. M. Lenczowski, J. W. Tichelaar, M J. Lizak, J. A. Whitsett, A. Koretsky, H. E. Varmus, *Genes Dev.*, **2001**, *15*, 3249-3262.
- [11] (a) M. Perucho, M. Goldfarb, K. Shimizu, C. Lama, J. Fogh, M. Wigler, *Cell*, **1981**, *27*, 467-476; (b) T. G. Krontiris, G. M. Cooper, *Proc. Natl. Acad. Sci. USA.*, **1981**, *78*, 1181-1184; (c) C. Shih, L. C. Padhy, M. Murray, R. A. Weinberg, *Nature*, **1981**, *290*, 261-264.
- [12] (a) W. H. Kirsten, L. A. Mayer, *J. Natl. Cancer Inst.*, **1969**, *43*, 735-746; (b) J. J. Harvey, *Nature*, **1964**, *204*, 1104-1105.
- [13] J. Downward, *Nat. Rev. Cancer*, **2003**, *3*, 11-22.
- [14] Y. Mitsuchi, J. R. Testa, *Am. J. Med. Genet.*, **2002**, *115*, 183-188.
- [15] W. M. Grady, S. D. Markowitz, *Annu. Rev. Genomics Hum. Genet.*, **2002**, *3*, 101-128.
- [16] E. M. Jaffee, R. H. Hruban, M. Canto, S. E. Kern, *Cancer Cell*, **2002**, *2*, 25-28.
- [17] (a) L. B. Eckert, G. A. Repasky, A. S. Ülkü, A. McFall, H. Zhou, C. I. Sartor, C. J. Der, *Cancer Res.*, **2004**, *64*, 4585-4592; (b) G. J. Clark, C. J. Der, *Breast Cancer Res. Treat.*, **1995**, *35*, 133-144; (c) J. Manelsohn, J. Baselga, *Oncogene*, **2000**, *19*, 6550-6565.

-
- [18] (a) I. R. Vetter, A. Wittinghofer, *Science*, **2001**, *294*, 1299-1304; (b) G. W. Reuther, C. J. Der, *Curr. Opin. Cell Biol.*, **2000**, *12*, 157-165; (c) Y. Takai, T. Sasaki, T. Matozaki, *Physiol. Rev.*, **2001**, *81*, 153-208.
- [19] J. Colicelli, *Sci. STKE*, **2004**, *250(re13)*, 1-31.
- [20] (a) W. Kolch, *Biochem. J.* **2000**, *351*, 289-305; (b) S. Marcus, A. Polverino, E. Chang, D. Robbins, M. H. Cobb, *Proc. Natl. Acad. Sci. USA.*, **1995**, *92*, 6180-6184.
- [21] J. Yan, S. Roy, A. Apolloni, A. Lane, J. F. Hancock, *J. Biol. Chem.*, **1998**, *273*, 24052-24056.
- [22] A. Rebollo, C. Martínez-A, *Blood*, **1999**, *9*, 2971-2980.
- [23] M. Malumbres, M. Barbacid, *Nat. Rev. Cancer*, **2003**, *3*, 7-12.
- [24] I. A. Prior, J. F. Hancock. *J. Cell Sci.*, **2001**, *114*, 1603-1608.
- [25] (a) J. F. Hancock, A. I. Magee, J. E. Childs, C. J. Marshall, *Cell*, **1989**, *57*, 1167-1177; (b) B. M. Willumsen, A. Christensen, N. L. Hubbert, A. G. Papageorge, *Nature*, **1984**, *310*, 583-586.
- [26] O. Rocks, A. Peyker, P. I. Bastiaens, *Curr. Opin. Cell Biol.*, **2006**, *18*, 351-357.
- [27] W. K. Schmidt, A. Tam, K. F. Kamada, S. Michaelis, *Proc. Nat. Acad. Sci. USA.*, **1998**, *95*, 11175-11180; (b) A. Tam, F. J. Nouvet, K. F. Kamada, H. Slunt, S. S. Sisodia, S. Michaelis, *J. Cell Biol.*, **1998**, *142*, 635-649.
- [28] (a) C. A. Hrycyna, S. K. Sapperstein, S. Clarke, S. Michaelis, *EMBO J.*, **1991**, *10*, 1699-1709; (b) Q. Dai, E. Choy, V. Chiu, J. Romano, S. R. Slivka, S. A. Seitz, S. Michaelis, M. R. Philips, *J. Biol. Chem.*, **1998**, *273*, 15030-15034.
- [29] E. Choy, V. K. Chiu, J. Silletti, M. Feoktistov, T. Morimoto, D. Michaelson, I. E. Ivanov, M. R. Philips, *Cell*, **1999**, *98*, 69-80.
- [30] (a) J. F. Hancock, H. Paterson, C. J. Marshall, *Cell*, **1990**, *63*, 133-139; (b) J. F. Hancock, K. Cadwallader, H. Paterson, C. J. Marshall, *EMBO J.*, **1991**, *10*, 4033-4039.
- [31] A. Apolloni, I. A. Prior, M. Lindsay, R. G. Parton, J. F Hancock, *Mol. Cell. Biol.*, **2000**, *20*, 2475-2487.
- [32] (a) V. L. Boyartchuk, M. N. Ashby, J. Rine, *Science*, **1997**, *275*, 1796-1800; (b) M. O. Bergo, P. Ambroziak, C. Gregory, A. George, J. C. Otto, E. Kim, H. Nagase, P. J. Casey, A. Balmain, S. G. Young, *Mol. Cell. Biol.*, **2002**, *22*, 171-181.
- [33] J. F. Hancock., *Nat. Rev. Mol. Cell Biol.*, **2003**, *4*, 373-384.
- [34] L. E. P. Dietrich, C. Ungermann, *EMBO J.*, **2004**, *5*, 1053-1057.
- [35] K. Simons, E. Ikonen, *Nature*, **1997**, *387*, 569-572.
- [36] (a) J. S. Goodwin, K. R. Drake, C. Rogers, L. Wright, J. Lippincott-Schwartz, M. R. Philips, A. K. Kenworthy, *J. Cell Biol.*, **2005**, *170*, 261-272; (b) O. A. Rocks, Peyker, M. Kahms, P. J. Verveer, C. Koerner, M. Lumbierres, J. Kuhlmann, H. Waldmann, A. Wittinghofer, P. I. H. Bastiaens, *Science*, **2005**, *307*, 1746-1752.

-
- [37] (a) M. Mehring, *Principles of High Resolution NMR in Solids, 2nd edition*. **1983**, Springer, Berlin;
(b) K. Schmidt-Rohr, H.W. Spiess, *Multidimensional Solid-State NMR and Polymers*. **1994**, Academic Press, London.
- [38] O. Zerbe, *BioNMR in Drug Research*, **2002**, Wiley-VCH Verlag, Weinheim.
- [39] H. W. Spiess, *NMR: Basic Principles and Progress*, **1978**, 15, 55.
- [40] (a) E. F. Pai, W. Kabsch, U. Krengel, K. C. Holmes, J. John, A. Wittinghofer, *Nature*, **1989**, 341, 209-214; (b) M. V. Milburn, L. Tong, A. M. deVos, A. Brunger, Z. Yamaizumi, S. Nishimura, S. H. Kim, *Science*, **1990**, 247, 939-945; (c) A. T. Brunger, M. V. Milburn, L. Tong, A. M. deVos, J. Jancarik, Z. Yamaizumi, S. Nishimura, E. Ohtsuka, S. H. Kim, *Proc. Natl. Acad. Sci. USA.*, **1990**, 87, 4849-4853. (d) U. Krengel, L. Schlichting, A. Scherer, R. Schumann, M. Frech, J. John, W. Kabsch, E. F. Pai, A. Wittinghofer, *Cell*, **1990**, 62, 539-548; (d) P. J. Kraulis, P. J. Dommelle, S. L. Campbell-Burk, T. V. Akenn, E. D. Laue, *Biochemistry*, **1994**, 33, 3515-3531.
- [41] (a) R. Thapar, J. G. Williams, S. L. Campbell, *J. Mol. Biol.*, **2004**, 343, 1391-1408; (b) M. Spoerner, C. Herrmann, I. R. Vetter, H. R. Kalbitzer, A. Wittinghofer, *Proc. Natl. Acad. Sci. USA.*, **2001**, 98, 4944-4949.
- [42] Part of the dynamical studies results has been published, see: G. Reuther, K.-T. Tan, A. Vogel, C. Nowak, K. Arnold, J. Kuhlmann, H. Waldmann, D. Huster, *J. Am Chem. Soc.*, **2006**, 128, 13840-13846.
- [43] (a) P. McGeady, S. Kuroda, K. Shimizu, Y. Takai, M. H. Gelb, *J. Biol. Chem.*, **1995**, 270, 26347-26351; (b) T. C. Turek, I. Gaon, D. Gamache, M. D. Distefano, *Bioorg. Med. Chem. Lett.*, **1997**, 7, 2125-2130; (c) I. Gaon, T. C. Turek, V. A. Weller, R. L. Edelstein, S. K. Singh, M. D. Distefano, *J. Org. Chem.*, **1996**, 61, 7738-7745; (d) R. L. Edelstein, M. S. Distefano, *Biochem. Biophys. Res. Commun.*, **1997**, 235, 377-382.
- [44] B. Bader, K. Kuhn, D. J. Owen, H. Waldmann, A. Wittinghofer, J. Kuhlmann, *Nature*, **2000**, 403, 223 -226.
- [45] G. T. Hermanson, *Bioconjugate Techniques*, **1996**, Academic Press, London.
- [46] (a) T. Wieland, J. Lewalter, C. Birr, *Liebigs Ann. Chem.*, **1970**, 740, 31-47; (b) A. N. Semenov, K. Y. Gordeev, *Int. J. Pept. Protein Res.*, **1995**, 45, 303-304; (c) C. R. Millington, R. Quarrell, G. Lowe, *Tetrahedron Lett.*, **1998**, 39, 7201-7204.
- [47] (a) I. C. P. Smith, I. H. Ekiel, in *Phosphorous-31 NMR, Principles and Applications*, D. G. Gorenstein, Ed., Academic Press, New York, **1984**, pp 447-475; (b) R. G. Griffin, *Methods Enzymol.*, **1981**, 72, 108-174; J. Seelig, *Biochim. Biophys. Acta.*, **1978**, 515, 105-140; (c) H. Saitô, I. Ando, A. Naito, in *Solid State NMR spectroscopy for Biopolymers: Principles and Applications*, Springer, The Netherlands, **2006**, pp 59-88.
- [48] P. R. Cullis, B. de Kruijff, *Biochim. Biophys. Acta.*, **1979**, 559, 399-420.
- [49] (a) D. S. Wishart, B. D. Sykes, *Methods Enzymol.*, **1994**, 239, 363-392; (b) S. Spera, A. Bax, *J. Am. Chem. Soc.* **1991**, 113, 5490-5492; (c) H. Saitô, *Magn. Reson. Chem.*, **1986**, 24, 835-852.

-
- [50] D. Huster, *Prog. Nucl. Magn. Reson. Spectrosc.*, **2005**, *46*, 79-107.
- [51] (a) A. Pines, M. G. Gibby, J. S. Waugh, *J. Chem. Phys.*, **1973**, *59*, 569-590; (b) M. J. Duer, in *Introduction to Solid-State NMR Spectroscopy*. Blackwell Publishing, Oxford, **2004**, pp 96-110.
- [52] The reference chemical shift values for the respective backbone geometries were taken from the BioMagResBank. <http://www.bmrb.wisc.edu/>.
- [53] (a) C. W. Lee, R. G. Griffin, *Biophys. J.*, **1989**, *55*, 355-358; (b) N. M. Szeverenyi, M. J. Sullivan, G. E. Maciel, *J. Magn. Reson.*, **1982**, *47*, 462-475.
- [54] (a) D. Suter, R. R. Ernst, *Phys. Rev. B*, **1985**, *32*, 5608-5627; (b) D. Huster, X. Yao, M. Hong, *J. Am. Chem. Soc.*, **1998**, *124*, 874-883.
- [55] (a) <http://spin.niddk.nih.gov/NMRPipe/talos/>; (b) G. Cornilescu, F. Delaglio, A. Bax, *J. Biomol. NMR*, **1999**, *13*, 289-302.
- [56] (a) S. Luca, J. F. White, A. K. Sohal, D. V. Filippov, J. H. van Boom, R. Grisshammer, M. Baldus, *Proc. Natl. Acad. Sci. USA.*, **2003**, *100*, 10706-10711; (b) A. T. Petkova, Y. Ishii, J. J. Balbach, O. N. Antzutkin, R. D. Leapman, F. Delaglio, R. Tycko, *Proc. Natl. Acad. Sci. USA.*, **2002**, *99*, 16742-16747; (c) S. Sharpe, W.-M. Yau, R. Tycko, *Biochemistry*, **2006**, *45*, 918-933.
- [57] (a) M. M. Javadpour, M. Eilers, M. Groesbeek, S. O. Smith, *Biophys. J.*, **1999**, *77*, 1609-1618; (b) B. K. Ho, R. Brasseur, *BMC Struct. Biol.*, **2005**, *5*, 14.
- [58] (a) M. Hong, J. D. Gross, W. HU, R. G. Griffin, *J. Magn. Reson.*, **1998**, *135*, 169-177; (b) D. P. Weliky, R. Tycko, *J. Am. Chem. Soc.*, **1996**, *118*, 8487-8488; (c) J. Heller, D. D. Laws, M. Tomaselli, D. S. King, D. E. Wemmer, A. Pines, R. H. Havlin, E. Oldfield, *J. Am. Chem. Soc.*, **1997**, *119*, 7827-7831.
- [59] (a) D. Huster, A. Vogel, C. Katzka, H. A. Scheidt, H. Binder, S. Dante, T. Gutberlet, O. Zschörnig, H. Waldmann, K. Arnold, *J. Am. Chem. Soc.*, **2003**, *125*, 4070-4079; (b) D. Huster, K. Kuhn, D. Kadereit, H. Waldmann, K. Arnold, *Angew. Chem. Int. Ed.*, **2001**, *40*, 1056-1058.
- [60] W. C. Wimley, S. H. White, *Nat. Struct. Biol.*, **1996**, *3*, 842-848.
- [61] R. Thapar, J. G. Williams, S. L. Campbell, *J. Mol. Biol.*, **2004**, *343*, 1391-1408.
- [62] M. J. Hope, M. B. Bally, G. Webb, P. R. Cullis, *Biochim. Biophys. Acta.*, **1985**, *812*, 55-65.
- [63] E. Sternin, M. Bloom, L. MacKay, *J. Magn. Reson.*, **1983**, *55*, 274-282.
- [64] M. Lafleur, B. Fine, E. Sternin, P. R. Cullis, M. Bloom, *Biophys. J.*, **1989**, *56*, 1037-1041.
- [65] (a) A. Vogel, C. P. Katzka, H. Waldmann, K. Arnold, M. F. Brown, D. Huster, *J. Am. Chem. Soc.*, **2005**, *127*, 12263-12272; (b) H. I. Petrache, S. W. Dodd, M. F. Brown, *Biophys. J.*, **2000**, *79*, 3172-3192.
- [66] B. W. Koenig, H. H. Strey, K. Gawrisch, *Biophys. J.*, **1997**, *73*, 1954-1966.
- [67] J. Huang, G. W. Feigenson, *Biophys. J.*, **1999**, *76*, 2142-2157.
- [68] M. F. Brown, A. A. Ribeiro, G. D. Williams, *Proc. Natl. Acad. Sci. USA.*, **1983**, *80*, 4325-4329.
- [69] M. F. Brown, R. L. Thurmond, S. W. Dodd, D. Otten, K. Beyer, *J. Am. Chem. Soc.*, **2002**, *124*, 8471-8484.

-
- [70] M. Hong, J. D. Gross, R. G. Griffin, *J. Phys. Chem.*, **1997**, *101*, 5869-5874.
- [71] G. M. Clore, A. Szabo, A. Bax, L. E. Kay, P. C. Driscoll, A. M. Gronenborn, *J. Am. Chem. Soc.*, **1990**, *112*, 4989-4991.
- [72] A. G. III. Palmer, J. Williams, A. McDermott, *J. Phys. Chem.*, **1996**, *100*, 13293-13310.
- [73] S. Shahinian, J. R. Silvius, *Biochemistry*, **1995**, *34*, 3813-3822.
- [74] T. J. Zahn, M. Eilers, Z. Guo, M. B. Ksebati, M. Simon, J. D. Scholten, S. O. Smith, R. A. Gibbs, *J. Am. Chem. Soc.*, **2000**, *122*, 7153-7164.
- [75] A. C. Rowat, J. H. Davis, *Biochim. Biophys. Acta.*, **2004**, *1661*, 178-187.
- [76] (a) D. Huster, L. Xiao, M. Hong, *Biochemistry*, **2001**, *40*, 7662-7674; (b) L. A. Colnago, K. G. Valentine, S. J. Opella, *Biochemistry*, **1987**, *26*, 847-854; (c) H. Saito, T. Tsuchida, K. Ogawa, T. Arakawa, S. Yamaguchi, S. Tuzi, *Biochim. Biophys. Acta.*, **2002**, *1565*, 97-106.
- [77] G. Reuther, K.-T. Tan, J. Kohler, C. Nowak, A. Pampel, K. Arnold, J. Kuhlmann, H. Waldmann, D. Huster, *Angew. Chem., Int. Ed.*, **2006**, *45*, 5387-5390.
- [78] S. H. White, A. S. Ladokhin, S. Jayasinghe, K. Hristova, *J. Biol. Chem.*, **2001**, *276*, 32395-32398.
- [79] R. Thapar, J. G. Williams, S. L. Campbell, *J. Mol. Biol.*, **2004**, *343*, 1391-1408.

Chapter B

Synthesis and Biochemical Studies of Rab GGTase Inhibitors

1 Introduction

Over the past centuries, science and technology have improved the life quality of human beings tremendously. From transportation, entertainment, medicine and to every daily activity, science and technology have shaped the fate of human beings from the beginning of life till the end of the day. The life span of human beings has been prolonged because of the advancement of medicine and development of new drugs. However, there are still many diseases such as HIV and Alzheimer's disease that can not be cured. To tackle these diseases, chemical biology has come into play from the end of the last century.

Chemical biology is a rapidly developing discipline, which attempts to answer biological questions by directly probing living systems at the chemical level. In contrast to research using biochemistry, genetics, or molecular biology, where mutagenesis can provide a modified version of the organism or cell of interest for further studies, chemical biological studies probe systems *in vitro* and *in vivo* with chemical entities that have been designed for a specific purpose or identified on the basis of biochemical or cell-based screening. Because of the nearly limitless number of chemicals available, this approach has become increasingly popular and useful in basic research, especially so for drug discovery and design.

A century of genetics-based interrogations of life has shown that perturbing life processes and observing the consequences can provide illuminating insights. Based on that, advances in diversity-oriented organic synthesis coupled with rapidly developing methodology and techniques of biological science should enable the chemical biology approach to be practical to explore all facets of biology with small-molecule modulators. In general, the chemical biology approach by using small molecules has become a promising tool to cure lethal diseases of human beings in recent years.

2 Background

2.1 Vesicular Transport in Eukaryotic Cells

One of the significant features distinguishing eukaryotic and prokaryotic cells is that the eukaryotic cells contain phospholipid membrane enclosed organelles such as mitochondria, endoplasmic reticulum (ER) and Golgi apparatus. Each of these organelles functions distinctively and occupies an irreplaceable position in eukaryotic cells. For example, the Golgi apparatus is responsible for processing and sorting of proteins received from the ER before being transported to their eventual destinations, and ER's function is to facilitate protein folding and transport of synthesized proteins. The defect of any one of these organelles will cause the cell to function ineffectively or even cell death.¹

For a cell to execute its functions properly, each of its numerous substances must be localized at the correct cellular compartments and plasma membrane. Unlike prokaryotic cells which do not contain membrane-bound compartments, the existence of a membrane surrounding the eukaryotic organelles has restricted the free movement of large molecules such as proteins, lipids, hormone and other essential substances from one compartment to another. With the exception of water, oxygen and some other small and non-polar molecules which are able to diffuse across phospholipids membranes, most of the larger polar molecules like proteins, ions and glucose pass through the membrane via different pathways. Molecules such as ions and glucose can be transported across membrane by the assistance of ion channel proteins and glucose symporter.² For the super-sized molecules like proteins, passing through the membrane by channel proteins is not possible. The mechanism by which proteins and other large molecules are transported to different compartments is called vesicular transport.

Vesicular transport³ plays a central role in the interaction of cells with their environment and the coordination of each organelle. Besides being the route by which proteins and peptides are released into the surrounding milieu, it is also the process by which

receptors, ion channels, ion pumps and other important receptor proteins are presented at the surface of the plasma membrane and different compartments. Therefore, the selectivity of such transport is critical in maintaining the functional organization of the cell and contact with its surroundings. Hormone receptor proteins, for example, must be delivered to the plasma membrane if the cell is to recognize hormones. As for the corrected folding of nascent proteins which require post-translational modification, these must be transported from ER to Golgi apparatus for further phosphorylation, glycosylation or lipidation. In vesicular transport, proteins are surrounded and transported within vesicles made up of at least one phospholipids bilayer, so the specificity of transport is based on the selective packaging of intended cargo into vesicles and the regulating proteins localized outside the vesicles that recognize and fuse only with the appropriate target membrane.

Protein trafficking (Figure 1) is highly regulated by various proteins at different steps. In general, this trafficking pathway can be divided into four steps: vesicle budding from a parent compartment, vesicle movement in the cytosol, vesicular tethering/docking with target membrane, and vesicle fusion to target membrane. In each step, different proteins are involved in regulating and coordinating the process. The absence or defect of anyone of the regulating proteins will have serious consequence to this process, or even render the termination of the whole transport event.

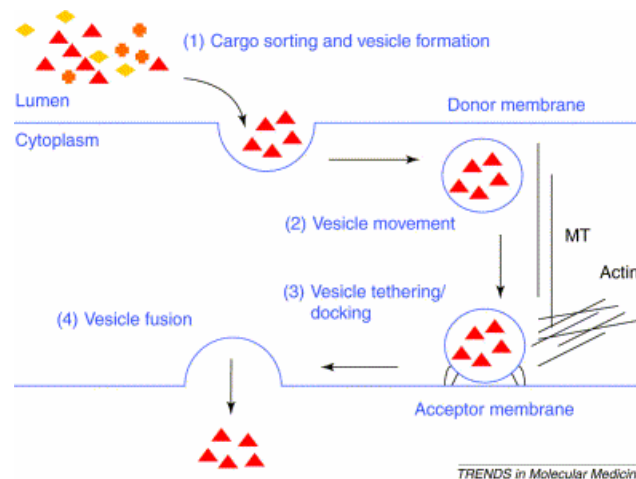


Figure 1. Schematic illustration of protein trafficking pathway.⁴

2.2 The Roles of Rab Proteins in Protein Trafficking

Of the many proteins which participate in regulating this biologically important process, Rab proteins have clearly emerged to be the proteins which occupy the critical position in protein trafficking, due to their importance and influence in all steps of trafficking.⁵ Furthermore, from the genomic perspective, Rab proteins have also appeared to be conserved throughout eukaryotic cell evolution and play a critical role in shaping the current vesicular trafficking pathways.⁶

Rab proteins belong to the largest family of the Ras superfamily of small GTPases. More than 60 Rab proteins have been described in mammalian cells, each with a specific subcellular localization, trafficking pathways, and many with specific patterns of tissue distribution (Table 1).⁷

Table 1. The human Rab GTPase family: nomenclature, localization and function.⁴

Rab	Rab localization	Possible function
Rab 1	ER-Golgi Intermediate compartment, cis-Golgi	ER-Golgi, intra-Golgi transport
Rab 2	ER-Golgi Intermediate compartment, cis-Golgi	Golgi-ER retrograde transport
Rab 3a	SV, secretory granules, PM	Regulated neurotransmitter release
Rab 5a	EE, CCV, PM, SV	PM-EE transport, EE-EE fusion
Rab 6a	ER, Golgi, TGN	Retrograde Golgi-ER, intra-Golgi traffic, Golgi-ER vesicles
Rab 27	Lysosome-like organelles: melanosomes, cytolytic granules	Lytic granule release, melanosome transport

Abbreviations: EE, early endosomes; CCV, clathrin-coated vesicles; PM, plasma membrane; TGN, trans-Golgi network; SV, synaptic vesicles

Rab proteins act predominantly as positive regulators, where their depletion leads to blocked or reduced transport *in vivo* or *in vitro*. Different kinds of Rab proteins regulate the transport of proteins from different compartments. For example, Rab 1 and Rab 2 play a role in ER to Golgi transit, whereas, Rab 3 is associated with secretory vesicles and has a role in regulated secretion of hormones and neurotransmitters.⁸ The characteristic functions of Rab proteins in the trafficking pathway have rendered Rab proteins to be essential at all levels and steps of vesicular transport.

2.2.1 Rab proteins assisted vesicle formation

The proteins that are found to be involved in vesicle formation belong to vesicle-coated protein complexes, namely, Clathrin-, COPI-, COPII-coated protein complex and their subunit proteins.⁹ However, recent *in vivo* and *in vitro* studies have shown that Rab also plays a crucial role in this process. One revealing finding on the mechanism by which Rab may be involved is that the Rab 11 effector, Rabphilin-11 together with a vesicle coat component Sec 13 of the coat complex COPII is responsible for triggering vesicle formation from ER to Golgi.¹⁰ Furthermore, Rab 11, Rabphilin-11 and Sec 13 may also function together in the formation of trans-Golgi network vesicles (Figure 2).¹¹

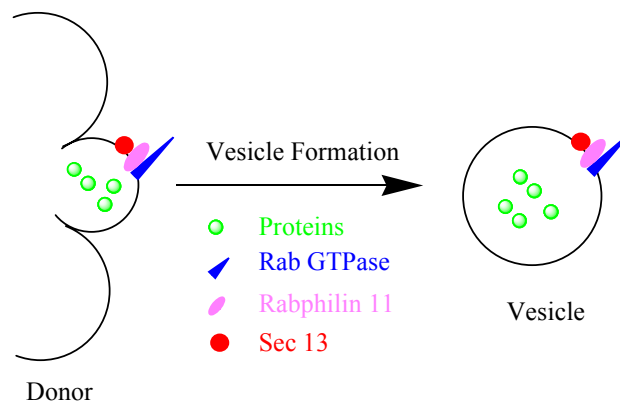


Figure 2. Rab proteins assisted vesicle formation.

2.2.2 Rab proteins mediated vesicle motility

In protein transport, both microtubules and actin cytoskeleton serve as rails for the movement of vesicles and organelles, using kinesin and myosin based motors, respectively.¹² The suggestion that Rab proteins are involved in vesicle motility along microtubules is supported by several evidences. First, the discovery of a Golgi-associated Rab protein, Rab 6, binding to a member of the kinesin family subsequently termed Rabkinesin-6 appears to play a role in cytokinesis, a process involving membrane transport events (Figure 3).¹³ Another Rab 6 effector candidate, GAPCenA, provides an additional connection between Rabs and microtubules. This putative effector is associated with the centrosome and is involved in microtubule nucleation, suggesting a possible role for Rab 6 in Golgi dynamics.¹⁴

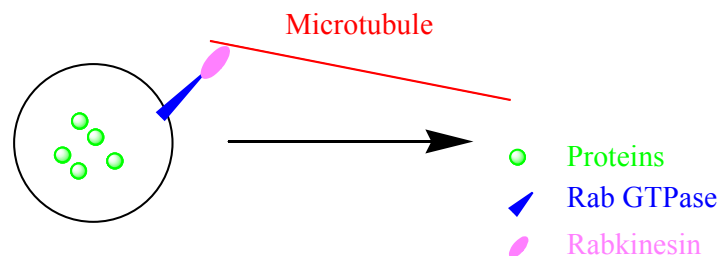


Figure 3. Rab proteins mediated vesicle motility.

2.2.3 Rab proteins regulate vesicle docking

To ensure that membrane traffic proceeds in an orderly manner, transport vesicles must be highly selective in recognizing the correct target membrane with which to fuse. This crucial recognition step and docking of vesicles to the target compartment is an established role for Rabs. A number of Rab effectors are implicated in such a function. One current proposed vesicle docking model suggests that Rab recruit proteins containing coiled-coil domains to form the sites for vesicle docking and extended rod structures to

bridge the two proximal membranes which can facilitate the membrane fusion process (Figure 4).¹⁵

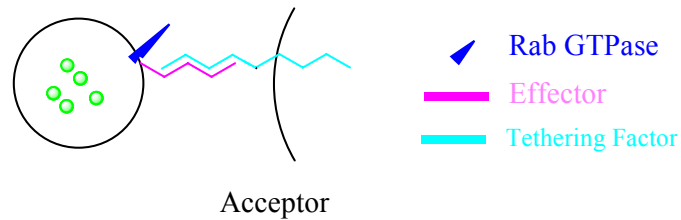


Figure 4. Vesicle docking regulated by Rabs.

One example supporting this model is the Rabaptin 5 complex, which interacts preferentially with endosome-associated Rab 5.¹⁶ Rabaptin 5 has two distinct Rab binding sites that could, in principle, dock two separate endosomes together. Rab 5 also interacts with EEA 1, an early endosome-associated protein that contains long stretches that form the coiled coil domain. EEA 1 can bring endosomes together and acts as an upstream regulator of fusion proteins.

2.2.4 Rab proteins regulate vesicle fusion

The final step of vesicular transport is assigned to a family of conserved membrane proteins termed SNAREs (soluble *N*-ethylmaleimide-sensitive-factor attachment protein receptor). Specific combinations of SNAREs that reside on vesicles (v-SNAREs) and SNAREs that associate with target membrane (t-SNAREs) form complexes that can drive membrane fusion.¹⁷ The participation of Rabs in this step was thought to be upstream to the SNARE complex formation. Recent information about the interaction of Rab effectors with other proteins pointed out that Rabs have a direct role in SNARE complex formation, and give new clues regarding their mode of interaction.¹⁸

A plausible model for Rab function in vesicle fusion, through the interaction with a Sec-1-like protein, suggests that Rabs recruits an effector, which interacts with a Sec 1-like protein (Figure 5). Sec 1 is the prototypic t-SNARE protector. This protein binds directly and tightly to the t-SNARE on the presynaptic plasma membrane, syntaxin-1A. Binding

of Sec 1 to syntaxin-1A blocks v-SNARE and t-SNARE interaction and therefore prevents the fusion of the vesicle with the target membrane. The interaction of the effector with the Sec 1 protein induces the exposure of the t-SNARE to its complementary set and allows it to form a complex with the v-SNARE, an event that results in membrane fusion.¹⁹

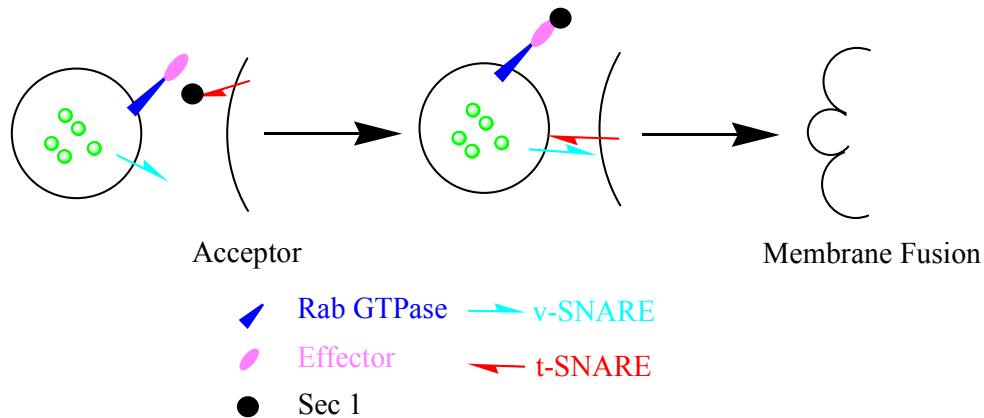


Figure 5. Rab proteins regulate vesicle fusion.

2.3.1 Upstream regulation of Rab proteins

Like their counterparts in the Ras GTPases superfamily, the cycling between the GTP- and GDP-bound forms is an essential feature of the mode of operation for Rab proteins. This is regulated by three factors: (i) a guanine nucleotide exchange factor (GEF) that stimulates the release of GDP and favoring the formation of a Rab-GTP complex, (ii) a GTPase activating protein (GAP) which catalyzes the hydrolysis of γ -phosphate from GTP to GDP, and (iii) a guanine nucleotide dissociation inhibitor (GDI) that inhibits the release of GDP.^{5, 20}

When Rab proteins are delivered to their respective compartment, they are in the inactive GDP-bound state. Once Rabs are bound to a vesicle surface, they can be activated by the replacement of GDP with GTP catalyzed by GEF. Rab bound to GTP are in the active conformation and can now interact with or recruit Rab effectors on target membranes to

facilitate various vesicular processes like vesicle movement, tethering/docking and fusion. After the Rabs have accomplished their task of aiding membrane fusion, the Rab GTPase is hydrolyzed to the GDP-bound form with the assistance of GAP. The Rabs can then be recycled back to their membrane of origin. The participation of GEF and GAP is necessary, since most GTPase have slow intrinsic rates of GTP hydrolysis and nucleotide exchange, and thus require accessory factors that stimulate these reactions. GDI is necessary for the recycling pathway. This enzyme inhibits the exchange of GDP to GTP to prolong the inactive state, and delivers the Rab to its initial membrane. GDI binding also helps to emulsify lipid-modified Rab, thus promoting the introduction of Rab into the membrane and subsequent dissociation from the membrane surface (Figure 6).²¹

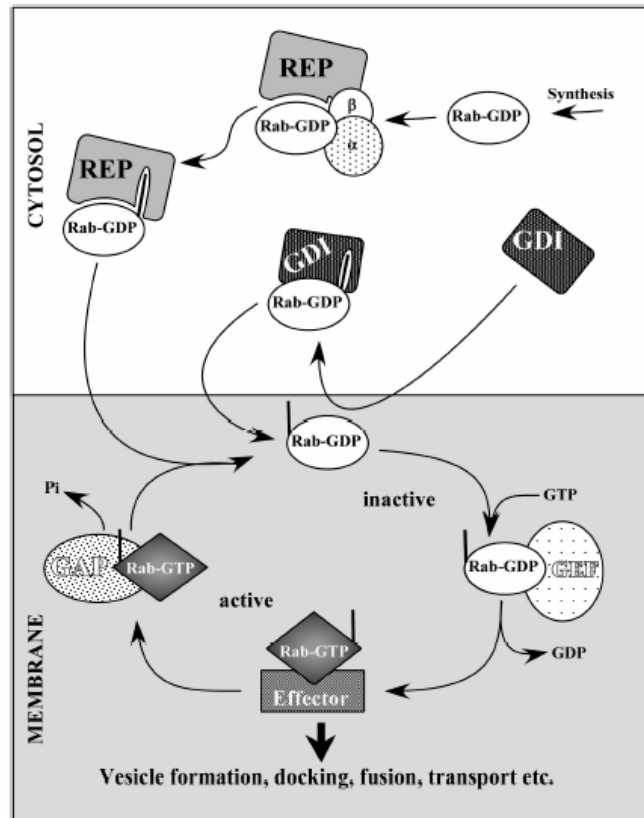


Figure 6. Rab prenylation, delivery to membranes and the GTPase cycle.²²

2.4.1 Post-translational modification of Rab proteins

The influence and the importance of Rab proteins for the vesicular trafficking pathway can only be realized if the proteins are post-translationally modified. In this modification, two 20 carbon geranylgeranyl groups (with the exception of a few members of the over 60 mammalian Rab with only one geranylgeranyl group) are attached to a cysteine at or near the carboxyl terminus of the protein via a thioether. The amino acid sequences of Rab proteins are most dissimilar near their C-terminal tails. Experiments indicate that the tail determines the intracellular location of each family member, presumably by enabling the protein to bind to complementary proteins on the surface of the appropriate organelle.²³ This transformation is essential to initiate the role of Rab and to move the proteins from the cytosol to different membrane compartments according to the type of Rab.

The post-translational modification of Rabs is carried out by Rab geranylgeranyltransferase (Rab GGTase).²⁴ In contrast to other members of the Ras family which require only the farnesyltransferase (FTase) or geranylgeranyltransferase I (GGTase I) to catalyze the transformation, the decoration of the Rab C-terminus requires not only Rab GGTase and geranylgeranyl pyrophosphate (GGPP), but also another enzyme called REP (Rab Escort Protein).^{21, 25} The need for the REP as an additional factor in posttranslational lipidation is unique to the Rab family, since other prenylating enzymes only recognize a specific C-terminal sequence motif (CAAX) of the modified proteins (mainly Ras GTPase).

2.5.1 The Rab pathway as a target for disease therapy

It is clear that due to the importance of Rab proteins in the vesicular trafficking pathway, the dysfunction of Rab proteins and its related proteins lead to serious diseases. To date, several diseases have been found to be linked to the Rab transport pathway.

One example implicated in human genetic disease is Rab 27a. Griscelli syndrome (GS) is a rare autosomal recessive disorder characterized by pigment dilution of the hair (silvery hair), owing to the accumulation of pigment in melanocytes.^{26, 27} In the absence of Rab 27a, melanosomes undertake bi-directional transport along microtubules, but are unable to bind to actin in the cell periphery, resulting in their net accumulation in the perinuclear region.

In addition to GS caused by Rab 27a, loss-of-function mutations in REP 1, one of two REP isoforms, leads to choroideremia (CHM).²⁸ CHM is an X-linked form of retinal degeneration of slow onset and progression, with affected males suffering blindness by middle age. Pathology results from degeneration of retinal pigment epithelium (RPE) and the two adjacent cell layers, the choroid and the retinal photoreceptor cells. CHM cells retain the ability of processing Rabs because of the presence of REP 2, which could explain the limited nature of the CHM phenotype. However, REP 2 compensation is not absolute as CHM lymphoblast cell lines exhibit an excess of unprenylated Rab 27a when compared with the wild type. Loss of REP 1 in CHM does not result in complete loss of Rab 27a function in all tissues.²⁹

The phenotype of the naturally-occurring mouse mutant, *gunmetal* (*gm*), is caused by a mutation in the *Rggta* (Rab GGTase α -subunit) gene, and is considered a model for Hermansky–Pudlak syndrome (HPS). HPS is a rare autosomal recessive, genetically heterogeneous disorder characterized by partial albinism, tendency for bleeding, and lysosomal accumulation of ceroid lipofuscin. This phenotype reflects defects in lysosome and lysosome-like organelles such as melanosomes and platelet-dense granules. *Gm* mice contain a splice-site mutation in the *Rggta* gene that results in a lowering of Rab GGTase activity to approximately 20% of the wild type.³⁰ It is likely that the *gm* phenotype results from partial defects in prenylation and function of multiple Rabs, as in CHM.

2.6.1 Rab GGTase as an apoptotic target

More recently, studies have shown that inhibition of Rab GGTase induces the onset of p53-independent proapoptotic activity and validated for the first time that this enzyme is a promising therapeutically relevant target for cancer therapy.³¹

Using a chemical genetic approach, some previously validated farnesyltransferase inhibitors (FTIs) have been identified to trigger p53-independent apoptosis in *C. elegans*, which was mimicked by knockdown of endosomal trafficking Rab proteins, the HOPS complex and notably the enzyme Rab GGTase.³² These FTIs were found to inhibit mammalian Rab GGTase with potencies that correlated with their proapoptotic activity. Knockdown of Rab GGTase by siRNA induced apoptosis in mammalian cancer cell lines, and both Rab GGTase α and β subunits were overexpressed in several tumour tissues. These results indicated Rab GGTase, and by extension endosomal vesicular trafficking pathways, as a therapeutically relevant target for modulation of apoptosis.

The findings of this work have two implications for identifying novel targets for cancer therapy. The first major implication for cancer therapy is the identification of a novel p53-independent pathway for inducing apoptosis in cancer cells. Strong evidence has been provided that inhibition of Rab GGTase, which results in blocking the posttranslational modification of Rab proteins, leads to programmed cell death, suggesting that interfering with endosomal vesicular trafficking pathways is a novel approach to cancer chemotherapy. Although the Rab GTPases could be considered as targets for developing novel proapoptotic anticancer drugs, Rab GGTase is clearly a better target for structure-based rational drug design, since its structure and biochemistry have been studied.³³ Furthermore, because of active site similarities with FTase and GGTase I,³⁴ one can build on the extensive experience with the design of FTase and GGTase I inhibitor to design selective Rab GGTase inhibitors.³⁵

The other major implication of the findings is that certain FTIs can potently inhibit Rab GGTase, suggesting that these compounds have targets other than FTase that contribute

to their antitumor activity, particularly their proapoptotic activity. This is important since it demonstrates for the first time that, though FTIs were designed and identified to inhibit selectively FTase, they can recognize other targets; in this case, a related prenyltransferase family member, Rab GGTase. Furthermore, at present, it is not known why some tumor cells are sensitive, whereas others are not. The discovery that certain FTIs can potently inhibit Rab GGTase opens a new avenue to address this important question. It would, therefore, be very important to determine whether there is a correlation between the levels of expression of Rab GGTase α and β subunits and/or inhibition of Rab GGTase and clinical activities/toxicities seen in clinical trials.

2.7.1 Regulation of Rab GGTase activity to study endosomal vesicular trafficking and cancer

One of many possible ways to study the functions and mechanisms of vesicular transport diseases is to reduce or knockdown the activity of Rabs and its related proteins. By inhibiting Rabs activity, the outcome on the phenotype and transport pathways in the corresponding cell can be observed easily. This knockdown approach can be done in two ways either by chemical biology or genetic methods.³⁶ The chemical biology approach normally involves the use of small molecules to inhibit a particular function or activity of a protein, and thus the concomitant consequences of the inhibition can be observed. The genetic approach mainly involves the use of gene mutation to produce a mutated protein or knockout the proteins completely from the cell.

There are several advantages in using the chemical biology approach to study the function of Rab in trafficking pathways over the classical genetic means. The effect of small molecules towards the protein functions is reversible, as the effect can be removed metabolically or by washing. In addition temporal control of the experiment is possible as the small molecules can be added at any time during the experiment. Furthermore, the effect of small molecules against the target proteins is always very fast.

By employing the chemical biology approach, a variety of upstream regulating proteins can be used to study the mechanism of vesicular trafficking pathways and disease. However, a potential target for Rabs regulations must fulfill several criteria. First, the underlying proteins must be specific, interacting only with Rab GTPase. Second, by inhibiting the corresponding proteins, the functions of other proteins should not be affected. Third, the protein involved should preferentially function in a catalytic manner towards Rabs. Among the many upstream regulators of Rabs, such as Rab GGTase, REP, GDI, GAP and GEF, Rab GGTase appears to be the best candidate for this chemical biology study.

Inhibiting the post-translational modification activity of Rab GGTase will only affect Rab. As mentioned before, inhibiting the activity of Rab GGTase will hamper the lipidation of the C-terminus of Rabs which means that the Rab proteins will not be able to associate with vesicle membrane. GAP and GEF are not suitable in the studies due to their general interaction with other members of Ras GTPase super family. Inhibiting the GAP and GEF can cause general knockdown of activity of many proteins and renders many proteins within the Ras family to be inactive.

The usage of small molecules to inhibit Rab GGTase should give some insight into Rabs localization in various membrane compartments and the biological response of to non-lipidated Rab in protein trafficking. Furthermore, the development of inhibitors against Rab GGTase allows the study of some diseases known to be related to the protein, such as Hermansky–Pudlak syndrome, Paget’s disease and cancer.

3 Aim of the Dissertation

While now, there are only very few publications reporting the chemical biology approach, where small molecules altering the activities of Rab GGTase are used to study the functions and effects of Rabs in protein trafficking.³⁷ Compared to various effective and specific inhibitors discovered for FTase and GGTase I, the identification of potent inhibitors for Rab GGTase has lagged behind and proceeded very slowly. This is despite the relative importance of Rab GGTase, which is linked with some skeletal diseases, such as excessive osteoclast-mediated bone resorption which can cause tumor-induced osteolysis and post-menopausal osteoporosis. Furthermore, recent studies have shown that inhibition of Rab GGTase induces the onset of p53-independent proapoptotic activity and validated for the first time that this enzyme is a promising therapeutically relevant target for cancer therapy.

In order to study how the inhibition of Rab GGTase influence the activity of Rab proteins in detail and its relationship with diseases, chemical biology means will be used to study the influence of different inhibitors towards Rab GGTase and finally to Rabs. So far, only two compounds that affect Rab GGTase activity have previously been described, and neither shows a high degree of potency or specificity for Rab GGTase.³⁸

The aim of this thesis is to develop a compound library, which contains potential inhibiting effects against Rab GGTase over FTase and GGTase I. Recent findings³¹ have raised the concerns over the high-potency dual inhibition of Rab GGTase and FTase. The findings showed that dual inhibition of FTase and Rab GGTase by multiple compounds with diverse structures, indicating that it is not unusual for a compound to interact with both proteins. The common but not universal potential crossreactivity of antiproliferative and proapoptotic effect of some FTIs with Rab GGTase has prompted us to re-assess the previously validated FTase inhibitor, Peptidocinnamin E (Figure 7), as a lead structure for this thesis.³⁹

Pepticcinnamin E is a natural occurring bisubstrate inhibitor of FTase. It has been shown to act as FTase inhibitor with $IC_{50} = 42 \mu\text{M}$. It consists of three amino acids as central core, an ester functionalized C-terminus and a α - β unsaturated phenyl capped N-terminus.⁴⁰

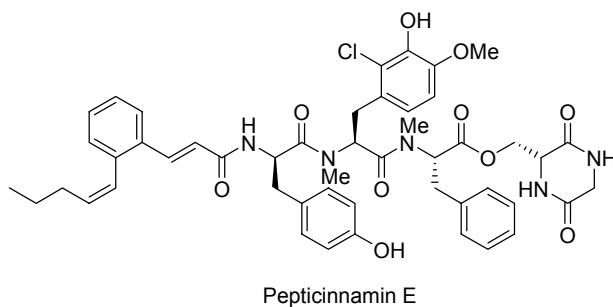


Figure 7. Structure of Pepticcinnamin E.

In this project, derivatives of Pepticcinnamin E should be prepared through solid phase peptide synthesis strategy (SPPS). The synthesized peptide-based inhibitors should be screened against Rab GGTase using a continuous fluorometric assay. Kinetic studies of a selected potent inhibitor should be probed to determine the mode of inhibition, such as competitive inhibition or non-competitive inhibition. In addition, a selected set of inhibitors should be subjected to *in vivo* study and selectivity screening against FTase and GGTase I.

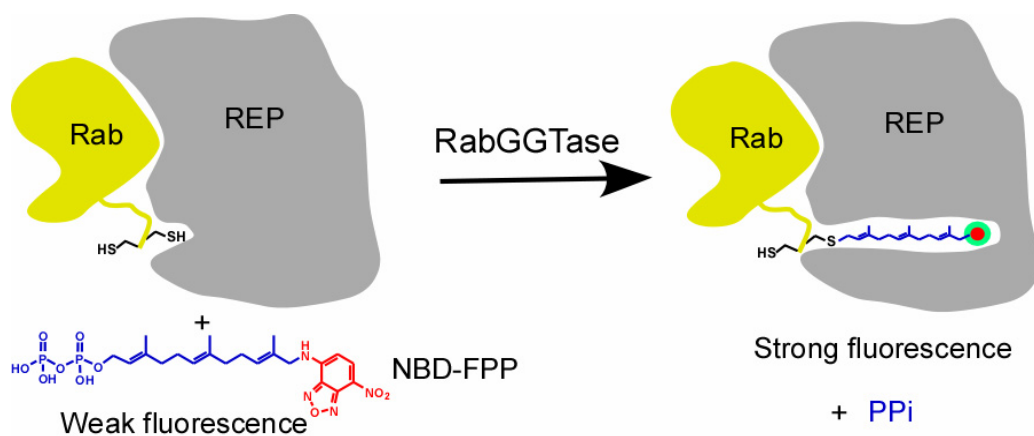
4 Results and Discussion

4.1.1 Fluorescence assay of Rab GGTase

Enzymatic studies and the search for potent, specific inhibitors of Rab prenylation led us to consider alternatives to the existing radioactivity-based and HPLC assays for Rab GGTase activity, which are discontinuous, laborious, and poorly amenable to miniaturization and parallelization.⁴¹ Continuous fluorescence assays are much better suited for high-throughput screening and characterization of potential inhibitors. Efficient continuous fluorescence assays for FTase and GGTase I that utilize the fluorescence changes of a dansylated pentapeptide containing the CAAX motif following prenylation have been reported previously.⁴² These are presumed to take advantage of the increase in hydrophobicity of the acceptor peptide following incorporation of an isoprenoid moiety in the vicinity of an environmentally sensitive dye like dansyl. However, this concept of intramolecular fluorescence enhancement cannot be directly applied to Rab GGTase, which recognizes the Rab:REP complex instead of a short peptide. Although a modified set-up for a fluorescence assay with semisynthetic Rab 7 protein substrates that have a fluorescence label at the C terminus has been reported,⁴³ it gave a fluorescent change of less than a factor of 2. This is probably due to the fact that the hydrophobic geranylgeranyl groups are buried in REP to increase the solubility of prenylated Rab proteins. In addition, construction of fluorescent protein sensors requires labor-intensive screening for fluorophores and labeling positions.

In this project, it is very helpful that a rapid, sensitive and homogeneous assay is available to screen large amounts of inhibitors in a very short time towards the activity of Rab GGTase enzyme. Hence, a recently reported continuous fluorometric assay for Rab GGTase by Wu et. al.⁴⁴ is used in our studies to determine the inhibitors activities towards Rab GGTase. In this assay, a fluorophore is incorporated into the soluble isoprenoid donor that will undergo strong changes of fluorescence during the prenylation reaction. Towards this end, a fluorescent analogue of geranylgeranyl pyrophosphate, {3,7,11-trimethyl-12-(7-nitrobenzo[1,2,5]oxadiazol-4-ylamino)dodeca-2,6,10-trien-1}

pyrophosphate (NBD-FPP) **1**, which has been demonstrated to be a lipid donor for Rab GGTase and GGTase I, was prepared.⁴⁵ This phosphoisoprenoid was used to develop the solution-based Rab prenylation assay (Scheme 1).



Scheme 1. Schematic illustration of fluorescent prenylation sensor.

The purpose of incorporating a NBD fluorescent group at terminal carbon of farnesyl pyrophosphate is that the fluorescent intensity of NBD group in water is very low, but it has very high fluorescent intensity in hydrophobic environment. By using this property of the NBD group, the inhibition of Rab GGTase can be determined by calculating the increment of fluorescence intensity. The rate of fluorescence intensity increment will be very low, if an inhibitor gives an inhibition at low concentration. The idea of attaching a NBD fluorophore group at the farnesyl pyrophosphate rather than a native substrate geranylgeranyl pyrophosphate (GGPP) is to compensate for the length of one isoprene unit by the introduction of NBD group. The active site of Rab GGTase and hydrophobic pocket of REP will be too small for a NBD-GGPP if the underlying substrate is used.

Upon incorporation of the NBD-farnesyl group into Rab proteins, an increase in fluorescence intensity over time with excitation at 479 nm and emission at 520 nm is observed (Figure 8). Fluorescence emission spectra taken before and after the reaction show a shift of the emission maximum from 547 to 525 nm as well as a 23-fold enhancement of fluorescence intensity at 525 nm. This dramatic increase in fluorescence

is a consequence of the Rab-conjugated NBD-farnesyl group's binding into the hydrophobic pocket on REP. In this case, REP plays the dual role of both Rab chaperone and conjugated fluorescent isoprenoid trapper, enhancing its fluorescence in the process.⁴⁶

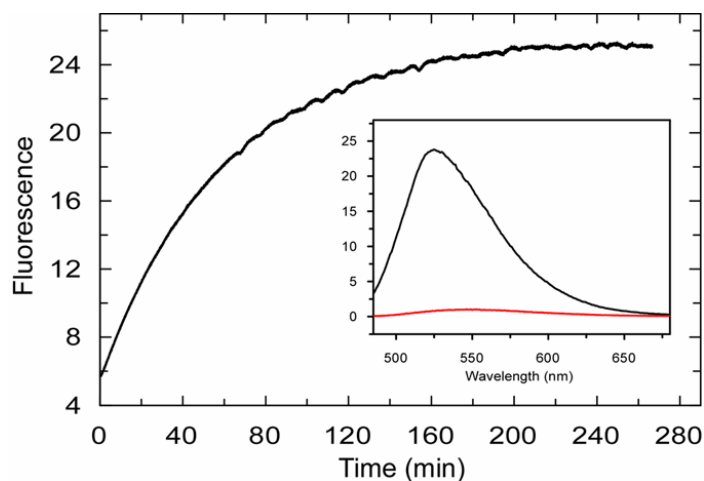


Figure 8. Time-course of the fluorescence change upon prenylation of the Rab7:REP-1 complex catalyzed by Rab GGTase in the presence of NBD-FPP.

4.1.2 Synthesis of the fluorescence substrate NBD-FPP 1

Rab 7, Rep 1 and Rab GGTase proteins were obtained by protein expression strategy and provided by group Dr. Kirill Alexandrov. Fluorescent substrate NBD-FPP **1** was prepared by means of chemical synthesis. The synthesis of **1** (Figure 9) involves several functional group manipulations and requires eight synthetic steps starting from commercially available farnesyl alcohol.

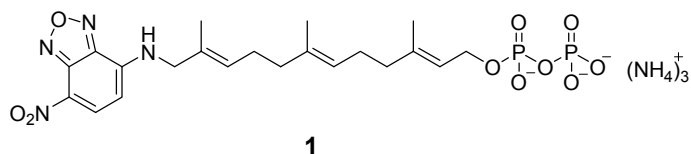
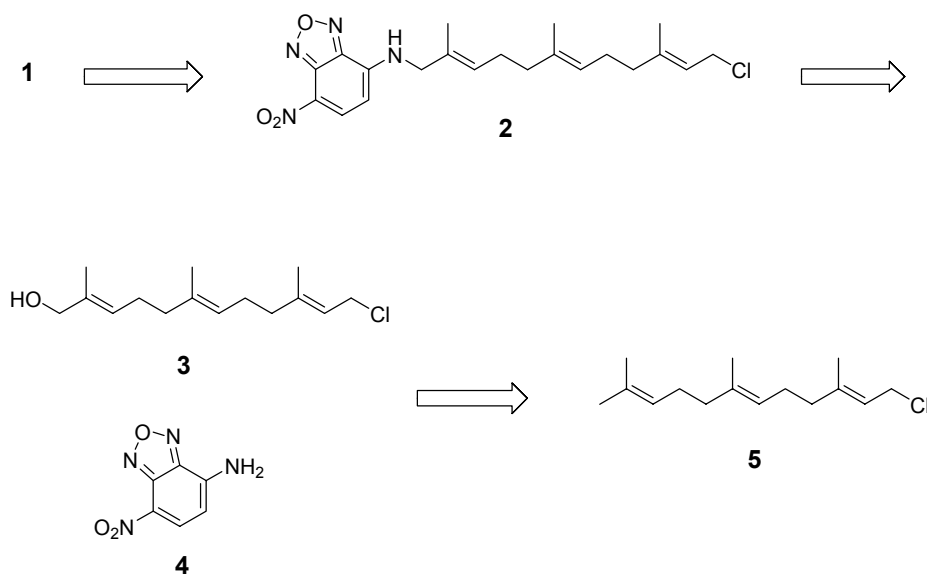


Figure 9. Structure of NBD-FPP **1**.

The plan for the synthesis of fluorescent substrate **1** was first designed to obtain the desired product in 3 steps as illustrated by retro analysis in Scheme 2.

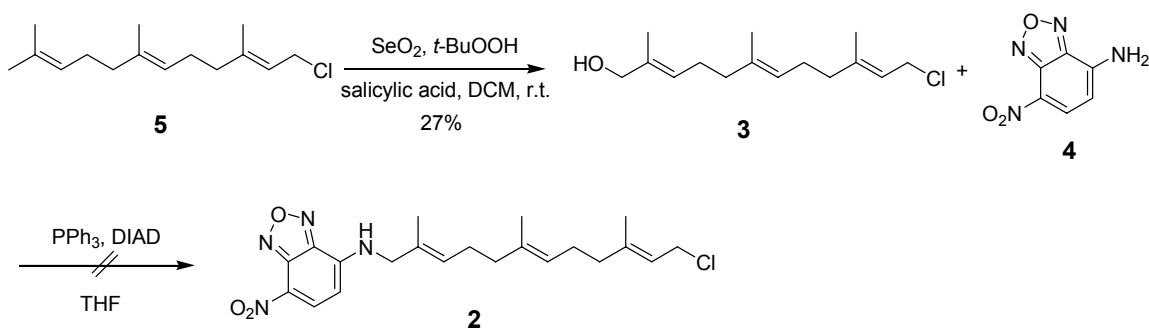


Scheme 2. Retro synthetic analysis of **1**.

The fluorescent product **1** can be envisioned to be obtained through nucleophilic substitution of **2** using a pyrophosphate salt to give **1**. The intermediate **2** can be synthesized through Mitsunobu reaction by coupling of **3** and **4**. The starting material for this synthetic route can be derived from commercially available compound **5**. The main advantage of this synthetic route is its short and succinct synthetic steps. However, allylic oxidation of **5** and subsequent Mitsunobu reaction might cause some side reactions or even destroy the intermediates, as the allylic chloride is a reactive compound.

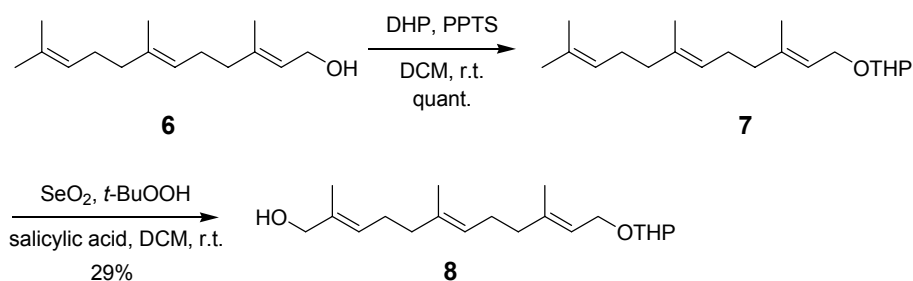
Allylic oxidation of **5** was performed using SeO_2 /t-BuOOH/salicylic acid in DCM to furnish **3** in 27% yield. Following oxidation of **5**, **3** was subjected to Mitsunobu reaction employing DIAD and PPh_3 reagents to introduce fluorescence substrate **4**, which was prepared by reacting NBD-Cl with ammonia, to replace the alcohol. Unfortunately, no desired product **2** was obtained in this reaction. In addition, no starting material **3** was recovered from the reaction as observed by the TLC. Several attempts to vary the reaction conditions by changing the addition sequence were futile. The failure to obtain **2**

might be due to the formation of undesired ylide side product which is a very common reaction between reactive allylic chloride and PPh_3 (Scheme 3).⁴⁷ Compound **3** can react with PPh_3 and DIAD at the same time with its two functional groups, OH and Cl. In this case, the stoichiometric PPh_3 was consumed by forming a side product ylide with allylic chloride moiety and thus renders the Mitsunobu reaction impossible to proceed with the allylic alcohol functional group.



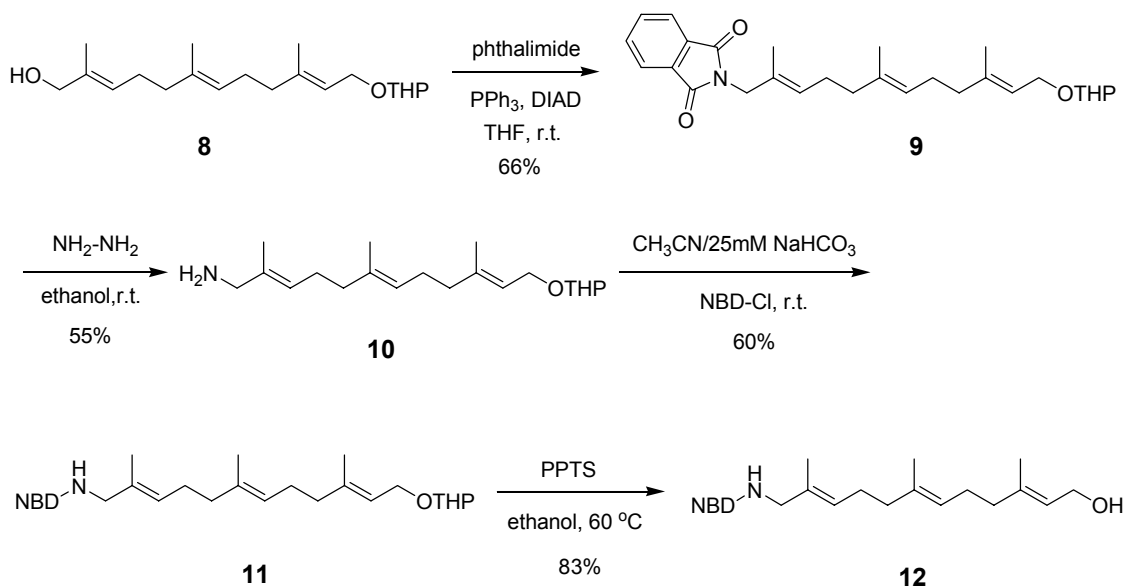
Scheme 3. Attempted synthesis of compound **2**.

After disappointing efforts to synthesize **1** in a shorter route, a previously reported synthetic protocol was adapted to prepare the fluorescent target **1**.⁴⁸ Before functional group manipulation at the terminal carbon of farnesyl alcohol **6**, compound **6** was protected with THP in order to avoid any side reaction in the next few steps of synthesis. Protection of **6** with THP and catalytic amount of PPTS gave compound **7** in quantitative yield without the need for the further purification. Functionalization at the terminal carbon of **7** was carried out using the allylic oxidation reaction employing SeO_2 / t -BuOOH/salicylic acid to give **8** in 29% yield. This step must be carefully monitored by TLC, as prolonged reaction time can increase the formation of side products from over oxidation of starting material to obtain more than one allylic alcohol at other allylic positions. The low yield of this step is generally attributed to this reason (Scheme 4).



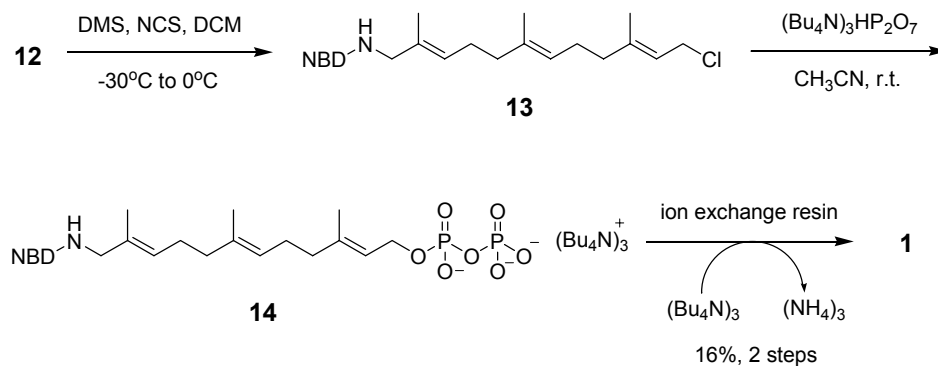
Scheme 4. Synthesis of allylic alcohol **8**.

Compound **8** was converted to **9** by employing Mitsunobu reaction using PPh_3 , phthalimide, and DIAD as reagents to give product **9** in 66% yield. **9** was then treated with hydrazine in ethanol overnight at room temperature to furnish **10** in 55% yield. The resultant white suspension formed when hydrazine reacts with the phthalimide group was easily separated by filtration. Incorporation of the NBD group on allylic amine **10** was achieved using 25mM NaHCO_3 and NBD chloride in CH_3CN at room temperature to give **11** in 60% yield. Deprotection of the THP group on **11** using PPTS at 60°C resulted in 83% yield of **12** (Scheme 5).



Scheme 5. Synthesis of fluorophore incorporated allylic alcohol **12**.

Chlorination of **12** was performed using DMS and NCS as a chlorinating agent at DCM to give compound **13** without any purification. Compared to its precursors which are stable at room temperature and can be kept for very long time, **13** is acid sensitive due to its farnesyl chain and the very reactive allylic chloride. After simple workup, NBD attached allylic chloride **13** was treated subsequently with $(\text{Bu}_4\text{N})_3\text{HP}_2\text{O}_7$ in CH_3CN at room temperature overnight. The resulting tetrabutylammonium NBD-FPP **14** was converted to the ammonium salt by passing **13** through a cation ion-exchange resin to give the target product NBD-FPP **1** in 16 % yield over two steps (Scheme 6). The NBD-FPP **1** is both acid and base labile and can only be stored between pH 7-10.



Scheme 6. Synthesis of fluorophore incorporated farnesyl pyrophosphate **1**.

4.2 Synthesis of Rab GGTase Inhibitors

4.2.1 Synthetic plan

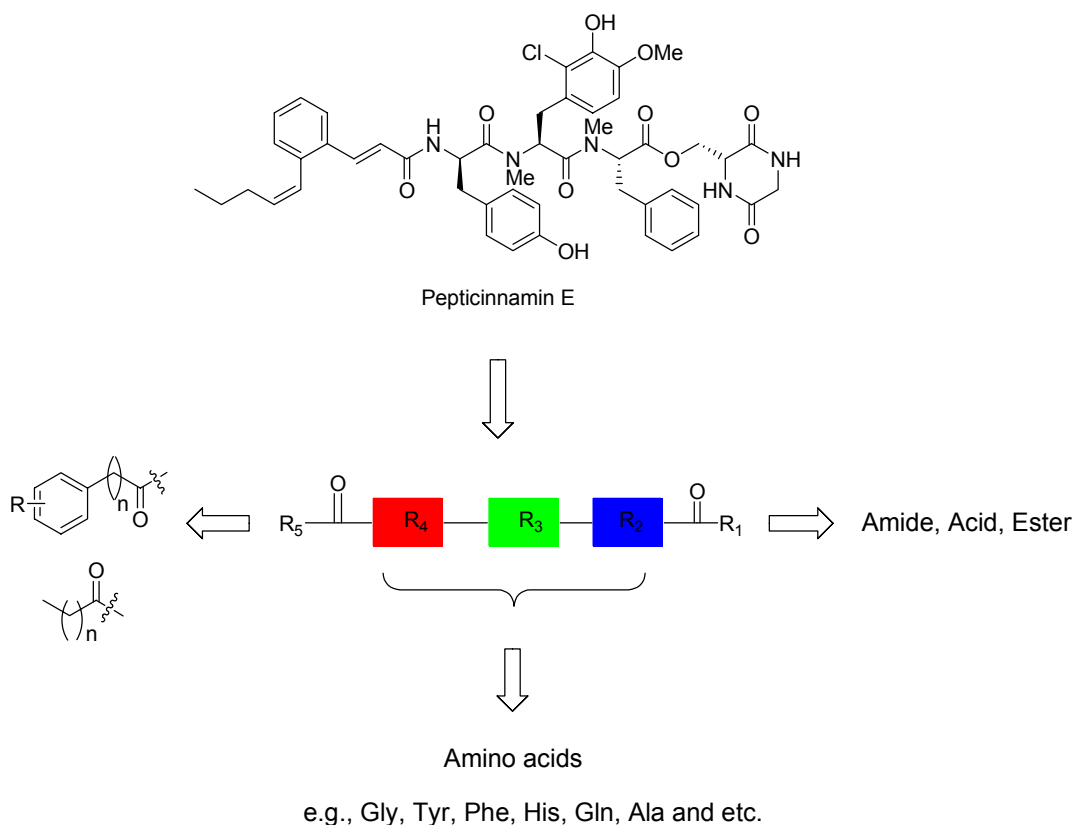
For the generation of compound libraries, it is particularly useful to apply solid phase synthesis strategies. The solid support can be easily separated and sorted into different portions to react with different building blocks or starting materials to afford highly diverse derivatives. In this dissertation, the synthesis of Rab GGTase inhibitors was carried out on solid supports. The synthesis of the Rab GGTase inhibitors was conducted together with Dr. Ester Rozas Guiu.

A straightforward modification strategy of the lead structure Pepticcinnamin E was envisioned by dividing the structure into three regions, N-terminus, C-terminus and a three amino acids central core. The compounds library of Pepticcinnamin E can be synthesized by means of the building block strategy. This strategy is the best method to construct a highly diverse library, as every position of the derivatives can be modified easily and freely by introducing different substrates which are compatible to the reaction condition.

The diversity of three amino acids central core can be introduced by adding different amino acids during the course of the synthesis. The central core amino acid residues of the lead structure are basically derivatives of tyrosine and phenylalanine. In order to cover broad range of derivatives, aliphatic residues and other natural amino acids were also considered and introduced during the synthesis.

Two different approaches were considered for the modifications of the N-terminus. The first approach introduced greater variety of aromatic functionalities which shows good binding properties with the zinc ion in Rab GGTase active site. The second approach was based on the introduction of aliphatic residues such as long aliphatic chains which are similar to the lipid substrate of Rab proteins with the aim of promoting competition with the substrate. Moreover, to study the influence of the C-terminus, this position was

further modified by introducing a wide spectrum of diverse amide, acid, and ester functionalities (Scheme 7).



Scheme 7. Modifications of Pepticcinnamin E.

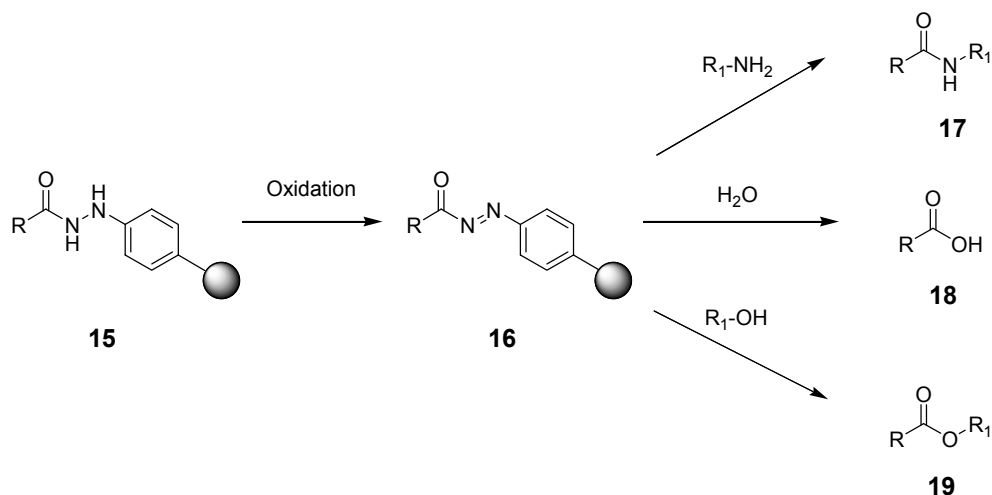
4.2.2 Choice of linkers

Since the first disclosure of solid phase synthesis by R. B. Merrifield,⁴⁹ a great number of linkers⁵⁰ (more than 200) have been developed over the past decades in order to allow many multi-step organic syntheses to be performed and the use of a broad range of reagents, allowing cleavages in a very selective manner. Most of the linkers used in the synthesis are either acid or base labile which means that the product attached to the solid support can be released under acid or base condition. There is another class of linkers which is inert to acid and base condition, but can be cleaved off by various nucleophiles after activation of the linker. This type of linker is called safety catch linker.

Safety catch linker not only represents a novel class of temporary protecting group to the target molecule, but also presents itself as a superior set of linker in diversity-oriented synthesis. Safety catch linker strategies in which a stable linkage is activated for cleavage by a discrete chemical modification have proven to be particularly useful in the synthesis of compound libraries. These linkers are often compatible with a broad range of reactions, yet target compounds can be released from solid support under mild conditions after the activating step. In addition, the activation step can potentially provide a reactive linkage functionality for cleavage with diverse nucleophiles. Therefore, an additional element of diversity can be added to the structure of the target compounds in the cleavage step.⁵¹

In order to introduce large diversity on the C-terminus of Rab GGTase inhibitors, the hydrazine linker was used in the synthesis of compounds library and attached to the C-terminus of the peptides. The hydrazine linker has been used in the synthesis of several base and acid labile lipopeptides. The linker is stable to Fmoc and Boc deprotection conditions.⁵²

The hydrazine linker **15** is suitable for the synthesis of Rab GGTase inhibitors as it presents great versatility and allows the creation of a wide variety of functional groups ranging from esters, amides, and acids at the C-terminus. The product can be released from the solid support via activation of the linker and subsequent nucleophilic addition. The activation of hydrazine linker **15** can be effected by very mild oxidation condition employing NBS/pyridine or Cu(OAc)₂.⁵³ The activated intermediate **16** can be subjected to different nucleophiles like amines, alcohols or water to release the product from the solid support (Scheme 8).

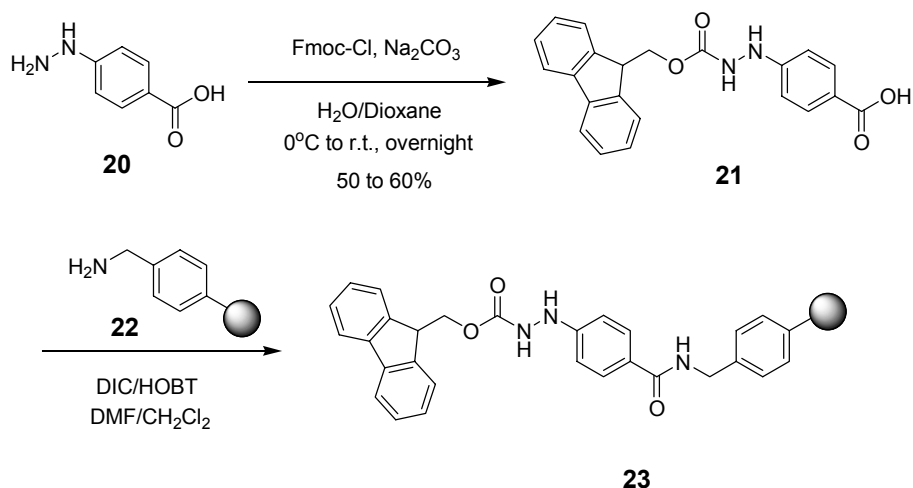


Scheme 8. Oxidative cleavage of hydrazine linker to obtain amide, carboxylic acid, and ester derivatives.

The preparation of Rab GGTase inhibitors library was carried out using the Fmoc-protecting strategy. The hydrazine linker is highly compatible to the Fmoc-deprotection conditions. Furthermore, the deprotection of the Fmoc group can be achieved in very short time to afford total deprotection.

4.2.3 Synthesis of the hydrazine linker **21** and loading to the resin

The linker was prepared by protection of 4-hydrazine benzoic acid **20** with the Fmoc group. The protection was carried out in water and dioxane using Fmoc-Cl and Na_2CO_3 overnight to give Fmoc-protected hydrazine linker **21** in $\approx 50\%$ yield (Scheme 9). Amino methylated polystyrene resin **22** was chosen as a solid support for the loading of the linker **21**. The reason to use this resin was that the formation of amide bond between linker and solid support can be sustained in the subsequent elongation, deprotection and cleavage condition.



Scheme 9. Synthesis of Fmoc-protected hydrazine linker **21** and loading to the resin **22**.

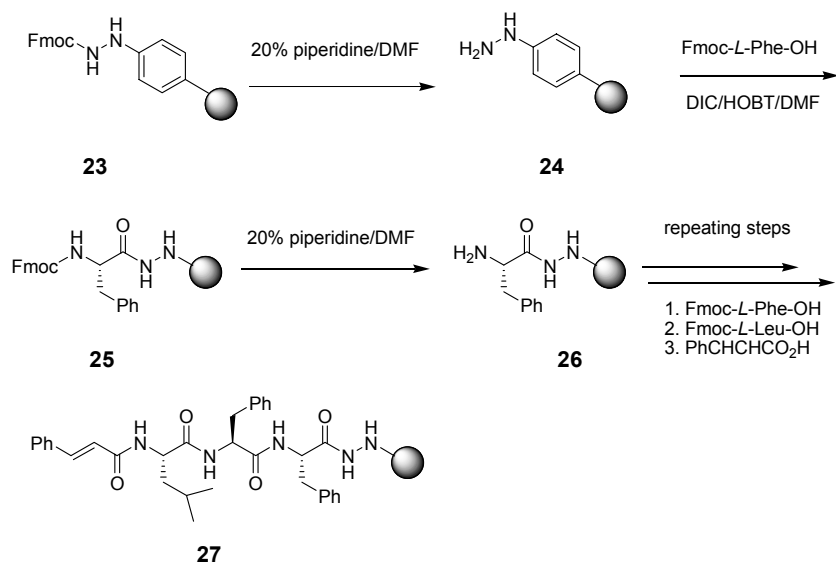
Two coupling conditions using different coupling reagents were surveyed to find out the best loading conditions. The loading of the first substances to the resin is very critical, as low loading and side product formation can render a low yield to the subsequent coupling reaction and difficult purification of the desired product. Table 2 outlines the loading condition using HOBT/HBTU/DIPEA and DIC/HOBT respectively. In general, the coupling of the linker to the resin using either method gave similar results. DIC/HOBT was chosen as the standard coupling method for loading of the linker to the resin due to the lower cost and since the method does not involve the addition of DIPEA base which can cause partial deprotection of Fmoc group and racemization of amino acids. The loading of the linker to the resin was achieved using DIC/HOBT in DCM and DMF overnight to obtain 90 to 100% loading yield. The loading of the linker to the resin was determined by measuring UV absorption intensity at wavelength 301 nm of deprotected Fmoc group.⁵⁴

Table 2. Comparison of two coupling methods.

Entry	Coupling condition	Loading yield
1	HOBT/HBTU/DIPEA	85-100%
2	DIC/HOBT	90-100%

4.2.4 Incorporation of amino acids and the N-terminal substrates

The Fmoc group of the hydrazine resin **23** was deprotected using 20% piperidine in DMF to give **24** prior to the introduction of amino acids. A DIC and HOBt coupling cocktail dissolved in DMF was the standard coupling condition for the incorporation of all amino acids and N-terminal substrates. After deprotection, Fmoc-protected phenylalanine was introduced to the resin using the standard coupling cocktail for 2 hours at room temperature. The reaction was monitored by the Kaiser test until it was completed. Typically this peptide coupling reaction can be completed within one hour; however, an additional hour was added to ensure that all the free amine on the resin has been reacted. Following that, the resin was washed with DCM and DMF to get rid of the excess amino acid and coupling reagents. The resin **25** was then subjected to another round of Fmoc deprotection using the standard deprotection cocktail to give resin **26**. The coupling/washing/deprotection process was repeated until three Fmoc-protected amino acids and the N-terminal carboxylic acid substrates were introduced (Scheme 10). This solid phase peptide strategy was applied to prepare all the peptides used for the screening of Rab GGTase inhibitors. By using this strategy, numerous diverse Pepticinnamin E derivatives were obtained in a very short time.



Scheme 10. General scheme for the synthesis of peptides.

In this compound library, 16 different substrates were introduced at N-terminal position of the peptides. Figure 10 shows all the carboxylic acids in this peptide library. The N-terminus of the peptides contain great variety of aromatic substrates from compounds **N-i** to **N-xii**, in which compound **N-vii** and **N-xi** were the byproducts from compound **N-ii** and **N-xi** respectively, after release from the resin using NBS/pyridine condition. The N-terminus of the peptides also included zinc ion binding functionality, such as compound **N-x**, **N-viii** and **N-xiii**. Various long aliphatic chains residues were also integrated in this library, such as compound **N-viii**, **N-xv** and **N-xvi**.

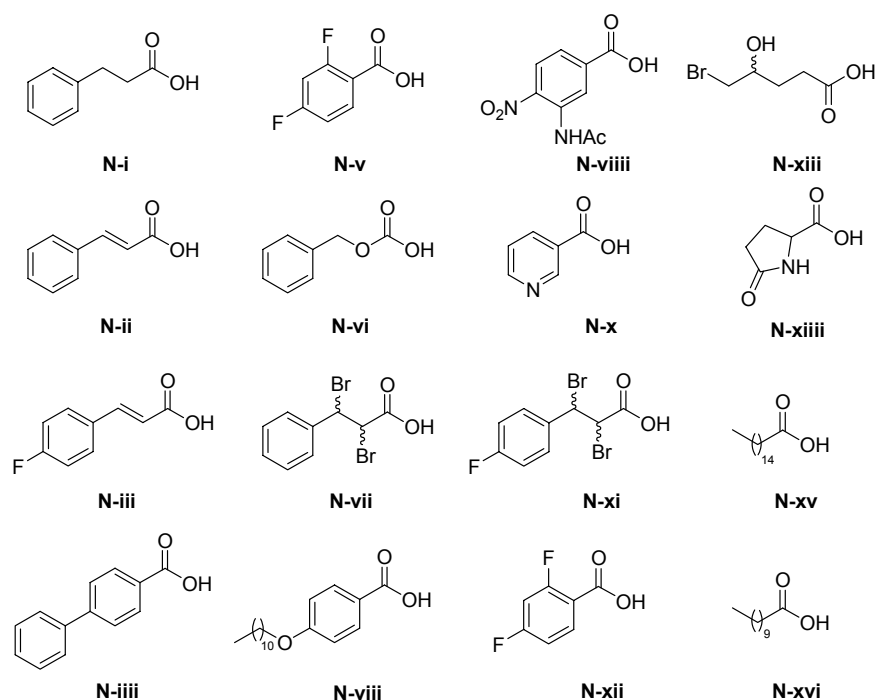


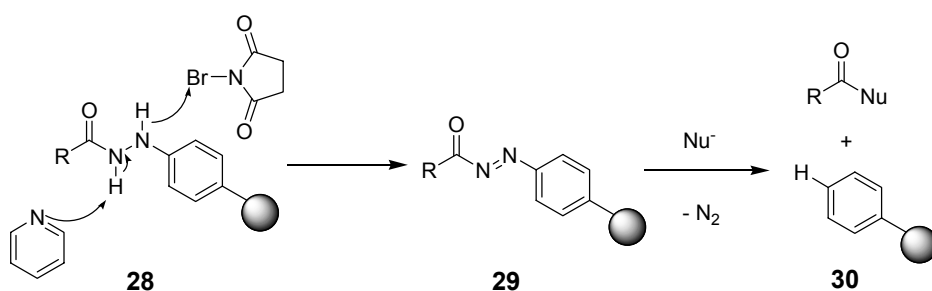
Figure 10. 16 different substrates were placed in N-terminus of peptide sequences in the compound library.

Various amino acids were placed in different positions of the peptide sequences to expand the diversity of the library. L-phenylalanine, L-tyrosine, L-serine, L-leucine, L-glutamine, L-glutamic acid, L-arginine and L-histidine were introduced at the second position of the peptide sequences. At the 3rd position of the peptide sequences, glycine, L-phenylalanine, L-leucine, L-serine, L-alanine, L-histidine, D-valine, L-isoleucine, L-

lysine and L-tyrosine were incorporated in the sequence. L-leucine, L-serine, L-alanine, L-phenylalanine, L-threonine, D-alanine, L-lysine, L-isoleucine, glycine, L-tyrosine and L-histidine were placed at the 4th position of the peptide sequence.

4.2.5 Oxidative cleavage by NBS

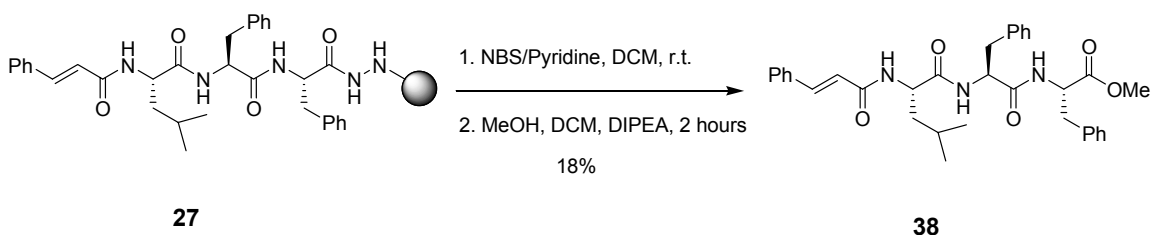
After completion of the peptide synthesis, the product must be released from the resin. Two oxidative cleavage methods were used to release the peptides from the solid support. The first oxidative release condition was the treatment of resin bound peptide with NBS/pyridine. The NBS/pyridine oxidative cleavage is a two step reaction involving oxidation of the hydrazine linker **28** utilizing NBS/pyridine and nucleophilic displacement of reactive acyldiazine **29** to give the desire product. The driving force of this reaction is the generation of nitrogen gas and aryl resin **30** after nucleophilic addition (Scheme 11).



Scheme 11. Mechanism of oxidative cleavage by NBS.

Peptide bound resin **27** was treated with 2 equivalents of NBS and pyridine in DCM for 5 minutes. The resultant yellow solution was filtered and the resin was washed with DCM. The release of peptide was achieved by treating methanol and DIPEA in DCM to the acyldiazine for 2 hours to furnish product **38** in 18% yield (Scheme 12) after purification. Besides methanol, substrates such as water, ammonia, aniline, benzyl amine and etc. can also be applied as nucleophiles. Some nucleophiles such as water which are not able to dissolve in DCM were dissolved in dioxane. The addition of base is only applicable to oxygen nucleophiles, nitrogen nucleophiles do not require the introduction of additional

amine base. Extending the reaction time did not improve the yield of the product. Around 250 peptides were prepared by using this oxidative cleavage method. Deprotection of all the protecting groups was carried out with deprotection cocktail TFA/TES/H₂O (50/1/1) in one hour.



Scheme 12. Release of product **38** from hydrazine linker using NBS with MeOH as nucleophile.

Figure 11 displays the LC_{MS} trace of crude product **38**. The peak at 9.59 minutes corresponds to product **38** with the molecular mass of 570 and 592 (plus a proton [569+H] and sodium atom [569+ Na] respectively).

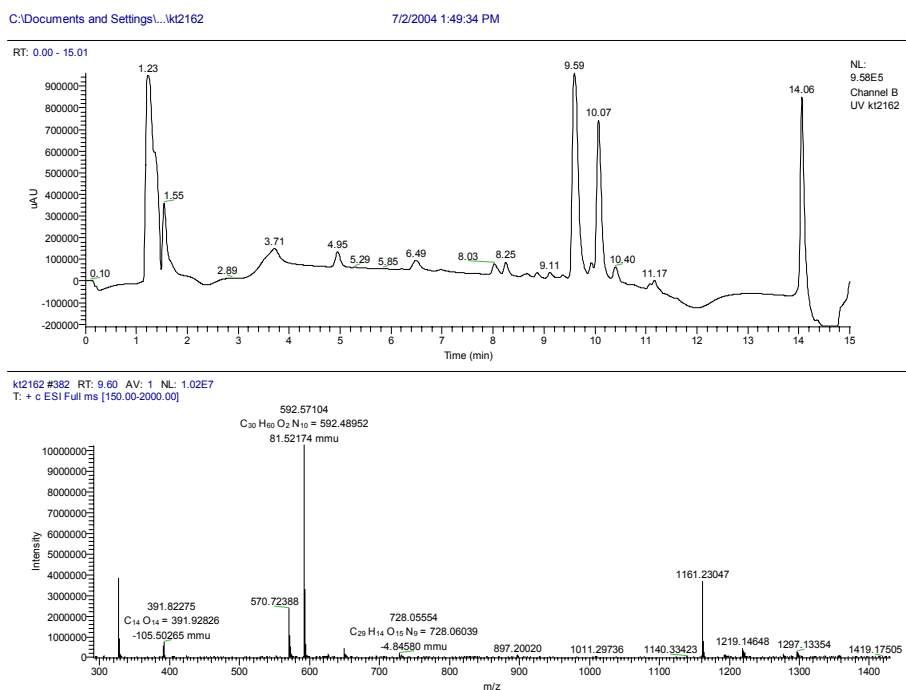


Figure 11. LC_{MS} trace of crude product **38**

Table 3 shows some of the peptides obtained using the NBS/pyridine oxidative cleavage strategy.

Table 3. Various peptides prepared using NBS oxidative condition

Entry	Nr.	R ₅	R ₄	R ₃	R ₂	R ₁	Yield %
1	39		L-Leu	L-Phe	L-Phe	OH	3
2	40		L-Pro	Gly	L-Phe		28
3	41		L-Ala	Gly	L-Tyr	OH	7
4	42		D-Ala	L-Phe	L-Gln		3
5	43		D-Ala	L-Phe	L-Gln	NH	5
6	44		L-Ala	L-Phe	L-Gln		1
7	45		L-Ile	L-Ala	L-Gln		1
8	46		L-Tyr	Gly-	L-Tyr		10
9	47		L-Tyr	Gly-	L-Tyr		7
10	48		L-Tyr	L-Tyr	L-Tyr		4
11	49		L-Ile	D-Val	L-Gln		6
12	50		L-Ser	Gly	L-Ser		6

In general, amine nucleophiles gave higher yield than alcohol nucleophiles. This difference of yield can be attributed to the better nucleophilicity of the nitrogen atom than the oxygen atom. Figure 12 shows the nucleophiles used in the NBS/pyridine cleavage condition. More than 30 different alcohol and amine nucleophiles were used to perform the nucleophilic displacement reaction to release the peptides from the solid support. The amine nucleophiles consist of aromatic and aliphatic amines. The alcohol nucleophiles consist of only aliphatic alcohol.

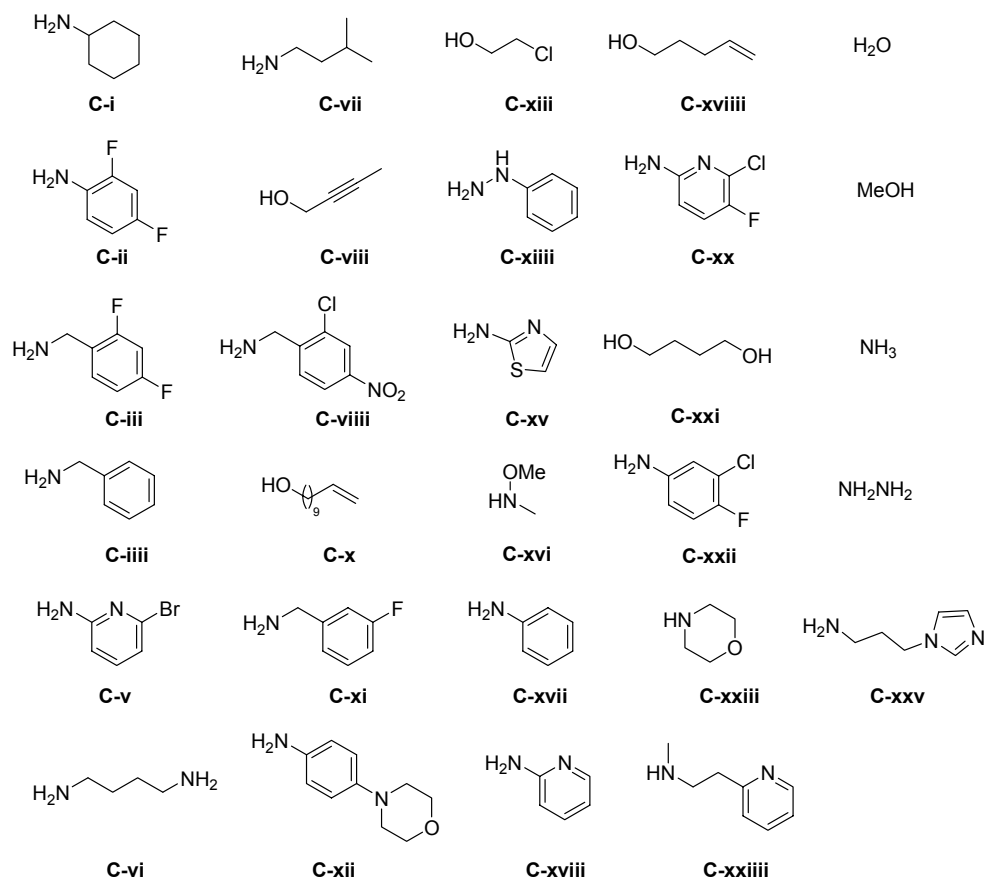
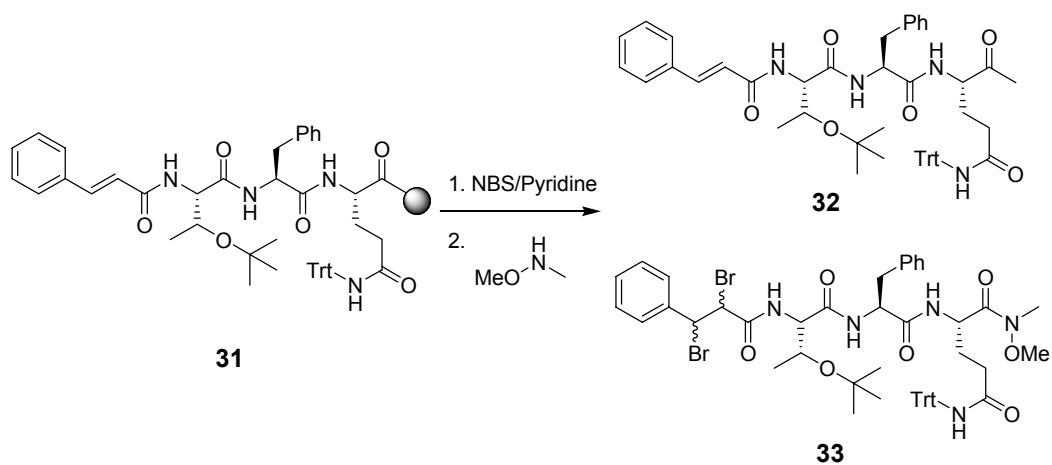


Figure 12. Nucleophiles used in the NBS/pyridine nucleophilic release condition.

Although 250 peptides have been synthesized using this cleavage method, the yield from this cleavage condition is not satisfactory. Some of the peptides released from the solid support using the NBS/pyridine method gave less than 2% yield. In addition to this problem, the NBS/pyridine cleavage method also introduced side reactions to the peptide if double bonds were presented in the peptide sequence. For example, peptide **31** which consists of a double bond at the N-terminal substrate was brominated to give side product **33** during oxidative cleavage (Scheme 13). Figure 13 and 14 shows the crude LC_MS traces of **32** and **33**, respectively. Figure 13 shows the small peak at 11.02 corresponding to **32** with the molecular mass of 865 plus a sodium atom [865+Na]; whereas Figure 14 shows the higher peak at 11.34 belonging to the side product **33**, the mass spectrum shows a typical dibromo pattern with 1:2:1 isotope distribution and molecular mass of 1048 [1023+Na].



Scheme 13. Side product **33** from NBS/pyridine cleavage condition of compound **31**.

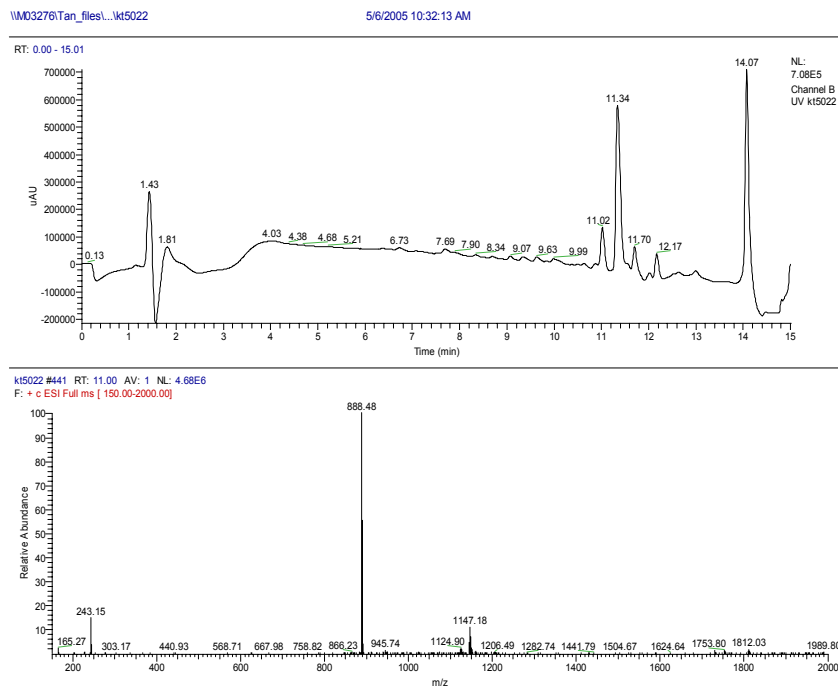


Figure 13. LC_MS trace of crude compound **32**.

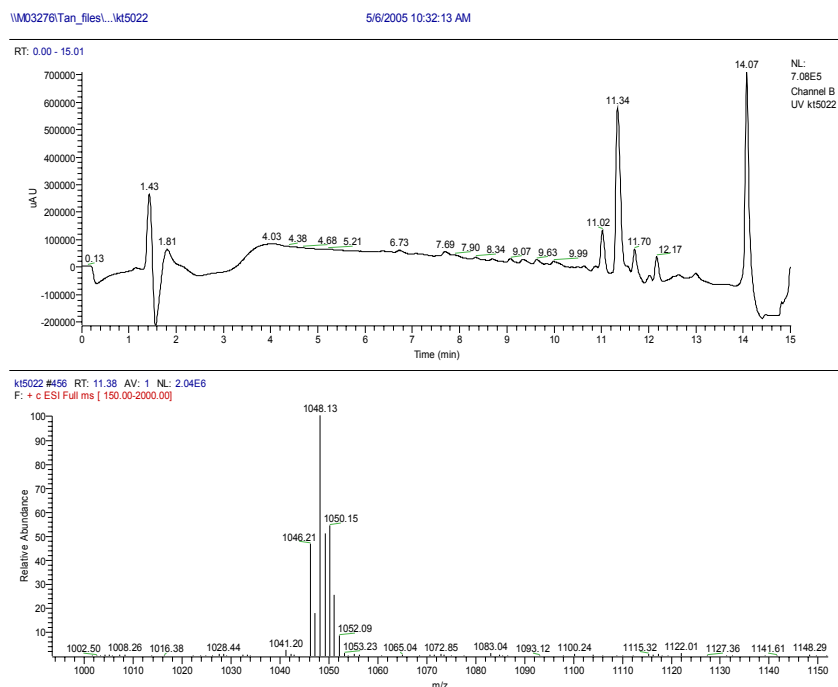


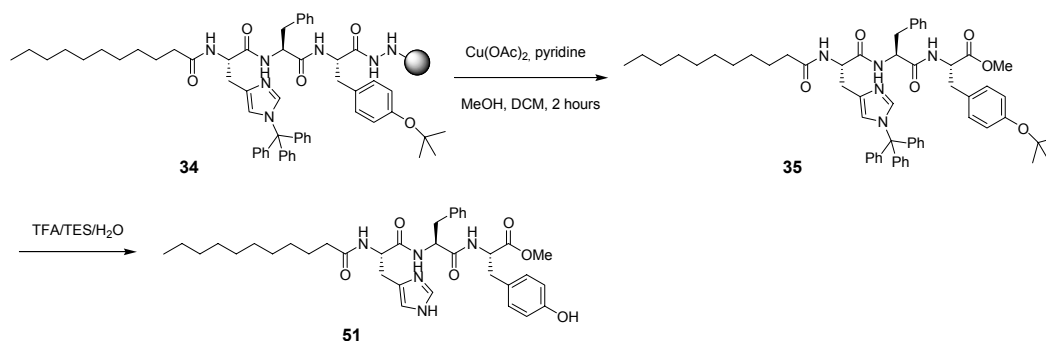
Figure 14. LC_MS trace of crude material **33**.

In order to overcome this problem, an alternative cleavage method was considered to boost the yield and reduce the side reaction.

4.2.6 Oxidative cleavage by $\text{Cu}(\text{OAc})_2$

The oxidative cleavage reaction performed by $\text{Cu}(\text{OAc})_2$ is a one step reaction involving the addition of $\text{Cu}(\text{OAc})_2$ to oxidize the hydrazine linker and *in situ* nucleophilic addition to release the peptide from the solid support. In contrast to the NBS/pyridine approach, only catalytic amount of $\text{Cu}(\text{OAc})_2$ is required for the oxidative process. The Cu(II) specie can be regenerated by the oxidation of Cu(I) in the solution by O_2 . Peptide **36** is one of the 130 peptides released from the resin employing $\text{Cu}(\text{OAc})_2$. The resin **34** was treated with 0.5 equivalent of $\text{Cu}(\text{OAc})_2$ and 1 mL of methanol in 2 mL DCM with 10 equivalents of pyridine for two hours to give peptide **35**. In this cleavage condition, utilization of DIPEA and Et_3N as base did not give any desired product. If the nucleophiles are amines, the addition of pyridine is not necessary. The excess amine,

pyridine and $\text{Cu}(\text{OAc})_2$ in the reaction mixture can be washed away by extraction with 1M HCl. Deprotection of all the protecting groups was carried out with deprotection cocktail TFA/TES/ H_2O (50/1/1) in one hour to give product **51** in 25% yield after purification (Scheme 14). The oxidative release of peptides from resin using $\text{Cu}(\text{OAc})_2$ condition gave very clean LC_MS trace with only desired product and deprotected protecting group. Figure 15 shows the crude LC_MS trace of peptide **51**. The peak at 7.57 minutes corresponds to **51** with the molecular mass of 648 plus a proton $[647+\text{H}]^+$.



Scheme 14. Oxidative release and cleavage of protecting groups of compound **51** with TFA/TES/ H_2O .

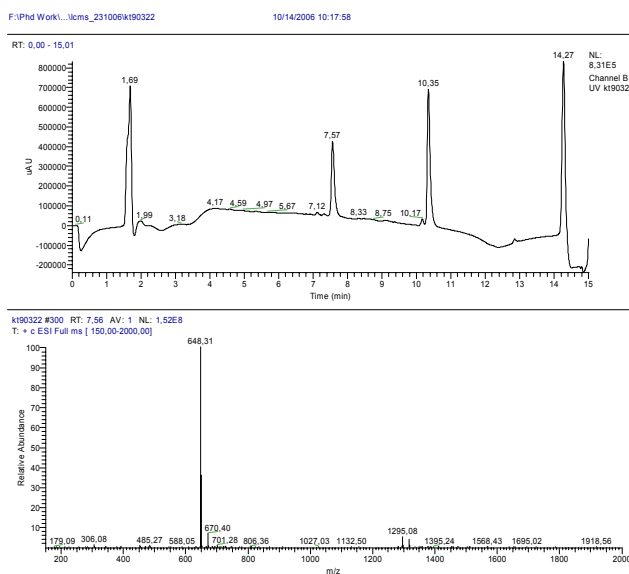


Figure 15. LC_MS trace of crude material **51**.

Table 4 shows some of the peptides released from the solid support using the Cu(OAc)₂ method. In general, fewer side products were observed by using the Cu(OAc)₂ oxidative condition.

Table 4. Various peptides prepared using Cu(OAc)₂ oxidative condition

Entry	Nr.	R ₅	R ₄	R ₃	R ₂	R ₁	Yield %
1	52		L-Tyr	L-His	L-Tyr	NH	2
2	53		L-Tyr	L-His	L-Tyr		20
3	54		L-Tyr	L-His	L-Tyr		22
4	55		L-Tyr	L-His	L-Tyr		7
5	56		L-His	L-His	L-His	OH	20
6	57		L-His	L-His	L-His	OMe	11
7	58		L-His	L-His	L-His	NH	7
8	59		L-His	L-His	L-Tyr		12
9	60		L-His	L-His	L-Tyr		15
10	61		L-Tyr	L-His	L-Tyr		20
11	62		L-His	Gly	L-Tyr		2
12	63		L-His	L-His	L-Ser		26
13	64		L-His	β-Ala	L-Tyr	OMe	4
14	65		L-His	β-Ala	L-Tyr	NH	1
15	66		L-His	β-Ala	L-Tyr		6
16	67		L-His	L-Phe	L-Tyr		13

Figure 16 shows 12 different nucleophiles used in the $\text{Cu}(\text{OAc})_2$ cleavage condition to release the peptides from the solid support. 10 equivalents of nucleophiles (relative to the resin) were used in the reaction except water, methanol and ammonia which 1 mL of solution was added to the reaction condition.

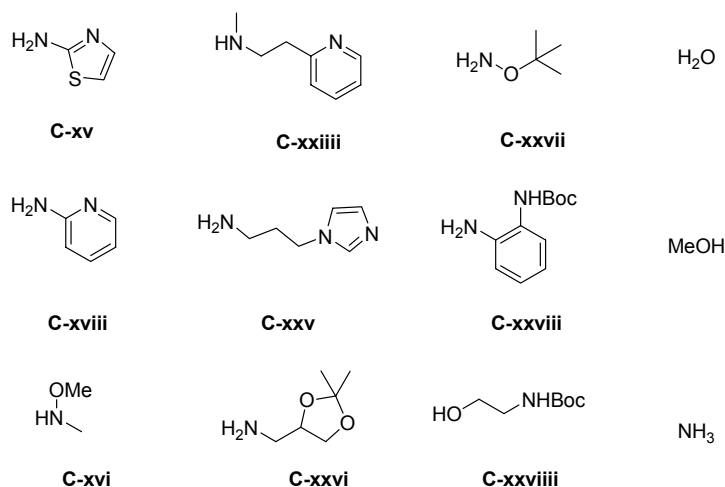
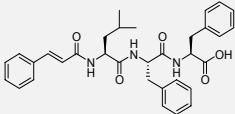


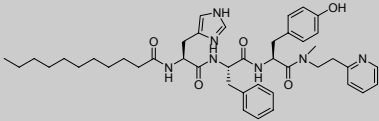
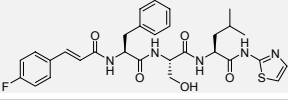
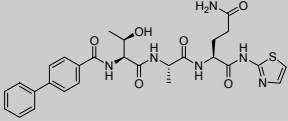
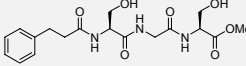
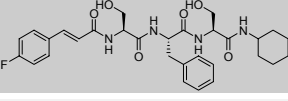
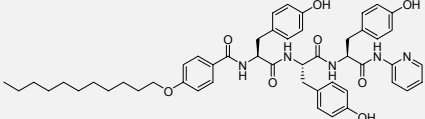
Figure 16. Nucleophiles used in the $\text{Cu}(\text{OAc})_2$ peptides release condition.

4.2.7 Comparison of the NBS and the $\text{Cu}(\text{OAc})_2$ oxidative cleavage condition

The efficiency of the oxidative nucleophilic release of peptides from solid support employing NBS and $\text{Cu}(\text{OAc})_2$ was studied by comparison the yield of the two cleavage conditions. Table 5 compares the yield of the peptides released from the NBS and $\text{Cu}(\text{OAc})_2$ conditions respectively after HPLC purification.

Table 5. Comparison of the efficient oxidative release of peptides by the NBS and $\text{Cu}(\text{OAc})_2$ conditions.

Entry	Nr.	Peptides	NBS (Yield) %	$\text{Cu}(\text{OAc})_2$ (Yield) %
1	39		3	5

2	81		7	18
3	141		3	15
4	187		6	16
5	260		2	5
6	280		2	16
7	346		2	12

In general, $\text{Cu}(\text{OAc})_2$ oxidative cleavage condition gave higher yield after HPLC purification. When amine substrates were used as nucleophiles in the two oxidative cleavage conditions, the difference of the yield is more pronounced than the alcohol nucleophiles. For example, the yield for peptides at entries 1 and 5 is similar, either the peptides were released from the solid support by NBS or $\text{Cu}(\text{OAc})_2$ methods. The yield for $\text{Cu}(\text{OAc})_2$ oxidative cleavage condition is around 10 % higher than NBS condition if amine substrates were used as nucleophiles. The reasons of the lower yield for NBS condition are probably due to the production of mono- and dibrominated sideproduct for the olefinic substrates and generation of acyldiazine radical from NBS.

4.2.8 Summary and Discussion of the peptide library synthesis

382 peptides were produced in total by both NBS and $\text{Cu}(\text{OAc})_2$ oxidative release condition. Among these 382 compounds, 250 peptide inhibitors were generated by NBS oxidative release approach. 16 different carboxylic derivatives were introduced at the N-terminus of the peptides in which both zinc ion binding and long lipid chain residues were included at the N-terminus. 12 natural and 4 non-natural amino acids were incorporated at various positions of the peptides. More than 30 different amine and

alcohol nucleophiles were applied to the C-terminus of the peptides. The yield of the peptides generated by two oxidative released condition ranges from as low as 1% to 30 % with purity of most peptides greater than 95% after purification. All the peptides prepared using NBS and $\text{Cu}(\text{OAc})_2$ cleavage conditions are listed in appendix.

The successful synthesis of 382 Rab GGTase peptide inhibitors has demonstrated that the hydrazine linker is an excellent linker for the preparation of compounds library, especially peptides library. The linker is acid and base stable but labile to mild oxidation method. By using this synthesis strategy, large number of peptide inhibitors can be assembled in a very short time. In this project, the diversity of the peptide library was achieved through the addition of different nucleophiles at C-terminus of peptides by oxidative nucleophilic reaction and building block strategy.

The LC_MS trace of the crude peptides after oxidative release from solid support showed relatively clean spectra which make the purification of the crude material easier. If the olefinic functionality containing peptides were treated with NBS, the major side reaction was the addition of mono- or dibromo to the olefin. This side reaction can be avoided by releasing the peptides from the resin using the $\text{Cu}(\text{OAc})_2$ conditions.

The use of $\text{Cu}(\text{OAc})_2$ cleavage condition for the synthesis of peptide library has several advantages over NBS condition. The yield for the $\text{Cu}(\text{OAc})_2$ cleavage condition is normally higher than the NBS condition. There is fewer side products observed in the crude LC-MS trace for $\text{Cu}(\text{OAc})_2$ condition. Unlike NBS condition, the oxidative cleavage reaction performed by $\text{Cu}(\text{OAc})_2$ is a one step reaction involving *in situ* nucleophilic addition to release the peptide from the solid support. This property makes the $\text{Cu}(\text{OAc})_2$ oxidative condition easier to handle than the NBS condition, as one reaction step of addition of NBS and washing avoided. Furthermore, the $\text{Cu}(\text{OAc})_2$ oxidative condition exists the opportunity to be optimized and performed in a automatic peptide synthesizer which can render the synthesis of peptide library more efficient and time saving.

4.3 Biochemical Investigation of Rab GGTase Inhibitors

4.3.1 *In vitro* screening of the peptide library

382 peptides were subjected to *in vitro* screening to identify the potential inhibitors of Rab GGTase. The screening of inhibitors was performed in 96 well plates using a continuous fluorometric assay for Rab GGTase developed by Wu et. al.⁴⁴ The *in vitro* screening was first carried out with 50 μM concentration of inhibitors and in the presence of 0.01 % detergent Triton X-100. IC_{50} values were determined subsequently for compounds showing >50% inhibition at 50 μM . The screening was performed in duplicate. Around 160 compounds were screened at 100 μM .

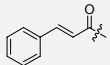
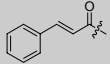
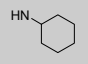
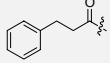
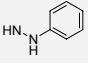
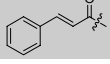
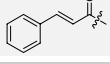
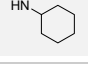
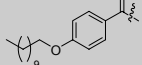
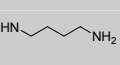
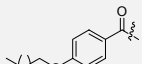
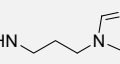
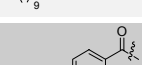

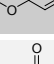
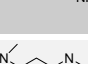
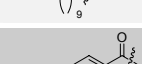
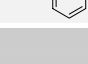
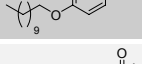
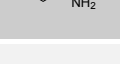
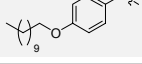
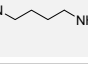
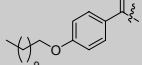
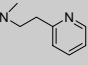
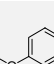
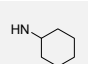
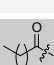
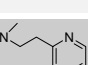
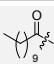
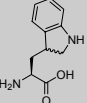
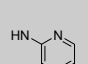
The screening protocol is briefly described here. 50 μL of 0.4 μM Rab GGTase and 4 μM NBD-FPP **1** was added to the well followed by 0.5 μL of inhibitor in 10 mM DMSO solution. The solution was mixed well and incubated at 37°C for two minutes. 50 μL of 4 μM Rab-7:REP-1 cocktail solution was added to the same well. The measurement was started immediately. Instead of 0.5 μL inhibitor, the positive control of the assay was carried out with the addition 0.5 μL DMSO.

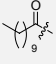
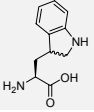
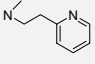
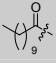
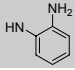
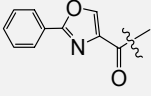
During the screening of the inhibitors using this assay, fluorescent bleaching of NBD-FPP **1** in the measurement was observed in every case. The fluorescent bleaching of NBD-FPP **1** is depending upon the type and concentration of inhibitors. To take into account the fluorescent bleaching effect during the measurement, two negative controls were included in the screening. In one negative control, the same concentration and volume of inhibitors was introduced to 50 μL of 0.4 μM Rab GGTase and 4 μM NBD-FPP **1** cocktail solution and 50 μL of buffer solution. The other negative control involved the addition of DMSO to buffer solution and Rab GGTase and NBD-FPP **1** cocktail solution.

18 compounds were identified in the screening to inhibit the biological activity of Rab GGTase to less than 50% at 50 μM concentration (for the inhibition activity of all the

compounds, see appendix). The compounds were selected to determine their IC₅₀ against Rab GGTase. Table 6 shows IC₅₀ values and structure of the inhibitors.

Table 6. Structure of peptide inhibitors and their IC₅₀ values

Entry	Nr.	R ₅	R ₄	R ₃	R ₂	R ₁	IC ₅₀ (μ M)
1	38		L-Leu	L-Phe	L-Phe	OMe	61.9 \pm 9.9
2	71		L-Leu	L-Phe	L-Phe		71.5 \pm 11
3	72		L-Ala	L-Phe	L-Gln		37.4 \pm 5.4
4	73		L-Phe	L-Phe	L-Tyr	OH	42.6 \pm 6.4
5	74		L-Phe	L-Phe	L-Tyr		68.7 \pm 12
6	75		L-His	L-His	L-His		13.3 \pm 22
7	76		L-His	L-His	L-His		20.5 \pm 1.7
8	69		L-His	L-Tyr	L-Phe		14.0 \pm 4.0
9	59		L-His	L-His	L-Tyr		4.8 \pm 0.6
10	48		L-Tyr	L-Tyr	L-Tyr		28.2 \pm 3.1
11	77		L-Tyr	L-Tyr	L-Tyr		8.8 \pm 0.5
12	78		L-His	L-His	L-His		24.7 \pm 1.7
13	79		L-His	L-Tyr	L-Phe		20.5 \pm 4.1
14	80		L-Tyr	L-His	L-Tyr		2.4 \pm 0.5
15	81		L-His	L-Phe	L-Tyr		0.96 \pm 0.1
16	82			L-His	L-His		27.8 \pm 1.8

17	83			L-His	L-His		31.7 ± 2.3
18	84		L-His	L-His	L-Ser		35.3 ± 4.2
19	EGR 1120		L-His	Gly	L-His(Trt)	OH	21

The IC₅₀ values of the inhibitors were measured using five different concentrations, 100 μM, 50 μM, 25 μM, 12.5 μM and 6.25 μM respectively. For compounds **59**, **80**, and **81**, the IC₅₀ values were measured using seven different concentrations, 10 μM, 5 μM, 2.5 μM, 1.25 μM, 0.625 μM, 0.3125 μM and 0.1562 μM respectively.

Three peptides, **38** (61.9 μM), **71** (71.5 μM) and **74** (68.7 μM), exhibited IC₅₀ value of more than 50 μM. The high IC₅₀ value of these three compounds did not coordinate well with the screening results which showing these three compounds have exhibited the remaining Rab GGTase < 50%. This might be due to the precipitation of the inhibitors at higher concentration which cause partial scattering of fluorescent, therefore giving high IC₅₀ value.

Seven peptides, **72** (37.4 μM), **73** (42.6 μM), **48** (28.2 μM), **78** (24.7 μM), **82** (27.8 μM), **83** (31.7 μM) and **84** (35.3 μM) gave IC₅₀ value in between 20 μM and 50 μM. These seven peptides showed moderate inhibition activity against Rab GGTase. Another four compounds which have shown IC₅₀ value in between 10 μM to 20 μM are **75** (13.3 μM), **76** (20.5 μM), **69** (14.0 μM), **79** (20.5 μM) respectively.

Three peptides were identified to have IC₅₀ value of less than 10 μM. They are **59** (4.8 μM), **80** (2.4 μM), and **81** (0.96 μM). Especially **81**, it has IC₅₀ value of nanomolar concentration. These three peptides are the most potent inhibitors identified so far. Figure 17 shows 4 nonlinear fitting curves from the selected inhibitors.

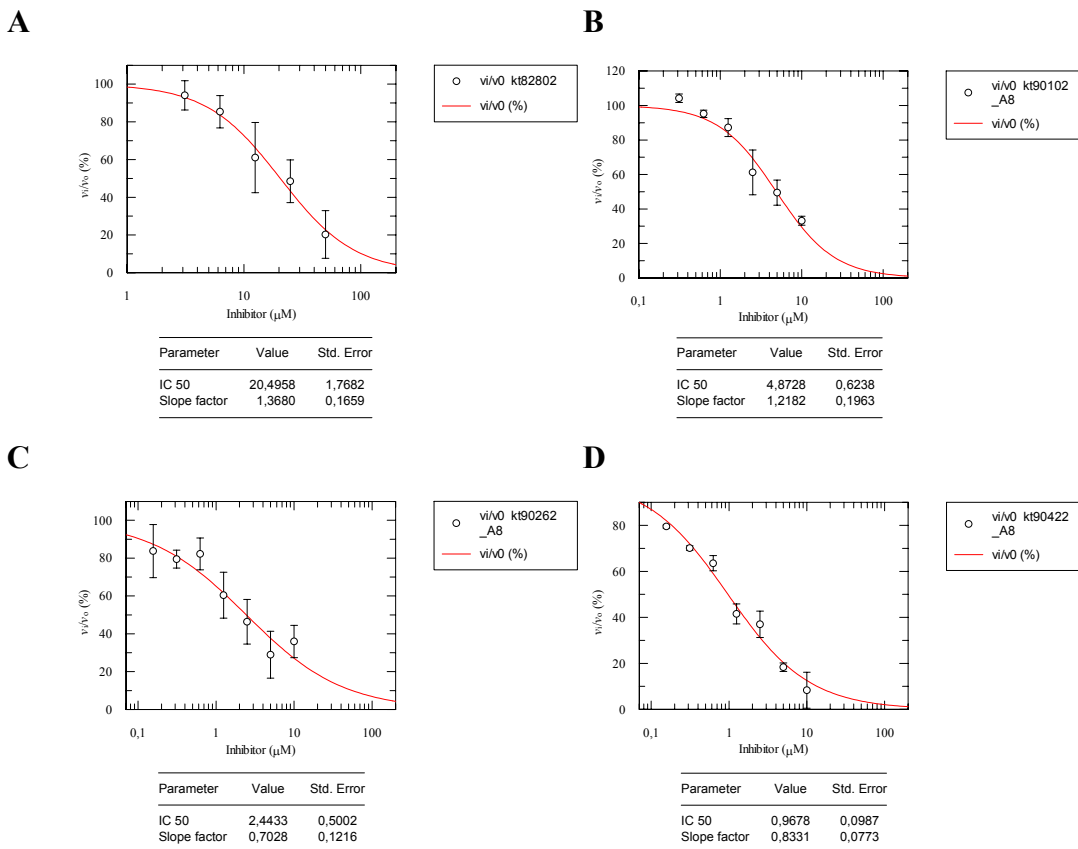


Figure 17. Nonlinear fitting curve of compounds A) **76**, B) **59**, C) **80** and D) **81** showing the IC_{50} values and their slope factors.

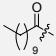
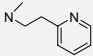
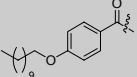
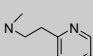
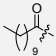
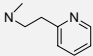
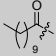
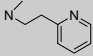
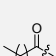
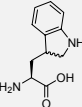
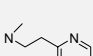
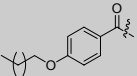
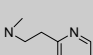
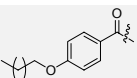
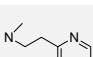
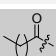
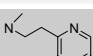
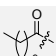
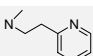
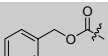
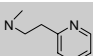
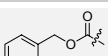
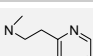
Most of the nonlinear fitting curves of the inhibitors have the slope factors between 0.7 to 2 in which clearly indicated that the compounds are not likely to be false positive inhibitors. The IC_{50} values of the active peptides against Rab GGTase were re-evaluated again using the robot-assisted screening and the results showed very close match to the activity and IC_{50} value measured manually.

4.3.2 Structure activity relationship (SAR) of inhibitors

Compound **81** is the most potent *in vitro* Rab GGTase inhibitors identified so far in this peptide library. The characteristic features of **81** are its long lipid chain at the N-terminus, R_5 position, and N-Methyl 2-ethyl pyridine moiety at its C-terminus, R_1 position. The other two potent inhibitors, **59** and **80** have similar features as **81** with the differences of

type and sequence of amino acids in the peptide central core. Table 7 compares 12 peptides in the compound library consisting of N-Methyl 2-ethyl pyridine moiety at R₁ position, with various substitutes at R₅ and different amino acids at R₂, R₃ and R₄ position.

Table 7. Structure activity relationship (SAR) analysis of peptides constitute fix moiety at R₁ position and variable building block at R₂, R₃ R₄ and R₅

Entry	Nr.	R ₅	R ₄	R ₃	R ₂	R ₁	IC ₅₀ (μM)
1	59		L-His	L-His	L-Tyr		4.8 ± 0.6
2	78		L-His	L-His	L-His		24.7 ± 1.7
3	80		L-Tyr	L-His	L-Tyr		2.4 ± 0.5
4	81		L-His	L-Phe	L-Tyr		0.96 ± 0.1
5	83			L-His	L-His		31.7 ± 2.3
6	85		L-Tyr	L-Tyr	L-Tyr		100 % ^a
7	86		L-His	L-Tyr	L-Phe		100 % ^a
8	87		L-Tyr	L-His	L-His		34% ^a
10	68		L-His	L-His	L-Ser		66% ^a
11	88		L-His	Gly	L-Tyr		85% ^a
12	89		L-His	β-Ala	L-Tyr		86% ^a

a: Entries 6 to 12 show the remaining Rab GGTase activity in percentage. IC₅₀ was not measured.

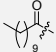
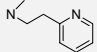
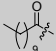
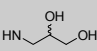
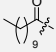
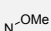
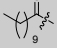
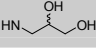
Placing the long lipid chain at R₅ position increases significantly the inhibition activity of peptides against Rab GGTase. This rationale is supported by the fact that all the peptides in entries 1 to 5 of Table 7 have one lipid chain at its N-terminus. The peptides without the lipid chain substituent at the R₅ position, entries 11 to 12, show little inhibition of Rab GGTase activity. Different lipid chain groups also contribute to distinctive IC₅₀ value.

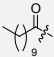
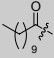
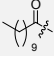
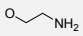
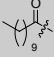
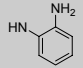
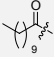
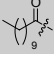
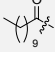
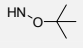
For example, entry 2 of Table 7 consists of a 4-undecyloxybenzoic group at R₅ position gives higher IC₅₀ value to the undecyl lipid chain. The reason for peptides containing long alkyl groups presenting better inhibition activity and IC₅₀ value might be due to the insertion of the lipid chain into the Rab GGTase active site which consists of a long and large tunnel for the binding to native substrate GGPP.

The type and sequence of amino acids are also the important factors contributing to the biological activity of the peptides. For example, entries 1, 3, 4, 5, 8 and 10 of Table 7 have the same functional group at the R₁ and R₅ position, yet the bioactivity of these 6 substrates to Rab GGTase are very different. Though entries 1 and 10 in Table 7 differ only at R₂ position with entry 1 consists of a L-tyrosine and entry 10 has a L-serine, the difference of the bioactivity is significant. Entry 1 which is **59** has IC₅₀ of about 5 μM, entry 10 which is **68** does not inhibit Rab GGTase very much with remaining Rab GGTase of 66% at 100 μM. Another example comes from entries 2 and 6. By changing all the amino acids from L-histidine (peptide **78**) to L-tyrosine (peptide **85**), the inhibition activity against Rab GGTase decreases from 24.7 μM to no inhibition, even at 50 μM.

It is also noteworthy to compare the influence of various substituents at the R₁ position of the C-terminus to understand the structure activity relationship of the peptides against Rab GGTase. Table 8 shows the peptides consists of the same moieties at R₅, R₄, R₃ and R₂ position, but variable at R₁ position.

Table 8. Comparison the effect of various substituents at R₁ position towards the understanding of structure activity relationship.

Entry	Nr.	R ₅	R ₄	R ₃	R ₂	R ₁ ^b	% ^c Rab GGTase Activity
1	81		L-His	L-Phe	L-Tyr		0.96 ± 0.1 ^a
2	90		L-His	L-Phe	L-Tyr		46%
3	91		L-His	L-Phe	L-Tyr		41%
4	92		L-His	L-Phe	L-Tyr		100%

5	93		L-His	L-Phe	L-Tyr	NH	100%
6	51		L-His	L-Phe	L-Tyr	OMe	100%
7	94		L-His	L-Phe	L-Tyr		60%
8	95		L-His	L-Phe	L-Tyr		76%
9	96		L-His	L-Phe	L-Tyr	OH	37%
10	98		L-His	L-Phe	L-Tyr	NH-OH	58%
11	97		L-His	L-Phe	L-Tyr		78%

a: IC₅₀ value; b: Entries 2 and 4 are diastereoisomer with the variable stereochemistry at the C-terminal secondary alcohol. c: The screening was performed at 50 μM.

Table 8 contains a series of peptides with different substitution at R₁ position. The inhibition activity of entry 1, compound **81**, against Rab GGTase is the most potent in this series of peptides with IC₅₀ value of 0.96 μM. Entries 4, 5 and 6 show no inhibition for Rab GGTase. Entries 2, 3, 7, 9 and 10 give similar inhibition activity for Rab GGTase. Inhibition activity of entries 8 and 11 for Rab GGTase is comparable.

From the different bioactivity results presented in Table 8, chemical moieties at the R₁ position play a decisive role in shaping the potency of inhibitors. In general, chemical moieties containing potential zinc ion binding functional group provide better inhibition activity. This argument is supported by good inhibition results shown in entries 1, 2, 3, 7, 9 and 10, and *vice versa* from the counter examples shown by entries 2, 3 and 4. Entry 10 has a hydroxamic group at the R₁ position which is believed to be able to coordinate to the zinc ion in the active site of Rab GGTase. The bioactivity of the peptide for the enzyme decreases by 20%, if the hydroxamic group was protected with tert butyl group (entry 11). This finding further verifies that a potential zinc ion coordinating residue gives positive enhancement for the inhibition activity of peptides. Different diastereoisomers also affect inhibition activity. Entries 2 and 4 show the difference of inhibition activity by 50%. These two peptides have identical sequence and chemical moiety at R₁ position, except the stereochemistry conformation at secondary alcohol (The

relative and absolute stereochemistry of entries 2 and 4 were not determined). This result indicated that having the right conformation of the chemical moiety at R₁ position can facilitate better coordination of ligand to the zinc ion with which increase the bioactivity.

In summary of the *in vitro* screening results from Table 6, 7, 8 and activity data in the appendix, a few conclusions from structure activity relationship analysis can be drawn:

- (1) A change of chemical moiety profoundly influences the inhibition activity of peptides, especially the chemical moieties position at R₁ and R₅.
- (2) Substrates containing long lipid chain at the N-terminus confer better inhibition activity against Rab GGTase. It is preferable and essential to have this long aliphatic chain to gain good bioactivity. This is believed that the long lipid chain fit nicely to the binding pocket of Rab GGTase which encloses a deep, large and hydrophobic active site for GGPP. The insertion of long lipid chain to the binding pocket gives hydrophobic interaction between the lipid chain and the binding site. This conclusion is confirmed by many of low IC₅₀ inhibitors having lipid containing peptides at R₅ position. Incorporation of an extra aryl ring is not beneficial to the increase of bioactivity against Rab GGTase as the entire moiety may become too long to fit into the Rab GGTase pocket.
- (3) In vitro screening results from a series of peptides in Table 6 and 8 show that chemical moiety at R₁ position which is able to chelate or bind to metal give better inhibitor bioactivity. Out of the 382 peptides screened, N-Methyl 2-ethyl pyridine substrate at R₁ position is the most promising candidate for the further development of more potent inhibitor.
- (4) The type and sequence of amino acids play very significant role in determining the bioactivity of peptides. Most of the potent peptides identified contain at least one histidine, and the best amino acids in peptides identified

so far containing L-histidine at 4th position, L-phenylalanine at 3rd position and L-tyrosine at 2nd position of the peptide sequence. Incorporation of L-histidine at 2nd position of the peptide increases the IC₅₀ value.

- (5) Majority of the peptides containing amino acids such as L-alanine, L-leucine and L-serine in this chemical library show no activity against Rab GGTase. Therefore, it is reasonable to conclude that by placing a zinc ion chelating amino acids such as L-histidine can improve the interaction of peptides with the enzyme. This argument can be supported that most of the peptides showing low IC₅₀ in the screening have at least one L-histidine in the peptide central core.

Figure 18 shows the summary of the structure activity relationships (SAR) for the peptide library. The SAR outlines some essential amino acids and chemical moieties at the peptide in order to give potent inhibition activity towards Rab GGTase.

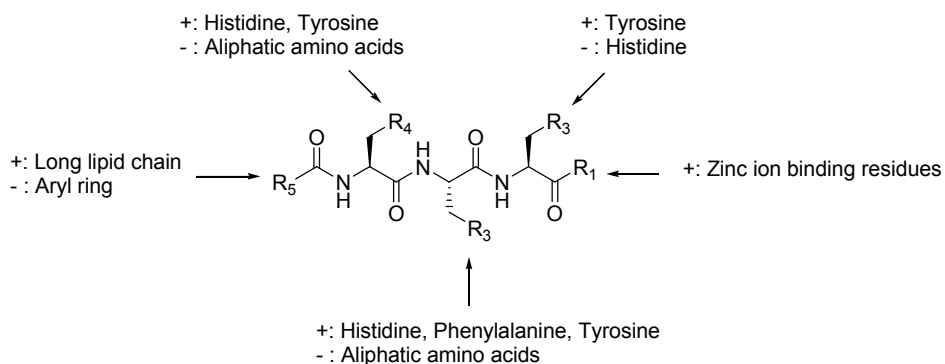


Figure 18. Structure activity relationship (SAR) of peptide library. + : Positive effect, - : Negative effect.

4.3.3 *In vivo* study of peptide inhibitors

Six selected *in vitro* potent peptide inhibitors, **77**, **75**, **76**, **80**, **59**, and **81** were subjected to *in vivo* study to identify active peptide inhibitors towards Rab GGTase in COS-7 cell. The principles of the *in vivo* testing are briefly described in the following paragraphs.

Approximately 24 hours after beginning of transfection, the cells were rinsed with fresh medium and inhibitors were added to the medium in various concentration. After another 24 hours of incubation with inhibitors, COS-7 cell lysates were collected and assayed for the presence of unprenylated Rab. An *in vitro* assay was carried out to assess the amount of unprenylated Rab in the lysate and to measure the *in vivo* inhibition of Rab prenylation.

The assay contains 4 μM Biotin-GPP, 3 μM Rab GGTase and 2 μM REP-1. These reagents are made up into a stock solution at room temperature. Lysate was then added and incubated at room temperature for 30 minutes. The reaction was stopped by the addition of 5 μL of sample buffer. Samples are boiled for 2 minutes and subsequently resolved by SDS-PAGE, Western Blot and probed with strepavidin-horse radish peroxidase (Strepavidin-HRS). If the protein, Rab GGTase, is inhibited inside the cell, the *in vitro* prenylation assay will show a positive result which should have a prenylated YFP-Rab7 blot band. If a compound tested does not inhibit the protein, then the YFP-Rab7 will be prenylated inside the COS-7 cell, as such no YFP-Rab7 band should be observed. The *in vivo* experiment was conducted by Dr. Christine Delon from Department of Physical Biochemistry, Max-Planck Institute, Dortmund.

Figure 19 shows the results of the *in vivo* testing. The peptides were screened at three different concentrations, 100 μM , 50 μM and 10 μM respectively. The blot bands where the peptides showed *in vivo* activity toward Rab GGTase correspond to the biotin prenylated YFP-Rab7 protein with strepavidin. Compactin which inhibits the synthesis of isoprenyl lipid was added as a positive control. Negative control was done with only DMSO.

All the six compounds tested were not cytotoxic to the COS-7 cells. Three peptide inhibitors, **59**, **80** and **81**, were identified to be *in vivo* active against Rab GGTase in COS-7 cell. These three peptide inhibitors all exhibited inhibition of Rab GGTase at 100 μM . **59** and **80** also showed *in vivo* activity against Rab GGTase at 50 μM , although the band color is not as intense as those shown at 100 μM . The three peptide inhibitors did not exhibit any inhibition at 10 μM as shown from Figure 19.

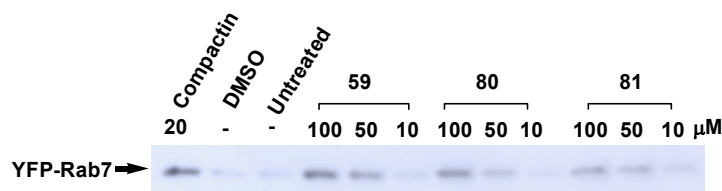


Figure 19. Western Blot of the *in vivo* assay. Cells over-expressing YFP-Rab7 were treated with 20 μM compactin, which inhibits the synthesis of isoprenyl lipid, as a positive control and with 1/1000v/v DMSO as a negative control. The inhibitors were screened at three different concentrations, 100 μM , 50 μM and 10 μM . Cell lysates were prenylated *in vitro* with Biotin labeled geranylgeranyl analogs, resolved by SDS-PAGE, Western blotted and analyzed with HRP-Streptavidin. The bands correspond to YFP-Rab7.

The estimated IC_{50} values of the three *in vivo* active compounds were calculated by integration of the band intensity. By fitting the data to the quadratic equation using Grafit, the estimated IC_{50} values of **59**, **80** and **81** are 47 μM , 60 μM and 52 μM respectively.

4.3.4 Selectivity studies of inhibitors towards Rab GGTase, FTase and GGTase I

Three selected compounds, **59**, **80** and **81**, were subjected to SDS-PAGE end-point gel assays for their selective inhibitory activity studies towards two other prenyltransferase, FTase and GGTase I. The IC_{50} values of the three selected compounds towards Rab GGTase were also determined using gel assay to give supplementary data for the 96-well plate format assay and also to have standard comparison with FTase and GGTase I.

The assay was performed using the same principle as in 96-well plate format. In an eppendorf tube, protein substrate GST-Rho A and GST-K Ras, and prenyltransferases GGTase I and FTase were incubated with inhibitors in buffer and 5% DMSO at 37°C for 2 minutes respectively. Fluorescent substrates NBD-FPP and NBD-GPP of GGTase I and FTase respectively were added to the mixture to initiate the prenylation reaction. The reaction mixture was incubated at 37°C for 10 minutes and quenched by addition of excess SDS-PAGE buffer. The reaction mixture was then subjected to SDS-PAGE to determine the fluorescent intensity of bands corresponding to the NBD-isoprenylated GTPase in the gel. The fluorescent intensity was determined by the integration of the corresponding bands. IC₅₀ of the peptide inhibitors towards Rab GGTase were determined in the same manner as FTase and GGTase I.

Table 9 shows the IC₅₀ values of three inhibitors towards FTase, GGTase I and Rab GGTase determined by SDS-PAGE assay. The selectivity data of a previously identified inhibitor, **EGR 1120**, towards these three prenyltransferase was included for comparison. The IC₅₀ value determined using gel assay were highly comparable to the value established by 96-well plate format. In general, the IC₅₀ value determined using SDS-PAGE gel assay was about 2 times higher than the results derived from 96-well plate assay. The consistent difference of plate format and gel assay for three structurally similar inhibitors indicates that the assay used for the screening of Rab GGTase inhibitors is indeed very reliable.

Table 9. Comparison of IC₅₀ values of inhibitors towards FTase, GGTase I and Rab GGTase using 96-well plate format continuous fluorescence assay and SDS-PAGE assay

Inhibitors	Rab GGTase		FTase (Gel assay)	GGTase I (Gel assay)
	Plate assay	Gel assay		
81	0.97 ± 0.1	2.7 ± 0.2	29 ^a	>100
80	2.4 ± 0.7	4.4 ± 0.4	42 ^b	>100
59	4.9 ± 0.6	10 ± 0.9	36	61
EGR 1120	21	14	14	5.2

a: The inhibitor showed about 50% inhibition at the range of 6-100 μM concentration; b: The inhibitor showed about 50% inhibition at the range of 25-100 μM concentration

As shown in Table 9, **81** and **80** exhibit very high inhibitory selectivity towards Rab GGTase over GGTase I. The IC₅₀ of both inhibitors towards GGTase I are above 100 μM concentration which makes **81** and **80** at least 50 and 20 times (compared with gel assay) more specific towards Rab GGTase over GGTase I respectively. Compound **59** is not so selective, as it exhibits IC₅₀ value towards Rab GGTase at 10 μM and GGTase I at 61 μM.

The three peptides exhibit similar IC₅₀ value towards FTase. The IC₅₀ of **81** and **80** towards FTase gave 50% inhibition of the enzyme at the range of 6-100 μM for **81** and 25-100 μM for **80**. The reasons of this inhibition pattern still remain unknown. Third peptide **59** shows good nonlinear regression curve and give IC₅₀ of FTase at 36 μM. Due to the structural similarity of the three peptides used for selectivity measurement, one can assume that **80** and **81** will also exhibit IC₅₀ value between 30 μM to 40 μM to FTase.

The three peptides were also compared with the previously identified potent peptide inhibitor **EGR 1120** of Rab GGTase. At the concentration of 50 μM, **EGR 1120** does not show high selectivity for all three enzymes. Both **81** and **80** showed excellent inhibition of Rab GGTase activity at 50 μM where enzyme activity drops to 20% and below. FTase was also inhibited to around 50 % activity. However, the inhibition ability of **80** and **81** towards GGTase I is very weak, as the enzyme still exhibited around 85 % activity at 50

μM (Figure 20). On the other hand, **59** shows strong inhibition at $50 \mu\text{M}$ towards all three enzymes. The selectivity experiments were performed by Yaowen Wu.

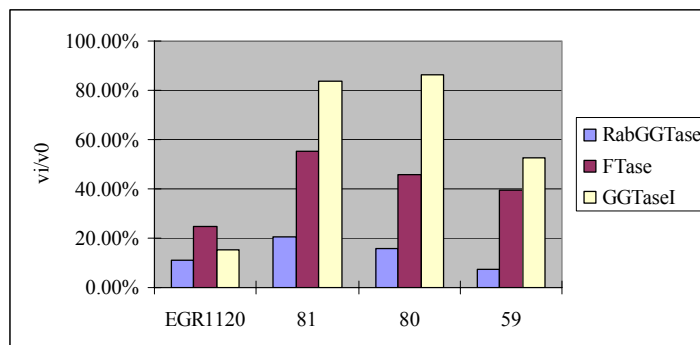


Figure 20. Initial reaction velocity of four inhibitors **EGR 1120**, **81**, **80** and **59** at $50 \mu\text{M}$.

In summary, the three inhibitors, **59**, **80**, and **81**, show generally high inhibition specificity towards Rab GGTase. The peptides do not inhibit FTase and GGTase I at low micro molar concentration. The high specificity of these three peptides promised potential usage as selective molecular sensor to study biological pathway involving Rab proteins over Ras and Rho proteins in cell and molecular biology.

4.3.5 Kinetic analysis of compound **81** towards Rab GGTase inhibition

The most potent *in vitro* compound **81** in this peptide library was subjected to kinetic studies in order to determine the possible mode of inhibition. The experiment was conducted with NBD-FPP **1** at different concentration together with a constant concentration of Rab-7:REP-1 at $1.2 \mu\text{M}$ and Rab GGTase at $0.08 \mu\text{M}$ respectively. The concentration of inhibitor **81** used in this experiment was $4 \mu\text{M}$ and $8 \mu\text{M}$ respectively. The profile of Lineweaver-Burk plot suggested that **81** is a non-competitive inhibitor with respect to NBD-FPP, as it has the intercept point at X-axis (Figure 21).

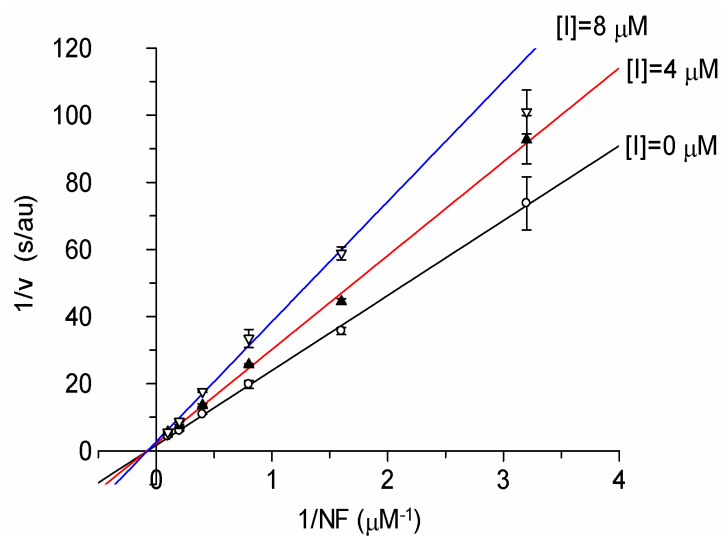


Figure 21. Lineweaver-Burk plot against NBD-FPP with constant concentration of Rab7:REP-1 of 1.2 μM and 0.08 μM Rab GGTase. The concentrations of inhibitor **81** were as indicated in the plot.

A titration experiment was performed to determine the K_d value of inhibitor **81** with Rab GGTase and also to confirm the mode of inhibition (non-competitive inhibitor of Rab GGTase) as obtained from Lineweaver-Burk plot. Figure 22 shows the raw data for a titration of NBD-FPP:Rab GGTase with **81** and finally with GGPP.

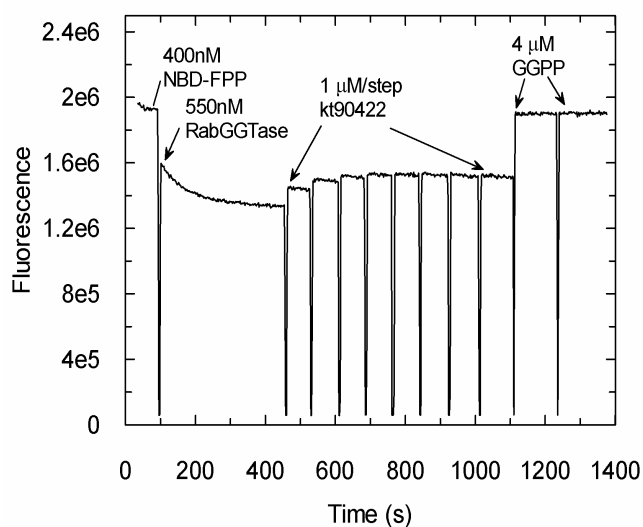


Figure 22. Titration curve of NBD-FPP:Rab GGTase with **81** and finally with GGPP.

The initial level of the fluorescence signal in Figure 22 represents the fluorescence of free NBD-FPP (400 nM). In the first step, Rab GGTase was added to a final concentration of 550 nM. Subsequently, **81** was titrated into the cuvette in 1 μ M units each addition. Finally, GGPP was added to a final concentration of 4 μ M.

As shown in Figure 22, the fluorescence signal decreased dramatically after the addition of Rab GGTase to NBD-FPP, suggesting binding of NBD-FPP **1** to Rab GGTase. With an increasing concentration of **81** in the solution, there was a dose-dependent increase in fluorescence, consistent with dissociation of the NBD-FPP from Rab GGTase. This displacement of NBD-FPP **1** reached saturation after 5 μ M of inhibitor was added. At this point an excess of GGPP was added to the reaction, the fluorescence increased to the level of free NBD-FPP, indicating that the NBD-FPP **1** was then fully displaced.

This initial displacement of NBD-FPP **1** suggests that binding of **81** to Rab GGTase might occur at a site close to the lipid substrate binding site and has influenced the lipid substrate binding with Rab GGTase at the beginning of titration. The saturation of fluorescent signal after addition of 5 μ M inhibitor further verified that **81** is indeed a non-competitive inhibitor to Rab GGTase. This finding is also consistent with that from the enzyme kinetics experiment using Lineweaver-Burk plot, indicating **81** is mostly non-competitive to the lipid substrate of Rab GGTase, hence, NBD-FPP **1**.

Fitting of the data from titration experiment (Figure 22) by numerical simulation to a non-competitive model led to a K_d value of 645 nM for the interaction of **81** with Rab GGTase (Figure 23). Titrations were fitted using the quadratic equation in the program Grafit 5 (Erithacus Software). The fits were performed using a model file that allows simulation and fitting to a set of numerical equations.

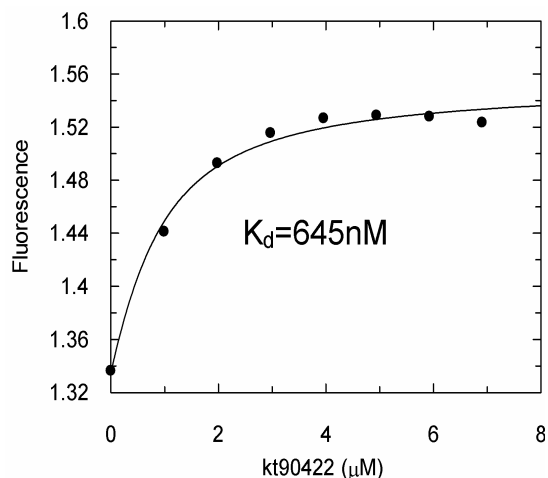


Figure 23. The raw data from Figure 22 were fitted by numerical simulation to a non-competitive model to give a K_d value of 645 nM for compound **81** with Rab GGTase.

A further titration experiment was conducted to elucidate the binding of **81** to Rab GGTase. An independent co-titration experiment was performed in which Rab GGTase was titrated into 200 nM NBD-FPP **1** in the absence of **81** (open circle), in the presence of 2 μ M (filled triangle) and 5 μ M **81** (filled square) respectively (Figure 24).

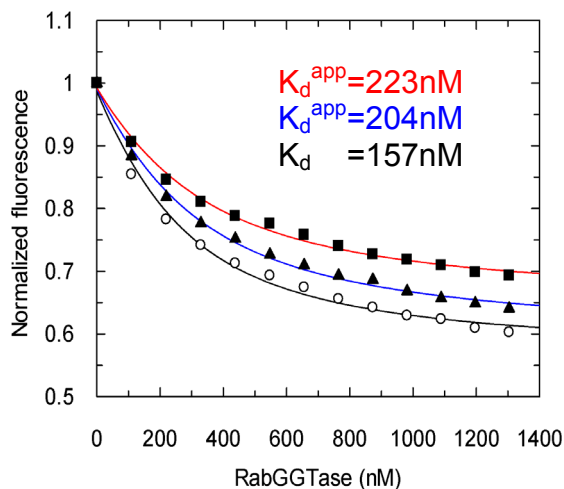


Figure 24. Titration of 200 nM solution of NBD-FPP with Rab GGTase in the absence of **81** (open circle and white line) and in the presence of 2 μ M (filled triangle and blue line) and 5 μ M **81** (filled square and red line). The data were fitted with a quadratic equation to give apparent K_d values. The fluorescence of NBD was excited at 479 nm, and the data collected at 547 nm.

A similar inhibition trend was observed when the titration in the presence of **81** was compared with the free titration (in the absence of an inhibitor). When the data was fitted to a quadratic equation, an apparent K_d value of 157 nM was obtained for NBD-FPP **1** with Rab GGTase in the absence of the inhibitor, and apparent K_d value of 204 nM and 223 nM in the presence of 2 μ M and 5 μ M of **81** respectively. The similar apparent K_d value in the absence and presence of the inhibitor indicate that the inhibitor does not weaken the affinity of NBD-FPP **1** binding to Rab GGTase and it is independent of inhibitor's concentration. This data provides further evidence that **81** is a non-competitive inhibitor towards Rab GGTase.

Fitting the data obtained above by numerical simulation (Figure 24) to a non-competitive model led to a genuine K_d value of 486 nM for the interaction of **81** with Rab GGTase (Figure 25). This result correlates very closely with the affinity of **81** to Rab GGTase obtained from Figure 22 ($K_d = 645$ nM).

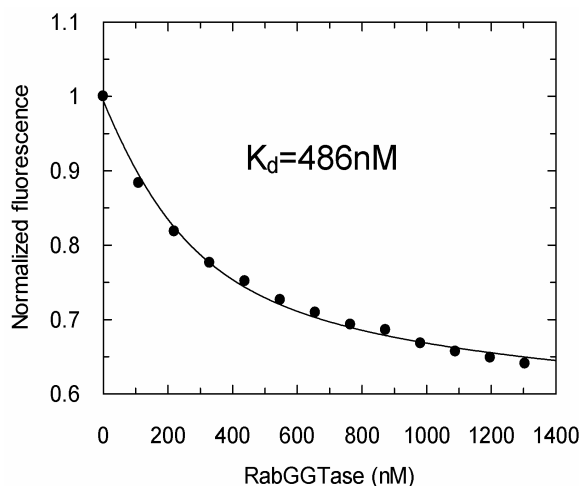


Figure 25. Numerical simulation of **81** to a non-competitive model to give a K_d value of 486 nM to Rab GGTase.

The data shown from the Lineweaver-Burk plot and two different titration experiments indicate that **81** should be a non-competitive inhibitor of Rab GGTase. The two different titration methods gave similar K_d values and complement each other by providing valid

kinetic data of **81** to Rab GGTase. From the titration results obtained from Figure 22, the binding site of **81** might be very close to prenyl binding site of Rab GGTase due to the initial displacement of NBD-FPP **1** from the enzyme. Further details on the inhibitor binding site in Rab GGTase can only be disclosed with more biochemistry experiments and X-ray crystallography. The kinetic experiments were performed by Yaowen Wu

4.3.6 Summary and discussions of biochemical investigation of Rab GGTase inhibitors

Out of the 382 peptides screened, 18 peptides were found to be active against Rab GGTase. The IC₅₀ of these peptide inhibitors were determined and one of them, **81**, gave an IC₅₀ value as low as 0.96 μM. Structure activity relationship analysis of the peptide library revealed that peptides containing long lipid chains at its N-terminus and moieties with metal chelating ability at C-terminus were found to be the most active substrates to inhibit Rab GGTase. Furthermore, incorporation of L-histidine amino acid together with the long lipid chain and zinc ion chelating residues improves the IC₅₀ value. This is probably due to the potential binding of L-histidine to the zinc ion in the Rab GGTase pocket.

Three compounds, **59**, **80** and **81**, were found to have *in vivo* activity against Rab GGTase. Selectivity screening of these three peptides against FTase, GGTase I and Rab GGTase using gel assay showed that the peptides selectively inhibit Rab GGTase, but gave no inhibition against GGTase I and only moderate activity against FTase. The kinetic analysis of **81** by titration and Lineweaver-Burk plot confirmed that the inhibitor is a non-competitive inhibitor of Rab GGTase with respect to the fluorophore lipid substrate **1**.

From the bioactivity results presented in Table 7, 8, 9 and in appendix, the initial approach of incorporation a long lipid chain residues in the peptides works very well. The large hydrophobicity of long lipid chain can impart the driving force to the peptides to diffuse the inhibitors to the hydrophobic pocket of Rab GGTase. In contrast to Rab

GGTase, FTase and GGTase I which known as the CAAX prenylases, both recognize the tetrapeptide motif CAAX at the C-terminus of their substrates and catalyze the transfer of FPP and GGPP to the cysteine residues. The different catalytic nature of three prenyltransferases has helped to explain the high inhibition specificity of three peptides **59**, **80** and **81** towards Rab GGTase over FTase and GGTase I. **59**, **80** and **81** do not contain any simple aliphatic amino acids and cysteine, therefore the low bioactivity of these three peptides towards FTase and GGTase I could be understood.

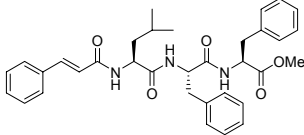
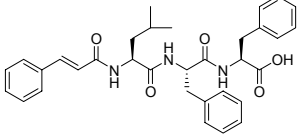
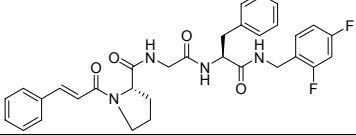
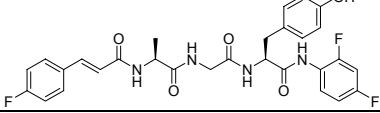
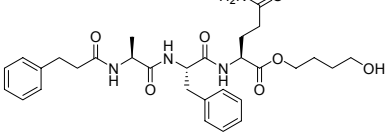
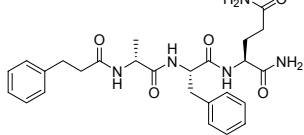
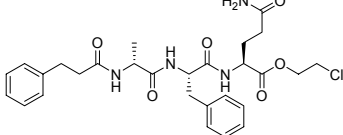
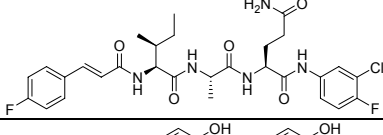
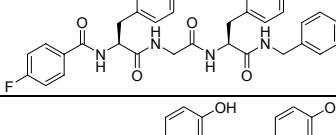
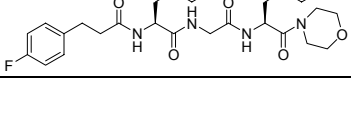
Several potent peptide inhibitors for Rab GGTase have been successfully optimized and synthesized starting from a previously validated FTase peptides library.⁵⁵ The synthetic modification of the FTase inhibitors based on the incorporation of long lipid chain moiety and potential zinc ion binding residues have diluted the effect of cross-activity for FTIs with Rab GGTase. This results demonstrat that cross-activity of FTIs with Rab GGTase and GGTase I can be modulated by rationale design of inhibitors.

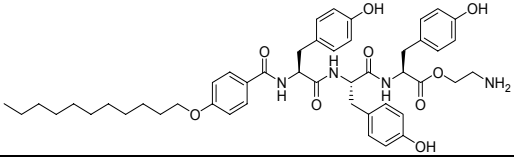
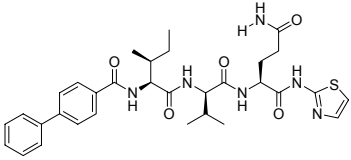
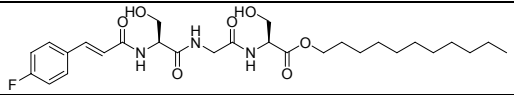
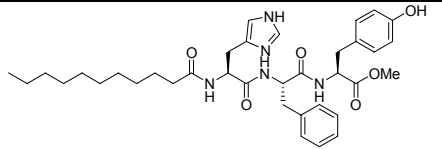
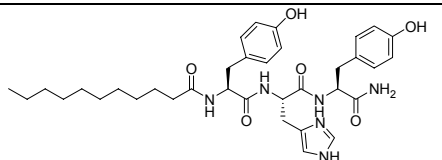
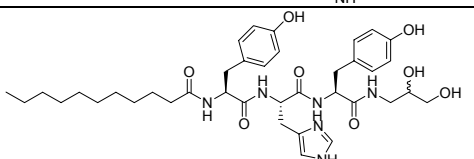
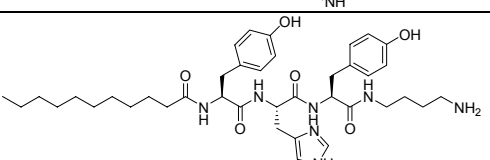
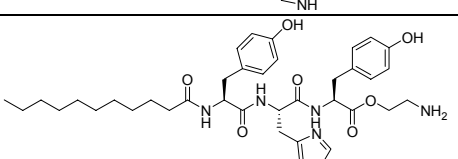
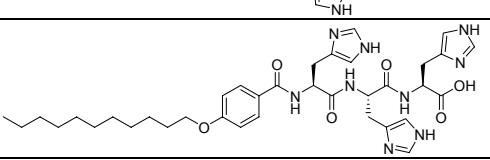
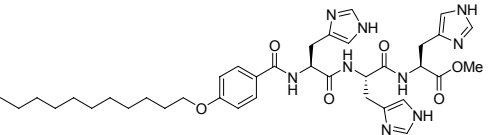
5 Conclusions and Outlook

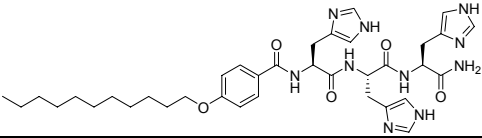
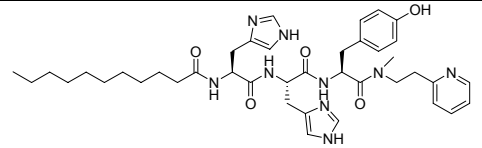
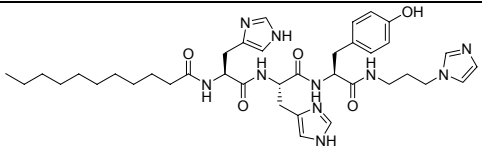
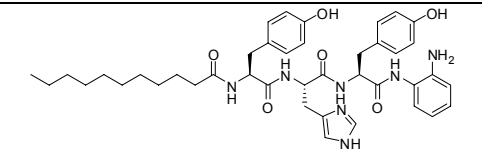
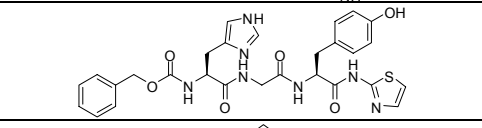
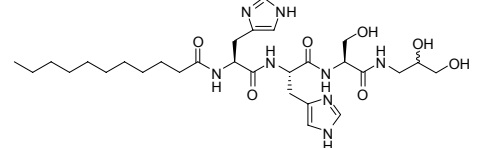
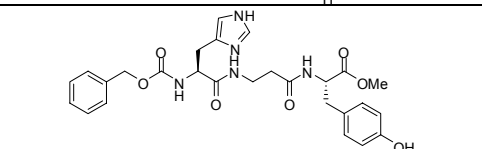
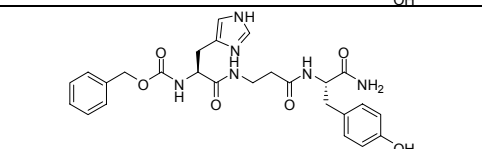
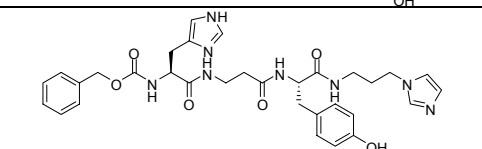
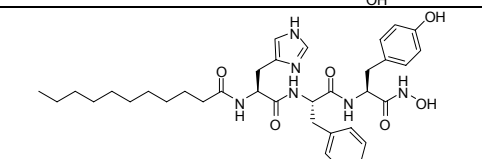
In conclusion, the synthesis of Pepticcinnamine E derivatives using safety catch linker and building block strategy has successfully generated 382 peptides with different chemical functionalities at N-terminus and C-terminus with the incorporation of various amino acids at the peptides central core. The bioactivity screen of these peptides has revealed several potent and selective inhibitors against Rab GGTase over FTase and GGTase I. The identification of three *in vivo* active peptides **59**, **80** and **81** in this peptides library has increased the value of the work.

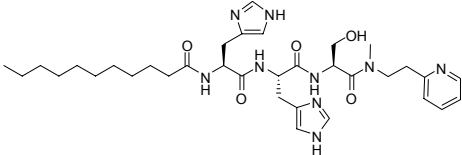
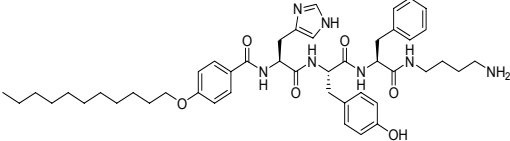
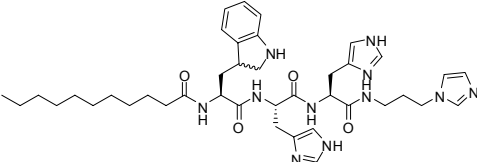
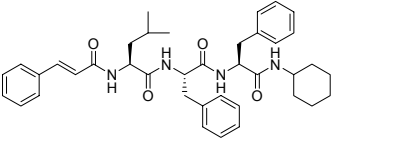
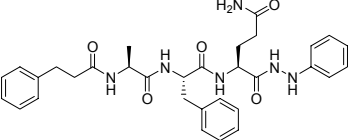
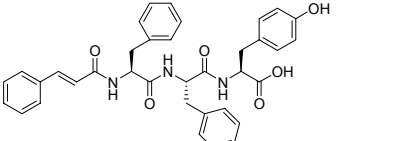
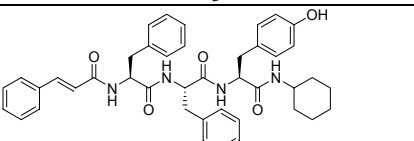
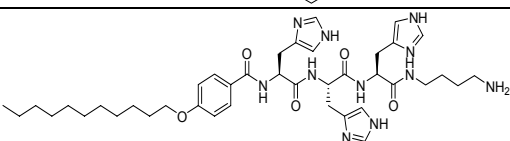
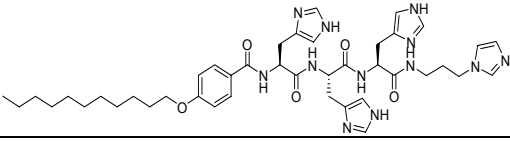
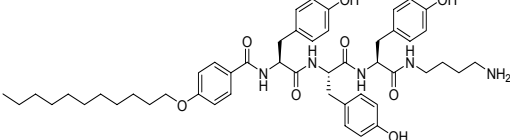
The future work for this project will be the modification of N-terminus and C-terminus moieties together with the amino acids sequence of the derivatives, based on the identified potent *in vitro* peptide inhibitors, **59**, **80** and **81** to increase the bioactivity of the peptides and at the same time improve the inhibition selectivity of Rab GGTase over FTase and GGTase I. The binding site of the inhibitors should also be characterized to facilitate the search for more potent and selective inhibitors.

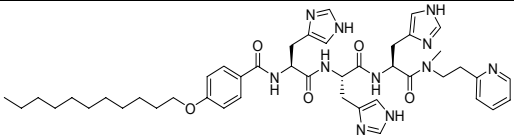
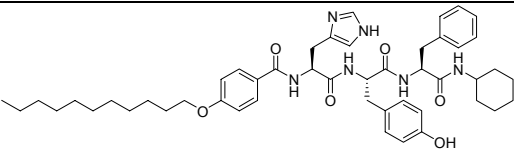
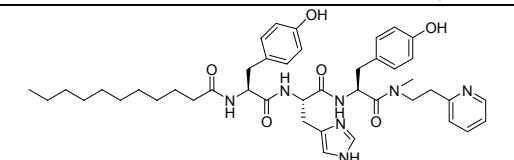
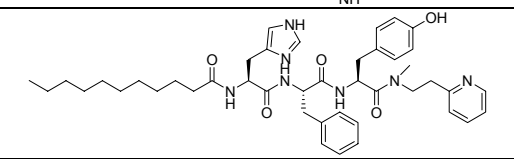
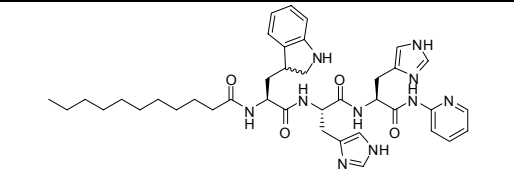
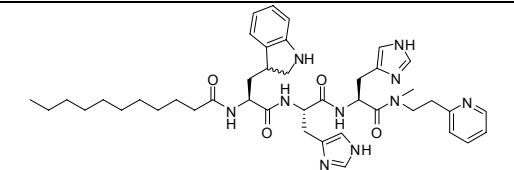
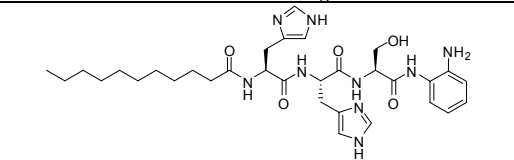
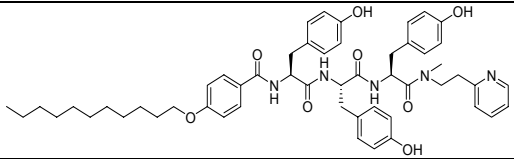
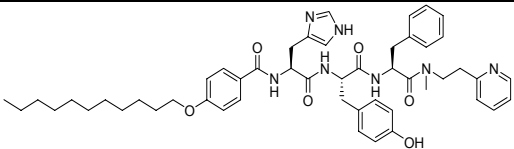
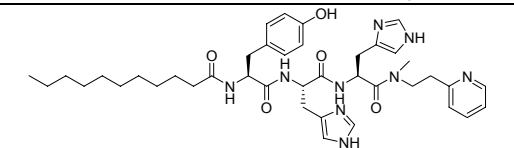
6 Appendix

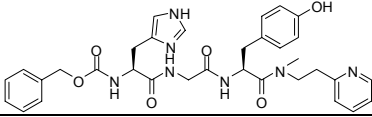
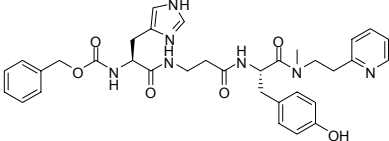
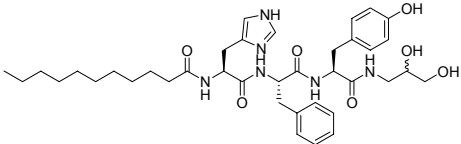
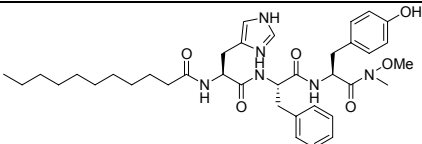
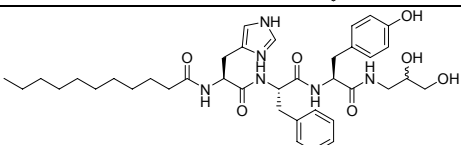
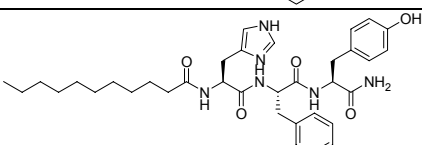
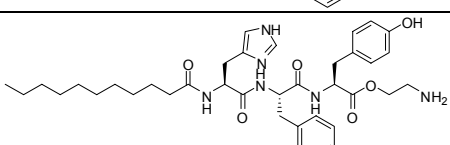
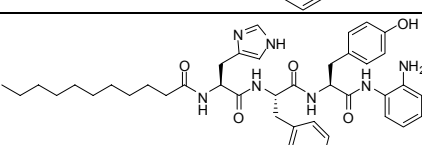
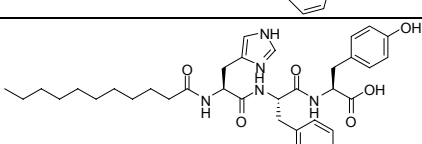
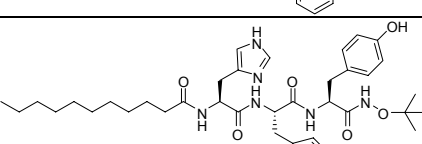
Entries	Nr.	Peptides	Yield (Purity) %	Rab GGTase Activity % (IC ₅₀)
1	38		18 (> 95)	5 (62 μM)
2	39		3 (> 95)	39 ^a
3	40		28 (> 85)	24 ^a
4	41		23 (> 90)	-6 ^a
5	42		3 (> 95)	4 ^a
6	43		5 (> 95)	113 ^a
7	44		1 (> 95)	95 ^a
8	45		1 (> 95)	64 ^a
9	46		10 (> 95)	123 ^b
10	47		7 (> 95)	94 ^b

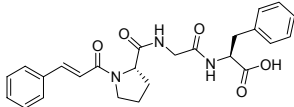
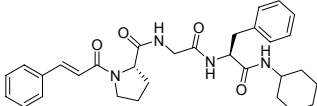
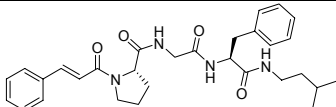
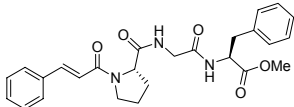
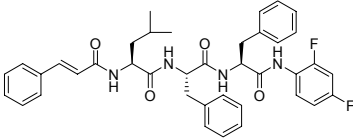
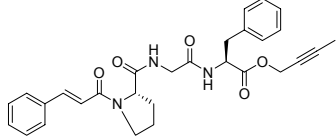
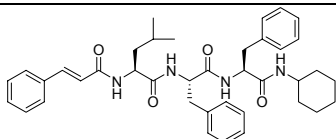
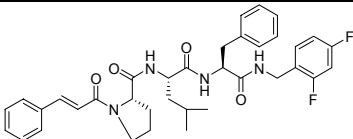
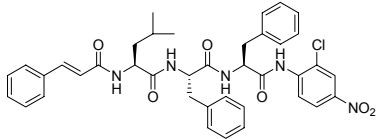
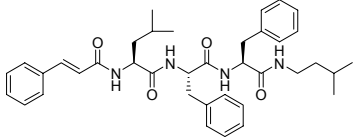
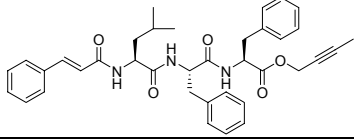
Entries	Nr.	Peptides	Yield (Purity) %	Rab GGTase Activity % (IC ₅₀)
11	48		4 (> 95)	26 (28 μM) ^b
12	49		6 (> 95)	60 ^a
13	50		6 (> 95)	86 ^b
14	51		25 (> 95)	100 ^b
15	52		2 (> 95)	92 ^b
16	53		20 (> 95)	106 ^b
17	54		22 (> 95)	68 ^b
18	55		7 (> 95)	60 ^b
19	56		20 (> 95)	45 ^b
20	57		11 (> 95)	86 ^b

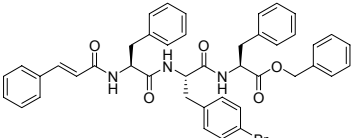
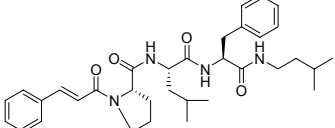
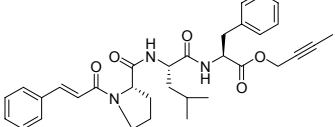
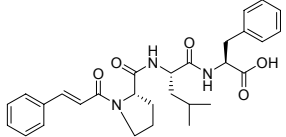
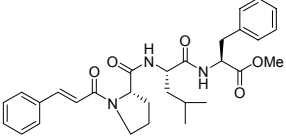
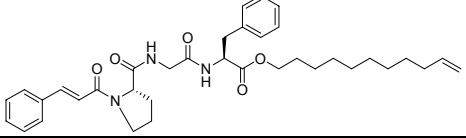
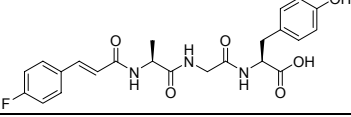
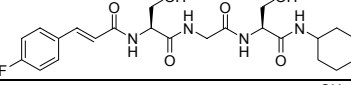
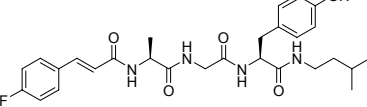
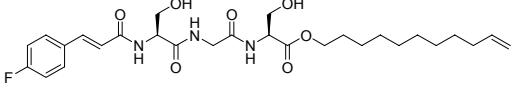
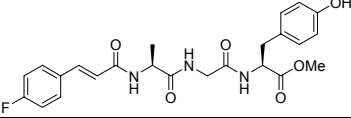
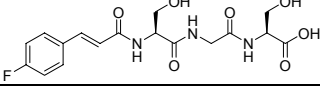
Entries	Nr.	Peptides	Yield (Purity) %	Rab GGTase Activity % (IC ₅₀)
21	58		7 (> 95)	98 ^b
22	59		12 (> 95)	2 (5 μM) ^b
23	60		15 (> 95)	92 ^b
24	61		20 (> 85)	77 ^b
25	62		2 (> 95)	87 ^b
26	63		26 (> 95)	75 ^b
27	64		4 (> 95)	88 ^b
28	65		1 (> 95)	89 ^b
29	66		6 (> 95)	88 ^b
30	67		13 (> 95)	58 ^b

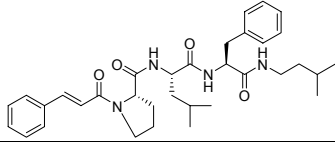
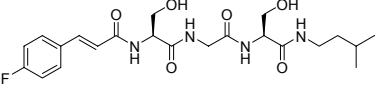
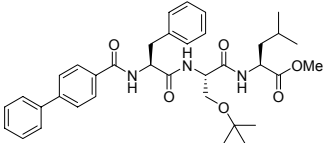
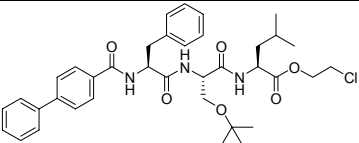
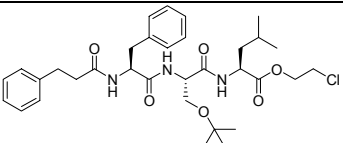
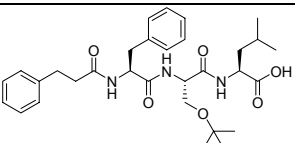
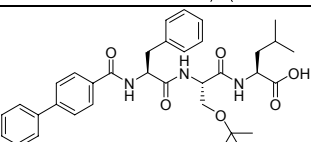
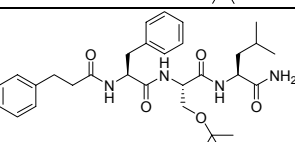
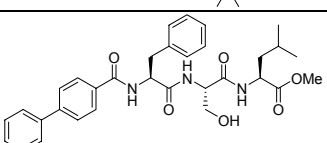
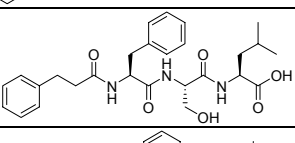
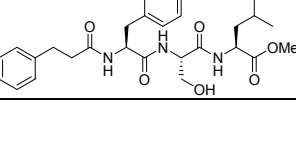
Entries	Nr.	Peptides	Yield (Purity) %	Rab GGTase Activity % (IC ₅₀)
31	68		6 (> 95)	66 ^b
32	69		6 (> 95)	-40 (14 μM) ^b
33	70		20 (> 95)	34 ^b
34	71		18 (> 95)	13 (71 μM)
35	72		2 (> 95)	-14 (37 μM)
36	73		12 (> 95)	11 (42 μM)
37	74		2 (> 95)	20 (68 μM)
38	75		20 (> 95)	-43 (13 μM) ^b
39	76		21 (> 95)	4 (20 μM) ^b
40	77		18 (> 95)	17 (8 μM) ^b

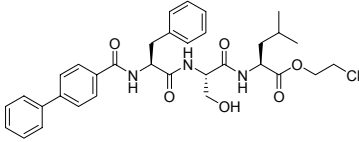
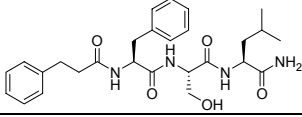
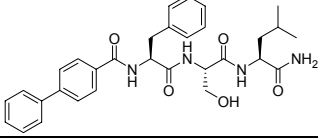
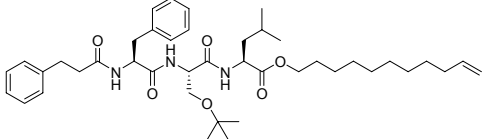
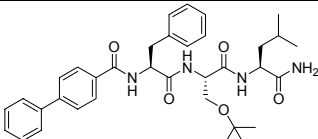
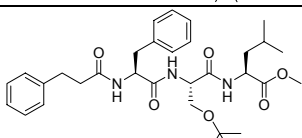
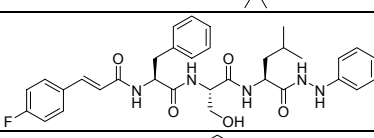
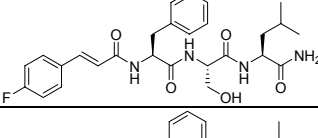
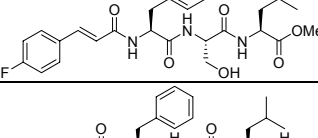
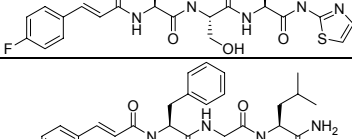
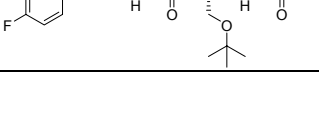
Entries	Nr.	Peptides	Yield (Purity) %	Rab GGTase Activity % (IC ₅₀)
41	78		25 (> 95)	-35 (24 μM) ^b
42	79		1 (> 85)	30 (20 μM) ^b
43	80		12 (> 85)	18 (2 μM) ^b
44	81		18 (> 95)	23 (1 μM) ^b
45	82		9 (> 95)	17 (28 μM) ^b
46	83		14 (> 95)	36 (31 μM) ^b
47	84		23 (> 85)	33 (35 μM) ^b
48	85		2 (> 95)	104 ^b
49	86		2 (> 95)	104 ^b
50	87		10 (> 95)	34 ^b

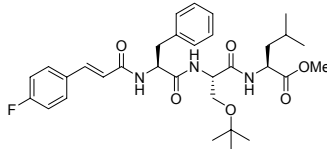
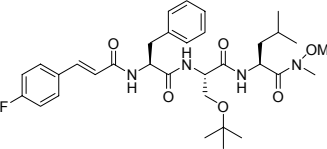
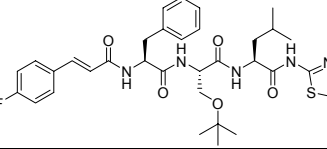
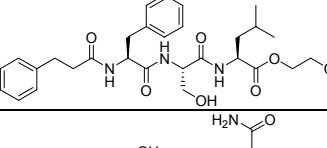
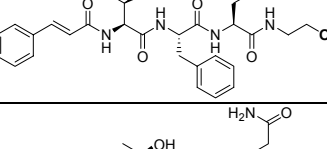
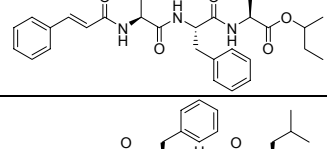
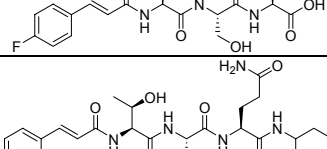
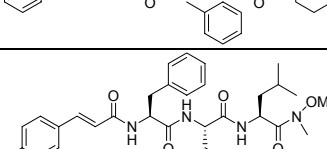
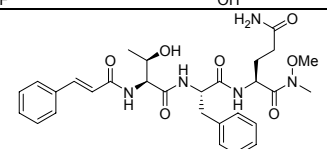
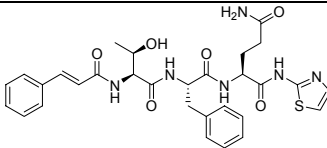
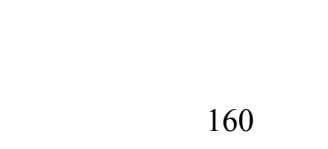
Entries	Nr.	Peptides	Yield (Purity) %	Rab GGTase Activity % (IC ₅₀)
51	88		2 (> 95)	85 ^b
52	89		1 (> 95)	86 ^b
53	90		3 (> 95)	47 ^b
54	91		1 (> 95)	41 ^b
55	92		35 (> 95)	100 ^b
56	93		13 (> 95)	100 ^b
57	94		12 (> 95)	60 ^b
58	95		5 (> 95)	76 ^b
59	96		22 (> 95)	37 ^b
60	97		5 (> 95)	78 ^b

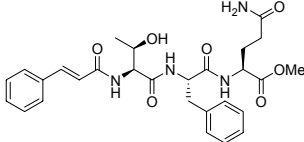
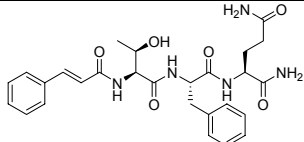
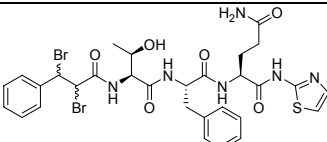
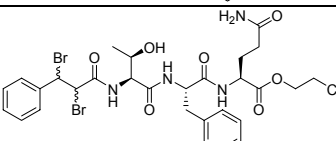
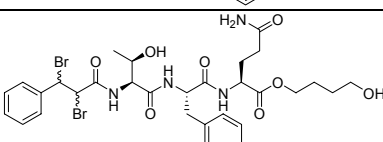
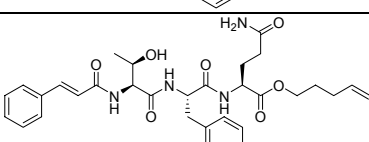
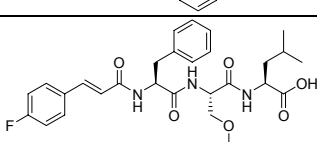
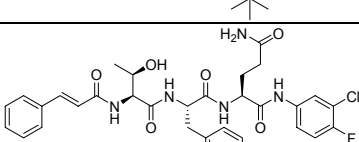
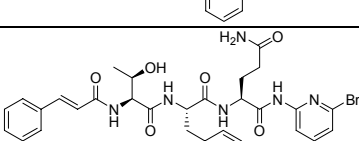
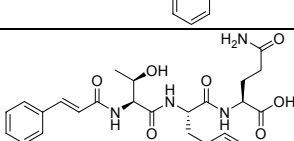
Entries	Nr.	Peptides	Yield (Purity) %	Rab GGTase Activity % (IC ₅₀)
61	98		45 (> 95)	42 ^a
62	99		22 (> 95)	35 ^a
63	100		42 (> 95)	45 ^a
64	101		32 (> 95)	102 ^a
65	102		18 (> 95)	82 ^a
66	103		19 (> 95)	43 ^a
67	104		31 (> 95)	72 ^a
68	105		31 (> 95)	49 ^a
69	106		17 (> 80)	90 ^a
70	107		20 (> 90)	112 ^a
71	108		5 (> 95)	62 ^a

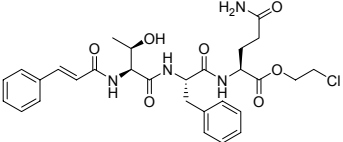
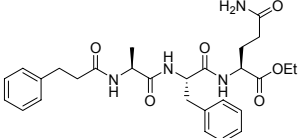
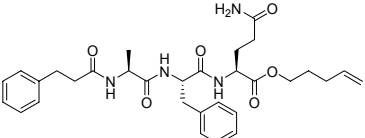
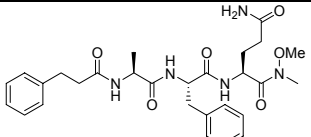
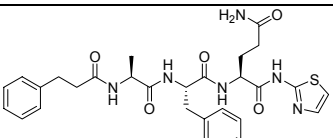
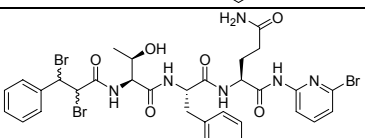
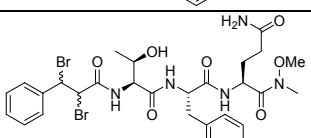
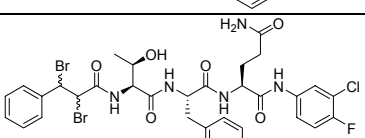
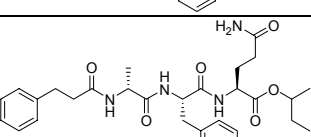
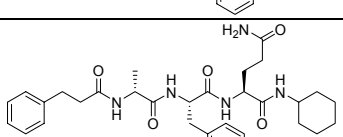
Entries	Nr.	Peptides	Yield (Purity) %	Rab GGTase Activity % (IC ₅₀)
72	109		6 (> 90)	40 ^a
73	110		34 (> 95)	106 ^a
74	111		16 (> 95)	95 ^a
75	112		7 (> 95)	49 ^a
76	113		16 (> 95)	75 ^a
77	114		6 (> 80)	86 ^a
78	115		7 (> 95)	44 ^a
79	116		8 (> 95)	51 ^a
80	117		8 (> 95)	41 ^a
81	118		3 (> 95)	-9 ^a
82	119		10 (> 80)	66 ^a
83	120		6 (> 95)	89 ^a

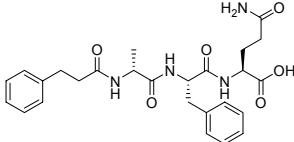
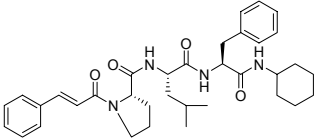
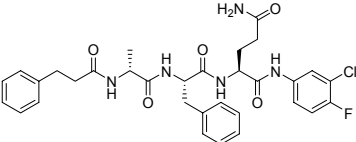
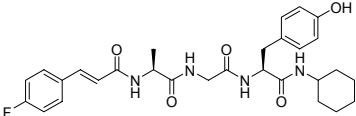
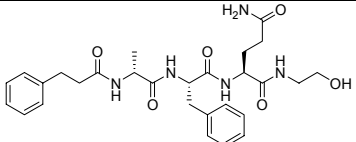
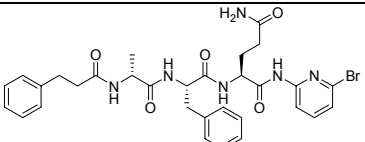
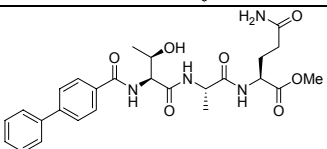
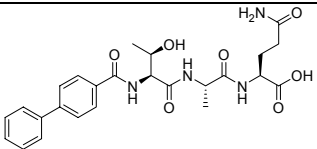
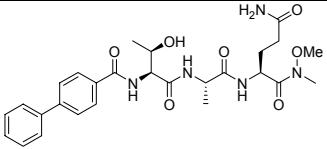
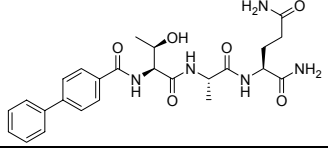
Entries	Nr.	Peptides	Yield (Purity) %	Rab GGTase Activity % (IC ₅₀)
84	121		20 (> 95)	130 ^a
85	122		17 (> 90)	92 ^a
86	123		29 (> 95)	97 ^a
87	124		16 (> 95)	117 ^a
88	125		14 (> 95)	77 ^a
89	126		16 (> 95)	66 ^a
90	127		8 (> 95)	50 ^a
91	128		30 (> 95)	76 ^a
92	129		29 (> 95)	91 ^a
93	130		10 (> 95)	81 ^a
94	131		25 (> 95)	63 ^a

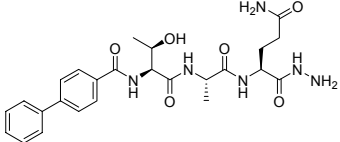
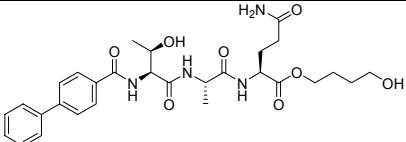
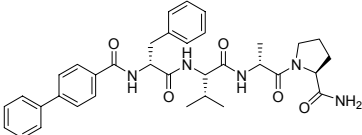
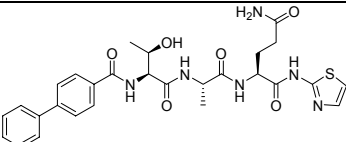
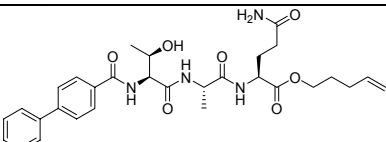
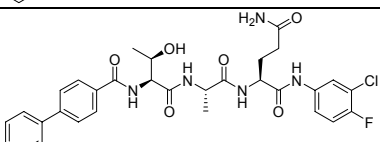
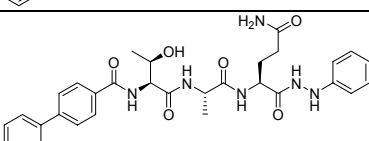
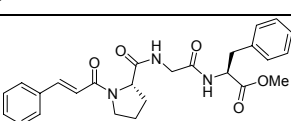
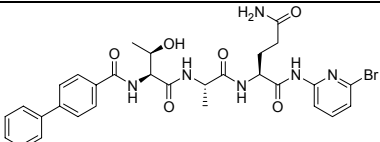
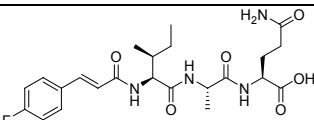
Entries	Nr.	Peptides	Yield (Purity) %	Rab GGTase Activity % (IC ₅₀)
95	132		10 (> 95)	8 ^a
96	133		20 (> 90)	93 ^a
97	134		20 (> 95)	97 ^a
98	135		6 (> 95)	90 ^a
99	136		26 (> 95)	93 ^a
100	137		30 (> 95)	92 ^a
101	138		1 (> 90)	74 ^a
102	139		3 (> 90)	63 ^a
103	140		3 (> 95)	83 ^a
104	141		3 (> 95)	93 ^a
105	142		8 (> 95)	138 ^a

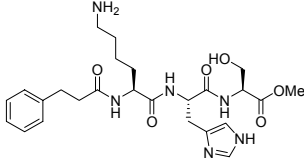
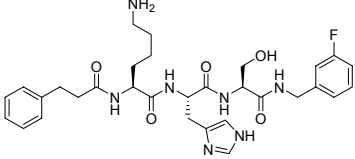
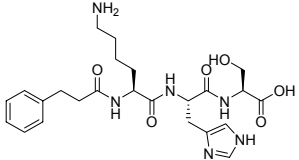
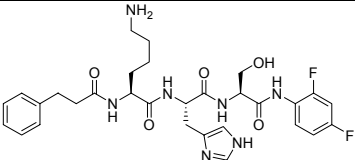
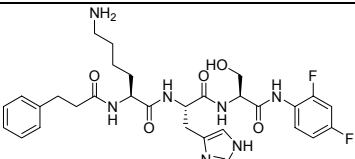
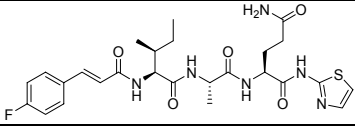
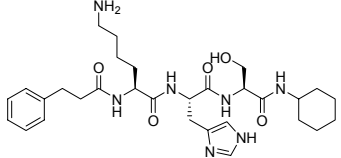
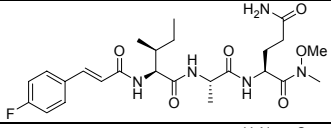
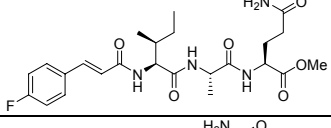
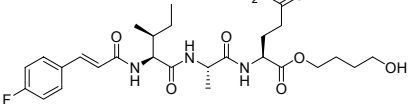
Entries	Nr.	Peptides	Yield (Purity) %	Rab GGTase Activity % (IC ₅₀)
106	143		7 (> 95)	98 ^a
107	144		3 (> 95)	80 ^a
108	145		5 (> 95)	70 ^a
109	146		7 (> 95)	52 ^a
110	147		5 (> 90)	93 ^a
111	148		1 (> 90)	52 ^a
112	149		3 (> 95)	80 ^a
113	150		1 (> 95)	52 ^a
114	151		5 (> 95)	13 ^a
115	152		1 (> 95)	66 ^a
116	153		2 (> 95)	66 ^a

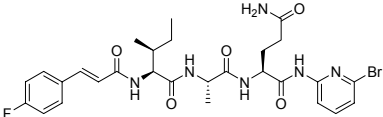
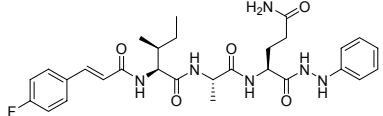
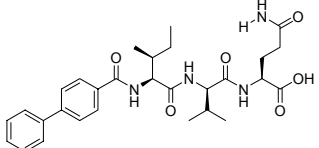
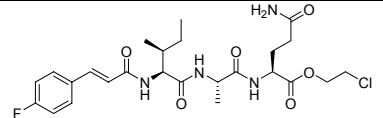
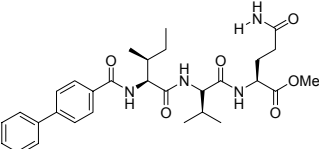
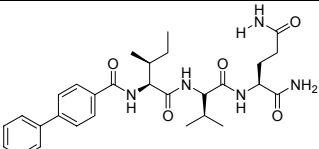
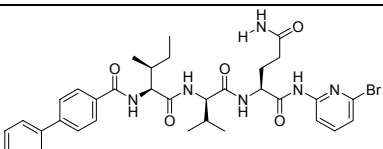
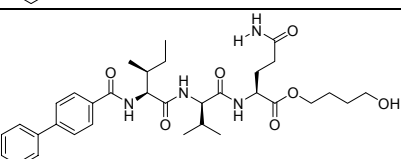
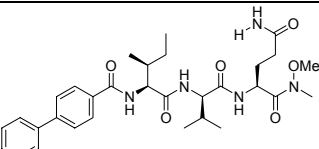
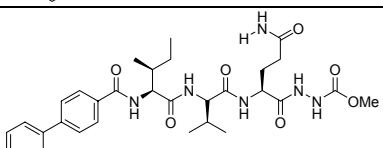
Entries	Nr.	Peptides	Yield (Purity) %	Rab GGTase Activity % (IC ₅₀)
117	154		2 (> 95)	77 ^a
118	155		1 (> 85)	65 ^a
119	156		3 (> 95)	40 ^a
120	157		1 (> 90)	7 ^a
121	158		4 (> 95)	60 ^a
122	159		2 (> 95)	64 ^a
123	160		3 (> 90)	52 ^a
124	161		2 (> 90)	50 ^a
125	162		2 (> 95)	53 ^a
126	163		2 (> 95)	59 ^a

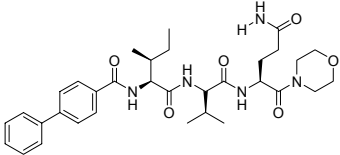
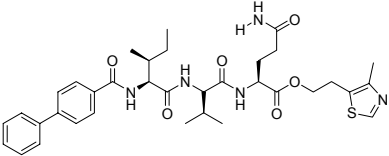
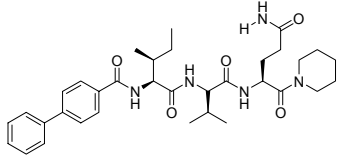
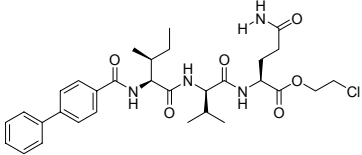
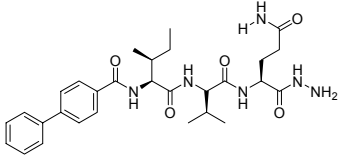
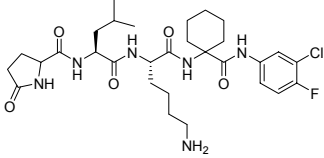
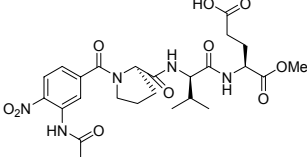
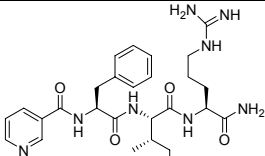
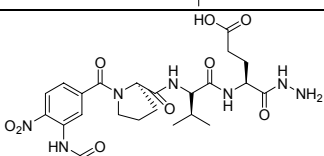
Entries	Nr.	Peptides	Yield (Purity) %	Rab GGTase Activity % (IC ₅₀)
127	164		1 (> 95)	66 ^a
128	165		4 (> 95)	88 ^a
129	166		2 (> 95)	49 ^a
130	167		6 (> 95)	69 ^a
131	168		4 (> 95)	99 ^a
132	169		2 (> 95)	59 ^a
133	170		8 (> 95)	75 ^a
134	171		1 (> 95)	16 ^a
135	172		1 (> 95)	108 ^a
136	173		2 (> 95)	-68 ^a

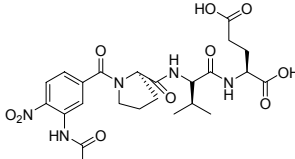
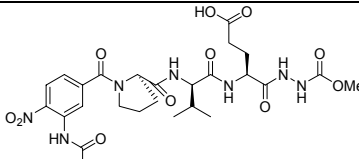
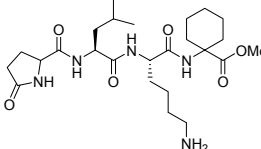
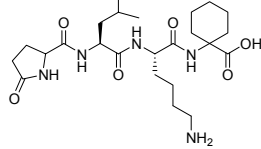
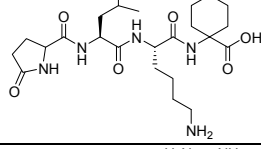
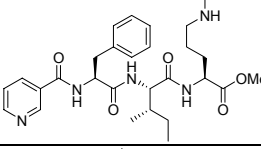
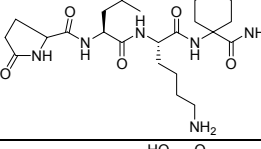
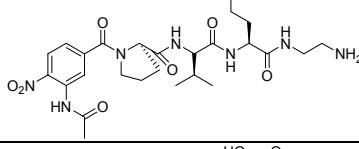
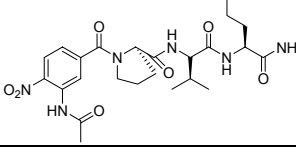
Entries	Nr.	Peptides	Yield (Purity) %	Rab GGTase Activity % (IC ₅₀)
137	174		6 (> 95)	62 ^a
138	175		12 (> 95)	142 ^a
139	176		1 (> 95)	63 ^a
140	177		9 (> 85)	17 ^a
141	178		1 (> 95)	70 ^a
142	179		1 (> 95)	71 ^a
143	180		2 (> 85)	38 ^a
144	181		6 (> 95)	45 ^a
145	182		7 (> 95)	71 ^a
146	183		8 (> 80)	77 ^a

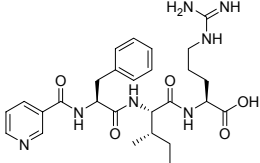
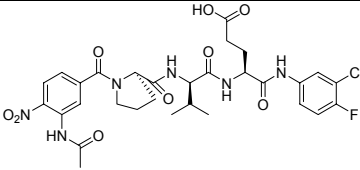
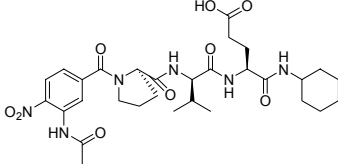
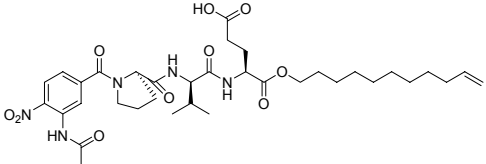
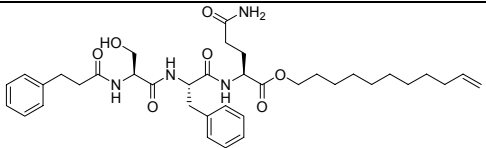
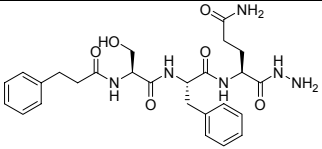
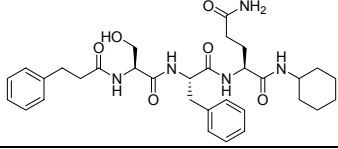
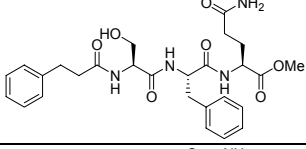
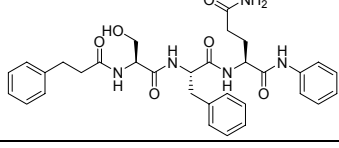
Entries	Nr.	Peptides	Yield (Purity) %	Rab GGTase Activity % (IC ₅₀)
147	184		3 (> 85)	38 ^a
148	185		4 (> 95)	47 ^a
149	186		25 (> 95)	81 ^a
150	187		6 (> 95)	80 ^a
151	188		4 (> 95)	92 ^a
152	189		5 (> 95)	-61 ^a
153	190		1 (> 85)	65 ^a
154	191		5 (> 95)	99 ^a
155	192		6 (> 70)	45 ^a
156	193		1 (> 95)	66 ^a

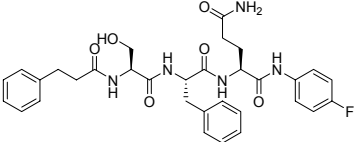
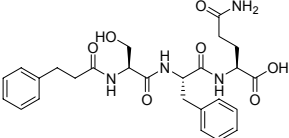
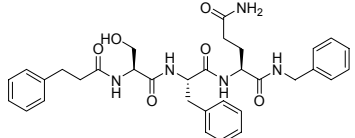
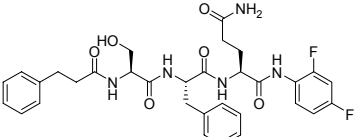
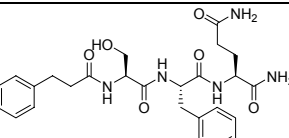
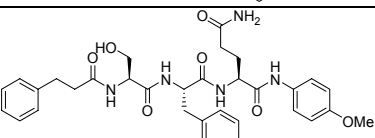
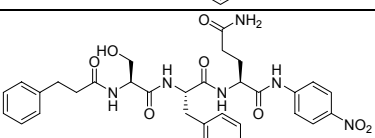
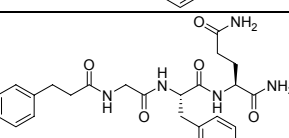
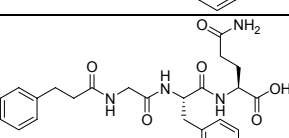
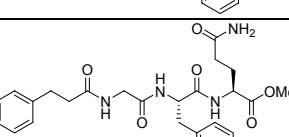
Entries	Nr.	Peptides	Yield (Purity) %	Rab GGTase Activity % (IC ₅₀)
157	194		10 (> 85)	88 ^a
158	195		25 (> 85)	93 ^a
159	196		6 (> 95)	80 ^a
160	197		4 (> 90)	78 ^a
161	198		1 (> 95)	89 ^a
162	199		1 (> 95)	40 ^a
163	200		3 (> 95)	94 ^a
164	201		1 (> 95)	54 ^a
165	202		1 (> 95)	58 ^a
166	203		1 (> 85)	81 ^a

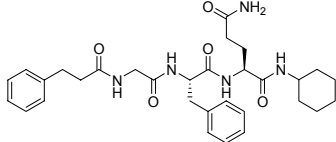
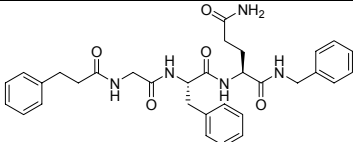
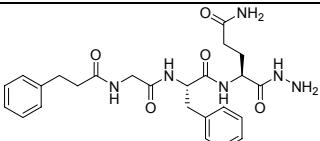
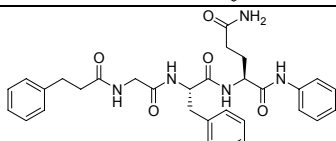
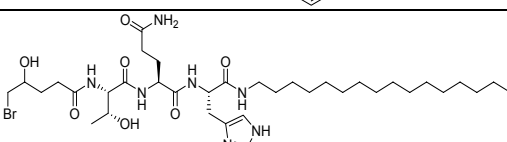
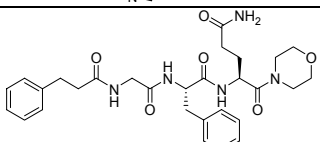
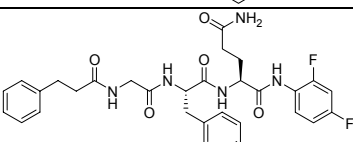
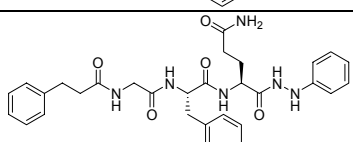
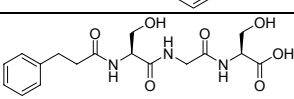
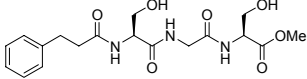
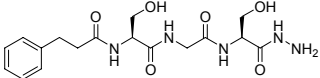
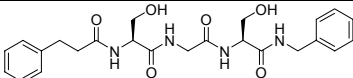
Entries	Nr.	Peptides	Yield (Purity) %	Rab GGTase Activity % (IC ₅₀)
167	204		1 (> 90)	95 ^a
168	205		1 (> 80)	93 ^a
169	206		3 (> 95)	89 ^a
170	207		1 (> 70)	-81 ^a
171	208		2 (> 80)	83 ^a
172	209		5 (> 90)	102 ^a
173	210		1 (> 80)	89 ^a
174	211		3 (> 95)	96 ^a
175	212		5 (> 95)	105 ^a
176	213		2 (> 95)	101 ^a

Entries	Nr.	Peptides	Yield (Purity) %	Rab GGTase Activity % (IC ₅₀)
177	214		7 (> 90)	98 ^a
178	215		1 (> 95)	52 ^a
179	216		3 (> 95)	87 ^a
180	217		2 (> 80)	101 ^a
181	218		1 (> 70)	85 ^a
182	219		6 (> 80)	81 ^a
183	220		3 (> 95)	112 ^a
184	221		5 (> 75)	94 ^a
185	222		7 (> 95)	111 ^a

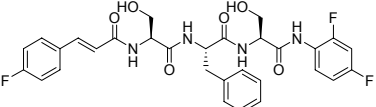
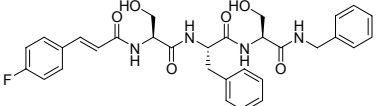
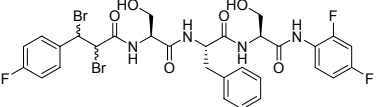
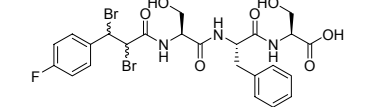
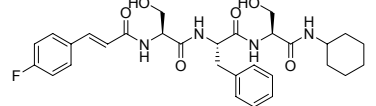
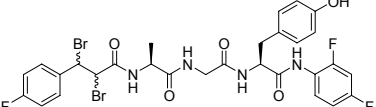
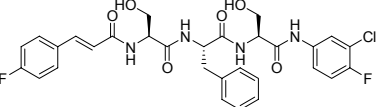
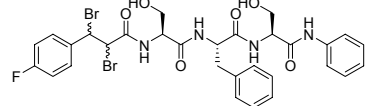
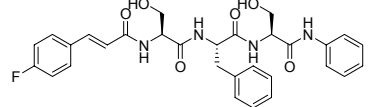
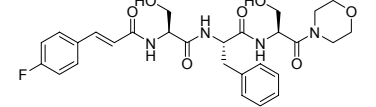
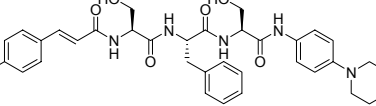
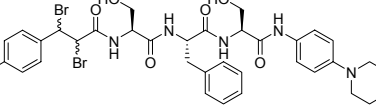
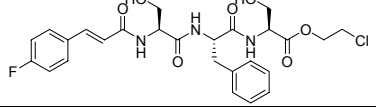
Entries	Nr.	Peptides	Yield (Purity) %	Rab GGTase Activity % (IC ₅₀)
186	223		6 (> 95)	128 ^a
187	224		5 (> 95)	107 ^a
188	225		8 (> 95)	118 ^a
189	226		34 (> 95)	120 ^a
190	227		30 (> 95)	116 ^a
191	228		4 (> 95)	110 ^a
192	229		5 (> 85)	99 ^a
193	230		1 (> 95)	80 ^a
194	231		3 (> 95)	97 ^a

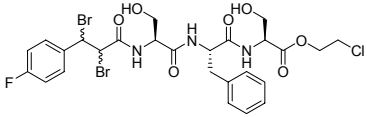
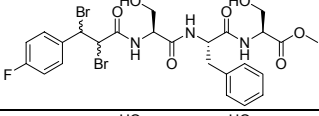
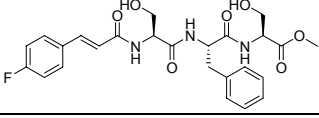
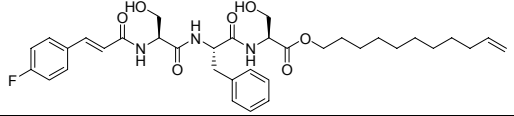
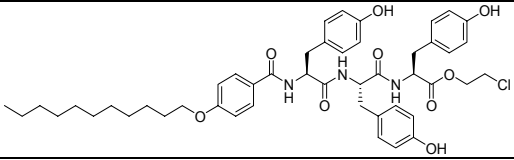
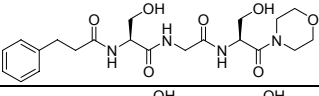
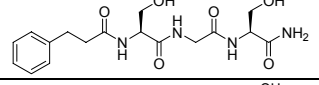
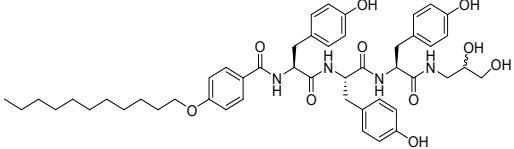
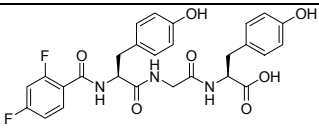
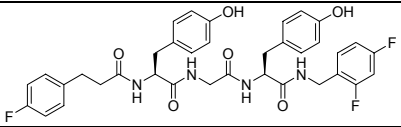
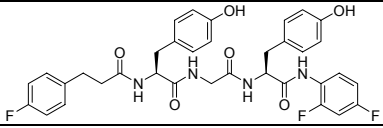
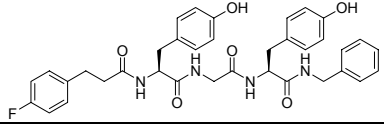
Entries	Nr.	Peptides	Yield (Purity) %	Rab GGTase Activity % (IC ₅₀)
195	232		8 (> 95)	127 ^a
196	233		10 (> 95)	87 ^a
197	234		7 (> 95)	114 ^a
198	235		1 (> 80)	-22 ^a
199	236		3 (> 95)	110 ^a
200	237		12 (> 70)	93 ^a
201	238		4 (> 85)	80 ^a
202	239		9 (> 95)	112 ^a
203	240		15 (> 95)	98 ^a

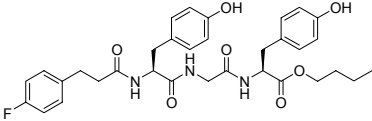
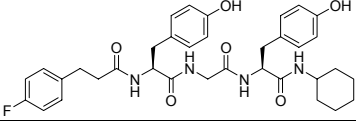
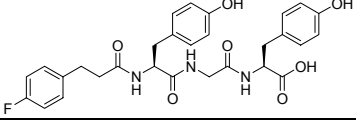
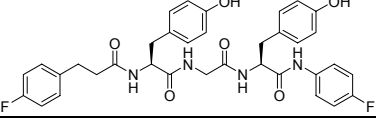
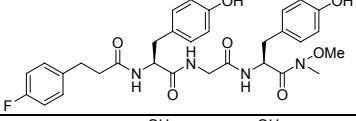
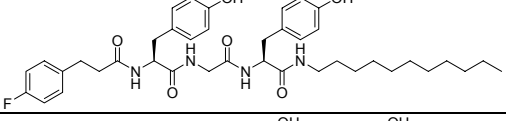
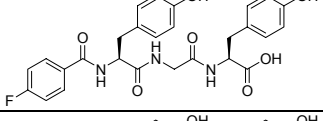
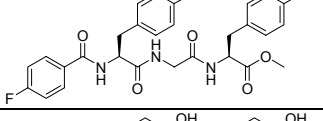
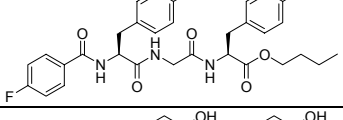
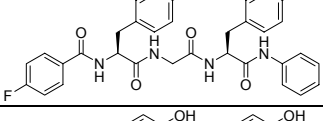
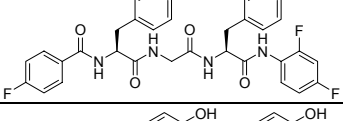
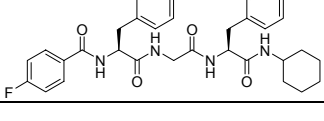
Entries	Nr.	Peptides	Yield (Purity) %	Rab GGTase Activity % (IC ₅₀)
204	241		14 (> 95)	116 ^a
205	242		4 (> 95)	121 ^a
206	243		10 (> 95)	104 ^a
207	244		10 (> 95)	105 ^a
208	245		15 (> 95)	127 ^a
209	246		8 (> 95)	93 ^a
210	247		8 (> 95)	121 ^b
211	248		3 (> 85)	95 ^b
212	249		3 (> 95)	79 ^b
213	250		6 (> 95)	82 ^b

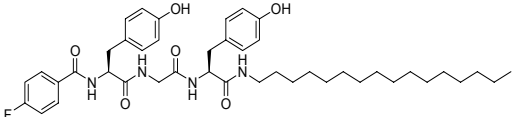
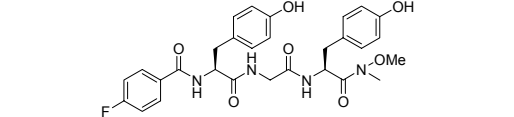
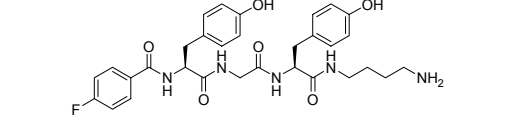
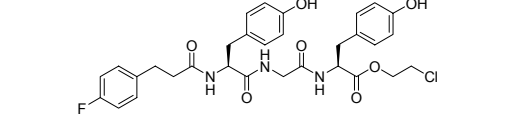
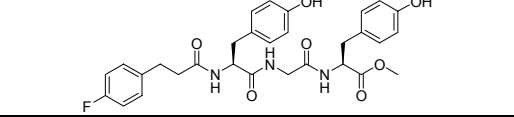
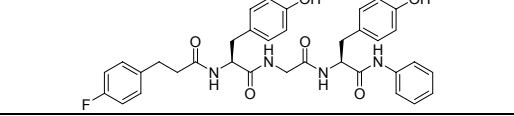
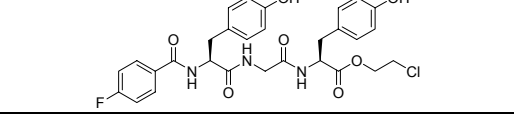
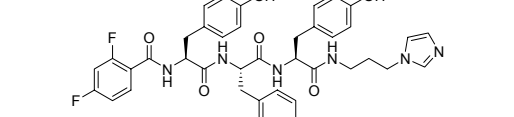
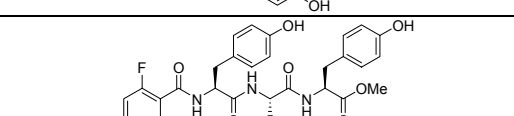
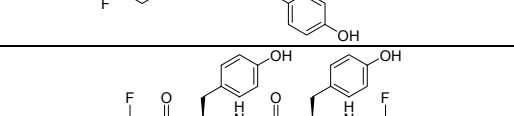
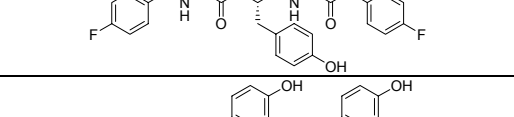
Entries	Nr.	Peptides	Yield (Purity) %	Rab GGTase Activity % (IC ₅₀)
214	251		6 (> 95)	75 ^b
215	252		7 (> 95)	102 ^b
216	253		6 (> 85)	84 ^b
217	254		8 (> 95)	94 ^b
218	255		1 (> 95)	82 ^b
219	256		2 (> 95)	91 ^b
220	257		11 (> 95)	99 ^b
221	258		1 (> 95)	80 ^b
222	259		4 (> 95)	91 ^b
223	260		2 (> 95)	87 ^b
224	261		6 (> 80)	81 ^b
225	262		7 (> 95)	92 ^b

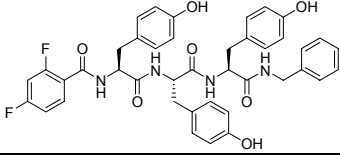
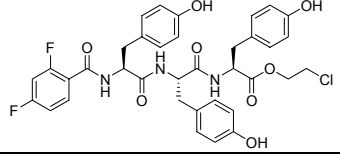
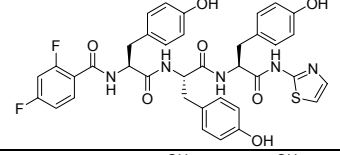
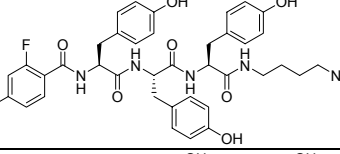
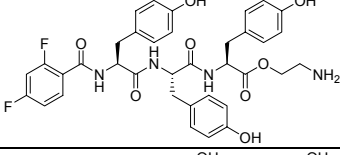
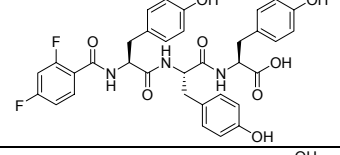
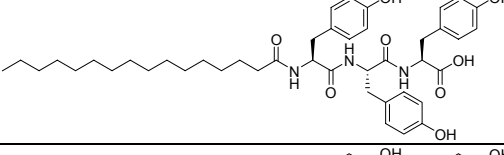
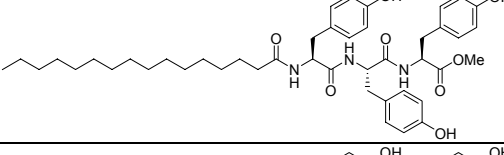
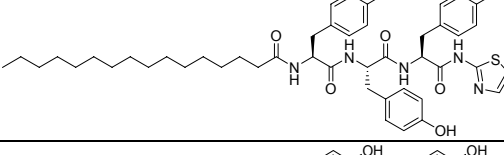
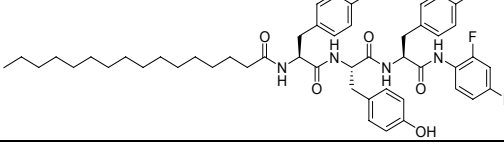
Entries	Nr.	Peptides	Yield (Purity) %	Rab GGTase Activity % (IC ₅₀)
226	263		6 (> 95)	81 ^b
227	264		3 (> 95)	91 ^b
228	265		17 (> 95)	118 ^b
229	266		9 (> 95)	124 ^b
230	267		11 (> 95)	125 ^b
231	268		8 (> 95)	88 ^b
232	269		15 (> 95)	107 ^b
233	270		3 (> 95)	107 ^b
234	271		1 (> 95)	78 ^b
235	272		1 (> 95)	91 ^b
236	273		6 (> 95)	100 ^b
237	274		4 (> 95)	100 ^b
238	275		2 (> 95)	96 ^b

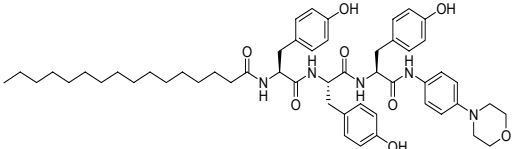
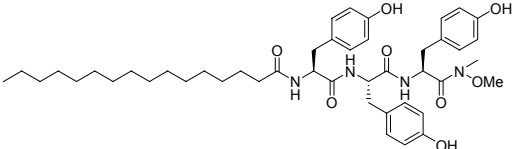
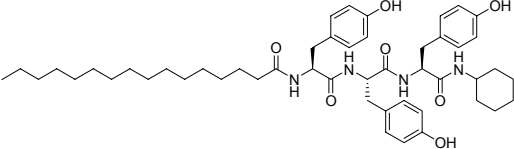
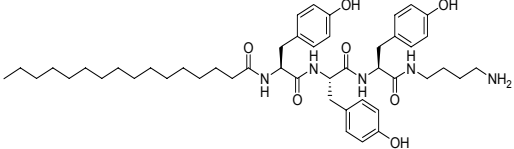
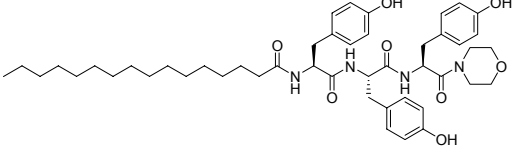
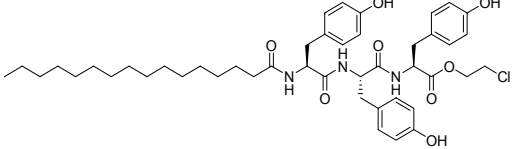
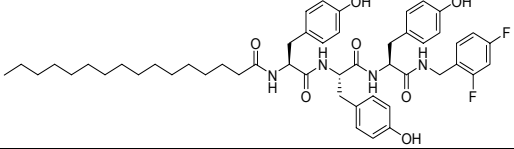
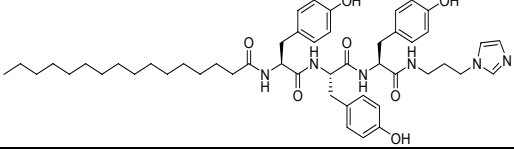
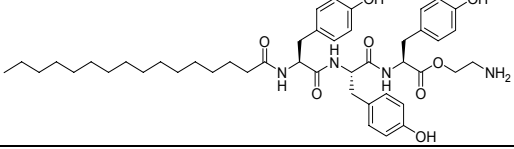
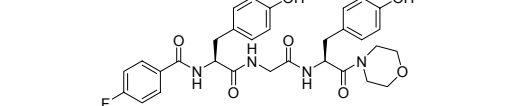
Entries	Nr.	Peptides	Yield (Purity) %	Rab GGTase Activity % (IC ₅₀)
239	276		10 (> 95)	120 ^b
240	277		13 (> 95)	99 ^b
241	278		5 (> 95)	119 ^b
242	279		1 (> 95)	96 ^b
243	280		2 (> 95)	112 ^b
244	281		3 (> 95)	86 ^b
245	282		8 (> 95)	110 ^b
246	283		3 (> 80)	115 ^b
247	284		4 (> 95)	116 ^b
248	285		3 (> 95)	100 ^b
249	286		5 (> 95)	96 ^b
250	287		3 (> 85)	63 ^b
251	288		4 (> 95)	84 ^b

Entries	Nr.	Peptides	Yield (Purity) %	Rab GGTase Activity % (IC ₅₀)
252	289		2 (> 95)	88 ^b
253	290		2 (> 95)	82 ^b
254	291		5 (> 95)	81 ^b
255	292		1 (> 95)	85 ^b
256	293		4 (> 95)	114 ^b
257	294		2 (> 95)	103 ^b
258	295		2 (> 95)	91 ^b
259	296		12 (> 95)	127 ^b
260	297		15 (> 95)	100 ^b
261	298		20 (> 95)	103 ^b
262	299		22 (> 95)	57 ^b
263	300		22 (> 95)	90 ^b

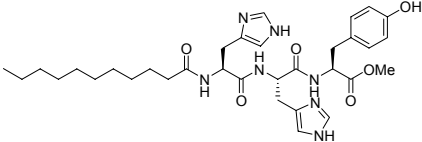
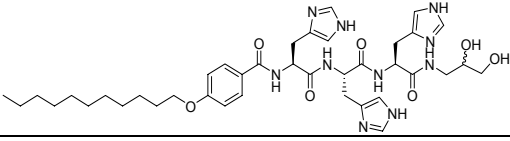
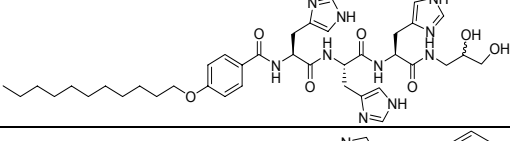
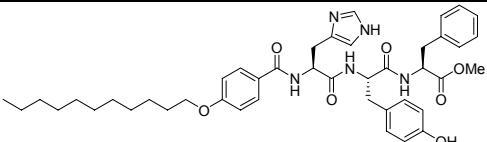
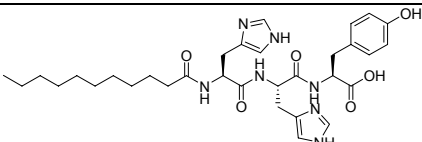
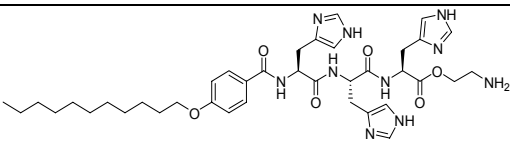
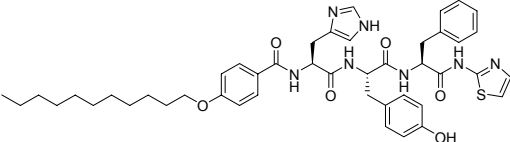
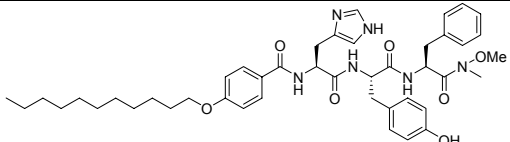
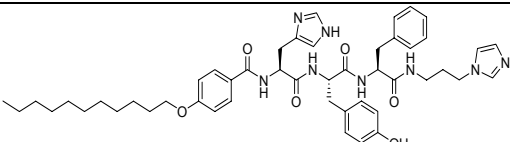
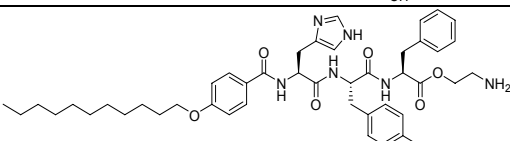
Entries	Nr.	Peptides	Yield (Purity) %	Rab GGTase Activity % (IC ₅₀)
264	301		8 (> 95)	60 ^b
265	302		16 (> 85)	91 ^b
266	303		17 (> 95)	81 ^b
267	304		12 (> 95)	85 ^b
268	305		9 (> 95)	100 ^b
269	306		10 (> 95)	124 ^b
270	307		26 (> 95)	91 ^b
271	308		8 (> 90)	93 ^b
272	309		3 (> 95)	57 ^b
273	310		9 (> 90)	96 ^b
274	311		11 (> 95)	85 ^b
275	312		6 (> 95)	87 ^b

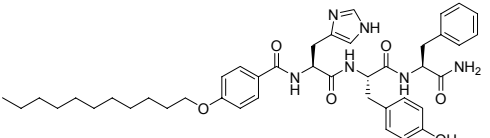
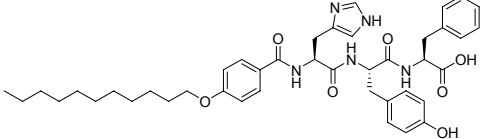
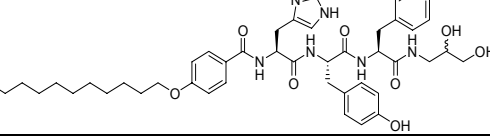
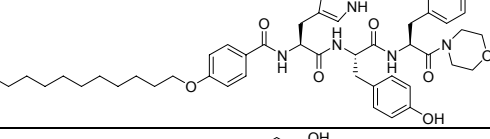
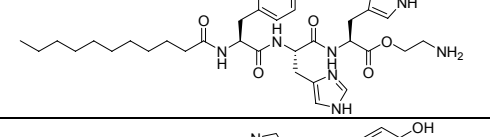
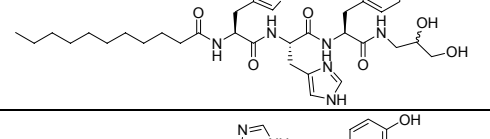
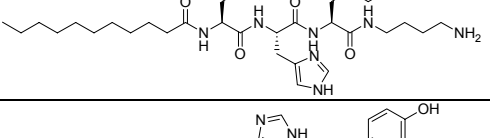
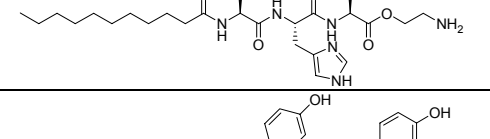
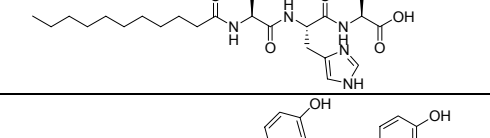
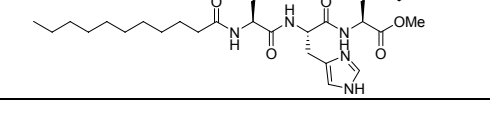
Entries	Nr.	Peptides	Yield (Purity) %	Rab GGTase Activity % (IC ₅₀)
276	313		4 (> 95)	136 ^b
277	314		11 (> 85)	94 ^b
278	315		15 (> 90)	98 ^b
279	316		4 (> 95)	69 ^b
280	317		19 (> 85)	99 ^b
281	318		16 (> 95)	78 ^b
282	319		1 (> 95)	79 ^b
283	320		3 (> 95)	89 ^b
284	321		1 (> 95)	61 ^b
285	322		3 (> 90)	111 ^b
286	323		1 (> 90)	114 ^b

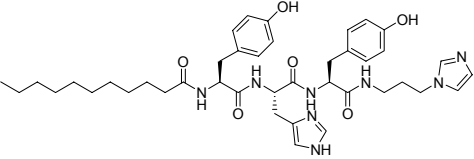
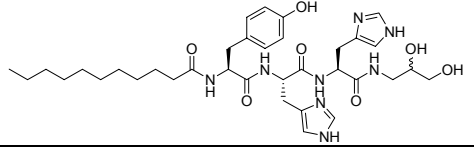
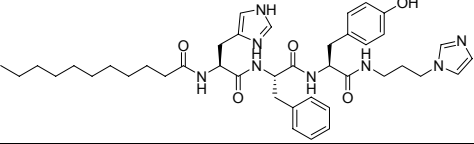
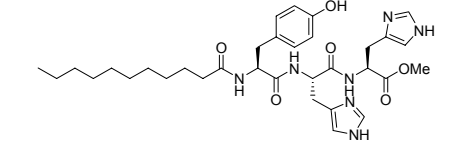
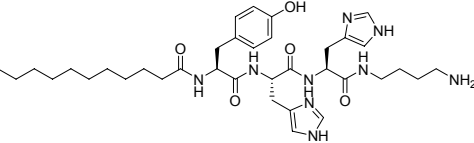
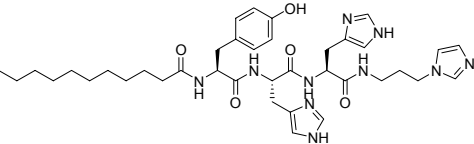
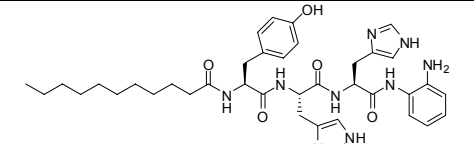
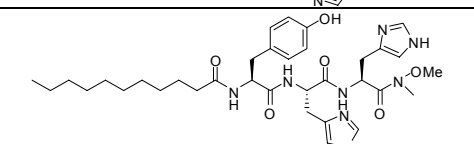
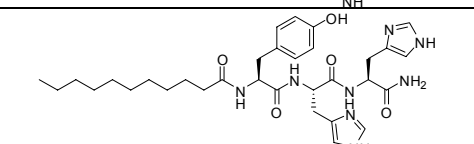
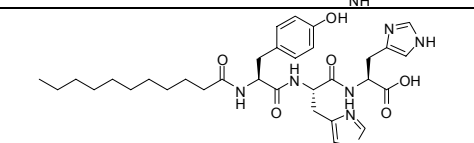
Entries	Nr.	Peptides	Yield (Purity) %	Rab GGTase Activity % (IC ₅₀)
287	324		3 (> 95)	113 ^b
288	325		2 (> 95)	92 ^b
289	326		3 (> 95)	99 ^b
290	327		20 (> 95)	85 ^b
291	328		1 (> 95)	97 ^b
292	329		32 (> 95)	88 ^b
293	330		7 (> 80)	65 ^b
294	331		8 (> 80)	94 ^b
295	332		10 (> 85)	103 ^b
296	333		5 (> 95)	82 ^b

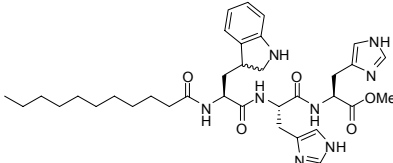
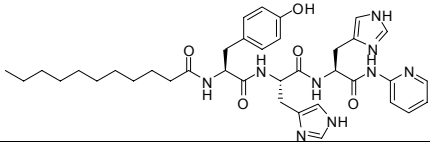
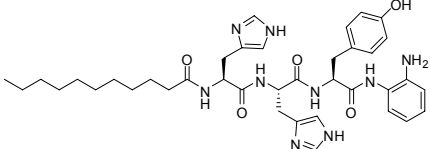
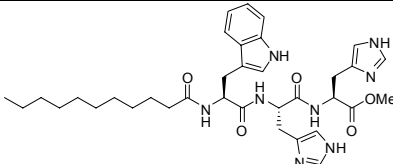
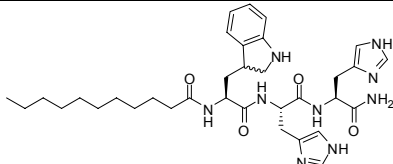
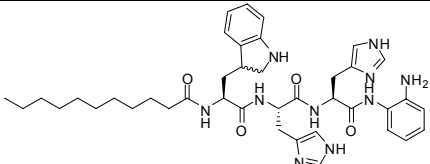
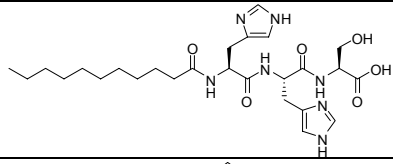
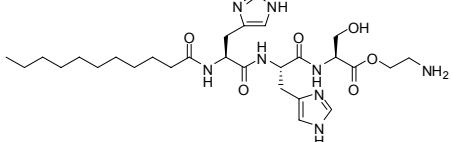
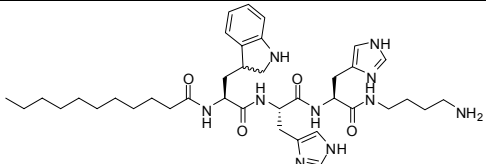
Entries	Nr.	Peptides	Yield (Purity) %	Rab GGTase Activity % (IC ₅₀)
297	334		8 (> 90)	96 ^b
298	335		15 (> 95)	97 ^b
299	336		7 (> 95)	98 ^b
300	337		20 (> 95)	63 ^b
301	338		18 (> 95)	106 ^b
302	339		8 (> 95)	104 ^b
303	340		7 (> 95)	64 ^b
304	341		17 (> 95)	100 ^b
305	342		7 (> 95)	76 ^b
306	343		5 (> 95)	95 ^b

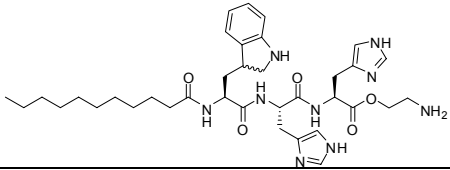
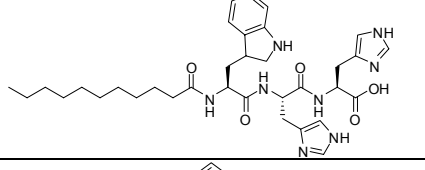
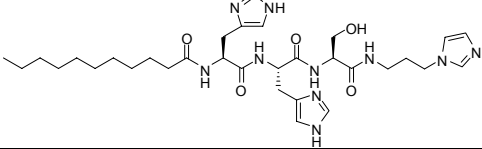
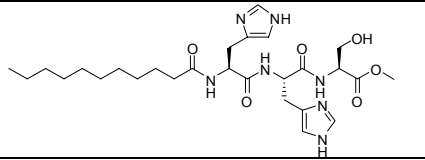
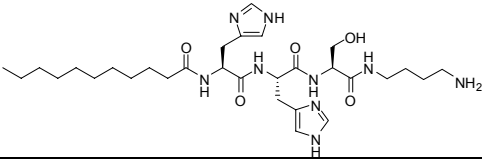
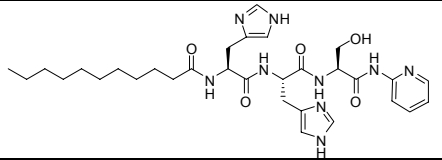
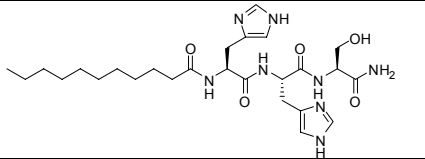
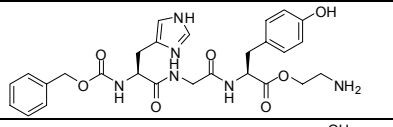
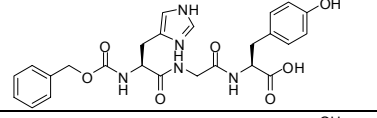
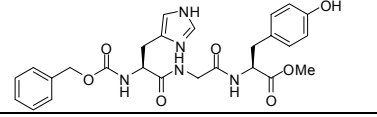
Entries	Nr.	Peptides	Yield (Purity) %	Rab GGTase Activity % (IC ₅₀)
307	344		22 (> 95)	65 ^b
308	345		8 (> 95)	86 ^b
309	346		2 (> 95)	114 ^b
310	347		4 (> 95)	114 ^b
311	348		6 (> 95)	130 ^b
312	349		12 (> 95)	123 ^b
313	350		12 (> 95)	138 ^b
314	351		15 (> 95)	114 ^b
315	352		9 (> 95)	101 ^b
316	353		19 (> 95)	113 ^b

Entries	Nr.	Peptides	Yield (Purity) %	Rab GGTase Activity % (IC ₅₀)
317	354		16 (> 95)	63 ^b
318	355		12 (> 95)	114 ^b
319	356		13 (> 95)	98 ^b
320	357		10 (> 95)	86 ^b
321	358		16 (> 95)	45 ^b
322	359		7 (> 95)	58 ^b
323	360		4 (> 95)	132 ^b
324	361		4 (> 95)	189 ^b
325	362		4 (> 85)	174 ^b
326	363		1 (> 95)	43 ^b

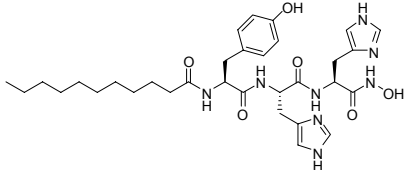
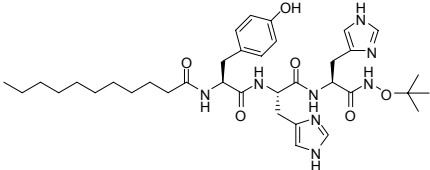
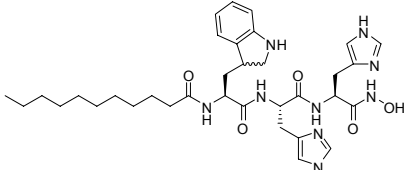
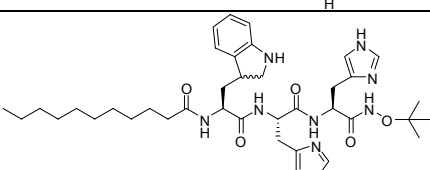
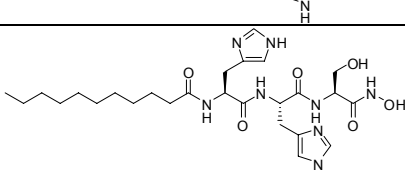
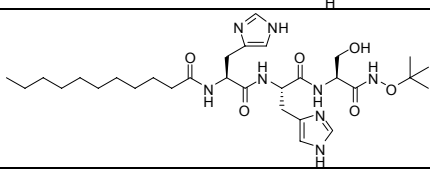
Entries	Nr.	Peptides	Yield (Purity) %	Rab GGTase Activity % (IC ₅₀)
327	364		3 (> 95)	93 ^b
328	365		8 (> 95)	80 ^b
329	366		9 (> 90)	59 ^b
330	367		5 (> 95)	100 ^b
331	368		3 (> 90)	64 ^b
332	369		17 (> 95)	104 ^b
333	370		13 (> 95)	70 ^b
334	371		8 (> 95)	68 ^b
335	372		12 (> 95)	52 ^b
336	373		23 (> 95)	75 ^b

Entries	Nr.	Peptides	Yield (Purity) %	Rab GGTase Activity % (IC ₅₀)
337	374		18 (> 95)	97 ^b
338	375		20 (> 95)	98 ^b
339	376		32 (> 95)	113 ^b
340	377		5 (> 90)	65 ^b
341	378		20 (> 95)	70 ^b
342	379		16 (> 95)	65 ^b
343	380		3 (> 95)	41 ^b
344	381		1 (> 95)	34 ^b
345	382		4 (> 85)	46 ^b
346	383		8 (> 85)	75 ^b

Entries	Nr.	Peptides	Yield (Purity) %	Rab GGTase Activity % (IC ₅₀)
347	384		5 (> 90)	100 ^b
348	385		11 (> 85)	63 ^b
349	386		23 (> 85)	80 ^b
350	387		1 (> 95)	87 ^b
351	388		4 (> 95)	55 ^b
352	389		13 (> 95)	43 ^b
353	390		18 (> 95)	95 ^b
354	391		13 (> 95)	90 ^b
355	392		18 (> 95)	68 ^b

Entries	Nr.	Peptides	Yield (Purity) %	Rab GGTase Activity % (IC ₅₀)
356	393		5 (> 85)	63 ^b
357	394		7 (> 95)	38 ^b
358	395		13 (> 95)	68 ^b
359	396		23 (> 85)	87 ^b
360	397		26 (> 95)	90 ^b
361	398		8 (> 85)	65 ^b
362	399		3 (> 95)	75 ^b
363	400		3 (> 95)	112 ^b
364	401		4 (> 95)	91 ^b
365	402		3 (> 95)	102 ^b

Entries	Nr.	Peptides	Yield (Purity) %	Rab GGTase Activity % (IC ₅₀)
366	403		3 (> 95)	89 ^b
367	404		4 (> 95)	87 ^b
368	405		2 (> 95)	80 ^b
369	406		3 (> 90)	87 ^b
370	407		1 (> 95)	87 ^b
371	408		5 (> 95)	93 ^b
372	409		3 (> 95)	77 ^b
373	410		2 (> 95)	72 ^b
374	411		1 (> 95)	67 ^b
375	412		10 (> 95)	70 ^b
376	413		5 (> 95)	80 ^b

Entries	Nr.	Peptides	Yield (Purity) %	Rab GGTase Activity % (IC ₅₀)
377	414		6 (> 95)	57 ^b
378	415		5 (> 95)	53 ^b
379	416		5 (> 85)	45 ^b
380	417		5 (> 95)	54 ^b
381	418		6 (> 95)	67 ^b
382	419		4 (> 95)	74 ^b

a: The screening was performed at 100 μ M without negative control

b: The screening was performed at 50 μ M with negative control

7 Experimental Part

5.1.1 Materials and Methods

Nuclear Magnetic Resonance Spectroscopy

^1H and ^{13}C NMR spectra were recorded on one of the following instruments: Varian Mercury 400, Bruker DRX 400 and Bruker DRX 500 with tetramethylsilane as the internal reference. The chemical shifts are provided in ppm and the coupling constants in Hz. The following abbreviations for multiplicities are used: *s*, singlet; *d*, doublet; *dd*, double doublet; *dt*, doublet triplet; *t*, triplet; *q*, quadruplet; *m*, multiplet; *br*, broad. The ^1H and ^{13}C spectra are calibrated to the solvent signals of CDCl_3 (7.26 ppm and 77.00 ppm), DMSO (2.50 ppm, 39.43 ppm) and MeOH (3.31 ppm, 49.05 ppm).

High Resolution Mass Spectrometry

High resolution mass spectra (HR-MS, 70 eV) were measured on a Jeol SX 102A spectrometer by using fast atom bombardment (FAB) techniques and on Thermo Orbitrap coupled to Thermo Accela HPLC machine by using electron spray ionization technique (ESI) The matrix used for FAB was 3-nitrobenzylalcohol (3-NBA).

Reversed-Phase High-Pressure Liquid Chromatography

Analytical HPLC was recorded on an Agilent HPLC (1100 series machine). The standard gradient began at 10% acetonitrile and was raised to 90% over 15 min. After 3 min at 90% acetonitrile, the column was washed for 5 min with 100% acetonitrile. The column was then equilibrated for 3 min with 10% acetonitrile. TFA (0.1% v/v) was added to the HPLC solvents. Analytical HPLC-MS measurements were recorded on an Agilent HPLC (1100 series) coupled to a Finnigan LCQ ESI spectrometer. The column used is indicated in parenthesis. Preparative HPLC was run on an Agilent HPLC (1100 series) and Waters HPLC 2767 using a 125/21 NUCLEODUR C18 and C4 Gravity, 5 μ (Macherey-Nagel column)

Thin-Layer Chromatography (TLC)

Thin-layer chromatography (TLC) plates were obtained from Merck (Silica gel 60, F254). The TLCs were visualized by UV light ($\lambda = 254$ nm, 366 nm) or by staining with KMnO_4 solution. The solvent system and R_f values are noted for the synthesized compounds.

Flash Chromatography

Flash column chromatography was performed using flash silica gel (Merck, Darmstadt, 40-64 μM) with pressure ranging from 0.5 - 1.0 bar.

Ultraviolet Spectroscopy

UV/VIS spectra were measured with a Cary 100 Spectrometer (Varian Inc.).

Optical Rotation

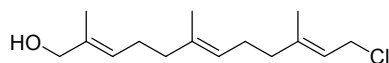
Optical rotations were measured with a Schmidt + Haensch Polartronic HH8 polarimeter at 589 nm. Concentrations are given in g/100 ml.

Chemicals

Chemicals were obtained from the following suppliers and used without further purification: Acros, Aldrich, Fluka, Novabiochem, Senn Chemicals. The solid support was purchased from Novabiochem. With the exception of DMF and NMP, all solvents were distilled prior to use following standard protocols. Dry DMF was purchased from Fluka.

5.2.2 Experimental procedures and analytical data

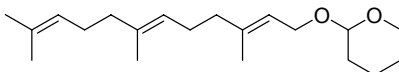
HO-Far-Cl (3)



To *trans-trans*-farnesyl chloride **5** (0.72 g, 3 mmol) was dissolved in 6 mL CH₂Cl₂ at room temperature, *t*-BuOOH (1.08 g, 12 mmol, 70 % aqueous solution), SeO₂ (33 mg, 0.3 mmol) and salicylic acid (39 mg, 0.3 mmol) were added respectively. The reaction mixture was stirred vigorously at room temperature for 2.5 hours. The excess *t*-BuOOH was co-evaporated with toluene. The residue was re-dissolved in Et₂O and the organic phase was washed with saturated solution of NaHCO₃, brine and dried over MgSO₄. The solution was filtered and concentrated *in vacuo*. The crude product was purified by silica gel chromatography to obtain 200 mg of **3** as colourless oil.

Yield = 27 %; **R_f** = 0.4 (cyclohexane : Ethyl acetate = 4:1); **¹H NMR** (400 MHz, CDCl₃): δ = 5.44 (ddt, *J* = 7.9, 2.5, 1.2 Hz, 1H), 5.38 (ddt, *J* = 7.0, 2.6, 1.2 Hz, 1H), 5.10 (dt, *J* = 6.7, 1.1 Hz, 1H), 4.09 (d, *J* = 7.9 Hz, 2H), 3.99 (s, 2H), 2.17-1.98 (m, 8H), 1.72 (s, 3H), 1.66 (s, 3H), 1.60 (s, 3H) ppm; **¹³C NMR** (100 MHz, CDCl₃): δ = 142.6, 135.2, 134.7, 125.9, 123.7, 120.3, 68.9, 41.1, 39.3, 39.2, 26.1, 26.0, 16.0, 16.0, 13.6 ppm.

Far-OTHP (7)

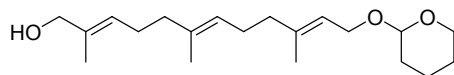


To *trans-trans*-farnesol (4.4 g, 20 mmol) in 20 mL CH₂Cl₂ was added 2,3-dihydropyran (DHP) (2.6 g, 30 mmol) and pyridinium-*para*-toluenesulfonate (PPTS) (0.5 g, 2 mmol) at room temperature and stirred overnight. The mixture was washed with saturated solution of NaHCO₃, brine, and dried over MgSO₄. The solution was filtered and concentrated under reduced pressure to obtain 5.7 g (100%) of **7** as colourless oil.

Yield = Quantitative; **R_f** = 0.7 (cyclohexane : Ethyl acetate = 4:1); **¹H NMR** (400 MHz, CDCl₃): δ = 5.37 (dq, *J* = 7.5, 1.3 Hz, 1H), 5.16-5.04 (m, 2H), 4.63 (dd, *J* = 4.2, 2.8 Hz, 1H), 4.24 (ddd, *J* = 11.9, 6.4, 0.7 Hz, 1H), 4.03 (ddd, *J* = 11.9, 7.4, 0.5 Hz, 1H), 3.90 (ddd, *J* = 11.3, 7.6, 3.7 Hz, 1H), 3.55-3.47 (m, 1H), 2.18-2.01 (m, 6H), 2.01-1.93 (m, 2H), 1.90-1.78 (m, 1H),

1.78-1.70 (m, 1H), 1.68 (s, 6H), 1.60 (s, 6H), 1.58-1.46 (m, 4H) ppm; ^{13}C NMR (100 MHz, CDCl_3): δ = 140.2, 135.2, 131.2, 124.3, 123.8, 120.6, 97.7, 63.6, 62.2, 39.7, 39.6, 30.7, 26.7, 26.3, 25.6, 25.5, 19.6, 17.6, 16.4, 16.0 ppm.

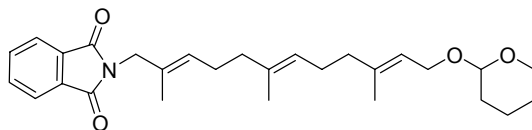
HO-Far-OTHP (8)



To THP protected *trans-trans*-farnesol **7** (5.7 g, 20 mmol) was dissolved in 40 mL CH_2Cl_2 at room temperature, *t*-BuOOH (7.2 g, 80 mmol, 70 % aqueous solution), SeO_2 (221 mg, 2 mmol) and salicylic acid (276 mg, 2 mmol) were added respectively. The reaction mixture was stirred vigorously at room temperature for 2.5 hours. The excess *t*-BuOOH was co-evaporated with toluene. The residue was re-dissolved in Et_2O and the organic phase was washed with saturated solution of NaHCO_3 , brine and dried over MgSO_4 . The solution was filtered and concentrated *in vacuo*. The crude product was purified by silica gel chromatography to obtain 1.7 g of **8** as colourless oil.

Yield = 27 %; **R_f** = 0.2 (cyclohexane : Ethyl acetate = 4:1); ^1H NMR (400 MHz, CDCl_3): δ = 5.46-5.28 (m, 2H), 5.11 (dt, J = 6.7, 6.5, 1.1 Hz, 1H), 4.62 (t, J = 4.2 Hz, 1H), 4.23 (dd, J = 11.6, 6.6 Hz, 1H), 4.03 (dd, J = 12.5, 6.7 Hz, 1H), 3.99 (s, 2H), 3.89 (ddd, J = 10.9, 7.5, 3.2 Hz, 1H), 3.56-3.45 (m, 1H), 2.17-1.97 (m, 8H), 1.91-1.77 (m, 1H), 1.68 (s, 3H), 1.66 (s, 3H), 1.60 (s, 3H), 1.59-1.48 (m, 4H) ppm.

Phthalimide-Far-OTHP (9)

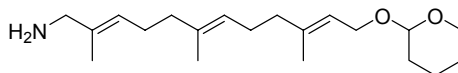


To a 20 mL solution of **2** (1.7 g, 5.3 mmol), phthalimide (853 mg, 5.8 mmol) and PPh_3 (1.5 g, 5.8 mmol) in THF were added DIAD (1.17 g, 5.8 mmol) dropwise for 0.5 hour at room temperature and the reaction mixture was stirred overnight. The mixture was evaporated to dryness and Et_2O was added to precipitate Ph_3PO . The white suspension was filtered and the filtrate was

concentrated *in vacuo*. The crude product was purified by silica gel chromatography to obtain 1.6 g of **9** as colourless oil.

Yield = 66 %; **R_f** = 0.3 (cyclohexane : Ethyl acetate = 6:1); **¹H NMR** (400 MHz, CDCl₃): δ = 7.85 (dd, *J* = 5.4, 3.0 Hz, 2H), 7.71 (dd, *J* = 5.4, 3.0 Hz, 2H), 5.40-5.27 (m, 2H), 5.10-5.03 (m, 1H), 4.62 (dd, *J* = 4.3, 2.8 Hz, 1H), 4.22 (dd, *J* = 12.4, 5.8 Hz, 1H), 4.19 (s, 2H), 4.02 (dd, *J* = 11.7, 7.2 Hz, 1H), 3.89 (ddd, *J* = 11.2, 7.4, 3.5 Hz, 1H), 3.59-3.43 (m, 1H), 2.25-1.91 (m, 8H), 1.90-1.78 (m, 1H), 1.77-1.68 (m, 1H), 1.66 (s, 3H), 1.64 (s, 3H), 1.56 (s, 3H), 1.56-1.51 (m, 4H) ppm; **¹³C NMR** (100 MHz, CDCl₃): δ = 168.2, 140.1, 134.7, 133.8, 132.1, 129.1, 127.4, 124.2, 123.2, 120.6, 97.7, 63.6, 62.2, 44.9, 39.5, 39.1, 30.7, 26.9, 26.4, 25.5, 19.6, 15.9, 14.6 ppm; **HRMS** (FAB, *m*-NBA) *m/z* calc. for C₂₈H₃₇NO₄ 451.2723, found 452.2786 [M+H]⁺.

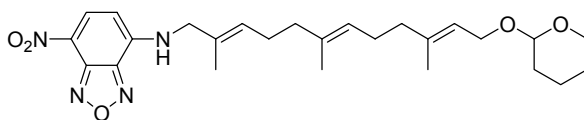
NH₂-Far-OTHP (**10**)



To a 40 mL ethanol solution of **9** (1.6 g, 3.5 mmol) was added hydrazine and the reaction mixture was stirred at room temperature overnight. The solution was evaporated to dryness. 100 mL CH₂Cl₂ was added and the white solid was filtered. The filtrate was concentrated *in vacuo* and purified by silica gel chromatography to obtain 600 mg of **10** as colourless oil.

Yield = 53 %; **R_f** = 0.25 (Ethyl acetate : Et₃N = 99:1); **¹H NMR** (400 MHz, CDCl₃): δ = 5.36 (ddq *J* = 8.7, 5.0, 1.2, 1.2, 1.2 Hz, 1H), 5.32-5.24 (m, 1H), 5.11 (dt, *J* = 6.8, 6.6, 1.1 Hz, 1H), 4.62 (dd, *J* = 4.2, 2.8 Hz, 1H), 4.23 (ddd, *J* = 11.7, 6.3, 0.6 Hz, 1H), 4.03 (dd, *J* = 11.9, 7.4 Hz, 1H), 3.89 (ddd, *J* = 11.1, 7.6, 3.5 Hz), 3.55-3.46 (m, 1H), 3.18 (s, 2H), 2.22-1.95 (m, 8H), 1.93-1.70 (m, 2H), 1.68 (s, 3H), 1.64 (s, 3H), 1.60 (s, 3H), 1.58-1.47 (m, 4H) ppm; **¹³C NMR** (100 MHz, CDCl₃): δ = 140.1, 139.8, 134.9, 124.4, 124.0, 120.6, 97.8, 63.6, 62.2, 49.7, 39.6, 39.4, 30.7, 26.3, 26.2, 25.5, 19.6, 16.4, 16.0, 14.5 ppm; **HRMS** (FAB, *m*-NBA) *m/z* calc. for C₂₀H₃₅NO₂ 321.2668, found 322.2756 [M+H]⁺.

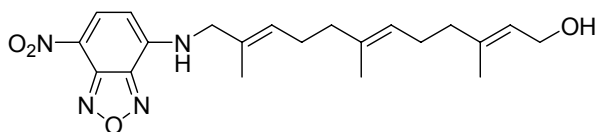
NBD-Far-OTHP (**11**)



To a solution of **10** (600 mg, 1.8 mmol) in 30 mL acetonitrile/25mM NaHCO₃ (1:1) was added NBD-Cl (335 mg, 1.8 mmol) at room temperature. The reaction mixture was stirred for one hour, another equivalent of NBD-Cl (335 mg, 1.8 mmol) was added and the mixture was stirred overnight. The mixture was poured into 200 mL CH₂Cl₂ and extracted twice with brine. The organic solution was dried over MgSO₄ and concentrated *in vacuo*. The crude product was purified by silica gel chromatography to obtain 543 mg of **11** as red brown oil.

Yield = 60 %; **R_f** = 0.1 (CH₂Cl₂); **¹H NMR** (400 MHz, CDCl₃): δ = 8.47 (d, *J* = 9.1 Hz, 1H), 6.19 (d, *J* = 8.6 Hz, 1H), 5.53-5.45 (m, 1H), 5.38-5.30 (m, 1H,), 5.14-5.06 (m, 1H), 4.62 (dd, *J* = 4.2, 2.8 Hz, 1H), 4.24 (ddd, *J* = 11.9, 6.2, 0.7 Hz, 1H), 4.09-4.02 (m, 1H), 4.02-3.99 (m, 2H), 3.94-3.85 (m, 1H), 3.59-3.44 (m, 1H), 2.45-1.92 (m, 8H), 1.92-1.78 (m, 2H), 1.73 (s, 3H), 1.67 (d, *J* = 0.6 Hz, 3H), 1.60 (d, *J* = 0.8 Hz, 3H), 1.58-1.47 (m, 4H) ppm; **¹³C NMR** (100 MHz, CDCl₃): δ = 143.8, 140.8, 139.8, 136.2, 134.3, 132.9, 129.3, 128.8, 128.5, 124.6, 120.7, 99.1, 97.9, 63.7, 62.4, 51.5, 39.5, 39.0, 30.7, 26.2, 26.2, 25.4, 19.6, 16.4, 15.9, 14.7 ppm.

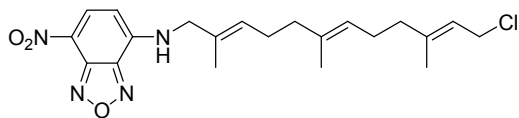
NBD-Far-OH (**12**)



To a solution of **11** (543mg, 1.1 mmol) in 20 mL ethanol was added pyridinium-*para*-toluenesulfonate (PPTS) (562 mg, 2.24 mmol). The reaction mixture was stirred at 60°C for 2 hours and poured into 200 mL Et₂O. The mixture was washed twice with brine and dried over MgSO₄. The organic solution was filtered and evaporated to dryness. The crude product was purified by silica gel chromatography to obtain 370 mg of **12** as red brown oil.

Yield = 83 %; **R_f** = 0.3 (cyclohexane : Ethyl acetate = 2:1); **¹H NMR** (400 MHz, CDCl₃): δ = 8.46 (d, *J* = 8.6 Hz, 1H), 6.72 (t, *J* = 4.9, 4.9 Hz, 1H), 6.16 (d, *J* = 8.6 Hz, 1H), 5.45 (dt, *J* = 7.1, 7.1, 1.0 Hz, 1H), 5.37 (dt, *J* = 7.0, 7.0, 1.3 Hz, 1H), 5.08 (dt, *J* = 6.8, 6.6, 1.0 Hz, 1H), 4.17 (d, *J* = 6.8 Hz, 2H), 4.00 (d, *J* = 5.5 Hz, 2H), 2.28-2.05 (m, 6H), 2.03-1.96 (m, 2H), 1.73 (s, 3H), 1.66 (s, 3H), 1.59 (s, 3H) ppm; **¹³C NMR** (100 MHz, CDCl₃): δ = 144.2, 144.0, 139.2, 136.3, 134.3, 128.8, 128.5, 124.5, 124.2, 123.4, 123.1, 99.1, 59.4, 51.3, 39.3, 38.9, 26.0, 26.0, 16.2, 15.9, 14.7 ppm; **HRMS** (FAB, *m*-NBA) *m/z* calc. for C₂₁H₂₈N₄O₄ 400.2111, found 400.2126 [M]⁺.

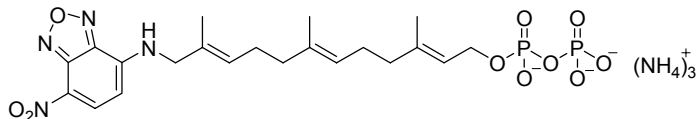
NBD-Far-Cl (13)



To NCS (40 mg, 0.30 mmol) in dry CH_2Cl_2 under argon atmosphere was added Dimethylsulfide (DMS) (42 mg, 0.67 mmol) dropwise at -30°C . The mixture was stirred for 5 minutes at 0°C and cooled again to -30°C . A solution of the alcohol **12** (120 mg, 0.30 mmol) in 1 mL dry CH_2Cl_2 was added and the mixture was stirred for 2 hours at 0°C . The mixture was poured into CH_2Cl_2 and the organic phase was washed twice with brine, dried with MgSO_4 and concentrated *in vacuo*. The crude product **13** was used for the next step without further purification.

Yield: quantitative; $R_f = 0.4$ (cyclohexane : ethyl acetate = 3:1); $^1\text{H NMR}$ (500 MHz, CDCl_3): $\delta = 1.55$ (br, 3H), 1.67 (d, $J = 1.0$, 3H), 1.70 (br, 3H), 1.96-2.16 (m, 8H), 4.03 (d, $J = 7.8$ Hz, 2H), 4.05 (d, $J = 8.0$ Hz, 2H), 5.04 (qt, $J = 6.4, 1.0$ Hz, 1H), 5.38 (qt, $J = 8.0, 1.2$ Hz, 1H) 5.47 (qt, $J = 6.6, 0.9$ Hz, 1H), 6.18 (d, $J = 8.7$ Hz, 1H), 6.78 (d, $J = 5.8$), 8.41 (d, $J = 8.7$ Hz) ppm.

NBD-Far-OPP (1)

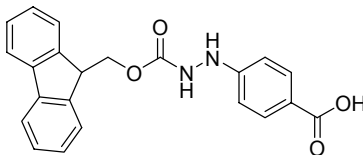


A solution of the compound **13** (125 mg, 0.3 mmol) was added to a solution of $(\text{Bu}_4\text{N})_3\text{HP}_2\text{O}_7$ (540 mg, 0.6 mmol) in dry CH_3CN (2 mL). The mixture was stirred for 4 hours at room temperature and the solvent was evaporated. The residue was dissolved in ammonium bicarbonate buffer (25 mM)/isorporpanol (39:1, 4 mL). The resulting solution was passed through a 1 x 8 cm Dowex 50X8 ion exchange column (NH_4^+ form), and lyophilization of the eluent yielded an orange solid. The sample was purified with a C18-Sep-Pak[®] cartridge and a linear gradient elution starting from ammonium bicarbonate buffer (25 mM) to CH_3CN to yield pure pyrophosphate **1** as an orange solid (10 mg, 16 % from alcohol **12**).

Yield = 16 % (2 steps, from alcohol **12**); $^1\text{H NMR}$ (200 MHz, D_2O): $\delta = 1.52$ (s, 6H), 1.94 (t, $J = 7.3$ Hz), 2.04 (dt, $J = 7.3$ Hz, $J = 7.0$ Hz, 2H), 3.90 (s, 2H), 4.29 (t, $J = 6.9$ Hz, 2H), 5.26 (t, $J =$

6.9 Hz, 1H), 5.32 (t, $J = 7.0$ Hz, 1H), 6.13 (d, $J = 8.7$ Hz, 1H), 8.25 (d, $J = 8.7$ Hz) ppm; ^{31}P NMR (162 MHz, D_2O): $\delta = -9.20$ (dd, $J = 22.2, 2.8$ Hz, 1P), -9.72 (dd, $J = 21.0, 2.0$ Hz, 1P) ppm.

General procedure (GP 1) for the synthesis of hydrazine linker 21



To hydrazinebenzoic acid (4 g, 26 mmol) in dioxane (30 mL) was added Na_2CO_3 (5.3 g, 50 mmol) in H_2O (90 mL). The clear solution was cooled at ice-bath and Fmoc chloride (7.3 g, 28 mol) in dioxane (30 mL) was added slowly. The reaction mixture was stirred at 0°C for 0.5 hour and room temperature overnight. The reaction mixture was extracted three times with diethyl ether and the organic phase was discarded. The remained aqueous/dioxane phase was acidific with 1M HCl till pH 1. Ethyl acetate was added and the aqueous phase was extracted three times with ethyl acetate. The collected organic phase was washed with brine, dried over MgSO_4 , filtered and concentrated *in vacuo*. The crude product was dissolved in minimum methanol followd by addition of ethyl acetate until cloudly. The solution was let to stand overnight until the formation of precipitate. The solid was filtered and collected to give 50 % yield of colourless solid.

Yield = 50 %; **R_f** = 0.4 (CH_2Cl_2 : Methanol = 9:1); ^1H NMR (500 MHz, CDCl_3): $\delta = 7.82$ (d, $J = 7.7$ Hz, 2H), 7.69 (d, $J = 7.2$ Hz, 2H), 7.42 (t, $J = 7.1$ Hz, 2H), 7.33 (t, $J = 7.0$ Hz, 1H), 6.66 (d, $J = 8.2$ Hz, 2H), 4.54 (d, $J = 5.8$ Hz, 2H), 4.25 (t, $J = 5.8$ Hz, 1H) ppm.

Determination of Fmoc-loading. Resin (1-2 mg) was weighed into a volumetric flask and filled with 3 mL 20% piperidine in DMF. After 20 minutes of gentile agitation, 1 mL was transferred to a quartz UV cuvette and diltuted to 3 mL with DMF. The absorbance was measured against reference at $\lambda = 301$ nm. The loading C_L is determined according to Beer's Law, $A = \epsilon cd$, where $\epsilon = 7800$ at 301 nm.

$$C_L = \frac{C_v \times V}{M} = \frac{A \times 9 \times 1000}{7800 \times M}$$

where C_V is the volume concentration, A is the absorbance, d is the path length of the UV cuvette, V is the total volume, M is the mass of the resin.

Determination of Theoretical Loading. The theoretical loading of the resin was determined according to the following formula:

$$\text{Loading}_{\text{new}} (\text{mol/g}) = \frac{\text{loading}_{\text{old}} (\text{mol/g})}{1 + \Delta \times \text{loading}_{\text{old}} (\text{mol/g})}$$

Where $\text{loading}_{\text{old}}$ is the previous loading and Δ is the mass difference of the added compound to the resin.

General procedure (GP 2) for the synthesis of the peptide libraries

Coupling using DIC/HOBT activation. The Fmoc-amino acid to be coupled (3 equivalents relative to resin loading) was dissolved in dry DMF, followed by addition of HOBT (3 equivalents) and DIC (3 equivalents). The mixture was stirred for 1 minute and added to the hydrazine resin at room temperature. The mixture was shaken at room temperature for 2 hours. The resin was filtered, washed three times with DMF, three times with CH_2Cl_2 , and three times with DMF.

Removal of Fmoc protecting group. The resin (200 mg, average loading 0.66 mmol/g) was washed 3 times with 3 mL 20% piperidine/DMF (5 minutes each time) to remove the Fmoc group from the amino acid. Subsequently, the resin was washed again three times with DMF, three times with CH_2Cl_2 , three times with DMF (each time 2 to 5 mL).

General procedure (GP 3) for the release of peptides using NBS/pyridine/nucleophile

To 250 mg peptidyl hydrazine resin (initial loading 0.66 mmol/g) was added NBS (58 mg, 0.33 mmol) and pyridine (26 mg, 0.33 mmol) in CH_2Cl_2 (2 mL). The reaction mixture was shaken for 5 minutes at room temperature. The resin was filtered and washed four times with CH_2Cl_2 . Nucleophiles (10 equivalents, 1.65 mmol) in 2 mL CH_2Cl_2 was added to the NBS/pyridine pretreated resin and shaken for 2 hours. The resin was filtered and washed four times with CH_2Cl_2 . The filtrate was washed with 1M HCl (5 mL) and brine. The organic layer was

evaporated to dryness. The crude product was treated with deprotection cocktail TFA/TES/H₂O (50/1/1, 5 mL) for 1 hour to cleave the protecting group. The reaction mixture was concentrated *in vacuo* and purified by preparative HPLC. The deprotection cocktail was used in every case, unless otherwise stated.

Remarks: For small hydrophilic nucleophiles such as H₂O and NH₃, 1 mL of the substrates was mixed with 2 mL of dioxane. For alcohol nucleophiles and amine nucleophiles containing HCl salt, additional 10 equivalents of DIPEA were added. Dioxane can be used as a solvent if the nucleophile cannot dissolve in CH₂Cl₂.

General procedure (GP 4) for the release of peptides using Cu(OAc)₂/pyridine/nucleophiles

To 250 mg peptidyl hydrazine resin (initial loading 0.66 mmol/g) in CH₂Cl₂ (2 mL) was added Cu(OAc)₂ (15 mg, 0.8 mmol), pyridine (130 mg, 1.65 mmol) and nucleophiles (10 equivalents, 1.65 mmol). The reaction mixture was shaken for 2 hours at room temperature under oxygen. The resin was filtered and washed four times with CH₂Cl₂. The filtrate was washed with 1M HCl (5 mL), brine. The organic layer was evaporated to dryness. The crude product was treated with deprotection cocktail TFA/TES/H₂O (50/1/1, 5 mL) for 1 hour to cleave the protecting group. The reaction mixture was concentrated *in vacuo* and purified by preparative HPLC. The deprotection cocktail was used in every case, unless otherwise stated.

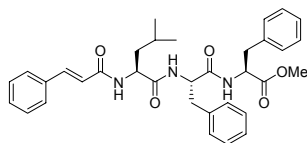
Remarks: For small hydrophilic nucleophiles such as H₂O and NH₃, 1 mL of the substrates was mixed with 2 mL of dioxane. Dioxane can be used as a solvent if the nucleophile cannot dissolve in CH₂Cl₂. Pyridine was not added for amine nucleophiles.

General procedure (GP 5) for the synthesis of C-terminal hydroxyl amide peptides

To 250 mg peptidyl hydrazine resin (initial loading 0.66 mmol/g) in dioxane (2 mL) was added Cu(OAc)₂ (15 mg, 0.8 mmol), pyridine (130 mg, 1.65 mmol) and H₂O (1 mL). The reaction mixture was shaken for 2 hours at room temperature under oxygen. The resin was filtered and washed with four times with CH₂Cl₂. The filtrate was washed with 1M HCl (5 mL), brine, and concentrated *in vacuo*. The resulting crude material was reacted with NH₂-O^tBu.HCl (20 mg, 0.165 mmol), EDC.HCl (47 mg, 0.247 mmol), HOBT (38 mg, 0.247 mmol) and Et₃N (25 mg, 0.247 mmol) overnight at room temperature. The reaction mixture was washed two times with 0.5

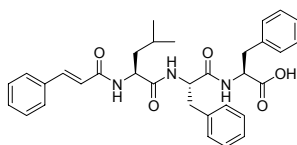
M H₂SO₄ (5 mL each), brine, and concentrated *in vacuo*. The protection group of crude material was cleaved off using 5 mL TFA/CH₂Cl₂ (50/50) for 48 hours. The reaction mixture was concentrated *in vacuo* and purified by preparative HPLC.

Analytical data of compound 38



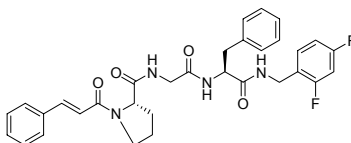
Peptide **38** was synthesized and released from solid support according to **GP 2** and **GP 3**. **Yield** = 18 %; **Purity** > 95% (LC_MS); **LC-MS** (C18, ESI_MS) 570.0 [M+H]⁺, 592.2 [M+Na]⁺; R_t = 9.79 min; ¹H NMR (400 MHz, CDCl₃): δ = 7.63 (d, *J* = 15.6 Hz, 1H), 7.51-7.48 (m, 2H), 7.37-7.36 (m, 3H), 7.23-7.14 (m, 8H), 7.00 (dd, *J* = 7.64, 1.76 Hz, 2H), 6.38 (d, *J* = 15.6 Hz, 1H), 4.80-4.75 (m, 1H), 4.71-4.67 (m, 1H), 4.61-4.56 (m, 1H), 3.66 (s, 1H), 3.09-2.98 (m, 4H), 1.64-1.59 (m, 2H), 1.54-1.50 (m, 1H), 0.92 (d, *J* = 4.4 Hz, 1H), 0.90 (d, *J* = 4.6 Hz, 1H) ppm; ¹³C NMR (100 MHz, CDCl₃): δ = 172.2, 171.5, 170.4, 166.2, 142.2, 136.4, 135.8, 134.8, 130.1, 129.5, 129.3, 129.0, 128.8, 128.7, 128.1, 127.3, 127.1, 120.0, 54.6, 53.5, 52.4, 52.0, 41.1, 38.2, 38.1, 25.0, 23.0, 22.3 ppm.

Analytical data of compound 39



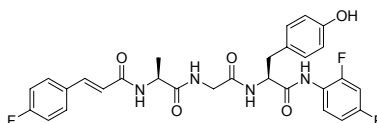
Peptide **39** was synthesized and released from solid support according to **GP 2** and **GP 3**. **Yield** = 5 %; **Purity** > 95% (LC_MS); **LC-MS** (C18, ESI_MS) 556.5 [M+H]⁺, 578.7 [M+Na]⁺; R_t = 8.87 min.

Analytical data of compound 40



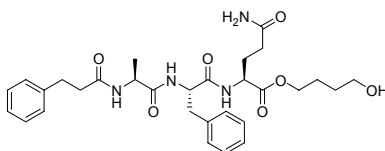
Peptide **40** was synthesized and released from solid support according to **GP 2** and **GP 3**. **Yield** = 28 %; **Purity** > 95% (LC_MS); **LC-MS** (C18, ESI_MS) 575.0 [M+H]⁺, 597.2 [M+Na]⁺; R_t = 8.58 min; **¹H NMR** (400 MHz, CDCl₃): δ = 7.65 (d, *J* = 15.3 Hz, 1H), 7.47-7.45 (m, 2H), 7.35-7.34 (m, 3H), 7.21-7.14 (m, 1H), 7.12-7.03 (m, 5H), 6.82-6.78 (m, 2H), 6.70 (d, *J* = 15.4 Hz, 1H), 4.60 (dd, *J* = 15.1, 7.3 Hz, 1H), 4.46 (s, 2H), 4.37 (dd, *J* = 16.3, 8.0 Hz, 1H), 3.70- 3.61 (m, 2H), 3.13-3.10(m, 1H), 3.06-2.99 (m, 1H), 2.15-2.08 (m, 2H), 2.06-1.98 (m, 2H) ppm; **¹³C NMR** (100 MHz, CDCl₃): δ = 172.7, 170.7, 169.3, 166.1, 162.7 and 162.6 (d, C-F), 160.2 and 160.2 (d, C-F), 143.9, 134.5, 130.1, 129.3, 129.0, 128.8, 128.3, 128.0, 126.6, 117.2, 113.4, 111.3, 111.0, 60.8, 49.8, 47.6, 43.2, 37.8, 31.3, 28.3, 25.1 ppm.

Analytical data of compound 41



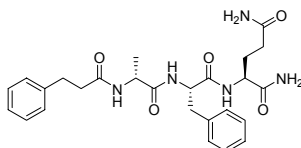
Peptide **41** was synthesized and released from solid support according to **GP 2** and **GP 3**. **Yield** = 23 %; **Purity** > 90% (LC_MS); **LC-MS** (C18, ESI_MS) 568.9 [M+H]⁺; R_t = 7.84 min.

Analytical data of compound 42



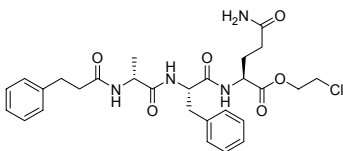
Peptide **42** was synthesized and released from solid support according to **GP 2** and **GP 3**. **Yield** = 3 %; **Purity** > 95% (LC_MS); **LC-MS** (C18, ESI_MS) 569.1 [M+H]⁺, 591.3 [M+Na]⁺; R_t = 7.00 min; **¹H NMR** (400 MHz, CD₃OD): δ = 7.64-6.88 (m, 10H), 4.63 (dd, *J* = 9.8, 4.7 Hz, 1H), 4.42 (dd, *J* = 9.4, 4.6 Hz, 1H), 4.23-4.10 (m, 3H), 3.58 (t, *J* = 6.31 Hz, 2H), 3.26 (dd, *J* = 13.7, 5.0 Hz, 1H), 2.99-2.80 (m, 4H), 2.58-2.44 (m, 2H), 2.37-2.19 (m, 2H), 2.09-1.96 (m, 1H), 1.79-1.66 (m, 2H), 1.65-1.55 (m, 2H), 1.06 (d, *J* = 7.1 Hz, 3H) ppm.

Analytical data of compound 43



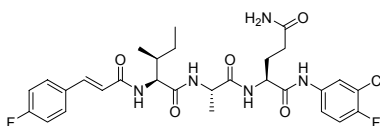
Peptide **43** was synthesized and released from solid support according to **GP 2** and **GP 3**. **Yield** = 5 %; **Purity** > 95% (LC_MS); **LC-MS** (C18, ESI_MS) 496.2 [M+H]⁺, 518.3 [M+Na]⁺; R_t = 6.48 min; **¹H NMR** (400 MHz, CD₃OD): δ = 7.75-6.75 (m, 10H), 4.55 (dd, *J* = 10.3, 5.0 Hz, 1H), 4.32 (dd, *J* = 9.6, 4.2 Hz, 1H), 4.14 (q, *J* = 7.0 Hz, 1H), 3.25 (dd, *J* = 14.0, 5.0 Hz, 1H), 2.91 (dd, *J* = 14.2, 10.0 Hz, 1H), 2.88-2.82 (m, 2H), 2.48 (dd, *J* = 8.9, 6.7 Hz, 2H), 2.30 (t, *J* = 7.4 Hz, 2H), 2.25-2.13 (m, 1H), 2.08-1.95 (m, 1H), 1.08 (d, *J* = 7.4 Hz, 3H); **¹³C NMR** (100 MHz, CD₃OD): δ = 177.9, 176.3, 176.1, 175.3, 173.6, 142.3, 138.6, 130.2, 129.5, 129.4, 129.4, 127.8, 127.1, 56.3, 54.4, 50.9, 38.3, 37.8, 32.9, 32.6, 28.8, 17.2 ppm.

Analytical data of compound 44



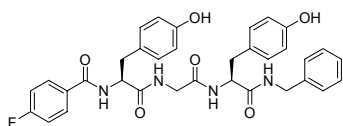
Peptide **44** was synthesized and released from solid support according to **GP 2** and **GP 3**. **Yield** = 1 %; **Purity** > 95% (LC_MS); **LC-MS** (C18, ESI_MS) 559.3 [M+H]⁺, 581.3 [M+Na]⁺; R_t = 7.53 min.

Analytical data of compound 45



Peptide **45** was synthesized and released from solid support according to **GP 2** and **GP 3**. **Yield** = 1 %; **Purity** > 95% (LC_MS); **LC-MS** (C18, ESI_MS) 606.5 [M+H]⁺, 628.6 [M+Na]⁺; R_t = 8.39 min.

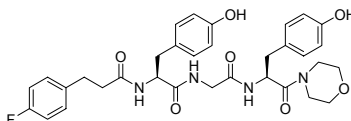
Analytical data of compound 46



Peptide **46** was synthesized and released from solid support according to **GP 2** and **GP 3**. **Yield** = 10 %; **Purity** > 95% (LC_MS); **LC-MS** (C18, ESI_MS) 613.0 [M+H]⁺, 635.2 [M+Na]⁺; R_t =

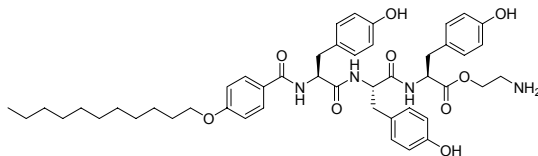
7.93 min; $^1\text{H NMR}$ (400 MHz, DMSO- D_6): δ = 9.16 (s, 1H), 9.12 (s, 1H), 8.60 (d, J = 8.1 Hz, 1H), 8.42 (t, J = 6.0, 6.0 Hz, 1H), 8.29 (t, J = 5.7, 5.7 Hz, 1H), 8.02 (d, J = 8.4 Hz, 1H), 7.86 (dd, J = 8.9, 5.5 Hz, 2H), 7.35-7.22 (m, 4H), 7.23-7.16 (m, 1H), 7.14-7.08 (m, 4H), 6.99 (d, J = 8.5 Hz, 2H), 6.62 (d, J = 8.5 Hz, 4H), 4.57 (ddd, J = 11.5, 7.9, 3.9 Hz, 1H), 4.45 (dt, J = 8.5, 8.4, 5.7 Hz, 1H), 4.28 (dd, J = 15.2, 6.1 Hz, 1H), 4.20 (dd, J = 15.2, 5.8 Hz, 1H), 3.80 (dd, J = 16.5, 6.1 Hz, 1H), 3.63 (dd, J = 16.5, 5.4 Hz, 1H), 3.00 (dd, J = 13.9, 4.1 Hz, 1H), 2.95-2.82 (m, 2H), 2.72 (dd, J = 13.6, 8.8 Hz, 1H) ppm; $^{13}\text{C NMR}$ (100 MHz, DMSO- D_6): δ = 171.7, 170.7, 168.3, 165.2, 162.5, 155.6, 155.5, 138.9, 130.0, 129.9, 129.9, 128.3, 128.0, 127.6, 126.8, 126.4, 115.0, 114.8, 114.8, 114.7, 55.4, 54.4, 41.9, 41.8, 36.9, 36.0 ppm; $^{19}\text{F NMR}$ (188 MHz, DMSO- D_6): δ = -109.5 ppm; $[\alpha]_{\text{D}}^{20}$ = -8.0° (C = 0.6, DMSO).

Analytical data of compound 47



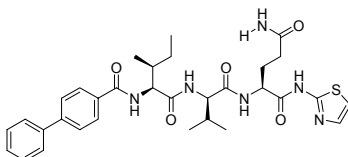
Peptide **47** was synthesized and released from solid support according to **GP 2** and **GP 3**. **Yield** = 7 %; **Purity** > 95% (LC_MS); **LC-MS** (C18, ESI_MS) 621.1 $[\text{M}+\text{H}]^+$, 643.3 $[\text{M}+\text{Na}]^+$; R_t = 7.40 min; $^1\text{H NMR}$ (400 MHz, DMF- D_7): δ = 9.54 (br s, 1H), 8.39 (t, J = 5.7, 5.7 Hz, 1H, CO-NH), 8.30 (d, J = 7.5 Hz, 1H), 8.20 (s, 1H), 7.42-7.32 (m, 2H), 7.27-7.18 (m, 6H), 7.00-6.83 (m, 4H), 5.12 (dt, J = 14.4, 7.2, 7.2 Hz, 1H), 4.70 (ddd, J = 9.2, 7.6, 4.9 Hz, 1H), 4.08 (dd, J = 16.7, 6.1 Hz, 1H), 3.92 (dd, J = 16.7, 5.5 Hz, 1H), 3.68-3.52 (m, 6H), 3.53-3.41 (m, 1H), 3.40-3.32 (m, 1H), 3.22 (dd, J = 13.9, 4.9 Hz, 1H), 3.15-3.09 (m, 1H), 3.05-2.95 (m, 4H), 2.72-2.58 (m, 2H) ppm; $^{13}\text{C NMR}$ (100 MHz, DMF- D_7): δ = 172.4, 172.4, 170.0, 168.8, 157.1, 156.8, 130.9, 130.6, 130.5, 130.4, 128.7, 128.0, 115.5, 115.4, 115.3, 115.1, 66.6, 66.6, 55.7, 50.5, 47.2, 42.7, 42.5, 37.9, 37.6, 37.0, 35.6 ppm.

Analytical data of compound 48



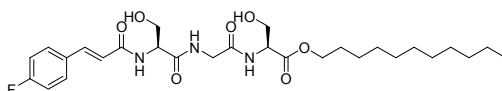
Peptide **48** was synthesized and released from solid support according to **GP 2** and **GP 3**. **Yield** = 4 %; **Purity** > 95% (LC_MS); **LC-MS** (C4, ESI_MS) 825.3 [M+H]⁺, 847.4 [M+Na]⁺; R_t = 8.55 min.

Analytical data of compound 49



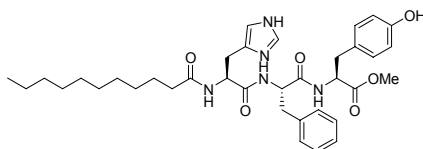
Peptide **49** was synthesized and released from solid support according to **GP 2** and **GP 3**. **Yield** = 6 %; **Purity** > 95% (LC_MS); **LC-MS** (C18, ESI_MS) 621.3 [M+H]⁺, 643.3 [M+Na]⁺; R_t = 8.49 min.

Analytical data of compound 50



Peptide **50** was synthesized and released from solid support according to **GP 2** and **GP 3**. **Yield** = 6 %; **Purity** > 95% (LC_MS); **LC-MS** (C18, ESI_MS) 552.0 [M+H]⁺, 574.3 [M+Na]⁺; R_t = 10.23 min.

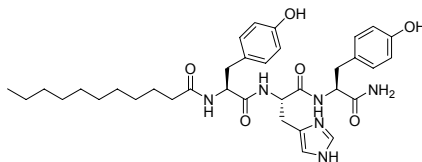
Analytical data of compound 51



Peptide **51** was synthesized and released from solid support according to **GP 2** and **GP 4**. **Yield** = 25 %; **Purity** > 95% (LC_MS); **LC-MS** (C4, ESI_MS) 648.3 [M+H]⁺, 670.4 [M+Na]⁺; R_t = 7.55 min; ¹H NMR (400 MHz, DMSO-D₆): δ = 8.86 (s, 1H), 8.50 (d, *J* = 7.4 Hz, 1H), 7.99 (d, *J* = 8.3 Hz, 1H), 7.93 (d, *J* = 8.0 Hz, 1H), 7.26-7.14 (m, 8H), 6.97 (d, *J* = 8.4 Hz, 2H), 6.64 (d, *J* = 8.4 Hz, 2H), 4.59-4.47 (m, 2H), 4.39 (q, *J* = 7.4 7.2 Hz, 1H), 3.55 (s, 3H), 2.98 (dd, *J* = 10.4, 3.9 Hz, 1H), 2.93 (dd, *J* = 11.7, 6.8 Hz, 1H), 2.85 (dd, *J* = 11.0, 7.3 Hz, 2H), 2.78 (dd, *J* = 13.6, 4.1 Hz,

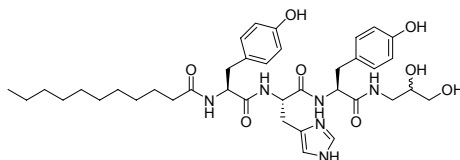
2H), 2.01 (t, $J = 7.4$ Hz, 1H), 1.36 (p, $J = 7.4$ Hz, 2H), 1.28-1.16 (m, 14H), 1.14-1.08 (m, 2H), 0.83 (t, $J = 6.8$ Hz, 3H) ppm; $[\alpha]_D^{20} = -5.0^\circ$ (C = 2.2, DMSO).

Analytical data of compound 52



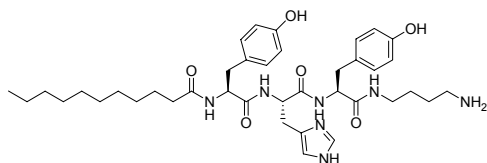
Peptide **52** was synthesized and released from solid support according to **GP 2** and **GP 4**. **Yield** = 2 %; **Purity** > 95% (LC_MS); **LC-MS** (C4, ESI_MS) 649.3 [M+H]⁺, 671.4 [M+Na]⁺; $R_t = 6.88$ min.

Analytical data of compound 53 (two diastereoisomers)



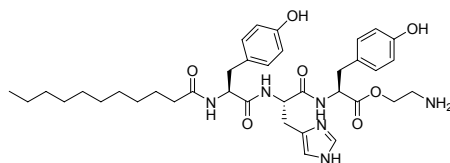
Peptide **53** was synthesized and released from solid support according to **GP 2** and **GP 4**. **Yield** = 20 %; **Purity** > 95% (LC_MS); **LC-MS** (C4, ESI_MS) 723.3 [M+H]⁺, 745.4 [M+Na]⁺; $R_t = 6.58$ min; **¹H NMR** (400 MHz, DMSO- D_6): $\delta = 9.18$ (br s, 1H), 9.14 (br s, 1H), 8.93 (s, 1H), 8.23 (d, $J = 8.0$ Hz, 1H), 8.07 (dd, $J = 10.2, 5.3$ Hz, 1H), 8.00 (d, $J = 7.5$ Hz, 1H), 7.96 (d, $J = 7.9$ Hz, 1H), 7.30 (s, 1H), 7.02 (d, $J = 8.39$ Hz, 4H), 6.64 (d, $J = 8.1$ Hz, 2H), 6.62 (d, $J = 8.3$ Hz, 1H), 4.57 (dd, $J = 14.0, 7.6$ Hz, 1H), 4.45-4.39 (m, 1H), 4.36 (ddd, $J = 11.2, 7.8, 3.5$ Hz, 1H), 3.55-3.42 (m, 1H), 3.34-3.10 (m, 3H), 3.11-2.91 (m, 3H), 2.91-2.77 (m, 2H), 2.72 (dd, $J = 13.9, 8.3$ Hz, 1H), 2.60 (dd, $J = 13.9, 10.5$ Hz, 1H), 2.01 (t, $J = 7.2, 7.2$ Hz, 1H), 1.52-1.31 (m, 2H), 1.31-1.01 (m, 14H), 0.85 (t, $J = 6.8, 6.8$ Hz, 3H) ppm; **¹³C NMR** (100 MHz, DMSO- D_6): $\delta = 172.4, 171.7, 171.3, 171.2, 169.3, 155.7, 155.6, 133.5, 129.9, 129.8, 129.0, 127.8, 127.2, 127.2, 116.8, 114.7, 114.6, 70.1, 70.1, 63.4, 63.4, 54.3, 54.2, 51.2, 42.1, 41.9, 36.8, 36.7, 36.7, 36.1, 35.0, 31.2, 28.8, 28.8, 28.6, 28.5, 28.3, 26.9, 25.1, 21.9, 13.8$ ppm; **HRMS** (FAB, *m*-NBA) m/z calc. for $C_{38}H_{54}N_6O_8$ 722.4003, found 723.4063 [M+H]⁺; $[\alpha]_D^{20} = +13.1^\circ$ (C = 1.6, DMSO).

Analytical data of compound 54



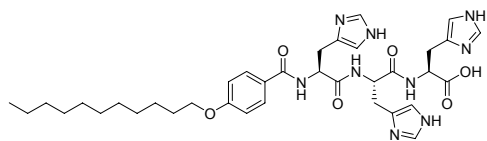
Peptide **54** was synthesized and released from solid support according to **GP 2** and **GP 4**. **Yield** = 22 %; **Purity** > 95% (LC_MS); **LC-MS** (C4, ESI_MS) 720.4 [M+H]⁺, 742.4 [M+Na]⁺; R_t = 5.95 min; ¹H NMR (400 MHz, DMSO-D₆): δ = 9.21 (br s, 1H), 8.95 (d, *J* = 0.9 Hz, 1H), 8.27 (d, *J* = 8.1 Hz, 1H), 8.06 (t, *J* = 5.6, 5.6 Hz, 1H), 7.99 (d, *J* = 4.5 Hz, 1H), 7.97 (d, *J* = 4.3 Hz, 1H), 7.78 (br s, 3H), 7.29 (s, 1H), 7.04-6.97 (m, 4H), 6.75-6.52 (m, 4H), 4.56 (dt, *J* = 8.0, 8.0, 5.8 Hz, 1H), 4.45-4.23 (m, 2H), 3.49 (s, 4H), 3.16-3.02 (m, 2H), 3.02-2.90 (m, 2H), 2.88-2.67 (m, 5H), 2.60 (dd, *J* = 14.1, 10.4 Hz, 1H), 2.01 (t, *J* = 7.0, 7.0 Hz, 2H), 1.52-1.30 (m, 6H), 1.30-1.01 (m, 14H), 0.85 (t, *J* = 6.8, 6.8 Hz, 3H) ppm; ¹³C NMR (100 MHz, DMSO-D₆): δ = 172.4, 171.8, 170.7, 169.3, 155.8, 155.6, 133.5, 129.9, 129.8, 129.1, 127.8, 127.2, 116.7, 114.8, 114.6, 54.4, 54.3, 51.3, 38.4, 37.8, 36.9, 36.0, 35.0, 31.2, 28.8, 28.8, 28.6, 28.5, 28.4, 26.8, 25.7, 25.1, 24.3, 21.9, 13.8 ppm; **HRMS** (FAB, *m*-NBA) *m/z* calc. for C₃₉H₅₇N₇O₆ 719.4370, found 719.4377 [M]⁺; [α]_D²⁰ = + 7.0° (C = 1.8, DMSO).

Analytical data of compound 55



Peptide **55** was synthesized and released from solid support according to **GP 2** and **GP 4**. **Yield** = 7 %; **Purity** > 95% (LC_MS); **LC-MS** (C4, ESI_MS) 693.3 [M+H]⁺, 715.4 [M+Na]⁺; R_t = 6.11 min; [α]_D²⁰ = + 7.0° (C = 0.5, DMSO).

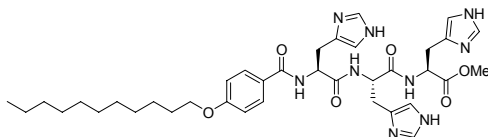
Analytical data of compound 56



Peptide **56** was synthesized and released from solid support according to **GP 2** and **GP 4**. **Yield** = 20 %; **Purity** > 95% (LC_MS); **LC-MS** (C4, ESI_MS) 704.3 [M+H]⁺, 726.4 [M+Na]⁺; R_t = 7.81

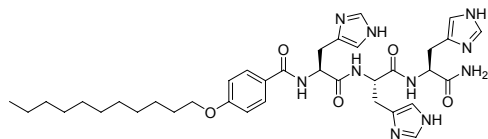
min; $^1\text{H NMR}$ (400 MHz, DMSO- D_6): δ = 8.75 (s, 1H), 8.73 (s, 1H), 8.70 (s, 1H), 8.54 (d, J = 5.3 Hz, 1H), 8.52 (d, J = 5.8 Hz, 1H), 8.26 (d, J = 7.5 Hz, 1H), 7.78 (d, J = 8.7 Hz, 2H), 7.30 (s, 1H), 7.26 (s, 2H), 6.97 (d, J = 8.8 Hz, 2H), 4.79-4.60 (m, 1H), 4.60-4.42 (m, 2H), 4.01 (t, J = 6.5, 6.5 Hz, 2H), 3.39-2.83 (m, 6H), 1.83-1.57 (m, 2H), 1.47-1.35 (m, 2H), 1.35-1.18 (m, 16H), 0.85 (t, J = 6.8, 6.8 Hz, 3H) ppm; $^{13}\text{C NMR}$ (100 MHz, DMSO- D_6): δ = 171.7, 170.4, 169.7, 166.0, 161.2, 158.3, 158.0, 133.8, 133.8, 130.5, 129.9, 129.7, 129.2, 125.4, 116.7, 116.6, 113.8, 67.6, 52.8, 51.8, 51.6, 31.1, 28.8, 28.6, 28.5, 28.4, 25.3, 21.9, 13.8 ppm; **HRMS** (FAB, *m*-NBA) m/z calc. for $\text{C}_{36}\text{H}_{49}\text{N}_9\text{O}_6$ 703.3806, found 704.3914 $[\text{M}+\text{H}]^+$; $[\alpha]_{\text{D}}^{20}$ = -11.4° (C = 1.6, DMSO).

Analytical data of compound 57



Peptide **57** was synthesized and released from solid support according to **GP 2** and **GP 4**. **Yield** = 3 %; **Purity** > 95% (LC_MS); **LC-MS** (C4, ESI_MS) 718.3 $[\text{M}+\text{H}]^+$, 740.4 $[\text{M}+\text{Na}]^+$; R_t = 7.66 min; $^1\text{H NMR}$ (400 MHz, DMSO- D_6): δ = 8.86 (s, 3H), 8.61 (d, J = 7.7 Hz, 1H), 8.53 (d, J = 7.7 Hz, 1H), 8.36 (d, J = 7.9 Hz, 1H), 7.76 (d, J = 8.8 Hz, 2H), 7.35 (s, 1H), 7.28 (d, J = 3.2 Hz, 2H), 6.96 (d, J = 8.9 Hz, 2H), 4.69-4.63 (m, 1H), 4.61-4.50 (m, 2H), 3.99 (t, J = 6.5 Hz, 2H), 3.18-2.95 (m, 6H), 3.60 (s, 3H), 1.73-1.65 (m, 2H), 1.44-1.33 (m, 2H), 1.34-1.18 (m, 16H), 0.83 (t, J = 6.8 Hz, 3H) ppm; $[\alpha]_{\text{D}}^{20}$ = -15.8° (C = 0.8, DMSO).

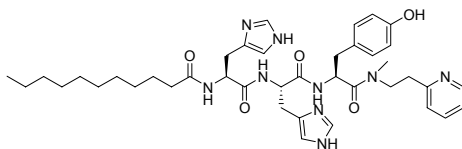
Analytical data of compound 58



Peptide **58** was synthesized and released from solid support according to **GP 2** and **GP 4**. **Yield** = 7 %; **Purity** > 95% (LC_MS); **LC-MS** (C4, ESI_MS) 703.4 $[\text{M}+\text{H}]^+$, 725.5 $[\text{M}+\text{Na}]^+$; R_t = 7.72 min; $^1\text{H NMR}$ (400 MHz, DMSO- D_6): δ = 8.85 (s, 1H), 8.80 (s, 1H), 8.53 (d, J = 7.3 Hz, 1H), 8.30 (d, J = 7.2 Hz, 1H), 7.76 (s, 1H), 7.74 (s, 1H), 7.52 (s, 1H), 7.31-7.25 (m, 4H), 6.97 (d, J = 8.9 Hz, 2H), 4.69-4.62 (m, 1H), 4.55-4.49 (m, 1H), 4.45 (dd, J = 13.5, 7.6 Hz, 1H), 3.99 (t, J =

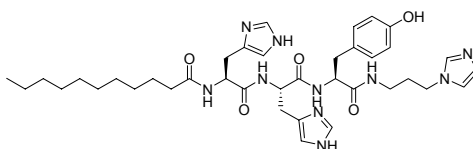
6.5 Hz, 2H), 3.16-3.04 (m, 3H), 3.03-2.91 (m, 3H), 1.74-1.66 (m, 2H), 1.44-1.34 (m, 2H), 1.34-1.21 (m, 16H), 0.83 (t, $J = 6.8$ Hz, 3H) ppm; $[\alpha]_D^{20} = -5.3^\circ$ (C = 0.3, DMSO).

Analytical data of compound 59



Peptide **59** was synthesized and released from solid support according to **GP 2** and **GP 4**. **Yield** = 12 %; **Purity** > 95% (LC_MS); **LC-MS** (C4, ESI_MS) 742.3 $[M+H]^+$, 764.4 $[M+Na]^+$; $R_t = 5.41$ min; **1H NMR** (400 MHz, DMSO- D_6): $\delta = 8.96$ (s, 1H), 8.94 (s, 1H), 8.20-8.10 (m, 2H), 7.36-7.21 (m, 5H), 7.01-6.96 (m, 2H), 6.67-6.60 (m, 2H), 4.73-4.66 (m, 1H), 4.60-4.50 (m, 2H), 3.76-3.67 (m, 1H), 3.49 (t, $J = 7.5$ Hz, 1H), 3.10-2.95 (m, 3H), 2.90-2.81 (m, 2H), 2.75 (s, 3H), 2.70-2.64 (m, 1H), 2.06-2.01 (m, 2H), 1.45-1.33 (m, 2H), 1.29-1.14 (m, 14H), 1.14-1.09 (m, 2H), 0.83 (t, $J = 6.8$ Hz, 3H) ppm; **^{13}C NMR** (100 MHz, DMSO- D_6): $\delta = 172.5, 170.0, 169.1, 166.2, 162.1, 155.9, 133.6, 130.0, 130.0, 128.8, 127.4, 126.8, 123.1, 122.3, 121.7, 116.7, 116.6, 116.6, 114.8, 51.4, 50.7, 49.7, 40.3, 34.9, 31.1, 28.8, 28.8, 28.6, 28.6, 28.5, 28.4, 24.9, 21.9, 13.8$ ppm; **HRMS** (ESI) m/z calc. for $C_{40}H_{55}N_9O_5$ 741.4326, found 742.4404 $[M+H]^+$; $[\alpha]_D^{20} = -0.8^\circ$ (C = 0.9, DMSO).

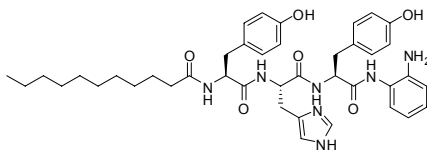
Analytical data of compound 60



Peptide **60** was synthesized and released from solid support according to **GP 2** and **GP 4**. **Yield** = 15 %; **Purity** > 95% (LC_MS); **LC-MS** (C4, ESI_MS) 731.5 $[M+H]^+$, 753.4 $[M+Na]^+$; $R_t = 5.11$ min; **1H NMR** (400 MHz, DMSO- D_6): $\delta = 8.95$ (s, 1H), 8.91 (t, $J = 1.3$ Hz, 2H), 8.20 (d, $J = 7.8$ Hz, 1H), 8.16 (d, $J = 8.6$ Hz, 1H), 8.14 (d, $J = 7.7$ Hz, 2H), 7.67 (s, 1H), 7.64 (s, 1H), 7.25 (d, $J = 3.5$ Hz, 2H), 6.99 (d, $J = 8.5$ Hz, 2H), 6.62 (d, $J = 8.4$ Hz, 2H), 4.59-4.48 (m, 2H), 4.31 (q, $J = 7.3$ Hz, 1H), 4.01 (t, $J = 7.1$ Hz, 2H), 3.11-3.01 (m, 3H), 3.01-2.89 (m, 3H), 2.89-2.83 (m, 1H), 2.81 (d, $J = 6.3$ Hz, 1H), 2.74 (dd, $J = 13.7, 7.8$ Hz, 1H), 2.04 (t, $J = 7.5$ Hz, 2H), 1.88-1.80 (m,

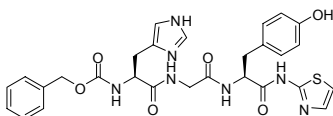
2H), 1.41-1.33 (m, 2H), 1.30-1.13 (m, 14H), 1.14-1.07 (m, 2H), 0.83 (t, $J = 6.8$ Hz, 3H) ppm; $[\alpha]_D^{20} = -3.9^\circ$ (C = 1.3, DMSO).

Analytical data of compound 61



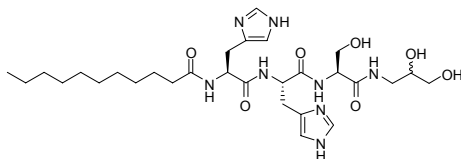
Peptide **61** was synthesized and released from solid support according to **GP 2** and **GP 4**. **Yield** = 20 %; **Purity** > 85% (LC_MS); **LC-MS** (C4, ESI_MS) 740.3 $[M+H]^+$, 762.5 $[M+Na]^+$; $R_t = 7.19$ min; **1H NMR** (400 MHz, DMSO- D_6): $\delta = 9.28$ (s, 1H), 8.94 (s, 1H), 8.94 (s, 1H), 8.32 (d, $J = 8.0$ Hz, 1H), 8.15 (d, $J = 6.9$ Hz, 1H), 7.97 (t, $J = 7.4$ Hz, 1H), 7.60 (dd, $J = 6.0, 3.1$ Hz, 1H), 7.32 (s, 1H), 7.29 (dd, $J = 6.1, 3.0$ Hz, 1H), 7.06 (d, $J = 8.4$ Hz, 2H), 7.00 (d, $J = 8.5$ Hz, 2H), 6.98-6.88 (m, 2H), 6.66 (d, $J = 8.5$ Hz, 2H), 6.60 (d, $J = 6.5$ Hz, 2H), 4.61 (dd, $J = 14.6, 8.0$ Hz, 1H), 4.55 (dd, $J = 14.5, 7.4$ Hz, 1H), 4.39-4.32 (m, 1H), 3.13-3.04 (m, 2H), 3.00-2.91 (m, 2H), 2.90-2.78 (m, 2H), 2.00 (t, $J = 7.3$ Hz, 2H), 1.39-1.31 (m, 2H), 1.28-1.13 (m, 14H), 1.12-1.04 (m, 2H), 0.86-0.81 (m, 3H) ppm; $[\alpha]_D^{20} = +20.0^\circ$ (C = 1.7, DMSO).

Analytical data of compound 62



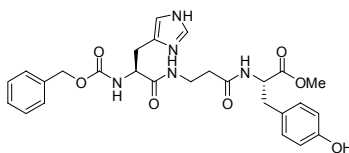
Peptide **62** was synthesized and released from solid support according to **GP 2** and **GP 4**. **Yield** = 2 %; **Purity** > 95% (LC_MS); **LC-MS** (C18, ESI_MS) 592.1 $[M+H]^+$, 614.1 $[M+Na]^+$; $R_t = 5.81$ min.

Analytical data of compound 63



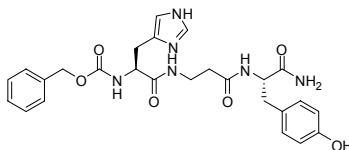
Peptide **63** was synthesized and released from solid support according to **GP 2** and **GP 4**. **Yield** = 26 %; **Purity** > 95% (LC_MS); **LC-MS** (C4, ESI_MS) 621.3 [M+H]⁺, 643.4 [M+Na]⁺; R_t = 5.52 min; **¹H NMR** (400 MHz, DMSO-D₆): δ = 8.90 (s, 1H), 8.90 (s, 1H), 8.19 (s, 1H), 8.17 (s, 1H), 8.15 (s, 1H), 7.96 (dd, *J* = 9.2, 5.6 Hz, 1H), 7.32 (s, 1H), 7.28 (s, 1H), 4.61 (dd, *J* = 13.2, 7.4 Hz, 1H), 4.54 (dt, *J* = 8.4 5.4 Hz, 1H), 4.25 (dq, *J* = 5.6, 2.6 Hz, 1H), 3.58 (dq, *J* = 11.2, 5.5 Hz, 2H), 3.52-3.45 (m, 1H), 3.28 (dd, *J* = 5.3, 2.5 Hz, 2H), 3.26-3.18 (m, 1H), 3.10 (dd, *J* = 15.1, 5.5 Hz, 1H), 3.07-2.98 (m, 2H), 2.88 (dd, *J* = 15.2, 8.9 Hz, 1H), 2.05 (t, *J* = 7.4 Hz, 2H), 1.38 (p, *J* = 7.4 Hz, 2H), 1.27-1.15 (m, 14H), 1.14-1.08 (m, 2H), 0.83 (t, *J* = 6.8 Hz, 3H) ppm; [α]_D²⁰ = -3.8° (C = 2.6, DMSO).

Analytical data of compound 64



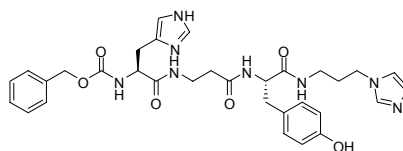
Peptide **64** was synthesized and released from solid support according to **GP 2** and **GP 4**. **Yield** = 5 %; **Purity** > 95% (LC_MS); **LC-MS** (C18, ESI_MS) 538.2 [M+H]⁺, 560.2 [M+Na]⁺; R_t = 5.62 min.

Analytical data of compound 65



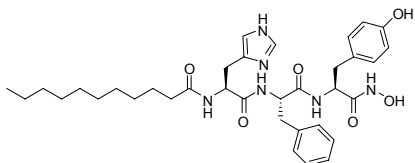
Peptide **65** was synthesized and released from solid support according to **GP 2** and **GP 4**. **Yield** = 1 %; **Purity** > 95% (LC_MS); **LC-MS** (C18, ESI_MS) 523.2 [M+H]⁺, 545.2 [M+Na]⁺; R_t = 5.04 min.

Analytical data of compound 66



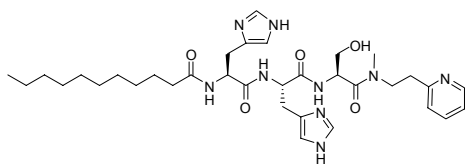
Peptide **66** was synthesized and released from solid support according to **GP 2** and **GP 4**. **Yield** = 6 %; **Purity** > 95% (LC_MS); **LC-MS** (C18, ESI_MS) 631.2 [M+H]⁺, 653.3 [M+Na]⁺; R_t = 4.37 min.

Analytical data of compound 67



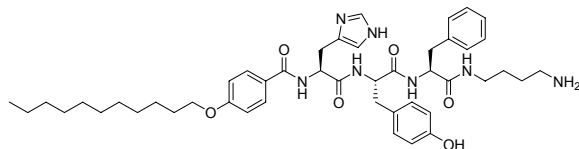
Peptide **67** was synthesized and released from solid support according to **GP 2** and **GP 5**. **Yield** = 13 %; **Purity** > 95% (LC_MS); **LC-MS** (C4, ESI_MS) 649.4 [M+H]⁺, 671.3 [M+Na]⁺; R_t = 9.87 min; ¹H NMR (400 MHz, DMSO-D₆): δ = 10.58 (s, 1H), 8.86 (s, 1H), 8.27 (d, *J* = 8.0 Hz, 1H), 7.99 (d, *J* = 8.4 Hz, 1H), 7.87 (d, *J* = 8.0 Hz, 1H), 7.19 (d, *J* = 6.2 Hz, 2H), 7.15 (d, *J* = 7.0 Hz, 2H), 6.98 (d, *J* = 8.4 Hz, 2H), 6.62 (d, *J* = 8.3 Hz, 2H), 4.55 (dt, *J* = 8.5, 8.3 Hz, 1H), 4.49 (dt, *J* = 8.6 4.5 Hz, 1H), 4.29 (q, *J* = 7.7 Hz, 1H), 3.00-2.91 (m, 2H), 2.85-2.72 (m, 3H), 2.68 (dd, *J* = 13.9, 7.5 Hz, 1H), 2.01 (t, *J* = 7.5 Hz, 1H), 1.40-1.31 (m, 1H), 1.30-1.15 (m, 14H), 1.14-1.08 (m, 2H), 0.83 (t, *J* = 6.7Hz, 3H) ppm; [α]_D²⁰ = - 14.1° (C = 1.1, DMSO).

Analytical data of compound 68



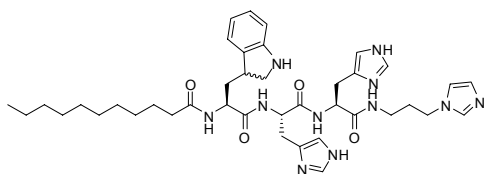
Peptide **68** was synthesized and released from solid support according to **GP 2** and **GP 4**. **Yield** = 6 %; **Purity** > 95% (LC_MS); **LC-MS** (C4, ESI_MS) 666.3 [M+H]⁺, 688.4 [M+Na]⁺; R_t = 5.25 min.

Analytical data of compound 69



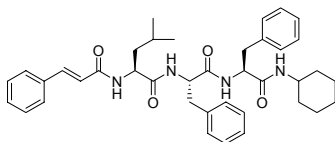
Peptide **69** was synthesized and released from solid support according to **GP 2** and **GP 3**. **Yield** = 6 %; **Purity** > 95% (LC_MS); **LC-MS** (C4, ESI_MS) 810.5 [M+H]⁺, 832.5 [M+Na]⁺; R_t = 7.70 min; ¹H NMR (400 MHz, DMSO-D₆): δ = 9.13 (d, *J* = 5.5 Hz, 1H), 8.65 (tt, *J* = 7.8 1.3 Hz, 1H), 8.36 (d, *J* = 8.0 Hz, 1H), 8.26 (d, *J* = 8.1 Hz, 1H), 8.17 (d, *J* = 6.8 Hz, 1H), 8.15 (d, *J* = 6.8 Hz, 1H), 7.92 (t, *J* = 5.7 Hz, 1H), 7.81 (s, 1H), 7.57 (d, *J* = 8.9 Hz, 2H), 7.26-7.12 (m, 7H), 6.93 (d, *J* = 9.0 Hz, 2H), 6.83 (d, *J* = 8.5 Hz, 2H), 6.41 (d, *J* = 8.4 Hz, 2H), 4.77 (dt, *J* = 9.0, 5.7 Hz, 1H), 4.47-4.35 (m, 2H), 4.00 (t, *J* = 6.5 Hz, 2H), 3.15-3.05 (m, 2H), 3.25-3.20 (m, 2H), 3.02-2.88 (m, 4H), 2.84-2.68 (m, 4H), 1.71 (p, *J* = 6.8 Hz, 2H), 1.48-1.31 (m, 4H), 1.32-1.22 (m, 16H), 0.83 (t, *J* = 6.6 Hz, 3H) ppm; [α]_D²⁰ = + 5.5° (C = 0.4, DMSO).

Analytical data of compound 70



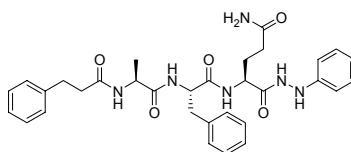
Peptide **70** was synthesized and released from solid support according to **GP 2** and **GP 4**. **Yield** = 20 %; **Purity** > 95% (LC_MS); **LC-MS** (C4, ESI_MS) 756.4 [M+H]⁺, 778.4 [M+Na]⁺; R_t = 5.26 min.

Analytical data of compound 71



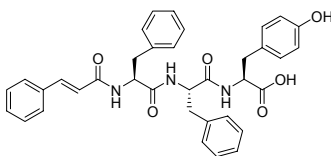
Peptide **71** was synthesized and released from solid support according to **GP 2** and **GP 3**. **Yield** = 18 %; **Purity** > 95% (LC_MS); **LC-MS** (C18, ESI_MS) 637.2 [M+H]⁺, 659.4 [M+Na]⁺; R_t = 10.40 min; ¹³C NMR (100 MHz, CDCl₃): δ = 172.5, 170.9, 169.8, 166.1, 141.5, 141.5, 139.6, 136.9, 136.4, 135.0, 132.6, 129.9, 129.6, 129.5, 129.0, 128.5, 128.0, 126.8, 54.4, 54.4, 52.0, 48.4, 42.3, 39.2, 39.2, 32.9, 32.7, 30.8, 25.7, 25.1, 23.1, 22.7 ppm.

Analytical data of compound 72



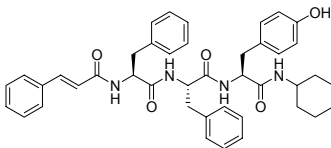
Peptide **72** was synthesized and released from solid support according to **GP 2** and **GP 3**. **Yield** = **Purity** > 95% (LC_MS); 2 %; **LC-MS** (C18, ESI_MS) 587.3 [M+H]⁺, 609.4 [M+Na]⁺; R_t = 7.41 min.

Analytical data of compound **73**



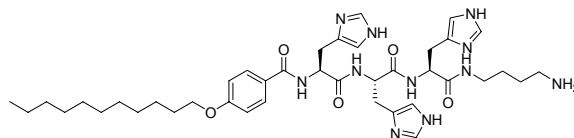
Peptide **73** was synthesized and released from solid support according to **GP 2** and **GP 3**. **Yield** = 12 %; **Purity** > 95% (LC_MS); **LC-MS** (C18, ESI_MS) 606.0 [M+H]⁺, 628.2 [M+Na]⁺; R_t = 8.41 min; ¹H NMR (400 MHz, CD₃OD): δ = 7.58-7.49 (m, 2H), 7.46 (d, *J* = 15.7 Hz, 1H, Ph-CH=), 7.42-7.35 (m, 3H), 7.26-7.08 (m, 10H), 7.03 (d, *J* = 8.6 Hz, 2H), 6.70 (d, *J* = 8.6 Hz, 2H), 6.55 (d, *J* = 15.7 Hz, 1H), 4.71 (dd, *J* = 9.4, 5.3 Hz, 1H), 4.64 (dd, *J* = 8.7, 5.3 Hz, 1H), 4.57 (dd, *J* = 7.9, 5.5 Hz, 3H), 3.17-3.02 (m, 3H), 2.97-2.78 (m, 3H) ppm; ¹³C NMR (100 MHz, CD₃OD): δ = 174.4, 173.2, 172.9, 168.3, 142.4, 138.5, 138.2, 136.2, 131.4, 130.9, 130.4, 130.2, 130.0, 129.4, 129.4, 128.9, 128.9, 127.7, 127.6, 121.3, 116.3, 116.3, 56.0, 55.7, 55.4, 38.9, 38.6, 37.7 ppm.

Analytical data of compound **74**



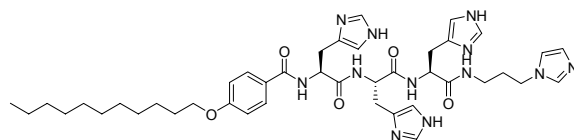
Peptide **74** was synthesized and released from solid support according to **GP 2** and **GP 3**. **Yield** = 2 %; **Purity** > 95% (LC_MS); **LC-MS** (C18, ESI_MS) 687.1 [M+H]⁺, 709.4 [M+Na]⁺; R_t = 12.11 min.

Analytical data of compound **75**



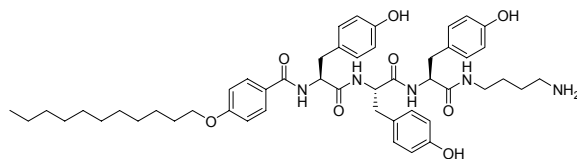
Peptide **75** was synthesized and released from solid support according to **GP 2** and **GP 4**. **Yield** = 20 %; **Purity** > 95% (LC_MS); **LC-MS** (C4, ESI_MS) 774.4 [M+H]⁺, 796.4 [M+Na]⁺; R_t = 5.43 min; **¹H NMR** (400 MHz, DMSO-D₆): δ = 8.91 (d, *J* = 0.8 Hz, 1H), 8.89 (s, 1H), 8.85 (s, 1H), 8.56 (d, *J* = 7.6 Hz, 1H), 8.35 (d, *J* = 7.7 Hz, 2H), 8.12 (t, *J* = 5.6, 5.6 Hz, 1H), 7.82 (br s, 3H), 7.75 (d, *J* = 8.8 Hz, 2H), 7.31 (s, 1H), 7.29 (s, 2H), 6.95 (d, *J* = 8.9 Hz, 2H), 4.71-4.62 (m, 1H), 4.54 (dd, *J* = 13.3, 7.8 Hz, 1H), 4.48 (dd, *J* = 13.8, 7.9 Hz, 1H), 3.99 (t, *J* = 6.5, 6.5 Hz, 2H), 3.24-3.05 (m, 5H), 3.05-2.90 (m, 3H), 2.85-2.68 (m, 2H), 1.75-1.63 (m, 2H), 1.57-1.43 (m, 2H), 1.43-1.34 (m, 4H), 1.34-1.16 (m, 16H), 0.83 (t, *J* = 6.8, 6.8 Hz, 3H) ppm; **¹³C NMR** (100 MHz, DMSO-D₆): δ = 170.5, 169.7, 169.5, 166.2, 161.2, 158.6, 158.3, 133.7, 133.7, 129.9, 129.4, 129.2, 125.4, 116.7, 116.6, 116.5, 113.7, 67.6, 52.5, 51.9, 51.9, 38.3, 38.0, 31.1, 28.8, 28.6, 28.5, 28.4, 26.9, 26.9, 26.5, 26.5, 26.1, 25.7, 25.3, 24.3, 21.9, 13.8 ppm; **HRMS** (FAB, *m*-NBA) *m/z* calc. for C₄₀H₅₉N₁₁O₅ 773.4701, found 774.4810 [M+H]⁺; [α]_D²⁰ = -12.3° (C = 1.8, DMSO).

Analytical data of compound 76



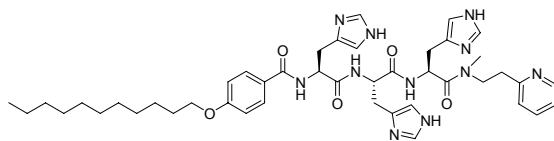
Peptide **76** was synthesized and released from solid support according to **GP 2** and **GP 4**. **Yield** = 21 %; **Purity** > 95% (LC_MS); **LC-MS** (C4, ESI_MS) 811.5 [M+H]⁺, 833.5 [M+Na]⁺; R_t = 5.45 min; **¹H NMR** (400 MHz, DMSO-D₆): δ = 8.98 (s, 1H), 8.90 (d, *J* = 0.8 Hz, 1H), 8.89 (d, *J* = 0.8 Hz, 1H), 8.84 (s, 1H), 8.58 (d, *J* = 7.8 Hz, 1H), 8.42 (d, *J* = 7.5 Hz, 1H), 8.39 (d, *J* = 7.6 Hz, 1H), 8.21 (t, *J* = 5.6 Hz, 1H), 7.75 (d, *J* = 8.8 Hz, 2H), 7.70 (t, *J* = 1.4 Hz, 1H), 7.63 (t, *J* = 1.3 Hz, 1H), 7.32 (s, 1H), 7.29 (s, 2H), 6.95 (d, *J* = 8.9 Hz, 2H), 4.70-4.63 (m, 1H), 4.54 (dt, *J* = 7.9, 4.9 Hz, 1H), 4.46 (dd, *J* = 13.9, 7.7 Hz, 1H), 4.12 (t, *J* = 6.8, Hz, 2H), 3.99 (t, *J* = 6.5 Hz, 2H), 3.20-2.94 (m, 6H), 1.95-1.86 (m, 2H), 1.69 (p, *J* = 6.6 Hz, 2H), 1.43-1.34 (m, 2H), 1.34-1.21 (m, 16H), 0.83 (t, *J* = 6.8 Hz, 3H) ppm; [α]_D²⁰ = -17.1° (C = 1.9, DMSO).

Analytical data of compound 77



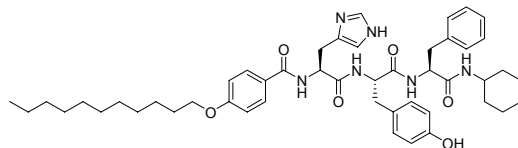
Peptide **77** was synthesized and released from solid support according to **GP 2** and **GP 3**. **Yield** = 18 %; **Purity** > 95% (LC_MS); **LC-MS** (C4, ESI_MS) 852.4 [M+H]⁺, 874.6 [M+Na]⁺; R_t = 8.39 min; **¹H NMR** (400 MHz, DMSO-D₆): δ = 9.11 (s, 2H), 8.32 (d, *J* = 8.1 Hz, 1H), 7.98 (d, *J* = 8.2 Hz, 1H), 7.94 (d, *J* = 8.0 Hz, 1H) 7.77-7.72 (m, 3H), 7.05 (d, *J* = 8.5 Hz, 2H), 7.02-6.92 (m, 6H), 6.64 (d, *J* = 8.5 Hz, 2H), 6.60 (d, *J* = 8.5 Hz, 2H), 6.54 (d, *J* = 8.50 Hz, 2H), 4.58-4.46 (m, 1H), 4.40 (dt, *J* = 8.4, 8.3, 5.0 Hz, 1H), 4.34 (dd, *J* = 14.2, 8.1 Hz, 1H), 4.00 (t, *J* = 6.5, 6.5 Hz, 2H), 3.15-2.92 (m, 2H), 2.89-2.79 (m, 4H), 2.79-2.62 (m, 4H), 1.82-1.63 (m, 2H), 1.51-1.35 (m, 4H), 1.33-1.20 (m, 18H), 0.84 (t, *J* = 7.0, 7.0 Hz, 3H) ppm; **¹³C NMR** (100 MHz, DMSO-D₆): δ = 171.4, 170.5, 170.4, 165.8, 160.9, 155.6, 155.6, 155.5, 130.0, 129.9, 129.1, 128.3, 127.4, 127.4, 125.9, 114.7, 114.7, 113.7, 67.5, 55.0, 54.2, 54.1, 38.4, 37.7, 36.9, 36.5, 36.5, 35.7, 35.7, 31.1, 28.8, 28.6, 28.5, 28.4, 25.7, 25.3, 24.2, 21.9, 13.8 ppm; **HRMS** (FAB, *m*-NBA) *m/z* calc. for C₄₉H₆₅N₅O₈ 851.4833, found 852.4888 [M+H]⁺; [α]_D²⁰ = -28.3° (C = 1.3, DMSO).

Analytical data of compound 78



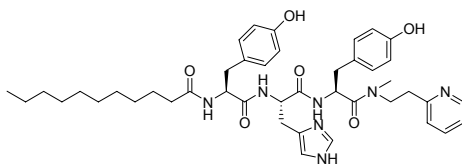
Peptide **78** was synthesized and released from solid support according to **GP 2** and **GP 3**. **Yield** = 25 %; **Purity** > 95% (LC_MS); **LC-MS** (C4, ESI_MS) 822.4 [M+H]⁺, 844.4 [M+Na]⁺; R_t = 5.71 min.

Analytical data of compound 79



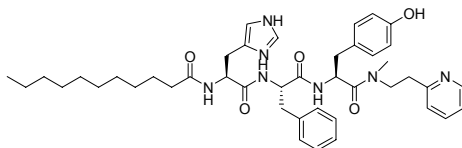
Peptide **79** was synthesized and released from solid support according to **GP 2** and **GP 3**. **Yield** = 1 %; **Purity** > 85% (LC_MS); **LC-MS** (C4, ESI_MS) 821.3 [M+H]⁺; R_t = 8.68 min.

Analytical data of compound 80



Peptide **80** was synthesized and released from solid support according to **GP 2** and **GP 4**. **Yield** = 12 %; **Purity** > 85% (LC_MS); **LC-MS** (C4, ESI_MS) 768.3 [M+H]⁺, 790.4 [M+Na]⁺; R_t = 6.41 min; **¹H NMR** (400 MHz, DMSO-D₆): δ = 9.22 (s, 1H), 9.12 (s, 1H), 8.96 (d, *J* = 1.0 Hz, 1H), 8.48 (dd, *J* = 14.0, 5.0 Hz, 1H), 8.21 (d, *J* = 6.77 Hz, 2H), 7.95 (d, *J* = 8.02 Hz, 1H), 7.78-7.66 (m, 1H), 7.35-7.19 (m, 3H), 7.00 (d, *J* = 8.6 Hz, 2H), 6.98 (d, *J* = 8.2 Hz, 2H), 6.66-6.58 (m, 4H), 4.71 (q, *J* = 7.3 Hz, 1H), 4.57 (dd, *J* = 13.8, 7.1 Hz, 1H), 4.35 (ddd, *J* = 10.7, 8.3, 3.9 Hz, 1H), 3.70 (ddd, *J* = 12.5, 8.5, 6.1 Hz, 2H), 3.49 (t, *J* = 8.0 Hz, 2H), 3.06-2.99 (m, 1H), 2.94 (dd, *J* = 15.1, 7.6 Hz, 1H), 2.88-2.79 (m, 2H), 2.71-2.65 (m, 1H), 2.59 (dd, *J* = 13.9, 10.5 Hz, 1H), 1.99 (t, *J* = 7.4 Hz, 2H), 1.38-1.30 (m, 2H), 1.27-1.04 (m, 14H), 0.83 (t, *J* = 6.8 Hz, 3H) ppm; **¹³C NMR** (100 MHz, DMSO-D₆): δ = 173.2, 172.4, 171.4, 169.8, 156.7, 156.4, 143.3, 134.3, 130.8, 130.8, 130.8, 130.6, 129.6, 128.6, 119.4, 117.6, 115.6, 115.4, 55.0, 53.0, 51.8, 41.1, 36.9, 35.8, 35.6, 31.9, 29.6, 29.5, 29.4, 29.3, 29.1, 25.9, 22.7, 14.6 ppm; **HRMS** (ESI) *m/z* calc. for C₄₃H₅₇N₇O₆ 767.4370, found 768.4455 [M+H]⁺; [α]_D²⁰ = +12.7° (C = 0.8, DMSO).

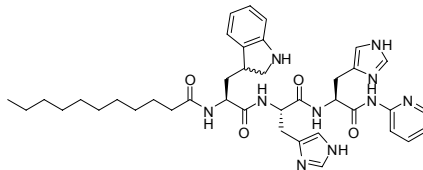
Analytical data of compound 81



Peptide **81** was synthesized and released from solid support according to **GP 2** and **GP 4**. **Yield** = 18 %; **Purity** > 95% (LC_MS); **LC-MS** (C4, ESI_MS) 752.3 [M+H]⁺, 774.4 [M+Na]⁺; R_t = 6.62 min; **¹H NMR** (400 MHz, DMSO-D₆): δ = 8.92 (dd, *J* = 2.8, 1.3 Hz, 1H), 8.49 (dd, *J* = 16.9, 5.5 Hz, 1H), 8.44-8.40 (m, 1H), 8.01 (dd, *J* = 8.3, 2.0 Hz, 1H), 7.83 (d, *J* = 7.9 Hz, 1H), 7.78 (d, *J* = 7.8 Hz, 1H), 7.33-7.10 (m, 10H), 6.98 (d, *J* = 8.5 Hz, 1H), 6.98 (d, *J* = 8.5 Hz, 1H), 6.63 (d, *J* = 8.5 Hz, 1H), 6.63 (d, *J* = 8.5 Hz, 1H), 4.73 (q, *J* = 7.4 Hz, 1H), 4.59-4.54 (m, 1H), 4.54-4.49 (m, 1H), 3.68 (ddd, *J* = 12.7, 8.4, 6.5 Hz, 2H), 3.46-3.39 (m, 2H), 3.01-2.91 (m, 2H), 2.87-2.75 (m, 3H), 2.74-2.71 (m, 3H), 2.64 (dd, *J* = 13.4, 6.7 Hz, 1H), 2.02 (t, *J* = 7.4 Hz, 2H), 1.40-1.32 (m, 2H), 1.29-1.08 (m, 14H), 0.83 (t, *J* = 6.7 Hz, 3H); **¹³C NMR** (100 MHz, DMSO-D₆): δ = 172.2,

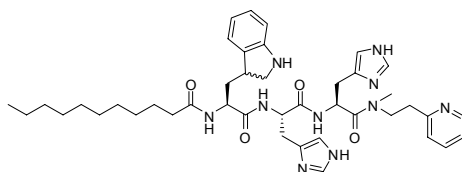
172.2, 170.4, 170.4, 170.0, 169.6, 169.6, 155.8, 137.8, 137.1, 136.9, 133.5, 130.0, 129.4, 129.3, 129.1, 129.1, 127.8, 127.7, 127.0, 126.1, 126.1, 123.7, 123.3, 121.9, 121.7, 117.3, 116.6, 114.8, 53.3, 53.3, 53.2, 51.0, 51.0, 51.0, 47.3, 37.3, 36.6, 36.6, 35.9, 34.9, 34.8, 33.3, 31.1, 28.8, 28.7, 28.6, 28.6, 28.5, 28.4, 26.7, 26.7, 26.7, 26.7, 24.9, 21.9, 13.8 ppm; **HRMS** (ESI) m/z calc. for $C_{43}H_{57}N_7O_5$ 751.4421, found 752.4504 $[M+H]^+$; $[\alpha]_D^{20} = -5.9^\circ$ (C = 1.6, DMSO).

Analytical data of compound **82**



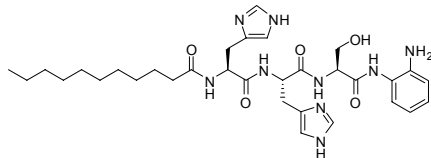
Peptide **82** was synthesized and released from solid support according to **GP 2** and **GP 4**. **Yield** = 9 %; **Purity** > 95% (LC_MS); **LC-MS** (C4, ESI_MS) 725.4 $[M+H]^+$, 747.5 $[M+Na]^+$; R_t = 6.01 min; **1H NMR** (400 MHz, DMSO- D_6): δ = 8.95 (d, J = 1.4 Hz, 1H), 8.94 (d, J = 1.2 Hz, 1H), 8.39 (d, J = 7.5 Hz, 1H), 8.31 (d, J = 6.7 Hz, 1H), 8.15 (d, J = 7.2 Hz, 1H), 7.39-7.35 (m, 2H), 7.31 (d, J = 6.9 Hz, 2H), 7.12 (d, J = 7.3 Hz, 2H), 7.04 (d, J = 7.0 Hz, 2H), 6.97 (d, J = 7.0 Hz, 2H), 6.68-6.57 (m, 3H), 4.60-4.49 (m, 2H), 4.32-4.24 (m, 1H), 3.23-3.04 (m, 4H), 3.03-2.93 (m, 2H), 2.20-2.05 (m, 2H), 2.04-1.87 (m, 1H), 1.74-1.59 (m, 1H), 1.55-1.42 (m, 2H), 1.28-1.17 (m, 16H), 0.84-0.79 (m, 3H) ppm; $[\alpha]_D^{20} = -3.2^\circ$ (C = 0.7, DMSO).

Analytical data of compound **83**



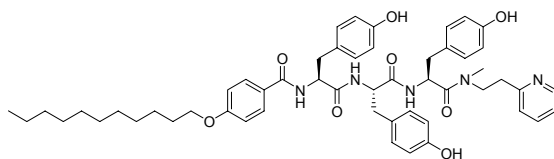
Peptide **83** was synthesized and released from solid support according to **GP 2** and **GP 4**. **Yield** = 14 %; **Purity** > 95% (LC_MS); **LC-MS** (C4, ESI_MS) 767.4 $[M+H]^+$, 789.4 $[M+Na]^+$; R_t = 5.57 min.

Analytical data of compound **84**



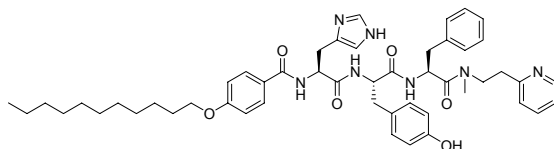
Peptide **84** was synthesized and released from solid support according to **GP 2** and **GP 4**. **Yield** = 23 %; **Purity** > 85% (LC_MS); **LC-MS** (C4, ESI_MS) 638.3 [M+H]⁺, 660.3 [M+Na]⁺; R_t = 5.83 min; **¹H NMR** (400 MHz, DMSO-D₆): δ = 9.32 (s, 1H), 8.94-8.93 (m, 2H), 8.93 (s, 2H), 8.27 (d, *J* = 7.84 Hz, 1H), 8.20 (d, *J* = 6.9 Hz, 1H), 8.16 (d, *J* = 7.9 Hz, 1H), 7.63 (dd, *J* = 6.0, 3.1 Hz, 1H), 7.35 (d, *J* = 3.3 Hz, 2H), 7.32-7.29 (m, 3H), 7.07 (dd, *J* = 7.8, 1.4 Hz, 1H), 6.92 (dt, *J* = 8.0, 1.5 Hz, 1H), 6.71 (dd, *J* = 8.0, 1.3 Hz, 1H), 6.53 (dt, *J* = 7.6, 1.4 Hz, 1H), 4.72-4.62 (m, 1H), 4.59-4.52 (m, 1H), 4.44 (q, *J* = 5.7, 5.6 Hz, 1H), 3.88 (dd, *J* = 5.2, 2.7 Hz, 1H), 3.74 (dd, *J* = 10.8, 5.6 Hz, 1H), 3.66 (dd, *J* = 10.8, 5.6 Hz, 1H), 3.18 (dd, *J* = 15.7, 5.7 Hz, 1H), 3.13-2.98 (m, 2H), 2.89 (dd, *J* = 15.3, 9.4 Hz, 1H), 2.05 (t, *J* = 7.4 Hz, 2H), 1.42-1.34 (m, 1H), 1.29-1.14 (m, 14H), 1.14-1.09 (m, 2H), 0.89-0.78 (m, 3H) ppm.

Analytical data of compound 85



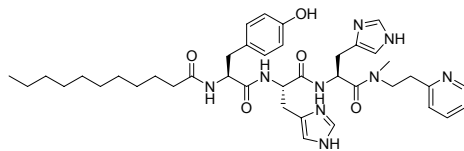
Peptide **85** was synthesized and released from solid support according to **GP 2** and **GP 3**. **Yield** = 2 %; **Purity** > 95% (LC_MS); **LC-MS** (C4, ESI_MS) 900.3 [M+H]⁺, 922.5 [M+Na]⁺; R_t = 8.88 min.

Analytical data of compound 86



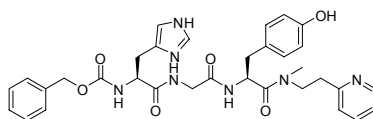
Peptide **86** was synthesized and released from solid support according to **GP 2** and **GP 3**. **Yield** = 2 %; **Purity** > 95% (LC_MS); **LC-MS** (C4, ESI_MS) 858.3 [M+H]⁺, 880.5 [M+Na]⁺; R_t = 7.45 min.

Analytical data of compound 87



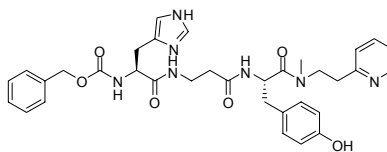
Peptide **87** was synthesized and released from solid support according to **GP 2** and **GP 4**. **Yield** = 10 %; **Purity** > 95% (LC_MS); **LC-MS** (C4, ESI_MS) 742.4 [M+H]⁺, 764.4 [M+Na]⁺; R_t = 5.67 min; **¹H NMR** (400 MHz, DMSO-D₆): δ = 8.96 (d, *J* = 1.3 Hz, 1H), 8.95 (d, *J* = 1.3 Hz, 1H), 8.55 (d, *J* = 4.0 Hz, 1H), 8.28 (d, *J* = 7.8 Hz, 2H), 7.93 (d, *J* = 7.7 Hz, 1H), 7.52-7.16 (m, 5H), 6.98 (d, *J* = 8.6 Hz, 2H), 6.60 (d, *J* = 8.5 Hz, 2H), 5.14-4.76 (m, 1H), 4.56-4.47 (m, 1H), 4.38-4.26 (m, 1H), 3.80-3.63 (m, 4H), 3.53-3.43 (m, 1H), 3.12-2.93 (m, 6H), 2.92 (s, 3H), 2.84-2.73 (m, 3H), 2.55 (dd, *J* = 13.7, 11.0 Hz, 1H), 1.99 (dt, *J* = 7.4, 7.4, 2.9 Hz, 2H), 1.51-1.28 (m, 2H), 1.28-1.01 (m, 14H), 0.83 (t, *J* = 6.9, 6.9 Hz, 3H) ppm; **¹³C NMR** (100 MHz, DMSO-D₆): δ = 172.5, 171.8, 170.6, 169.4, 158.2, 157.9, 155.6, 142.2, 133.6, 133.6, 129.8, 129.0, 128.7, 127.7, 124.2, 124.1, 117.1, 116.7, 114.6, 54.2, 53.5, 51.4, 51.3, 35.0, 34.9, 31.1, 28.8, 28.7, 28.6, 28.5, 28.4, 26.7, 26.5, 26.3, 26.2, 25.0, 21.9, 13.8 ppm; **HRMS** (FAB, *m*-NBA) *m/z* calc. for C₄₀H₅₅N₉O₅ 741.4326, found 741.4352 [M]⁺; found 742.4373 [M+H]⁺; [α]_D²⁰ = - 7.6° (C = 0.6, DMSO).

Analytical data of compound 88



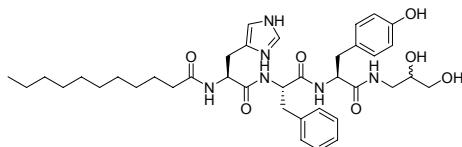
Peptide **88** was synthesized and released from solid support according to **GP 2** and **GP 4**. **Yield** = 2 %; **Purity** > 95% (LC_MS); **LC-MS** (C18, ESI_MS) 628.2 [M+H]⁺, 650.2 [M+Na]⁺; R_t = 4.72 min.

Analytical data of compound 89



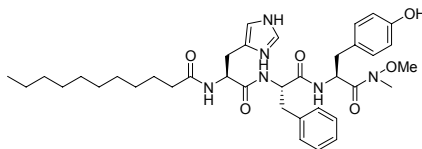
Peptide **89** was synthesized and released from solid support according to **GP 2** and **GP 4**. **Yield** = 1 %; **Purity** > 95% (LC_MS); **LC-MS** (C18, ESI_MS) 642.2 [M+H]⁺, 664.3 [M+Na]⁺; R_t = 4.75 min.

Analytical data of compound 90



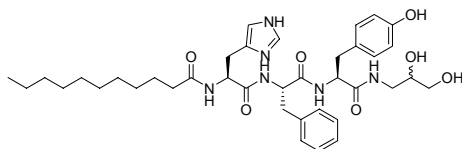
Peptide **90** was synthesized and released from solid support according to **GP 2** and **GP 4**. **Yield** = 3 %; **Purity** > 95% (LC_MS); **LC-MS** (C4, ESI_MS) 707.4 [M+H]⁺, 729.4 [M+Na]⁺; R_t = 6.32 min.

Analytical data of compound 91



Peptide **91** was synthesized and released from solid support according to **GP 2** and **GP 4**. **Yield** = 1 %; **Purity** > 95% (LC_MS); **LC-MS** (C4, ESI_MS) 677.3 [M+H]⁺, 699.4 [M+Na]⁺; R_t = 7.40 min.

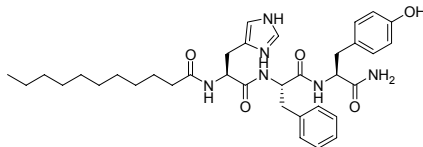
Analytical data of compound 92



Peptide **92** was synthesized and released from solid support according to **GP 2** and **GP 4**. **Yield** = 35 %; **Purity** > 95% (LC_MS); **LC-MS** (C4, ESI_MS) 707.4 [M+H]⁺, 729.4 [M+Na]⁺; R_t = 6.89 min; ¹H NMR (400 MHz, DMSO-D₆): δ = 8.86 (s, 1H), 8.17 (dd, *J* = 8.2, 2.3 Hz, 1H), 7.99 (d, *J* = 8.3 Hz, 1H), 7.88 (dd, *J* = 7.8, 2.2 Hz, 1H), 7.82 (dt, *J* = 5.8, 2.8 Hz, 1H), 7.22-7.12 (m, 6H), 6.99 (dd, *J* = 8.4, 1.4 Hz, 2H), 6.61 (d, *J* = 8.4 Hz, 2H), 4.55 (dt, *J* = 8.7, 5.5 Hz, 1H), 4.50-4.44 (m, 1H), 4.44-4.37 (m, 1H), 3.43 (td, *J* = 15.9, 5.2 Hz, 1H), 3.28-3.22 (m, 2H), 3.21-3.13 (m,

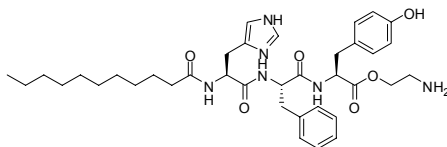
1H), 3.03-2.91 (m, 3H), 2.88-2.68 (m, 3H), 2.01 (t, $J = 7.4$, Hz, 2H), 1.36 (p, $J = 7.5$ Hz, 2H), 1.29-1.16 (m, 16H), 1.13-1.07 (m, 2H), 0.83 (t, $J = 6.8$ Hz, 3H) ppm; $[\alpha]_D^{20} = -4.9^\circ$ (C = 3.7, DMSO).

Analytical data of compound 93



Peptide **93** was synthesized and released from solid support according to **GP 2** and **GP 4**. **Yield** = 13 %; **Purity** > 95% (LC_MS); **LC-MS** (C4, ESI_MS) 633.3 $[M+H]^+$, 655.4 $[M+Na]^+$; $R_t = 7.12$ min; **1H NMR** (400 MHz, DMSO- D_6): $\delta = 8.86$ (s, 1H), 8.11 (d, $J = 8.1$ Hz, 1H), 8.01 (d, $J = 8.3$ Hz, 1H), 7.94 (d, $J = 7.9$ Hz, 1H), 7.26 (br s, 1H), 7.24-7.13 (m, 5H), 7.04 (br s, 1H), 7.01 (d, $J = 8.5$ Hz, 2H), 6.63 (d, $J = 8.52$ Hz, 2H), 4.56 (dt, $J = 8.5, 8.5, 5.5$ Hz, 1H), 4.48 (dt, $J = 8.4, 8.4, 4.6$ Hz, 1H), 4.36 (dt, $J = 8.2, 8.2, 5.5$ Hz, 1H), 3.04-2.92 (m, 2H), 2.93-2.77 (m, 3H), 2.72 (dd, $J = 14.1, 8.5$ Hz, 1H), 2.03 (t, $J = 7.4, 7.4$ Hz, 2H), 1.50-1.31 (m, 2H), 1.31-1.07 (m, 14H), 0.85 (t, $J = 6.8, 6.8$ Hz, 3H) ppm; **^{13}C NMR** (100 MHz, DMSO- D_6): $\delta = 172.5, 172.2, 170.3, 169.9, 155.6, 137.3, 133.6, 129.9, 129.5, 129.0, 127.8, 127.6, 126.1, 116.6, 114.7, 54.0, 53.8, 51.1, 37.2, 36.7, 34.9, 31.1, 28.9, 28.8, 28.6, 28.5, 28.4, 26.8, 24.9, 21.9, 13.8$ ppm; **HRMS** (FAB, *m*-NBA) m/z calc. for $C_{35}H_{48}N_6O_5$ 632.3686, found 633.3773 $[M+H]^+$; $[\alpha]_D^{20} = -7.5^\circ$ (C = 1.2, DMSO).

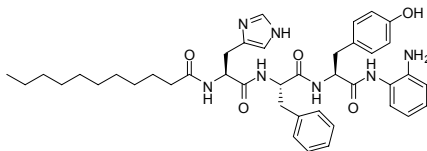
Analytical data of compound 94



Peptide **94** was synthesized and released from solid support according to **GP 2** and **GP 4**. **Yield** = 12 %; **Purity** > 95% (LC_MS); **LC-MS** (C4, ESI_MS) 676.4 $[M+H]^+$, 677.4 $[M+Na]^+$; $R_t = 6.31$ min; **1H NMR** (400 MHz, DMSO- D_6): $\delta = 8.86$ (s, 1H), 8.45 (d, $J = 7.6$ Hz, 1H), 8.01 (d, $J = 8.3$ Hz, 1H), 7.95 (d, $J = 8.1$ Hz, 1H), 7.25-7.14 (m, 6H), 6.99 (d, $J = 8.5$ Hz, 2H), 6.65 (d, $J = 8.5$ Hz, 2H), 4.57-4.48 (m, 2H), 4.22 (td, $J = 11.3, 5.5$ Hz, 1H), 4.18-4.11 (m, 1H), 3.05 (dd, $J = 8.1, 5.4$ Hz, 2H), 3.00 (dd, $J = 9.7, 4.7$ Hz, 1H), 2.98-2.91 (m, 2H), 2.85 (dd, $J = 14.4, 8.5$ Hz, 1H),

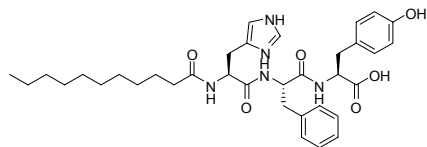
2.81-2.72 (m, 2H), 2.01 (t, $J = 7.5$ Hz, 2H), 1.40-1.31 (m, 2H), 1.28-1.16 (m, 14H), 1.13-1.08 (m, 2H), 0.83 (t, $J = 6.8$ Hz, 3H) ppm; $[\alpha]_D^{20} = -4.5^\circ$ (C = 0.9, DMSO).

Analytical data of compound 95



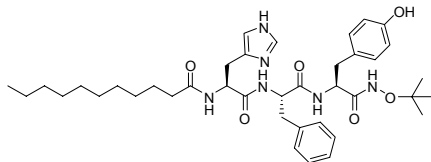
Peptide **95** was synthesized and released from solid support according to **GP 2** and **GP 4**. **Yield** = 5 %; **Purity** > 95% (LC_MS); **LC-MS** (C4, ESI_MS) 724.3 [M+H]⁺, 746.4 [M+Na]⁺; $R_t = 7.49$ min; **¹H NMR** (400 MHz, DMSO-D₆): $\delta = 9.15$ (s, 1H), 8.90 (d, $J = 1.3$ Hz, 1H), 8.35 (d, $J = 7.4$ Hz, 1H), 8.01 (d, $J = 8.3$ Hz, 1H), 7.93 (d, $J = 7.9$ Hz, 1H), 7.23-7.17 (m, 6H), 7.16-7.12 (m, 1H), 7.06 (d, $J = 8.5$ Hz, 2H), 6.98 (dd, $J = 7.8, 1.4$ Hz, 1H), 6.69 (dd, $J = 8.0, 1.3$ Hz, 1H), 6.66 (d, $J = 8.5$ Hz, 2H), 4.61-4.52 (m, 3H), 3.05-2.91 (m, 3H), 2.88-2.77 (m, 3H), 2.02 (t, $J = 7.4$ Hz, 2H), 1.41-1.32 (m, 2H), 1.26-1.16 (m, 14H), 1.14-1.08 (m, 2H), 0.83 (t, $J = 6.8$ Hz, 3H) ppm; $[\alpha]_D^{20} = +2.1^\circ$ (C = 2.3, DMSO).

Analytical data of compound 96



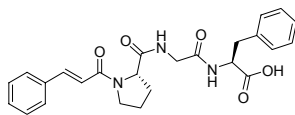
Peptide **96** was synthesized and released from solid support according to **GP 2** and **GP 4**. **Yield** = 22 %; **Purity** > 95% (LC_MS); **LC-MS** (C4, ESI_MS) 634.3 [M+H]⁺, 656.3 [M+Na]⁺; $R_t = 7.29$ min; **¹H NMR** (400 MHz, DMSO-D₆): $\delta = 8.76$ (s, 1H), 8.36 (d, $J = 7.7$ Hz, 1H), 7.96 (d, $J = 8.3$ Hz, 1H), 7.90 (d, $J = 8.1$ Hz, 1H), 7.22-7.14 (m, 6H), 7.00 (d, $J = 8.5$ Hz, 2H), 6.64 (d, $J = 8.5$ Hz, 2H), 4.58-4.49 (m, 2H), 4.36 (dt, $J = 7.9, 5.7$ Hz, 1H), 3.00 (dd, $J = 14.0, 4.2$ Hz, 1H), 2.95 (dd, $J = 8.9, 5.8$ Hz, 1H), 2.91 (dd, $J = 7.4, 5.9$ Hz, 1H), 2.82 (dd, $J = 8.6, 5.6$ Hz, 1H), 2.80-2.73 (m, 2H), 2.01 (t, $J = 7.4$ Hz, 2H), 1.40-1.32 (m, 2H), 1.28-1.17 (m, 14H), 1.14-1.08 (m, 2H), 0.83 (t, $J = 6.8$ Hz, 3H) ppm; $[\alpha]_D^{20} = -0.4^\circ$ (C = 1.7, DMSO).

Analytical data of compound 97



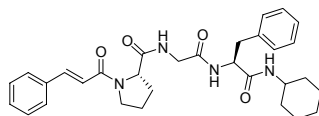
Peptide **97** was synthesized and released from solid support according to **GP 2** and **GP 5**. **Yield** = 5 %; **Purity** > 95% (LC_MS); **LC-MS** (C4, ESI_MS) 705.4 [M+H]⁺, 727.4 [M+Na]⁺; R_t = 7.67 min; ¹H NMR (400 MHz, DMSO-D₆): δ = 8.85 (s, 1H), 8.35 (d, *J* = 8.1 Hz, 1H), 7.97 (d, *J* = 8.4 Hz, 1H), 7.82 (d, *J* = 8.0 Hz, 1H), 7.22-7.14 (m, 5H), 7.00 (d, *J* = 8.5 Hz, 2H), 6.63 (d, *J* = 8.5 Hz, 2H), 4.56 (dd, *J* = 8.8, 5.2 Hz, 1H), 4.50 (dd, *J* = 7.9, 4.4 Hz, 1H), 4.36 (q, *J* = 7.5 Hz, 1H), 3.00-2.91 (m, 2H), 2.83-2.68 (m, 4H), 2.01 (t, *J* = 7.5 Hz, 2H), 1.40-1.32 (m, 2H), 1.29-1.15 (m, 14H), 1.13-1.07 (m, 2H), 1.05-1.03 (m, 9H), 0.83 (t, *J* = 6.8 Hz, 3H) ppm; [α]_D²⁰ = - 8.4° (C = 0.5, DMSO).

Analytical data of compound **98**



Peptide **98** was synthesized and released from solid support according to **GP 2** and **GP 3**. **Yield** = 45 %; **Purity** > 95% (LC_MS); **LC-MS** (C18, ESI_MS) 450.5 [M+H]⁺, 472.4 [M+Na]⁺; R_t = 7.15 min; ¹H NMR (400 MHz, CD₃OD): δ = 7.61 (d, *J* = 15.5 Hz, 1H), 7.58-7.55 (m, 2H), 7.38-7.36 (m, 3H), 7.21 (d, *J* = 4.46 Hz, 5H), 6.97 (d, *J* = 15.5 Hz, 1H), 4.68 (dd, *J* = 8.6, 5.2 Hz, 1H), 4.49 (dd, *J* = 8.3, 5.2 Hz, 1H), 3.96 (d, *J* = 17.0 Hz, 1H), 3.90-3.80 (m, 2H), 3.75 (d, *J* = 17.0 Hz, 1H), 3.24 (dd, *J* = 14.0, 5.2 Hz, 1H), 3.11 (dd, *J* = 14.0, 8.7 Hz, 1H), 2.26-2.20 (m, 1H), 2.19-2.09 (m, 1H), 2.06-1.99 (m, 2H) ppm.

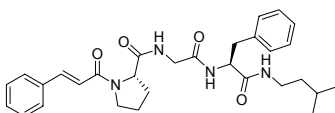
Analytical data of compound **99**



Peptide **99** was synthesized and released from solid support according to **GP 2** and **GP 3**. **Yield** = 22 %; **Purity** > 95% (LC_MS); **LC-MS** (C18, ESI_MS) 531.7 [M+H]⁺, 553.5 [M+Na]⁺; R_t = 8.52 min; ¹H NMR (400 MHz, CD₃OD): δ = 7.67 (d, *J* = 15.5 Hz, 1H), 7.60-7.57 (m, 2H), 7.40-

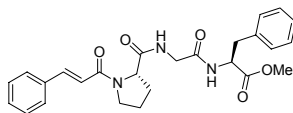
7.36 (m, 3H), 7.23-7.19(m, 5H), 7.01 (d, $J = 15.5$ Hz, 1H), 4.56 (dd, $J = 9.1, 5.9$ Hz, 1H), 4.46 (dd, $J = 8.2, 5.3$ Hz, 1H), 3.93-3.82 (m, 2H), 3.78 (d, $J = 3.7$ Hz, 2H), 3.64-3.58 (m, 1H), 3.24 (dd, $J = 13.8, 5.8$ Hz, 1H), 3.05 (dd, $J = 13.8, 9.2$ Hz, 1H), 2.32-2.27 (m, 1H), 2.16 -1.98 (m, 3H), 1.82-1.68 (m, 5H), 1.36-1.12 (m, 5H) ppm; ^{13}C NMR (100 MHz, CD_3OD): $\delta = 175.8, 172.3, 171.5, 167.7, 144.4, 138.7, 136.2, 132.2, 130.2, 130.0, 129.4, 129.2, 127.7, 119.3, 62.8, 56.5, 50.1, 49.3, 43.9, 39.0, 33.6, 33.5, 30.5, 26.6, 26.1, 26.1, 26.1$ ppm.

Analytical data of compound 100



Peptide **100** was synthesized and released from solid support according to **GP 2** and **GP 3**. **Yield** = 42 %; **Purity** > 95% (LC_MS); **LC-MS** (C18, ESI_MS) 519.7 $[\text{M}+\text{H}]^+$, 541.5 $[\text{M}+\text{Na}]^+$; $R_t = 8.55$ min; ^1H NMR (400 MHz, CD_3OD): $\delta = 7.66$ (d, $J = 15.5$ Hz, 1H), 7.60-7.56 (m, 2H), 7.39-7.37 (m, 3H), 7.24-7.12 (m, 5H), 7.00 (d, $J = 15.5$ Hz, 1H), 4.57 (dd, $J = 9.3, 5.6$ Hz, 1H), 4.45 (dd, $J = 8.3, 5.3$ Hz, 1H), 3.94-3.84 (m, 2H), 3.82 (d, $J = 16.9$ Hz, 1H), 3.75 (d, $J = 16.9$ Hz, 1H), 3.26 (dd, $J = 13.9, 5.7$ Hz, 1H), 3.20 (dt, $J = 7.1, 7.1, 2.4$ Hz, 2H), 3.06 (dd, $J = 13.9, 9.3$ Hz, 1H) 2.30-2.25 (m, 1H), 2.18-2.10(m, 1H), 2.08-1.99 (m, 2H), 1.61-1.50 (m, 1H), 1.36 (m, 2H), 0.89 (d, $J = 1.4$ Hz, 3H), 0.88 (d, $J = 1.4$ Hz, 3H) ppm; ^{13}C NMR (100 MHz, CD_3OD): $\delta = 175.8, 173.2, 171.6, 167.7, 144.4, 138.8, 136.2, 131.2, 130.2, 130.0, 129.4, 129.2, 127.7, 119.3, 62.8, 56.6, 43.9, 39.1, 38.8, 38.8, 30.5, 26.7, 26.1, 22.8, 22.8$ ppm.

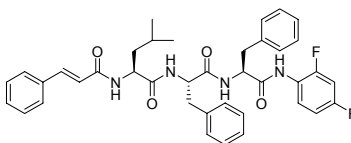
Analytical data of compound 101



Peptide **101** was synthesized and released from solid support according to **GP 2** and **GP 3**. **Yield** = 32 %; **Purity** > 95% (LC_MS); **LC-MS** (C18, ESI_MS) 464.3 $[\text{M}+\text{H}]^+$, 464.4 $[\text{M}+\text{Na}]^+$; $R_t = 7.82$ min; ^1H NMR (400 MHz, CD_3OD): $\delta = 7.61$ (d, $J = 15.5$ Hz, 1H), 7.56-7.54 (m, 2H), 7.38-7.34 (m, 3H), 7.21-7.14 (m, 5H), 6.97 (d, $J = 15.5$ Hz, 1H), 4.68 (dd, $J = 8.3, 6.0$ Hz, 1H), 4.48 (dd, $J = 8.3, 5.3$ Hz, 1H), 3.94 (d, $J = 17.0$ Hz, 1H), 3.88-3.81 (m, 2H), 3.76 (d, $J = 17.0$ Hz, 1H), 3.68 (s, 3H), 3.20 (dd, $J = 13.9, 6.0$ Hz, 1H), 3.10 (dd, $J = 13.8, 8.4$ Hz, 1H), 2.26-2.22 (m, 1H), 2.17-2.13 (m, 1H), 2.05-2.01 (m, 2H) ppm; ^{13}C NMR (100 MHz, CD_3OD): $\delta = 175.3, 173.3,$

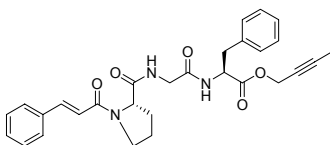
171.6, 167.5, 144.3, 138.2, 136.2, 131.1, 130.2, 129.9, 129.4, 129.2, 127.8, 119.3, 62.3, 55.4, 52.7, 43.5, 43.1, 38.4, 30.5, 26.0 ppm.

Analytical data of compound 102



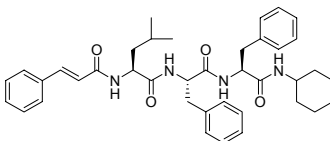
Peptide **102** was synthesized and released from solid support according to **GP 2** and **GP 3**. **Yield** = 18 %; **Purity** > 95% (LC_MS); **LC-MS** (C18, ESI_MS) 667.7 [M+H]⁺, 689.7 [M+Na]⁺; R_t = 9.81 min.

Analytical data of compound 103



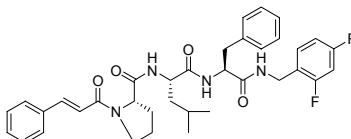
Peptide **103** was synthesized and released from solid support according to **GP 2** and **GP 3**. **Yield** = 19 %; **Purity** > 95% (LC_MS); **LC-MS** (C18, ESI_MS) 502.4 [M+H]⁺, 524.5 [M+Na]⁺; R_t = 8.47 min; ¹H NMR (400 MHz, CDCl₃): δ = 7.70 (d, *J* = 15.4 Hz, 1H), 7.51-7.48 (m, 3H), 7.37-7.36 (m, 3H), 7.23-7.28 (m, 2H), 7.13-7.12 (m, 2H), 6.71 (d, *J* = 15.4 Hz, 1H), 4.86 (dd, *J* = 6.5, 6.1 Hz, 1H), 4.66 (q, *J* = 2.4 Hz, 1H), 4.63 (q, *J* = 2.4 Hz, 1H), 4.61-4.58 (m, 1H), 4.14 (dd, *J* = 16.8, 7.1 Hz, 1H), 3.79-3.73 (m, 2H), 3.66 (dd, *J* = 16.6, 8.2 Hz, 1H), 3.20 (dd, *J* = 13.9, 5.9 Hz, 1H), 3.10 (dd, *J* = 13.9, 6.5 Hz, 1H), 2.36-2.31 (m, 1H), 2.17-2.10 (m, 1H), 2.04-1.96 (m, 2H), 1.84 (t, *J* = 2.4 Hz, 3H) ppm; ¹³C NMR (100 MHz, CDCl₃): δ = 172.0, 170.7, 169.0, 166.3, 143.8, 135.8, 134.7, 130.0, 129.4, 128.8, 128.4, 128.0, 126.9, 117.4, 83.7, 72.6, 60.5, 53.5, 53.3, 47.5, 43.1, 37.5, 27.8, 25.0, 3.6 ppm.

Analytical data of compound 104



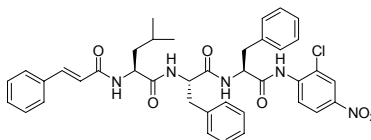
Peptide **104** was synthesized and released from solid support according to **GP 2** and **GP 3**. **Yield** = 31 %; **Purity** > 85% (LC_MS); **LC-MS** (C18, ESI_MS) 637.6 [M+H]⁺, 659.7 [M+Na]⁺; R_t = 10.20 min; ¹³C NMR (100 MHz, CDCl₃): δ = 172.4, 170.9, 169.9, 165.9, 141.2, 136.4, 136.1, 134.8, 129.7, 129.4, 129.3, 128.8, 128.4, 128.3, 128.2, 127.8, 126.7, 126.6, 54.2, 54.0, 51.7, 48.3, 39.3, 39.1, 32.6, 32.4, 25.4, 24.9, 22.8, 22.5 ppm.

Analytical data of compound 105



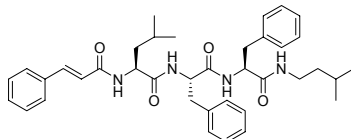
Peptide **105** was synthesized and released from solid support according to **GP 2** and **GP 3**. **Yield** = 31 %; **Purity** > 95% (LC_MS); **LC-MS** (C18, ESI_MS) 631.7 [M+H]⁺, 653.7 [M+Na]⁺; R_t = 9.33 min; ¹H NMR (400 MHz, CDCl₃): δ = 7.74 (d, *J* = 15.4 Hz, 1H), 7.54-7.52 (m, 2H), 7.40-7.39 (m, 2H), 7.28-7.12 (m, 5H), 6.90-6.82 (m, 3H), 6.73 (d, *J* = 15.4 Hz, 1H), 4.70 (dd, *J* = 14.6, 7.7 Hz, 1H), 4.55 (dd, *J* = 14.3, 5.4 Hz, 1H), 4.46-4.39 (m, 2H), 4.20-4.11 (m, 3H), 3.75-3.71 (m, 1H), 3.68-3.64 (m, 1H), 3.21 (dd, *J* = 14.1, 5.9 Hz, 1H), 3.13 (dd, *J* = 14.1, 7.5 Hz, 1H), 2.05-1.97 (m, 3H), 1.89-1.83 (m, 1H), 1.53-1.44 (m, 2H), 1.37-1.32 (m, 1H), 0.84 (d, *J* = 6.24 Hz, 3H), 0.77 (d, *J* = 6.03 Hz, 3H) ppm; ¹³C NMR (100 MHz, CDCl₃): δ = 172.1, 171.7, 170.7, 166.7, 162.9 and 162.8 (d, C-F), 160.4 and 160.3 (d, C-F), 144.3, 136.8, 134.4, 130.3, 129.2, 129.1, 128.9, 128.4, 128.0, 126.6, 117.0, 111.3, 111.0, 60.3, 53.8, 53.3, 47.6, 39.8, 37.3, 31.4, 27.3, 24.9, 22.8, 21.4 ppm.

Analytical data of compound 106



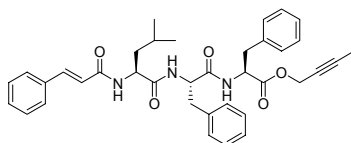
Peptide **106** was synthesized and released from solid support according to **GP 2** and **GP 3**. **Yield** = 17 %; **Purity** > 80% (LC_MS); **LC-MS** (C18, ESI_MS) 711.3 [M+H]⁺, 732.7 [M+Na]⁺; R_t = 10.43 min.

Analytical data of compound 107



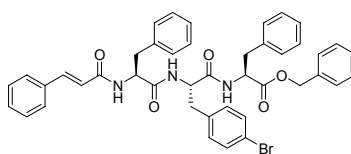
Peptide **107** was synthesized and released from solid support according to **GP 2** and **GP 3**. **Yield** = 20 %; **Purity** > 90% (LC_MS); **LC-MS** (C18, ESI_MS) 625.7[M+H]⁺, 647.6 [M+Na]⁺; R_t = 10.15 min; **¹H NMR** (400 MHz, CDCl₃): δ = 7.59 (d, *J* = 15.7 Hz, 1H), 7.51-7.49 (m, 1H), 7.33-7.26 (m, 4H), 7.21-7.10 (m, 6H), 7.08-7.01 (m, 1H), 6.99-6.96 (m, 3H), 6.81 (d, *J* = 15.8 Hz, 1H), 5.24-5.17 (m, 2H), 5.09-5.03 (m, 1H), 3.29-3.25 (m, 2H), 3.08-2.93 (m, 2H), 1.73-1.67 (m, 2H), 1.47-1.39 (m, 1H), 1.29-1.23 (m, 2H), 0.93 (d, *J* = 5.91 Hz, 5H), 0.83-0.81 (m, 8H) ppm; **¹³C NMR** (100 MHz, CDCl₃): δ = 172.2, 170.9, 170.6, 165.8, 140.8, 136.7, 136.1, 135.0, 129.5, 129.4, 129.3, 128.7, 128.3, 128.3, 128.2, 127.8, 126.5, 121.5, 54.1, 53.8, 51.7, 42.5, 39.3, 39.0, 38.0, 37.8, 25.6, 25.0, 22.9, 22.8, 22.5, 22.4 ppm.

Analytical data of compound 108



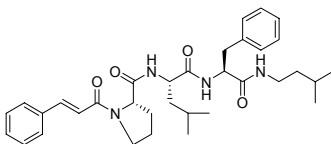
Peptide **108** was synthesized and released from solid support according to **GP 2** and **GP 3**. **Yield** = 5 %; **Purity** > 95% (LC_MS); **LC-MS** (C18, ESI_MS) 608.5 [M+H]⁺, 630.6 [M+Na]⁺; R_t = 9.99 min; **¹H NMR** (400 MHz, CDCl₃): δ = 7.61 (d, *J* = 15.6 Hz, 1H), 7.55-7.47 (m, 2H), 7.40-7.37 (m, 3H), 7.24-7.14 (m, 8H), 7.04-7.00 (m, 2H), 6.34 (d, *J* = 15.6 Hz, 1H), 4.80 (dd, *J* = 13.40, 5.92 Hz, 1H), 4.68-4.63 (m, 2H), 4.62-4.06 (m, 1H), 4.57-4.49 (m, 1H), 3.13-3.08 (m, 2H), 3.05-3.00 (m, 2H), 1.87 (t, *J* = 2.4, 2.4 Hz, 3H), 1.64-1.58 (m, 2H), 0.91 (d, *J* = 3.8 Hz, 1H), 0.90 (d, *J* = 3.8 Hz, 1H) ppm; **¹³C NMR** (100 MHz, CDCl₃): δ = 171.9, 170.2, 170.1, 165.9, 142.0, 136.3, 135.4, 134.5, 129.9, 129.3, 129.3, 128.8, 128.6, 128.5, 127.8, 127.1, 126.9, 119.7, 83.9, 72.5, 54.4, 53.6, 53.1, 51.7, 40.7, 37.9, 37.6, 24.7, 22.8, 22.0, 3.6 ppm.

Analytical data of compound 109



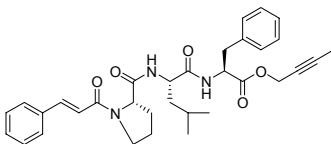
Peptide **109** was synthesized and released from solid support according to **GP 2** and **GP 3**. **Yield** = 6 %; **Purity** > 90% (LC_MS); **LC-MS** (C18, ESI_MS) 758.3 [M+H]⁺, 782.4 [M+Na]⁺; R_t = 10.77 min; **¹H NMR** (400 MHz, CDCl₃): δ = 7.57 (d, *J* = 15.3 Hz, 1H), 7.29-6.88 (m, 24H), 6.26 (d, *J* = 15.4 Hz), 5.11 (s, 2H), 4.76-4.74 (m, 1H), 4.684.66 (m, 1H), 4.51-4.45 (m, 1H), 3.08-2.83 (m, 6H) ppm.

Analytical data of compound 110



Peptide **110** was synthesized and released from solid support according to **GP 2** and **GP 3**. **Yield** = 34 %; **Purity** > 95% (LC_MS); **LC-MS** (C18, ESI_MS) 575.7 [M+H]⁺, 597.7 [M+Na]⁺; R_t = 9.57 min; **¹H NMR** (400 MHz, CDCl₃): δ = 7.78 (d, *J* = 15.5 Hz, 1H), 7.60-7.50 (m, 2H), 7.44-7.37 (m, 3H), 7.25-7.13 (m, 5H), 6.76 (d, *J* = 15.4 Hz, 1H), 4.68 (dt, *J* = 8.5, 8.5, 5.7 Hz, 1H), 4.53 (dd, *J* = 7.8, 3.8 Hz, 1H), 4.20-4.10 (m, 1H), 3.86-3.76 (m, 1H), 3.76-3.67 (m, 1H), 3.38-3.17 (m, 6H), 3.12 (dd, *J* = 14.09, 8.50 Hz, 1H), 2.29-2.14 (m, 1H), 2.14-1.99 (m, 3H), 1.65-1.42 (m, 3H), 1.42-1.28 (m, 3H), 0.89 (d, *J* = 1.78 Hz, 3H), 0.87 (d, *J* = 1.81 Hz, 3H), 0.85 (d, *J* = 6.37 Hz, 3H), 0.78 (d, *J* = 6.23 Hz, 3H) ppm; **¹³C NMR** (100 MHz, CDCl₃): δ = 172.2, 171.6, 170.9, 166.8, 144.5, 137.2, 134.4, 130.4, 129.1, 128.9, 128.4, 128.1, 126.6, 116.9, 60.7, 54.0, 53.3, 47.6, 39.8, 38.0, 37.8, 37.3, 27.7, 25.6, 25.0, 24.9, 22.9, 22.4, 22.3, 21.4 ppm.

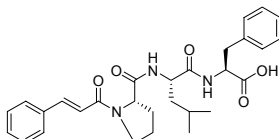
Analytical data of compound 111



Peptide **111** was synthesized and released from solid support according to **GP 2** and **GP 3**. **Yield** = 16 %; **Purity** > 95% (LC_MS); **LC-MS** (C18, ESI_MS) 558.7 [M+H]⁺, 580.6 [M+Na]⁺; R_t = 9.33 min; **¹H NMR** (400 MHz, CDCl₃): δ = 7.74 (d, *J* = 15.5 Hz, 1H), 7.59-7.47 (m, 2H), 7.42-7.36 (m, 3H), 7.31-7.27 (m, 2H), 7.26-7.15 (m, 3H), 6.74 (d, *J* = 15.4 Hz, 1H), 4.88 (dt, *J* = 7.8, 6.0, 6.0 Hz, 1H), 4.70 (q, *J* = 2.5, 2.4, 2.4 Hz, 1H), 4.69-4.64 (m, 2H), 4.30 (ddd, *J* = 9.1, 7.5, 5.5 Hz, 1H), 3.76-3.72 (m, 1H), 3.69-3.60 (m, 1H), 3.21 (dd, *J* = 13.9, 5.8 Hz, 1H), 3.11 (dd, *J* =

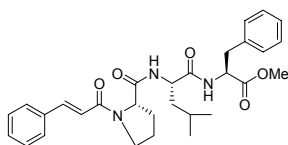
13.9, 6.7 Hz, 1H), 2.43-2.35 (m, 1H), 2.21-1.98 (m, 2H), 1.87 (t, $J = 2.4, 2.4$ Hz, 3H), 1.70-1.62 (m, 1H), 1.60-1.42 (m, 2H), 0.86 (d, $J = 6.4$ Hz, 3H), 0.82 (d, $J = 6.4$ Hz, 3H) ppm; ^{13}C NMR (100 MHz, CDCl_3): $\delta = 171.6, 171.4, 170.7, 166.4, 143.6, 135.8, 134.7, 130.0, 129.4, 128.8, 128.4, 128.0, 126.9, 117.5, 83.7, 72.6, 59.9, 53.6, 52.9, 52.1, 47.4, 40.0, 37.6, 27.0, 25.0, 24.8, 22.8, 21.7, 3.6$ ppm.

Analytical data of compound 112



Peptide **112** was synthesized and released from solid support according to **GP 2** and **GP 3**. **Yield** = 7 %; **Purity** > 95% (LC_MS); **LC-MS** (C18, ESI_MS) 506.6 $[\text{M}+\text{H}]^+$, 528.7 $[\text{M}+\text{Na}]^+$; $R_t = 8.07$ min; ^1H NMR (400 MHz, CDCl_3): $\delta = 7.74$ (d, $J = 15.5$ Hz, 1H), 7.58-7.48 (m, 2H), 7.42-7.34 (m, 3H), 7.25-7.15 (m, 5H), 6.73 (d, $J = 15.5$ Hz, 1H), 4.79 (dd, $J = 13.7, 6.2$ Hz, 1H), 4.64-4.61 (m, 1H), 4.41-4.23 (m, 1H), 3.70-3.60 (m, 2H), 3.23 (dd, $J = 13.8, 5.1$ Hz, 1H), 3.06 (dd, $J = 13.9, 7.2$ Hz, 1H), 2.40-2.21 (m, 1H), 2.21-2.03 (m, 2H), 1.61-1.40 (m, 4H), 0.85 (d, $J = 6.14$ Hz, 3H), 0.81 (d, $J = 6.30$ Hz, 3H) ppm.

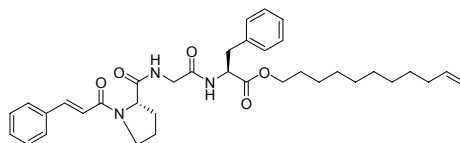
Analytical data of compound 113



Peptide **113** was synthesized and released from solid support according to **GP 2** and **GP 3**. **Yield** = 16 %; **Purity** > 95% (LC_MS); **LC-MS** (C18, ESI_MS) 520.8 $[\text{M}+\text{H}]^+$, 542.6 $[\text{M}+\text{Na}]^+$; $R_t = 8.80$ min; ^1H NMR (400 MHz, CDCl_3): $\delta = 7.74$ (d, $J = 15.4$ Hz, 1H), 7.60-7.50 (m, 2H), 7.44-7.37 (m, 3H), 7.31-7.26 (m, 2H), 7.24-7.11 (m, 3H), 6.74 (d, $J = 15.4$ Hz, 1H), 4.84 (dd, $J = 13.7, 6.6$ Hz, 1H), 4.67 (dd, $J = 8.1, 2.1$ Hz, 1H), 4.30 (ddd, $J = 9.1, 7.5, 5.3$ Hz, 1H), 3.79-3.72 (m, 1H), 3.71 (s, 3H), 3.69-3.59 (m, 1H), 3.18 (dd, $J = 13.95, 5.79$ Hz, 1H), 3.08 (dd, $J = 13.89, 6.71$ Hz, 1H), 2.46-2.30 (m, 1H), 2.21-1.80 (m, 4H), 1.74-1.61 (m, 1H), 1.60-1.40 (m, 1H), 0.86 (d, $J = 6.43$ Hz, 3H), 0.82 (d, $J = 6.42$ Hz, 3H) ppm; ^{13}C NMR (100 MHz, CDCl_3): $\delta = 171.8,$

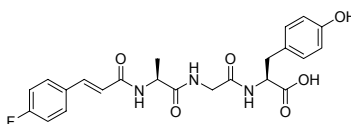
171.5, 171.4, 166.4, 143.6, 136.0, 134.7, 130.1, 129.2, 128.8, 128.4, 128.0, 126.9, 117.5, 59.9, 53.4, 52.2, 52.1, 47.4, 39.9, 37.8, 27.0, 25.0, 24.8, 22.8, 21.7 ppm.

Analytical data of compound 114



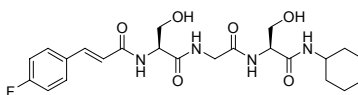
Peptide **114** was synthesized and released from solid support according to **GP 2** and **GP 3**. **Yield** = 6 %; **Purity** > 80% (LC_MS); **LC-MS** (C18, ESI_MS) 602.7 [M+H]⁺, 624.7 [M+Na]⁺; R_t = 11.48 min; ¹H NMR (400 MHz, CDCl₃): δ = 7.70 (d, *J* = 15.4 Hz, 1H), 7.53-7.45 (m, 2H), 7.41-7.32 (m, 3H), 7.25-7.16 (m, 3H), 7.13-7.07 (m, 2H), 6.71 (d, *J* = 15.4 Hz, 1H), 5.81 (ddt, *J* = 16.9, 10.2, 6.7, 6.7 Hz, 1H), 4.99 (ddt, *J* = 17.0, 2.1, 1.5, 1.5 Hz, 1H), 4.93 (ddt, *J* = 10.2, 2.28, 1.2, 1.2 Hz, 1H), 4.80 (dd, *J* = 6.5, 6.3 Hz, 1H), 4.61 (dd, *J* = 7.7, 3.5 Hz, 1H), 4.14 (dd, *J* = 16.9, 7.8 Hz, 1H, Gly-α-H), 4.02 (dt, *J* = 6.7, 6.7, 2.8 Hz, 2H), 3.81-3.73 (m, 1H), 3.77 (dd, *J* = 16.8, 5.2 Hz, 1H), 3.70-3.60 (m, 1H), 3.15 (dd, *J* = 13.8, 6.0 Hz, 1H), 3.09 (dd, *J* = 13.8, 6.4 Hz, 1H), 2.09-1.93 (m, 2H), 1.60-1.45 (m, 2H), 1.44-1.33 (m, 2H), 1.33-1.18 (m, 14H) ppm; ¹³C NMR (100 MHz, CDCl₃): δ = 171.9, 171.5, 168.8, 166.3, 143.6, 139.1, 136.0, 134.8, 130.0, 129.3, 128.8, 128.4, 128.0, 126.8, 117.5, 114.1, 65.5, 60.5, 53.4, 47.5, 43.2, 37.8, 33.7, 29.4, 29.1, 29.0, 28.9, 28.4, 27.7, 25.7, 25.7, 25.1 ppm.

Analytical data of compound 115



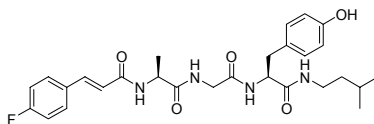
Peptide **115** was synthesized and released from solid support according to **GP 2** and **GP 3**. **Yield** = 7 %; **Purity** > 95% (LC_MS); **LC-MS** (C18, ESI_MS) 458.1 [M+H]⁺, 480.2 [M+Na]⁺; R_t = 6.38 min.

Analytical data of compound 116



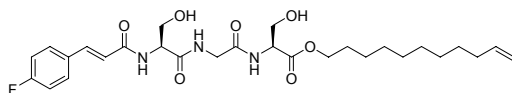
Peptide **116** was synthesized and released from solid support according to **GP 2** and **GP 3**. **Yield** = 8 %; **Purity** > 95% (LC_MS); **LC-MS** (C18, ESI_MS) 479.3 [M+H]⁺, 501.4 [M+Na]⁺; R_t = 6.50 min

Analytical data of compound 117



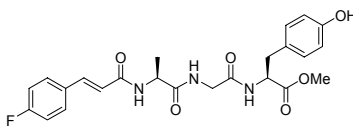
Peptide **117** was synthesized and released from solid support according to **GP 2** and **GP 3**. **Yield** = 8 %; **Purity** > 95% (LC_MS); **LC-MS** (C18, ESI_MS) 527.5 [M+H]⁺, 549.5 [M+Na]⁺; R_t = 7.47 min.

Analytical data of compound 118



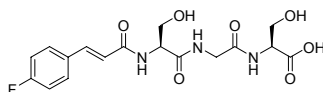
Peptide **118** was synthesized and released from solid support according to **GP 2** and **GP 3**. **Yield** = 3 %; **Purity** > 95% (LC_MS); **LC-MS** (C18, ESI_MS) 550.1 [M+H]⁺, 572.2 [M+Na]⁺; R_t = 9.61 min.

Analytical data of compound 119



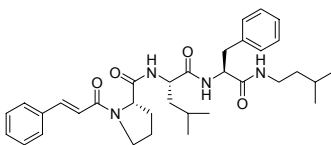
Peptide **119** was synthesized and released from solid support according to **GP 2** and **GP 3**. **Yield** = 10 %; **Purity** > 80% (LC_MS); **LC-MS** (C18, ESI_MS) 472.2 [M+H]⁺, 494.4 [M+Na]⁺; R_t = 6.83 min.

Analytical data of compound 120



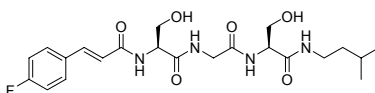
Peptide **120** was synthesized and released from solid support according to **GP 2** and **GP 3**. **Yield** = 6 %; **Purity** > 80% (LC_MS); **LC-MS** (C18, ESI_MS) 397.9 [M+H]⁺; R_t = 5.43 min.

Analytical data of compound 121



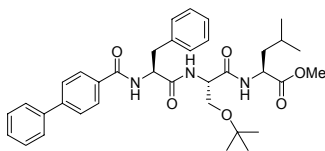
Peptide **121** was synthesized and released from solid support according to **GP 2** and **GP 3**. **Yield** = 20 %; **Purity** > 95% (LC_MS); **LC-MS** (C18, ESI_MS) 575.7 [M+H]⁺, 597.7 [M+Na]⁺; R_t = 9.57 min.

Analytical data of compound 122



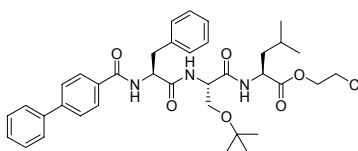
Peptide **122** was synthesized and released from solid support according to **GP 2** and **GP 3**. **Yield** = 17 %; **Purity** > 90% (LC_MS); **LC-MS** (C18, ESI_MS) 467.3 [M+H]⁺, 489.4 [M+Na]⁺; R_t = 6.53 min.

Analytical data of compound 123



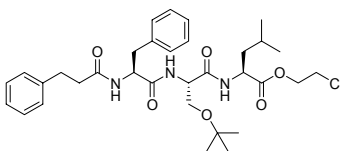
Peptide **123** was synthesized and released from solid support according to **GP 2** and **GP 3**. **Yield** = 29 %; **Purity** > 95% (LC_MS); **LC-MS** (C18, ESI_MS) 616.3 [M+H]⁺, 638.4 [M+Na]⁺; R_t = 10.64 min.

Analytical data of compound 124



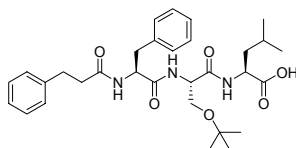
Peptide **124** was synthesized and released from solid support according to **GP 2** and **GP 3**. **Yield** = 16 %; **Purity** > 95% (LC_MS); **LC-MS** (C18, ESI_MS) 664.2 [M+H]⁺, 686.4 [M+Na]⁺; R_t = 10.95 min.

Analytical data of compound 125



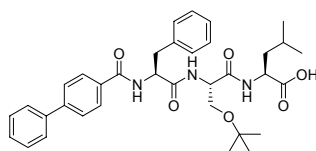
Peptide **125** was synthesized and released from solid support according to **GP 2** and **GP 3**. **Yield** = 14 %; **Purity** > 95% (LC_MS); **LC-MS** (C18, ESI_MS) 638.4 [M+Na]⁺; R_t = 10.32 min.

Analytical data of compound 126



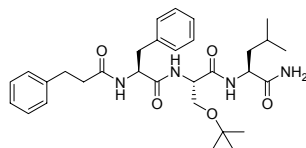
Peptide **126** was synthesized and released from solid support according to **GP 2** and **GP 3**. **Yield** = 16 %; **Purity** > 95% (LC_MS); **LC-MS** (C18, ESI_MS) 554.1 [M+H]⁺, 576.3 [M+Na]⁺; R_t = 9.09 min.

Analytical data of compound 127



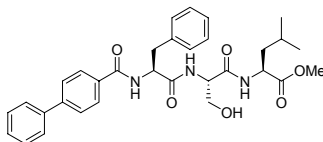
Peptide **127** was synthesized and released from solid support according to **GP 2** and **GP 3**. **Yield** = 8 %; **Purity** > 95% (LC_MS); **LC-MS** (C18, ESI_MS) 602.0 [M+H]⁺, 624.3 [M+Na]⁺; R_t = 9.79 min.

Analytical data of compound 128



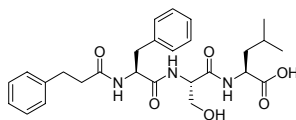
Peptide **128** was synthesized and released from solid support according to **GP 2** and **GP 3**. **Yield** = 30 %; **Purity** > 95% (LC_MS); **LC-MS** (C18, ESI_MS) 553.4 [M+H]⁺, 575.4 [M+Na]⁺; R_t = 8.79 min.

Analytical data of compound 129



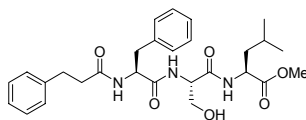
Peptide **129** was synthesized and released from solid support according to **GP 2** and **GP 3**. **Yield** = 29 %; **Purity** > 95% (LC_MS); **LC-MS** (C18, ESI_MS) 560.2 [M+H]⁺, 582.2 [M+Na]⁺; R_t = 9.12 min.

Analytical data of compound 130



Peptide **130** was synthesized and released from solid support according to **GP 2** and **GP 3**. **Yield** = 10 %; **Purity** > 95% (LC_MS); **LC-MS** (C18, ESI_MS) 498.1 [M+H]⁺, 520.2 [M+Na]⁺; R_t = 7.74 min.

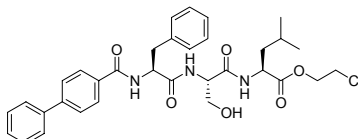
Analytical data of compound 131



Peptide **131** was synthesized and released from solid support according to **GP 2** and **GP 3**. **Yield** = 25 %; **Purity** > 95% (LC_MS); **LC-MS** (C18, ESI_MS) 512.2 [M+H]⁺, 534.3 [M+Na]⁺; R_t = 8.37 min; ¹H NMR (400 MHz, CD₃OD): δ = 7.30-7.06 (m, 10H), 4.64 (dd, *J* = 9.3, 5.2 Hz, 1H), 4.49 (dd, *J* = 8.7, 6.1 Hz, 1H), 4.43 (t, *J* = 5.4, 5.4 Hz, 1H), 3.77 (d, *J* = 5.4 Hz, 2H), 3.71 (s,

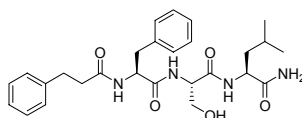
3H), 3.14 (dd, $J = 13.9, 5.2$ Hz, 1H), 2.87 (dd, $J = 14.0, 9.3$ Hz, 1H), 2.78 (dt, $J = 7.4, 7.4, 1.7$ Hz, 2H), 2.45 (dt, $J = 7.6, 7.6, 1.9$, 2H), 1.82-1.52 (m, 3H), 0.96 (d, $J = 6.4$ Hz, 3H), 0.92 (d, $J = 6.3$ Hz, 3H) ppm; ^{13}C NMR (100 MHz, CD_3OD): $\delta = 175.3, 174.5, 173.7, 172.1, 142.1, 138.4, 130.3, 129.5, 129.4, 129.3, 127.7, 127.1, 63.1, 56.6, 56.1, 52.7, 52.3, 41.5, 38.6, 32.7, 25.9, 23.3, 21.9$ ppm.

Analytical data of compound 132



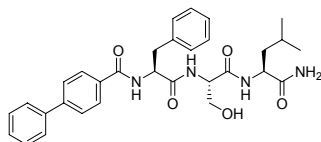
Peptide **132** was synthesized and released from solid support according to **GP 2** and **GP 3**. **Yield** = 10 %; **Purity** > 95% (LC_MS); **LC-MS** (C18, ESI_MS) 608.3 $[\text{M}+\text{H}]^+$, 630.3 $[\text{M}+\text{Na}]^+$; $R_t = 9.52$ min; ^1H NMR (400 MHz, CD_3OD): $\delta = 7.85\text{-}7.77$ (m, 2H), 7.73-7.62 (m, 4H), 7.50-7.42 (m, 2H), 7.41-7.14 (m, 6H), 4.89 (dd, $J = 9.5, 5.2$ Hz, 1H), 4.58-4.46 (m, 2H), 4.44-4.29 (m, 2H), 3.84 (d, $J = 5.6$ Hz, 2H), 3.76 (t, $J = 5.5, 5.5$ Hz, 2H), 3.10 (dd, $J = 13.9, 9.4$ Hz, 2H), 1.82-1.57 (m, 3H), 0.96 (d, $J = 6.4$ Hz, 3H), 0.93 (d, $J = 6.3$ Hz, 3H) ppm; ^{13}C NMR (100 MHz, CD_3OD): $\delta = 173.9, 173.6, 172.2, 170.1, 145.9, 141.2, 138.6, 133.8, 130.4, 130.0, 129.5, 129.1, 129.1, 128.1, 128.0, 127.8, 66.1, 63.1, 56.8, 56.7, 52.4, 42.6, 41.5, 38.5, 25.9, 23.2, 22.0$ ppm.

Analytical data of compound 133



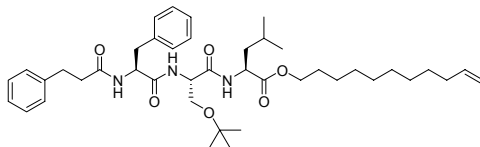
Peptide **133** was synthesized and released from solid support according to **GP 2** and **GP 3**. **Yield** = 20 %; **Purity** > 90% (LC_MS); **LC-MS** (C18, ESI_MS) 497.1 $[\text{M}+\text{H}]^+$, 519.2 $[\text{M}+\text{Na}]^+$; $R_t = 7.37$ min.

Analytical data of compound 134



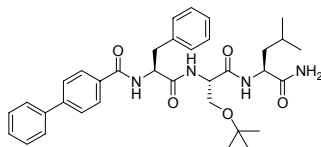
Peptide **134** was synthesized and released from solid support according to **GP 2** and **GP 3**. **Yield** = 20 %; **Purity** > 95% (LC_MS); **LC-MS** (C18, ESI_MS) 545.1 [M+H]⁺, 567.2 [M+Na]⁺; R_t = 8.17 min.

Analytical data of compound 135



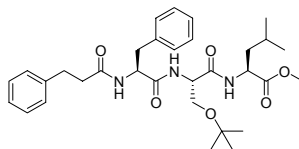
Peptide **135** was synthesized and released from solid support according to **GP 2** and **GP 3**. **Yield** = 6 %; **Purity** > 95% (LC_MS); **LC-MS** (C18, ESI_MS) 706.4 [M+H]⁺, 728.5 [M+Na]⁺; R_t = 13.23 min.

Analytical data of compound 136



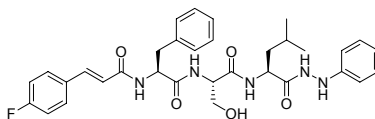
Peptide **136** was synthesized and released from solid support according to **GP 2** and **GP 3**. **Yield** = 26 %; **Purity** > 95% (LC_MS); **LC-MS** (C18, ESI_MS) 601.2 [M+H]⁺, 623.3 [M+Na]⁺; R_t = 9.56 min.

Analytical data of compound 137



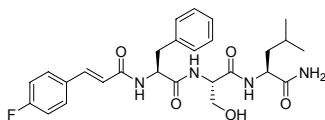
Peptide **137** was synthesized and released from solid support according to **GP 2** and **GP 3**. **Yield** = 30 %; **Purity** > 95% (LC_MS); **LC-MS** (C18, ESI_MS) 568.5 [M+H]⁺, 590.4 [M+Na]⁺; R_t = 9.93 min.

Analytical data of compound 138



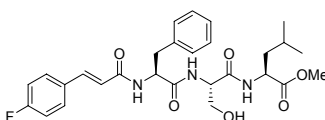
Peptide **138** was synthesized and released from solid support according to **GP 2** and **GP 3**. **Yield** = 1 %; **Purity** > 90% (LC_MS); **LC-MS** (C18, ESI_MS) 604.1 [M+H]⁺, 626.3 [M+Na]⁺; R_t = 8.59 min.

Analytical data of compound 139



Peptide **139** was synthesized and released from solid support according to **GP 2** and **GP 3**. **Yield** = 3 %; **Purity** > 90% (LC_MS); **LC-MS** (C18, ESI_MS) 513.1 [M+H]⁺, 535.2 [M+Na]⁺; R_t = 7.55 min; **¹H NMR** (400 MHz, CD₃OD): δ = 7.60-7.53 (m, 2H), 7.47 (d, *J* = 15.8 Hz, 1H, Ph-CH=), 7.31-7.25 (m, 5H), 7.15-7.08 (m, 2H), 6.58 (d, *J* = 15.9 Hz, 1H), 4.72 (dd, *J* = 9.0, 5.5 Hz, 1H), 4.45-4.31 (m, 2H), 3.85 (dd, *J* = 10.7, 5.3 Hz, 1H), 3.72 (dd, *J* = 10.7, 6.3 Hz, 1H), 3.21 (dd, *J* = 14.0, 5.4 Hz, 1H), 2.99 (dd, *J* = 14.0, 9.0 Hz, 1H), 1.88-1.53 (m, 3H), 0.95 (d, *J* = 6.2 Hz, 3H), 0.91 (d, *J* = 6.2 Hz, 3H) ppm; **¹³C NMR** (100 MHz, CD₃OD): δ = 177.7, 173.9, 172.4, 168.6, 141.3, 138.3, 131.0, 130.9, 130.3, 129.5, 127.9, 121.1, 117.0, 116.7, 62.9, 56.8, 53.1, 41.5, 38.6, 25.9, 23.7, 21.6 ppm.

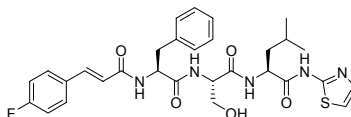
Analytical data of compound 140



Peptide **140** was synthesized and released from solid support according to **GP 2** and **GP 3**. **Yield** = 3 %; **Purity** > 95% (LC_MS); **LC-MS** (C18, ESI_MS) 528.1 [M+H]⁺, 550.2 [M+Na]⁺; R_t = 8.46 min; **¹H NMR** (400 MHz, CD₃OD): δ = 7.64-7.51 (m, 2H), 7.46 (d, *J* = 15.8 Hz, 1H), 7.30-7.16 (m, 5H), 7.15-7.07 (m, 2H), 6.57 (d, *J* = 15.8 Hz, 1H), 4.76 (dd, *J* = 9.1, 5.3 Hz, 1H), 4.54-4.37 (m, 2H), 3.79 (d, *J* = 5.5 Hz, 2H), 3.70 (s, 3H), 3.23 (dd, *J* = 14.0, 5.3 Hz, 1H), 2.98 (dd, *J* = 14.0, 9.1 Hz, 1H), 1.76-1.51 (m, 3H), 0.94 (d, *J* = 6.4 Hz, 3H), 0.91 (d, *J* = 6.3 Hz, 3H) ppm; **¹³C NMR**

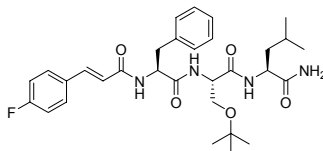
NMR (100 MHz, CD₃OD): δ = 174.5, 173.7, 172.2, 168.5, 141.2, 138.4, 131.0, 130.9, 130.3, 129.5, 127.8, 121.1, 116.9, 116.7, 63.0, 56.8, 56.7, 56.5, 52.7, 41.6, 38.7, 25.9, 23.3, 21.9 ppm.

Analytical data of compound 141



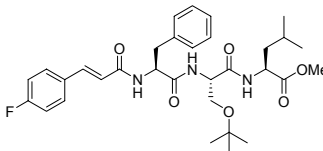
Peptide **141** was synthesized and released from solid support according to **GP 2** and **GP 3**. **Yield** = 3 %; **Purity** > 95% (LC_MS); **LC-MS** (C18, ESI_MS) 596.2 [M+H]⁺, 618.2 [M+Na]⁺; R_t = 8.55 min; **¹H NMR** (400 MHz, CD₃OD): δ = 7.63-7.51 (m, 1H), 7.47 (d, *J* = 15.8 Hz, 1H), 7.44 (d, *J* = 3.63 Hz, 1H), 7.29-7.15 (m, 6H), 7.15-7.06 (m, 2H), 6.57 (d, *J* = 15.7 Hz, 1H), 4.80-4.73 (m, 1H), 4.70-4.63 (m, 1H), 4.46 (t, *J* = 5.8, 5.8 Hz, 1H), 3.87 (dd, *J* = 10.6, 5.6 Hz, 1H), 3.77 (dd, *J* = 10.7, 6.1 Hz, 1H), 3.23 (dd, *J* = 14.0, 5.3 Hz, 1H), 2.99 (dd, *J* = 14.0, 9.1 Hz, 1H), 1.92-1.55 (m, 3H), 0.99-0.92 (m, 6H) ppm; **¹³C NMR** (100 MHz, CD₃OD): δ = 173.9, 172.6, 172.5, 168.5, 166.3, 159.9, 141.2, 138.3, 138.3, 131.0, 130.9, 130.3, 129.5, 127.8, 116.9, 116.7, 114.9, 62.9, 56.6, 56.5, 53.3, 41.5, 38.7, 25.9, 23.5, 21.8 ppm.

Analytical data of compound 142



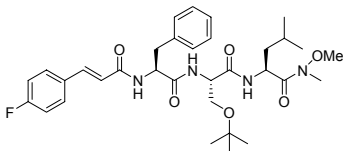
Peptide **142** was synthesized and released from solid support according to **GP 2** and **GP 3**. **Yield** = 8 %; **Purity** > 95% (LC_MS); **LC-MS** (C18, ESI_MS) 569.3 [M+H]⁺, 591.3 [M+Na]⁺; R_t = 8.85 min.

Analytical data of compound 143



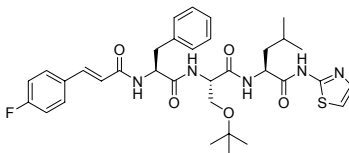
Peptide **143** was synthesized and released from solid support according to **GP 2** and **GP 3**. **Yield** = 7 %; **Purity** > 95% (LC_MS); **LC-MS** (C18, ESI_MS) 584.3 [M+H]⁺, 606.3 [M+Na]⁺; R_t = 9.93 min.

Analytical data of compound 144



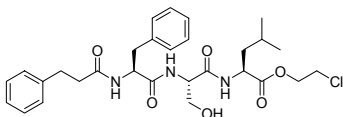
Peptide **144** was synthesized and released from solid support according to **GP 2** and **GP 3**. **Yield** = 3 %; **Purity** > 95% (LC_MS); **LC-MS** (C18, ESI_MS) 613.1 [M+H]⁺, 635.3 [M+Na]⁺; R_t = 9.71 min.

Analytical data of compound 145



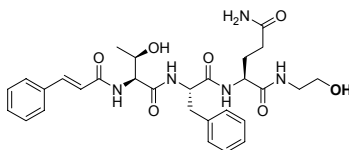
Peptide **145** was synthesized and released from solid support according to **GP 2** and **GP 3**. **Yield** = 5 %; **Purity** > 95% (LC_MS); **LC-MS** (C18, ESI_MS) 652.3 [M+H]⁺, 674.3 [M+Na]⁺; R_t = 9.99 min.

Analytical data of compound 146



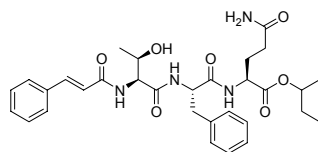
Peptide **146** was synthesized and released from solid support according to **GP 2** and **GP 3**. **Yield** = 7 %; **Purity** > 95% (LC_MS); **LC-MS** (C18, ESI_MS) 560.4 [M+H]⁺, 582.3 [M+Na]⁺; R_t = 8.84 min.

Analytical data of compound 147



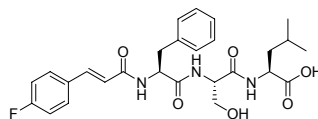
Peptide **147** was synthesized and released from solid support according to **GP 2** and **GP 3**. **Yield** = 5 %; **Purity** > 90% (LC_MS); **LC-MS** (C18, ESI_MS) 568.7 [M+H]⁺, 593.4 [M+Na]⁺; R_t = 5.37 min.

Analytical data of compound 148



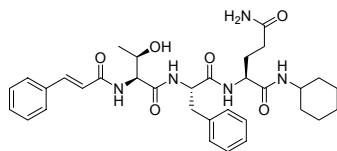
Peptide **148** was synthesized and released from solid support according to **GP 2** and **GP 3**. **Yield** = 1 %; **Purity** > 90% (LC_MS); **LC-MS** (C18, ESI_MS) 581.2 [M+H]⁺, 603.2 [M+Na]⁺; R_t = 7.69 min.

Analytical data of compound 149



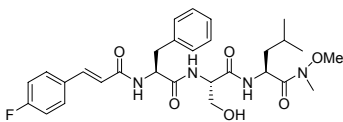
Peptide **149** was synthesized and released from solid support according to **GP 2** and **GP 3**. **Yield** = 3%; **Purity** > 95% (LC_MS); **LC-MS** (C18, ESI_MS) 514.2 [M+H]⁺, 536.2 [M+Na]⁺; R_t = 7.91 min; ¹H NMR (400 MHz, CD₃OD): δ = 7.60-7.53 (m, 2H), 7.46 (d, *J* = 16.0 Hz, 1H), 7.32-7.17 (m, 6H), 7.15-7.07 (m, 1H), 6.57 (d, *J* = 15.8 Hz, 1H), 4.80-4.70 (m, 1H), 4.51-4.39 (m, 2H), 3.79 (d, *J* = 5.1 Hz, 2H), 3.27-3.18 (m, 1H), 2.98 (dd, *J* = 13.9, 9.2 Hz, 1H), 1.89-1.48 (m, 3H), 0.95 (d, *J* = 6.4 Hz, 3H), 0.92 (d, *J* = 6.4 Hz, 3H) ppm.

Analytical data of compound 150



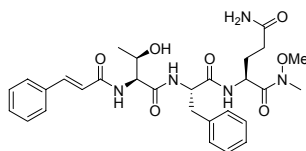
Peptide **150** was synthesized and released from solid support according to **GP 2** and **GP 3**. **Yield** = 1 %; **Purity** > 95% (LC_MS); **LC-MS** (C18, ESI_MS) 606.3 [M+H]⁺, 628.3 [M+Na]⁺; R_t = 7.50 min.

Analytical data of compound 151



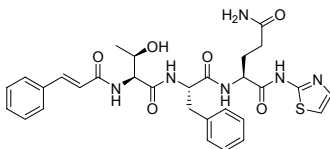
Peptide **151** was synthesized and released from solid support according to **GP 2** and **GP 3**. **Yield** = 5 %; **Purity** > 95% (LC_MS); **LC-MS** (C18, ESI_MS) 556.9 [M+H]⁺, 579.2 [M+Na]⁺; R_t = 8.48 min; ¹H NMR (400 MHz, CD₃OD): δ = 7.60-7.52 (m, 2H), 7.46 (d, *J* = 15.8 Hz, 1H), 7.33-7.15 (m, 6H), 7.15-7.07 (m, 1H), 6.56 (d, *J* = 15.8 Hz, 1H), 4.99-4.90 (m, 1H), 4.79 (dd, *J* = 9.4, 5.2 Hz, 1H), 4.45 (t, *J* = 5.4, 5.4 Hz, 1H), 3.81 (s, 3H), 3.78 (t, *J* = 5.4, 5.4 Hz, 2H), 3.24 (dd, *J* = 14.1, 5.1 Hz, 1H), 3.19 (s, 3H), 2.97 (dd, *J* = 14.1, 9.2 Hz, 1H₂), 1.84-1.39 (m, 3H), 0.94 (d, *J* = 6.6 Hz, 3H), 0.94 (d, *J* = 6.5 Hz, 3H) ppm; ¹³C NMR (100 MHz, CD₃OD): δ = 173.7, 172.1, 170.7, 168.4, 141.1, 138.5, 131.0, 130.9, 130.3, 129.5, 127.8, 121.2, 116.9, 116.7, 63.2, 62.0, 56.6, 56.3, 49.7, 41.5, 38.8, 26.0, 23.7, 21.8 ppm.

Analytical data of compound 152



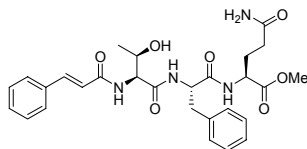
Peptide **152** was synthesized and released from solid support according to **GP 2** and **GP 3**. **Yield** = 1 %; **Purity** > 95% (LC_MS); **LC-MS** (C18, ESI_MS) 568.0 [M+H]⁺, 690.2 [M+Na]⁺; R_t = 6.76 min.

Analytical data of compound 153



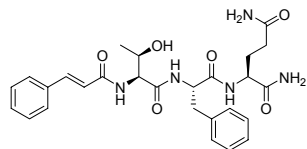
Peptide **153** was synthesized and released from solid support according to **GP 2** and **GP 3**. **Yield** = 2 %; **Purity** > 95% (LC_MS); **LC-MS** (C18, ESI_MS) 607.2 [M+H]⁺, 629.2 [M+Na]⁺; R_t = 7.13 min.

Analytical data of compound 154



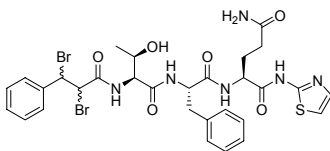
Peptide **154** was synthesized and released from solid support according to **GP 2** and **GP 3**. **Yield** = 2 %; **Purity** > 95% (LC_MS); **LC-MS** (C18, ESI_MS) 539.1 [M+H]⁺, 561.2 [M+Na]⁺; R_t = 6.93 min.

Analytical data of compound 155



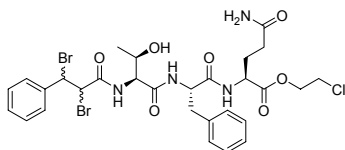
Peptide **155** was synthesized and released from solid support according to **GP 2** and **GP 3**. **Yield** = 1 %; **Purity** > 85% (LC_MS); **LC-MS** (C18, ESI_MS) 524.1 [M+H]⁺, 546.2 [M+Na]⁺; R_t = 6.39 min.

Analytical data of compound 156



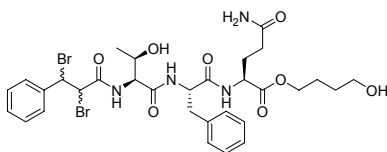
Peptide **156** was synthesized and released from solid support according to **GP 2** and **GP 3**. **Yield** = 3 %; **Purity** > 95% (LC_MS); **LC-MS** (C18, ESI_MS) 767.0 [M+H]⁺, 788.9 [M+Na]⁺; R_t = 7.75 min.

Analytical data of compound 157



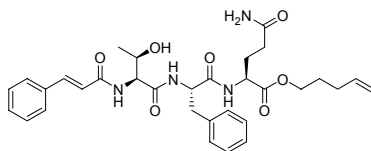
Peptide **157** was synthesized and released from solid support according to **GP 2** and **GP 3**. **Yield** = 1 %; **Purity** > 90% (LC_MS); **LC-MS** (C18, ESI_MS) 747.0 [M+H]⁺, 769.0 [M+Na]⁺; R_t = 8.07 min.

Analytical data of compound 158



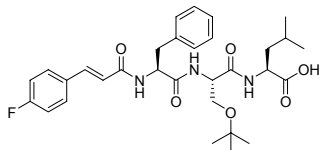
Peptide **158** was synthesized and released from solid support according to **GP 2** and **GP 3**. **Yield** = 4 %; **Purity** > 95% (LC_MS); **LC-MS** (C18, ESI_MS) 757.1 [M+H]⁺, 779.0 [M+Na]⁺; R_t = 7.38 min.

Analytical data of compound 159



Peptide **159** was synthesized and released from solid support according to **GP 2** and **GP 3**. **Yield** = 2 %; **Purity** > 95% (LC_MS); **LC-MS** (C18, ESI_MS) 593.4 [M+H]⁺, 615.3 [M+Na]⁺; R_t = 7.89 min.

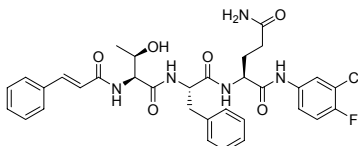
Analytical data of compound 160



Peptide **160** was synthesized and released from solid support according to **GP 2** and **GP 3**. **Yield** = 3 %; **Purity** > 90% (LC_MS); **LC-MS** (C18, ESI_MS) 570.0 [M+H]⁺, 592.3 [M+Na]⁺; R_t =

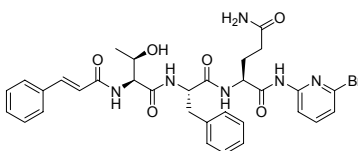
9.11 min; $^1\text{H NMR}$ (400 MHz, CD_3OD): $\delta = 7.58\text{-}7.53$ (m, 2H), 7.48 (d, $J = 15.7$ Hz, 1H), 7.33-7.16 (m, 6H), 7.15-7.08 (m, 1H), 6.57 (d, $J = 15.7$ Hz, 1H), 4.80-4.76 (m, 1H), 4.52-4.41 (m, 2H), 3.71 (dd, $J = 9.0, 4.4$ Hz, 1H), 3.55 (dd, $J = 8.8, 5.4$ Hz, 1H), 3.28-3.23 (m, 1H), 2.98 (dd, $J = 14.2, 9.5$ Hz, 1H), 1.88-1.46 (m, 3H), 1.15 (s, 9H), 0.94 (d, $J = 6.33$ Hz, 3H), 0.92 (d, $J = 6.27$ Hz, 3H) ppm.

Analytical data of compound 161



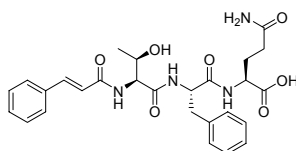
Peptide **161** was synthesized and released from solid support according to **GP 2** and **GP 3**. **Yield** = 2 %; **Purity** > 90% (LC_MS); **LC-MS** (C18, ESI_MS) 652.2 $[\text{M}+\text{H}]^+$, 674.3 $[\text{M}+\text{Na}]^+$; $R_t = 8.03$ min.

Analytical data of compound 162



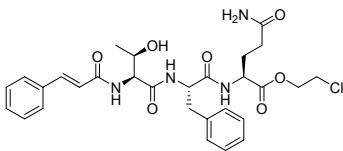
Peptide **162** was synthesized and released from solid support according to **GP 2** and **GP 3**. **Yield** = 2 %; **Purity** > 95% (LC_MS); **LC-MS** (C18, ESI_MS) 679.1 $[\text{M}+\text{H}]^+$, 703.2 $[\text{M}+\text{Na}]^+$; $R_t = 7.77$ min.

Analytical data of compound 163



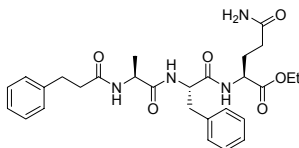
Peptide **163** was synthesized and released from solid support according to **GP 2** and **GP 3**. **Yield** = 2 %; **Purity** > 95% (LC_MS); **LC-MS** (C18, ESI_MS) 525.0 $[\text{M}+\text{H}]^+$, 547.2 $[\text{M}+\text{Na}]^+$; $R_t = 6.64$ min.

Analytical data of compound 164



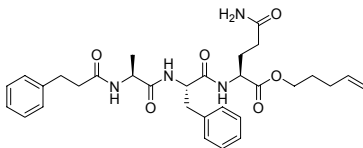
Peptide **164** was synthesized and released from solid support according to **GP 2** and **GP 3**. **Yield** = 1 %; **Purity** > 95% (LC_MS); **LC-MS** (C18, ESI_MS) 587.3 [M+H]⁺, 609.3 [M+Na]⁺; R_t = 7.39 min.

Analytical data of compound 165



Peptide **165** was synthesized and released from solid support according to **GP 2** and **GP 3**. **Yield** = 4 %; **Purity** > 95% (LC_MS); **LC-MS** (C18, ESI_MS) 525.2 [M+H]⁺, 547.2 [M+Na]⁺; R_t = 7.34 min; ¹H NMR (400 MHz, CD₃OD): δ = 7.65-6.77 (m, 10H), 4.62 (dd, *J* = 9.9, 4.9 Hz, 1H), 4.40 (dd, *J* = 9.5, 4.6 Hz, 1H), 4.17 (d, *J* = 7.1 Hz, 1H), 4.17 (q, *J* = 7.1 Hz, 2H), 3.24 (dd, *J* = 14.0, 4.8 Hz, 1H), 2.92-2.81 (m, 3H), 2.54-2.42 (m, 2H), 2.34-2.28 (m, 2H), 2.27-2.16 (m, 1H), 2.06-1.92 (m, 1H), 1.26 (t, *J* = 7.1 Hz, 3H), 1.06 (d, *J* = 7.1 Hz, 3H) ppm; ¹³C NMR (100 MHz, CD₃OD): δ = 177.6, 175.2, 175.1, 173.5, 172.8, 142.3, 138.5, 130.3, 129.5, 129.4, 129.3, 127.7, 127.2, 62.4, 55.6, 53.5, 50.7, 38.4, 38.2, 32.6, 32.5, 28.3, 17.5, 14.5 ppm.

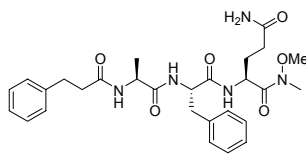
Analytical data of compound 166



Peptide **166** was synthesized and released from solid support according to **GP 2** and **GP 3**. **Yield** = 2 %; **Purity** > 95% (LC_MS); **LC-MS** (C18, ESI_MS) 565.3 [M+H]⁺, 587.3 [M+Na]⁺; R_t = 8.03 min; ¹H NMR (400 MHz, CD₃OD): δ = 7.58-6.91 (m, 10H), 5.90-5.69 (m, 1H), 5.19-4.92 (m, 2H), 4.62 (dd, *J* = 10.5, 4.6 Hz, 1H), 4.41 (dd, *J* = 9.6, 4.5 Hz, 1H), 4.20-4.07 (m, 3H), 2.98-

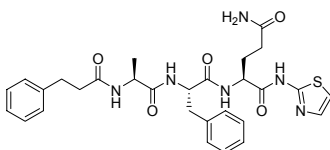
2.77 (m, 3H), 2.48 (d, $J = 8.31$ Hz, 2H), 2.36-2.26 (m, 2H), 2.28-2.17 (m, 1H), 2.17-2.08 (m, 2H), 2.06-1.95 (m, 1H), 1.77-1.69 (m, 2H), 1.05 (d, $J = 6.9$ Hz, 3H) ppm.

Analytical data of compound 167



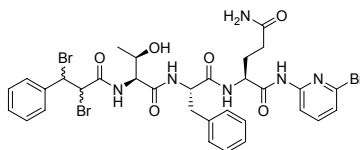
Peptide **167** was synthesized and released from solid support according to **GP 2** and **GP 3**. **Yield** = 6 %; **Purity** > 95% (LC_MS); **LC-MS** (C18, ESI_MS) 540.3 [M+H]⁺, 562.3 [M+Na]⁺; $R_t = 6.86$ min; **¹H NMR** (400 MHz, CD₃OD): $\delta = 7.65$ - 6.74 (m, 10H), 4.61 (dd, $J = 9.8, 5.0$ Hz, 1H), 4.20 (q, $J = 7.3$ Hz, 1H), 3.80 (s, 3H), 3.27-3.11 (m, 4H), 2.95-2.81 (m, 3H), 2.52-2.44 (m, 2H), 2.34-2.27 (m, 2H), 2.15-2.05 (m, 1H), 1.97-1.85 (m, 1H), 1.07 (d, $J = 7.2$ Hz, 3H) ppm; **¹³C NMR** (100 MHz, CD₃OD): $\delta = 177.7, 177.1, 177.1, 175.1, 173.3, 142.3, 138.5, 130.4, 129.5, 129.4, 129.4, 127.7, 127.2, 60.8, 55.6, 50.6, 50.5, 38.5, 38.2, 32.7, 32.6, 28.4, 24.2, 17.7$ ppm.

Analytical data of compound 168



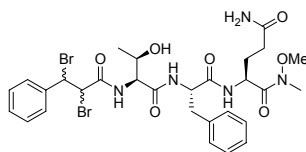
Peptide **168** was synthesized and released from solid support according to **GP 2** and **GP 3**. **Yield** = 4 %; **Purity** > 95% (LC_MS); **LC-MS** (C18, ESI_MS) 579.2 [M+H]⁺, 601.2 [M+Na]⁺; $R_t = 7.25$ min; **¹H NMR** (400 MHz, CD₃OD): $\delta = 7.44$ (d, $J = 3.6$ Hz, 1H), 7.30-7.09 (m, 11H), 4.72-4.50 (m, 2H), 4.19 (q, $J = 7.2$ Hz, 1H), 3.25 (dd, $J = 14.0, 5.0$ Hz, 1H), 2.92 (dd, $J = 14.1, 9.8$ Hz, 1H), 2.87-2.78 (m, 2H), 2.52-2.44 (m, 2H), 2.35 (t, $J = 7.37$ Hz, 2H), 2.29-2.17 (m, 1H), 2.14-2.03 (m, 1H), 1.10 (d, $J = 7.1$ Hz, 3H) ppm; **¹³C NMR** (100 MHz, CD₃OD): $\delta = 177.6, 175.7, 175.3, 173.7, 171.2, 160.3, 142.2, 138.4, 138.3, 137.7, 130.3, 129.4, 129.4, 129.3, 127.8, 127.1, 56.0, 54.3, 50.9, 38.3, 38.0, 32.6, 32.5, 24.2, 17.4$ ppm.

Analytical data of compound 169



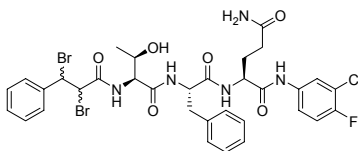
Peptide **169** was synthesized and released from solid support according to **GP 2** and **GP 3**. **Yield** = 2 %; **Purity** > 95% (LC_MS); **LC-MS** (C18, ESI_MS) 840.9 [M+H]⁺, 860.9 [M+Na]⁺; R_t = 8.44 min.

Analytical data of compound 170



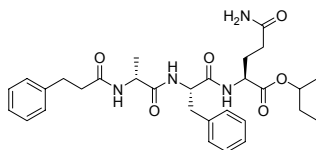
Peptide **170** was synthesized and released from solid support according to **GP 2** and **GP 3**. **Yield** = 8 %; **Purity** > 95% (LC_MS); **LC-MS** (C18, ESI_MS) 727.8 [M+H]⁺, 750.0 [M+Na]⁺; R_t = 7.49 min.

Analytical data of compound 171



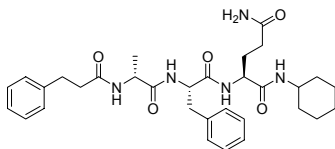
Peptide **171** was synthesized and released from solid support according to **GP 2** and **GP 3**. **Yield** = 1 %; **Purity** > 95% (LC_MS); **LC-MS** (C18, ESI_MS) 812.0 [M+H]⁺, 834.0 [M+Na]⁺; R_t = 8.65 min.

Analytical data of compound 172



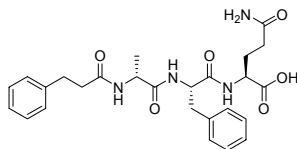
Peptide **172** was synthesized and released from solid support according to **GP 2** and **GP 3**. **Yield** = 1 %; **Purity** > 95% (LC_MS); **LC-MS** (C18, ESI_MS) 553.2 [M+H]⁺, 575.2 [M+Na]⁺; R_t = 7.89 min.

Analytical data of compound 173



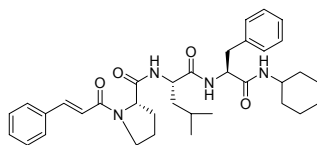
Peptide **173** was synthesized and released from solid support according to **GP 2** and **GP 3**. **Yield** = 2 %; **Purity** > 95% (LC_MS); **LC-MS** (C18, ESI_MS) 578.3 [M+H]⁺, 600.4 [M+Na]⁺; R_t = 7.69 min.

Analytical data of compound 174



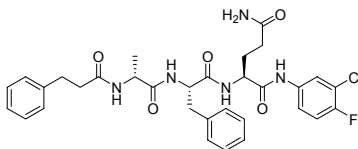
Peptide **174** was synthesized and released from solid support according to **GP 2** and **GP 3**. **Yield** = 6 %; **Purity** > 95% (LC_MS); **LC-MS** (C18, ESI_MS) 497.1 [M+H]⁺, 519.2 [M+Na]⁺; R_t = 6.75 min; **¹H NMR** (400 MHz, CD₃OD): δ = 7.37-7.00 (m, 10H), 4.62 (dd, *J* = 10.0, 4.7 Hz, 1H), 4.41 (dd, *J* = 9.4, 4.3 Hz, 1H), 4.17 (q, *J* = 7.2 Hz, 1H), 3.24 (dd, *J* = 14.0, 4.7 Hz, 1H), 2.88 (dd, *J* = 14.0, 8.8 Hz, 1H), 2.88-2.82 (m, 2H), 2.47 (dd, *J* = 8.6, 6.7 Hz, 2H), 2.31 (t, *J* = 7.35 Hz, 2H), 2.29-2.18 (m, 1H), 2.07-1.92 (m, 1H), 1.05 (d, *J* = 7.2 Hz, 3H) ppm; **¹³C NMR** (100 MHz, CD₃OD): δ = 177.8, 175.2, 175.1, 174.4, 173.5, 142.3, 138.5, 130.4, 129.4, 129.4, 129.4, 127.7, 127.1, 55.6, 53.3, 50.7, 38.4, 38.2, 32.6, 28.5, 24.2, 17.6 ppm.

Analytical data of compound 175



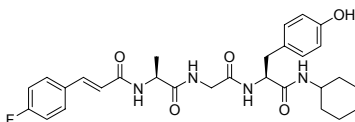
Peptide **175** was synthesized and released from solid support according to **GP 2** and **GP 3**. **Yield** = 12 %; **Purity** > 95% (LC_MS); **LC-MS** (C18, ESI_MS) 587.8 [M+H]⁺, 609.7 [M+Na]⁺; R_t = 9.65 min.

Analytical data of compound 176



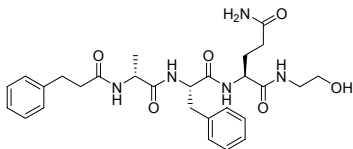
Peptide **176** was synthesized and released from solid support according to **GP 2** and **GP 3**. **Yield** = 1 %; **Purity** > 95% (LC_MS); **LC-MS** (C18, ESI_MS) 624.3 [M+H]⁺, 646.2 [M+Na]⁺; R_t = 8.28 min; ¹H NMR (400 MHz, CD₃OD): δ = 7.94 (dd, *J* = 6.8, 2.7 Hz, 1H), 7.61-7.51 (m, 1H), 7.32-7.02 (m, 11H), 4.55 (dd, *J* = 10.0, 4.6 Hz, 1H), 4.46 (dd, *J* = 9.8, 4.4 Hz, 1H), 4.17 (q, *J* = 7.1 Hz, 1H), 3.30-3.19 (m, 1H), 2.96 (dd, *J* = 14.2, 9.9 Hz, 1H), 2.86-2.71 (m, 2H), 2.50-2.22 (m, 5H), 2.20-2.08 (m, 1H), 1.14 (d, *J* = 7.1 Hz, 3H) ppm; ¹³C NMR (100 MHz, CD₃OD): δ = 177.7, 176.6, 175.3, 173.8, 171.0, 144.2, 142.2, 138.5, 130.2, 129.5, 129.4, 129.2, 127.9, 127.1, 123.2, 121.4, 121.3, 117.6, 117.4, 56.8, 55.1, 51.0, 38.1, 35.4, 32.8, 32.4, 28.5, 17.1 ppm.

Analytical data of compound 177



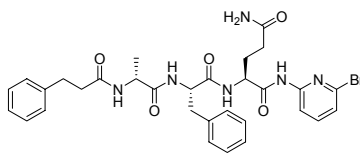
Peptide **177** was synthesized and released from solid support according to **GP 2** and **GP 3**. **Yield** = 9 %; **Purity** > 85% (LC_MS); **LC-MS** (C18, ESI_MS) 539.2 [M+H]⁺, 561.3 [M+Na]⁺; R_t = 7.65 min.

Analytical data of compound 178



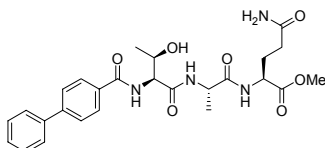
Peptide **178** was synthesized and released from solid support according to **GP 2** and **GP 3**. **Yield** = 1 %; **Purity** > 95% (LC_MS); **LC-MS** (C18, ESI_MS) 540.5 [M+H]⁺; R_t = 5.42 min.

Analytical data of compound 179



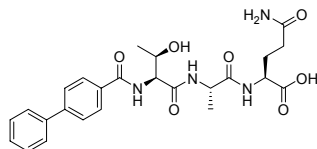
Peptide **179** was synthesized and released from solid support according to **GP 2** and **GP 3**. **Yield** = 1 %; **Purity** > 95% (LC_MS); **LC-MS** (C18, ESI_MS) 651.3 [M+H]⁺, 673.2 [M+Na]⁺; R_t = 7.96 min.

Analytical data of compound 180



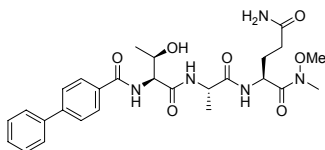
Peptide **180** was synthesized and released from solid support according to **GP 2** and **GP 3**. **Yield** = 1 %; **Purity** > 85% (LC_MS); **LC-MS** (C18, ESI_MS) 513.2 [M+H]⁺, 535.2 [M+Na]⁺; R_t = 6.78 min.

Analytical data of compound 181



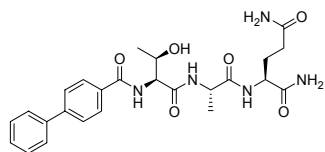
Peptide **181** was synthesized and released from solid support according to **GP 2** and **GP 3**. **Yield** = 6 %; **Purity** > 95% (LC_MS); **LC-MS** (C18, ESI_MS) 499.0 [M+H]⁺, 521.2 [M+Na]⁺; R_t = 6.55 min; **¹H NMR** (400 MHz, CD₃OD): δ = 7.98 (d, *J* = 8.2 Hz, 2H), 7.76 (d, *J* = 8.2 Hz, 2H), 7.68 (d, *J* = 7.4 Hz, 2H), 7.47 (t, *J* = 7.5, 7.5 Hz, 2H), 7.39 (t, *J* = 7.2, 7.2 Hz, 1H), 4.63 (d, *J* = 4.2 Hz, 1H), 4.50-4.36 (m, 2H), 4.36-4.27 (m, 1H), 2.46-2.28 (m, 2H), 2.28-2.19 (m, 1H), 2.01-1.87 (m, 1H), 1.43 (d, *J* = 7.1 Hz, 3H), 1.29 (d, *J* = 6.3 Hz, 3H); **¹³C NMR** (100 MHz, CD₃OD): δ = 174.9, 172.6, 172.6, 169.4, 167.5, 146.0, 141.2, 133.7, 130.0, 129.1, 129.1, 128.1, 128.1, 68.8, 60.5, 53.2, 50.6, 32.7, 28.7, 20.2, 17.6 ppm.

Analytical data of compound 182



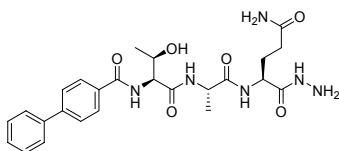
Peptide **182** was synthesized and released from solid support according to **GP 2** and **GP 3**. **Yield** = 7 %; **Purity** > 95% (LC_MS); **LC-MS** (C18, ESI_MS) 542.0 [M+H]⁺, 564.2 [M+Na]⁺; R_t = 6.65 min.

Analytical data of compound 183



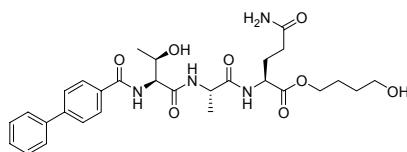
Peptide **183** was synthesized and released from solid support according to **GP 2** and **GP 3**. **Yield** = 8 %; **Purity** > 80% (LC_MS); **LC-MS** (C18, ESI_MS) 498.1 [M+H]⁺, 520.2 [M+Na]⁺; R_t = 6.39 min; ¹H NMR (400 MHz, CD₃OD): δ = 7.99 (d, *J* = 8.2 Hz, 2H), 7.76 (d, *J* = 8.2 Hz, 2H), 7.68 (dd, *J* = 8.4, 1.1 Hz, 2H), 7.47 (t, *J* = 7.7 Hz, 2H), 7.40 (d, *J* = 7.5 Hz, 1H), 4.63 (d, *J* = 4.1 Hz, 1H), 4.40-4.26 (m, 3H), 2.45-2.25 (m, 2H), 2.22-2.10 (m, 1H), 2.02-1.89 (m, 1H), 1.43 (d, *J* = 7.21 Hz, 3H), 1.30 (d, *J* = 6.39 Hz, 3H); ¹³C NMR (100 MHz, CD₃OD): δ = 177.8, 176.3, 175.0, 173.1, 170.1, 146.1, 141.2, 133.7, 130.0, 129.1, 129.1, 128.1, 128.1, 68.9, 60.6, 54.1, 51.2, 32.7, 28.9, 20.3, 17.3 ppm.

Analytical data of compound 184



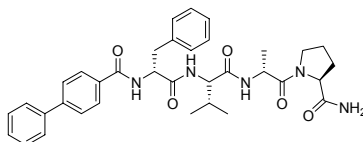
Peptide **184** was synthesized and released from solid support according to **GP 2** and **GP 3**. **Yield** = 3 %; **Purity** > 85% (LC_MS); **LC-MS** (C18, ESI_MS) 513.2 [M+H]⁺, 535.3 [M+Na]⁺; R_t = 6.07 min.

Analytical data of compound 185



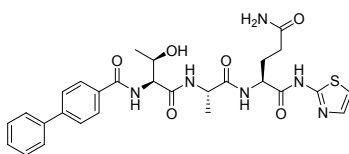
Peptide **185** was synthesized and released from solid support according to **GP 2** and **GP 3**. **Yield** = 4 %; **Purity** > 95% (LC_MS); **LC-MS** (C18, ESI_MS) 571.1 [M+H]⁺, 593.3 [M+Na]⁺; R_t = 6.63 min.

Analytical data of compound 186



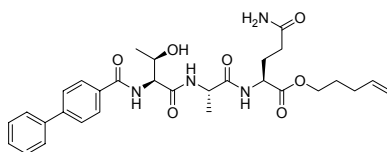
Peptide **186** was synthesized and released from solid support according to **GP 2** and **GP 3**. **Yield** = 25 %; **Purity** > 95% (LC_MS); **LC-MS** (C18, ESI_MS) 612.1 [M+H]⁺, 634.3 [M+Na]⁺; R_t = 8.15 min; ¹H NMR (400 MHz, DMSO-D₆): Major isomer δ = 8.65 (dd, *J* = 8.4, 3.6 Hz, 1H), 8.22 (d, *J* = 8.8 Hz, 1H), 7.90 (d, *J* = 5.4 Hz, 1H), 7.88 (d, *J* = 5.4 Hz, 1H), 7.78-7.69 (m, 5H), 7.49 (t, *J* = 7.5 Hz, 2H), 7.43-7.37 (m, 3H), 7.25 (t, *J* = 7.52 Hz, 2H), 4.89-4.81 (m, 1H), 4.28-4.23 (m, 1H), 4.21-4.16 (m, 1H), 3.11 (dd, *J* = 13.6, 4.7 Hz, 1H), 3.01 (dd, *J* = 13.5, 10.7 Hz, 1H), 2.05-1.79 (m, 4H), 1.79-1.68 (m, 1H), 1.21 (d, *J* = 6.8 Hz, 3H), 0.82 (d, *J* = 6.4 Hz, 3H), 0.80 (d, *J* = 6.5 Hz, 3H) ppm; **HRMS** (ESI) *m/z* calc. for C₃₅H₄₁N₅O₅ 611.3108, found 612.3179 [M+H]⁺.

Analytical data of compound 187



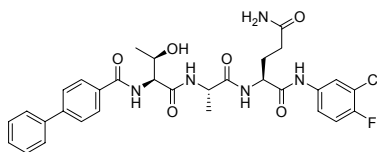
Peptide **187** was synthesized and released from solid support according to **GP 2** and **GP 3**. **Yield** = 6 %; **Purity** > 95% (LC_MS); **LC-MS** (C18, ESI_MS) 581.1 [M+H]⁺, 603.1 [M+Na]⁺; R_t = 7.09 min.

Analytical data of compound 188



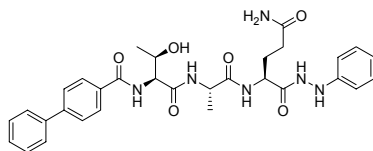
Peptide **188** was synthesized and released from solid support according to **GP 2** and **GP 3**. **Yield** = 4 %; **Purity** > 95% (LC_MS); **LC-MS** (C18, ESI_MS) 567.2 [M+H]⁺, 589.2 [M+Na]⁺; R_t = 7.68 min.

Analytical data of compound 189



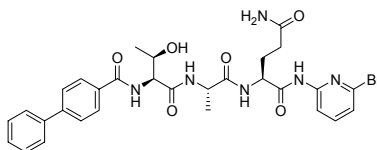
Peptide **189** was synthesized and released from solid support according to **GP 2** and **GP 3**. **Yield** = 5 %; **Purity** > 95% (LC_MS); **LC-MS** (C18, ESI_MS) 626.2 [M+H]⁺, 648.2 [M+Na]⁺; R_t = 7.99 min.

Analytical data of compound 190



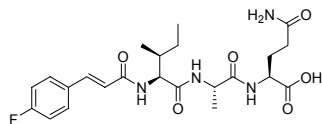
Peptide **190** was synthesized and released from solid support according to **GP 2** and **GP 3**. **Yield** = 1 %; **Purity** > 85% (LC_MS); **LC-MS** (C18, ESI_MS) 589.2 [M+H]⁺, 611.2 [M+Na]⁺; R_t = 7.18 min.

Analytical data of compound 192



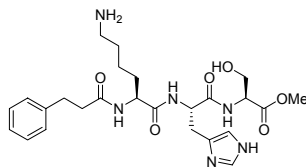
Peptide **192** was synthesized and released from solid support according to **GP 2** and **GP 3**. **Yield** = 6 %; **Purity** > 70% (LC_MS); **LC-MS** (C18, ESI_MS) 653.0 [M+H]⁺, 675.1 [M+Na]⁺; R_t = 7.67 min.

Analytical data of compound 193



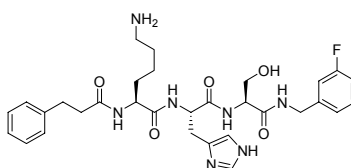
Peptide **193** was synthesized and released from solid support according to **GP 2** and **GP 3**. **Yield** = 1 %; **Purity** > 95% (LC_MS); **LC-MS** (C18, ESI_MS) 479.3 [M+H]⁺, 501.4 [M+Na]⁺; R_t = 6.79 min.

Analytical data of compound 194



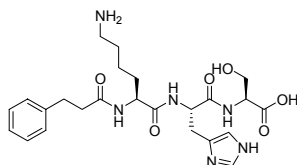
Peptide **194** was synthesized and released from solid support according to **GP 2** and **GP 3**. **Yield** = 10 %; **Purity** > 85% (LC_MS); **LC-MS** (C18, ESI_MS) 517.8 [M+H]⁺, 540.1 [M+Na]⁺; R_t = 1.32 min.

Analytical data of compound 195



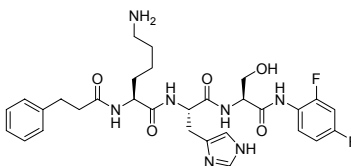
Peptide **195** was synthesized and released from solid support according to **GP 2** and **GP 3**. **Yield** = 25 %; **Purity** > 85% (LC_MS); **LC-MS** (C18, ESI_MS) 610.4 [M+H]⁺; R_t = 4.52 min.

Analytical data of compound 196



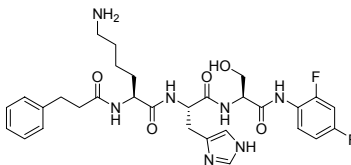
Peptide **196** was synthesized and released from solid support according to **GP 2** and **GP 3**. **Yield** = 6 %; **Purity** > 95% (LC_MS); **LC-MS** (C18, ESI_MS) 503.3 [M+H]⁺; R_t = 2.23 min.

Analytical data of compound 197



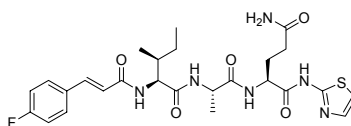
Peptide **197** was synthesized and released from solid support according to **GP 2** and **GP 3**. **Yield** = 4 %; **Purity** > 90% (LC_MS); **LC-MS** (C18, ESI_MS) 614.3 [M+H]⁺, 636.4 [M+Na]⁺; R_t = 4.07 min.

Analytical data of compound 198



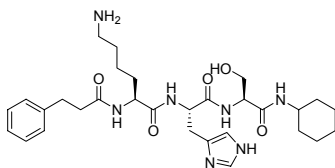
Peptide **198** was synthesized and released from solid support according to **GP 2** and **GP 3**. **Yield** = 1 %; **Purity** > 95% (LC_MS); **LC-MS** (C18, ESI_MS) 614.3 [M+H]⁺, 636.3 [M+Na]⁺; R_t = 4.46 min.

Analytical data of compound 199



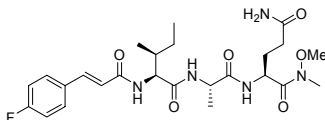
Peptide **199** was synthesized and released from solid support according to **GP 2** and **GP 3**. **Yield** = 1 %; **Purity** > 95% (LC_MS); **LC-MS** (C18, ESI_MS) 561.5 [M+H]⁺, 583.4 [M+Na]⁺; R_t = 7.27 min.

Analytical data of compound 200



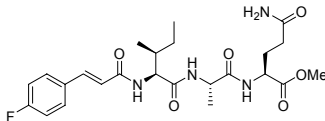
Peptide **200** was synthesized and released from solid support according to **GP 2** and **GP 3**. **Yield** = 3 %; **Purity** > 95% (LC_MS); **LC-MS** (C18, ESI_MS) 584.6 [M+H]⁺, 606.7 [M+Na]⁺; R_t = 4.18 min.

Analytical data of compound 201



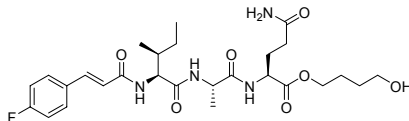
Peptide **201** was synthesized and released from solid support according to **GP 2** and **GP 3**. **Yield** = 1 %; **Purity** > 95% (LC_MS); **LC-MS** (C18, ESI_MS) 522.3 [M+H]⁺, 544.4 [M+Na]⁺; R_t = 6.87 min.

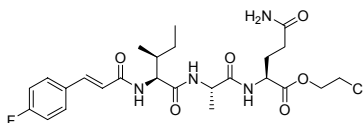
Analytical data of compound 202



Peptide **202** was synthesized and released from solid support according to **GP 2** and **GP 3**. **Yield** = 1 %; **Purity** > 95% (LC_MS); **LC-MS** (C18, ESI_MS) 493.4 [M+H]⁺, 515.4 [M+Na]⁺; R_t = 7.03 min.

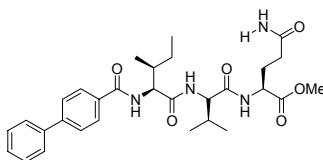
Analytical data of compound 203





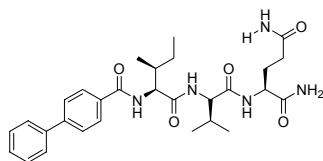
Peptide **207** was synthesized and released from solid support according to **GP 2** and **GP 3**. **Yield** = 1 %; **Purity** > 70% (LC_MS); **LC-MS** (C18, ESI_MS) 541.4 [M+H]⁺, 563.5 [M+Na]⁺; R_t = 7.46 min.

Analytical data of compound 208



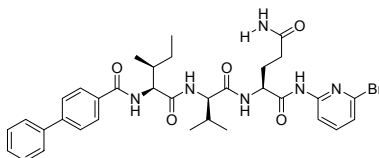
Peptide **208** was synthesized and released from solid support according to **GP 2** and **GP 3**. **Yield** = 2 %; **Purity** > 80% (LC_MS); **LC-MS** (C18, ESI_MS) 553.4 [M+H]⁺, 575.4 [M+Na]⁺; R_t = 8.37 min.

Analytical data of compound 209



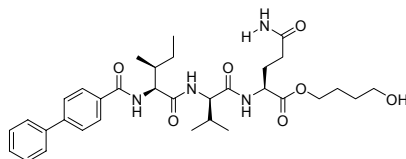
Peptide **209** was synthesized and released from solid support according to **GP 2** and **GP 3**. **Yield** = 5 %; **Purity** > 90% (LC_MS); **LC-MS** (C18, ESI_MS) 538.3 [M+H]⁺, 560.3 [M+Na]⁺; R_t = 9.70 min.

Analytical data of compound 210



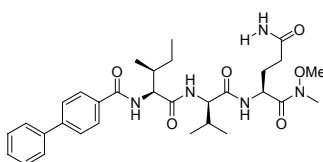
Peptide **210** was synthesized and released from solid support according to **GP 2** and **GP 3**. **Yield** = 1 %; **Purity** > 80% (LC_MS); **LC-MS** (C18, ESI_MS) 693.5 [M+H]⁺, 715.4 [M+Na]⁺; R_t = 11.91 min.

Analytical data of compound 211



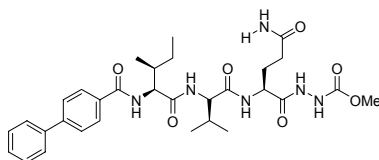
Peptide **211** was synthesized and released from solid support according to **GP 2** and **GP 3**. **Yield** = 3 %; **Purity** > 95% (LC_MS); **LC-MS** (C18, ESI_MS) 611.5 [M+H]⁺, 633.4 [M+Na]⁺; R_t = 10.37 min.

Analytical data of compound 212



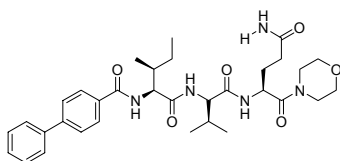
Peptide **212** was synthesized and released from solid support according to **GP 2** and **GP 3**. **Yield** = 5 %; **Purity** > 95% (LC_MS); **LC-MS** (C18, ESI_MS) 582.3 [M+H]⁺, 604.4 [M+Na]⁺; R_t = 10.44 min.

Analytical data of compound 213



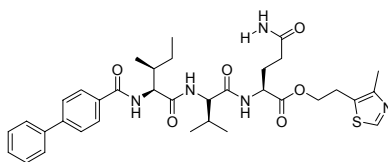
Peptide **213** was synthesized and released from solid support according to **GP 2** and **GP 3**. **Yield** = 2 %; **Purity** > 95% (LC_MS); **LC-MS** (C18, ESI_MS) 611.4 [M+H]⁺, 633.4 [M+Na]⁺; R_t = 7.87 min.

Analytical data of compound 214



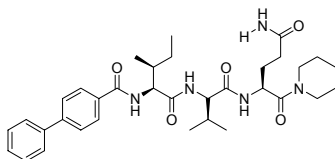
Peptide **214** was synthesized and released from solid support according to **GP 2** and **GP 3**. **Yield** = 7 %; **Purity** > 90% (LC_MS); **LC-MS** (C18, ESI_MS) 608.3 [M+H]⁺, 630.4 [M+Na]⁺; R_t = 7.96 min.

Analytical data of compound 215



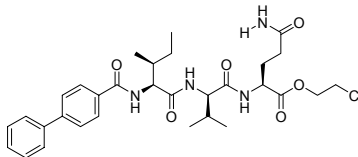
Peptide **215** was synthesized and released from solid support according to **GP 2** and **GP 3**. **Yield** = 1 %; **Purity** > 95% (LC_MS); **LC-MS** (C18, ESI_MS) 664.4 [M+H]⁺, 686.4 [M+Na]⁺; R_t = 10.71 min.

Analytical data of compound 216



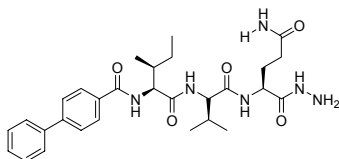
Peptide **216** was synthesized and released from solid support according to **GP 2** and **GP 3**. **Yield** = 3 %; **Purity** > 95% (LC_MS); **LC-MS** (C18, ESI_MS) 606.5 [M+H]⁺, 628.5 [M+Na]⁺; R_t = 11.03 min.

Analytical data of compound 217



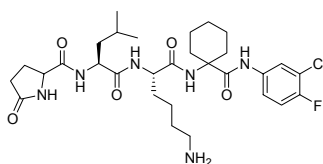
Peptide **217** was synthesized and released from solid support according to **GP 2** and **GP 3**. **Yield** = 2 %; **Purity** > 80% (LC_MS); **LC-MS** (C18, ESI_MS) 601.6 [M+H]⁺, 623.5 [M+Na]⁺; R_t = 11.55 min.

Analytical data of compound 218



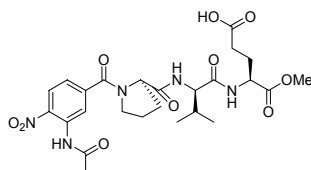
Peptide **218** was synthesized and released from solid support according to **GP 2** and **GP 3**. **Yield** = 1 %; **Purity** > 70% (LC_MS); **LC-MS** (C18, ESI_MS) 553.4 [M+H]⁺, 575.5 [M+Na]⁺; R_t = 9.30 min.

Analytical data of compound 219



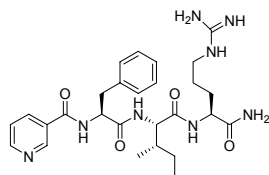
Peptide **219** was synthesized and released from solid support according to **GP 2** and **GP 3**. **Yield** = 6 %; **Purity** > 80% (LC_MS); **LC-MS** (C18, ESI_MS) 623.5 [M+H]⁺, 645.3 [M+Na]⁺; R_t = 6.30 min.

Analytical data of compound 220



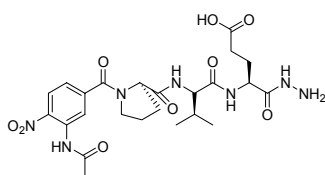
Peptide **220** was synthesized and released from solid support according to **GP 2** and **GP 3**. **Yield** = 3 %; **Purity** > 95% (LC_MS); **LC-MS** (C18, ESI_MS) 564.2 [M+H]⁺, 586.3 [M+Na]⁺; R_t = 6.64 min.

Analytical data of compound 221



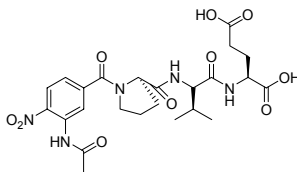
Peptide **221** was synthesized and released from solid support according to **GP 2** and **GP 3**. **Yield** = 5 %; **Purity** > 75% (LC_MS); **LC-MS** (C18, ESI_MS) 539.3 [M+H]⁺, 561.3 [M+Na]⁺; R_t = 4.90 min.

Analytical data of compound 222



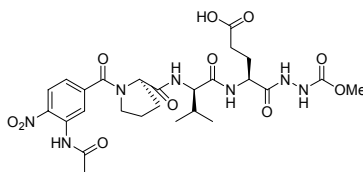
Peptide **222** was synthesized and released from solid support according to **GP 2** and **GP 3**. **Yield** = 7 %; **Purity** > 95% (LC_MS); **LC-MS** (C18, ESI_MS) 564.4 [M+H]⁺, 586.4 [M+Na]⁺; R_t = 5.65 min.

Analytical data of compound 223



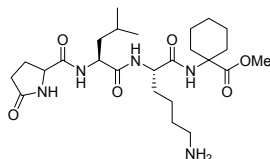
Peptide **223** was synthesized and released from solid support according to **GP 2** and **GP 3**. **Yield** = 6 %; **Purity** > 95% (LC_MS); **LC-MS** (C18, ESI_MS) 550.2 [M+H]⁺, 572.3 [M+Na]⁺; R_t = 6.27 min.

Analytical data of compound 224



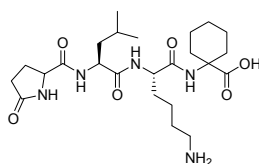
Peptide **224** was synthesized and released from solid support according to **GP 2** and **GP 3**. **Yield** = 5 %; **Purity** > 95% (LC_MS); **LC-MS** (C18, ESI_MS) 622.0 [M+H]⁺, 644.2 [M+Na]⁺; R_t = 6.09 min.

Analytical data of compound 225



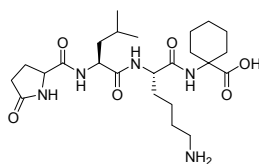
Peptide **225** was synthesized and released from solid support according to **GP 2** and **GP 3**. **Yield** = 8 %; **Purity** > 95% (LC_MS); **LC-MS** (C18, ESI_MS) 510.4 [M+H]⁺, 532.4 [M+Na]⁺; R_t = 5.47 min.

Analytical data of compound 226



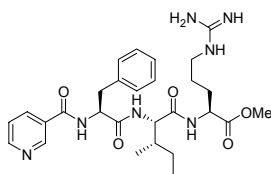
Peptide **226** was synthesized and released from solid support according to **GP 2** and **GP 3**. **Yield** = 34 %; **Purity** > 95% (LC_MS); **LC-MS** (C18, ESI_MS) 496.4 [M+H]⁺, 518.4 [M+Na]⁺; R_t = 5.15 min.

Analytical data of compound 227



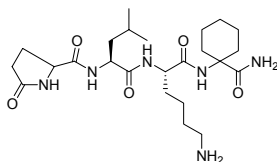
Peptide **227** was synthesized and released from solid support according to **GP 2** and **GP 3**. **Yield** = 30 %; **Purity** > 95% (LC_MS); **LC-MS** (C18, ESI_MS) 496.4 [M+H]⁺, 518.4 [M+Na]⁺; R_t = 5.15 min.

Analytical data of compound 228



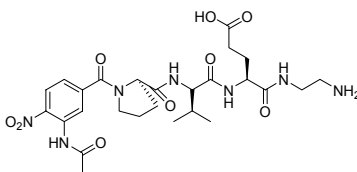
Peptide **228** was synthesized and released from solid support according to **GP 2** and **GP 3**. **Yield** = 4 %; **Purity** > 95% (LC_MS); **LC-MS** (C18, ESI_MS) 554.4 [M+H]⁺; R_t = 5.76 min.

Analytical data of compound 229



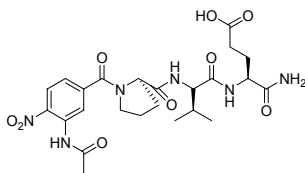
Peptide **229** was synthesized and released from solid support according to **GP 2** and **GP 3**. **Yield** = 5 %; **Purity** > 95% (LC_MS); **LC-MS** (C18, ESI_MS) 495.4 [M+H]⁺, 517.4 [M+Na]⁺; R_t = 4.54 min.

Analytical data of compound 230



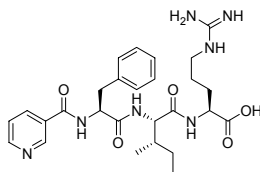
Peptide **230** was synthesized and released from solid support according to **GP 2** and **GP 3**. **Yield** = 1 %; **Purity** > 85% (LC_MS); **LC-MS** (C18, ESI_MS) 592.2 [M+H]⁺; R_t = 7.14 min.

Analytical data of compound 231



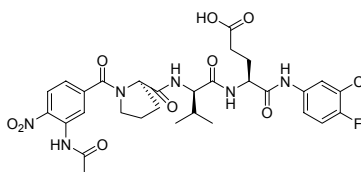
Peptide **231** was synthesized and released from solid support according to **GP 2** and **GP 3**. **Yield** = 3 %; **Purity** > 95% (LC_MS); **LC-MS** (C18, ESI_MS) 549.0 [M+H]⁺, 571.3 [M+Na]⁺; R_t = 5.86 min.

Analytical data of compound 232



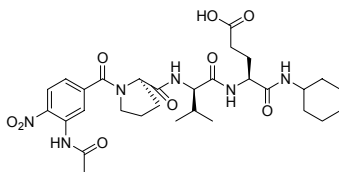
Peptide **232** was synthesized and released from solid support according to **GP 2** and **GP 3**. **Yield** = 8 %; **Purity** > 95% (LC_MS); **LC-MS** (C18, ESI_MS) 540.4 [M+H]⁺; R_t = 5.08 min.

Analytical data of compound 233



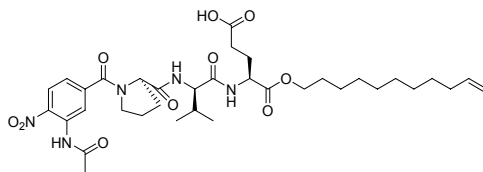
Peptide **233** was synthesized and released from solid support according to **GP 2** and **GP 3**. **Yield** = 10 %; **Purity** > 95% (LC_MS); **LC-MS** (C18, ESI_MS) 677.0 [M+H]⁺, 699.2 [M+Na]⁺; R_t = 7.88 min.

Analytical data of compound 234



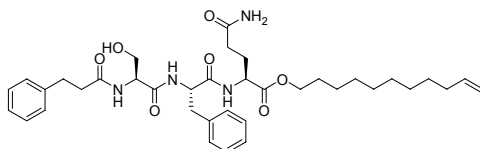
Peptide **234** was synthesized and released from solid support according to **GP 2** and **GP 3**. **Yield** = 7 %; **Purity** > 95% (LC_MS); **LC-MS** (C18, ESI_MS) 631.2 [M+H]⁺, 653.3 [M+Na]⁺; R_t = 7.30 min.

Analytical data of compound 235



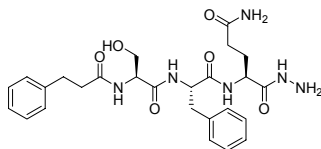
Peptide **235** was synthesized and released from solid support according to **GP 2** and **GP 3**. **Yield** = 1 %; **Purity** > 80% (LC_MS); **LC-MS** (C18, ESI_MS) 702.4 [M+H]⁺, 724.4 [M+Na]⁺; R_t = 10.05 min.

Analytical data of compound 236



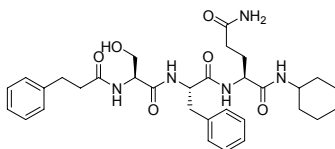
Peptide **236** was synthesized and released from solid support according to **GP 2** and **GP 3**. **Yield** = 3 %; **Purity** > 95% (LC_MS); **LC-MS** (C18, ESI_MS) 665.5 [M+H]⁺, 687.5 [M+Na]⁺; R_t = 10.10 min.

Analytical data of compound 237



Peptide **237** was synthesized and released from solid support according to **GP 2** and **GP 3**. **Yield** = 12 %; **Purity** > 70% (LC_MS); **LC-MS** (C18, ESI_MS) 527.2 [M+H]⁺, 549.3 [M+Na]⁺; R_t = 6.16 min.

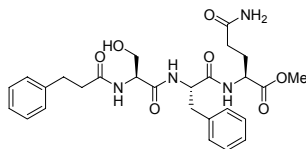
Analytical data of compound 238



Peptide **238** was synthesized and released from solid support according to **GP 2** and **GP 3**. **Yield** = 4 %; **Purity** > 85% (LC_MS); **LC-MS** (C18, ESI_MS) 594.3 [M+H]⁺, 616.3 [M+Na]⁺; R_t = 7.56 min; ¹H NMR (400 MHz, DMSO-D₆): δ = 8.01 (d, *J* = 7.7 Hz, 1H), 7.96 (d, *J* = 8.2 Hz, 1H), 7.93 (d, *J* = 7.4 Hz, 1H), 7.61 (d, *J* = 7.8 Hz, 1H), 7.29-7.13 (m, 10H), 6.74 (s, 1H), 5.02 (t, *J* = 5.60 Hz, 1H), 4.48 (dt, *J* = 8.6, 4.69 Hz, 1H), 4.28 (q, *J* = 6.3 Hz, 1H), 4.17 (dt, *J* = 8.3, 5.7 Hz, 1H), 3.48 (t, *J* = 5.30 Hz, 2H), 3.06 (dd, *J* = 14.0, 4.4 Hz, 1H), 2.84 (dd, *J* = 13.9, 8.9 Hz,

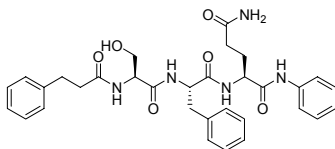
1H), 2.80-2.74 (m, 2H), 2.45-2.39 (m, 2H), 2.09-1.98 (m, 2H), 1.92-1.78 (m, 1H), 1.79-1.60 (m, 5H), 1.59-1.48 (m, 1H), 1.34-1.04 (m, 5H) ppm; **HRMS** (ESI) m/z calc. for $C_{32}H_{43}N_5O_6$ 593.3213, found 594.3286 $[M+H]^+$.

Analytical data of compound 239



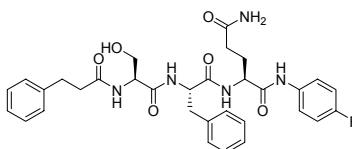
Peptide **239** was synthesized and released from solid support according to **GP 2** and **GP 3**. **Yield** = 9 %; **Purity** > 95% (LC_MS); **LC-MS** (C18, ESI_MS) 527.2 $[M+H]^+$, 549.3 $[M+Na]^+$; R_t = 6.93 min.

Analytical data of compound 240



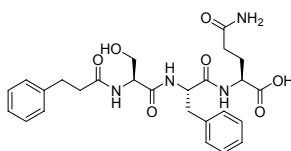
Peptide **240** was synthesized and released from solid support according to **GP 2** and **GP 3**. **Yield** = 15 %; **Purity** > 95% (LC_MS); **LC-MS** (C18, ESI_MS) 588.3 $[M+H]^+$, 610.3 $[M+Na]^+$; R_t = 7.59 min; **1H NMR** (400 MHz, DMSO- D_6): δ = 9.87 (s, 1H), 8.19 (d, J = 7.7 Hz, 1H), 8.02 (d, J = 7.8 Hz, 1H), 7.96 (d, J = 7.6 Hz, 1H), 7.62 (dd, J = 8.6, 1.1 Hz, 2H), 7.35-7.12 (m, 15H), 7.09-7.04 (m, 1H), 6.79 (s, 1H), 5.01 (t, J = 5.4 Hz, 1H), 4.54 (dt, J = 8.6, 4.3 Hz, 1H), 4.36 (dt, J = 8.0, 5.6 Hz, 1H), 4.30 (q, J = 6.1 Hz, 1H), 3.50 (t, J = 5.6 Hz, 2H), 3.10 (dd, J = 14.0, 4.4 Hz, 1H), 2.86 (dd, J = 13.9, 9.0 Hz, 1H), 2.80-2.75 (m, 2H), 2.47-2.38 (m, 2H), 2.18-2.10 (m, 2H), 2.03-1.92 (m, 1H), 1.91-1.79 (m, 1H) ppm; **HRMS** (ESI) m/z calc. for $C_{32}H_{37}N_5O_6$ 587.2744, found 588.2814 $[M+H]^+$.

Analytical data of compound 241



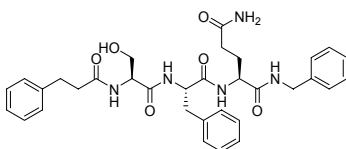
Peptide **241** was synthesized and released from solid support according to **GP 2** and **GP 3**. **Yield** = 14 %; **Purity** > 95% (LC_MS); **LC-MS** (C18, ESI_MS) 606.2 [M+H]⁺, 628.3 [M+Na]⁺; R_t = 7.69 min; **¹H NMR** (400 MHz, CD₃OD): δ = 9.93 (s, 1H), 8.20 (d, *J* = 7.6 Hz, 1H), 8.02 (d, *J* = 8.0 Hz, 1H), 7.97 (s, 1H), 7.95 (s, 2H), 7.64 (dd, *J* = 9.1, 5.0 Hz, 2H), 7.34-7.07 (m, 12H), 6.79 (s, 1H), 5.01 (t, *J* = 5.5 Hz, 1H), 4.53 (dt, *J* = 8.4, 8.2, 4.5 Hz, 1H), 4.40-4.21 (m, 2H), 3.50 (t, *J* = 5.8 Hz, 2H), 3.09 (dd, *J* = 13.8, 4.4 Hz, 1H), 2.88-2.82 (m, 1H), 2.77 (t, *J* = 8.0 Hz, 2H), 2.46-2.38 (m, 2H), 2.23-2.05 (m, 2H), 2.04-1.91 (m, 1H), 1.91-1.78 (m, 1H) ppm; **¹³C NMR** (100 MHz, CD₃OD): δ = 173.3, 171.6, 170.6, 170.2, 169.7, 141.1, 137.4, 129.1, 128.1, 128.0, 127.8, 126.1, 125.7, 121.0, 120.9, 115.2, 115.0, 61.5, 54.9, 53.8, 53.1, 36.5, 35.6, 31.2, 30.8, 27.5 ppm; **¹⁹F NMR** (188 MHz, CD₃OD): δ = -119.4, -119.5, -119.5, -119.5, -119.5, -119.6, -119.6 ppm; **HRMS** (FAB, *m*-NBA) *m/z* calc. for C₃₂H₃₆FN₅O₆ 605.2650, found 606.2750 [M+H]⁺.

Analytical data of compound 242



Peptide **242** was synthesized and released from solid support according to **GP 2** and **GP 3**. **Yield** = 4 %; **Purity** > 95% (LC_MS); **LC-MS** (C18, ESI_MS) 513.3 [M+H]⁺, 535.2 [M+Na]⁺; R_t = 6.61 min.

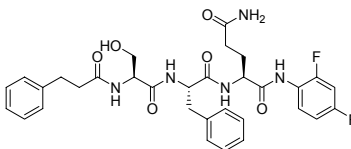
Analytical data of compound 243



Peptide **243** was synthesized and released from solid support according to **GP 2** and **GP 3**. **Yield** = 10 %; **Purity** > 95% (LC_MS); **LC-MS** (C18, ESI_MS) 602.3 [M+H]⁺, 624.4 [M+Na]⁺; R_t = 7.52 min; **¹H NMR** (400 MHz, DMSO-D₆): δ = 8.22 (t, *J* = 6.0 Hz, 1H), 8.07 (d, *J* = 7.9 Hz, 1H), 8.01 (d, *J* = 7.9 Hz, 1H), 7.90 (d, *J* = 7.6 Hz, 1H), 7.34-7.09 (m, 15H), 6.74 (s, 1H), 4.98 (t, *J* = 5.4 Hz, 1H), 4.50 (dt, *J* = 8.6, 4.6 Hz, 1H), 4.32-4.18 (m, 4H), 3.45 (t, *J* = 5.9 Hz, 2H), 3.06 (dd, *J* = 14.1, 4.5 Hz, 1H), 2.82 (dd, *J* = 14.0, 9.1 Hz, 1H), 2.78-2.72 (m, 2H), 2.40 (dt, *J* = 7.5, 1.7

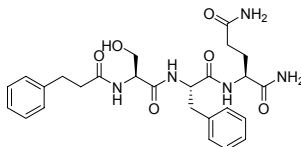
Hz, 2H), 2.10-2.04 (m, 2H), 1.97-1.85 (m, 1H), 1.80-1.69 (m, 1H) ppm; **HRMS** (ESI) m/z calc. for $C_{33}H_{39}N_5O_6$ 601.2900, found 602.2973 $[M+H]^+$.

Analytical data of compound 244



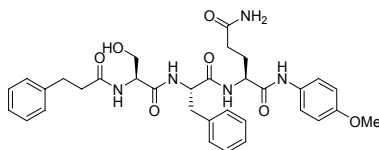
Peptide **244** was synthesized and released from solid support according to **GP 2** and **GP 3**. **Yield** = 10 %; **Purity** > 95% (LC_MS); **LC-MS** (C18, ESI_MS) 624.4 $[M+H]^+$, 646.5 $[M+Na]^+$; R_t = 7.69 min; **1H NMR** (400 MHz, DMSO- D_6): δ = 9.71 (s, 1H), 8.25 (d, J = 7.7 Hz, 1H), 7.98 (d, J = 8.0 Hz, 1H), 7.92 (d, J = 7.7 Hz, 1H), 7.79 (dt, J = 9.0, 6.3 Hz, 1H), 7.37-7.13 (m, 13H), 7.08 (t, J = 8.8 Hz, 1H), 6.80 (s, 1H), 4.96 (t, J = 5.45 Hz, 1H), 4.55 (dt, J = 8.6, 4.7 Hz, 1H), 4.47 (td, J = 8.1, 5.6 Hz, 1H), 4.29 (q, J = 6.1 Hz, 1H), 3.48 (t, J = 5.7 Hz, 2H), 3.09 (dd, J = 13.8, 4.3 Hz, 1H), 2.84 (dd, J = 13.9, 9.0 Hz, 1H), 2.80-2.75 (m, 2H), 2.42 (dt, J = 7.3, 1.5 Hz, 2H), 2.16 (td, J = 9.4, 6.3 Hz, 2H), 2.05-1.91 (m, 1H), 1.91-1.78 (m, 1H) ppm; **HRMS** (ESI) m/z calc. for $C_{32}H_{35}F_2N_5O_6$ 623.2555, found 624.2628 $[M+H]^+$.

Analytical data of compound 245



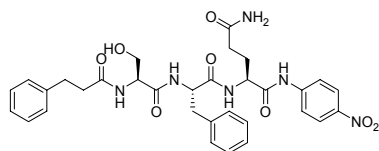
Peptide **245** was synthesized and released from solid support according to **GP 2** and **GP 3**. **Yield** = 15 %; **Purity** > 95% (LC_MS); **LC-MS** (C18, ESI_MS) 512.2 $[M+H]^+$, 534.2 $[M+Na]^+$; R_t = 6.40 min; **1H NMR** (400 MHz, DMSO- D_6): δ = 8.07 (d, J = 7.7 Hz, 1H), 7.95 (d, J = 2.9 Hz, 1H), 7.93 (d, J = 2.4 Hz, 1H), 7.33-7.12 (m, 10H), 7.09 (d, J = 7.0 Hz, 2H), 6.75 (s, 1H), 4.48 (dt, J = 9.3, 4.8 Hz, 1H), 4.29 (q, J = 6.32 Hz, 1H), 4.14 (dt, J = 8.6, 5.2 Hz, 1H), 3.48 (dd, J = 5.9, 3.4 Hz, 2H), 3.08 (dd, J = 13.9, 4.4 Hz, 1H), 2.85 (dd, J = 14.0, 9.3 Hz, 1H), 2.80-2.74 (m, 2H), 2.42 (dt, J = 7.4, 1.8 Hz, 2H), 2.07 (t, J = 8.14 Hz, 2H), 1.96-1.85 (m, 1H), 1.79-1.65 (m, 1H) ppm; **HRMS** (ESI) m/z calc. for $C_{26}H_{33}N_5O_6$ 511.2431, found 512.2503 $[M+H]^+$.

Analytical data of compound 246



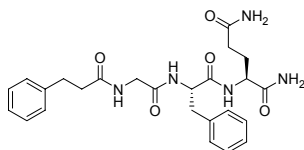
Peptide **246** was synthesized and released from solid support according to **GP 2** and **GP 3**. **Yield** = 8 %; **Purity** > 95% (LC_MS); **LC-MS** (C18, ESI_MS) 618.3 [M+H]⁺, 640.3 [M+Na]⁺; *R*_t = 7.52 min; **¹H NMR** (400 MHz, DMSO-*D*₆): δ = 9.72 (s, 1H), 8.16 (d, *J* = 7.7 Hz, 1H), 8.02 (d, *J* = 7.8 Hz, 1H), 7.95 (d, *J* = 7.5 Hz, 1H), 7.52 (d, *J* = 9.1 Hz, 2H), 7.30-7.11 (m, 10H), 6.89 (d, *J* = 9.1 Hz, 2H), 6.78 (s, 1H), 5.01 (t, *J* = 5.0 Hz, 1H), 4.53 (dt, *J* = 8.8, 4.26 Hz, 1H), 4.37-4.25 (m, 2H), 3.72 (s, 3H), 3.50 (t, *J* = 5.6 Hz, 2H), 3.09 (dd, *J* = 14.0, 4.4 Hz, 1H), 2.88-2.83 (m, 1H), 2.78 (t, *J* = 7.5 Hz, 2H), 2.43 (dd, *J* = 8.8, 5.9 Hz, 2H), 2.16-2.09 (m, 2H), 2.02-1.91 (m, 1H), 1.89-1.77 (m, 1H) ppm; **HRMS** (ESI) *m/z* calc. for C₃₃H₃₉N₅O₇ 617.2849, found 618.2922 [M+H]⁺.

Analytical data of compound 247



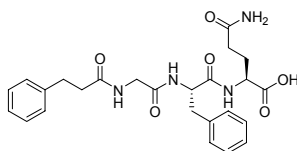
Peptide **247** was synthesized and released from solid support according to **GP 2** and **GP 3**. **Yield** = 8 %; **Purity** > 95% (LC_MS); **LC-MS** (C18, ESI_MS) 633.0 [M+H]⁺, 655.2 [M+Na]⁺; *R*_t = 7.72 min; **¹H NMR** (400 MHz, DMF-*D*₇): δ = 10.39 (s, 1H), 8.32 (d, *J* = 6.9 Hz, 2H), 8.25 (d, *J* = 9.2 Hz, 2H), 8.08 (d, *J* = 7.0 Hz, 1H), 8.02 (d, *J* = 9.3 Hz, 2H), 7.45 (s, 1H), 7.36-7.09 (m, 10H), 6.88 (s, 1H), 5.31 (t, *J* = 5.4, 5.4 Hz, 1H), 4.61 (dt, *J* = 9.0, 9.0, 4.4 Hz, 1H), 4.52-4.39 (m, 2H), 3.75 (dt, *J* = 11.2, 5.7, 5.7 Hz, 1H), 3.65 (dt, *J* = 10.8, 5.5, 5.5 Hz, 1H), 3.23 (dd, *J* = 14.0, 4.2 Hz, 1H), 3.01 (dd, *J* = 14.0, 9.2 Hz, 1H), 2.83 (t, *J* = 8.2 Hz, 2H), 2.54 (dd, *J* = 8.6, 6.5 Hz, 2H), 2.32 (t, *J* = 7.5, 7.5 Hz, 2H), 2.18 (dt, *J* = 13.1, 7.2, 7.2 Hz, 1H), 2.01 (dt, *J* = 16.3, 7.4, 7.4 Hz, 1H) ppm; **¹³C NMR** (100 MHz, DMF-*D*₇): δ = 174.4, 172.9, 171.9, 171.8, 171.8, 145.7, 143.3, 142.0, 138.3, 129.7, 128.7, 128.7, 128.6, 126.8, 126.3, 125.2, 119.7, 62.7, 56.2, 55.6, 54.7, 37.6, 37.2, 32.0, 31.7, 27.9 ppm; **[α]_D²⁰** = -6.2° (C = 0.4, DMSO).

Analytical data of compound 248



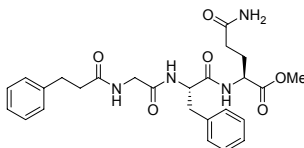
Peptide **248** was synthesized and released from solid support according to **GP 2** and **GP 3**. **Yield** = 3 %; **Purity** > 85% (LC_MS); **LC-MS** (C18, ESI_MS) 482.0 [M+H]⁺, 504.1 [M+Na]⁺; R_t = 6.45 min; **¹H NMR** (400 MHz, DMF-D₇): δ = 8.42-8.35 (m, 2H), 8.23 (d, *J* = 7.9 Hz, 1H), 7.57 (s, 1H), 7.52-7.29 (m, 10H), 7.24 (s, 1H), 6.96 (s, 1H), 4.74 (dt, *J* = 9.2, 9.1, 4.5 Hz, 1H), 4.47 (dt, *J* = 8.6, 8.5, 4.7 Hz, 1H), 4.02 (dd, *J* = 16.3, 5.5 Hz, 1H), 3.90 (dd, *J* = 16.3, 5.7 Hz, 1H), 3.35 (dd, *J* = 13.9, 4.5 Hz, 1H), 3.01 (t, *J* = 8.4, 8.4 Hz, 2H), 2.69 (t, *J* = 8.4, 8.4 Hz, 2H), 2.41 (t, *J* = 7.6, 7.6 Hz, 2H), 2.27 (dt, *J* = 13.2, 7.7, 7.7 Hz, 1H), 2.07 (dt, *J* = 16.3, 7.4, 7.4 Hz, 1H) ppm; **¹³C NMR** (100 MHz, DMF-D₇): δ = 174.7, 173.9, 173.1, 171.5, 170.4, 142.1, 138.6, 129.7, 128.7, 128.7, 128.6, 126.7, 126.3, 55.4, 53.4, 43.2, 37.5, 37.4, 32.1, 31.6, 28.4 ppm.

Analytical data of compound 249



Peptide **249** was synthesized and released from solid support according to **GP 2** and **GP 3**. **Yield** = 3 %; **Purity** > 95% (LC_MS); **LC-MS** (C18, ESI_MS) 483.0 [M+H]⁺, 505.1 [M+Na]⁺; R_t = 6.76 min

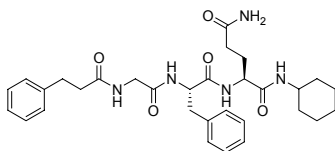
Analytical data of compound 250



Peptide **250** was synthesized and released from solid support according to **GP 2** and **GP 3**. **Yield** = 6 %; **Purity** > 95% (LC_MS); **LC-MS** (C18, ESI_MS) 497.1 [M+H]⁺, 519.2 [M+Na]⁺; R_t = 6.90 min; **¹H NMR** (400 MHz, DMF-D₇): δ = 8.57 (d, *J* = 7.4 Hz, 1H), 8.28 (t, *J* = 5.5, 5.5 Hz, 1H), 8.19 (d, *J* = 8.4 Hz, 1H), 7.57 (s, 1H), 7.50-7.26 (m, 10H), 6.99 (s, 1H), 4.83 (dt, *J* = 8.7, 8.7, 4.6 Hz, 1H), 4.53 (dt, *J* = 8.9, 8.9, 5.1 Hz, 1H), 4.00 (dd, *J* = 16.5, 5.7 Hz, 1H), 3.91 (dd, *J* = 16.5, 5.6 Hz, 1H), 3.83 (s, 3H), 3.34 (dd, *J* = 13.8, 4.5 Hz, 1H), 3.11-3.07 (m, 1H), 3.01 (t, *J* =

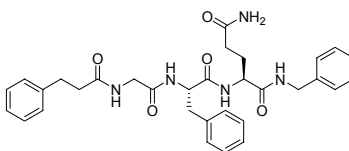
8.1, 8.1 Hz, 2H), 2.69 (t, $J = 8.3$, 8.3 Hz, 2H), 2.45 (t, $J = 7.2$, 7.2 Hz, 2H), 2.26 (dt, $J = 13.1$, 12.8, 7.7 Hz, 1H), 2.08 (dt, $J = 14.2$, 7.7, 7.7 Hz, 1H) ppm; ^{13}C NMR (100 MHz, DMF- D_7): $\delta = 174.2$, 172.7, 171.8, 169.6, 142.1, 138.4, 129.8, 128.7, 128.7, 128.5, 126.7, 126.3, 54.6, 52.6, 51.9, 43.0, 37.9, 37.6, 31.6, 31.6, 27.4 ppm.

Analytical data of compound 251



Peptide **251** was synthesized and released from solid support according to **GP 2** and **GP 3**. **Yield** = 6 %; **Purity** > 95% (LC_MS); **LC-MS** (C18, ESI_MS) 564.2 $[\text{M}+\text{H}]^+$, 586.4 $[\text{M}+\text{Na}]^+$; $R_t = 7.57$ min; ^1H NMR (400 MHz, DMF- D_7): $\delta = 8.36$ (d, $J = 5.4$ Hz, 1H), 8.32 (d, $J = 7.4$ Hz, 1H), 8.22 (d, $J = 8.0$ Hz, 1H), 7.64 (d, $J = 7.9$ Hz, 1H), 7.58 (s, 1H), 7.51-7.32 (m, 10H), 6.95 (s, 1H), 4.75 (ddd, $J = 9.1$, 7.8, 4.5 Hz, 1H), 4.47 (dt, $J = 8.3$, 8.3, 4.9 Hz, 1H), 4.06 (dd, $J = 16.4$, 5.7 Hz, 1H), 3.93 (dd, $J = 16.2$, 5.6 Hz, 1H), 3.85-3.71 (m, 1H), 3.36 (dd, $J = 13.9$, 4.4 Hz, 1H), 3.12 (dd, $J = 13.9$, 7.8 Hz, 1H), 3.04 (t, $J = 8.3$, 8.3 Hz, 2H), 2.71 (t, $J = 8.3$, 8.3 Hz, 2H), 2.41 (t, $J = 7.6$, 7.6 Hz, 2H), 2.29-2.18 (m, 1H), 2.16-2.02 (m, 1H), 2.01-1.90 (m, 2H), 1.90-1.81 (m, 2H), 1.77-1.66 (m, 1H), 1.58-1.22 (m, 5H) ppm; ^{13}C NMR (100 MHz, DMF- D_7): $\delta = 174.7$, 173.0, 171.3, 170.6, 170.4, 142.0, 138.5, 129.7, 128.7, 128.7, 128.6, 126.7, 126.3, 55.4, 53.5, 48.4, 43.2, 37.6, 37.4, 32.9, 32.9, 32.1, 31.6, 28.6, 25.9, 25.2, 25.2 ppm.

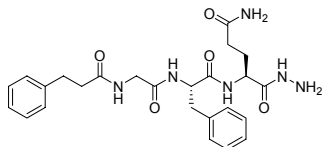
Analytical data of compound 252



Peptide **252** was synthesized and released from solid support according to **GP 2** and **GP 3**. **Yield** = 7 %; **Purity** > 95% (LC_MS); **LC-MS** (C18, ESI_MS) 572.2 $[\text{M}+\text{H}]^+$, 594.4 $[\text{M}+\text{Na}]^+$; $R_t = 7.46$ min; ^1H NMR (400 MHz, DMF- D_7): $\delta = 8.37$ -8.30 (m, 3H), 8.27 (t, $J = 6.0$, 6.0 Hz, 1H), 7.55 (br s, 1H), 7.51-7.32 (m, 15H), 6.95 (br s, 1H), 4.79 (ddd, $J = 9.0$, 7.6, 4.7 Hz, 1H), 4.58 (dd, $J = 8.6$, 4.3 Hz, 1H), 4.55 (d, $J = 5.9$ Hz, 2H), 4.03 (dd, $J = 16.4$, 5.6 Hz, 1H), 3.93 (dd, $J = 16.4$, 5.7 Hz, 1H), 3.36 (dd, $J = 13.9$, 4.7 Hz, 1H), 3.13 (dd, $J = 14.0$, 9.0 Hz, 1H), 3.05 (t, $J = 7.5$, 7.5 Hz, 2H), 2.71-2.65 (m, 2H), 2.43 (t, $J = 8.9$, 8.9 Hz, 2H), 2.32 (ddt, $J = 8.6$, 8.6, 5.1, 3.5 Hz, 1H),

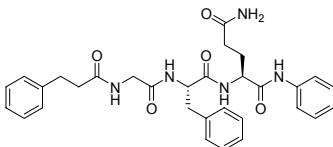
2.21-2.03 (m, 1H) ppm; ^{13}C NMR (100 MHz, DMF- D_7): δ = 174.6, 173.0, 171.8, 171.6, 170.3, 142.0, 140.1, 138.5, 129.7, 128.7, 128.7, 128.7, 128.6, 127.6, 127.1, 126.7, 126.3, 55.3, 53.7, 43.1, 42.8, 37.5, 37.5, 32.1, 31.6, 28.4 ppm.

Analytical data of compound 253



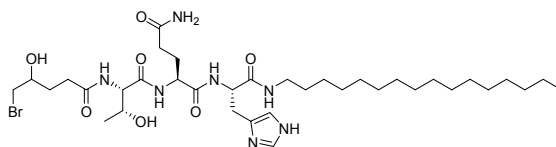
Peptide **253** was synthesized and released from solid support according to **GP 2** and **GP 3**. **Yield** = 6 %; **Purity** > 85% (LC_MS); **LC-MS** (C18, ESI_MS) 497.0 $[\text{M}+\text{H}]^+$, 519.1 $[\text{M}+\text{Na}]^+$; R_t = 6.24 min.

Analytical data of compound 254



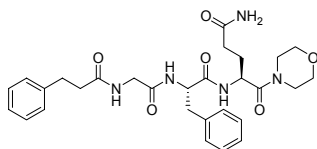
Peptide **254** was synthesized and released from solid support according to **GP 2** and **GP 3**. **Yield** = 8 %; **Purity** > 95% (LC_MS); **LC-MS** (C18, ESI_MS) 558.2 $[\text{M}+\text{H}]^+$, 580.4 $[\text{M}+\text{Na}]^+$; R_t = 7.57 min; ^1H NMR (400 MHz, DMF- D_7): δ = 9.80 (s, 1H), 8.54-8.36 (m, 3H), 7.97 (d, J = 1.2 Hz, 1H), 7.95 (d, J = 1.1 Hz, 1H), 7.61 (br s, 1H), 7.54-7.20 (m, 15H), 7.00 (br s, 1H), 4.78 (ddd, J = 9.2, 7.3, 4.4 Hz, 1H), 4.65 (ddd, J = 8.9, 7.9, 4.8 Hz, 1H), 4.09 (dd, J = 16.2, 5.4 Hz, 1H), 3.95 (dd, J = 16.2, 5.7 Hz, 1H), 3.40 (dd, J = 14.0, 4.3 Hz, 1H), 3.16 (dd, J = 14.0, 9.3 Hz, 1H), 3.03-2.96 (m, 2H), 2.76-2.57 (m, 2H), 2.50 (t, J = 7.3, 7.3 Hz, 1H), 2.39 (ddt, J = 13.6, 13.6, 7.5, 5.9 Hz, 1H), 2.31-2.12 (m, 1H) ppm; ^{13}C NMR (100 MHz, DMF- D_7): δ = 174.5, 173.2, 171.6, 170.9, 170.7, 142.0, 139.7, 138.4, 129.7, 129.0, 128.7, 128.6, 128.6, 126.8, 126.3, 123.8, 119.8, 55.7, 54.4, 43.3, 37.5, 37.4, 32.1, 31.5, 28.1 ppm.

Analytical data of compound 255



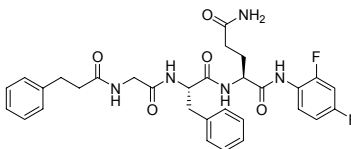
Peptide **255** was synthesized and released from solid support according to **GP 2** and **GP 3**. **Yield** = 1 %; **Purity** > 95% (LC_MS); **LC-MS** (C18, ESI_MS) 788.3 [M+H]⁺, 810.4 [M+Na]⁺; R_t = 8.19 min.

Analytical data of compound 256



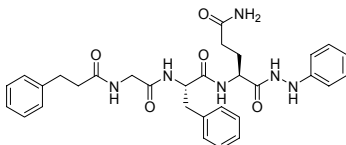
Peptide **256** was synthesized and released from solid support according to **GP 2** and **GP 3**. **Yield** = 2 %; **Purity** > 95% (LC_MS); **LC-MS** (C18, ESI_MS) 552.1 [M+H]⁺, 574.3 [M+Na]⁺; R_t = 6.83 min.

Analytical data of compound 257



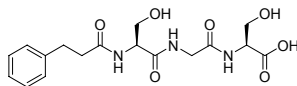
Peptide **257** was synthesized and released from solid support according to **GP 2** and **GP 3**. **Yield** = 11 %; **Purity** > 95% (LC_MS); **LC-MS** (C18, ESI_MS) 594.0 [M+H]⁺, 616.3 [M+Na]⁺; R_t = 7.65 min; ¹H NMR (400 MHz, DMSO-D₆): δ = 9.69 (s, 1H), 8.35 (d, *J* = 7.6 Hz, 1H), 8.10-8.04 (m, 2H), 7.79 (dt, *J* = 9.0, 6.2 Hz, 1H), 7.36-7.12 (m, 15H), 4.57 (dt, *J* = 8.7, 4.2 Hz, 1H), 4.47 (td, *J* = 8.1, 5.4 Hz, 1H), 3.73 (dd, *J* = 16.4, 5.8 Hz, 1H), 3.57 (dd, *J* = 16.5, 5.6 Hz, 1H), 3.05 (dd, *J* = 13.6, 4.4 Hz, 1H), 2.84-2.73 (m, 3H), 2.44-2.34 (m, 2H), 2.18 (td, *J* = 8.6 5.9 Hz, 2H), 2.07-1.94 (m, 1H), 1.93-1.83 (m, 1H) ppm; [α]_D²⁰ = + 6.0° (C = 0.4, DMSO).

Analytical data of compound 258



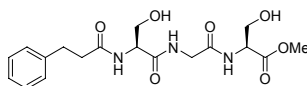
Peptide **258** was synthesized and released from solid support according to **GP 2** and **GP 3**. **Yield** = 1 %; **Purity** > 95% (LC_MS); **LC-MS** (C18, ESI_MS) 573.1 [M+H]⁺, 595.3 [M+Na]⁺; R_t = 7.50 min.

Analytical data of compound 259



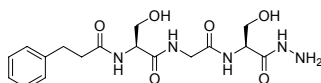
Peptide **259** was synthesized and released from solid support according to **GP 2** and **GP 3**. **Yield** = 4 %; **Purity** > 95% (LC_MS); **LC-MS** (C18, ESI_MS) 382.0 [M+H]⁺, 404.2 [M+Na]⁺; R_t = 5.56 min.

Analytical data of compound 260



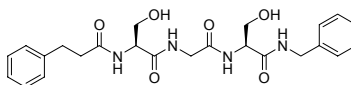
Peptide **260** was synthesized and released from solid support according to **GP 2** and **GP 3**. **Yield** = 2 %; **Purity** > 95% (LC_MS); **LC-MS** (C18, ESI_MS) 396.0 [M+H]⁺; R_t = 5.79 min.

Analytical data of compound 261



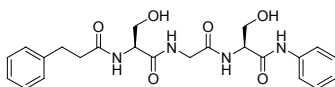
Peptide **261** was synthesized and released from solid support according to **GP 2** and **GP 3**. **Yield** = 6 %; **Purity** > 80% (LC_MS); **LC-MS** (C18, ESI_MS) 396.0 [M+H]⁺, 418.2 [M+Na]⁺; R_t = 4.90 min.

Analytical data of compound 262



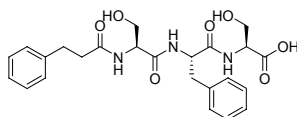
Peptide **262** was synthesized and released from solid support according to **GP 2** and **GP 3**. **Yield** = 7 %; **Purity** > 95% (LC_MS); **LC-MS** (C18, ESI_MS) 471.1 [M+H]⁺, 493.2 [M+Na]⁺; R_t = 6.57 min.

Analytical data of compound 263



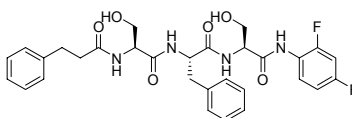
Peptide **263** was synthesized and released from solid support according to **GP 2** and **GP 3**. **Yield** = 6 %; **Purity** > 95% (LC_MS); **LC-MS** (C18, ESI_MS) 457.0 [M+H]⁺; R_t = 6.63 min.

Analytical data of compound 264



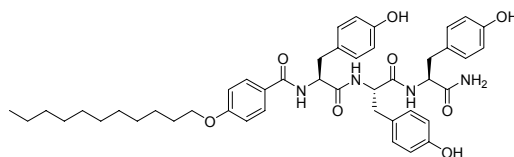
Peptide **264** was synthesized and released from solid support according to **GP 2** and **GP 3**. **Yield** = 3 %; **Purity** > 95% (LC_MS); **LC-MS** (C18, ESI_MS) 472.0 [M+H]⁺, 494.2 [M+Na]⁺; R_t = 6.63 min.

Analytical data of compound 265



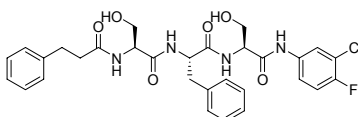
Peptide **265** was synthesized and released from solid support according to **GP 2** and **GP 3**. **Yield** = 17 %; **Purity** > 95% (LC_MS); **LC-MS** (C18, ESI_MS) 583.0 [M+H]⁺, 605.3 [M+Na]⁺; R_t = 7.81 min; **¹H NMR** (400 MHz, DMSO-D₆): δ = 9.65 (s, 1H), 8.19 (d, *J* = 7.6 Hz, 1H), 7.99 (d, *J* = 8.0 Hz, 1H), 7.92 (d, *J* = 7.6 Hz, 1H), 7.82 (dt, *J* = 9.0 6.2 Hz, 1H), 7.35-7.12 (m, 14H), 7.11-7.04 (m, 1H), 5.07 (t, *J* = 5.5 Hz, 1H), 4.91 (t, *J* = 5.5 Hz, 1H), 4.60 (dd, *J* = 8.5, 4.1 Hz, 1H), 4.55 (dd, *J* = 13.5, 5.8 Hz, 1H), 4.28 (q, *J* = 6.0 Hz, 1H), 3.68 (dt, *J* = 5.6 1.9 Hz, 2H), 3.47 (t, *J* = 5.8 Hz, 2H), 3.10 (dd, *J* = 13.9, 4.2 Hz, 1H), 2.84 (dd, *J* = 13.8, 9.1 Hz, 1H), 2.78 (t, *J* = 7.9 Hz, 2H), 2.43 (dt, *J* = 7.6 2.1 Hz, 2H) ppm; [α]_D²⁰ = -9.7° (C = 0.7, DMSO).

Analytical data of compound 266



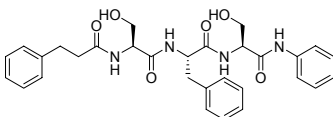
Peptide **266** was synthesized and released from solid support according to **GP 2** and **GP 3**. **Yield** = 9 %; **Purity** > 95% (LC_MS); **LC-MS** (C4, ESI_MS) 781.1 [M+H]⁺, 803.5 [M+Na]⁺; R_t = 9.77 min; **¹H NMR** (400 MHz, DMSO-D₆): δ = 9.11 (s, 1H), 9.07 (s, 1H), 9.07 (s, 1H), 8.28 (d, *J* = 8.2 Hz, 1H), 7.95 (d, *J* = 7.7 Hz, 1H), 7.87 (d, *J* = 8.3 Hz, 1H), 7.71 (d, *J* = 8.8 Hz, 2H), 7.03 (d, *J* = 8.5 Hz, 2H), 6.99-6.91 (m, 6H), 6.61 (d, *J* = 8.5 Hz, 2H), 6.57 (d, *J* = 8.4 Hz, 2H), 6.52 (d, *J* = 8.4 Hz, 2H), 4.54-4.47 (m, 1H), 4.40-4.29 (m, 2H), 3.98 (t, *J* = 6.5 Hz, 2H), 2.92-2.77 (m, 4H), 2.76-2.61 (m, 2H), 1.73-1.65 (m, 2H), 1.44-1.34 (m, 2H), 1.35-1.18 (m, 16H), 0.83 (t, *J* = 6.8 Hz, 3H) ppm; [α]_D²⁰ = -42.9° (C = 0.4, DMSO).

Analytical data of compound **267**



Peptide **267** was synthesized and released from solid support according to **GP 2** and **GP 3**. **Yield** = 11 %; **Purity** > 95% (LC_MS); **LC-MS** (C18, ESI_MS) 599.0 [M+H]⁺, 621.2 [M+Na]⁺; R_t = 8.31 min; **¹H NMR** (400 MHz, DMSO-D₆): δ = 10.09 (s, 1H), 8.15 (d, *J* = 7.5 Hz, 1H), 8.02 (d, *J* = 7.8 Hz, 1H), 7.98-7.94 (m, 2H), 7.53 (ddd, *J* = 9.0, 4.3, 2.6 Hz, 1H), 7.37 (t, *J* = 9.0 Hz, 1H), 7.28-7.12 (m, 12H), 5.07 (t, *J* = 5.5 Hz, 1H), 4.94 (t, *J* = 5.5 Hz, 1H), 4.56 (dt, *J* = 8.9, 4.4 Hz, 1H), 4.40 (q, *J* = 6.0 Hz, 1H), 4.28 (q, *J* = 6.2 Hz, 1H), 3.66 (t, *J* = 6.2 Hz, 2H), 3.48 (t, *J* = 5.9 Hz, 2H), 3.09 (dd, *J* = 14.0, 4.3 Hz, 1H), 2.85 (dd, *J* = 14.0, 9.0 Hz, 1H), 2.78 (t, *J* = 7.9 Hz, 2H), 2.43 (dt, *J* = 7.5, 1.4 Hz, 2H) ppm; [α]_D²⁰ = -12.1° (C = 0.6, DMSO).

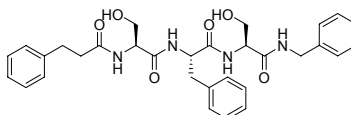
Analytical data of compound **268**



Peptide **268** was synthesized and released from solid support according to **GP 2** and **GP 3**. **Yield** = 8 %; **Purity** > 95% (LC_MS); **LC-MS** (C18, ESI_MS) 547.0 [M+H]⁺, 569.3 [M+Na]⁺; R_t = 7.73 min; **¹H NMR** (400 MHz, DMSO-D₆): δ = 9.81 (s, 1H), 8.10 (d, *J* = 7.7 Hz, 1H), 8.01 (d, *J* = 7.8 Hz, 1H), 7.94 (d, *J* = 7.5 Hz, 1H), 7.63 (d, *J* = 1.1 Hz, 1H), 7.61 (d, *J* = 1.0 Hz, 1H), 7.32-7.11 (m, 14H), 7.06-7.01 (m, 1H), 5.01 (t, *J* = 5.5 Hz, 1H), 4.94 (t, *J* = 5.5 Hz, 1H), 4.55 (dt, *J* =

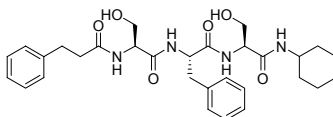
9.1 4.4 Hz, 1H), 4.43 (q, $J = 5.9$ Hz, 1H), 4.27 (q, $J = 6.2$ Hz, 1H), 3.65 (t, $J = 5.7$ Hz, 2H), 3.47 (t, $J = 6.0$ Hz, 2H), 3.08 (dd, $J = 13.9, 4.2$ Hz, 1H), 2.84 (dd, $J = 13.8, 9.0$ Hz, 1H), 2.78 (t, $J = 7.9$ Hz, 2H), 2.41 (dt, $J = 7.6, 1.5$ Hz, 2H) ppm; $[\alpha]_D^{20} = -15.0^\circ$ (C = 0.4, DMSO).

Analytical data of compound 269



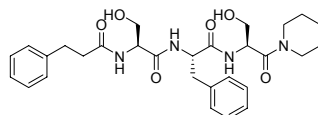
Peptide **269** was synthesized and released from solid support according to **GP 2** and **GP 3**. **Yield** = 15 %; **Purity** > 95% (LC_MS); **LC-MS** (C18, ESI_MS) 561.1 [M+H]⁺, 583.3 [M+Na]⁺; $R_t = 7.62$ min; **¹H NMR** (400 MHz, DMSO- D_6): $\delta = 8.22$ (t, $J = 5.9, 5.9$ Hz, 1H), 8.04 (s, 1H), 8.02 (s, 1H), 7.92 (d, $J = 7.6$ Hz, 1H), 7.39-7.10 (m, 15H), 4.94 (br s, 1H), 4.56 (dt, $J = 8.6, 8.4, 4.6$ Hz, 1H), 4.39-4.22 (m, 4H), 3.61 (d, $J = 5.6$ Hz, 2H), 3.46 (d, $J = 5.5$ Hz, 2H), 3.32 (d, $J = 1.3$ Hz, 2H), 3.08 (dd, $J = 14.0, 4.7$ Hz, 1H), 2.84 (dd, $J = 14.0, 9.1$ Hz, 1H), 2.77 (t, $J = 7.9, 7.9$ Hz, 1H), 2.42 (dt, $J = 7.7, 7.7, 2.3$ Hz, 1H) ppm; **¹³C NMR** (100 MHz, DMSO- D_6): $\delta = 171.5, 170.6, 170.1, 169.6, 141.1, 139.0, 137.5, 129.1, 128.1, 128.0, 128.0, 127.8, 126.8, 126.5, 126.0, 125.7, 61.5, 61.5, 55.2, 54.9, 53.8, 41.9, 36.9, 36.6, 30.8$ ppm; **HRMS** (FAB, *m*-NBA) m/z calc. for $C_{31}H_{36}N_4O_6$ 560.2635, found 561.2694 [M+H]⁺; $[\alpha]_D^{20} = +1.6^\circ$ (C = 0.8, DMSO).

Analytical data of compound 270



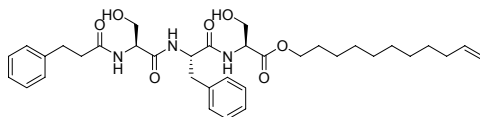
Peptide **270** was synthesized and released from solid support according to **GP 2** and **GP 3**. **Yield** = 3 %; **Purity** > 95% (LC_MS); **LC-MS** (C18, ESI_MS) 553.2 [M+H]⁺, 575.3 [M+Na]⁺; $R_t = 7.67$ min.

Analytical data of compound 271



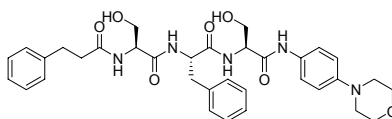
Peptide **271** was synthesized and released from solid support according to **GP 2** and **GP 3**. **Yield** = 1 %; **Purity** > 95% (LC_MS); **LC-MS** (C18, ESI_MS) 539.2 [M+H]⁺, 561.4 [M+Na]⁺; R_t = 7.22 min.

Analytical data of compound 272



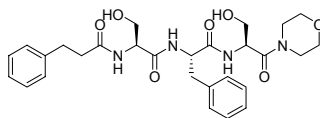
Peptide **272** was synthesized and released from solid support according to **GP 2** and **GP 3**. **Yield** = 1 %; **Purity** > 95% (LC_MS); **LC-MS** (C18, ESI_MS) 624.1 [M+H]⁺, 646.4 [M+Na]⁺; R_t = 10.54 min.

Analytical data of compound 273



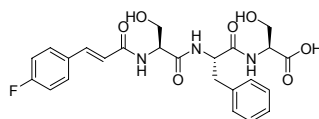
Peptide **273** was synthesized and released from solid support according to **GP 2** and **GP 3**. **Yield** = 6 %; **Purity** > 95% (LC_MS); **LC-MS** (C18, ESI_MS) 632.1 [M+H]⁺, 654.3 [M+Na]⁺; R_t = 7.13 min.

Analytical data of compound 274



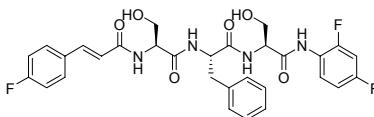
Peptide **274** was synthesized and released from solid support according to **GP 2** and **GP 3**. **Yield** = 4 %; **Purity** > 95% (LC_MS); **LC-MS** (C18, ESI_MS) 541.1 [M+H]⁺, 563.3 [M+Na]⁺; R_t = 6.80 min.

Analytical data of compound 275



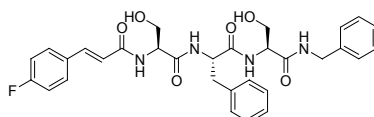
Peptide **275** was synthesized and released from solid support according to **GP 2** and **GP 3**. **Yield** = 2 %; **Purity** > 95% (LC_MS); **LC-MS** (C18, ESI_MS) 488.0 [M+H]⁺, 510.2 [M+Na]⁺; R_t = 6.95 min.

Analytical data of compound 276



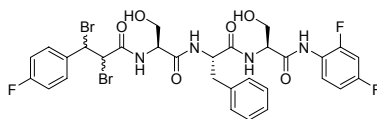
Peptide **276** was synthesized and released from solid support according to **GP 2** and **GP 3**. **Yield** = 10 %; **Purity** > 95% (LC_MS); **LC-MS** (C18, ESI_MS) 599.0 [M+H]⁺, 621.2 [M+Na]⁺; R_t = 7.99 min; ¹H NMR (400 MHz, DMSO-D₆): δ = 9.64 (s, 1H), 8.19 (d, *J* = 7.8 Hz, 1H), 8.11 (d, *J* = 7.7 Hz, 1H), 8.07 (d, *J* = 8.2 Hz, 1H), 7.81 (dt, *J* = 9.1, 6.3 Hz, 1H), 7.62 (d, *J* = 5.5 Hz, 1H), 7.59 (d, *J* = 5.4 Hz, 1H), 7.40 (d, *J* = 15.7 Hz, 1H), 7.33-7.02 (m, 11H), 6.75 (d, *J* = 15.8 Hz, 1H), 5.05 (t, *J* = 5.5 Hz, 1H), 4.97 (t, *J* = 5.5 Hz, 1H), 4.60 (dt, *J* = 8.7, 4.2 Hz, 1H), 4.53 (dd, *J* = 13.3, 5.9 Hz, 1H), 4.40 (q, *J* = 6.0, 5.9 Hz, 1H), 3.66 (t, *J* = 6.3 Hz, 2H), 3.54 (t, *J* = 5.8 Hz, 2H), 3.09 (dd, *J* = 13.9, 4.5 Hz, 1H), 2.83 (dd, *J* = 14.1, 9.1 Hz, 1H) ppm; [α]_D²⁰ = + 1.4° (C = 0.5, DMSO).

Analytical data of compound 277



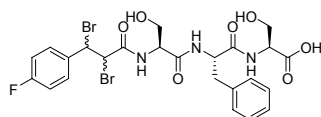
Peptide **277** was synthesized and released from solid support according to **GP 2** and **GP 3**. **Yield** = 13 %; **Purity** > 95% (LC_MS); **LC-MS** (C18, ESI_MS) 577.1 [M+H]⁺, 599.3 [M+Na]⁺; R_t = 7.81 min; ¹H NMR (400 MHz, DMSO-D₆): δ = 8.21 (t, *J* = 6.1 Hz, 1H), 8.13 (d, *J* = 4.2 Hz, 1H), 8.11 (d, *J* = 4.6 Hz, 1H), 8.05 (d, *J* = 8.0 Hz, 1H), 7.61 (d, *J* = 5.5 Hz, 1H), 7.59 (d, *J* = 5.5 Hz, 1H), 7.39 (d, *J* = 15.8 Hz, 1H), 7.32-7.09 (m, 14H), 6.74 (d, *J* = 15.8 Hz, 1H), 4.56 (dt, *J* = 8.5 4.3 Hz, 1H), 4.39 (q, *J* = 6.0 Hz, 1H), 4.31-4.27 (m, 4H), 3.60 (d, *J* = 5.6 Hz, 2H), 3.54 (d, *J* = 7.0 Hz, 2H), 3.07 (dd, *J* = 13.9, 4.4 Hz, 1H), 2.82 (dd, *J* = 14.1, 9.3 Hz, 1H) ppm; [α]_D²⁰ = + 7.4° (C = 0.7, DMSO).

Analytical data of compound 278



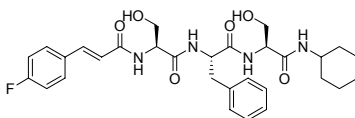
Peptide **278** was synthesized and released from solid support according to **GP 2** and **GP 3**. **Yield** = 5 %; **Purity** > 95% (LC_MS); **LC-MS** (C18, ESI_MS) 758.7 [M+H]⁺, 780.9 [M+Na]⁺; R_t = 8.63 min.

Analytical data of compound 279



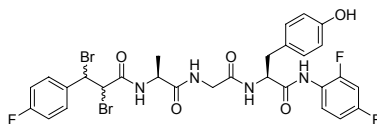
Peptide **279** was synthesized and released from solid support according to **GP 2** and **GP 3**. **Yield** = 1 %; **Purity** > 95% (LC_MS); **LC-MS** (C18, ESI_MS) 647.8 [M+H]⁺, 669.8 [M+Na]⁺; R_t = 7.68 min.

Analytical data of compound 280



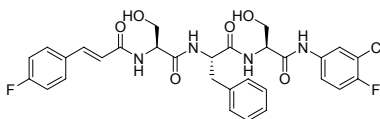
Peptide **280** was synthesized and released from solid support according to **GP 2** and **GP 3**. **Yield** = 2 %; **Purity** > 95% (LC_MS); **LC-MS** (C18, ESI_MS) 569.1 [M+H]⁺, 591.3 [M+Na]⁺; R_t = 7.89 min.

Analytical data of compound 281



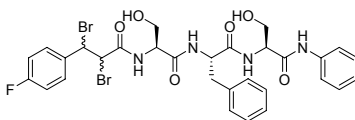
Peptide **281** was synthesized and released from solid support according to **GP 2** and **GP 3**. **Yield** = 3 %; **Purity** > 95% (LC_MS); **LC-MS** (C18, ESI_MS) 728.8 [M+H]⁺, 750.9 [M+Na]⁺; R_t = 8.35 min.

Analytical data of compound 282



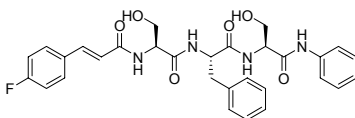
Peptide **282** was synthesized and released from solid support according to **GP 2** and **GP 3**. **Yield** = 8 %; **Purity** > 95% (LC_MS); **LC-MS** (C18, ESI_MS) 615.0 [M+H]⁺, 637.2 [M+Na]⁺; R_t = 8.41 min.

Analytical data of compound 283



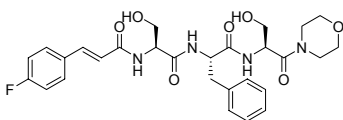
Peptide **283** was synthesized and released from solid support according to **GP 2** and **GP 3**. **Yield** = 3 %; **Purity** > 80% (LC_MS); **LC-MS** (C18, ESI_MS) 722.8 [M+H]⁺, 744.9 [M+Na]⁺; R_t = 8.55 min.

Analytical data of compound 284



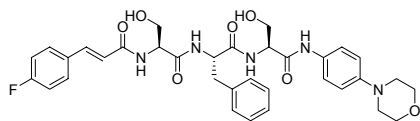
Peptide **284** was synthesized and released from solid support according to **GP 2** and **GP 3**. **Yield** = 4 %; **Purity** > 95% (LC_MS); **LC-MS** (C18, ESI_MS) 563.0 [M+H]⁺, 585.1 [M+Na]⁺; R_t = 7.91 min.

Analytical data of compound 285



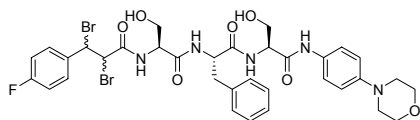
Peptide **285** was synthesized and released from solid support according to **GP 2** and **GP 3**. **Yield** = 3 %; **Purity** > 95% (LC_MS); **LC-MS** (C18, ESI_MS) 557.0 [M+H]⁺, 579.2 [M+Na]⁺; R_t = 6.95 min.

Analytical data of compound 286



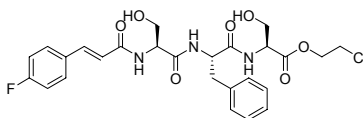
Peptide **286** was synthesized and released from solid support according to **GP 2** and **GP 3**. **Yield** = 5 %; **Purity** > 95% (LC_MS); **LC-MS** (C18, ESI_MS) 648.0 [M+H]⁺, 670.1 [M+Na]⁺; R_t = 7.31 min.

Analytical data of compound 287



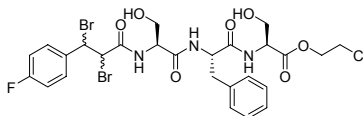
Peptide **287** was synthesized and released from solid support according to **GP 2** and **GP 3**. **Yield** = 3 %; **Purity** > 85% (LC_MS); **LC-MS** (C18, ESI_MS) 808.0 [M+H]⁺, 830.0 [M+Na]⁺; R_t = 8.00 min.

Analytical data of compound 288



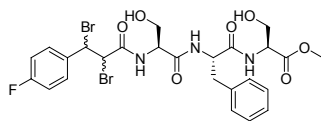
Peptide **288** was synthesized and released from solid support according to **GP 2** and **GP 3**. **Yield** = 4 %; **Purity** > 95% (LC_MS); **LC-MS** (C18, ESI_MS) 550.0 [M+H]⁺; R_t = 7.74 min.

Analytical data of compound 289



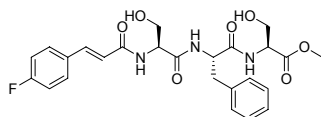
Peptide **289** was synthesized and released from solid support according to **GP 2** and **GP 3**. **Yield** = 2 %; **Purity** > 95% (LC_MS); **LC-MS** (C18, ESI_MS) 709.8 [M+H]⁺, 731.8 [M+Na]⁺; R_t = 8.42 min.

Analytical data of compound 290



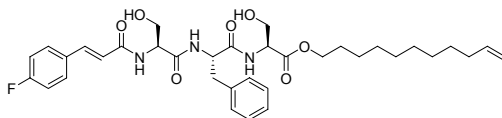
Peptide **290** was synthesized and released from solid support according to **GP 2** and **GP 3**. **Yield** = 2 %; **Purity** > 95% (LC_MS); **LC-MS** (C18, ESI_MS) 661.8 [M+H]⁺, 683.8 [M+Na]⁺; R_t = 7.98 min.

Analytical data of compound 291



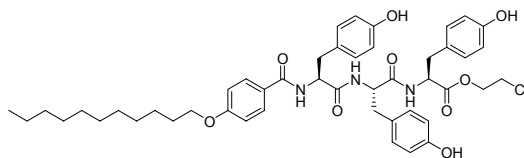
Peptide **291** was synthesized and released from solid support according to **GP 2** and **GP 3**. **Yield** = 5 %; **Purity** > 95% (LC_MS); **LC-MS** (C18, ESI_MS) 502.0 [M+H]⁺, 524.2 [M+Na]⁺; R_t = 7.25 min.

Analytical data of compound 292



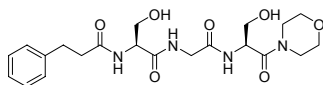
Peptide **292** was synthesized and released from solid support according to **GP 2** and **GP 3**. **Yield** = 1 %; **Purity** > 95% (LC_MS); **LC-MS** (C18, ESI_MS) 640.1 [M+H]⁺, 662.3 [M+Na]⁺; R_t = 10.56 min.

Analytical data of compound 293



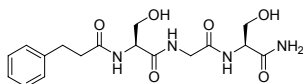
Peptide **293** was synthesized and released from solid support according to **GP 2** and **GP 3**. **Yield** = 4 %; **Purity** > 95% (LC_MS); **LC-MS** (C4, ESI_MS) 844.3 [M+H]⁺, 866.4 [M+Na]⁺; R_t = 10.31 min.

Analytical data of compound 294



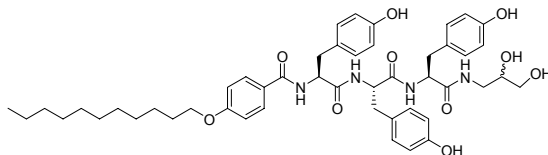
Peptide **294** was synthesized and released from solid support according to **GP 2** and **GP 3**. **Yield** = 2 %; **Purity** > 95% (LC_MS); **LC-MS** (C18, ESI_MS) 451.1 [M+H]⁺, 473.2 [M+Na]⁺; R_t = 5.55 min.

Analytical data of compound 295



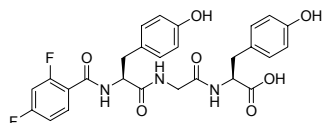
Peptide **295** was synthesized and released from solid support according to **GP 2** and **GP 3**. **Yield** = 2 %; **Purity** > 95% (LC_MS); **LC-MS** (C18, ESI_MS) 381.0 [M+H]⁺; R_t = 5.52 min.

Analytical data of compound 296



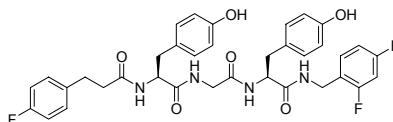
Peptide **296** was synthesized and released from solid support according to **GP 2** and **GP 3**. **Yield** = 12 %; **Purity** > 95% (LC_MS); **LC-MS** (C4, ESI_MS) 855.3 [M+H]⁺, 877.5 [M+Na]⁺; R_t = 9.52 min; ¹H NMR (400 MHz, DMSO-D₆): δ = 9.13 (s, 1H), 9.08 (s, 1H), 9.08 (s, 1H), 8.28 (d, *J* = 8.3 Hz, 1H), 8.01 (d, *J* = 7.5 Hz, 1H), 7.91 (d, *J* = 8.3 Hz, 1H), 7.78 (t, *J* = 5.7 Hz, 1H), 7.73 (d, *J* = 8.8 Hz, 2H), 7.06 (d, *J* = 8.5 Hz, 2H), 7.02-6.94 (m, 6H), 6.63 (d, *J* = 8.3 Hz, 2H), 6.59 (d, *J* = 8.5 Hz, 2H), 6.53 (d, *J* = 8.4 Hz, 2H), 4.67 (d, *J* = 4.8 Hz, 1H), 4.57-4.50 (m, 1H), 4.46 (dd, *J* = 12.0, 5.9 Hz, 1H), 4.43-4.37 (m, 2H), 4.00 (t, *J* = 6.5 Hz, 2H), 3.44 (qd, *J* = 9.8, 4.9 Hz, 1H), 3.25 (td, *J* = 11.3, 5.6 Hz, 2H), 3.21-3.13 (m, 1H), 3.01-2.94 (m, 1H), 2.92-2.78 (m, 4H), 2.75-2.63 (m, 2H), 1.71 (p, *J* = 6.8 Hz, 2H), 1.47-1.36 (m, 2H), 1.35-1.23 (m, 16H), 0.83 (t, *J* = 6.8 Hz, 3H) ppm; [α]_D²⁰ = -38.8° (C = 0.7, DMSO).

Analytical data of compound 297



Peptide **297** was synthesized and released from solid support according to **GP 2** and **GP 3**. **Yield** = 15 %; **Purity** > 95% (LC_MS); **LC-MS** (C18, ESI_MS) 541.9 [M+H]⁺, 564.1 [M+Na]⁺; R_t = 7.28 min; **¹H NMR** (400 MHz, DMSO-D₆): δ = 9.18 (s, 1H), 9.15 (s, 1H), 8.33 (d, *J* = 5.5 Hz, 1H), 8.31-8.28 (m, 1H), 8.27 (d, *J* = 3.2 Hz, 1H), 8.05 (d, *J* = 8.0 Hz, 1H), 7.61 (dt, *J* = 8.5, 6.7 Hz, 1H), 7.35-7.28 (m, 1H), 7.15 (dt, *J* = 8.6 2.5 Hz, 1H), 7.07 (d, *J* = 8.4 Hz, 2H), 7.00 (d, *J* = 8.4 Hz, 2H), 6.64 (d, *J* = 8.5 Hz, 2H), 6.64 (d, *J* = 8.5 Hz, 2H), 4.61 (dt, *J* = 9.5 4.4 Hz, 1H), 4.36 (dt, *J* = 8.5 5.4 Hz, 1H), 3.79 (dd, *J* = 16.7, 5.7 Hz, 1H), 3.68 (dd, *J* = 16.6, 5.6 Hz, 1H), 2.99 (dd, *J* = 13.9, 4.1 Hz, 1H), 2.93 (dd, *J* = 14.0, 5.3 Hz, 1H), 2.84-2.73 (m, 2H) ppm; **HRMS** (ESI) *m/z* calc. for C₂₇H₂₅F₂N₃O₇ 541.5001, found 542.1733 [M+H]⁺; [α]_D²⁰ = + 8.5° (C = 0.9, DMSO).

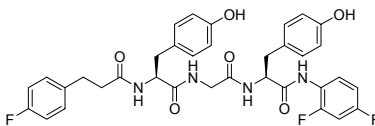
Analytical data of compound **298**



Peptide **298** was synthesized and released from solid support according to **GP 2** and **GP 3**. **Yield** = 20 %; **Purity** > 95% (LC_MS); **LC-MS** (C18, ESI_MS) 677.1 [M+H]⁺, 699.3 [M+Na]⁺; R_t = 8.45 min; **¹H NMR** (400 MHz, DMSO-D₆): δ = 9.16 (br d, *J* = 14.8 Hz, 1H), 8.43 (t, *J* = 5.9, 5.9 Hz, 1H), 8.17 (t, *J* = 5.7, 5.7 Hz, 1H), 8.07 (d, *J* = 8.1 Hz, 1H), 8.04 (d, *J* = 8.1 Hz, 1H), 7.33-6.84 (m, 9H), 6.64 (d, *J* = 0.9 Hz, 2H), 6.62 (d, *J* = 0.9 Hz, 2H), 4.53-4.34 (m, 2H), 4.28 (dd, *J* = 15.3, 5.9 Hz, 1H), 4.19 (dd, *J* = 15.1, 5.2 Hz, 1H), 3.78 (dd, *J* = 16.6, 6.0 Hz, 1H), 3.59 (dd, *J* = 16.5, 5.4 Hz, 1H), 2.89 (s, 3H), 2.90-2.84 (m, 2H), 2.73 (d, *J* = 0.6 Hz, 3H), 2.72-2.60 (m, 4H), 2.33 (dt, *J* = 7.6, 7.4, 2.2 Hz, 2H) ppm; **¹³C NMR** (100 MHz, DMSO-D₆): δ = 171.7, 171.2, 170.9, 168.3, 162.4, 162.2, 162.1, 161.6, 160.9, 160.8, 159.9, 159.8, 159.2, 158.4, 158.3, 155.7, 155.6, 137.2, 137.2, 130.2, 130.2, 130.1, 130.1, 129.9, 129.9, 129.7, 129.6, 127.9, 127.5, 122.0, 122.0, 121.9, 121.8, 114.8, 114.8, 114.7, 114.6, 111.0, 111.0, 110.8, 110.8, 103.6, 103.3, 103.0, 54.4, 54.3, 41.8, 36.8, 36.6, 36.5, 35.6, 35.3, 35.2, 30.6, 29.8 ppm; **¹⁹F NMR** (188 MHz, DMSO-D₆): δ = -112.745, -112.783, -112.825, -112.867, -112.910, -115.048, -115.089, -115.139, -115.183, -117.862, -117.893, -117.909, -117.939, -117.969, -117.985, -118.016; **HRMS** (FAB,

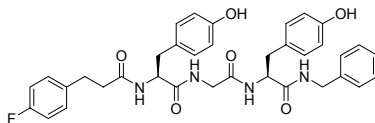
m-NBA) *m/z* calc. for C₃₆H₃₅F₃N₄O₆ 676.2509, found 677.2606 [M+H]⁺; [α]_D²⁰ = + 2.6° (C = 1.6, DMSO).

Analytical data of compound 299



Peptide **299** was synthesized and released from solid support according to **GP 2** and **GP 3**. **Yield** = 22 %; **Purity** > 95% (LC_MS); **LC-MS** (C18, ESI_MS) 663.0 [M+H]⁺, 685.2 [M+Na]⁺; R_t = 8.48 min; **¹H NMR** (400 MHz, DMSO-D₆): δ = 9.80 (s, 1H), 9.15 (s, 1H), 9.12 (s, 1H), 8.15 (t, *J* = 5.7, 5.7 Hz, 1H), 8.10 (d, *J* = 8.0 Hz, 1H), 8.04 (d, *J* = 8.1 Hz, 1H), 7.66 (dt, *J* = 8.9, 8.9, 6.2 Hz, 1H), 7.28 (ddd, *J* = 10.9, 9.0, 2.9 Hz, 1H), 7.16-6.85 (m, 9H), 6.63 (d, *J* = 8.5 Hz, 2H), 6.61 (d, *J* = 8.5 Hz, 2H), 4.67 (dt, *J* = 8.8, 8.7, 5.7 Hz, 1H), 4.39 (ddd, *J* = 10.0, 8.2, 4.5 Hz, 1H), 3.77 (dd, *J* = 16.7, 5.9 Hz, 1H), 3.59 (dd, *J* = 16.7, 5.5 Hz, 1H), 2.94 (dd, *J* = 13.7, 5.1 Hz, 1H), 2.89-2.83 (m, 1H), 2.78 (dd, *J* = 13.7, 9.0 Hz, 1H), 2.66 (t, *J* = 7.7, 7.7 Hz, 2H), 2.60 (dd, *J* = 13.8, 9.9 Hz, 1H), 2.31 (dt, *J* = 7.6, 7.3, 1.44 Hz, 2H) ppm; **¹³C NMR** (100 MHz, DMSO-D₆): δ = 171.6, 171.2, 170.3, 168.5, 161.6, 159.2, 155.7, 155.6, 137.2, 137.2, 130.0, 129.9, 129.7, 129.6, 127.9, 127.2, 126.0, 125.9, 125.9, 114.8, 114.7, 114.6, 54.5, 54.2, 41.7, 36.9, 36.6, 36.5, 35.6 ppm; **¹⁹F NMR** (188 MHz, DMSO-D₆): δ = -114.7, -114.7, -114.7, -114.7, -114.8, -114.8, -117.8, -117.9, -117.9, -117.9, -118.0, -119.0, -119.1, -119.1, -119.1 ppm; **HRMS** (FAB, *m*-NBA) *m/z* calc. for C₃₅H₃₃F₃N₄O₆ 662.2352, found 663.2459 [M+H]⁺; [α]_D²⁰ = + 11.0° (C = 1.4, DMSO).

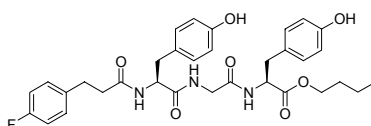
Analytical data of compound 300



Peptide **300** was synthesized and released from solid support according to **GP 2** and **GP 3**. **Yield** = 22 %; **Purity** > 95% (LC_MS); **LC-MS** (C18, ESI_MS) 641.1 [M+H]⁺, 663.3 [M+Na]⁺; R_t = 8.25 min; **¹H NMR** (400 MHz, DMSO-D₆): δ = 9.17 (s, 1H), 9.15 (s, 1H), 8.42 (t, *J* = 6.0, 6.0 Hz, 1H), 8.16 (t, *J* = 5.7, 5.7 Hz, 1H), 8.07 (d, *J* = 8.0 Hz, 1H), 8.02 (d, *J* = 8.2 Hz, 1H), 7.95 (s, 1H), 7.31-6.92 (m, 13H), 6.64 (d, *J* = 3.2 Hz, 2H), 6.62 (d, *J* = 3.2 Hz, 2H), 4.49-4.42 (m, 1H), 4.40 (ddd, *J* = 9.8, 8.0, 4.40 Hz, 1H), 4.29 (dd, *J* = 15.2, 5.9 Hz, 1H), 4.21 (dd, *J* = 15.3, 5.7 Hz,

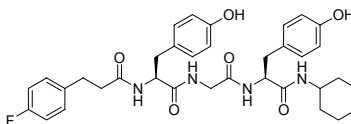
1H), 3.78 (dd, $J = 16.5, 6.0$ Hz, 1H), 3.59 (dd, $J = 16.6, 5.4$ Hz, 1H), 2.94-2.84 (m, 2H), 2.72-2.64 (m, 3H), 2.64-2.58 (m, 1H), 2.33 (dt, $J = 7.6, 7.3, 1.6$ Hz, 2H₂) ppm; ¹³C NMR (100 MHz, DMSO-D₆): $\delta = 171.6, 171.2, 170.7, 168.3, 159.2, 155.7, 155.6, 138.9, 137.2, 137.2, 129.9, 129.9, 129.7, 129.6, 128.0, 126.8, 126.5, 114.8, 114.7, 114.6, 54.4, 54.3, 41.8, 36.9, 36.6, 36.5, 35.6$ ppm; ¹⁹F NMR (188 MHz, DMSO-D₆): $\delta = -117.8, -117.8, -117.8, -117.9, -117.9, -117.9, -118.0$ ppm; HRMS (FAB, *m*-NBA) m/z calc. for C₃₆H₃₇FN₄O₆ 640.2697, found 641.2761 [M+H]⁺; $[\alpha]_D^{20} = +5.8^\circ$ (C = 1.4, DMSO).

Analytical data of compound 301



Peptide **301** was synthesized and released from solid support according to **GP 2** and **GP 3**. **Yield** = 8 %; **Purity** > 95% (LC_MS); **LC-MS** (C18, ESI_MS) 608.1 [M+H]⁺, 630.2 [M+Na]⁺; R_t = 8.78 min; ¹H NMR (400 MHz, DMSO-D₆): $\delta = 9.20$ (s, 1H), 9.14 (s, 1H), 8.19 (d, $J = 5.6$ Hz, 1H), 8.16 (d, $J = 7.4$ Hz, 1H), 8.06 (d, $J = 7.9$ Hz, 1H), 7.12 (d, $J = 5.8$ Hz, 1H), 7.10 (d, $J = 5.6$ Hz, 1H), 7.03 (d, $J = 9.0$ Hz, 2H), 7.01-6.96 (m, 6H), 6.65 (d, $J = 8.5$ Hz, 2H), 6.62 (d, $J = 8.5$ Hz, 2H), 4.43-4.34 (m, 2H), 3.97 (t, $J = 6.4$ Hz, 2H), 3.76 (dd, $J = 16.5, 6.0$ Hz, 1H), 3.63 (dd, $J = 16.7, 5.3$ Hz, 1H), 2.90-2.82 (m, 3H), 2.72-2.64 (m, 3H), 2.37-2.30 (m, 2H), 1.51-1.38 (m, 2H), 1.28-1.18 (m, 2H), 0.84 (t, $J = 7.3$ Hz, 3H) ppm; $[\alpha]_D^{20} = +14.0^\circ$ (C = 0.1, DMSO).

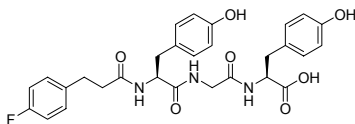
Analytical data of compound 302



Peptide **302** was synthesized and released from solid support according to **GP 2** and **GP 3**. **Yield** = 16 %; **Purity** > 85% (LC_MS); **LC-MS** (C18, ESI_MS) 633.1 [M+H]⁺, 655.3 [M+Na]⁺; R_t = 8.34 min; ¹H NMR (400 MHz, DMSO-D₆): $\delta = 9.14$ (s, 1H), 9.12 (s, 1H), 8.17 (t, $J = 5.7$ Hz, 1H), 8.06 (d, $J = 8.1$ Hz, 1H), 7.89 (d, $J = 8.3$ Hz, 1H), 7.68 (d, $J = 7.8$ Hz, 1H), 7.12 (d, $J = 5.6$ Hz, 1H), 7.10 (d, $J = 5.6$ Hz, 1H), 7.04 (d, $J = 8.9$ Hz, 2H), 7.00 (d, $J = 6.7$ Hz, 2H), 6.97 (d, $J = 6.9$ Hz, 2H), 6.63 (d, $J = 8.5$ Hz, 2H), 6.62 (d, $J = 8.5$ Hz, 2H), 4.44-4.32 (m, 2H), 3.73 (dd, $J = 16.6, 5.9$ Hz, 1H), 3.56 (dd, $J = 16.5, 5.5$ Hz, 1H), 3.52-3.42 (m, 1H), 2.88 (dd, $J = 13.8, 4.2$ Hz,

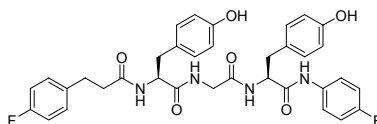
1H), 2.81 (dd, $J = 13.7, 5.7$ Hz, 1H), 2.72-2.66 (m, 3H), 2.63 (dd, $J = 9.9, 3.8$ Hz, 1H), 2.37-2.31 (m, 2H) ppm; $[\alpha]_D^{20} = +7.0^\circ$ (C = 0.9, DMSO)

Analytical data of compound 303



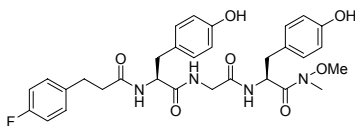
Peptide **303** was synthesized and released from solid support according to **GP 2** and **GP 3**. **Yield** = 1 7%; **Purity** > 95% (LC_MS); **LC-MS** (C18, ESI_MS) 552.0 [M+H]⁺, 574.2 [M+Na]⁺; $R_t = 7.36$ min; **¹H NMR** (400 MHz, DMSO-D₆): $\delta = 8.17$ (t, $J = 5.8$ Hz, 1H), 8.06 (d, $J = 8.0$ Hz, 1H), 7.99 (d, $J = 7.9$ Hz, 1H), 7.12 (d, $J = 5.6$ Hz, 1H), 7.10 (d, $J = 5.6$ Hz, 1H), 7.06-6.96 (m, 7H), 6.67-6.60 (m, 5H), 4.40 (ddd, $J = 9.9, 8.1, 4.4$ Hz, 1H), 4.34 (dt, $J = 8.3, 5.3$ Hz, 1H), 3.76 (dd, $J = 16.7, 6.0$ Hz, 1H), 3.61 (dd, $J = 16.7, 5.5$ Hz, 1H), 2.93 (dd, $J = 14.0, 5.2$ Hz, 1H), 2.87 (dd, $J = 14.1, 4.4$ Hz, 1H), 2.78 (dd, $J = 13.8, 8.5$ Hz, 1H), 2.72-2.64 (m, 3H), 2.60 (dd, $J = 14.1, 4.3$ Hz, 1H), 2.56-2.54 (m, 1H), 2.33 (dt, $J = 7.6, 2.0$ Hz, 2H) ppm; $[\alpha]_D^{20} = +20.8^\circ$ (C = 0.8, DMSO).

Analytical data of compound 304



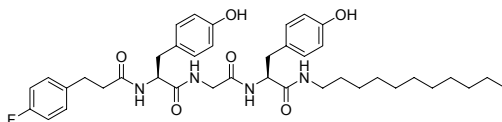
Peptide **304** was synthesized and released from solid support according to **GP 2** and **GP 3**. **Yield** = 12 %; **Purity** > 95% (LC_MS); **LC-MS** (C18, ESI_MS) 645.1 [M+H]⁺, 667.2 [M+Na]⁺; $R_t = 8.49$ min; **¹H NMR** (400 MHz, DMSO-D₆): $\delta = 10.00$ (s, 1H), 9.16 (s, 1H), 9.14 (s, 1H), 8.20 (t, $J = 5.7$ Hz, 1H), 8.14 (d, $J = 7.8$ Hz, 1H), 8.07 (d, $J = 8.1$ Hz, 1H), 7.60 (d, $J = 5.0$ Hz, 1H), 7.57 (d, $J = 5.0$ Hz, 1H), 7.15-7.08 (m, 6H), 7.06-6.97 (m, 6H), 6.64 (d, $J = 4.6$ Hz, 2H), 6.62 (d, $J = 4.6$ Hz, 2H), 4.54 (dt, $J = 8.2, 5.8$ Hz, 1H), 4.40 (dt, $J = 9.8, 4.5$ Hz, 1H), 3.78 (dd, $J = 16.6, 5.9$ Hz, 1H), 3.61 (dd, $J = 16.5, 5.7$ Hz, 1H), 2.94 (dd, $J = 13.8, 5.6$ Hz, 1H), 2.88 (dd, $J = 14.0, 4.4$ Hz, 1H), 2.78 (dd, $J = 14.1, 8.6$ Hz, 1H), 2.74-2.58 (m, 3H), 2.38-2.28 (m, 2H) ppm; $[\alpha]_D^{20} = +26.8^\circ$ (C = 0.6, DMSO).

Analytical data of compound 305



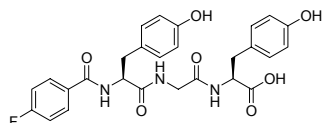
Peptide **305** was synthesized and released from solid support according to **GP 2** and **GP 3**. **Yield** = 9 %; **Purity** > 95% (LC_MS); **LC-MS** (C18, ESI_MS) 595.0 [M+H]⁺, 617.3 [M+Na]⁺; R_t = 7.68 min; **¹H NMR** (400 MHz, DMSO-D₆): δ = 9.18 (s, 1H), 9.13 (s, 1H), 8.13 (t, *J* = 5.9 Hz, 1H), 8.04 (d, *J* = 8.2 Hz, 1H), 7.12 (d, *J* = 5.7 Hz, 1H), 7.10 (d, *J* = 5.6 Hz, 1H), 7.03 (d, *J* = 9.0 Hz, 2H), 7.01-6.96 (m, 4H), 6.65 (d, *J* = 8.5 Hz, 2H), 6.62 (d, *J* = 8.5 Hz, 2H), 4.88 (s, 1H), 4.40 (ddd, *J* = 10.3, 8.3, 4.7 Hz, 1H), 3.76 (dd, *J* = 16.6, 5.9 Hz, 1H), 3.65 (s, 3H), 3.59 (dd, *J* = 17.0, 5.5 Hz, 1H), 3.07 (s, 3H), 2.87 (dd, *J* = 13.8, 4.4 Hz, 1H), 2.81 (dd, *J* = 13.7, 5.4 Hz, 1H), 2.72-2.62 (m, 3H), 2.61 (dd, *J* = 14.3, 10.0 Hz, 1H), 2.32 (dd, *J* = 8.1, 5.8 Hz, 2H) ppm; [α]_D²⁰ = +15.7° (C = 0.4, DMSO).

Analytical data of compound 306



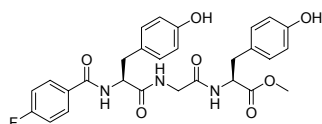
Peptide **306** was synthesized and released from solid support according to **GP 2** and **GP 3**. **Yield** = 10 %; **Purity** > 95% (LC_MS); **LC-MS** (C18, ESI_MS) 705.2 [M+H]⁺, 727.4 [M+Na]⁺; R_t = 10.52 min; **¹H NMR** (400 MHz, DMSO-D₆): δ = 9.14 (s, 1H), 9.12 (s, 1H), 8.16 (t, *J* = 5.6 Hz, 1H), 8.07 (d, *J* = 7.9 Hz, 1H), 7.91 (d, *J* = 8.2 Hz, 1H), 7.81 (t, *J* = 5.6 Hz, 1H), 7.12 (d, *J* = 5.7 Hz, 1H), 7.10 (d, *J* = 5.6 Hz, 1H), 7.03 (d, *J* = 8.9 Hz, 2H), 6.99 (d, *J* = 8.5 Hz, 2H), 6.98 (d, *J* = 8.4 Hz, 2H), 6.62 (d, *J* = 8.4 Hz, 2H), 6.62 (d, *J* = 8.5 Hz, 2H), 4.42-4.30 (m, 2H), 3.75 (dd, *J* = 16.6, 6.0 Hz, 1H), 3.55 (dd, *J* = 16.5, 5.4 Hz, 1H), 3.03 (dd, *J* = 13.0, 6.1 Hz, 1H), 2.95 (dd, *J* = 12.7, 5.8 Hz, 1H), 2.86 (dt, *J* = 13.6, 4.99 Hz, 2H), 2.74-2.64 (m, 2H), 2.62 (dd, *J* = 11.2, 7.3 Hz, 1H), 2.38-2.30 (m, 2H), 1.39-1.27 (m, 2H), 1.30-1.14 (m, 18H), 0.85 (t, *J* = 6.8 Hz, 3H) ppm; [α]_D²⁰ = +8.0° (C = 0.4, DMSO).

Analytical data of compound 307



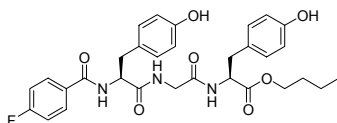
Peptide **307** was synthesized and released from solid support according to **GP 2** and **GP 3**. **Yield** = 26 %; **Purity** > 95% (LC_MS); **LC-MS** (C18, ESI_MS) 524.0 [M+H]⁺, 546.2 [M+Na]⁺; R_t = 7.31 min; **¹H NMR** (400 MHz, DMF-D₇): δ = 8.84 (d, *J* = 7.8 Hz, 1H), 8.53 (t, *J* = 5.7, 5.7 Hz, 1H), 7.86-7.67 (m, 4H), 7.42 (t, *J* = 8.8, 8.8 Hz, 2H), 7.35 (d, *J* = 8.4 Hz, 2H), 7.24 (d, *J* = 8.4 Hz, 2H), 6.89 (d, *J* = 8.4 Hz, 2H), 6.89 (d, *J* = 8.4 Hz, 2H), 4.91 (ddd, *J* = 10.3, 7.9, 4.5 Hz, 1H), 4.73 (dt, *J* = 8.1, 8.1, 5.2 Hz, 1H), 4.13 (dd, *J* = 16.8, 6.0 Hz, 1H), 3.96 (dd, *J* = 16.7, 5.4 Hz, 1H), 3.39 (dd, *J* = 13.9, 4.4 Hz, 1H), 3.27-3.14 (m, 2H), 3.14-3.07 (m, 1H) ppm; **¹³C NMR** (100 MHz, DMF-D₇): δ = 173.3, 172.3, 169.3, 166.3, 157.0, 156.8, 131.3, 131.3, 130.6, 130.6, 130.6, 130.5, 129.1, 128.2, 115.5, 115.5, 115.4, 115.3, 56.6, 54.6, 42.7, 37.0, 36.8 ppm; **HRMS** (ESI) *m/z* calc. for C₂₇H₂₆FN₃O₇ 523.1755, found 524.1824 [M+H]⁺.

Analytical data of compound 308



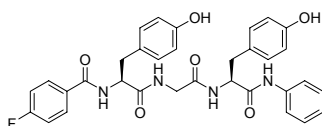
Peptide **308** was synthesized and released from solid support according to **GP 2** and **GP 3**. **Yield** = 8 %; **Purity** > 90% (LC_MS); **LC-MS** (C18, ESI_MS) 538.0 [M+H]⁺, 560.2 [M+Na]⁺; R_t = 7.71 min; **¹H NMR** (400 MHz, DMSO-D₆): δ = 9.19 (s, 1H), 9.10 (s, 1H), 8.58 (d, *J* = 8.0 Hz, 1H), 8.29 (t, *J* = 4.9 Hz, 1H), 8.16 (d, *J* = 7.6 Hz, 1H), 7.86 (d, *J* = 5.5 Hz, 1H), 7.83 (d, *J* = 5.5 Hz, 1H), 7.25 (t, *J* = 8.8 Hz, 2H), 7.09 (d, *J* = 8.4 Hz, 2H), 6.95 (d, *J* = 8.4 Hz, 2H), 6.61 (t, *J* = 8.2 Hz, 4H), 4.59-4.52 (m, 1H), 4.38 (dt, *J* = 8.2, 6.1 Hz, 1H), 3.76 (dd, *J* = 16.8, 6.0 Hz, 1H), 3.65 (dd, *J* = 16.8, 5.5 Hz, 1H), 3.30 (s, 3H), 2.98 (dd, *J* = 13.9, 3.9 Hz, 1H), 2.91-2.83 (m, 2H), 2.78 (dd, *J* = 13.6, 8.4 Hz, 1H) ppm; **HRMS** (FAB, *m*-NBA) *m/z* calc. for C₂₈H₂₈FN₃O₇ 537.1911, found 538.1965 [M+H]⁺; [α]_D²⁰ = - 5.1° (C = 0.6, DMSO).

Analytical data of compound 309



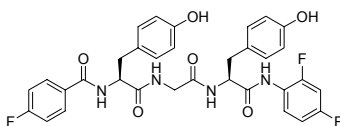
Peptide **309** was synthesized and released from solid support according to **GP 2** and **GP 3**. **Yield** = 3 %; **Purity** > 95% (LC_MS); **LC-MS** (C18, ESI_MS) 580.0 [M+H]⁺, 602.2 [M+Na]⁺; R_t = 8.45 min; **HRMS** (FAB, *m*-NBA) *m/z* calc. for C₃₁H₃₄FN₃O₇ 579.2381, found 580.2479 [M+H]⁺.

Analytical data of compound 310



Peptide **310** was synthesized and released from solid support according to **GP 2** and **GP 3**. **Yield** = 9 %; **Purity** > 90% (LC_MS); **LC-MS** (C18, ESI_MS) 599.1 [M+H]⁺, 621.2 [M+Na]⁺; R_t = 8.09 min; ¹H NMR (400 MHz, DMSO-D₆): δ = 9.94 (s, 1H), 9.15 (s, 1H), 9.11 (s, 1H), 8.60 (d, *J* = 8.1 Hz, 1H), 8.33 (t, *J* = 5.7, 5.7 Hz, 1H), 8.13 (d, *J* = 8.1 Hz, 1H), 7.86 (dd, *J* = 8.9, 5.5 Hz, 2H), 7.57 (dd, *J* = 8.6, 1.1 Hz, 2H), 7.32-7.21 (m, 4H), 7.11 (d, *J* = 8.5 Hz, 2H), 7.07-7.00 (m, 3H), 6.62 (d, *J* = 8.5 Hz, 2H), 6.62 (d, *J* = 8.5 Hz, 2H), 4.69-4.41 (m, 2H), 3.80 (dd, *J* = 16.2, 5.6 Hz, 1H), 3.66 (dd, *J* = 16.7, 5.7 Hz, 1H), 3.01 (dd, *J* = 13.9, 3.9 Hz, 1H), 2.95 (dd, *J* = 13.7, 5.4 Hz, 1H), 2.87 (dd, *J* = 13.8, 10.7 Hz, 1H), 2.78 (dd, *J* = 13.8, 8.8 Hz, 1H) ppm; ¹³C NMR (100 MHz, DMSO-D₆): δ = 171.8, 169.8, 168.4, 165.2, 155.7, 155.5, 138.5, 130.0, 129.9, 129.9, 129.8, 128.5, 128.3, 127.3, 123.3, 119.3, 115.0, 114.8, 114.8, 114.7, 55.4, 55.0, 41.9, 36.9, 36.0 ppm; **HRMS** (FAB, *m*-NBA) *m/z* calc. for C₃₃H₃₁FN₄O₆ 598.2228, found 598.2203 [M]⁺; 599.2280 [M+H]⁺; [α]_D²⁰ = +14.8° (C = 0.5, DMSO).

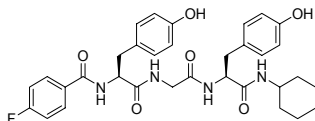
Analytical data of compound 311



Peptide **311** was synthesized and released from solid support according to **GP 2** and **GP 3**. **Yield** = 11 %; **Purity** > 95% (LC_MS); **LC-MS** (C18, ESI_MS) 635.0 [M+H]⁺, 657.2 [M+Na]⁺; R_t = 8.23 min; ¹H NMR (400 MHz, DMSO-D₆): δ = 9.81 (s, 1H), 9.15 (s, 1H), 9.11 (s, 1H), 8.58 (d, *J* = 8.1 Hz, 1H), 8.30 (t, *J* = 5.7 Hz, 1H), 8.12 (d, *J* = 8.2 Hz, 1H), 7.87 (d, *J* = 5.5 Hz, 1H), 7.85 (d, *J* = 5.5 Hz, 1H), 7.66 (dt, *J* = 9.0, 6.2 Hz, 1H), 7.33-7.22 (m, 3H), 7.11 (d, *J* = 8.5 Hz, 2H), 7.05 (d, *J* = 8.5 Hz, 2H), 6.63 (d, *J* = 8.4 Hz, 2H), 6.61 (d, *J* = 8.5 Hz, 2H), 4.69 (dt, *J* = 8.4 5.1

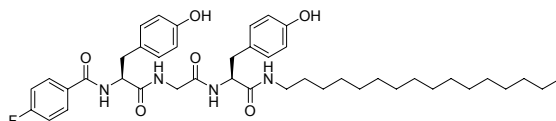
Hz, 1H), 4.58 (ddd, $J = 10.8, 8.3, 4.1$ Hz, 1H), 3.80 (dd, $J = 16.4, 5.6$ Hz, 1H), 3.66 (dd, $J = 16.7, 5.4$ Hz, 1H), 3.06-2.91 (m, 2H), 2.86 (dd, $J = 13.7, 10.88$ Hz, 1H), 2.78 (dd, $J = 13.8, 9.1$ Hz, 1H) ppm; $[\alpha]_D^{20} = +10.1^\circ$ ($C = 0.6$, DMSO).

Analytical data of compound 312



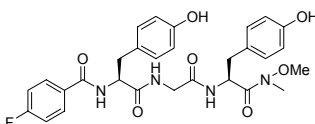
Peptide **312** was synthesized and released from solid support according to **GP 2** and **GP 3**. **Yield** = 6 %; **Purity** > 95% (LC_MS); **LC-MS** (C18, ESI_MS) 605.1 $[M+H]^+$, 627.3 $[M+Na]^+$; $R_t = 8.13$ min.

Analytical data of compound 313



Peptide **313** was synthesized and released from solid support according to **GP 2** and **GP 3**. **Yield** = 4 %; **Purity** > 95% (LC_MS); **LC-MS** (C18, ESI_MS) 747.2 $[M+H]^+$; $R_t = 12.35$ min.

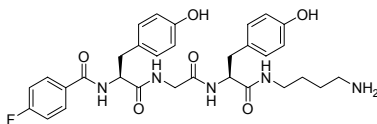
Analytical data of compound 314



Peptide **314** was synthesized and released from solid support according to **GP 2** and **GP 3**. **Yield** = 11 %; **Purity** > 85% (LC_MS); **LC-MS** (C18, ESI_MS) 567.0 $[M+H]^+$, 589.2 $[M+Na]^+$; $R_t = 7.48$ min; $^1\text{H NMR}$ (400 MHz, DMSO- D_6): $\delta = 9.16$ (s, 1H), 9.09 (s, 1H), 8.56 (d, $J = 8.2$ Hz, 1H), 8.25 (t, $J = 5.8$ Hz, 1H), 8.11 (d, $J = 8.7$ Hz, 1H), 7.85 (d, $J = 8.9$ Hz, 2H), 7.84 (d, $J = 8.8$ Hz, 2H), 7.25 (t, $J = 8.8$ Hz, 2H), 7.09 (d, $J = 8.5$ Hz, 2H), 6.95 (d, $J = 8.4$ Hz, 2H), 6.61 (d, $J = 8.5$ Hz, 2H), 6.60 (d, $J = 8.7$ Hz, 2H), 4.88 (s, 1H), 4.56 (ddd, $J = 11.0, 8.3, 3.9$ Hz, 1H), 3.76 (dd, $J = 17.2, 6.3$ Hz, 1H), 3.64 (s, 3H), 3.63 (dd, $J = 16.7, 5.6$ Hz, 1H), 3.30 (s, 3H), 2.97 (dd, J

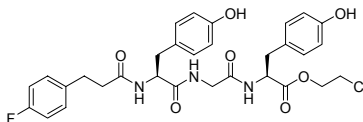
= 13.6, 3.8 Hz, 1H), 2.84 (dd, $J = 11.4, 9.0$ Hz, 1H), 2.79 (dd, $J = 14.2, 4.9$ Hz, 1H), 2.64 (dd, $J = 13.8, 8.7$ Hz, 1H) ppm; $[\alpha]_D^{20} = +0.6^\circ$ ($C = 0.9$, DMSO).

Analytical data of compound 315



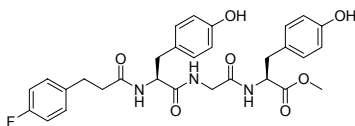
Peptide **315** was synthesized and released from solid support according to **GP 2** and **GP 3**. **Yield** = 15 %; **Purity** > 90% (LC_MS); **LC-MS** (C18, ESI_MS) 594.3 $[M+H]^+$, 616.3 $[M+Na]^+$; $R_t = 5.65$ min; **1H NMR** (400 MHz, DMSO- D_6): $\delta = 9.17$ (s, 1H), 9.14 (s, 1H), 8.61 (d, $J = 8.1$ Hz, 1H), 8.31 (t, $J = 5.6, 5.6$ Hz, 1H), 8.05-7.90 (m, 2H), 7.90-7.83 (m, 2H), 7.66 (br s, 2H), 7.38-7.21 (m, 2H), 7.11 (d, $J = 8.5$ Hz, 2H), 6.98 (d, $J = 8.5$ Hz, 2H), 6.62 (d, $J = 8.5$ Hz, 2H), 6.62 (d, $J = 8.5$ Hz, 2H), 4.56 (ddd, $J = 12.0, 8.0, 4.0$ Hz, 1H), 4.35 (dt, $J = 8.9, 8.7, 5.06$ Hz, 1H), 3.80 (dd, $J = 16.5, 6.0$ Hz, 1H), 3.58 (dd, $J = 16.6, 5.2$ Hz, 1H), 3.14-2.93 (m, 3H), 2.93-2.81 (m, 2H), 2.75 (s, 2H), 2.67 (dd, $J = 13.6, 9.0$ Hz, 1H), 1.62-1.30 (m, 4H) ppm; **^{13}C NMR** (100 MHz, DMSO- D_6): $\delta = 171.8, 170.7, 168.2, 165.3, 162.5, 155.6, 155.5, 130.0, 129.9, 129.8, 129.8, 128.2, 127.7, 115.0, 114.8, 114.7, 55.4, 54.4, 41.9, 38.4, 37.7, 37.0, 36.0, 25.8, 24.3$ ppm; **HRMS** (FAB, *m*-NBA) m/z calc. for $C_{31}H_{36}FN_5O_6$ 593.2650, found 594.2720 $[M]^+$; $[\alpha]_D^{20} = -2.8^\circ$ ($C = 0.9$, DMSO).

Analytical data of compound 316



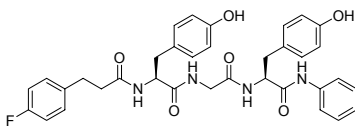
Peptide **316** was synthesized and released from solid support according to **GP 2** and **GP 3**. **Yield** = 4 %; **Purity** > 95% (LC_MS); **LC-MS** (C18, ESI_MS) 614.0 $[M+H]^+$; $R_t = 8.40$ min; **1H NMR** (400 MHz, DMF- D_7): $\delta = 8.37$ (t, $J = 5.7, 5.7$ Hz, 1H), 8.32 (dd, $J = 7.4, 5.4$ Hz, 2H), 7.48-7.31 (m, 2H), 7.29-7.17 (m, 6H), 7.02-6.85 (m, 4H), 4.75 (dt, $J = 7.8, 7.8, 6.1$ Hz, 1H), 4.71-4.66 (m, 1H), 4.51 (ddd, $J = 5.6, 4.2, 3.1$ Hz, 2H), 4.09 (dd, $J = 16.8, 6.0$ Hz, 1H), 4.01-3.90 (m, 3H), 3.30-3.15 (m, 3H), 3.02-2.95 (m, 3H), 2.65 (dd, $J = 8.6, 6.5$ Hz, 2H) ppm; **^{13}C NMR** (100 MHz, DMF- D_7): $\delta = 172.5, 172.4, 172.4, 171.8, 169.6, 157.1, 156.8, 130.6, 130.6, 130.4, 130.4, 128.7, 127.7, 115.6, 115.4, 115.3, 65.0, 55.7, 54.8, 49.7, 42.5, 37.6, 37.0, 36.8, 36.8$ ppm.

Analytical data of compound 317



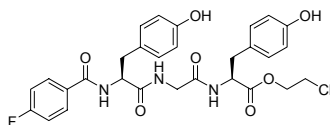
Peptide **317** was synthesized and released from solid support according to **GP 2** and **GP 3**. **Yield** = 19 %; **Purity** > 85% (LC_MS); **LC-MS** (C18, ESI_MS) 566.0 [M+H]⁺; R_t = 7.88 min; **¹H NMR** (400 MHz, DMF-D₇): δ = 8.24 (t, *J* = 5.8, 5.8 Hz, 1H), 8.19 (d, *J* = 7.8 Hz, 1H), 8.14 (d, *J* = 7.6 Hz, 1H), 7.30-7.13 (m, 6H), 6.83-6.66 (m, 4H), 4.77-4.37 (m, 2H), 4.23-3.70 (m, 2H), 3.64 (s, 3H), 3.05 (dd, *J* = 13.9, 4.8 Hz, 1H), 3.01-2.93 (m, 2H), 2.85-2.76 (m, 3H), 2.48 (dd, *J* = 8.7, 6.7 Hz, 2H) ppm; **¹³C NMR** (100 MHz, DMF-D₇): δ = 172.5, 172.4, 172.3, 169.4, 156.9, 156.6, 130.4, 130.4, 130.3, 130.2, 128.5, 127.6, 115.4, 115.2, 115.2, 115.0, 55.6, 54.6, 51.8, 42.4, 37.4, 36.8, 36.7, 36.7 ppm; [α]_D²⁰ = +12.4° (C = 0.9, DMSO).

Analytical data of compound 318



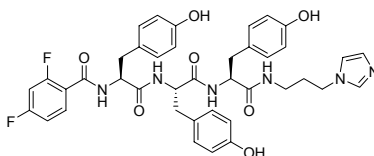
Peptide **318** was synthesized and released from solid support according to **GP 2** and **GP 3**. **Yield** = 16 %; **Purity** > 95% (LC_MS); **LC-MS** (C18, ESI_MS) 627.0 [M+H]⁺, 649.2 [M+Na]⁺; R_t = 8.36 min; **¹H NMR** (400 MHz, DMF-D₇): δ = 10.01 (s, 1H), 9.53 (s, 1H), 9.52 (s, 1H), 8.50 (t, *J* = 5.5, 5.5 Hz, 1H), 8.40 (d, *J* = 7.1 Hz, 1H), 8.22 (d, *J* = 7.9 Hz, 1H), 7.89 (d, *J* = 7.8 Hz, 2H), 7.56-7.41 (m, 2H), 7.38-7.17 (m, 9H), 6.91 (d, *J* = 8.3 Hz, 2H), 6.90 (d, *J* = 8.4 Hz, 2H), 4.85 (dt, *J* = 8.5, 8.5, 5.4 Hz, 1H), 4.68 (ddd, *J* = 9.3, 7.3, 4.9 Hz, 1H), 4.08 (dd, *J* = 16.6, 5.9 Hz, 1H), 3.92 (dd, *J* = 16.6, 5.3 Hz, 1H), 3.31 (dd, *J* = 13.9, 5.2 Hz, 1H), 3.24 (dd, *J* = 14.0, 4.9 Hz, 1H), 3.13 (dd, *J* = 13.8, 8.6 Hz, 1H), 3.04-2.96 (m, 3H), 2.67 (dd, *J* = 8.47, 6.58 Hz, 2H) ppm; **¹³C NMR** (100 MHz, DMF-D₇): δ = 172.9, 172.8, 170.6, 169.4, 156.9, 156.8, 139.7, 130.6, 130.6, 130.4, 130.3, 129.0, 128.6, 128.5, 123.8, 120.0, 115.5, 115.4, 115.3, 115.1, 56.3, 56.0, 43.1, 37.6, 37.4, 36.9, 36.8 ppm; [α]_D²⁰ = +27.0° (C = 0.8, DMSO).

Analytical data of compound 319



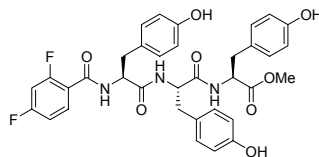
Peptide **319** was synthesized and released from solid support according to **GP 2** and **GP 3**. **Yield** = 1 %; **Purity** > 95% (LC_MS); **LC-MS** (C18, ESI_MS) 586.0 [M+H]⁺, 608.2 [M+Na]⁺; R_t = 8.13 min.

Analytical data of compound 320



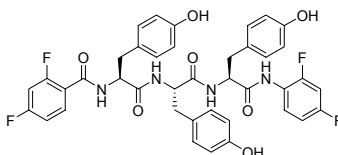
Peptide **320** was synthesized and released from solid support according to **GP 2** and **GP 3**. **Yield** = 3 %; **Purity** > 95% (LC_MS); **LC-MS** (C18, ESI_MS) 755.3 [M+H]⁺, 778.4 [M+Na]⁺; R_t = 5.90 min.

Analytical data of compound 321



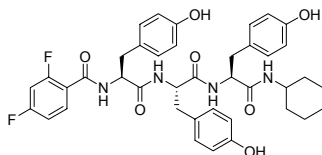
Peptide **321** was synthesized and released from solid support according to **GP 2** and **GP 3**. **Yield** = 1 %; **Purity** > 95% (LC_MS); **LC-MS** (C18, ESI_MS) 662.0 [M+H]⁺, 684.2 [M+Na]⁺; R_t = 7.84 min.

Analytical data of compound 322



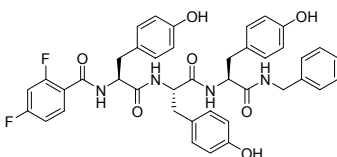
Peptide **322** was synthesized and released from solid support according to **GP 2** and **GP 3**. **Yield** = 3 %; **Purity** > 90% (LC_MS); **LC-MS** (C18, ESI_MS) 758.9 [M+H]⁺, 781.2 [M+Na]⁺; R_t = 8.39 min.

Analytical data of compound 323



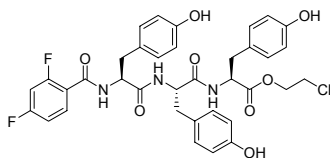
Peptide **323** was synthesized and released from solid support according to **GP 2** and **GP 3**. **Yield** = 1 %; **Purity** > 90% (LC_MS); **LC-MS** (C18, ESI_MS) 729.1 [M+H]⁺; R_t = 8.20 min.

Analytical data of compound 324



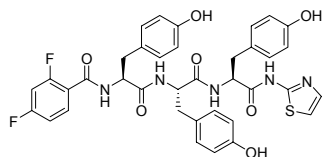
Peptide **324** was synthesized and released from solid support according to **GP 2** and **GP 3**. **Yield** = 3 %; **Purity** > 95% (LC_MS); **LC-MS** (C18, ESI_MS) 737.0 [M+H]⁺, 759.4 [M+Na]⁺; R_t = 8.14 min.

Analytical data of compound 325



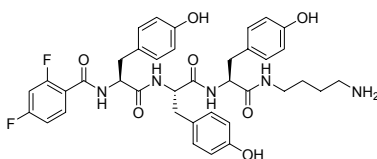
Peptide **325** was synthesized and released from solid support according to **GP 2** and **GP 3**. **Yield** = 2 %; **Purity** > 95% (LC_MS); **LC-MS** (C18, ESI_MS) 710.0 [M+H]⁺, 732.3 [M+Na]⁺; R_t = 8.17 min.

Analytical data of compound 326



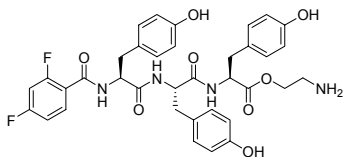
Peptide **326** was synthesized and released from solid support according to **GP 2** and **GP 3**. **Yield** = 3 %; **Purity** > 95% (LC_MS); **LC-MS** (C18, ESI_MS) 730.1 [M+H]⁺, 752.2 [M+Na]⁺; R_t = 7.81 min.

Analytical data of compound 327



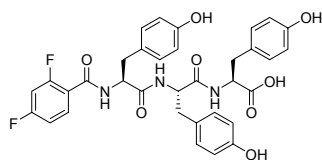
Peptide **327** was synthesized and released from solid support according to **GP 2** and **GP 3**. **Yield** = 20 %; **Purity** > 95% (LC_MS); **LC-MS** (C18, ESI_MS) 718.3 [M+H]⁺; R_t = 5.87 min.

Analytical data of compound 328



Peptide **328** was synthesized and released from solid support according to **GP 2** and **GP 3**. **Yield** = 1 %; **Purity** > 95% (LC_MS); **LC-MS** (C18, ESI_MS) 691.2 [M+H]⁺, 713.3 [M+Na]⁺; R_t = 5.92 min.

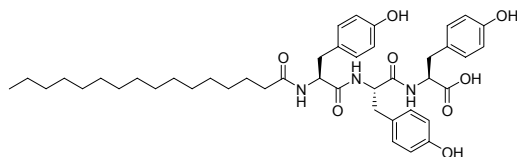
Analytical data of compound 329



Peptide **329** was synthesized and released from solid support according to **GP 2** and **GP 3**. **Yield** = 32 %; **Purity** > 95% (LC_MS); **LC-MS** (C18, ESI_MS) 648.0 [M+H]⁺, 670.2 [M+Na]⁺; R_t = 7.42 min; ¹H NMR (400 MHz, DMSO-D₆): δ = 9.15 (s, 2H), 8.20 (d, *J* = 7.7 Hz, 1H), 8.17 (dd, *J*

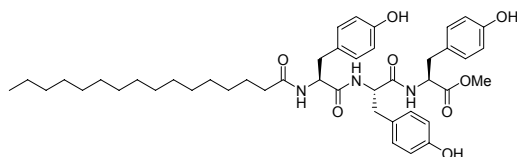
= 8.3, 3.6 Hz, 1H), 8.05 (d, $J = 8.3$ Hz, 1H), 7.56 (dt, $J = 8.5, 6.7$ Hz, 1H), 7.35-7.27 (m, 1H), 7.15 (dt, $J = 8.3, 2.00$ Hz, 1H), 7.07-6.98 (m, 6H), 6.66 (d, $J = 8.54$ Hz, 2H), 6.62 (d, $J = 5.3$ Hz, 2H), 6.60 (d, $J = 5.3$ Hz, 2H), 4.57 (dt, $J = 9.6, 4.2$ Hz, 1H), 4.51 (dt, $J = 8.7, 4.5$ Hz, 1H), 4.38 (dt, $J = 7.8, 5.8$ Hz, 1H), 2.99-2.87 (m, 3H), 2.83 (dd, $J = 13.9, 7.9$ Hz, 1H), 2.70 (dt, $J = 14.2, 9.5$ Hz, 2H) ppm; **HRMS** (ESI) m/z calc. for $C_{34}H_{31}F_2N_3O_8$ 647.2079, found 648.2150 $[M+H]^+$.

Analytical data of compound 330



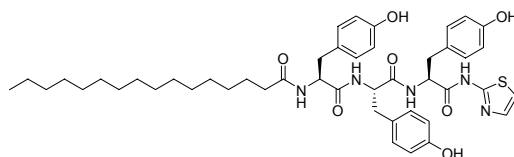
Peptide **330** synthesized and released from solid support according to **GP 2** and **GP 3**. **Yield** = 7 %; **Purity** > 80% (LC_MS); **LC-MS** (C4, ESI_MS) 746.1 $[M+H]^+$, 768.4 $[M+Na]^+$; $R_t = 9.95$ min; **1H NMR** (400 MHz, DMSO- D_6): $\delta = 9.18$ (s, 1H), 9.11 (s, 2H), 8.10 (d, $J = 7.3$ Hz, 1H), 7.94-7.67 (m, 2H), 7.05-6.93 (m, 6H), 6.69-6.55 (m, 6H), 4.43 (dt, $J = 8.3, 4.5$ Hz, 1H), 4.40-4.30 (m, 2H), 2.98-2.76 (m, 4H), 2.76-2.64 (m, 1H), 2.64-2.52 (m, 1H), 1.97 (t, $J = 8.2$ Hz, 2H), 1.42-1.30 (m, 2H), 1.29-1.13 (m, 24H), 1.13-1.03 (m, 2H), 0.85 (t, $J = 6.5$ Hz, 3H) ppm; **HRMS** (ESI) m/z calc. for $C_{43}H_{59}N_3O_8$ 745.4302, found 746.4374 $[M+H]^+$.

Analytical data of compound 331



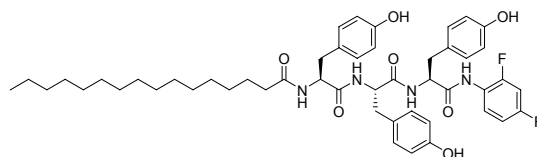
Peptide **331** was synthesized and released from solid support according to **GP 2** and **GP 3**. **Yield** = 8 %; **Purity** > 80% (LC_MS); **LC-MS** (C4, ESI_MS) 760.2 $[M+H]^+$, 782.5 $[M+Na]^+$; $R_t = 10.25$ min; **1H NMR** (400 MHz, DMSO- D_6): $\delta = 9.19$ (s, 1H), 9.10 (s, 1H), 9.06 (s, 1H), 8.27 (d, $J = 7.4$ Hz, 1H), 7.80 (dd, $J = 8.1, 6.2$ Hz, 2H), 7.04-6.86 (m, 6H), 6.63 (d, $J = 8.4$ Hz, 2H), 6.59 (d, $J = 8.4$ Hz, 2H), 6.57 (d, $J = 8.4$ Hz, 2H), 4.45-4.39 (m, 1H), 4.39-4.30 (m, 2H), 3.53 (s, 3H), 2.91-2.72 (m, 4H), 2.64 (dd, $J = 14.1, 8.9$ Hz, 1H), 2.52 (dd, $J = 12.4, 8.7$ Hz, 1H), 1.96 (t, $J = 7.4$ Hz, 2H), 1.42-1.28 (m, 2H), 1.29-1.10 (m, 24H), 1.11-1.00 (m, 2H), 0.83 (t, $J = 6.8$ Hz, 3H) ppm; **HRMS** (ESI) m/z calc. for $C_{44}H_{61}N_3O_8$ 759.4459, found 760.4531 $[M+H]^+$.

Analytical data of compound 332



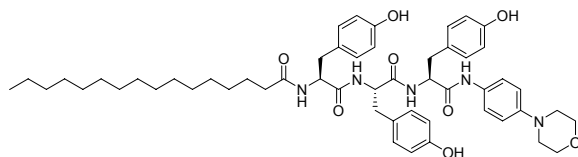
Peptide **332** was synthesized and released from solid support according to **GP 2** and **GP 3**. **Yield** = 10 %; **Purity** > 85% (LC_MS); **LC-MS** (C4, ESI_MS) 828.3 [M+H]⁺, 850.5 [M+Na]⁺; R_t = 10.43 min; **¹H NMR** (400 MHz, DMSO-D₆): δ = 12.22 (s, 1H), 9.18 (s, 1H), 9.08 (s, 2H), 8.27 (d, *J* = 7.4 Hz, 1H), 7.84 (d, *J* = 8.4 Hz, 1H), 7.76 (d, *J* = 8.0 Hz, 1H), 7.47 (d, *J* = 3.5 Hz, 1H), 7.22 (d, *J* = 3.5 Hz, 1H), 7.05 (d, *J* = 3.5 Hz, 2H), 6.95 (t, *J* = 8.7 Hz, 4H), 6.64 (d, *J* = 8.5 Hz, 2H), 6.59 (d, *J* = 8.5 Hz, 2H), 6.54 (d, *J* = 8.5 Hz, 2H), 4.70 (dd, *J* = 14.1, 7.6 Hz, 1H), 4.44 (dt, *J* = 8.3, 4.7 Hz, 1H), 4.39-4.32 (m, 1H), 3.00-2.75 (m, 4H), 2.67 (dd, *J* = 14.1, 8.6 Hz, 1H), 2.54 (dd, *J* = 12.8, 8.9 Hz, 1H), 1.97 (t, *J* = 7.5 Hz, 2H), 1.38-1.28 (m, 2H), 1.28-1.11 (m, 24H), 1.11-1.01 (m, 2H), 0.85 (t, *J* = 6.8 Hz, 3H) ppm; **HRMS** (ESI) *m/z* calc. for C₄₆H₆₁N₅O₇S 827.4292, found 828.4365 [M+H]⁺.

Analytical data of compound 333



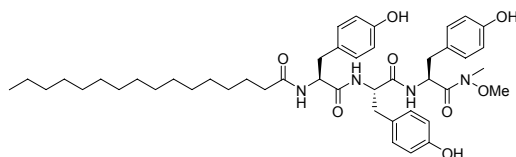
Peptide **333** was synthesized and released from solid support according to **GP 2** and **GP 3**. **Yield** = 5 %; **Purity** > 95% (LC_MS); **LC-MS** (C4, ESI_MS) 857.2 [M+H]⁺, 879.5 [M+Na]⁺; R_t = 10.63 min; **¹H NMR** (400 MHz, DMSO-D₆): δ = 9.73 (s, 1H), 9.14 (s, 1H), 9.07 (s, 1H), 9.06 (s, 1H), 8.16 (d, *J* = 7.9 Hz, 1H), 7.81 (dd, *J* = 13.4, 8.4 Hz, 2H), 7.67 (dt, *J* = 8.8, 6.2 Hz, 1H), 7.33-7.19 (m, 1H), 7.04 (d, *J* = 8.4 Hz, 4H), 6.98-6.90 (m, 5H), 6.63 (d, *J* = 8.5 Hz, 2H), 6.57 (d, *J* = 8.5 Hz, 2H), 6.55-6.52 (m, 2H), 4.67 (q, *J* = 7.9, 7.7 Hz, 1H), 4.41 (dt, *J* = 8.1, 4.4 Hz, 1H), 4.34 (dt, *J* = 9.6, 4.0 Hz, 1H), 2.98-2.73 (m, 4H), 2.65 (dd, *J* = 14.0, 8.6 Hz, 1H), 2.53 (dd, *J* = 13.4, 9.6 Hz, 1H), 1.95 (t, *J* = 7.4 Hz, 2H), 1.40-1.26 (m, 2H), 1.26-1.10 (m, 24H), 1.10-1.00 (m, 2H), 0.83 (t, *J* = 6.8 Hz, 3H) ppm; **HRMS** (ESI) *m/z* calc. for C₄₉H₆₂F₂N₄O₇ 856.4587, found 857.4659 [M+H]⁺.

Analytical data of compound 334



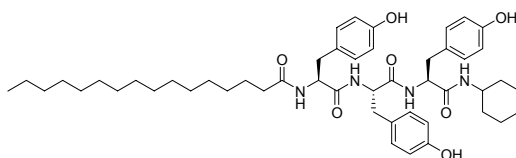
Peptide **334** was synthesized and released from solid support according to **GP 2** and **GP 3**. **Yield** = 8 %; **Purity** > 90% (LC_MS); **LC-MS** (C4, ESI_MS) 906.2 [M+H]⁺, 928.5 [M+Na]⁺; R_t = 10.36 min; ¹H NMR (400 MHz, DMSO-D₆): δ = 9.67 (s, 1H), 9.13 (s, 1H), 9.07 (s, 1H), 9.07 (s, 1H), 8.08 (d, *J* = 8.1 Hz, 1H), 7.85 (d, *J* = 8.1 Hz, 1H), 7.80 (d, *J* = 7.9 Hz, 1H), 7.38 (d, *J* = 9.0 Hz, 2H), 7.01 (d, *J* = 8.2 Hz, 2H), 6.94 (t, *J* = 7.7 Hz, 4H), 6.85 (d, *J* = 9.0 Hz, 2H), 6.61 (d, *J* = 8.4 Hz, 2H), 6.57 (d, *J* = 8.3 Hz, 2H), 6.54 (d, *J* = 8.5 Hz, 2H), 4.52 (q, *J* = 7.07 Hz, 1H), 4.43-4.29 (m, 2H), 3.72-3.68 (m, 4H), 3.03-3.00 (m, 4H), 2.95-2.73 (m, 4H), 2.67 (dd, *J* = 14.1, 8.2 Hz, 1H), 2.54 (dd, *J* = 14.3, 10.2 Hz, 1H), 1.96 (t, *J* = 7.15 Hz, 2H), 1.41-1.26 (m, 2H), 1.27-1.10 (m, 24H), 1.10-0.99 (m, 2H), 0.83 (t, *J* = 6.65 Hz, 3H) ppm; **HRMS** (ESI) *m/z* calc. for C₅₃H₇₁N₅O₈ 905.5303, found 905.5380 [M+H]⁺.

Analytical data of compound 335



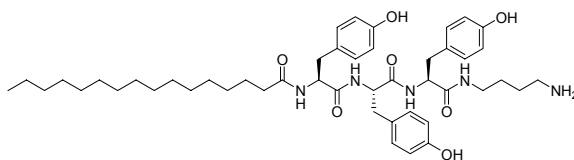
Peptide **335** was synthesized and released from solid support according to **GP 2** and **GP 3**. **Yield** = 15 %; **Purity** > 95% (LC_MS); **LC-MS** (C4, ESI_MS) 789.2 [M+H]⁺, 811.4 [M+Na]⁺; R_t = 10.34 min; ¹H NMR (400 MHz, DMSO-D₆): δ = 9.18 (s, 1H), 9.10 (s, 1H), 9.08 (s, 1H), 7.85 (d, *J* = 8.5 Hz, 1H), 7.74 (d, *J* = 8.1 Hz, 1H), 7.07-6.88 (m, 6H), 6.65 (d, *J* = 8.5 Hz, 2H), 6.59 (d, *J* = 8.3 Hz, 4H), 4.92 (br, 1H), 4.43 (dt, *J* = 8.4, 4.82 Hz, 1H), 4.35 (dt, *J* = 10.3, 4.0 Hz, 1H), 3.59 (s, 3H), 3.05 (s, 3H), 2.89-2.77 (m, 3H), 2.74-2.61 (m, 2H), 2.54 (dd, *J* = 12.2, 8.5 Hz, 1H), 1.97 (t, *J* = 7.3 Hz, 2H), 1.40-1.28 (m, 2H), 1.28-1.12 (m, 24H), 1.12-1.03 (m, 2H), 0.85 (t, *J* = 6.8 Hz, 3H) ppm; **HRMS** (ESI) *m/z* calc. for C₄₅H₆₄N₄O₈ 788.4724, found 789.4797 [M+H]⁺.

Analytical data of compound 336



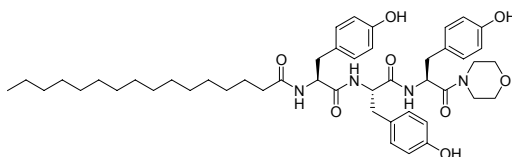
Peptide **336** was synthesized and released from solid support according to **GP 2** and **GP 3**. **Yield** = 7 %; **Purity** > 95% (LC_MS); **LC-MS** (C4, ESI_MS) 827.4 [M+H]⁺, 849.6 [M+Na]⁺; R_t = 10.71 min; **¹H NMR** (400 MHz, DMSO-D₆): δ = 9.12 (s, 1H), 9.11 (s, 1H), 9.08 (s, 1H), 7.90 (d, *J* = 8.3 Hz, 1H), 7.86 (d, *J* = 8.2 Hz, 1H), 7.81 (d, *J* = 7.9 Hz, 1H), 7.61 (d, *J* = 7.9 Hz, 1H), 6.97 (d, *J* = 8.5 Hz, 4H), 6.93 (d, *J* = 8.5 Hz, 2H), 6.62 (d, *J* = 8.5 Hz, 2H), 6.59 (d, *J* = 8.5 Hz, 2H), 6.59 (d, *J* = 8.5 Hz, 2H), 4.41-4.32 (m, 3H), 3.51-3.41 (m, 1H), 2.87-2.76 (m, 3H), 2.74-2.64 (m, 2H), 2.56 (dd, *J* = 13.8, 10.0 Hz, 1H), 1.98 (t, *J* = 7.3 Hz, 2H), 1.73-1.47 (m, 4H), 1.41-1.30 (m, 2H), 1.30-1.14 (m, 28H), 1.13-0.98 (m, 4H), 0.85 (t, *J* = 6.8 Hz, 3H) ppm; **HRMS** (ESI) *m/z* calc. for C₄₉H₇₀N₄O₇ 826.5245, found 827.5315 [M+H]⁺.

Analytical data of compound 337



Peptide **337** was synthesized and released from solid support according to **GP 2** and **GP 3**. **Yield** = 20 %; **Purity** > 95% (LC_MS); **LC-MS** (C4, ESI_MS) 816.4 [M+H]⁺, 838.5 [M+Na]⁺; R_t = 8.57 min; **¹H NMR** (400 MHz, DMSO-D₆): δ = 9.17 (s, 1H), 9.15 (s, 1H), 9.11 (s, 1H), 7.93 (d, *J* = 8.2 Hz, 1H), 7.88 (d, *J* = 8.3 Hz, 1H), 7.86 (d, *J* = 8.4 Hz, 1H), 7.75 (t, *J* = 5.6 Hz, 1H), 7.68 (br, 2H), 4.40-4.30 (m, 3H), 3.09-2.93 (m, 1H), 2.88-2.79 (m, 2H), 2.79-2.72 (m, 4H), 2.72-2.62 (m, 2H), 2.56 (dd, *J* = 13.8, 10.3 Hz, 1H), 1.99 (t, *J* = 7.3 Hz, 1H), 1.50-1.41 (m, 2H), 1.41-1.31 (m, 4H), 1.29-1.12 (m, 24H), 1.12-1.04 (m, 2H), 0.85 (t, *J* = 6.7 Hz, 3H) ppm; **HRMS** (ESI) *m/z* calc. for C₄₇H₆₉N₅O₇ 815.5197, found 816.5269 [M+H]⁺.

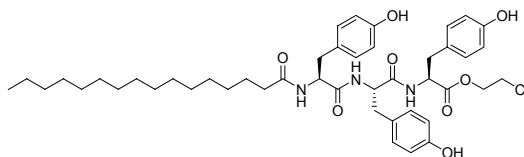
Analytical data of compound 338



Peptide **338** was synthesized and released from solid support according to **GP 2** and **GP 3**. **Yield** = 18 %; **Purity** > 95% (LC_MS); **LC-MS** (C4, ESI_MS) 815.2 [M+H]⁺, 837.5 [M+Na]⁺; R_t = 10.21 min; **¹H NMR** (400 MHz, DMSO-D₆): δ = 9.19 (s, 1H), 9.10 (s, 1H), 9.07 (s, 1H), 8.25 (d, *J* = 7.9 Hz, 1H), 7.84 (d, *J* = 8.4 Hz, 1H), 7.77 (d, *J* = 8.1 Hz, 1H), 6.99-6.91 (m, 6H), 6.64 (d, *J*

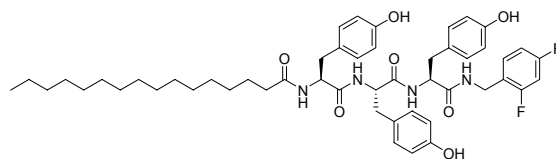
= 8.4 Hz, 2H), 6.58 (d, $J = 8.4$ Hz, 4H), 4.78 (dd, $J = 8.1, 7.8$ Hz, 1H), 4.41 (dt, $J = 8.3, 5.0$ Hz, 1H), 4.37-4.31 (m, 1H), 3.46 (dd, $J = 13.8, 8.0$ Hz, 1H), 3.43-3.36 (m, 2H), 3.27-3.22 (m, 1H), 3.17-3.08 (m, 1H), 3.05-2.97 (m, 1H), 2.86-2.76 (m, 3H), 2.74-2.62 (m, 2H), 2.54 (dd, $J = 14.0, 10.5$ Hz, 1H), 1.96 (t, $J = 7.3$ Hz, 2H), 1.38-1.28 (m, 2H), 1.28-1.11 (m, 24H), 1.10-1.02 (m, 2H), 0.83 (t, $J = 6.8$ Hz, 3H); **HRMS** (ESI) m/z calc. for $C_{47}H_{66}N_4O_8$ 814.4881, found 815.4953 $[M+H]^+$.

Analytical data of compound 339



Peptide **339** was synthesized and released from solid support according to **GP 2** and **GP 3**. **Yield** = 8 %; **Purity** > 95% (LC_MS); **LC-MS** (C4, ESI_MS) 808.2 $[M+H]^+$, 830.5 $[M+Na]^+$; R_t = 10.59 min; **1H NMR** (400 MHz, DMSO- D_6): δ = 9.19 (s, 1H), 9.10 (s, 1H), 9.06 (s, 1H), 8.34 (d, $J = 7.2$ Hz, 1H), 7.80 (d, $J = 8.4$ Hz, 1H), 7.79 (d, $J = 8.1$ Hz, 1H), 7.02-6.92 (m, 6H), 6.64 (d, $J = 8.40$ Hz, 2H), 6.59 (d, $J = 8.19$ Hz, 2H), 6.57 (d, $J = 7.62$ Hz, 2H), 4.47-4.38 (m, 2H), 4.38-4.30 (m, 1H), 4.22 (t, $J = 5.2$ Hz, 2H), 3.75-3.64 (m, 2H), 2.93-2.80 (m, 3H), 2.77 (dd, $J = 13.8, 4.0$ Hz, 1H), 2.64 (dd, $J = 14.1, 8.9$ Hz, 1H), 2.52 (dd, $J = 11.0, 7.3$ Hz, 1H), 1.95 (t, $J = 7.24$ Hz, 2H), 1.37-1.27 (m, 2H), 1.27-1.10 (m, 2H), 1.10-1.00 (m, 2H), 0.83 (t, $J = 6.79$ Hz, 3H) ppm; **HRMS** (ESI) m/z calc. for $C_{45}H_{62}ClN_3O_8$ 807.4225, found 808.4298 $[M+H]^+$.

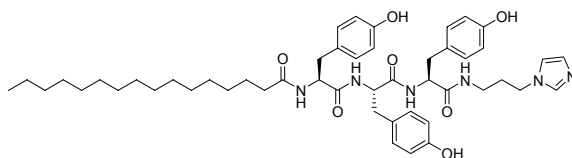
Analytical data of compound 340



Peptide **340** was synthesized and released from solid support according to **GP 2** and **GP 3**. **Yield** = 7 %; **Purity** > 95% (LC_MS); **LC-MS** (C4, ESI_MS) 871.3 $[M+H]^+$, 893.5 $[M+Na]^+$; R_t = 10.64 min; **1H NMR** (400 MHz, DMSO- D_6): δ = 9.18 (s, 1H), 9.11 (s, 1H), 9.08 (s, 1H), 8.30 (t, $J = 5.9$ Hz, 1H), 8.05 (d, $J = 7.9$ Hz, 1H), 7.85 (d, $J = 4.8$ Hz, 1H), 7.83 (d, $J = 4.3$ Hz, 1H), 7.20-7.13 (m, 1H), 6.99-6.91 (m, 9H), 6.63 (d, $J = 8.5$ Hz, 2H), 6.59 (d, $J = 8.5$ Hz, 2H), 6.59 (d, $J = 8.5$ Hz, 2H), 4.48-4.42 (m, 1H), 4.41-4.32 (m, 2H), 4.26 (dd, $J = 15.4, 6.0$ Hz, 1H), 4.16 (dd, $J =$

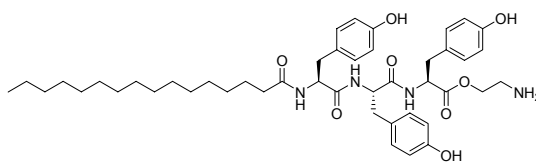
15.7, 5.2 Hz, 1H), 2.88-2.80 (m, 2H), 2.79-2.71 (m, 1H), 2.67 (dd, $J = 14.0, 8.8$ Hz, 1H), 2.55 (dd, $J = 12.2, 8.6$ Hz, 1H), 1.98 (t, $J = 7.4$ Hz, 2H), 1.39-1.27 (m, 2H), 1.28-1.13 (m, 24H), 1.13-1.03 (m, 2H), 0.85 (t, $J = 6.86$ Hz, 3H) ppm; **HRMS** (ESI) m/z calc. for $C_{50}H_{64}F_2N_4O_7$ 870.4743, found 871.4818 $[M+H]^+$.

Analytical data of compound 341



Peptide **341** was synthesized and released from solid support according to **GP 2** and **GP 3**. **Yield** = 17 %; **Purity** > 95% (LC_MS); **LC-MS** (C4, ESI_MS) 853.5 $[M+H]^+$, 875.6 $[M+Na]^+$; R_t = 8.69 min; **¹H NMR** (400 MHz, DMSO- D_6): δ = 9.19 (s, 2H), 8.88 (s, 1H), 8.02 (d, $J = 7.7$ Hz, 1H), 7.93-7.81 (m, 3H), 7.62 (d, $J = 13.5$ Hz, 2H), 7.00 (d, $J = 8.4$ Hz, 2H), 6.95 (d, $J = 8.4$ Hz, 4H), 6.64 (d, $J = 8.4$ Hz, 2H), 6.60 (d, $J = 8.4$ Hz, 4H), 4.42-4.28 (m, 3H), 4.00 (t, $J = 6.8$ Hz, 2H), 2.98 (dq, $J = 14.0, 6.7$ Hz, 2H), 2.89-2.79 (m, 2H), 2.79-2.62 (m, 3H), 2.57 (dd, $J = 13.9, 9.9$ Hz, 1H), 1.99 (t, $J = 7.21$ Hz, 2H), 1.90-1.77 (m, 2H), 1.42-1.30 (m, 2H), 1.30-1.13 (m, 24H), 1.12-1.04 (m, 2H), 0.85 (t, $J = 6.8$ Hz, 3H) ppm; **HRMS** (ESI) m/z calc. for $C_{49}H_{68}N_6O_7$ 852.5149, found 853.5222 $[M+H]^+$.

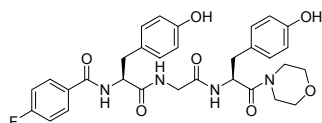
Analytical data of compound 342



Peptide **342** was synthesized and released from solid support according to **GP 2** and **GP 3**. **Yield** = 7 %; **Purity** > 95% (LC_MS); **LC-MS** (C4, ESI_MS) 789.4 $[M+H]^+$, 811.5 $[M+Na]^+$; R_t = 8.71 min; **¹H NMR** (400 MHz, DMSO- D_6): δ = 9.24 (s, 1H), 9.16 (s, 1H), 9.11 (s, 1H), 8.23 (d, $J = 7.6$ Hz, 1H), 7.88 (dd, $J = 8.2, 4.4$ Hz, 3H), 7.01-6.93 (m, 6H), 6.67 (d, $J = 8.4$ Hz, 2H), 6.62 (d, $J = 8.4$ Hz, 2H), 6.59 (d, $J = 8.4$ Hz, 2H), 4.50 (q, $J = 7.8, 7.6$ Hz, 1H), 4.45-4.38 (m, 1H), 4.38-4.31 (m, 1H), 4.23 (td, $J = 11.2, 5.4$ Hz, 1H), 4.16-4.10 (m, 1H), 3.05 (dd, $J = 10.0, 4.9$ Hz, 2H), 2.99 (dd, $J = 14.2, 5.6$ Hz, 1H), 2.85 (dd, $J = 14.5, 6.5$ Hz, 2H), 2.78 (dd, $J = 13.9, 4.1$ Hz, 1H), 2.66 (dd, $J = 13.9, 9.1$ Hz, 1H), 2.55 (dd, $J = 13.6, 9.4$ Hz, 1H), 1.99 (t, $J = 7.0$ Hz, 2H), 1.39-

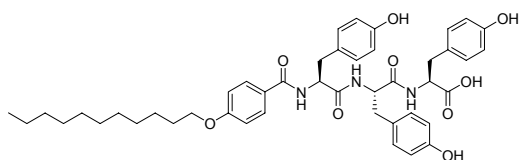
1.30 (m, 2H), 1.29-1.13 (m, 24H), 1.12-1.04 (m, 2H), 0.85 (t, $J = 6.86$ Hz, 3H) ppm; **HRMS** (ESI) m/z calc. for $C_{45}H_{64}N_4O_8$ 788.4724, found 789.4796 $[M+H]^+$.

Analytical data of compound 343



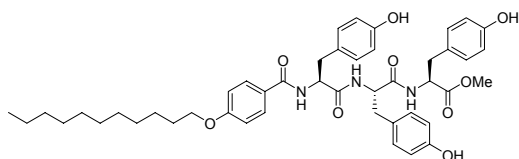
Peptide **343** was synthesized and released from solid support according to **GP 2** and **GP 3**. **Yield** = 5 %; **Purity** > 95% (LC_MS); **LC-MS** (C18, ESI_MS) 593.0 $[M+H]^+$, 615.3 $[M+Na]^+$; R_t = 7.83 min.

Analytical data of compound 344



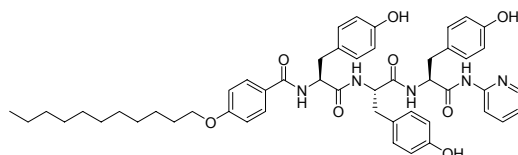
Peptide **344** was synthesized and released from solid support according to **GP 2** and **GP 3**. **Yield** = 22 %; **Purity** > 95% (LC_MS); **LC-MS** (C4, ESI_MS) 782.1 $[M+H]^+$, 804.4 $[M+Na]^+$; R_t = 9.87 min; **1H NMR** (400 MHz, DMSO- D_6): δ = 9.10 (d, $J = 1.8$ Hz, 1H), 9.09 (s, 1H), 8.31 (d, $J = 8.2$ Hz, 1H), 7.85 (d, $J = 8.1$ Hz, 1H), 7.74 (d, $J = 8.8$ Hz, 1H), 7.73 (d, $J = 8.8$ Hz, 1H), 7.05 (d, $J = 8.5$ Hz, 2H), 7.02-6.93 (m, 6H), 6.65 (d, $J = 8.5$ Hz, 2H), 6.62-6.53 (m, 6H), 4.57-4.49 (m, 1H), 4.36 (dt, $J = 8.2$ 5.2 Hz, 1H), 4.00 (dt, $J = 6.4$, 2.1 Hz, 2H), 2.96-2.85 (m, 3H), 2.85-2.77 (m, 2H), 2.72 (dd, $J = 15.6$, 6.5 Hz, 1H), 1.71 (p, $J = 6.4$ Hz, 2H), 1.47-1.35 (m, 2H), 1.37-1.20 (m, 16H), 0.85 (t, $J = 6.8$ Hz, 3H) ppm; **HRMS** (ESI) m/z calc. for $C_{45}H_{55}N_3O_9$ 781.3938, found 782.4013 $[M+H]^+$; $[\alpha]_D^{20} = -46.8^\circ$ (C = 1.3, DMSO).

Analytical data of compound 345



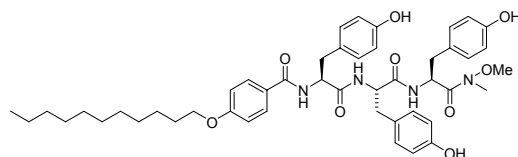
Peptide **345** was synthesized and released from solid support according to **GP 2** and **GP 3**. **Yield** = 8 %; **Purity** > 95% (LC_MS); **LC-MS** (C4, ESI_MS) 796.1 [M+H]⁺, 818.4 [M+Na]⁺; R_t = 10.15 min; ¹H NMR (400 MHz, DMSO-D₆): δ = 9.20 (s, 1H), 9.10 (s, 1H), 9.09 (s, 1H), 8.34 (d, J = 7.4 Hz, 1H), 8.27 (d, J = 8.2 Hz, 1H), 7.92 (d, J = 8.3 Hz, 1H), 7.73 (d, J = 8.9 Hz, 2H), 7.05 (d, J = 8.5 Hz, 2H), 6.96 (t, J = 8.6 Hz, 4H), 6.65 (d, J = 8.5 Hz, 2H), 6.59 (d, J = 8.5 Hz, 2H), 6.55 (d, J = 8.5 Hz, 2H), 4.56-4.44 (m, 1H), 4.37 (q, J = 7.0 6.7 Hz, 1H), 4.00 (t, J = 6.7 Hz, 2H), 3.55 (s, 3H), 2.92-2.83 (m, 4H), 2.80 (dd, J = 14.8, 4.5 Hz, 1H), 2.67 (dd, J = 12.5, 9.0 Hz, 1H), 1.71 (p, J = 6.1 Hz, 2H), 1.48-1.35 (m, 2H), 1.38-1.20 (m, 16H), 0.85 (t, J = 6.8 Hz, 3H) ppm; [α]_D²⁰ = -45.2° (C = 0.2, DMSO).

Analytical data of compound 346



Peptide **346** was synthesized and released from solid support according to **GP 2** and **GP 3**. **Yield** = 2 %; **Purity** > 95% (LC_MS); **LC-MS** (C4, ESI_MS) 858.4 [M+H]⁺, 880.4 [M+Na]⁺; R_t = 9.99 min.

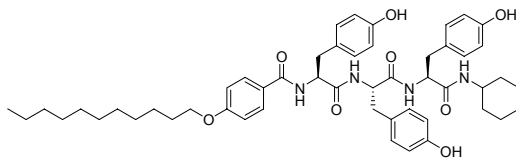
Analytical data of compound 347



Peptide **347** was synthesized and released from solid support according to **GP 2** and **GP 3**. **Yield** = 4 %; **Purity** > 95% (LC_MS); **LC-MS** (C4, ESI_MS) 825.1 [M+H]⁺, 847.4 [M+Na]⁺; R_t = 10.04 min; ¹H NMR (400 MHz, DMSO-D₆): δ = 9.18 (s, 1H), 9.08 (s, 1H), 9.07 (s, 1H), 8.29 (d, J = 8.1 Hz, 2H), 7.84 (d, J = 8.0 Hz, 1H), 7.73 (d, J = 8.9 Hz, 2H), 7.05 (d, J = 8.5 Hz, 2H), 6.98 (d, J = 8.5 Hz, 2H), 6.95 (d, J = 8.9 Hz, 2H), 6.65 (d, J = 8.5 Hz, 2H), 6.59 (d, J = 8.5 Hz, 2H), 6.52 (d, J = 8.5 Hz, 2H), 4.95-4.87 (m, 1H), 4.56-4.49 (m, 1H), 4.46 (dt, J = 8.8, 4.67 Hz, 1H), 4.00 (t, J = 6.6 Hz, 2H), 3.58 (s, 3H), 3.05 (s, 3H), 2.92-2.75 (m, 4H), 2.73-2.63 (m, 2H), 1.71 (

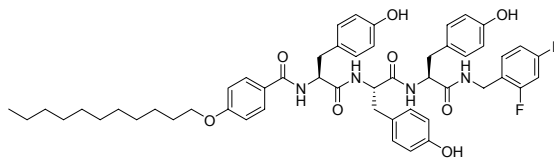
p, $J = 6.9$ Hz, 2H), 1.44-1.37 (m, 2H), 1.34-1.23 (m, 18H), 0.83 (t, $J = 6.8$ Hz, 3H) ppm; $[\alpha]_D^{20} = -32.0^\circ$ (C = 0.2, DMSO).

Analytical data of compound 348



Peptide **348** was synthesized and released from solid support according to **GP 2** and **GP 3**. **Yield** = 6 %; **Purity** > 95% (LC_MS); **LC-MS** (C4, ESI_MS) 863.3 [M+H]⁺, 885.6 [M+Na]⁺; $R_t = 10.39$ min; **¹H NMR** (400 MHz, DMSO-D₆): $\delta = 9.10$ (s, 1H), 9.07 (s, 1H), 9.06 (s, 1H), 8.28 (d, $J = 8.4$ Hz, 1H), 7.93 (d, $J = 8.3$ Hz, 1H), 7.89 (d, $J = 7.9$ Hz, 1H), 7.71 (d, $J = 8.8$ Hz, 2H), 7.59 (d, $J = 7.8$ Hz, 1H), 7.04 (d, $J = 8.5$ Hz, 2H), 6.97-6.91 (m, 4H), 6.61 (d, $J = 8.5$ Hz, 2H), 6.57 (d, $J = 8.5$ Hz, 2H), 6.51 (d, $J = 8.5$ Hz, 2H), 4.51 (dt, $J = 10.5, 4.0$ Hz, 1H), 4.39 (dd, $J = 12.2, 7.7$ Hz, 1H), 4.34 (dd, $J = 14.5, 6.9$ Hz, 1H), 3.98 (t, $J = 6.5$ Hz, 2H), 3.50-3.38 (m, 1H), 2.88 (dd, $J = 14.4, 4.5$ Hz, 1H), 2.83-2.74 (m, 3H), 2.73-2.63 (m, 2H), 1.73-1.45 (m, 6H), 1.44-1.34 (m, 2H), 1.33-1.15 (m, 16H), 1.14-0.94 (m, 4H), 0.85 (t, $J = 6.8$ Hz, 3H) ppm; $[\alpha]_D^{20} = -74.0^\circ$ (C = 0.3, DMSO).

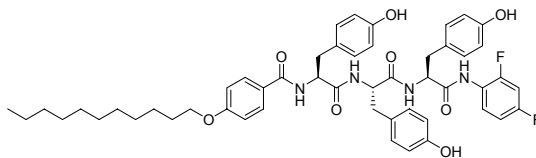
Analytical data of compound 349



Peptide **349** was synthesized and released from solid support according to **GP 2** and **GP 3**. **Yield** = 12 %; **Purity** > 95% (LC_MS); **LC-MS** (C4, ESI_MS) 907.2 [M+H]⁺, 929.4 [M+Na]⁺; $R_t = 10.35$ min; **¹H NMR** (400 MHz, DMSO-D₆): $\delta = 9.16$ (s, 1H), 9.07 (s, 1H), 9.07 (s, 1H), 8.29 (d, $J = 7.8$ Hz, 1H), 8.27 (d, $J = 10.4$ Hz, 1H), 8.09 (d, $J = 8.2$ Hz, 1H), 7.91 (d, $J = 7.9$ Hz, 1H), 7.71 (d, $J = 8.9$ Hz, 2H), 7.18-7.11 (m, 1H), 7.03 (d, $J = 8.5$ Hz, 2H), 6.99-6.87 (m, 8H), 6.61 (d, $J = 8.5$ Hz, 2H), 6.57 (d, $J = 8.5$ Hz, 2H), 6.51 (d, $J = 8.5$ Hz, 2H), 4.51 (ddd, $J = 10.3, 8.3, 4.1$ Hz, 1H), 4.46-4.38 (m, 2H), 4.25 (dd, $J = 15.6, 6.2$ Hz, 1H), 4.14 (dd, $J = 15.3, 5.5$ Hz, 1H), 3.98 (t, $J = 6.5$ Hz, 2H), 2.90-2.83 (m, 2H), 2.83-2.77 (m, 2H), 2.74 (dd, $J = 8.2, 5.4$ Hz, 1H), 2.66

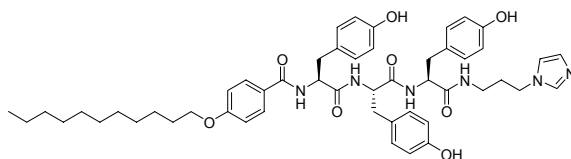
(dd, $J = 13.7, 8.1$ Hz, 1H), 1.73-1.65 (m, 2H), 1.43-1.34 (m, 2H), 1.34-1.19 (m, 16H), 0.85 (t, $J = 6.8$ Hz, 3H) ppm; $[\alpha]_D^{20} = -38.0^\circ$ (C = 0.8, DMSO).

Analytical data of compound 350



Peptide **350** was synthesized and released from solid support according to **GP 2** and **GP 3**. **Yield** = 12 %; **Purity** > 95% (LC_MS); **LC-MS** (C4, ESI_MS) 893.1 [M+H]⁺, 915.4 [M+Na]⁺; $R_t = 10.35$ min; **¹H NMR** (400 MHz, DMSO- D_6): $\delta = 9.74$ (s, 1H), 9.14 (s, 1H), 9.07 (s, 1H), 9.04 (s, 1H), 8.27 (d, $J = 8.3$ Hz, 1H), 8.21 (d, $J = 7.9$ Hz, 1H), 7.89 (d, $J = 8.2$ Hz, 1H), 7.71 (d, $J = 8.8$ Hz, 2H), 7.69-7.63 (m, 1H), 7.06-7.02 (m, 5H), 6.94 (d, $J = 8.5$ Hz, 2H), 6.93 (d, $J = 8.9$ Hz, 2H), 6.63 (d, $J = 8.5$ Hz, 2H), 6.57 (d, $J = 8.5$ Hz, 2H), 6.48 (d, $J = 8.4$ Hz, 2H), 4.67 (q, $J = 7.3$ Hz, 1H), 4.55-4.48 (m, 1H), 4.45 (dt, $J = 8.5, 4.6$ Hz, 1H), 3.98 (t, $J = 6.5$ Hz, 2H), 2.97-2.74 (m, 5H), 2.71-2.62 (m, 1H), 1.69 (p, $J = 6.4$ Hz, 2H), 1.45-1.33 (m, 2H), 1.36-1.19 (m, 16H), 0.85 (t, $J = 6.8$ Hz, 3H) ppm; $[\alpha]_D^{20} = -27.1^\circ$ (C = 0.8, DMSO).

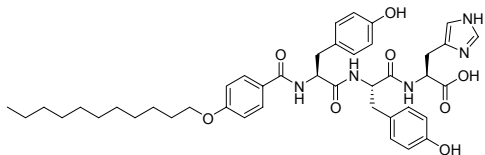
Analytical data of compound 351



Peptide **351** was synthesized and released from solid support according to **GP 2** and **GP 3**. **Yield** = 15 %; **Purity** > 95% (LC_MS); **LC-MS** (C4, ESI_MS) 889.4 [M+H]⁺, 911.5 [M+Na]⁺; $R_t = 8.45$ min; **¹H NMR** (400 MHz, DMSO- D_6): $\delta = 9.17$ (s, 1H), 9.11 (s, 2H), 8.84 (s, 1H), 8.33 (d, $J = 8.3$ Hz, 1H), 8.06 (d, $J = 7.5$ Hz, 1H), 7.96 (d, $J = 7.9$ Hz, 1H), 7.85 (t, $J = 5.77, 5.77$ Hz, 1H), 7.74 (d, $J = 8.8$ Hz, 2H), 7.61 (d, $J = 15.7$ Hz, 2H), 7.03 (d, $J = 8.5$ Hz, 2H), 6.97 (d, $J = 8.5$ Hz, 2H), 6.95 (d, $J = 1.2$ Hz, 2H), 6.93 (s, 2H), 6.64 (d, $J = 8.4$ Hz, 2H), 6.59 (d, $J = 8.5$ Hz, 2H), 6.54 (d, $J = 8.5$ Hz, 2H), 4.51 (ddd, $J = 10.2, 8.0, 4.6$ Hz, 1H), 4.42 (dt, $J = 8.4, 8.4, 5.0$ Hz, 1H), 4.31 (q, $J = 7.4, 7.4, 7.4$ Hz, 1H), 4.04-3.96 (m, 5H), 2.98 (dq, $J = 13.8, 13.8, 13.7, 6.8$ Hz, 2H), 2.91-2.80 (m, 6H), 2.79-2.63 (m, 2H), 1.94-1.77 (m, 2H), 1.76-1.65 (m, 2H), 1.47-1.36 (m, 2H), 1.34-1.20 (m, 18H), 0.85 (t, $J = 6.8, 6.8$ Hz, 3H) ppm; **¹³C NMR** (100 MHz, DMSO-

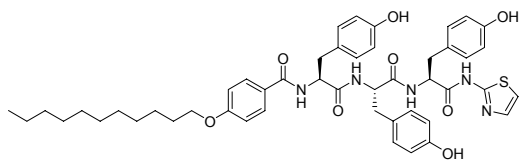
D₆): δ = 171.4, 170.7, 170.7, 165.8, 161.0, 155.7, 155.6, 155.5, 135.4, 130.0, 129.9, 129.9, 129.8, 129.1, 128.2, 127.3, 125.8, 121.5, 121.3, 120.7, 114.8, 114.7, 113.7, 67.5, 55.1, 54.5, 54.5, 54.1, 45.5, 36.6, 35.7, 34.9, 31.1, 29.4, 28.8, 28.6, 28.5, 28.4, 25.3, 21.9, 13.8 ppm; **HRMS** (FAB, *m*-NBA) *m/z* calc. for C₅₁H₆₄N₆O₈ 888.4786, found 889.4825 [M+H]⁺; $[\alpha]_D^{20}$ = - 16.6° (C = 0.9, DMSO).

Analytical data of compound 352



Peptide **352** was synthesized and released from solid support according to **GP 2** and **GP 3**. **Yield** = 9 %; **Purity** > 95% (LC_MS); **LC-MS** (C4, ESI_MS) 756.4 [M+H]⁺, 778.4 [M+Na]⁺; R_t = 8.64 min; **¹H NMR** (400 MHz, DMSO-D₆): δ = 9.10 (s, 1H), 8.66 (s, 1H), 8.37 (d, *J* = 8.5 Hz, 1H), 8.26 (d, *J* = 8.0 Hz, 1H), 7.94 (d, *J* = 8.1 Hz, 1H), 7.70 (d, *J* = 8.9 Hz, 2H), 7.25 (s, 1H), 7.02 (d, *J* = 8.4 Hz, 2H), 6.98 (d, *J* = 8.5 Hz, 1H), 6.94 (d, *J* = 8.9 Hz, 2H), 6.57 (d, *J* = 8.5 Hz, 2H), 6.54 (d, *J* = 8.5 Hz, 1H), 4.55-4.47 (m, 2H), 4.40 (dd, *J* = 12.7, 8.2 Hz, 1H), 3.99 (t, *J* = 6.5 Hz, 2H), 3.09 (dd, *J* = 15.1, 5.2 Hz, 1H), 2.96 (dd, *J* = 15.1, 7.9 Hz, 1H), 2.89 (t, *J* = 4.1 Hz, 1H), 2.85 (t, *J* = 4.3 Hz, 1H), 2.80-2.64 (m, 2H), 1.73-1.65 (m, 1H), 1.44-1.34 (m, 2H), 1.33-1.22 (m, 16H), 0.83 (t, *J* = 6.8 Hz, 3H) ppm; $[\alpha]_D^{20}$ = - 38.3° (C = 0.3, DMSO).

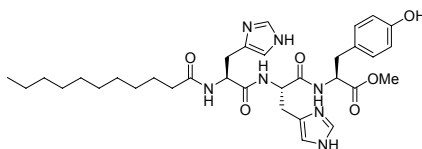
Analytical data of compound 353



Peptide **353** was synthesized and released from solid support according to **GP 2** and **GP 3**. **Yield** = 19 %; **Purity** > 95% (LC_MS); **LC-MS** (C4, ESI_MS) 864.3 [M+H]⁺, 886.4 [M+Na]⁺; R_t = 10.12 min; **¹H NMR** (400 MHz, DMSO-D₆): δ = 8.32 (d, *J* = 7.3 Hz, 1H), 8.28 (d, *J* = 8.4 Hz, 1H), 7.84 (d, *J* = 8.1 Hz, 1H), 7.72 (d, *J* = 8.7 Hz, 2H), 7.45 (d, *J* = 3.5 Hz, 1H), 7.20 (d, *J* = 3.5 Hz, 1H), 7.04 (d, *J* = 8.4 Hz, 2H), 6.94 (d, *J* = 8.4 Hz, 2H), 6.93 (d, *J* = 8.9 Hz, 2H), 6.62 (d, *J* = 8.3 Hz, 2H), 6.58 (d, *J* = 8.3 Hz, 2H), 6.47 (d, *J* = 8.3 Hz, 2H), 4.68 (dd, *J* = 14.5, 7.2 Hz, 1H),

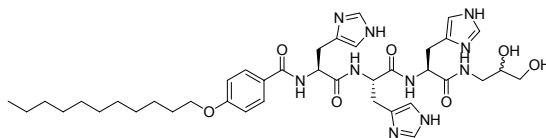
4.55-4.43 (m, 2H), 3.98 (t, $J = 6.4$ Hz, 2H), 2.97-2.92 (m, 1H), 2.89 (dd, $J = 13.9, 4.1$ Hz, 2H), 2.80 (dt, $J = 14.5, 14.1$ Hz, 2H), 2.67 (dd, $J = 14.1, 8.3$ Hz, 1H), 1.73-1.65 (m, 2H), 1.43-1.34 (m, 2H), 1.32-1.20 (m, 2H), 0.83 (t, $J = 6.6$ Hz, 3H) ppm; ^{13}C NMR (100 MHz, DMSO- D_6): $\delta = 171.2, 170.9, 170.0, 165.6, 160.9, 157.5, 155.8, 155.6, 155.4, 137.5, 130.1, 130.0, 129.9, 129.1, 128.4, 127.2, 126.8, 125.9, 114.8, 114.7, 114.6, 113.7, 113.7, 113.5, 67.5, 54.9, 54.3, 53.6, 36.6, 36.4, 35.7, 31.1, 28.8, 28.6, 28.6, 28.4, 25.3, 21.9, 13.8$ ppm; $[\alpha]_{\text{D}}^{20} = -14.8^\circ$ (C = 1.2, DMSO).

Analytical data of compound 354



Peptide **354** was synthesized and released from solid support according to **GP 2** and **GP 4**. **Yield** = 16 %; **Purity** > 95% (LC_MS); **LC-MS** (C4, ESI_MS) 638.3 $[\text{M}+\text{H}]^+$, 660.4 $[\text{M}+\text{Na}]^+$; $R_t = 5.77$ min; ^1H NMR (400 MHz, DMSO- D_6): $\delta = 8.88$ (s, 1H), 8.86 (s, 1H), 8.43 (d, $J = 7.3$ Hz, 1H), 8.24 (d, $J = 7.9$ Hz, 1H), 8.12 (d, $J = 7.9$ Hz, 1H), 7.26 (s, 1H), 7.21 (s, 1H), 6.97 (d, $J = 8.5$ Hz, 2H), 6.65 (d, $J = 8.5$ Hz, 2H), 4.59 (dt, $J = 8.0, 8.0, 5.7$ Hz, 1H), 4.52 (dt, $J = 8.4, 8.3, 5.7$ Hz, 1H), 4.40 (dd, $J = 14.0, 7.4$ Hz, 1H), 3.56 (s, 3H), 3.12-3.01 (m, 2H), 3.00-2.91 (m, 2H), 2.91-2.79 (m, 2H), 2.06 (t, $J = 7.5, 7.5$ Hz, 2H), 1.50-1.33 (m, 2H), 1.32-1.09 (m, 14H), 0.85 (t, $J = 6.8, 6.8$ Hz, 3H) ppm; ^{13}C NMR (100 MHz, DMSO- D_6): $\delta = 172.5, 171.5, 170.1, 169.8, 156.0, 133.8, 133.6, 133.6, 129.8, 129.6, 129.2, 126.6, 116.6, 115.0, 54.0, 51.7, 51.5, 51.3, 35.7, 35.0, 31.2, 28.9, 28.8, 28.6, 28.5, 28.4, 26.8, 26.7, 24.9, 21.9, 13.8$ ppm; **HRMS** (FAB, *m*-NBA) m/z calc. for $\text{C}_{33}\text{H}_{47}\text{N}_7\text{O}_6$ 637.3588, found 638.3646 $[\text{M}+\text{H}]^+$; $[\alpha]_{\text{D}}^{20} = -1.5^\circ$ (C = 1.1, DMSO).

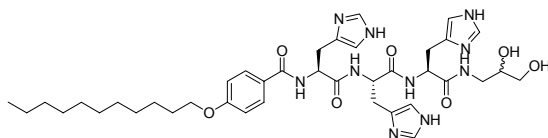
Analytical data of compound 355



Peptide **355** was synthesized and released from solid support according to **GP 2** and **GP 4**. **Yield** = 12 %; **Purity** > 95% (LC_MS); **LC-MS** (C4, ESI_MS) 777.3 $[\text{M}+\text{H}]^+$, 799.4 $[\text{M}+\text{Na}]^+$; $R_t = 7.64$ min; ^1H NMR (400 MHz, DMSO- D_6): $\delta = 8.89$ (s, 1H), 8.87 (s, 1H), 8.83 (s, 1H), 8.55 (d, J

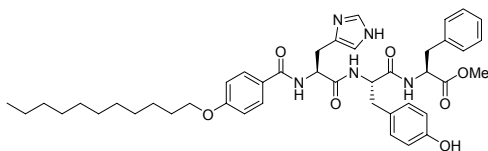
= 7.8 Hz, 1H), 8.33 (t, $J = 7.9, 7.9$ Hz, 2H), 8.06 (t, $J = 5.6, 5.6$ Hz, 1H), 7.77 (d, $J = 8.9$ Hz, 2H), 7.33 (s, 1H), 7.30 (s, 2H), 6.98 (d, $J = 8.9$ Hz, 2H), 4.72-4.65 (m, 1H), 4.61-4.51 (m, 2H), 4.01 (t, $J = 6.5, 6.5$ Hz, 2H), 3.56-3.41 (m, 2H), 3.33-3.21 (m, 2H), 3.21-3.16 (m, 1H), 3.17-3.06 (m, 3H), 3.06-2.92 (m, 3H), 1.82-1.59 (m, 2H), 1.46-1.36 (m, 2H), 1.35-1.20 (m, 14H), 0.85 (d, $J = 7.0$ Hz, 3H) ppm; **HRMS** (FAB, *m*-NBA) m/z calc. for $C_{39}H_{56}N_{10}O_7$ 776.4333, found 777.4422 $[M+H]^+$; $[\alpha]_D^{20} = -8.5^\circ$ (C = 0.4, DMSO).

Analytical data of compound 356



Peptide **356** was synthesized and released from solid support according to **GP 2** and **GP 4**. **Yield** = 13 %; **Purity** > 95% (LC_MS); **LC-MS** (C4, ESI_MS) 777.3 $[M+H]^+$; $R_t = 7.57$ min; **1H NMR** (400 MHz, DMSO- D_6): $\delta = 8.87$ (s, 1H), 8.86 (s, 1H), 8.80 (s, 1H), 8.55 (d, $J = 7.7$ Hz, 1H), 8.41-8.26 (m, 2H), 8.06 (t, $J = 5.5, 5.5$ Hz, 1H), 7.77 (d, $J = 8.8$ Hz, 2H), 7.32 (s, 1H), 7.30 (s, 2H), 6.98 (d, $J = 8.9$ Hz, 2H), 4.73-4.65 (m, 1H), 4.60-4.51 (m, 2H), 4.01 (t, $J = 6.5, 6.5$ Hz, 2H), 3.57-3.42 (m, 1H), 3.32-3.25 (m, 2H), 3.21-3.17 (m, 1H), 3.16-2.93 (m, 7H), 1.86-1.59 (m, 2H), 1.46-1.36 (m, 2H), 1.35-1.22 (m, 14H), 0.84 (t, $J = 7.0, 7.0$ Hz, 3H) ppm; **^{13}C NMR** (100 MHz, DMSO- D_6): $\delta = 170.5, 169.8, 169.7, 166.1, 161.2, 158.3, 133.8, 130.0, 129.2, 129.2, 125.4, 116.7, 116.6, 116.5, 113.8, 70.0, 69.9, 67.6, 63.4, 52.5, 52.4, 51.9, 42.1, 42.1, 31.1, 28.8, 28.6, 28.5, 28.4, 25.3, 21.9, 13.8$ ppm; **HRMS** (FAB, *m*-NBA) m/z calc. for $C_{39}H_{56}N_{10}O_7$ 776.4333, found 777.4413 $[M+H]^+$; $[\alpha]_D^{20} = -5.2^\circ$ (C = 0.8, DMSO).

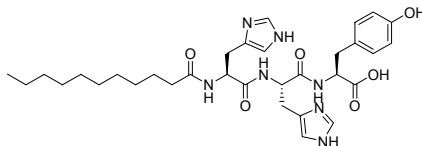
Analytical data of compound 357



Peptide **357** was synthesized and released from solid support according to **GP 2** and **GP 3**. **Yield** = 10 %; **Purity** > 95% (LC_MS); **LC-MS** (C4, ESI_MS) 754.3 $[M+H]^+$; $R_t = 8.93$ min; **1H NMR** (400 MHz, DMSO- D_6): $\delta = 9.14$ (s, 1H), 8.81 (s, 1H), 8.55 (d, $J = 7.5$ Hz, 1H), 8.43 (d, $J = 8.3$ Hz, 1H), 7.86 (d, $J = 7.9$ Hz, 1H), 7.77 (d, $J = 8.8$ Hz, 2H), 7.25 (d, $J = 6.4$ Hz, 2H), 7.21 (s, 2H),

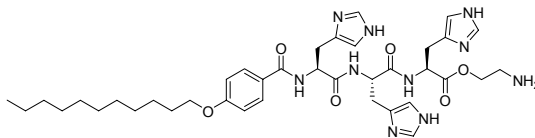
7.19 (s, 1H), 7.04-6.93 (m, 4H), 6.54 (d, $J = 8.5$ Hz, 2H), 4.73 (dt, $J = 9.1, 8.9, 5.3$ Hz, 1H), 4.54-4.41 (m, 2H), 4.02 (t, $J = 6.5, 6.5$ Hz, 2H), 3.57 (s, 3H), 3.14-2.99 (m, 3H), 2.96 (dd, $J = 13.9, 5.4$ Hz, 1H), 2.86 (dd, $J = 13.9, 4.3$ Hz, 1H), 2.68 (dd, $J = 14.0, 8.3$ Hz, 1H), 1.84-1.58 (m, 2H), 1.48-1.36 (m, 2H), 1.36-1.18 (m, 14H), 0.85 (t, $J = 6.8, 6.8$ Hz, 1H) ppm; ^{13}C NMR (100 MHz, DMSO- D_6): $\delta = 171.5, 170.9, 169.8, 165.8, 161.1, 155.6, 136.8, 130.0, 129.2, 128.9, 128.1, 127.1, 126.4, 125.5, 114.7, 113.7, 109.1, 67.6, 53.8, 53.5, 52.0, 51.7, 36.5, 31.1, 28.8, 28.6, 28.5, 28.4, 25.3, 21.9, 13.8$ ppm; HRMS (FAB, *m*-NBA) m/z calc. for $\text{C}_{43}\text{H}_{55}\text{N}_5\text{O}_7$ 753.4101, found 754.4174 $[\text{M}+\text{H}]^+$; $[\alpha]_{\text{D}}^{20} = -14.7^\circ$ ($C = 0.7$, DMSO).

Analytical data of compound 358



Peptide **358** was synthesized and released from solid support according to **GP 2** and **GP 4**. **Yield** = 16 %; **Purity** > 95% (LC_MS); **LC-MS** (C4, ESI_MS) 624.2 $[\text{M}+\text{H}]^+$, 646.4 $[\text{M}+\text{Na}]^+$; $R_t = 5.89$ min; ^1H NMR (400 MHz, DMSO- D_6): $\delta = 8.86$ (1H), 8.85 (1H), 8.25 (d, $J = 7.4$ Hz, 1H), 8.21 (d, $J = 7.9$ Hz, 1H), 8.12 (d, $J = 7.9$ Hz, 1H), 7.26 (s, 1H), 7.22 (s, 1H), 7.00 (d, $J = 8.4$ Hz, 2H), 6.64 (d, $J = 8.5$ Hz, 2H), 4.60 (dt, $J = 8.1, 8.0, 5.5$ Hz, 1H), 4.52 (dt, $J = 8.4, 8.3, 5.3$ Hz, 1H), 4.36 (dt, $J = 8.1, 8.0, 5.5$ Hz, 1H), 3.08 (dd, $J = 15.6, 5.1$ Hz, 1H), 1.45-1.35 (m, 2H), 1.33-1.05 (m, 14H), 0.85 (t, $J = 6.8, 6.8$ Hz, 3H) ppm; ^{13}C NMR (100 MHz, DMSO- D_6): $\delta = 172.5, 172.5, 170.1, 169.7, 155.9, 133.6, 133.6, 129.9, 129.6, 129.3, 127.0, 116.6, 114.9, 109.2, 53.9, 51.5, 51.4, 35.7, 35.0, 31.2, 28.9, 28.8, 28.6, 28.5, 28.4, 26.7, 26.7, 24.9, 21.9, 13.8$ ppm; HRMS (FAB, *m*-NBA) m/z calc. for $\text{C}_{32}\text{H}_{45}\text{N}_7\text{O}_6$ 623.3431, found 624.3506 $[\text{M}+\text{H}]^+$; $[\alpha]_{\text{D}}^{20} = +2.6^\circ$ ($C = 1.6$, DMSO).

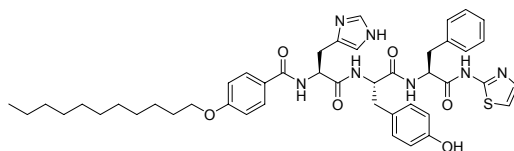
Analytical data of compound 359



Peptide **359** was synthesized and released from solid support according to **GP 2** and **GP 4**. **Yield** = 7 %; **Purity** > 95% (LC_MS); **LC-MS** (C4, ESI_MS) 747.2 $[\text{M}+\text{H}]^+$, 769.4 $[\text{M}+\text{Na}]^+$; $R_t = 6.65$

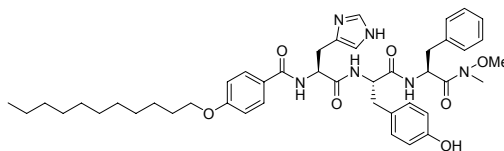
min; $^1\text{H NMR}$ (400 MHz, DMSO-D_6): $\delta = 8.85$ (s, 1H), 8.81 (s, 1H), 8.54 (t, $J = 6.5$ Hz, 1H), 8.37 (d, $J = 6.9$ Hz, 1H), 7.76 (s, 1H), 7.74 (s, 1H), 7.29 (s, 1H), 7.27 (s, 2H), 6.96 (d, $J = 8.9$ Hz, 2H), 4.66 (td, $J = 7.2, 5.2$ Hz, 1H), 4.55 (dt, $J = 8.1, 5.0$ Hz, 1H), 4.25 (t, $J = 5.2$ Hz, 1H), 3.99 (t, $J = 6.4$ Hz, 2H), 3.57-3.54 (m, 1H), 3.25-3.14 (m, 1H), 3.15-3.03 (m, 1H), 3.03-2.94 (m, 1H), 1.74-1.65 (m, 2H), 1.44-1.34 (m, 2H), 1.34-1.20 (m, 16H), 0.83 (t, $J = 6.8$ Hz, 3H) ppm; $[\alpha]_D^{20} = -19.2^\circ$ ($C = 0.4$, DMSO).

Analytical data of compound 360



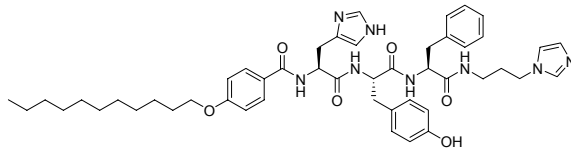
Peptide **360** was synthesized and released from solid support according to **GP 2** and **GP 3**. **Yield** = 4 %; **Purity** > 95% (LC_MS); **LC-MS** (C4, ESI_MS) 822.3 $[\text{M}+\text{H}]^+$; $R_t = 8.32$ min; $^1\text{H NMR}$ (400 MHz, DMSO-D_6): $\delta = 8.92$ (d, $J = 1.3$ Hz, 1H), 8.53 (d, $J = 7.3$ Hz, 1H), 8.48 (d, $J = 8.2$ Hz, 1H), 7.83 (d, $J = 8.2$ Hz, 1H), 7.77 (d, $J = 8.9$ Hz, 2H), 7.46 (d, $J = 3.5$ Hz, 1H), 7.34-7.21 (m, 7H), 7.21-7.13 (m, 1H), 6.96 (d, $J = 8.9$ Hz, 2H), 6.92 (d, $J = 8.5$ Hz, 2H), 6.44 (d, $J = 8.5$ Hz, 2H), 4.95-4.63 (m, 2H), 4.45 (dt, $J = 8.4, 8.4, 4.3$ Hz, 1H), 4.00 (t, $J = 6.5, 6.5$ Hz, 2H), 3.22-2.98 (m, 3H), 2.97-2.83 (m, 2H), 2.70 (dd, $J = 13.9, 8.4$ Hz, 1H), 1.75-1.64 (m, 2H), 1.47-1.34 (m, 2H), 1.34-1.13 (m, 16H), 0.82 (t, $J = 7.0, 7.0$ Hz, 3H) ppm; **HRMS** (FAB, *m*-NBA) *m/z* calc. for $\text{C}_{45}\text{H}_{55}\text{N}_7\text{O}_6\text{S}$ 821.3935, found 822.3965 $[\text{M}+\text{H}]^+$; $[\alpha]_D^{20} = -6.6^\circ$ ($C = 0.3$, DMSO).

Analytical data of compound 361



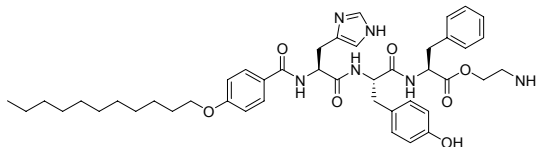
Peptide **361** was synthesized and released from solid support according to **GP 2** and **GP 3**. **Yield** = 4 %; **Purity** > 95% (LC_MS); **LC-MS** (C4, ESI_MS) 783.3 $[\text{M}+\text{H}]^+$; $R_t = 8.28$ min.

Analytical data of compound 362



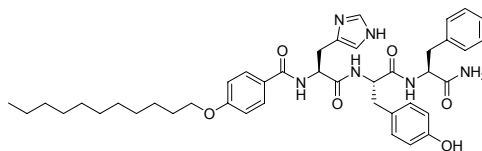
Peptide **362** was synthesized and released from solid support according to **GP 2** and **GP 3**. **Yield** = 4 %; **Purity** > 85% (LC_MS); **LC-MS** (C4, ESI_MS) 847.6 [M+H]⁺, 869.5 [M+Na]⁺; R_t = 6.94 min.

Analytical data of compound 363



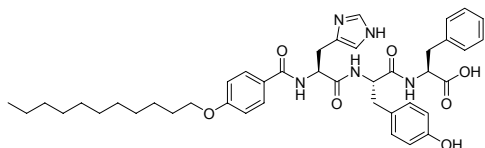
Peptide **363** was synthesized and released from solid support according to **GP 2** and **GP 3**. **Yield** = 1 %; **Purity** > 95% (LC_MS); **LC-MS** (C4, ESI_MS) 783.3 [M+H]⁺, 805.4 [M+Na]⁺; R_t = 7.79 min.

Analytical data of compound 364



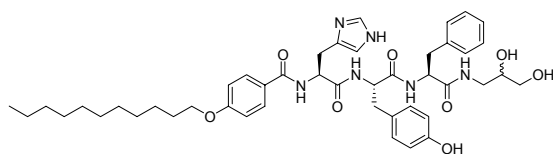
Peptide **364** was synthesized and released from solid support according to **GP 2** and **GP 3**. **Yield** = 3 %; **Purity** > 95% (LC_MS); **LC-MS** (C4, ESI_MS) 739.4 [M+H]⁺, 761.5 [M+Na]⁺; R_t = 8.01 min; ¹H NMR (400 MHz, DMSO-D₆): δ = 9.07 (s, 1H), 8.42 (d, *J* = 7.1 Hz, 1H), 8.14 (d, *J* = 7.8 Hz, 1H), 7.75 (d, *J* = 8.7 Hz, 2H), 7.28-7.12 (m, 7H), 7.06 (s, 1H), 6.97 (d, *J* = 8.9 Hz, 2H), 6.50 (d, *J* = 8.4 Hz, 2H), 4.67-4.59 (m, 1H), 4.46-4.30 (m, 2H), 4.00 (t, *J* = 6.3 Hz, 2H), 3.04-2.94 (m, 2H), 2.85-2.76 (m, 2H), 2.70-2.63 (m, 1H), 1.70 (p, *J* = 6.7 Hz, 2H), 1.44-1.35 (m, 2H), 1.34-1.21 (m, 16H), 0.83 (t, *J* = 6.7 Hz, 3H) ppm; [α]_D²⁰ = -13.0° (C = 0.2, DMSO).

Analytical data of compound 365



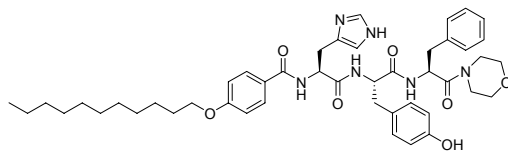
Peptide **365** was synthesized and released from solid support according to **GP 2** and **GP 3**. **Yield** = 8 %; **Purity** > 95% (LC_MS); **LC-MS** (C4, ESI_MS) 740.3 [M+H]⁺; R_t = 8.09 min; **¹H NMR** (500 MHz, DMSO-D₆): δ = 9.14 (d, *J* = 5.70 Hz, 1H), 8.39 (d, *J* = 7.6 Hz, 2H), 8.18 (t, *J* = 6.7, 6.7 Hz, 1H), 7.83 (s, 1H), 7.76 (d, *J* = 8.7 Hz, 2H), 7.58 (d, *J* = 8.7 Hz, 1H), 7.35-7.08 (m, 4H), 7.04-6.84 (m, 4H), 6.52 (d, *J* = 8.3 Hz, 2H), 4.64 (dd, *J* = 13.8, 8.0 Hz, 1H), 4.52-4.35 (m, 2H), 4.01 (t, *J* = 6.4, 6.4 Hz, 2H), 3.16-3.01 (m, 2H), 3.01-2.80 (m, 3H), 2.66 (dd, *J* = 14.3, 8.9 Hz, 1H), 1.86-1.60 (m, 2H), 1.49-1.36 (m, 2H), 1.36-1.15 (m, 16H), 0.85 (t, *J* = 6.8, 6.8 Hz, 3H) ppm; [α]_D²⁰ = + 16.3° (C = 0.6, DMSO).

Analytical data of compound 366



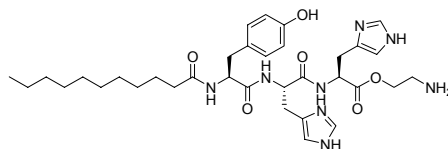
Peptide **366** was synthesized and released from solid support according to **GP 2** and **GP 3**. **Yield** = 9 %; **Purity** > 90% (LC_MS); **LC-MS** (C4, ESI_MS) 813.4 [M+H]⁺, 835.5 [M+Na]⁺; R_t = 8.47 min; **¹H NMR** (400 MHz, DMSO-D₆): δ = 9.12 (d, *J* = 5.5 Hz, 1H), 8.79-8.69 (m, 1H), 8.43 (d, *J* = 7.8 Hz, 1H), 8.22 (d, *J* = 8.2 Hz, 1H), 8.18-8.14 (m, 1H), 7.75 (d, *J* = 8.8 Hz, 2H), 7.57 (d, *J* = 8.8 Hz, 1H), 7.24-7.12 (m, 7H), 6.97 (d, *J* = 8.9 Hz, 2H), 6.90 (d, *J* = 8.4 Hz, 2H), 6.49 (d, *J* = 8.4 Hz, 2H), 4.71 (dt, *J* = 8.6 5.3 Hz, 1H), 4.57-4.45 (m, 1H), 4.39 (dt, *J* = 8.1 4.6 Hz, 1H), 4.00 (t, *J* = 6.4 Hz, 2H), 3.47-3.38 (m, 2H), 3.25 (dd, *J* = 5.5, 2.4 Hz, 1H), 3.24-3.20 (m, 2H), 3.19-3.13 (m, 1H), 3.07-2.94 (m, 3H), 2.85-2.74 (m, 2H), 2.70-2.62 (m, 1H), 1.70 (p, *J* = 6.8 Hz, 2H), 1.47-1.34 (m, 2H), 1.32-1.15 (m, 16H), 0.83 (t, *J* = 6.8 Hz, 3H) ppm; [α]_D²⁰ = - 6.5° (C = 0.7, DMSO).

Analytical data of compound 367



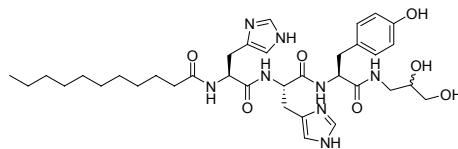
Peptide **367** was synthesized and released from solid support according to **GP 2** and **GP 3**. **Yield** = 5 %; **Purity** > 95% (LC_MS); **LC-MS** (C4, ESI_MS) 809.3 [M+H]⁺; R_t = 8.80 min.

Analytical data of compound 368



Peptide **368** was synthesized and released from solid support according to **GP 2** and **GP 4**. **Yield** = 3 %; **Purity** > 90% (LC_MS); **LC-MS** (C4, ESI_MS) 667.2 [M+H]⁺, 689.4 [M+Na]⁺; R_t = 5.39 min; ¹H NMR (400 MHz, DMSO-D₆): δ = 8.89 (s, 2H), 8.39 (d, *J* = 7.7 Hz, 1H), 8.34 (d, *J* = 8.0 Hz, 1H), 7.97 (d, *J* = 7.9 Hz, 1H), 7.30 (s, 1H), 7.28 (s, 1H), 6.97 (d, *J* = 8.5 Hz, 2H), 6.60 (d, *J* = 8.5 Hz, 2H), 4.66 (dd, *J* = 13.2, 7.8 Hz, 1H), 4.52 (dt, *J* = 8.4, 8.3, 5.4 Hz, 1H), 4.38-4.27 (m, 1H), 4.24 (t, *J* = 5.2, 5.2 Hz, 2H), 3.14-3.01 (m, 5H), 2.94 (dd, *J* = 15.0, 8.6 Hz, 1H), 2.78 (dd, *J* = 13.7, 4.0 Hz, 1H), 2.69-2.52 (m, 1H), 2.24-1.74 (m, 2H), 1.49-1.28 (m, 2H), 1.28-1.02 (m, 14H), 0.84 (t, *J* = 6.7, 6.7 Hz, 3H) ppm; **HRMS** (FAB, *m*-NBA) *m/z* calc. for C₃₄H₅₀N₈O₆ 666.3853, found 667.3948 [M+H]⁺; [α]_D²⁰ = -1.5° (C = 0.2, DMSO).

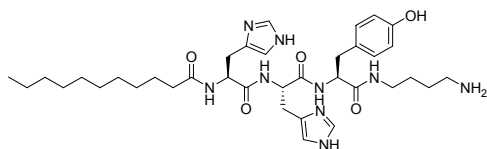
Analytical data of compound 369 (Two diastereoisomers)



Peptide **369** was synthesized and released from solid support according to **GP 2** and **GP 4**. **Yield** = 17 %; **Purity** > 95% (LC_MS); **LC-MS** (C4, ESI_MS) 697.3 [M+H]⁺, 719.5 [M+Na]⁺; R_t = 5.48 min; ¹H NMR (400 MHz, DMSO-D₆): δ = 8.68 (s, 1H), 8.65 (s, 1H), 7.24 (s, 1H), 7.16 (s, 1H), 7.02 (d, *J* = 8.49 Hz, 2H), 6.65 (d, *J* = 8.55 Hz, 2H), 4.59 (t, *J* = 6.3, 6.3 Hz, 1H), 4.54 (dd, *J* = 8.4, 6.2 Hz, 1H), 4.43 (ddd, *J* = 8.7, 6.4, 4.7 Hz, 1H), 3.65-3.53 (m, 1H), 3.48-3.29 (m, 2H), 3.22 (d, *J* = 5.6 Hz, 1H), 3.20-3.03 (m, 4H), 3.01-2.92 (m, 2H), 2.81 (dd, *J* = 13.9, 8.6 Hz, 1H),

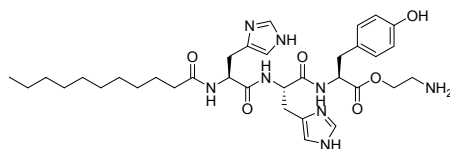
2.14 (t, $J = 7.9$, 7.9 Hz, 2H), 1.60-1.38 (m, 2H), 1.34-1.10 (m, 14H), 0.84 (t, $J = 6.9$, 6.9 Hz, 3H) ppm; ^{13}C NMR (100 MHz, DMSO- D_6): $\delta = 176.5$, 174.2, 172.4, 172.4, 171.6, 157.4, 135.1, 135.1, 135.1, 135.0, 131.4, 128.7, 128.7, 118.8, 118.4, 116.4, 116.4, 116.3, 71.9, 71.7, 64.9, 64.8, 56.9, 56.8, 53.7, 53.6, 43.5, 43.3, 38.1, 38.1, 36.7, 33.0, 30.7, 30.6, 30.4, 30.3, 28.2, 28.0, 28.0, 26.8, 23.7, 14.4 ppm; HRMS (FAB, *m*-NBA) m/z calc. for $\text{C}_{35}\text{H}_{52}\text{N}_8\text{O}_7$ 696.3959, found 697.4041 $[\text{M}+\text{H}]^+$.

Analytical data of compound 370



Peptide **370** was synthesized and released from solid support according to **GP 2** and **GP 4**. Yield = 13 %; Purity > 95% (LC_MS); LC-MS (C4, ESI_MS) 694.4 $[\text{M}+\text{H}]^+$, 716.5 $[\text{M}+\text{Na}]^+$; $R_t = 4.93$ min; ^1H NMR (400 MHz, DMSO- D_6): $\delta = 8.72$ (d, $J = 1.40$ Hz, 1H), 8.71 (d, $J = 1.39$ Hz, 1H), 7.24 (d, $J = 1.27$ Hz, 1H), 7.19 (d, $J = 1.27$ Hz, 1H), 7.02 (d, $J = 8.60$ Hz, 2H), 6.66 (d, $J = 8.6$ Hz, 2H), 4.60 (dd, $J = 7.4$, 5.8 Hz, 1H), 4.55 (dd, $J = 8.7$, 5.7 Hz, 1H), 4.40 (dd, $J = 8.1$, 6.9 Hz, 1H), 3.24-3.02 (m, 5H), 3.02-2.90 (m, 2H), 2.89-2.79 (m, 3H), 2.13 (t, $J = 8.1$, 8.1 Hz, 2H), 1.67-1.39 (m, 6H), 1.35-1.12 (m, 14H), 0.84 (t, $J = 6.9$, 6.9 Hz, 3H) ppm; ^{13}C NMR (100 MHz, DMSO- D_6): $\delta = 174.5$, 171.6, 170.4, 169.6, 155.4, 132.9, 132.9, 129.4, 129.0, 128.5, 126.7, 116.6, 116.4, 114.3, 54.9, 51.6, 51.6, 38.3, 37.5, 36.2, 34.6, 31.0, 28.6, 28.6, 28.4, 28.2, 25.9, 25.7, 25.1, 24.7, 23.7, 21.7, 12.4 ppm; HRMS (FAB, *m*-NBA) m/z calc. for $\text{C}_{36}\text{H}_{55}\text{N}_9\text{O}_5$ 693.4326, found 694.4418 $[\text{M}+\text{H}]^+$; $[\alpha]_D^{20} = -2.5^\circ$ ($C = 0.8$, DMSO).

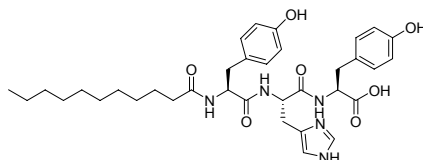
Analytical data of compound 371



Peptide **371** was synthesized and released from solid support according to **GP 2** and **GP 4**. Yield = 8 %; Purity > 95% (LC_MS); LC-MS (C4, ESI_MS) 667.3 $[\text{M}+\text{H}]^+$, 689.3 $[\text{M}+\text{Na}]^+$; $R_t = 5.00$ min; ^1H NMR (400 MHz, DMSO- D_6): $\delta = 8.82$ (s, 2H), 8.34 (d, $J = 7.6$ Hz, 1H), 8.25 (d, $J = 7.7$ Hz, 1H), 8.10 (d, $J = 7.8$ Hz, 1H), 7.22 (s, 1H), 7.19 (s, 1H), 6.97 (d, $J = 8.5$ Hz, 2H), 6.64 (d, J

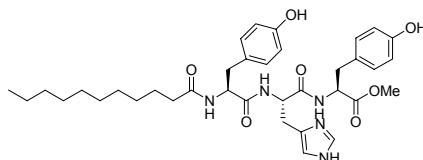
= 8.5 Hz, 2H), 4.56 (dt, $J = 8.2, 5.2$ Hz, 1H), 4.50 (dt, $J = 8.0, 4.2$ Hz, 1H), 4.25-4.11 (m, 2H), 3.07 (t, $J = 5.4$ Hz, 2H), 3.05-2.89 (m, 4H), 2.84 (dd, $J = 15.2, 9.2$ Hz, 2H), 2.04 (t, $J = 7.4$ Hz, 2H), 1.41-1.33 (m, 2H), 1.30-1.14 (m, 14H), 1.13-1.08 (m, 2H), 0.83 (t, $J = 6.8$ Hz, 3H) ppm; $[\alpha]_D^{20} = -1.6^\circ$ (C = 0.5, DMSO).

Analytical data of compound 372



Peptide **372** was synthesized and released from solid support according to **GP 2** and **GP 4**. **Yield** = 12 %; **Purity** > 95% (LC_MS); **LC-MS** (C4, ESI_MS) 650.3 [M+H]⁺, 672.3 [M+Na]⁺; $R_t = 6.90$ min; **¹H NMR** (400 MHz, DMSO-D₆): $\delta = 9.21$ (br s, 1H), 9.14 (br s, 1H), 8.80 (s, 1H), 8.25 (d, $J = 8.2$ Hz, 1H), 8.06 (d, $J = 7.5$ Hz, 1H), 7.94 (d, $J = 7.9$ Hz, 1H), 7.24 (s, 1H), 6.99 (d, $J = 8.4$ Hz, 2H), 6.98 (d, $J = 8.5$ Hz, 2H), 6.63 (d, $J = 8.5$ Hz, 2H), 6.60 (d, $J = 8.5$ Hz, 2H), 4.59 (dt, $J = 7.9, 7.6, 5.4$ Hz, 1H), 4.41-4.27 (m, 2H), 3.05 (dd, $J = 15.4, 5.3$ Hz, 1H), 2.96-2.85 (m, 2H), 2.85-2.74 (m, 2H), 2.58 (dd, $J = 13.8, 10.5$ Hz, 1H), 1.99 (dt, $J = 7.1, 6.9, 1.0$ Hz, 1H), 1.39-1.29 (m, 2H), 1.29-1.02 (m, 14H), 0.84 (t, $J = 6.8, 6.8$ Hz, 3H) ppm; **¹³C NMR** (100 MHz, DMSO-D₆): $\delta = 172.5, 172.4, 171.6, 169.6, 155.8, 155.6, 133.5, 129.9, 129.8, 129.4, 127.8, 127.0, 116.6, 114.9, 114.6, 54.2, 53.7, 51.2, 36.1, 35.7, 35.0, 31.1, 28.8, 28.8, 28.6, 28.5, 28.3, 27.0, 25.1, 21.9, 13.8$ ppm; **HRMS** (FAB, *m*-NBA) m/z calc. for C₃₅H₄₇N₅O₇ 649.3475, found 650.3561 [M+H]⁺; $[\alpha]_D^{20} = +13.1^\circ$ (C = 1.0, DMSO).

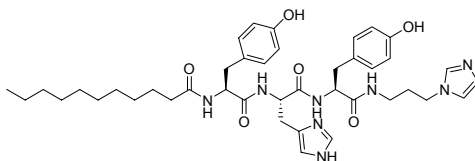
Analytical data of compound 373



Peptide **373** was synthesized and released from solid support according to **GP 2** and **GP 4**. **Yield** = 23 %; **Purity** > 95% (LC_MS); **LC-MS** (C4, ESI_MS) 664.3 [M+H]⁺, 686.3 [M+Na]⁺; $R_t = 7.00$ min; **¹H NMR** (400 MHz, DMSO-D₆): $\delta = 9.24$ (br s, 1H), 9.14 (br s, 1H), 8.92 (d, $J = 1.2$ Hz, 1H), 8.28 (d, $J = 8.1$ Hz, 1H), 8.26 (d, $J = 7.3$ Hz, 1H), 7.95 (d, $J = 7.9$ Hz, 1H), 7.27 (s, 1H),

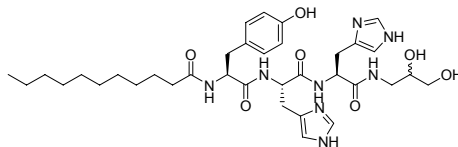
6.99 (d, $J = 8.5$ Hz, 2H), 6.95 (d, $J = 8.5$ Hz, 2H), 6.64 (d, $J = 8.5$ Hz, 2H), 6.60 (d, $J = 8.5$ Hz, 2H), 4.60 (dt, $J = 8.2, 8.2, 5.8$ Hz, 1H), 4.43-4.27 (m, 2H), 3.55 (s, 3H), 3.05 (dd, $J = 15.1, 5.6$ Hz, 1H), 2.95-2.81 (m, 3H), 2.78 (dd, $J = 14.2, 3.5$ Hz, 1H), 2.58 (dd, $J = 13.9, 10.3$ Hz, 1H), 2.00 (t, $J = 7.0, 7.0$ Hz, 2H), 1.49-1.29 (m, 2H), 1.29-1.01 (m, 14H), 0.83 (t, $J = 6.9, 6.9$ Hz, 3H) ppm; ^{13}C NMR (100 MHz, DMSO- D_6): $\delta = 172.4, 171.6, 171.5, 169.7, 155.9, 155.6, 133.5, 129.8, 129.0, 127.7, 126.6, 116.6, 114.9, 114.6, 54.3, 53.9, 51.7, 51.1, 36.1, 35.7, 35.0, 31.2, 28.8, 28.8, 28.6, 28.5, 28.4, 26.8, 25.1, 21.9, 13.8$ ppm; HRMS (FAB, *m*-NBA) m/z calc. for $\text{C}_{36}\text{H}_{49}\text{N}_5\text{O}_7$ 663.3632, found 664.3681 $[\text{M}+\text{H}]^+$; $[\alpha]_{\text{D}}^{20} = +13.1^\circ$ (C = 1.6, DMSO).

Analytical data of compound 374



Peptide **374** was synthesized and released from solid support according to **GP 2** and **GP 4**. Yield = 18 %; Purity > 95% (LC_MS); LC-MS (C4, ESI_MS) 757.4 $[\text{M}+\text{H}]^+$, 779.4 $[\text{M}+\text{Na}]^+$; $R_t = 6.07$ min; ^1H NMR (400 MHz, DMSO- D_6): $\delta = 8.92$ (s, 1H), 8.91 (d, $J = 1.0$ Hz, 2H), 8.29 (d, $J = 7.9$ Hz, 1H), 8.09 (t, $J = 5.7$ Hz, 1H), 8.02 (d, $J = 7.3$ Hz, 1H), 7.98 (d, $J = 7.8$ Hz, 1H), 7.65 (s, 1H), 7.62 (s, 1H), 7.27 (s, 1H), 6.99 (d, $J = 8.5$ Hz, 2H), 6.98 (d, $J = 8.5$ Hz, 2H), 6.63 (d, $J = 8.5$ Hz, 2H), 6.60 (d, $J = 8.5$ Hz, 2H), 4.55 (dt, $J = 8.1, 5.77$ Hz, 1H), 4.36-4.27 (m, 2H), 4.01 (t, $J = 7.0$ Hz, 2H), 3.09-2.99 (m, 2H), 2.98-2.89 (m, 2H), 2.86-2.73 (m, 4H), 2.59 (dd, $J = 13.8, 10.5$ Hz, 1H), 2.03-1.97 (m, 1H), 1.88-1.80 (m, 2H), 1.38-1.30 (m, 2H), 1.28-1.13 (m, 14H), 1.13-1.03 (m, 2H), 0.83 (t, $J = 6.9$ Hz, 3H) ppm; $[\alpha]_{\text{D}}^{20} = +6.6^\circ$ (C = 1.5, DMSO).

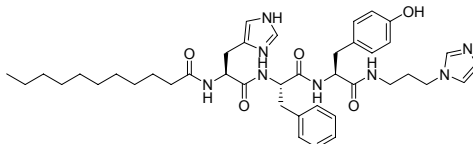
Analytical data of compound 375



Peptide **375** was synthesized and released from solid support according to **GP 2** and **GP 4**. Yield = 20 %; Purity > 95% (LC_MS); LC-MS (C4, ESI_MS) 697.4 $[\text{M}+\text{H}]^+$, 719.4 $[\text{M}+\text{Na}]^+$; $R_t = 5.85$ min; ^1H NMR (400 MHz, DMSO- D_6): $\delta = 8.90$ (s, 2H), 8.31 (d, $J = 8.0$ Hz, 1H), 8.21 (dd, $J =$

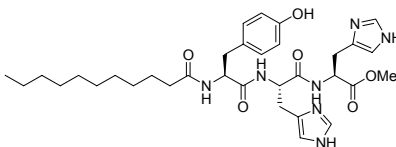
= 7.6, 2.9 Hz, 1H), 8.01 (t, $J = 5.1$ Hz, 1H), 7.95 (d, $J = 7.8$ Hz, 1H), 7.31 (s, 1H), 7.29 (s, 1H), 6.98 (d, $J = 8.5$ Hz, 2H), 6.60 (d, $J = 8.4$ Hz, 2H), 4.57-4.50 (m, 2H), 4.33 (ddd, $J = 11.6, 7.7, 3.9$ Hz, 1H), 3.50-3.43 (m, 1H), 3.31-3.19 (m, 3H), 3.12-3.04 (m, 2H), 3.01-2.91 (m, 3H), 2.79 (dd, $J = 14.0, 3.8$ Hz, 1H), 2.00 (dt, $J = 7.2, 2.7$ Hz, 2H), 1.37-1.29 (m, 2H), 1.27-1.13 (m, 14H), 1.11-1.04 (m, 2H), 0.84 (t, $J = 6.8$ Hz, 3H) ppm; $[\alpha]_D^{20} = +1.8^\circ$ (C = 1.6, DMSO).

Analytical data of compound 376



Peptide **376** was synthesized and released from solid support according to **GP 2** and **GP 4**. **Yield** = 32 %; **Purity** > 95% (LC_MS); **LC-MS** (C4, ESI_MS) 740.4 $[M+H]^+$, 763.4 $[M+Na]^+$; $R_t = 6.25$ min; **1H NMR** (400 MHz, DMSO- D_6): $\delta = 8.94$ (s, 1H), 8.90 (d, $J = 1.2$ Hz, 1H), 8.25 (d, $J = 7.7$ Hz, 1H), 8.07 (d, $J = 8.2$ Hz, 1H), 7.97 (t, $J = 5.7$ Hz, 1H), 7.93 (d, $J = 7.8$ Hz, 1H), 7.66 (s, 1H), 7.63 (s, 1H), 7.21-7.13 (m, 6H), 7.00 (d, $J = 8.5$ Hz, 2H), 6.63 (d, $J = 8.4$ Hz, 2H), 4.58-4.52 (m, 1H), 4.52-4.47 (m, 1H), 4.33 (q, $J = 7.4$ Hz, 1H), 4.00 (dt, $J = 6.8, 1.45$ Hz, 2H), 3.05-2.92 (m, 4H), 2.86-2.70 (m, 4H), 2.02 (t, $J = 7.4$ Hz, 2H), 1.88-1.79 (m, 2H), 1.36 (p, $J = 7.3$ Hz, 2H), 1.27-1.15 (m, 14H), 1.13-1.08 (m, 2H), 0.83 (t, $J = 6.8$ Hz, 3H) ppm; $[\alpha]_D^{20} = -8.4^\circ$ (C = 3.3, DMSO).

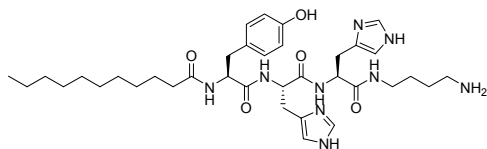
Analytical data of compound 377



Peptide **377** was synthesized and released from solid support according to **GP 2** and **GP 4**. **Yield** = 5 %; **Purity** > 90% (LC_MS); **LC-MS** (C4, ESI_MS) 638.4 $[M+H]^+$, 660.4 $[M+Na]^+$; $R_t = 6.03$ min; **1H NMR** (400 MHz, DMSO- D_6): $\delta = 8.86$ (s, 1H), 8.78 (s, 1H), 8.48 (d, $J = 7.8$ Hz, 1H), 8.30 (d, $J = 7.8$ Hz, 1H), 7.94 (d, $J = 7.8$ Hz, 1H), 7.31 (s, 1H), 7.27 (s, 1H), 6.98 (d, $J = 8.5$ Hz, 2H), 6.60 (d, $J = 8.5$ Hz, 2H), 4.57 (dt, $J = 7.7, 5.2$ Hz, 1H), 4.52 (dd, $J = 7.9, 2.1$ Hz, 1H), 4.33 (ddd, $J = 11.8, 7.6, 4.3$ Hz, 1H), 3.60 (s, 3H), 3.12 (dd, $J = 15.4, 5.5$ Hz, 2H), 3.03 (dd, $J = 15.7, 6.6$ Hz, 2H), 2.93 (dd, $J = 14.7, 7.3$ Hz, 1H), 2.79 (dd, $J = 13.9, 3.8$ Hz, 1H), 2.00 (dt, $J = 7.3,$

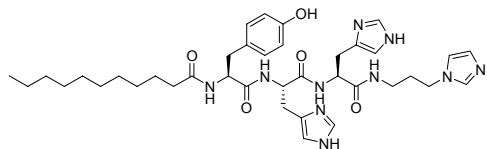
2.7 Hz, 2H), 1.38-1.29 (m, 2H), 1.28-1.13 (m, 14H), 1.11-1.05 (m, 2H), 0.84 (t, $J = 6.9$ Hz, 3H) ppm; $[\alpha]_D^{20} = -5.0^\circ$ (C = 0.4, DMSO).

Analytical data of compound 378



Peptide **378** was synthesized and released from solid support according to **GP 2** and **GP 4**. **Yield** = 20 %; **Purity** > 95% (LC_MS); **LC-MS** (C4, ESI_MS) 694.4 [M+H]⁺, 716.5 [M+Na]⁺; $R_t = 5.36$ min; **¹H NMR** (400 MHz, DMSO-D₆): $\delta = 8.94$ (s, 2H), 8.37 (d, $J = 7.5$ Hz, 1H), 8.24 (d, $J = 7.7$ Hz, 1H), 8.10 (t, $J = 5.5, 5.5$ Hz, 1H), 7.99 (d, $J = 7.7$ Hz, 1H), 7.84 (br s, 2H), 7.32 (s, 1H), 7.30 (s, 1H), 6.99 (d, $J = 8.48$ Hz, 2H), 6.61 (d, $J = 8.44$ Hz, 2H), 4.54 (dd, $J = 13.2, 7.7$ Hz, 1H), 4.49 (dd, $J = 13.4, 7.5$ Hz, 1H), 4.37-4.28 (m, 1H), 3.18-2.91 (m, 6H), 2.89-2.71 (m, 3H), 2.58 (dd, $J = 14.2, 10.1$ Hz, 1H), 2.01 (dt, $J = 7.2, 7.0, 3.0$ Hz, 2H), 1.55-1.45 (m, 2H), 1.45-1.38 (m, 2H), 1.38-1.30 (m, 2H), 1.29-1.02 (m, 14H), 0.85 (t, $J = 6.8, 6.8$ Hz, 3H) ppm; **¹³C NMR** (100 MHz, DMSO-D₆): $\delta = 172.6, 172.0, 169.7, 169.5, 158.6, 155.7, 133.7, 133.6, 129.8, 129.3, 129.2, 127.7, 116.7, 114.7, 54.4, 51.9, 51.7, 38.3, 38.0, 36.0, 35.0, 31.2, 28.9, 28.8, 28.6, 28.6, 28.4, 26.9, 26.4, 25.7, 25.0, 24.3, 22.0, 13.8$ ppm; **HRMS** (FAB, *m*-NBA) m/z calc. for C₃₆H₅₅N₉O₅ 693.4326, found 694.4382 [M+H]⁺; $[\alpha]_D^{20} = -1.1^\circ$ (C = 1.6, DMSO).

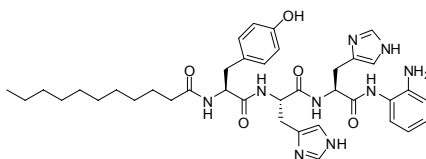
Analytical data of compound 379



Peptide **379** was synthesized and released from solid support according to **GP 2** and **GP 4**. **Yield** = 16 %; **Purity** > 95% (LC_MS); **LC-MS** (C4, ESI_MS) 731.4 [M+H]⁺, 753.4 [M+Na]⁺; $R_t = 5.40$ min; **¹H NMR** (400 MHz, DMSO-D₆): $\delta = 9.03$ (s, 1H), 8.94 (s, 2H), 8.39 (d, $J = 7.9$ Hz, 1H), 8.28 (d, $J = 7.7$ Hz, 1H), 8.16 (t, $J = 5.6, 5.6$ Hz, 1H), 7.99 (d, $J = 7.4$ Hz, 1H), 7.72 (t, $J = 1.5, 1.5$ Hz, 1H), 7.66 (t, $J = 1.4, 1.4$ Hz, 1H), 7.33 (s, 1H), 7.29 (s, 1H), 6.96 (d, $J = 8.5$ Hz, 2H), 6.59 (d, $J = 8.5$ Hz, 2H), 4.52 (dt, $J = 8.1, 8.0, 5.3$ Hz, 1H), 4.45 (dt, $J = 8.0, 7.9, 5.9$ Hz, 1H), 4.35-4.25 (m, 1H), 4.13 (t, $J = 7.1, 7.1$ Hz, 2H), 3.43-2.88 (m, 6H), 2.77 (dd, $J = 13.7, 4.5$ Hz,

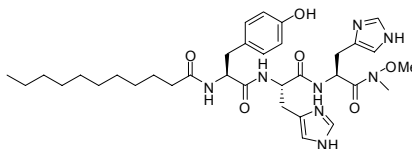
1H), 2.57 (dd, $J = 14.0, 10.5$ Hz, 1H), 2.10-1.96 (m, 2H), 1.96-1.86 (m, 2H), 1.40-1.28 (m, 2H), 1.28-1.00 (m, 14H), 0.83 (t, $J = 6.9, 6.9$ Hz, 3H) ppm; ^{13}C NMR (100 MHz, DMSO- D_6): $\delta = 172.7, 172.0, 169.9, 169.7, 155.6, 135.3, 133.7, 133.6, 129.7, 129.3, 129.2, 127.6, 121.7, 120.1, 116.7, 116.6, 114.6, 54.5, 52.1, 51.7, 45.8, 35.9, 35.2, 35.0, 31.1, 29.3, 28.8, 28.8, 28.6, 28.5, 28.4, 26.6, 26.3, 25.0, 21.9, 13.8$ ppm; HRMS (FAB, *m*-NBA) m/z calc. for $\text{C}_{38}\text{H}_{54}\text{N}_{10}\text{O}_5$ 730.4279, found 731.4353 $[\text{M}+\text{H}]^+$; $[\alpha]_{\text{D}}^{20} = -3.0^\circ$ ($C = 1.3$, DMSO).

Analytical data of compound 380



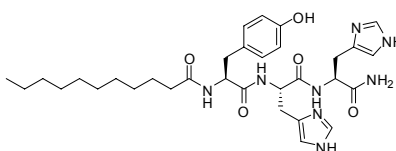
Peptide **380** was synthesized and released from solid support according to **GP 2** and **GP 4**. Yield = 3 %; Purity > 95% (LC_MS); LC-MS (C4, ESI_MS) 714.3 $[\text{M}+\text{H}]^+$, 736.3 $[\text{M}+\text{Na}]^+$; $R_t = 6.15$ min.

Analytical data of compound 381



Peptide **381** was synthesized and released from solid support according to **GP 2** and **GP 4**. Yield = 1 %; Purity > 95% (LC_MS); LC-MS (C4, ESI_MS) 667.3 $[\text{M}+\text{H}]^+$, 689.3 $[\text{M}+\text{Na}]^+$; $R_t = 5.92$ min

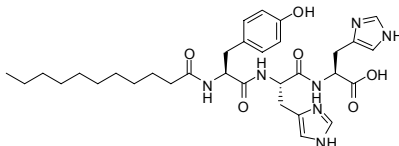
Analytical data of compound 382



Peptide **382** was synthesized and released from solid support according to **GP 2** and **GP 4**. Yield = 4 %; Purity > 85% (LC_MS); LC-MS (C4, ESI_MS) 623.4 $[\text{M}+\text{H}]^+$, 645.4 $[\text{M}+\text{Na}]^+$; $R_t = 5.90$ min; ^1H NMR (400 MHz, DMSO- D_6): $\delta = 8.87$ (s, 1H), 8.83 (s, 1H), 8.30 (d, $J = 7.6$ Hz, 1H),

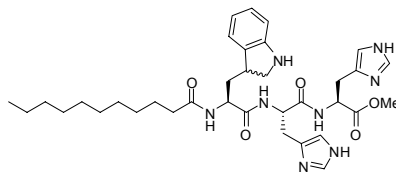
8.16 (d, $J = 7.7$ Hz, 1H), 7.97 (d, $J = 7.5$ Hz, 1H), 7.49 (s, 1H), 7.29 (s, 1H), 7.28 (s, 1H), 6.98 (d, $J = 8.5$ Hz, 2H), 6.60 (d, $J = 8.4$ Hz, 2H), 4.54-4.47 (m, 1H), 4.45 (dt, $J = 8.0, 5.4$ Hz, 1H), 4.32 (ddd, $J = 11.6, 7.9, 4.0$ Hz, 1H), 3.15-3.04 (m, 3H), 2.99-2.90 (m, 2H), 2.79 (dd, $J = 14.3, 4.3$ Hz, 1H), 2.00 (dt, $J = 7.5, 3.5$ Hz, 2H), 1.39-1.29 (m, 2H), 1.26-1.12 (m, 14H), 1.10-1.05 (m, 2H), 0.84 (t, $J = 6.9$ Hz, 3H) ppm; $[\alpha]_D^{20} = +10.0^\circ$ (C = 0.3, DMSO).

Analytical data of compound 383



Peptide **383** was synthesized and released from solid support according to **GP 2** and **GP 4**. **Yield** = 8 %; **Purity** > 85% (LC_MS); **LC-MS** (C4, ESI_MS) 624.3 $[M+H]^+$, 646.3 $[M+Na]^+$; $R_t = 6.23$ min; **1H NMR** (400 MHz, DMSO- D_6): $\delta = 8.78$ (s, 1H), 8.76 (s, 1H), 8.35 (d, $J = 7.9$ Hz, 1H), 8.23 (d, $J = 8.0$ Hz, 1H), 7.95 (d, $J = 7.9$ Hz, 1H), 7.29 (s, 1H), 7.25 (s, 1H), 6.99 (d, $J = 8.4$ Hz, 2H), 6.60 (d, $J = 8.4$ Hz, 2H), 4.55-4.46 (m, 2H), 4.37-4.30 (m, 1H), 3.14 (dd, $J = 15.0, 4.8$ Hz, 1H), 3.10 (dd, $J = 10.8, 5.0$ Hz, 1H), 3.03 (dd, $J = 16.8, 7.0$ Hz, 1H), 2.99 (dd, $J = 15.1, 8.2$ Hz, 1H), 2.95 (dd, $J = 15.2, 8.0$ Hz, 1H), 2.80 (dd, $J = 13.9, 3.8$ Hz, 1H), 1.99 (dt, $J = 7.2, 2.9$ Hz, 2H), 1.38-1.29 (m, 2H), 1.28-1.11 (m, 14H), 1.11-1.05 (m, 2H), 0.84 (t, $J = 6.8$ Hz, 3H) ppm; $[\alpha]_D^{20} = +1.5^\circ$ (C = 0.6, DMSO).

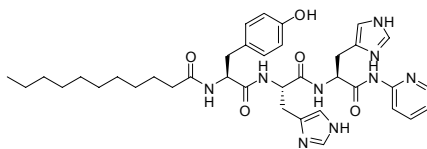
Analytical data of compound 384



Peptide **384** was synthesized and released from solid support according to **GP 2** and **GP 4**. **Yield** = 5 %; **Purity** > 90% (LC_MS); **LC-MS** (C4, ESI_MS) 663.4 $[M+H]^+$, 685.4 $[M+Na]^+$; $R_t = 5.77$ min; **1H NMR** (400 MHz, DMSO- D_6): $\delta = 8.99$ (d, $J = 1.3$ Hz, 1H), 8.98 (d, $J = 1.3$ Hz, 1H), 8.95 (d, $J = 1.3$ Hz, 1H), 8.94 (d, $J = 1.3$ Hz, 1H), 8.54 (dd, $J = 7.7, 4.6$ Hz, 1H), 8.38 (t, $J = 7.8$ Hz, 1H), 8.16 (dd, $J = 12.2, 7.4$ Hz, 1H), 7.39 (d, $J = 2.7$ Hz, 1H), 7.33-7.31 (m, 2H), 7.07-7.01 (m, 2H), 6.80-6.71 (m, 2H), 4.64-4.52 (m, 2H), 4.34-4.27 (m, 1H), 3.26-2.93 (m, 7H), 2.22-2.08

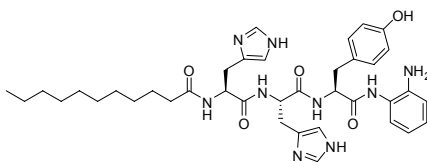
(m, 2H), 2.03-1.88 (m, 1H), 1.73-1.62 (m, 1H), 1.54-1.46 (m, 2H), 1.29-1.18 (m, 16H), 0.87-0.81 (m, 3H) ppm; $[\alpha]_D^{20} = -7.7^\circ$ (C = 0.4, DMSO).

Analytical data of compound 385



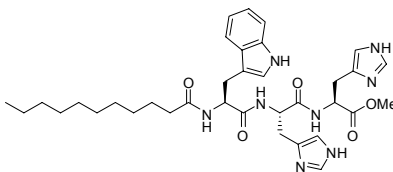
Peptide **385** was synthesized and released from solid support according to **GP 2** and **GP 4**. **Yield** = 11 %; **Purity** > 85% (LC_MS); **Purity** > 95% (LC_MS); **LC-MS** (C4, ESI_MS) 700.3 [M+H]⁺, 722.1 [M+Na]⁺; R_t = 6.09 min; **¹H NMR** (400 MHz, DMSO-D₆): δ = 8.90-8.87 (m, 2H), 8.36 (t, *J* = 7.6 Hz, 1H), 8.28 (d, *J* = 7.9 Hz, 1H), 7.99 (d, *J* = 8.3 Hz, 1H), 7.94 (d, *J* = 7.1 Hz, 1H), 7.82-7.73 (m, 1H), 7.34 (d, *J* = 7.9 Hz, 1H), 7.29 (d, *J* = 5.7 Hz, 1H), 7.16-7.09 (m, 1H), 6.98 (d, *J* = 8.5 Hz, 2H), 6.60 (d, *J* = 7.4 Hz, 2H), 4.59 (dd, *J* = 8.0, 5.6 Hz, 1H), 4.56-4.49 (m, 1H), 4.37-4.30 (m, 1H), 3.21-3.12 (m, 2H), 3.11-3.05 (m, 1H), 3.04-2.91 (m, 2H), 2.83-2.76 (m, 1H), 2.03-1.97 (m, 2H), 1.38-1.30 (m, 2H), 1.28-1.14 (m, 14H), 1.11-1.04 (m, 2H), 0.86-0.82 (m, 3H) ppm; $[\alpha]_D^{20} = +3.1^\circ$ (C = 0.6, DMSO).

Analytical data of compound 386



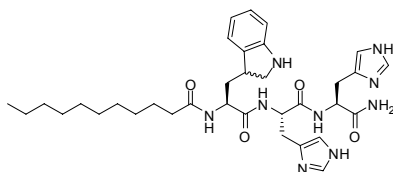
Peptide **386** was synthesized and released from solid support according to **GP 2** and **GP 4**. **Yield** = 23 %; **Purity** > 85% (LC_MS); **LC-MS** (C4, ESI_MS) 714.4 [M+H]⁺, 736.3 [M+Na]⁺; R_t = 5.89 min; **¹H NMR** (400 MHz, DMSO-D₆): δ = 8.94 (s, 1H), 8.93 (s, 1H), 8.25 (dd, *J* = 7.3, 3.1 Hz, 1H), 8.15 (dd, *J* = 12.4, 7.9 Hz, 1H), 7.61 (dd, *J* = 6.0, 3.1 Hz, 1H), 7.33-7.24 (m, 3H), 7.06 (d, *J* = 8.5 Hz, 1H), 6.97 (d, *J* = 8.5 Hz, 2H), 6.59 (d, *J* = 8.5 Hz, 2H), 4.60 (dt, *J* = 7.7, 5.9 Hz, 1H), 4.56-4.49 (m, 2H), 3.25 (dd, *J* = 13.8, 6.5 Hz, 1H), 3.17-2.99 (m, 3H), 2.86 (dd, *J* = 15.4, 9.7 Hz, 2H), 2.04 (dt, *J* = 7.8, 2.1 Hz, 2H), 1.41-1.33 (m, 2H), 1.28-1.15 (m, 14H), 1.13-1.09 (m, 2H), 0.85-0.81 (m, 3H) ppm; $[\alpha]_D^{20} = +4.5^\circ$ (C = 2.1, DMSO).

Analytical data of compound 387



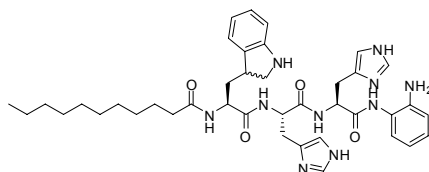
Peptide **387** was synthesized and released from solid support according to **GP 2** and **GP 4**. **Yield** = 1 %; **Purity** > 95% (LC_MS); **LC-MS** (C4, ESI_MS) 661.3 [M+H]⁺, 683.4 [M+Na]⁺; R_t = 6.43 min.

Analytical data of compound 388



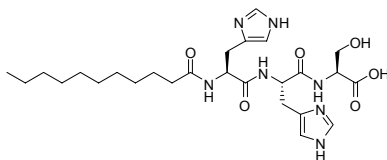
Peptide **388** was synthesized and released from solid support according to **GP 2** and **GP 4**. **Yield** = 4 %; **Purity** > 95% (LC_MS); **LC-MS** (C4, ESI_MS) 648.3 [M+H]⁺, 670.3 [M+Na]⁺; R_t = 5.67 min.

Analytical data of compound 389



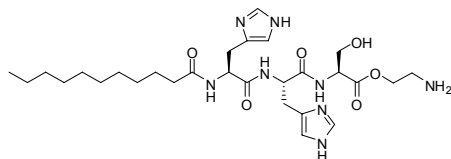
Peptide **389** was synthesized and released from solid support according to **GP 2** and **GP 4**. **Yield** = 13 %; **Purity** > 95% (LC_MS); **LC-MS** (C4, ESI_MS) 739.4 [M+H]⁺, 761.4 [M+Na]⁺; R_t = 5.99 min; **¹H NMR** (400 MHz, DMSO-D₆): δ = 8.91 (dd, *J* = 5.4, 1.3 Hz, 1H), 8.36-8.30 (m, 1H), 8.19 (dd, *J* = 12.0, 7.4 Hz, 1H), 7.59-7.54 (m, 2H), 7.36-7.29 (m, 3H), 7.25-7.21 (m, 2H), 7.06-7.00 (m, 2H), 6.79-6.72 (m, 2H), 5.41 (dd, *J* = 14.4, 7.7 Hz, 1H), 4.58 (dt, *J* = 8.0, 5.3 Hz, 1H), 4.34-4.26 (m, 1H), 3.52-3.42 (m, 2H), 3.33-3.20 (m, 2H), 3.19-3.10 (m, 2H), 3.03 (dd, *J* = 15.0, 8.2 Hz, 1H), 2.20-2.07 (m, 2H), 2.05-1.93 (m, 1H), 1.74-1.65 (m, 1H), 1.53-1.42 (m, 2H), 1.25-1.16 (m, 16H), 0.84-0.79 (m, 3H) ppm.

Analytical data of compound 390



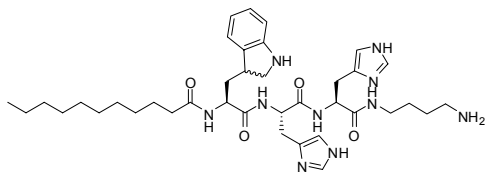
Peptide **390** was synthesized and released from solid support according to **GP 2** and **GP 4**. **Yield** = 18 %; **Purity** > 95% (LC_MS); **LC-MS** (C4, ESI_MS) 548.2 [M+H]⁺, 576.2 [M+Na]⁺; R_t = 5.83 min; **¹H NMR** (400 MHz, DMSO-D₆): δ = 8.86 (d, *J* = 1.2 Hz, 1H), 8.85 (d, *J* = 1.2 Hz, 1H), 8.24 (d, *J* = 7.7 Hz, 1H), 8.19 (d, *J* = 7.9 Hz, 1H), 8.14 (d, *J* = 7.8 Hz, 1H), 7.29 (s, 1H), 7.26 (s, 1H), 4.66 (dt, *J* = 8.0, 5.2 Hz, 1H), 4.52 (dt, *J* = 8.4, 5.7 Hz, 1H), 4.26 (td, *J* = 7.8, 4.4 Hz, 1H), 3.74 (dd, *J* = 10.9, 5.1 Hz, 1H), 3.63 (dd, *J* = 10.9, 3.8 Hz, 1H), 3.11 (dd, *J* = 15.4, 5.2 Hz, 1H), 3.02 (dd, *J* = 15.2, 5.5 Hz, 1H), 2.96 (dd, *J* = 15.3, 8.1 Hz, 1H), 2.87 (dd, *J* = 15.2, 8.6 Hz, 1H), 2.05 (t, *J* = 7.5 Hz, 2H), 1.42-1.34 (m, 2H), 1.30-1.15 (m, 14H), 1.15-1.10 (m, 2H), 0.83 (t, *J* = 6.8 Hz, 3H) ppm; [α]_D²⁰ = - 3.7° (C = 1.5, DMSO).

Analytical data of compound 391



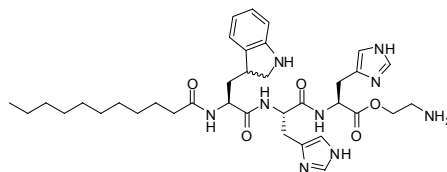
Peptide **391** was synthesized and released from solid support according to **GP 2** and **GP 4**. **Yield** = 13 %; **Purity** > 95% (LC_MS); **LC-MS** (C4, ESI_MS) 591.3 [M+H]⁺, 613.3 [M+Na]⁺; R_t = 4.92 min; **¹H NMR** (400 MHz, DMSO-D₆): δ = 8.92 (d, *J* = 1.1 Hz, 1H), 8.90 (d, *J* = 1.2 Hz, 1H), 8.36 (d, *J* = 7.7 Hz, 1H), 8.26 (d, *J* = 8.0 Hz, 1H), 8.16 (d, *J* = 7.8 Hz, 1H), 7.30 (s, 1H), 7.27 (s, 1H), 4.67 (dt, *J* = 8.4, 5.2 Hz, 1H), 4.52 (dt, *J* = 8.5, 5.3 Hz, 1H), 4.44 (td, *J* = 8.3, 4.2 Hz, 1H), 4.28-4.16 (m, 2H), 3.83 (dd, *J* = 11.1, 4.9 Hz, 1H), 3.65 (dd, *J* = 11.1, 3.9 Hz, 1H), 3.16-3.07 (m, 5H), 3.03 (dd, *J* = 15.3, 5.0 Hz, 1H), 2.96 (dd, *J* = 15.6, 8.7 Hz, 1H), 2.87 (dd, *J* = 15.1, 9.4 Hz, 1H), 2.05 (t, *J* = 7.5 Hz, 2H), 1.42-1.33 (m, 2H), 1.28-1.17 (m, 14H), 1.15-1.08 (m, 2H), 0.83 (t, *J* = 6.8 Hz, 3H) ppm; [α]_D²⁰ = - 3.1° (C = 1.2, DMSO).

Analytical data of compound 392



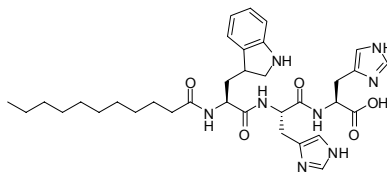
Peptide **392** was synthesized and released from solid support according to **GP 2** and **GP 4**. **Yield** = 18 %; **Purity** > 95% (LC_MS); **LC-MS** (C4, ESI_MS) 719.5 [M+H]⁺, 741.5 [M+Na]⁺; R_t = 5.27 min; ¹H NMR (400 MHz, DMSO-D₆): δ = 8.95 (dd, *J* = 2.3, 1.4 Hz, 1H), 8.91 (dd, *J* = 7.5, 1.3 Hz, 1H), 8.35 (dd, *J* = 7.4, 4.5 Hz, 1H), 8.25 (dd, *J* = 10.5, 7.7 Hz, 1H), 8.17 (dd, *J* = 13.3, 7.5 Hz, 1H), 8.04 (t, *J* = 5.5 Hz, 1H), 7.37-7.24 (m, 4H), 7.11-6.97 (m, 2H), 6.74-6.66 (m, 2H), 4.57-4.50 (m, 1H), 4.48-4.40 (m, 1H), 4.31-4.24 (m, 1H), 3.23-3.02 (m, 4H), 3.02-2.92 (m, 2H), 2.81-2.71 (m, 2H), 2.22-2.03 (m, 1H), 2.03-1.88 (m, 1H), 1.73-1.59 (m, 1H), 1.57-1.31 (m, 4H), 1.24-1.17 (m, 16H), 0.85-0.79 (m, 3H) ppm; [α]_D²⁰ = - 6.2° (C = 1.5, DMSO).

Analytical data of compound 393



Peptide **393** was synthesized and released from solid support according to **GP 2** and **GP 4**. **Yield** = 5 %; **Purity** > 85% (LC_MS); **LC-MS** (C4, ESI_MS) 692.3 [M+H]⁺, 714.5 [M+Na]⁺; R_t = 5.41 min.

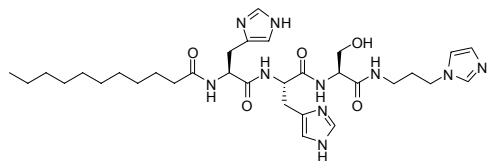
Analytical data of compound 394



Peptide **394** was synthesized and released from solid support according to **GP 2** and **GP 4**. **Yield** = 7 %; **Purity** > 95% (LC_MS); **LC-MS** (C4, ESI_MS) 649.4 [M+H]⁺, 671.3 [M+Na]⁺; R_t = 5.97 min; ¹H NMR (400 MHz, DMSO-D₆): δ = 8.94 (dd, *J* = 3.2, 1.2 Hz, 1H), 8.91 (dd, *J* = 6.4, 1.2 Hz, 1H), 8.40-8.28 (m, 1H), 8.14 (t, *J* = 7.8, 7.8 Hz, 1H), 7.36 (s, 1H), 7.30 (s, 1H), 7.02 (d, *J* = 7.0 Hz, 1H), 6.99-6.92 (m, 4H), 6.60 (d, *J* = 9.6 Hz, 1H), 4.58-4.50 (m, 2H), 4.26 (dd, *J* = 13.5,

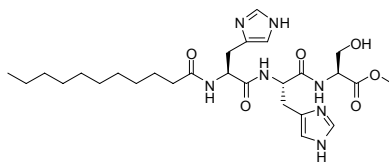
8.2 Hz, 1H), 3.16 (dd, $J = 8.7, 5.0$ Hz, 2H), 3.13-3.04 (m, 3H), 3.02-2.93 (m, 3H), 2.25-2.05 (m, 2H), 2.02-1.86 (m, 2H), 1.73-1.59 (m, 1H), 1.54-1.42 (m, 2H), 1.27-1.16 (m, 16H), 0.85-0.79 (m, 3H) ppm; $[\alpha]_D^{20} = -6.6^\circ$ (C = 0.5, DMSO).

Analytical data of compound 395



Peptide **395** was synthesized and released from solid support according to **GP 2** and **GP 4**. **Yield** = 13 %; **Purity** > 95% (LC_MS); **LC-MS** (C4, ESI_MS) 655.4 [M+H]⁺, 677.5 [M+Na]⁺; $R_t = 4.93$ min; **¹H NMR** (400 MHz, DMSO- D_6): $\delta = 8.98$ (s, 1H), 8.91 (s, 1H), 8.91 (s, 1H), 8.23 (d, $J = 7.8$ Hz, 1H), 8.18 (s, 1H), 8.16 (s, 1H), 8.13 (d, $J = 7.0$ Hz, 1H), 7.71 (t, $J = 1.6$ Hz, 1H), 7.65 (t, $J = 1.5$ Hz, 1H), 7.32 (s, 1H), 7.28 (s, 1H), 4.62 (dt, $J = 7.7, 5.5$ Hz, 1H), 4.53 (dt, $J = 8.5, 4.9$ Hz, 1H), 4.22-4.14 (m, 4H), 3.63 (dd, $J = 10.7, 5.7$ Hz, 1H), 3.58 (dd, $J = 10.8, 5.4$ Hz, 1H), 3.11 (dd, $J = 15.1, 5.2$ Hz, 1H), 3.04 (dd, $J = 10.9, 4.1$ Hz, 1H), 2.99 (dd, $J = 15.8, 7.1$ Hz, 1H), 2.87 (dd, $J = 15.2, 9.2$ Hz, 1H), 2.05 (t, $J = 7.3$ Hz, 2H), 1.98-1.90 (m, 2H), 1.43-1.31 (m, 2H), 1.28-1.16 (m, 14H), 1.14-1.09 (m, 2H), 0.83 (t, $J = 6.8$ Hz, 3H) ppm; $[\alpha]_D^{20} = -6.0^\circ$ (C = 1.2, DMSO).

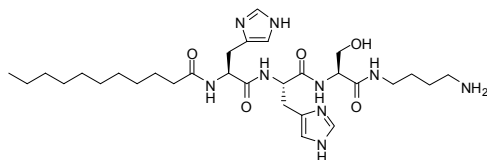
Analytical data of compound 396



Peptide **396** was synthesized and released from solid support according to **GP 2** and **GP 4**. **Yield** = 23 %; **Purity** > 85% (LC_MS); **LC-MS** (C4, ESI_MS) 562.2 [M+H]⁺, 584.4 [M+Na]⁺; $R_t = 5.61$ min; **¹H NMR** (400 MHz, DMSO- D_6): $\delta = 8.89$ (s, 1H), 8.87 (s, 1H), 8.38 (d, $J = 7.5$ Hz, 1H), 8.23 (d, $J = 7.9$ Hz, 1H), 8.14 (d, $J = 7.8$ Hz, 1H), 7.29 (s, 1H), 7.26 (s, 1H), 4.66 (dt, $J = 8.1, 5.5$ Hz, 1H), 4.52 (dt, $J = 8.2, 5.6$ Hz, 1H), 4.34 (td, $J = 7.6, 4.6$ Hz, 1H), 3.73 (dd, $J = 11.0, 5.0$ Hz, 1H), 3.61 (s, 3H), 3.61 (dd, $J = 11.0, 4.3$ Hz, 1H), 3.10 (dd, $J = 15.3, 5.3$ Hz, 1H), 3.02 (dd, $J = 15.3, 5.6$ Hz, 1H), 2.95 (dd, $J = 14.9, 8.1$ Hz, 1H), 2.87 (dd, $J = 15.4, 9.0$ Hz, 1H), 2.05

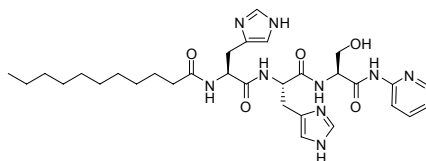
(t, $J = 7.4$ Hz, 2H), 1.42-1.34 (m, 2H), 1.27-1.17 (m, 14H), 1.15-1.10 (m, 2H), 0.83 (t, $J = 6.8$ Hz, 3H) ppm; $[\alpha]_D^{20} = -6.0^\circ$ (C = 2.2, DMSO).

Analytical data of compound 397



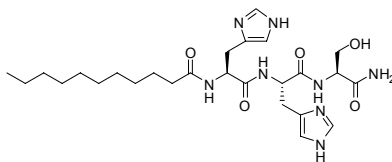
Peptide **397** was synthesized and released from solid support according to **GP 2** and **GP 4**. **Yield** = 26 %; **Purity** > 95% (LC_MS); **LC-MS** (C4, ESI_MS) 618.4 [M+H]⁺, 640.4 [M+Na]⁺; $R_t = 4.92$ min; **¹H NMR** (400 MHz, DMSO-D₆): $\delta = 8.91$ (s, 2H), 8.18 (t, $J = 7.8$ Hz, 2H), 8.10 (d, $J = 7.2$ Hz, 1H), 8.06 (t, $J = 5.6$ Hz, 1H), 7.81 (s, 2H), 7.32 (s, 1H), 7.28 (s, 1H), 4.61 (td, $J = 7.7, 5.75$ Hz, 1H), 4.53 (dt, $J = 8.6, 5.3$ Hz, 1H), 4.20 (q, $J = 5.6, 5.3$ Hz, 1H), 3.58 (dd, $J = 5.3, 2.7$ Hz, 2H), 3.16-2.96 (m, 3H), 2.87 (dd, $J = 15.3, 9.3$ Hz, 1H), 2.05 (t, $J = 7.4$ Hz, 2H), 1.58-1.47 (m, 2H), 1.47-1.40 (m, 2H), 1.36 (dd, $J = 14.7, 7.2$ Hz, 2H), 1.28-1.15 (m, 14H), 1.14-1.09 (m, 2H), 0.83 (t, $J = 6.8$ Hz, 3H) ppm; $[\alpha]_D^{20} = -5.9^\circ$ (C = 2.4, DMSO).

Analytical data of compound 398



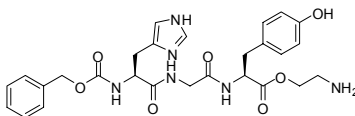
Peptide **398** was synthesized and released from solid support according to **GP 2** and **GP 4**. **Yield** = 8 %; **Purity** > 85% (LC_MS); **LC-MS** (C4, ESI_MS) 624.2 [M+H]⁺, 646.3 [M+Na]⁺; $R_t = 5.72$ min; **¹H NMR** (400 MHz, DMSO-D₆): $\delta = 10.46$ (s, 1H), 8.91 (s, 1H), 8.89 (s, 1H), 8.31 (ddd, $J = 4.8, 1.9, 0.9$ Hz, 1H), 8.24 (d, $J = 7.6$ Hz, 1H), 8.21 (d, $J = 7.5$ Hz, 1H), 8.14 (d, $J = 7.7$ Hz, 1H), 8.03 (d, $J = 8.4$ Hz, 1H), 7.80-7.74 (m, 1H), 7.33 (s, 1H), 7.29 (s, 1H), 7.11 (ddd, $J = 7.3, 4.9, 1.0$ Hz, 1H), 4.68 (dd, $J = 13.5, 7.5$ Hz, 1H), 4.57-4.51 (m, 2H), 3.76 (dd, $J = 10.9, 5.3$ Hz, 1H), 3.65 (dd, $J = 11.0, 4.9$ Hz, 1H), 3.13 (dd, $J = 15.1, 5.2$ Hz, 1H), 3.04 (dd, $J = 15.4, 6.1$ Hz, 1H), 3.00 (dd, $J = 15.3, 6.7$ Hz, 1H), 2.88 (dd, $J = 15.4, 8.1$ Hz, 1H), 2.05 (t, $J = 7.5$ Hz, 2H), 1.44-1.33 (m, 2H), 1.28-1.16 (m, 14H), 1.14-1.10 (m, 2H), 0.83 (t, $J = 6.8$ Hz, 3H) ppm; $[\alpha]_D^{20} = -7.5^\circ$ (C = 0.6, DMSO).

Analytical data of compound 399



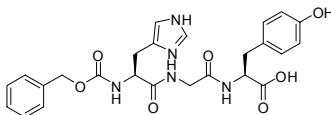
Peptide **399** was synthesized and released from solid support according to **GP 2** and **GP 4**. **Yield** = 3 %; **Purity** > 95% (LC_MS); **LC-MS** (C4, ESI_MS) 547.3 [M+H]⁺, 569.4 [M+Na]⁺; R_t = 5.60 min.

Analytical data of compound 400



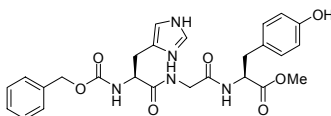
Peptide **400** was synthesized and released from solid support according to **GP 2** and **GP 4**. **Yield** = 3 %; **Purity** > 95% (LC_MS); **LC-MS** (C4, ESI_MS) 553.2 [M+H]⁺, 575.3 [M+Na]⁺; R_t = 4.35 min.

Analytical data of compound 401



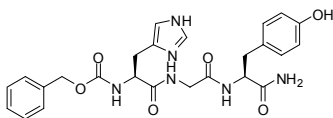
Peptide **401** was synthesized and released from solid support according to **GP 2** and **GP 4**. **Yield** = 4 %; **Purity** > 95% (LC_MS); **LC-MS** (C18, ESI_MS) 510.1 [M+H]⁺, 532.1 [M+Na]⁺; R_t = 5.29 min.

Analytical data of compound 402



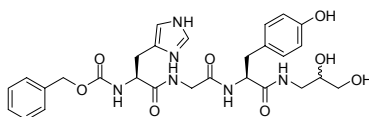
Peptide **402** was synthesized and released from solid support according to **GP 2** and **GP 4**. **Yield** = 3 %; **Purity** > 95% (LC_MS); **LC-MS** (C18, ESI_MS) 524.1 [M+H]⁺, 546.2 [M+Na]⁺; R_t = 5.71 min.

Analytical data of compound 403



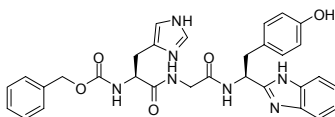
Peptide **403** was synthesized and released from solid support according to **GP 2** and **GP 4**. **Yield** = 3 %; **Purity** > 95% (LC_MS); **LC-MS** (C18, ESI_MS) 509.1 [M+H]⁺, 532.2 [M+Na]⁺; R_t = 5.03 min.

Analytical data of compound 404



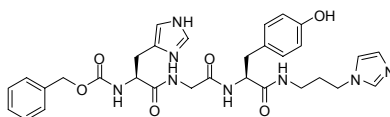
Peptide **404** was synthesized and released from solid support according to **GP 2** and **GP 4**. **Yield** = 4 %; **Purity** > 95% (LC_MS); **LC-MS** (C18, ESI_MS) 583.2 [M+H]⁺, 605.3 [M+Na]⁺; R_t = 4.93 min.

Analytical data of compound 405



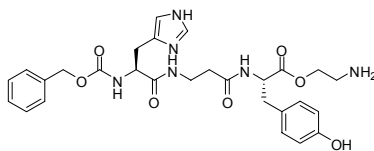
Peptide **405** was synthesized and released from solid support according to **GP 2** and **GP 4**. **Yield** = 2 %; **Purity** > 95% (LC_MS); **LC-MS** (C18, ESI_MS) 582.2 [M+H]⁺, 604.2 [M+Na]⁺; R_t = 5.03 min.

Analytical data of compound 406



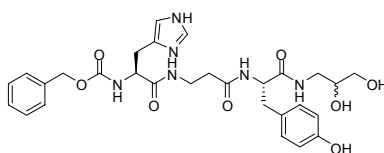
Peptide **406** was synthesized and released from solid support according to **GP 2** and **GP 4**. **Yield** = 3 %; **Purity** > 90% (LC_MS); **LC-MS** (C18, ESI_MS) 617.2 [M+H]⁺, 639.2 [M+Na]⁺; R_t = 4.35 min.

Analytical data of compound 407



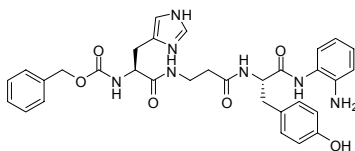
Peptide **407** was synthesized and released from solid support according to **GP 2** and **GP 4**. **Yield** = 1 %; **Purity** > 95% (LC_MS); **LC-MS** (C18, ESI_MS) 567.2 [M+H]⁺, 589.2 [M+Na]⁺; R_t = 4.44 min.

Analytical data of compound 408



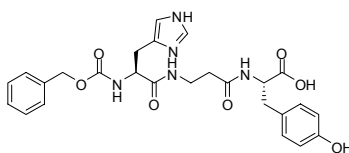
Peptide **408** was synthesized and released from solid support according to **GP 2** and **GP 4**. **Yield** = 5 %; **Purity** > 95% (LC_MS); **LC-MS** (C18, ESI_MS) 597.2 [M+H]⁺, 619.3 [M+Na]⁺; R_t = 4.92 min.

Analytical data of compound 409



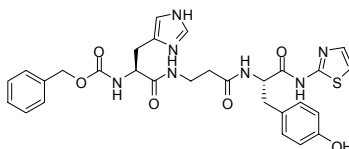
Peptide **409** was synthesized and released from solid support according to **GP 2** and **GP 4**. **Yield** = 3 %; **Purity** > 80% (LC_MS); **LC-MS** (C18, ESI_MS) 614.2 [M+H]⁺, 636.2 [M+Na]⁺; R_t = 5.59 min.

Analytical data of compound 410



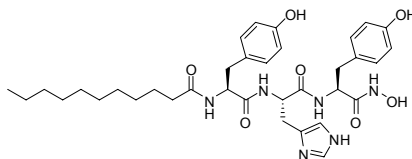
Peptide **410** was synthesized and released from solid support according to **GP 2** and **GP 4**. **Yield** = 2 %, **Purity** > 95% (LC_MS); **LC-MS** (C4, ESI_MS) 524.2 [M+H]⁺, 546.2 [M+Na]⁺; R_t = 5.32 min.

Analytical data of compound 411



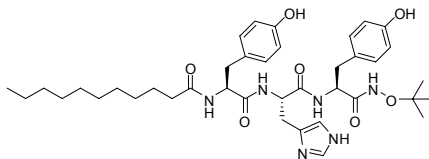
Peptide **411** was synthesized and released from solid support according to **GP 2** and **GP 4**. **Yield** = 1 %; **Purity** > 95% (LC_MS); **LC-MS** (C18, ESI_MS) 606.1 [M+H]⁺, 628.2 [M+Na]⁺; R_t = 5.78 min.

Analytical data of compound 412



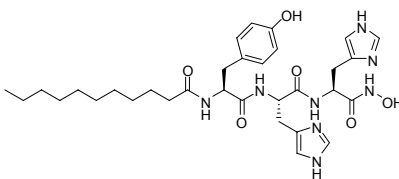
Peptide **412** was synthesized and released from solid support according to **GP 2** and **GP 5**. **Yield** = 10 %; **Purity** > 95% (LC_MS); **LC-MS** (C4, ESI_MS) 665.3 [M+H]⁺, 687.3 [M+Na]⁺; R_t = 6.89 min; ¹H NMR (400 MHz, DMSO-D₆): δ = 10.69 (s, 1H), 9.17 (s, 1H), 9.12 (s, 1H), 8.88 (s, 2H), 8.21 (d, *J* = 8.0 Hz, 1H), 8.05 (d, *J* = 7.9 Hz, 1H), 7.95 (d, *J* = 7.8 Hz, 1H), 7.26 (s, 1H), 7.00 (d, *J* = 8.6 Hz, 2H), 6.97 (d, *J* = 8.6 Hz, 2H), 6.62 (d, *J* = 8.3 Hz, 2H), 6.60 (d, *J* = 8.2 Hz, 2H), 4.55 (dd, *J* = 13.5, 7.6 Hz, 1H), 4.37-4.31 (m, 1H), 4.26 (q, *J* = 7.8, Hz, 1H), 3.02 (dd, *J* = 14.9, 5.5 Hz, 1H), 2.91 (dd, *J* = 15.1, 7.6 Hz, 1H), 2.79 (dd, *J* = 12.9, 5.5 Hz, 2H), 2.69 (dd, *J* = 12.7, 9.1 Hz, 2H), 1.99 (t, *J* = 7.0 Hz, 2H), 1.39-1.30 (m, 2H), 1.29-1.12 (m, 14H), 1.11-1.03 (m, 2H), 0.84 (t, *J* = 6.8 Hz, 3H) ppm; [α]_D²⁰ = + 7.7° (C = 0.8, DMSO).

Analytical data of compound 413



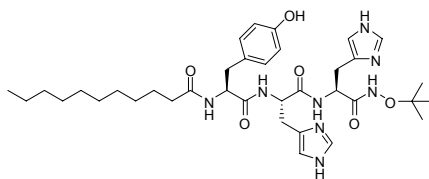
Peptide **413** was synthesized and released from solid support according to **GP 2** and **GP 5**. **Yield** = 5 %; **Purity** > 95% (LC_MS); **LC-MS** (C4, ESI_MS) 721.4 [M+H]⁺, 743.3 [M+Na]⁺; R_t = 7.25 min; **¹H NMR** (400 MHz, DMSO-D₆): δ = 10.55 (s, 1H), 9.17 (s, 1H), 9.11 (s, 1H), 8.87 (s, 1H), 8.22 (d, *J* = 8.17 Hz, 1H), 8.11 (d, *J* = 7.4 Hz, 1H), 7.94 (d, *J* = 8.1 Hz, 1H), 7.27 (s, 1H), 7.00 (d, *J* = 8.6 Hz, 2H), 7.00 (d, *J* = 8.5 Hz, 2H), 6.63 (d, *J* = 8.5 Hz, 2H), 6.60 (d, *J* = 8.5 Hz, 2H), 4.57 (q, *J* = 7.7 Hz, 1H), 4.38-4.29 (m, 2H), 3.02 (dd, *J* = 15.2, 5.6 Hz, 1H), 2.91 (dd, *J* = 15.4, 7.6 Hz, 1H), 2.83-2.70 (m, 3H), 2.63-2.54 (m, 1H), 1.99 (t, *J* = 7.4 Hz, 2H), 1.38-1.29 (m, 2H), 1.29-1.12 (m, 14H), 1.11-1.05 (m, 2H), 1.03 (s, 9H), 0.84 (t, *J* = 6.8 Hz, 3H) ppm; [α]_D²⁰ = + 11.2° (C = 0.4, DMSO).

Analytical data of compound 414



Peptide **414** was synthesized and released from solid support according to **GP 2** and **GP 5**. **Yield** = 6 %; **Purity** > 95% (LC_MS); **LC-MS** (C4, ESI_MS) 639.3 [M+H]⁺, 661.3 [M+Na]⁺; R_t = 6.00 min; **¹H NMR** (400 MHz, DMSO-D₆): δ = 8.89 (s, 1H), 8.85 (s, 1H), 8.28 (d, *J* = 3.7 Hz, 1H), 8.26 (d, *J* = 3.0 Hz, 1H), 7.95 (d, *J* = 7.5 Hz, 1H), 7.29 (s, 1H), 7.26 (s, 1H), 6.99 (d, *J* = 8.5 Hz, 2H), 6.60 (d, *J* = 8.5 Hz, 2H), 4.52 (td, *J* = 7.9, 5.6 Hz, 1H), 4.41 (dd, *J* = 14.2, 7.7 Hz, 1H), 4.36-4.30 (m, 1H), 3.08 (dd, *J* = 6.0, 3.2 Hz, 1H), 3.06-3.02 (m, 2H), 2.92 (dd, *J* = 14.9, 7.5 Hz, 2H), 2.79 (dd, *J* = 13.9, 3.8 Hz, 1H), 2.02-1.97 (m, 2H), 1.38-1.29 (m, 1H), 1.28-1.11 (m, 14H), 1.10-1.04 (m, 2H), 0.84 (t, *J* = 6.9 Hz, 3H) ppm; [α]_D²⁰ = + 0.6° (C = 0.5, DMSO).

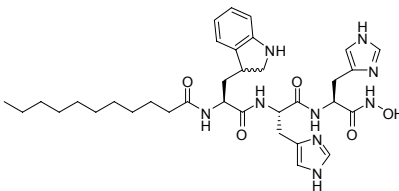
Analytical data of compound 415



Peptide **415** was synthesized and released from solid support according to **GP 2** and **GP 5**. **Yield** = 5 %; **Purity** > 95% (LC_MS); **LC-MS** (C4, ESI_MS) 695.4 [M+H]⁺, 717.4 [M+Na]⁺; R_t = 6.22 min; **¹H NMR** (400 MHz, DMSO-D₆): δ = 9.13 (s, 1H), 8.87 (s, 1H), 8.85 (s, 1H), 8.34 (d, *J* =

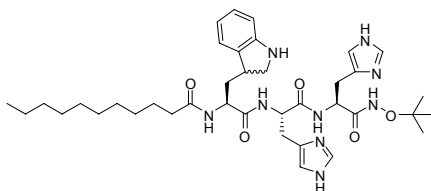
7.7 Hz, 1H), 8.28 (d, $J = 7.9$ Hz, 1H), 7.94 (d, $J = 7.5$ Hz, 1H), 7.33 (s, 1H), 7.27 (s, 1H), 6.99 (d, $J = 8.4$ Hz, 2H), 6.60 (d, $J = 8.5$ Hz, 2H), 4.54 (dd, $J = 13.5, 7.5$ Hz, 1H), 4.45 (q, $J = 7.2$ Hz, 1H), 4.37-4.30 (m, 1H), 3.10-3.06 (m, 1H), 3.05-3.01 (m, 2H), 2.97-2.89 (m, 2H), 2.79 (dd, $J = 13.9, 3.5$ Hz, 1H), 2.02-1.97 (m, 1H), 1.39-1.29 (m, 2H), 1.29-1.11 (m, 16H), 1.07 (s, 9H), 0.84 (t, $J = 6.8$ Hz, 3H) ppm.

Analytical data of compound 416



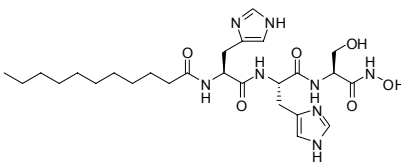
Peptide **416** was synthesized and released from solid support according to **GP 2** and **GP 3**. **Yield** = 5 %; **Purity** > 85% (LC_MS); **LC-MS** (C4, ESI_MS) 664.3 [M+H]⁺, 686.4 [M+Na]⁺; $R_t = 5.73$ min; **¹H NMR** (400 MHz, DMSO-D₆): $\delta = 8.90$ (s, 1H), 8.30 (d, $J = 7.8$ Hz, 1H), 8.14 (d, $J = 7.5$ Hz, 1H), 7.29 (d, $J = 4.7$ Hz, 2H), 6.93 (d, $J = 7.2$ Hz, 1H), 6.55 (d, $J = 6.7$ Hz, 1H), 4.57-4.50 (m, 1H), 4.37 (dd, $J = 14.9, 6.9$ Hz, 1H), 4.26 (dd, $J = 14.8, 7.9$ Hz, 1H), 3.14 (dd, $J = 13.6, 6.6$ Hz, 1H), 3.10-3.02 (m, 4H), 3.01-2.95 (m, 1H), 2.23-2.03 (m, 2H), 1.54-1.42 (m, 2H), 1.27-1.14 (m, 16H), 0.82 (dt, $J = 7.0, 2.4$ Hz, 3H) ppm; $[\alpha]_D^{20} = -8.0^\circ$ (C = 0.2, DMSO).

Analytical data of compound 417



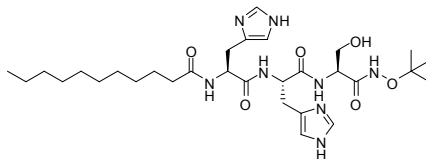
Peptide **417** was synthesized and released from solid support according to **GP 2** and **GP 5**. **Yield** = 5 %; **Purity** > 95% (LC_MS); **LC-MS** (C4, ESI_MS) 720.4 [M+H]⁺, 742.4 [M+Na]⁺; $R_t = 6.00$ min; **¹H NMR** (400 MHz, DMSO-D₆): $\delta = 8.90$ (s, 1H), 8.30 (d, $J = 7.8$ Hz, 1H), 8.14 (d, $J = 7.5$ Hz, 1H), 7.29 (d, $J = 4.7$ Hz, 2H), 6.93 (d, $J = 7.2$ Hz, 1H), 6.55 (d, $J = 6.7$ Hz, 1H), 4.57-4.50 (m, 1H), 4.37 (dd, $J = 14.9, 6.9$ Hz, 1H), 4.26 (dd, $J = 14.8, 7.9$ Hz, 1H), 3.14 (dd, $J = 13.6, 6.6$ Hz, 1H), 3.10-3.02 (m, 4H), 3.01-2.95 (m, 1H), 2.23-2.03 (m, 2H), 1.54-1.42 (m, 2H), 1.27-1.14 (m, 16H), 1.04 (s, 9H), 0.82 (dt, $J = 7.0, 2.4$ Hz, 3H) ppm; $[\alpha]_D^{20} = -6.5^\circ$ (C = 0.2, DMSO).

Analytical data of compound 418



Peptide **418** was synthesized and released from solid support according to **GP 2** and **GP 5**. **Yield** = 6 %; **Purity** > 95% (LC_MS); **LC-MS** (C4, ESI_MS) 563.3 [M+H]⁺, 585.3 [M+Na]⁺; R_t = 5.59 min; **¹H NMR** (400 MHz, DMSO-D₆): δ = 8.83 (s, 1H), 8.80 (s, 1H), 8.15 (s, 1H), 8.13 (s, 1H), 8.11 (d, *J* = 1.9 Hz, 1H), 7.27 (s, 1H), 7.26 (s, 1H), 4.59 (dd, *J* = 13.1, 7.1 Hz, 1H), 4.52 (dt, *J* = 8.1, 5.3 Hz, 1H), 4.15 (dd, *J* = 13.2, 5.8 Hz, 1H), 3.53 (d, *J* = 6.0 Hz, 1H), 3.06 (dd, *J* = 15.7, 5.9 Hz, 1H), 3.02 (dd, *J* = 16.3, 5.3 Hz, 1H), 2.96 (dd, *J* = 14.9, 7.3 Hz, 1H), 2.86 (dd, *J* = 15.1, 8.5 Hz, 1H), 2.05 (t, *J* = 7.4 Hz, 2H), 1.43-1.34 (m, 2H), 1.28-1.15 (m, 14H), 1.16-1.07 (m, 2H), 0.84 (t, *J* = 6.8 Hz, 3H) ppm; [α]_D²⁰ = - 8.7° (C = 0.4, DMSO).

Analytical data of compound 419



Peptide **419** was synthesized and released from solid support according to **GP 2** and **GP 5**. **Yield** = 4 %; **Purity** > 95% (LC_MS); **LC-MS** (C4, ESI_MS) 619.4 [M+H]⁺, 641.3 [M+Na]⁺; R_t = 5.85 min; **¹H NMR** (400 MHz, DMSO-D₆): δ = 8.83 (s, 1H), 8.14 (d, *J* = 7.8 Hz, 1H), 8.10 (d, *J* = 8.0 Hz, 1H), 7.28 (s, 1H), 7.26 (s, 1H), 4.60 (dd, *J* = 13.4, 6.8 Hz, 1H), 4.52 (dt, *J* = 8.2, 5.3 Hz, 1H), 4.18 (dd, *J* = 12.7, 6.4 Hz, 1H), 3.55 (d, *J* = 6.3 Hz, 2H), 3.06 (dd, *J* = 15.3, 5.6 Hz, 1H), 3.01 (dd, *J* = 15.1, 5.0 Hz, 1H), 2.97 (dd, *J* = 15.9, 5.7 Hz, 1H), 2.86 (dd, *J* = 15.2, 8.9 Hz, 1H), 2.05 (t, *J* = 7.4 Hz, 2H), 1.43-1.34 (m, 2H), 1.27-1.15 (m, 16H), 1.13 (s, 9H), 0.84 (t, *J* = 6.9 Hz, 3H) ppm; [α]_D²⁰ = - 16.0° (C = 0.1, DMSO).

General procedure for *in vitro* screening of peptides library (M)

The *in vitro* screening of peptides was performed in 96 microtiter plate. 50 μL of 0.4 μM Rab GGTase and 4 μM NBD-FPP **1** was added to the well followed by 0.5 μL of inhibitor in 10 mM DMSO solution. The solution was mixed, shaken and incubated at 37°C for two minutes. 50 μL

of 4 μM Rab-7:REP-1 cocktail solution was added to the same well. The measurement was started immediately.

Negative control for the bleaching of NBD-FPP 1 caused by inhibitors during *in vitro* screening (NC)

50 μL of 0.4 μM Rab GGTase and 4 μM NBD-FPP 1 was added to the well followed by 0.5 μL of inhibitor in 10 mM DMSO solution. The solution was mixed, shaken and incubated at 37°C for two minutes. 50 μL buffer (50 mM Hepes, 50 mM NaCl, 2 mM MgCl_2 , 5 mM DTE, 20 μM GDP, 0.01% Triton X-100, pH7.2) was added to the same well. The measurement was started immediately.

Positive control of measurement (PC)

50 μL of 0.4 μM Rab GGTase and 4 μM NBD-FPP 1 was added to the well followed by 0.5 μL of DMSO. The solution was mixed, shaken and incubated at 37°C for two minutes. 50 μL of 4 μM Rab-7:REP-1 cocktail solution was added to the same well. The measurement was started immediately.

Negative control for the bleaching of NBD-FPP 1 caused by DMSO during *in vitro* screening (NC_{DMSO})

50 μL of 0.4 μM Rab GGTase and 4 μM NBD-FPP 1 was added to the well followed by 0.5 μL DMSO. The solution was mixed, shaken and incubated at 37°C for two minutes. 50 μL buffer (50 mM Hepes, 50 mM NaCl, 2 mM MgCl_2 , 5 mM DTE, 20 μM GDP, 0.01% Triton X-100, pH7.2) was added to the same well. The measurement was started immediately.

% of remaining enzyme activity was determined by the following equation:

$$\% \text{ of remaining enzyme activity} = \frac{\text{M} - \text{NC}}{\text{PC} - \text{NC}_{\text{DMSO}}}$$

The IC_{50} was determined using non linear fitting curve based on the following equation with the program Grafit:

$$y = \frac{100\%}{1 + \left(\frac{X}{IC_{50}}\right)^s}$$

where y = enzyme inhibition = V_i/V_0 ($0 < y < 100$)
 x = inhibitor concentration
 s = slope factor

8 References

- [1] (a) J. M. Berg, J. L. Tymoczko, L. Stryer, *Biochemistry*, **2002**, New York: W. H. Freeman and Co., 5th ed.; (b) G. M. Cooper, *The Cell - A Molecular Approach*, **2000**, Sunderland (MA): Sinauer Associates, Inc.; 2nd ed.
- [2] H. Lodish, A. Berk, S. L. Zipursky, P. Matsudaira, D. Baltimore, J. E. Darnell, *Molecular Cell Biology*. **2000**, New York: W. H. Freeman & Co.; 4th ed.
- [3] (a) G. J. Siegal, B. W. Agranoff, R. W. Albers, S. K. Fisher, M. D. Uhler, *Basic Neurochemistry, Molecular, Cellular, and Medical Aspects* **1999**, Philadelphia: Lippincott, Williams & Wilkins; 6th ed.; (b) B. Alberts, A. Johnson, J. Lewis, M. Raff, K. Roberts, P. Walter, *Molecular Biology of the Cell*, **2002**, New York and London: Garland Science; 4th ed.
- [4] M. C. Seabra, E. H. Mules, A. N. Hume, *Trends Mol. Med.*, **2002**, *8*, 23-30.
- [5] N. Segev *Sci. STKE*, **2001**, re11.
- [6] J. B. Pereira-Leal, M. C. Seabra, *J. Mol. Biol.*, **2001**, *313*, 889-901.
- [7] H. Stenmark, V. M. Olkkonen, *Genome Biol.*, **2001**, *2*: reviews 3007.1-3007.7.
- [8] (a) E. J. Tisdale, J. R. Bourne, R. Khosravi-Far, C. J. Der, W. E. Balch, *J. Cell Biol.*, **1992**, *119*, 749-761; (b) G. Fischer von Mollard, B. Stahl, C. Li, T. Sudhof, R. Jahn, *Trends Biochem. Sci.*, **1994**, *19*, 164-168.
- [9] (a) C. Gurkan, S. M. Stagg, P. Lapointe, W. E. Balch, *Nat Rev Mol Cell Biol.*, **2006**, *7*, 727-738; (b) J. C. Dawson, J. A. Legg, L. M. Machesky, *Trends Cell Biol.*, **2006**, *16*, 493-498.
- [10] (a) A. Mammoto, T. Sasaki, Y. Kim, Y. Takai, *J. Biol. Chem.*, **2000**, *275*, 13167-13170; (b) C. Barlowe, L. Orci, T. Yeung, M. Hosobuchi, B. Hamamoto, N. Salama, M. F. Rexach, M. Ravazzola, M. Amherdt, R. Schekman, *Cell*, **1994**, *77*, 895-907.
- [11] K. Roberg, N. Rowley, C. Kaiser, *J. Cell Biol.*, **1997**, *137*, 1469-1482.
- [12] (a) G. Bloom, L. Goldstein, *J. Cell Biol.*, **1998**, *140*, 1277-1280; (b) R. D. Vale, R. A. Milligan, *Science*, **2000**, *288*, 88-95.
- [13] (a) A. Echard, F. Jollivet, O. Martinez, J. J. Lacapère, A. Rousselet, I. Janoueix-Lerosey, B. Goud, *Science*, **1998**, *279*, 580-585; (b) E. Hill, M. Clarke, F. A. Barr, *EMBO J.*, **2000**, *19*, 5711-5719.
- [14] M. H. Cuif, F. Possmayer, H. Zander, N. Bordes, F. Jollivet, A. Couedel-Courteille, I. Janoueix-Lerosey, G. Langsley, M. Bornens, B. Goud, *EMBO J.*, **1999**, *18*, 1772-1782.
- [15] M. Sogaard, K. Tani, R. R. Ye, S. Geromanos, P. Tempst, T. Kirchhausen, J. E. Rothman, T. Söllner, *Cell*, **1994**, *78*, 937-948; (b) S. R. Pfeffer, *Nature Cell Biol.*, **1999**, *1*, E17-E22.
- [16] (a) A. Simonsen, R. Lippe, S. Christoforidis, J. Gaullier, A. Brech, J. Callaghan, B. Toh, C. Murphy, M. Zerial, H. Stenmark, *Nature*, **1998**, *394*, 494-498; (b) S. Christoforidis, H. M. McBride, R. D. Burgoyne, M. Zerial, *Nature*, **1999**, *397*, 621-625; (c) M. A. Barbieri, S.

-
- Hoffenberg, R. Roberts, A. Mukhopadhyay, A. Pomrehn, B. F. Dickey, P. D. Stahl, *J. Biol. Chem.*, **1998**, *273*, 25850-25855.
- [17] W. J. Hong, *Biochim. Biophys. Acta.*, **2005**, *1744*, 120-144.
- [18] R. Jahn, T. C. Sudhof, *Annu. Rev. Biochem.*, **1999**, *68*, 863-911.
- [19] (a) A. Simonsen, J. M. Gaullier, A. D'Arrigo, H. Stenmark, *J. Biol. Chem.*, **1999**, *274*, 28857-28860; (b) E. Nielsen, S. Christoforidis, S. Uttenweiler-Joseph, M. Miaczynska, F. Dewitte, M. Wilm, B. Hoflack, M. Zerial, *J. Cell Biol.*, **2000**, *151*, 601-612.
- [20] (a) S. R. Pfeffer, A. B. Dirac-Svejstrup, T. Soldati, *J. Biol. Chem.*, **1995**, *270*, 17057-17059.
- [21] (a) D. A. Andres, M. C. Seabra, M. S. Brown, S. A. Armstrong, T. E. Smeland, F. P. M. Cremers, J. L. Goldstein, *Cell*, **1993**, *73*, 1091-1099; (b) J. C. Sanford, J. Yu, J. Y. Pan, M. Wessling-Resnick, *J. Biol. Chem.*, **1995**, *270*, 26904-26909.
- [22] R. S. Goody, A. Rak, K. Alexandrov, *Cell. Mol. Life Sci.*, **2005**, *62*, 1657-1670.
- [23] K. F. Leung, R. Baron, M. C. Seabra, *J. Lipid Res.*, **2006**, *47*, 467-475.
- [24] (a) M. C. Seabra, M. S. Brown, C. A. Slaughter, T. C. Sudhof, J. L. Goldstein, *Cell*, **1992**, *70*, 1049-1057; (b) M. C. Seabra, J. L. Goldstein, T. C. Sudhof, M. S. Brown, *J. Biol. Chem.*, **1992**, *267*, 14497-14503.
- [25] P. J. Casey, M. C. Seabra, *J. Biol. Chem.*, **1996**, *271*, 5289-5292.
- [26] (a) C. Griscelli, M. Prunieras, *Int. J. Dermatol.* **1978**, *17*, 788-791; (b) C. Klein, N. Philippe, F. Le Deist, S. Fraitag, C. Prost, A. Durandy, A. Fischer, C. Griscelli, *J. Pediatr.*, **1994**, *125*, 886-895.
- [27] (a) G. Ménasché, E. Pastural, J. Feldmann, S. Certain, F. Ersoy, S. Dupuis, N. Wulffraat, D. Bianchi, A. Fischer, F. Le Deist, G. de Saint Basile, *Nat. Genet.*, **2000**, *25*, 173-176; (b) S. M. Wilson, R. Yip, D. A. Swing, T. N. O'Sullivan, Y. Zhang, E. K. Novak, R. T. Swank, L. B. Russell, N. G. Copeland, N. A. Jenkins, *Proc. Natl. Acad. Sci. U S A.*, **2000**, *97*, 7933-7938.
- [28] M. C. Seabra, *Ophthalm. Genet.*, **1996**, *17*, 43-46.
- [29] M. C. Seabra, Y. K. Ho, J. S. Anant, *J. Biol. Chem.*, **1995**, *270*, 24420-24427.
- [30] (a) J. C. Detter, Q. Zhang, E. H. Mules, E. K. Novak, V. S. Mishra, W. Li, E. B. McMurtrie, V. T. Tchernev, M. R. Wallace, M. C. Seabra, R. T. Swank, S. F. Kingsmore, *Proc. Natl. Acad. Sci. USA.*, **2000**, *97*, 4144-4149; (b) M. Huizing, Y. Anikster, W. A. Gahl, *Traffic*, **2000**, *1*, 823-835; (c) R. T. Swank, E. K. Novak, M. E. McGarry, M. E. Rusiniak, L. Feng, *Pigment Cell Res.*, **1998**, *11*, 60-80.
- [31] (a) S. M. Sebt, *Cancer Cell*, **2005**, *7*, 297-300; (b) M. R. Lackner, R. M. Kindt, P. M. Carroll, K. Brown, M. R. Cancilla, C. Chen, H. de Silva, Y. Franke, B. Guan, T. Heuer, T. Hung, K. Keegan, J. M. Lee, V. Manne, C. O'Brien, D. Parry, J. J. Perez-Villar, R. K. Reddy, H. Xiao, H. Zhan, M. Cockett, G. Plowman, K. Fitzgerald, M. Costa, P. Ross-Macdonald, *Cancer Cell*, **2005**, *7*, 325-336.
- [32] I. M. Bell. *J. Med. Chem.*, **2004**, *47*, 1869-1878.

-
- [33] (a) F. Shen, M. C. Seabra, *J. Biol. Chem.*, **1996**, *271*, 3692-3698; (b) N. H. Thoma, A. Iakovenko, A. Kalinin, H. Waldmann, R. S. Goody, K. Alexandrov, *Biochemistry*, **2001**, *40*, 268-274; (c) N. H. Thoma, A. Niculae, R. S. Goody, K. Alexandrov, *J. Biol. Chem.*, **2001**, *276*, 48631-48636; (d) H. Zhang, M. C. Seabra, J. Deisenhofer, *Struct. Fold. Des.*, **2000**, *8*, 241-251.
- [34] C. L. Strickland, W. T. Windsor, R. Syto, L. Wang, R. Bond, Z. Wu, J. Schwartz, H. V. Le, L. S. Beese, P. C. Weber, *Biochemistry*, **1998**, *37*, 16601-16611.
- [35] T. S. Reid, L. S. Beese, *Biochemistry*, **2004**, *43*, 6877-6884.
- [36] T. U. Mayer, T. M. Kapoor, S. J. Haggarty, R. W. King, S. L. Schreiber, T. J. Mitchison, *Science*, **1999**, *286*, 971-974.
- [37] F. El Qualid, L. H. Cohen, G. A. van der Marel, M. Overhand, *Curr. Med. Chem.*, **2006**, *13*, 2385-2427.
- [38] (a) F. P. Coxon, M. H. Helfrich, B. Larijani, M. Muzylak, J. E. Dunford, D. Marshall, A. D. McKinnon, S. A. Nesbitt, M. A. Horton, M. C. Seabra, F. H. Ebetino, M. J. Rogers, *J. Biol. Chem.*, **2001**, *276*, 48213-48222; (b) Z. Ren, C. E. Elson, M. N. Gould, *Biochem. Pharmacol.*, **1997**, *54*, 113-120.
- [39] (a) M. Thutewohl, L. Kissau, B. Popkirova, I.-M. Karaguni, T. Nowak, M. Bate, J. Kuhlmann, O. Müller, H. Waldmann, *Bioorg. Med. Chem.*, **2003**, *11*, 2617-2626; (b) M. Thutewohl, L. Kissau, B. Popkirova, I.-M. Karaguni, T. Nowak, M. Bate, J. Kuhlmann, O. Müller, H. Waldmann, *Angew. Chem. Int. Ed.*, **2002**, *41*, 3616-3620.
- [40] K. Shiomi, H. Yang, J. Inokoshi, D. Van der Pyl, A. Nakagawa, H. Takeshima, S. Omura. *J. Antibiot.*, **1993**, *46*, 229-234.
- [41] (a) J. S. Anant, L. Desnoyers, M. Machius, B. Demeler, J. C. Hansen, K. D. Westover, J. Deisenhofer, M. C. Seabra, *Biochemistry*, **1998**, *37*, 12559-12568; (b) N. H. Thoma, A. Niculae, R. S. Goody, K. Alexandrov, *J. Biol. Chem.*, **2001**, *276*, 48631-48636.
- [42] (a) D. L. Pompliano, R. P. Gomez, N. J. Anthony, *J. Am. Chem. Soc.*, **1992**, *114*, 7945-7946; (b) W. C. Pickett, F. L. Zhang, C. Silverstrim, S. R. Schow, M. M. Wick, S. S. Kerwar, *Anal. Biochem.*, **1995**, *225*, 60-63.
- [43] T. Durek, K. Alexandrov, R. S. Goody, A. Hildebrand, I. Heinemann, H. Waldmann, *J. Am. Chem. Soc.*, **2004**, *126*, 16368-16378.
- [44] Y. W. Wu, H. Waldmann, R. Reents, F. H. Ebetino, R. S. Goody, K. Alexandrov, *ChemBioChem*, **2006**, *7*, 1859-1861.
- [45] B. Dursina, R. Reents, C. Delon, Y. Wu, M. Kulharia, M. Thutewohl, A. Veligodsky, A. Kalinin, V. Evstifeev, D. Ciobanu, S. E. Szedlaczek, H. Waldmann, R. S. Goody, K. Alexandrov, *J. Am. Chem. Soc.*, **2006**, *128*, 2822-2835.
- [46] (a) O. Pylypenko, A. Rak, R. Reents, A. Niculae, V. Sidorovitch, M. D. Cioaca, E. Bessolitsyna, N. H. Thoma, H. Waldmann, I. Schlichting, R. S. Goody, K. Alexandrov, *Mol. Cell*, **2003**, *11*, 483-494; (b) N. H. Thoma, A. Iakovenko, A. Kalinin, H. Waldmann, R. S. Goody, K. Alexandrov,

-
- Biochemistry*, **2001**, *40*, 268-274.
- [47] P. J. Murphy, S. E. Lee *J. Chem. Soc., Perkin Trans.*, **1999**, *1*, 3049 – 3066.
- [48] R. Reents, M. Wagner, S. Schlummer, J. Kuhlmann, H. Waldmann, *ChemBioChem*, **2005**, *6*, 86-94.
- [49] R. B. Merrifield, *J. Am. Chem. Soc.*, **1964**, *86*, 304-305.
- [50] F. Guillier, D. Orain, M. Bradley, *Chem. Rev.*, **2000**, *100*, 2091-2158.
- [51] (a) M. H. Todd, S. F. Oliver, C. Abell, *Org. Lett.*, **1999**, *1*, 1149-1151; (b) B. J. Backes, A. A. Virgilio, J. A. Ellman, *J. Am. Chem. Soc.* **1996**, *118*, 3055-3056.
- [52] C. R. Millington, R. Quarrell, G. Lowe, *Tetrahedron Lett.* **1998**, *39*, 7201-7204
- [53] (a) C. Peters, H. Waldmann, *J. Org. Chem.*, **2003**, *68*, 6053-6055; (b) J. A. Camarero, B. J. Hackel, J. J. De Yoreo, A. R. Mitchell, *J. Org. Chem.*, **2004**, *69*, 4145-4151.
- [54] J. Meienhofer, M. Waki, E. P. Heimer, T. J. Lambros, R. C. Makofske, C. -D. Chang, *Int. J. Pept. Prot. Res.*, **1979**, *13*, 35.
- [55] Michael Thutewohl, *Kombinatorische Festphasensynthese von Analoga des Farnesyltransferase-Inhibitors Peptidcinnamin E und deren biologische Evaluierung*, Phd Thesis, **2002**, Dortmund University.

Abbreviations

AcOH	Acetic acid
Ac ₂ O	Acetic anhydride
Aloc	Allyloxycarbonyl
Boc	<i>Tert</i> -butyl carboxycarbonyl
Calc.	Calculated
CH	Cyclohexane
COSY	COrrrelation SpectroscopY
CP	Cross-polarization
Da	Dalton
Dansyl	5-dimethylaminonaphtalene-1-sulfonyl
DIAD	Diisopropyl azodicarboxylate
DIC	<i>N,N'</i> -Di- <i>iso</i> -propylcarbodiimide
DIPEA	<i>N,N</i> -Diisopropylethylamine
DMAP	4-Dimethylaminopyridine
DMF	<i>N,N</i> -Dimethylformamide
DMPC	1,2-Dimyristoyl- <i>sn</i> -Glycero-3-Phosphocholine
DMS	Dimethyl sulfide
DMSO	Dimethyl sulfoxide
DNA	Deoxyribonucleic acid
EA	EtOAc Ethyl acetate
EI	Electron impact
Eq.	Equivalent
ER	Endoplasmic reticulum
ESI	Electron spray ionization
Et ₃ N	Triethyl amine
FAB	Fast atom bombardment
Fmoc	9-Fluorenylmethyloxycarbonyl
Fmoc-OSu	N-(9-Fluorenylmethoxycarbonyloxy) succinimide
GAP	GTPase activating protein

GC_MS	Gas chromatography mass spectrometry
GDP	Guanosine 5'-diphosphate
GTP	Guanosine 5'-triphosphate
GEF	Guanine nucleotide exchange factor
HBTU	O-(1H-benzotriazole-1-yl)-N,N,N',N'-tetramethyluronium hexafluorophosphate
HD	Hexadecyl
HetCor	Heteronuclear COrelated SpectroscopY
HOAT	1-hydroxy-7-azabenzotriazole
HOBT	1-Hydroxy-1H-benzotriazole
HPLC	High Performance Liquid Chromatography
Hz	Hertz
IC ₅₀	50% inhibitory concentration
LC_MS	Liquid Chromatography Mass Spectrometry
LRR	Leucine-rich repeats
MALDI	Matrix assisted laser desorption ionization
MAS	Magic angle spinning
MS	Mass spectrum
NBS	N-Bromosuccinimide
NCS	N-Chlorosuccinimide
NMR	Nuclear magnetic resonance
NOESY	Nuclear Overhauser Effect SpectroscopY
PCR	Polymerase chain reaction
PPh ₃	Triphenyl phosphine
PPTS	Pyridinium P-Toluenesulfonates
PS	Polystyrene
rac.	Racemic
Rf	Retention factor
Rt	Retention time
RT	Room temperature
SAR	Structure activity relationship

Sat.	Saturated
SDS	Sodium dodecylsulfate
<i>t</i> -Bu	Tert-butyl
TES	Triethylsilane
TFA	Trifluoro acetic acid
THP	Tetrahydropyran
THF	Tetrahydrofuran
TLC	Thin layer chromatography
TOCSY	TOTAL Correlated SpectroscopY
TOF	Time of flight
$[\alpha]_D^{20}$	Specific optical rotation

Summary of the Dissertation

The first half of this thesis is dedicated to dynamic and structural studies on the interaction between the C-terminus of the N-Ras protein with phospholipid membranes using solid-state NMR. In this work, three semi-synthetic N-Ras proteins were constructed by replacing the native palmitoyl chain with hexadecyl chain to give better stability. To facilitate the NMR study, the C-terminal N-Ras peptide was labeled in an alternating pattern with ^{13}C and ^{15}N to increase signal intensity and to suppress the background signals from the lipid matrix. Furthermore, the hexadecyl chain of the peptide was labeled with ^2H to study the dynamic behavior of the lipid chain in the phospholipid membrane. The proteins were synthesized using the chemical biology approach, through ligation of chemically synthesized labeled C-terminal lipidated peptide with the non-labeled N-terminal water-soluble N-Ras protein. The ligation strategy was done through the Michael addition of cysteine at C-terminal of soluble N-Ras protein to MIC group of labeled lipidated peptide. This synthetic method gave moderate yield which were sufficient for the solid state NMR study.

Different MAS NMR experiments such as Bloch-decay ^{13}C experiment, CP ^{13}C experiment, ^{13}C - ^{13}C and ^{13}C - ^1H correlation experiments were performed to establish the $^{13}\text{C}_{\alpha}$, $^{13}\text{C}_{\beta}$, ^{13}CO and $^1\text{H}_{\alpha}$ chemical shifts for the C-terminus of the membrane-bound N-Ras protein. The chemical shifts for the C-terminus of the membrane-bound N-Ras proteins determined in the MAS NMR experiments provided the input parameters for the structural calculations. The program package TALOS was used for the empirical prediction of Φ and Ψ backbone structure of the membrane-binding domain of Ras from the isotopic chemical shifts.

A simulated annealing protocol was used for structural calculations of the C-terminus of the membrane-bound lipidated Ras protein based on the torsion angle obtained from TALOS prediction. The computer simulation revealed that the global fold of the C terminus of the N-Ras protein in the membrane resembles a horseshoe. The membrane anchor of Ras has no regular α -helical or β -sheet motifs. The membrane topology of the

protein is determined by hydrophobic interactions between the lipidated cysteine and hydrophobic side chains. The lipid-binding domain is linked to the GTP-binding N-terminal region of the protein by a linker domain, which is putatively flexible. In contrast to H-Ras, there is currently no known structure (or no available structural studies) of the C-terminus of N-Ras. However, considering that there is 92 % sequence homology between H-Ras and N-Ras it can be assumed that these structures are very similar.

Deuterium-labeled hexadecyl lipid chain at cysteine 181 of N-Ras protein was used to obtain the dynamic information of the N-Ras lipid chain's interaction with phospholipid membranes. The dynamic results calculated from ^2H NMR indicate that the chain inserts into the hydrophobic membrane interior with almost no energy cost, thereby largely retaining its configurational entropy and leaving the host matrix relatively unchanged. The dynamic properties of this lipid chain completely differ from that of the phospholipid membrane, registering a comparatively low order parameter and high motional amplitude inside the phospholipid membrane.

The backbone and side chain molecular mobility of the seven isotopically labeled C-terminal amino acids of Ras were studied by ^{13}C MAS NMR spectroscopy. The order parameter of backbone and side chain was determined by 2D *dipolar coupling chemical-shift correlation experiment* (DIPSHIFT). The order parameter of farnesylated cysteine 186 is about 60% higher than that of hexadecylated cysteine 181. This observation suggested that the farnesyl modification of cysteine 186 is relatively rigid. In summary, the C-terminus of membrane-associated full length Ras protein shows a versatile dynamics.

The second half of the thesis dealt with the identification of peptide inhibitors of Rab GGTase, which is an enzyme of Rab proteins. The lead compound of the peptide inhibitors is the natural product Pepticinnamin E. The synthesis of peptides library employing hydrazine linker has shown to be an efficient method to generate a large compound library in a short time. By using this traceless linker, around 380 derivatives of Pepticinnamin E were generated. Two oxidation cleavage methods were used to released

the peptides from the solid support, namely, NBS/pyridine, and Cu(OAc)₂/pyridine leading to different derivatives at C-terminus of peptides.

Out of these 382 peptide inhibitors, 18 compounds have been found to be active against Rab GGTase, with IC₅₀ values between 1 μM to 70 μM. From the structure activity relationship analysis, peptides which contain a long lipid chain at its N-terminus and a moiety with metal chelating ability at C-terminus were found to be the most active substrate to inhibit Rab GGTase activity.

Three compounds, **59**, **80** and **81**, were found to have *in vivo* activity against Rab GGTase. These three peptides were subjected to selectivity screening to determine their potency against FTase, GGTase I and Rab GGTase. These three peptides have shown high inhibitory selectivity of Rab GGTase over FTase and GGTase I. Of which, **81**, which consists of these two features mentioned above, has IC₅₀ value of around 1 μM against the enzyme. The kinetic studies of **81** have revealed that the inhibitor is a non-competitive inhibitor of Rab GGTase with respect to the lipid substrate and has a K_d value of around 600 nM.

Zusammenfassung der Dissertation

Der erste Teil der Dissertation widmet sich dem Studium von Struktur und Dynamik des C-Terminus des N-Ras-Proteins in Phospholipid-Membranen mittels Festkörper-NMR-Techniken. In dieser Arbeit wurden drei semi-synthetische N-Ras-Proteine konstruiert, bei denen die Palmitoylgruppe durch eine Hexadecyleinheit ersetzt wurde, um eine bessere Stabilität zu gewährleisten. Zur Verstärkung der NMR-Signale des Proteins und zur Unterdrückung der Signale der Lipidmatrix, wurden mit ^{13}C - und ^{15}N -Isotopen angereicherte C-terminale N-Ras Peptide dargestellt. Darüber hinaus wurde die Hexadecylkette des Peptids mit ^2H markiert, um Informationen über die Dynamik des Proteins in Wechselwirkung mit Phospholipid-Membranen zu erhalten. Im Sinne einer chemisch-biologischen Fragestellung wurden zunächst durch chemische Synthese isotopenmarkierte C-terminale Peptide dargestellt und diese dann biochemisch mit dem wasserlöslichen N-Ras Protein über eine MIC-Ligation verknüpft. Die hierbei erzielte moderate Ausbeute war ausreichend, um die folgenden NMR-Studien durchzuführen.

Um die chemischen Verschiebungen von $^{13}\text{C}\alpha$, $^{13}\text{C}\beta$, ^{13}CO und $^1\text{H}\alpha$ des C-Terminus von membran-gebundenen N-Ras zuzuordnen, wurden mittels direkt angeregte ^{13}C -NMR Experiment, ^{13}C -Kreuzpolarisationsexperimente, ^{13}C - ^{13}C - und ^{13}C - ^1H Korrelations-experimente durchgeführt. Aus diesen Daten konnten mithilfe des TALOS-Programmpakets empirische Voraussagen der Phi (Φ)- und Psi (Ψ)-Rückgratstruktur der membranbindenden Domäne von N-Ras gemacht werden.

Auf den TALOS-Voraussagen über den Torsionswinkel basierend, wurde ein Strukturmodell des membran-gebundenen lipidierten Ras-Proteins berechnet. Der C-Terminus des membrangebundenen Ras Proteins ähnelt in seiner Struktur einem Hufeisen. Der Membrananker von Ras verfügt nicht über reguläre α -helikale oder β -Faltblatt-Motive. Die Membrantopologie des Proteins ist bestimmt durch hydrophobe Wechselwirkungen zwischen dem lipidierten Cystein und hydrophoben Seitenketten. Die lipidbindende Domäne ist mit der GTP-bindenden N-terminalen Region des Proteins über eine Linker-Domäne verknüpft, die mutmaßlich flexibel ist. Im Gegensatz zu H-Ras existiert gegenwärtig noch keine Struktur des N-Terminus von N-Ras. Dennoch kann bei einer Sequenzhomologität von 92 % von einer hohen strukturellen Ähnlichkeit ausgegangen werden.

Eine deuteriummarkierte Hexadecyl-Lipidkette an Cystein 181 von N-Ras wurde zur Gewinnung dynamischer Informationen über die Wechselwirkung von N-Ras-Lipidkette und Phospholipid-Membran eingesetzt. Aus ^2H -NMR-Experimenten berechnete Ergebnisse zur Dynamik deuten darauf hin, dass sich die Kette in die Hostmembran einbaut, wobei die Konfigurationsentropie größtenteils erhalten bleibt und die Lipidmembran relativ unverändert bleibt. Die dynamischen Eigenschaften dieser Lipidkette unterscheiden sich jedoch vollständig von denen einer Phospholipid-Membran, da ein niedriger Ordnungsparameter und eine hohe Bewegungsamplitude innerhalb der Phospholipid-Membran berechnet wurden.

Die molekulare Dynamik von Rückgrat und Seitenketten der sieben isotopen-markierten C-terminalen Aminosäuren von Ras wurden mittels ^{13}C -MAS-NMR untersucht. Hierbei wurde durch 2D DIPSHIFT-Experimente der Ordnungsparameter von Rückgrat und Seitenkette bestimmt. Für den Ordnungsparameter von farnesyliertem Cystein 181 wurde ein um etwa 60 % höher Wert als für hexadecyliertes Cystein 186 gefunden, was für eine relative hohe Rigidity der Farnesylmodifikation von Cystein 186 spricht. Zusammenfassend lässt sich sagen, dass der C-Terminus von membranassoziiertem Ras-Protein eine vielseitige Dynamik aufweist.

Die zweite Hälfte dieser Dissertation setzt sich mit der Identifikation von Peptidinhibitoren der Rab GGTase, einem Enzym der Rab-Proteine, auseinander. Als Leitstruktur für die Peptidinhibitoren dient der Naturstoff Pepticinnamin E. Es wurde gezeigt, dass die Festphasensynthese einer Peptidbibliothek unter Anwendung des Hydrazidlinkers eine effiziente Methode zur Herstellung einer großen Zahl von Substanzen in kurzer Zeit ermöglicht. Durch Nutzung dieses „spurlosen“ Linkers wurden etwa 380 Pepticinnamin-Derivate dargestellt. Zur Abspaltung der Peptide von der festen Phase wurden zwei Oxidationsmethoden angewandt, die zu unterschiedlichen Derivaten am C-Terminus der Peptide führten: NBS/Pyridin und $\text{Cu}(\text{OAc})_2$.

Bei 18 dieser 382 Peptidinhibitoren wurde eine inhibitorische Aktivität bei der Rab GGTase gefunden; in der Folge wurden IC_{50} -Werte zwischen $1\ \mu\text{M}$ und $70\ \mu\text{M}$ für diese Peptide bestimmt. Eine Analyse der Struktur-Aktivitäts-Beziehung ergab, dass Peptide mit langer Lipidkette am N-Terminus und Metall-chelatisierenden Eigenschaften am C-Terminus die höchste inhibitorische Aktivität bei Rab GGTase aufweisen. So wurde für die Verbindung **81**,

die diese beiden strukturellen Bedingungen erfüllt, ein IC_{50} -Wert von etwa $1\ \mu\text{M}$ gegen das Enzym bestimmt.

Drei Verbindungen, **59**, **80** und **81**, zeigten *in vivo* – Aktivität gegen Rab GGTase in der Zelle. In einem Selektivitäts-Screening zeigten diese Peptide eine hohe inhibitorische Selektivität gegen Rab GGTase im Vergleich zu FTase und GGTase I. Kinetische Untersuchungen mit **81** zeigen eine in Bezug auf das Lipidsubstrat nicht-kompetitive Inhibierung der Rab GGTase mit einem K_D -Wert von etwa $600\ \text{nM}$.

Acknowledgement

First of all, I would like to thank my Ph.D. advisor Prof. Dr. Herbert Waldmann for giving me an opportunity to work under his supervision in his group. I am grateful for his constant support, constructive guidance and active encouragement throughout the project work which helped me a lot in understanding the subject and undertaking several problems with fruitful solutions.

I wish to express my gratitude to Dr. Daniel Huster, Dr. Jürgen Kuhlmann, Guido Reuther and Christine Nowak for the nice collaborating work on the NMR project. Thousands of thanks go to YaoWen Wu, Dr. Christine Delon, Dr. Kirill Alexandrov and Prof. Dr. Roger Goody from Department of Physical Biochemistry for providing the necessary assistance in Rab GGTase project. I am deeply thankful to Dr. Sabine Arndt, Dr. Robin Bon, Dr. Ester Guiu Rozas and Stefan Wetzel for helping and working together with me in Rab GGTase team.

I would like to thank International Max-Planck Research School in Chemical Biology (IMPRS-CB) and also Max-Planck Society for their generous financial supports. I also want to show my sincere gratitude to Dr. Jutta Rötter and Frau Brigitte Rose for their kind official supports and helps.

I would like to thank all my colleagues at the Department of Chemical Biology who have contributed for a cooperative working environment along last four years, in special to those people working in Dortmund University lab, Réne Tannert, Matthias Mentel, Hao Tan, Dr. Masahito Yoshida, Dr. Samy Chamma, Dr. TaiShan Hu, Kirtikumar Jadhav and Dr Ivan Reis Correa.

Finally, I would like to express my greatest gratitude to my parents and siblings for their unconditional support. Especially, I would like to give my special thanks to my fiancée Xiaoi whose patient love enabled me to complete this work.

Curriculum Vitae

Name: Kui-Thong Tan

Date of Birth: 22.02.1978

Sex: Male

Nationalities: Malaysian

Education

- | | |
|-----------------|------------------------------------------------------------------------------------------------------------------------------------------------------------------------------------------------------------------------------------------------------------------------|
| 1985-1990 | Sekolah Rendah Jenis Kebangsaan (C) Tit Bin, Pantai Remis, Malaysia |
| 1991-1996 | Yik Ching High School, Pantai Remis, Malaysia |
| 1997-2001 | Bachelor of Science in Chemistry (Honours), National University of Singapore, Singapore |
| 06/2000-12/2000 | B. Sc (Honours) "Development of New Methods for Construction of α -Regioselective Homoallylic Alcohols" under the supervision of Prof. Dr. Teck Peng Loh in National University of Singapore, Singapore |
| 08/2003-09/2007 | Ph. D. thesis "Solid-State NMR Spectroscopy Studies of Human N-Ras Protein and Synthesis and Biochemical Studies of Rab GGTase Inhibitors" under the supervision of Prof. Dr. Herbert Waldmann in Max-Planck Institute of Molecular Physiology and Dortmund University |

International Publications

1. The first $\text{In}(\text{OTf})_3$ catalyzed conversion of kinetically formed homoallylic alcohols into the thermodynamically preferred regioisomers: Application to the synthesis of 22 α -sterols. Loh, T. P.; **Tan, K. T.**; Hu, Q.Y. *Angew. Chem., Int. Ed. Engl.* **2001**, *40*, 2921-2922.
2. Diverse cyclization catalyzed by $\text{In}(\text{OTf})_3$ from the convergent assembly of substituted tetrahydrofurans and tetrahydropyrans. Loh, T. P.; Hu, Q. Y.; **Tan, K. T.**; Cheng, H. S. *Org. Lett.* **2001**, *3*, 2669-2672.
3. Development of a Highly α -Regioselective Indium-Mediated Allylation Reaction in Water. Loh, T. P.; **Tan, K. T.**; Yang, J. Y.; Xiang, C. L. *Tet. Lett.* **2001**, *42*, 8701-8703.
4. A New Mechanistic Proposal for the Origin of α -Homoallylic Alcohols in Indium-Mediated Allylation Reaction in Water. Loh, T. P.; **Tan, K. T.**; Hu, Q. Y. *Tet. Lett.* **2001**, *42*, 8705-8708.
5. Homoallylic sterol/indium (III) Lewis acid: novel enantioselective allylation reagent system exhibiting α -regioselectivity. Loh, T. P.; Hu, Q. Y.; Chok, Y. K.; **Tan, K. T.** *Tet. Lett.* **2001**, *42*, 9277-9280.
6. The First Example of Enantioselective Allyl Transfer from a Linear Homoallylic Alcohol to an Aldehyde. Loh, T. P.; Lee, C. L. K.; **Tan, K. T.** *Org. Lett.* **2002**, *4*, 2985-2987
7. Development of General α -Regioselective Metal-mediated Allylation Reactions in Aqueous Media and a New Mechanistic Proposal for the Origin of α -Regioselectivity. **Tan, K. T.**, Chng, S. S., Cheng, H. S., Loh, T. P. *J. Am. Chem. Soc.* **2003**, *125*, 2958-2963
8. An Unusual Approach to the Synthesis of Enantiomerically Cis Linear Homoallylic Alcohols Based on the Steric Interaction Mechanism of Camphor Scaffold. Lee, C. L. K., Lee, C. H. A., **Tan, K. T.** Loh, T. P. *Org. Lett.* **2004**, *6*, 1281-1283
9. Catalytic Asymmetric Allylation of Aldehydes via a Chiral Indium(III) Complex. Teo, Y. C.; **Tan, K. T.**; Loh, T. P. *Chem. Commun.*, **2005**, 1318-1320
10. Molecular Dynamics of a Membrane Bound Lipid-Modified Human N-Ras Protein Determined by Solid-State NMR Spectroscopy. G. Reuther, **K.-T. Tan**, J. Köhler, C. Nowak, A. Pampel, K. Arnold, J. Kuhlmann, H. Waldmann, D. Huster. *Angew. Chem., Int. Ed. Engl.* **2006**, *45*, 5387-5390
11. The Lipidated Membrane Anchor of Full Length N-Ras Protein Shows an Extensive Dynamics as Revealed by Solid-State NMR Spectroscopy. G. Reuther, **K.-T. Tan**, A.

Vogel, C. Nowak, K. Arnold, J. Kuhlmann, H. Waldmann, D. Huster. *J. Am. Chem. Soc.* **2006**, *128*, 13840-13846

12. Flexibility of Ras Lipid Modifications Studied by ^2H Solid-State NMR and Molecular Dynamic Simulation. A. Vogel, **K.-T. Tan**, H. Waldmann, S. E. Feller, M. F. Brown, D. Huster. *Biophys. J.*, **2007**, *In press*
13. Membrane binding of a lipidated N-Ras protein studied in lipid monolayers. F. Bringezu, M. Majerowicz, S. Wen, G. Reuther, **K.-T. Tan**, J. Kuhlmann, H. Waldmann, and Daniel Huster, *Eur. Biophys. J.*, **2007**, *in press*
14. Interaction analysis of prenylated Rab GTPase with Rab escort protein and GDP dissociation inhibitor explains the need for both regulators. Y.-W. Wu, **K.-T. Tan**, H. Waldmann, R. S. Goody, K. Alexandrov. *Proc. Natl. Acad. Sci. USA.*, **2007**, *in press*